Deliverable 6.1:

Initial State of the Art

on Gas Transport in Clayey Materials

Work Package GAS

Document information

Project Acronym	**EURAD**
Project Title	**European Joint Programme on Radioactive Waste Management**
Project Type	**European Joint Programme (EJP)**
EC grant agreement No.	**847593**
Project starting / end date	**1st June 2019 – 30 May 2024**
Work Package No.	**6**
Work Package Title	**Mechanistic understanding of gas transport in clay materials**
Work Package Acronym	**GAS**
Deliverable No.	**6.1**
Deliverable Title	**Initial State-of-the-Art on Gas Transport in Clayey Materials**
Lead Beneficiary	**ONDRAF/NIRAS**
Contractual Delivery Date	**30 November 2020**
Actual Delivery Date	**17 November 2021**
Type	**Report**
Dissemination level	**PU**
Authors	LEVASSEUR Séverine **(ONDRAF/NIRAS),** COLLIN Frédéric **(ULiège),** DANIELS Katherine **(BGS),** DYMITROWSKA Magdalena **(IRSN),** HARRINGTON Jon **(UKRI-BGS),** JACOPS Elke **(SCK CEN),** KOLDITZ Olaf **(UFZ),** MARSCHALL Paul **(Nagra),** NORRIS Simon **(RWM),** SILLEN Xavier **(ONDRAF/NIRAS),** TALANDIER Jean **(Andra),** TRUCHE Laurent **(CNRS/UGrenoble),** WENDLING Jacques **(Andra)**

To be cited as:

Levasseur S., Collin F., Daniels K., Dymitrowska M., Harrington J., Jacops E., Kolditz O., Marschall P., Norris S., Sillen X., Talandier J., Truche L. and Wendling J. (2021). Initial State of the Art on Gas Transport in Clayey Materials. Deliverable D6.1 of the HORIZON 2020 project EURAD, Work Package Gas. EC Grant agreement no: 847593.

Disclaimer

All information in this document is provided 'as is' and no guarantee or warranty is given that the information is fit for any particular purpose. The user, therefore, uses the information at its sole risk and liability. For the avoidance of all doubts, the European Commission has no liability in respect of this document, which is merely representing the authors' view.

Acknowledgement

EURAD (Deliverable n° 6.1) – Initial State of the Art on Gas Transport in Clayey Materials
Dissemination level: PU
Date of issue of this report: 17/11/2021

Page ii

Status of deliverable		
	By	Date
Delivered (Lead Beneficiary)	ONDRAF/NIRAS	20/10/2020
Verified (WP Leader)	ONDRAF/NIRAS	30/11/2020
Reviewed (Reviewers)	WP Board	06/11/2020
	R. Winsley	29/01/2021
	O. Leupin	22/03/2021
	M.V. Villar	26/04/2021
Verifier (WP Leader)	ONDRAF/NIRAS	24/10/2021
Approved (PMO)	R. Winsley	17/11/2021
Submitted to EC (Coordinator)	Andra	17/11/2021

EURAD (Deliverable n° 6.1) – Initial State of the Art on Gas Transport in Clayey Materials
Dissemination level: PU
Date of issue of this report: **17/11/2021**

Page iii

Executive summary

Gas generation and transport through a repository is an important issue for the geological disposal of radioactive waste. Increasing the understanding of gas transport through low-permeability porous materials such as clayey materials is so considered as a high priority in the EURAD Roadmap, within the geoscience theme. Owing to their excellent properties for the confinement of contaminants, clays are considered as potential host rocks for geological disposal in several countries in Europe. Clay-based materials are also expected to be used in engineered barriers in most geological repository concepts under development.

Considerable amounts of gas can be generated in a geological repository for radioactive waste. The largest fraction of the gas is expected to be hydrogen produced through the anaerobic corrosion of steel and reactive metals present in the waste, in their packaging and in the engineered barrier system (EBS). Radiolysis and the degradation of organics also produce gas. Even though the gas production processes are generally slow, it is possible that gas could be generated at a faster rate than it can be removed through the engineered barrier components and the host rock without creating discrete, gas-specific pathways (e.g. fracturing or pathway dilation). In several disposal concepts, the potential for the release to the biosphere of gas containing volatile radionuclides is an area that requires consideration and therefore robust underpinning knowledge.

Consequently, a work package devoted to the mechanistic understanding of gas transport in clayey materials (WP GAS) has been included in the first European Joint Programme on Radioactive Waste Management (EURAD). The raison d'être of this WP is to provide answers to two key end-users' questions:

- How can gas migrate within the repository and which water soluble and volatile radionuclide transport could be associated with it?

- How and to what extend could the hydro-mechanical perturbations induced by gas affect barrier integrity and performance?

Building on previous efforts and projects such as the EC project FORGE, the work programme of the WP GAS of EURAD aims in first place to provide data and develop process-level models in support of the mechanistic understanding of transport processes in natural and engineered clayey materials, of their couplings with the mechanical behaviour and of their impact on the properties of these materials. Experimental work aims to determine for each identified gas transport regime the range of conditions under which that regime is possible, in clay materials that are representative of potential host rocks and clayey EBS components that are being used or considered within European geological disposal programmes. In this way, data will be obtained that are pertinent for materials and conditions of interest to all Member States.

In addition to the extension of the scientific database, desk work in the WP GAS aims to show how the knowledge gained from laboratory and in situ configurations is integrated in conceptualisations of gas transport through different components of a disposal system and how gas could affect (or not) the performance of the components and the system. This involves (i) the assembly of phenomenological descriptions (storyboards) of gas transport and of its likely consequences at the relevant scale for typical repository configurations and (ii) testing different approaches to represent the effects of gas at repository scale and to bound their consequences in terms of repository performance.

EURAD (Deliverable n° 6.1) – Initial State of the Art on Gas Transport in Clayey Materials
Dissemination level: PU
Date of issue of this report: 17/11/2021

Page v

EURAD Deliverable 6.1 – Initial State of the Art on Gas Transport in Clayey Materials

The present state-of-the-art report (SOTA) on gas transport through clayey materials has been written in the early stage of the project. Its structure is aligned with the work programme of the WP GAS. It aims to provide a general overview of the state of knowledge with respect to the main RD&D (research, development and demonstration) topics of the WP GAS, with sufficient context so that it can be of use to a lay audience with limited technical background, early-stage programmes, RD&D managers and the teams involved in EURAD. This report is the result of a common understanding, shared by the organisations involved in the WP GAS of the current state of the art on gas transport in clayey materials. Building upon the identification of key uncertainties, this SOTA can be used as a baseline against which WP progress can be measured.

This state-of-the-art report starts by drawing a broad picture of gas transport in the specific context of geological disposal. The role of clay barriers in repositories is explained. An overview of relevant clayey materials and their properties is given, focusing on the materials studied in the experimental and modelling programmes of the WP GAS of EURAD. Then, the report details the main gas transport mechanisms which are expected to take place in a disposal system in the post-closure phase: (i) the diffusive transport of dissolved gas, including retardation effects by physico-sorption of gas on the solid phase, when gas produced within the system can dissolve in the pore water and be transported by diffusion; (ii) visco-capillary flow and (iii) the formation of discrete gas-filled pathways, if a free gas phase develops as the gas production rate exceeds the rate at which gas can be dissolved and evacuated by diffusion. The consequences of the modes of gas transport are discussed in terms of temporary or permanent disturbance of porous media. The hydro-mechanical processes associated with formation of additional pathways through the materials, such as pathway dilation and the creation of discrete pathways, are described in detail. Beyond the disturbances of the materials by the different gas transport modes, the likely consequences on barrier integrity are examined. Finally the conceptualisations of gas transport at the scale of disposal systems and approaches that can be used for evaluating the impact of gas with respect to the functioning of different repositories are discussed. At each stage of the description of gas transport mechanisms, particular attention was paid to emphasising the interests and needs of the end-users in the context of geological disposal, as well as to highlighting the common understanding of these mechanisms and listing the knowledge gaps as these stood at the beginning of the WP GAS of EURAD. The compilation of all the research on the transport of gas in clayey materials detailed in this SOTA reveals a great diversity of experimental results in terms of observed phenomena and processes. The comparison of results (and experiments) is not trivial and different interpretations are sometimes possible to explain the observations of the same experiment. The lack of reproducibility and/or replication further compounds the experimental uncertainties. Next to their consolidation, the output of laboratory tests need to be transposed to the conditions, in particular the stress fields, prevailing in a deep geological repository. With respect to modelling of gas transfer in saturated clay materials, continuum and discrete approaches exist. For both, the transition from the laboratory to the in situ scale is still a challenging task. It is the ambition of the WP GAS to address these issues. This SOTA is thus a baseline for the research activities carried out within the WP GAS of EURAD and a yardstick to measure its progress.

At the end of the EURAD European Joint Programme (2024), a second version of the SOTA will be written, focusing on the integration of new developments, key findings and insights gained during the project and/or that could emerge between 2019 and 2024 outside EURAD, but also clearly identifying and formulating the uncertainties of all types with sufficient context and full transparency in order to make it as practical as possible for the end-users to later assess which of those uncertainties are the most relevant within their national programme and to devise the best ways to handle them. The ambition of this second SOTA is to make clear statements on scientific consensus that can support a shared vision on gas management, recognising differences between national programmes, *in varietate concordia*.

EURAD (Deliverable n° 6.1) – Initial State of the Art on Gas Transport in Clayey Materials
Dissemination level: PU
Date of issue of this report: 17/11/2021

Page vi

Table of contents

EURAD (Deliverable n° 6.1) – Initial State of the Art on Gas Transport in Clayey Materials
Dissemination level: PU
Date of issue of this report: **17/11/2021**

Page vii

EURAD (Deliverable n° 6.1) – Initial State of the Art on Gas Transport in Clayey Materials
Dissemination level: PU
Date of issue of this report: 17/11/2021

Page viii

EURAD (Deliverable n° 6.1) – Initial State of the Art on Gas Transport in Clayey Materials
Dissemination level: PU
Date of issue of this report: 17/11/2021

Page ix

EURAD (Deliverable n° 6.1) – Initial State of the Art on Gas Transport in Clayey Materials
Dissemination level: PU
Date of issue of this report: 17/11/2021

Page x

EURAD (Deliverable n° 6.1) – Initial State of the Art on Gas Transport in Clayey Materials
Dissemination level: PU
Date of issue of this report: 17/11/2021

Page xi

Acronyms

Organisations – The organisations involved in the Work Package Gas of the EURAD European Joint Programme are in bold.	
Aalto University	Aalto University (*Aalto-yliopisto / Aalto-universitetet*) (Finland)
Andra	National Agency for Radioactive Waste Management (*Agence Nationale pour la Gestion des Déchets Radioactifs*) (France)
BGE	Federal Company for Radioactive Waste Disposal mbH (*Bundesgesellschaft für Endlagerung*) (Germany)
BGR	Federal Institute for Geosciences and Natural Resources (*Bundesanstalt für Geowissenschaften und Rohstoffe*) (Germany)
BGS	British Geological Survey (UKRI) (United Kingdom)
CEA	Alternative energies and atomic energy commission (*Commissariat à l'énergie atomique et aux énergies alternatives*) (France)
CIEMAT	Centre for Energy, Environment and Technology (*Centro de Investigaciones Energéticas, Medioambientales y Tecnológicas*) (Spain)
CIMNE	International Centre for Numerical Methods in Engineering (Spain)
CNRS	*Centre national de la recherche scientifique* (France)
CNRS (ULorraine)	GeoRessources, depending on the University of Lorraine and CNRS (France)
CNRS (UPoitiers)	Institute of Chemistry of Materials and Media *(Institut de chimie des milieux et matériaux de Poitiers – IC2MP),* depending on the University of Poitiers, IMT Atlantique and CNRS (France)
CNRS (UGrenoble)	Institute of Earth Sciences (*Institut des sciences de la Terre – ISTerre*), depending on the University of Grenoble and CNRS(France)
CNRS (UNantes)	*Laboratoire de physique subatomique et des technologies associées – Subatech*) depending on the University of Nantes, IMT Atlantique and CNRS (Nantes, France)
COVRA	Central Organisation for Radioactive Waste (*Centrale Organisatie Voor Radioactief Afval*) (The Netherlands)
CTU	Czech Technical University (Czech Republic)
EC	European Commission
EDF	*Electricité de France* (France)
ENRESA	National Radioactive Waste Company (*Empresa Nacional de Residuos Radiactivos*) (Spain)
EPFL	*Ecole Polytechnique Fédérale de Lausanne* (Switzerland)
EURIDICE	European Underground Research Infrastructure for Disposal of nuclear waste in a Clay Environment (Belgium)

EURAD (Deliverable n° 6.1) – Initial State of the Art on Gas Transport in Clayey Materials
Dissemination level: PU
Date of issue of this report: **17/11/2021**

Page xiii

Organisations – The organisations involved in the Work Package Gas of the EURAD European Joint Programme are in bold.

FZJ	Jülich research centre (*Forschungszentrum Jülich GmbH*) (Germany)
GRS	*Gesellschaft für Anlagen- und Reaktorsicherheit* (Germany)
IRSN	Institute for radiation protection and nuclear safety (*Institut de radioprotection et de sûreté nucléaire*) (France)
IUPAC	International Union of Pure and Applied Chemistry
LEI	Lithuanian Energy Institute (Lithuania)
Nagra	National Cooperative for the Disposal of Radioactive Waste (*Nationale Genossenschaft für die Lagerung radioaktiver Abfälle*) (Switzerland)
NWMO	Nuclear Waste Management Organization (Canada)
ONDRAF/NIRAS	Belgian Agency for Radioactive Waste and Enriched Fissile Materials (*Organisme national des déchets radioactifs et des matières fissiles enrichies / Nationale instelling voor radioactief afval en verrijkte Splijtstoffen)* (Belgium)
POSIVA	Finnish expert organisation responsible for the final disposal of spent nuclear fuel of the owners (Finland)
PSI	Paul Scherrer Institute (Switzerland)
RWM	Radioactive Waste Management (United Kingdom)
RWTH	Aachen University (Germany)
SCK CEN	Belgian Nuclear Research Centre (*Studiecentrum voor Kernenergie / Centre d'Étude de l'énergie Nucléaire*) (Belgium)
SKB	Swedish Nuclear Fuel and Waste Management Company (*Svensk Kärnbränslehantering*) (Sweden)
SÚRAO	Radioactive Waste Repositories Authority (*Správa Úložišť Radioaktivních Odpadú*) (Czech Republic)
TU Delft	Delft University of Technology (*Technische Universiteit Delft*) (The Netherlands)
UFZ	Helmholtz Centre for Environmental Research (*Helmholtz Zentrum für Umweltforschung*) (Germany)
ÚJV Řež	Nuclear Physics Institute (Czech Republic)
ULiège	University of Liège (Belgium)
UPC	Technical University of Catalonia (*Universitat Politècnica de Catalunya*) (Spain)
ZHAW	Zurich University of Applied Sciences (Switzerland)

EURAD (Deliverable n° 6.1) – Initial State of the Art on Gas Transport in Clayey Materials
Dissemination level: PU
Date of issue of this report: **17/11/2021**

Page xiv

Projects / facilities	
ACED	RD&D work package of EURAD devoted to the assessment of chemical evolution of ILW and HLW disposal cells
Äspö HRL	Äspö hard rock laboratory in Sweden
BEACON	Bentonite mechanical evolution – *EC project (2017–2021)*
CARBOWASTE	Treatment and disposal of irradiated graphite and other carbonaceous waste – *EC project (2008–2013)*
CAST	Carbon-14 source term and fate – *EC project (2013–2018)*
DECOVALEX	Development of coupled models and their validation against experiments – *international research and model comparison collaboration, initiated in 1992*
DONUT	RD&D work package of EURAD devoted to the development and improvement of numerical methods and tools for modelling coupled processes
EURAD	European joint programme on radioactive waste management – *EC funded (2019–2024)*
EURATOM	European atomic energy community
FEBEX	Full-scale engineered barriers experiment in crystalline host rock – *EC project (1996-1999)*
FEBEX II	Full-scale engineered barriers experiment in crystalline host rock phase II – *EC project (2000-2004)*
FORGE	Fate of repository gases. Investigation of process of gas generation and transport and their potential impact on a disposal system – *EC project (2009–2013)*
GAMBIT club	A consortium of radioactive waste management agencies: SKB, Andra, ENRESA, JNC (Japanese organisation), Nagra, and Posiva
GRIMSEL Test Site (GTS)	International underground research laboratory located in the Swiss Alps
HADES URL	High-activity disposal experimental site – underground research laboratory in Mol (Belgium)
HITEC	RD&D work package of EURAD devoted to the study of the influence of temperature on clay-based material behaviour
Lasgit	Large scale gas injection test (full-scale demonstration project performed at the Äspö hard rock laboratory in Sweden
MEGAS	Modelling and experiments on gas migration in repository host rocks (under the umbrella of the PEGASUS EC project) – *EC project (1992–1997)*
MHM URL	Meuse/Haute-Marne underground research laboratory in France
MIND	Microbiology in nuclear waste disposal – *EC project (2014-2018)*
Mont Terri URL	Underground research laboratory in Switzerland
NF-PRO	Understanding and physical and numerical modelling of the key processes in the near field and their coupling for different host rocks and repository strategies – *EC project (2004–2007)*

EURAD (Deliverable n° 6.1) – Initial State of the Art on Gas Transport in Clayey Materials
Dissemination level: PU
Date of issue of this report: 17/11/2021

Page xv

Projects / facilities	
PAMINA	Performance assessment methodologies in application to guide the development of the safety case – *EC project (2006–2009)*
PEBS	Long-term performance of engineered barrier systems (EBS) – *EC project (2010-2014)*
PEGASUS	Project on the effects of gas in underground storage facilities for radioactive waste – *EC umbrella project (1991–1998)*
PROGRESS	Research into gas generation and migration in radioactive waste repository systems – *EC project (1996–1999)*
RESEAL	A large scale in situ demonstration test for repository sealing in an argillaceous host rock – *EC project (1996–1999) (2000–2005)*
SELFRAC	Fractures and self-healing within the excavation disturbed zone in clays – *EC project (2002–2003)*
TIMODAZ	Thermal impact on the damaged zone around a radioactive waste disposal in clay host rocks – *EC project (2006–2010)*
Tournemire	Tournemire tunnel and experimental station, underground laboratory, France
UMAN	Work package of EURAD devoted to the understanding of uncertainty, risk and safety

Other acronyms	
BC	Boom Clay
BCV	Czech bentonite
BJH method	Barrett, Joyner and Halenta method
COx	Callovo-Oxfordian claystone
DWP	Disposal Waste Package
EBS	Engineered barrier system
EDZ	Excavation damaged zone
EGTS	Engineered gas transport system
FDT method	Fluid displacement technique with Kerdane
FEBEX bentonite	Bentonite extracted from the Cortijo de Archidona deposit (Spain) (sometimes also called 'Serrata clay' to reflect its geographical origin)
FEM	Finite element method
FIB-nt	Focused ion beam nano-tomography
FIB-SEM	Focused ion beam scanning electron microscopy

EURAD (Deliverable n° 6.1) – Initial State of the Art on Gas Transport in Clayey Materials
Dissemination level: PU
Date of issue of this report: 17/11/2021

Page xvi

Other acronyms	
GDF	Geological disposal facility (also called 'repository')
HLW	High-level waste
HMC	Hydro-mechanical and chemical
HPC	High-performance-computing
HR-SEM	High-resolution SEM
ILW	Long-lived intermediate-level waste
L/ILW	Low- and intermediate-level waste
LVDT	Linear variable differential transformer
MEX	Model-experiment-exercises
MIP	Mercury intrusion porosimetry
MLA	Machine learning algorithms
MOF	Metal organic framework
MX-80	Granular Wyoming sodium bentonite
NMR	Nuclear magnetic resonance
OCR	Over-consolidation ratio
OPA	Opalinus Clay
PA	Performance assessment
RD&D	Research, development, and demonstration
RE	Nationally funded research entity
REV	Representative elementary volume
RH	Relative humidity
RN	Radionuclide
S/B mixture	Mixture of quartz sand and bentonite in different proportions
SEM	Scanning electron microscopy
SF	Spent fuel
SOTA	State-of-the-art report
STEM	Scanning transmission electron microscopy
STP	Standard temperature and pressure
TEM	Transmission electron microscopy
THMC	Thermo-hydro-mechanical and chemical
TSO	Technical support organisation

EURAD (Deliverable n° 6.1) – Initial State of the Art on Gas Transport in Clayey Materials
Dissemination level: PU
Date of issue of this report: 17/11/2021

Page xvii

Other acronyms	
UILW	Unshielded intermediate-level waste
URL	Underground research laboratory
WMO	Waste management organisation
WP	Work package
XCT	X-ray computed tomography
XRD	X-ray diffraction
μ-CT	X-ray micro-computed tomography

EURAD (Deliverable n° 6.1) – Initial State of the Art on Gas Transport in Clayey Materials
Dissemination level: PU
Date of issue of this report: 17/11/2021

Page xviii

Symbols

Many authors from different research fields have contributed to this state-of-the-art report. As each research field has its own notations, compiling a list of common symbols was not straightforward. The following symbols are used throughout most of the document while the symbols in Sections 2.5 and 3.3 may differ.

Symbol	Parameter	Unit
C_c	Compression index	–
$C_{c,sat}$	Compression index for the saturated sample	–
C_p	Pore compressibility	1/Pa
C_s	Swelling index	–
D_0	Diffusion coefficient in free water	m²/s
D_{app}	Apparent diffusion coefficient	m²/s
D_{eff}	Effective diffusion coefficient	m²/s
D_p	Pore diffusion coefficient	m²/s
e	Void ratio	–
k	Intrinsic permeability	m²
k_g	Gas permeability	m²
k_w	Water permeability	m²
k_{rg}	Gas relative permeability	–
k_{rw}	Water relative permeability	–
K	Hydraulic conductivity	m/s
K_h	Horizontal hydraulic conductivity	m/s
K_v	Vertical hydraulic conductivity	m/s
K_0	Coefficient of earth pressure at rest	–
m, n	van Genuchten shape parameters	–
P	Pressure	Pa
P_b	Gas breakthrough pressure	Pa
P_c	Capillary pressure	Pa
P_g	Gas pressure	Pa
P_r	Gas entry pressure	Pa
P_w	Water pressure	Pa

EURAD (Deliverable n° 6.1) – Initial State of the Art on Gas Transport in Clayey Materials
Dissemination level: PU
Date of issue of this report: **17/11/2021**

Page xix

Symbol	Parameter	Unit
s	Suction	Pa
$S_{r,w}$	Degree of saturation of the porous media (also called 'water saturation')	–
T	Temperature	°C
ε	Strain	–
μ_g	Dynamic viscosity of the gas phase	Pa.s
μ_w	Dynamic viscosity of liquid water	Pa.s
μ_{nwf}	Viscosity of the non-wetting fluid	Pa.s
μ_{wf}	Viscosity of the wetting fluid	Pa.s
ρ_d	Dry density[1]	kg/m^3 or g/cm^3 or Mg/m^3
ρ_s	Solid density	kg/m^3
ρ_w	Density of water	kg/m^3
σ	Total stress	Pa
σ'	Effective stress	Pa
σ_H	Major horizontal stress	Pa
σ_h	Minor horizontal stress	Pa
σ_v	Vertical stress	Pa
ϕ	Porosity	–

[1] Three units are commonly used for dry density.

EURAD (Deliverable n° 6.1) – Initial State of the Art on Gas Transport in Clayey Materials
Dissemination level: PU
Date of issue of this report: **17/11/2021**

Page xx

1.   Introduction

Deep geological repositories for the disposal of radioactive waste generally rely on a multi-barrier system to isolate the waste from the biosphere. This multi-barrier system typically comprises the natural geological barrier provided by the repository host rock and its surroundings and an engineered barrier system (EBS) (Box 1). The EBS represents the man-made, engineered materials placed within a repository, including, among others and depending on the disposal concept, waste canisters, buffer materials, backfill and seals. This multi-barrier principle creates an overall robustness of the system that enhances confidence that the waste will be successfully contained, as the natural barrier provides a stable environment that allows the EBS to function for hundreds to many thousands of years, depending on the disposal concept. Owing to their excellent properties for the confinement of contaminants among which their very low permeability, their sorption capacity and their swelling/self-sealing capacity, clay-based materials are considered for use as part of the engineered barriers in about all repository designs under development (Box 2). Clay formations are also considered as potential hosts for geological disposal in several countries in Europe (Box 3).

Considerable amounts of gas can be generated in a repository containing radioactive waste. The largest fraction of the gas is expected to be hydrogen produced by the anaerobic corrosion of steel and reactive metals present in the waste, in their packaging and in the EBS. The degradation of organics and radiolysis also produce gas. Even though the gas production processes are generally slow it is important to verify that these will not be detrimental to the good functioning of the disposal system. The low permeability of clays that is favourable with respect to the containment function of a repository also limits the evacuation of the generated gas. It is possible that gas could be generated at a faster rate that it can be removed through the engineered barrier components, resulting in the development of a pressurised gas phase within the repository. The accumulated gas could then escape from repository by creating discrete, gas-specific pathways (e.g. fracturing or pathway dilation) through the EBS and/or the host rock. In addition, the potential release to the biosphere of gas containing volatile radionuclides is also an issue that needs to be considered.

To evaluate the impact of gas on the functioning of deep geological repositories, adequate understanding of possible gas transport modes through clay barriers is essential. Building on previous efforts and projects such as FORGE[2], the work programme of the WP GAS of EURAD aims to provide data and develop process-level models in support of the mechanistic understanding of transport processes in natural and engineered clayey materials that are being used or considered within European geological disposal programmes.

---

[2] The FORGE project (Fate Of Repository GasES) was funded by the European Commission and ran between February 2009 and September 2013. It involved a pan-European consortium, involving international radioactive waste management organisations, regulators and academia, drawn together to progress on key research issues related to the generation and the transport of repository gases.

EURAD (Deliverable n° 6.1) – Initial State of the Art on Gas Transport in Clayey Materials
Dissemination level: PU
Date of issue of this report: **17/11/2021**   Page 1

Box 1 – Geological disposal system

A geological disposal system consists of the waste, the engineered barriers and the host rock. Each of these elements fulfils, separately or in complementary fashion, multiple safety functions. It is the whole system that must be considered when assessing the safety of the system and not each system component separately.
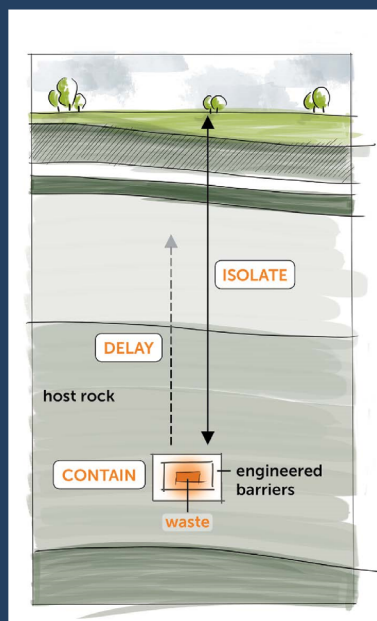
Assessing the safety of a disposal system requires that a **safety case** be developed together with supporting **safety assessment.** As defined by IAEA, "the safety case is the collection of scientific, technical, administrative, and managerial arguments and evidence in support of the safety of a disposal facility, covering the suitability of the site and the design, construction and operation of the facility, the assessment of radiation risks and assurance of the adequacy and quality of all of the safety-related work associated with the disposal facility. Safety assessment, an integral part of the safety case, is driven by a systematic assessment of radiation hazards and is an important component of the safety case." (IAEA 2012)

EURAD (Deliverable n° 6.1) – Initial State of the Art on Gas Transport in Clayey Materials
Dissemination level: PU
Date of issue of this report: **17/11/2021**

Page 2

Box 2 – Clay as material for engineered barriers

The favourable properties of clay (low permeability, self-sealing, stability) make it a material of choice for engineered barriers. Clay is mainly used as:

- buffer material: the empty space between the disposal package and the host rock is filled with clay (in granular form, pellets and/or blocks). For instance, bentonite, a swelling clay, is used as buffer material filling the voidage between the disposal packages and the host rock in the disposal facility designs selected in Finland, Sweden and Switzerland.

- backfill material: clay (for instance in the form of blocks or pellets) is used to fill excavated spaces (placement rooms, access ways), sometimes in combination with other materials.

- sealing material: clay, sometimes in combination with other materials, is used to isolate parts of the disposal facility. Seals are works of limited dimensions with specific purpose placed at key locations of the disposal facility. For instance, in France, the seals aim to limit water flow within the underground facilities.
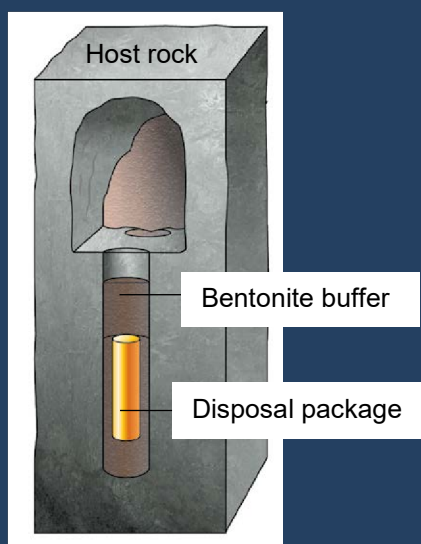
Example of placement of disposal package in a geological disposal facility (source: NWMO).

*Industrial robot **backfilling** a gallery with bentonite blocks. Remaining voids (between the rock surface and the blocks) will be filled with bentonite pellets (source: SKB).*
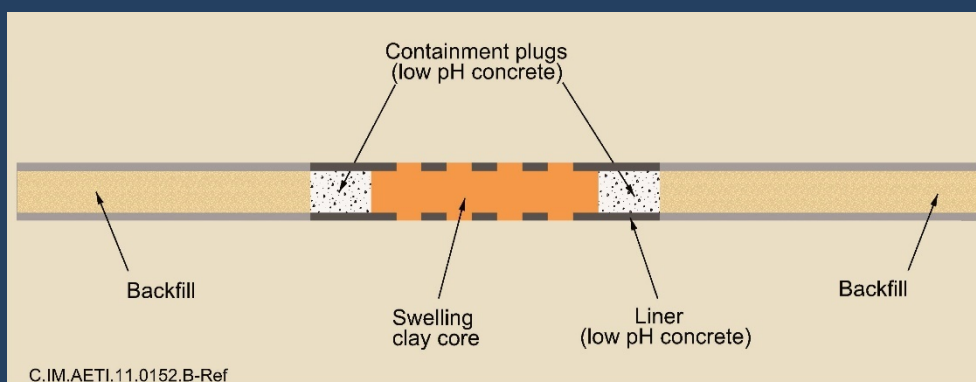
Reference drift sealing and backfilling concept (France). The seal is composed of a swelling clay core (bentonite) with two low pH concrete containment plugs, one at each end. The remaining part of the drift is backfilled with the original excavated material (argillites) (source: Andra).

EURAD (Deliverable n° 6.1) – Initial State of the Art on Gas Transport in Clayey Materials
Dissemination level: PU
Date of issue of this report: 17/11/2021

Page 3

Box 3 – Clays as host formations

In Europe, France and Switzerland have chosen to dispose of their high-level and long-lived intermediate-level radioactive waste in indurated clays, respectively in the Callovo-Oxfordian and Opalinus Clay formations; in Switzerland, Opalinus Clay is also the proposed host formation for low- and intermediate-level waste. For Belgium, the technical solution recommended for the long-term management of high-level and long-lived low- and intermediate-level waste is geological disposal in poorly indurated clay (Boom Clay or Ypresian clays). The Netherlands also considers clays as a potential host formation for the disposal of all types of radioactive waste.

The research and development studies performed over several decades have highlighted the clays' favourable properties:

- **very little water movement**: thanks to their low permeability, there is practically no water movement in clays. Radionuclide and chemical contaminant transport via this medium is thus strongly delayed.

- **diffusive transport**: given the limited water movement, transport in clays is essentially diffusive, which means species migrate primarily under the influence of their concentration gradient, and very little under the influence of the pore water movement.

- **retention capacity**: clays have a strong retention capacity for many radionuclides and chemical contaminants. Their migration through clays is thus considerably delayed.

- **buffer effect**: clays display a significant buffer effect with regard to chemical perturbations. The thickness of the clay that is chemically perturbed by the disposal facility is therefore very limited.

- **self-sealing capacity**: clays show a high capacity for self-sealing. Any fractures and fissures that occur, in particular those created by excavation activities, close quite rapidly.

- **stability**: the selected clay host rocks – and therefore their favourable properties – have remained unchanged over millions of years. The migration of natural chemical species through these clay host rocks has remained diffusive during at least the last million years.

- **vertical homogeneity**: radionuclide and chemical contaminant transport properties are very homogeneous almost throughout the entire thickness of the selected clay host rocks.

- **lateral continuity**: clays are present within simple geological structures, with a significant lateral continuity, which facilitates their large scale characterisation.

1.1   Work Package's raison d'être

The Work Package 6 'Mechanistic understanding of gas transport in clayey materials' (WP GAS) aims:

- To improve the mechanistic understanding of gas transport processes in natural and engineered clayey materials, their couplings with the mechanical behaviour and their impact on the properties of these materials;

- To evaluate the gas transport regimes that can be active at the scale of a geological disposal system and their potential impact on barrier integrity and repository performance.

The first raison d'être of this WP is to provide results that are applicable to a wide range of national programmes. This is possible because the results of previous efforts on the identification and characterisation of the possible gas transport processes suggest that the mechanisms at play in different clays are generally similar, while the conditions (gas pressure, stresses/deformations, saturations, …)

EURAD (Deliverable n° 6.1) – Initial State of the Art on Gas Transport in Clayey Materials
Dissemination level: PU
Date of issue of this report: 17/11/2021

Page 4

for the transition from one transport regime (diffusion, two-phase flow, pathway dilation and fracturing) to another strongly depend on the specific properties of a given clayey material.

The second raison d'être of this WP is to transfer knowledge gained from laboratory and in situ experiments to configurations that are commonly found in current repository designs, to address key questions from the end-users:

- How could gas be transported throughout the disposal system and which water soluble and volatile radionuclide transport could be associated with it?

- How and to what extent could the hydro-mechanical perturbations induced by gas affect barrier integrity and long-term repository performance?

This WP is built up heavily on the results, return of experience and conclusions from the past FORGE EC project. The experimental investigation of gas transport in FORGE sometimes revealed complex mechanisms, e.g. the development of discrete, unstable pathways controlled by the mechanical behaviour of the porous media. However, it was also suggested that this complexity can be addressed as long as one can bound the effects of these mechanisms using simpler and robust descriptions for evaluation purposes. The WP GAS of EURAD aims then at increasing the confidence in the overall understanding of gas behaviour in clayey materials gained from FORGE and improving its integration in the conceptualisation process for the different components of a disposal system. This should in turn support and justify the use of robust evaluation approaches and confirm the expert judgment at the end of FORGE that gas is not a showstopper for geological disposal but a question of managing uncertainties[3].

The WP is linked to EURAD Roadmap Theme 4 – Geoscience to understand rock properties, radionuclide transport and long-term geological evolution – Phases 1-2 (https://ejp-eurad.eu/roadmap).

1.2   Objective of the state-of-the-art report

Written in the early stage of the WP GAS, this state-of-the-art report (SOTA) on gas transport through clayey materials (Deliverable 6.1) aims to provide:

- A synthesis of the state of knowledge on gas transport processes that may occur through clayey materials as well as descriptions of gas-induced impacts on barrier integrity (including self-sealing processes);

- An overview of the current conceptualisations of gas transport through geological disposal systems and related processes and an overview of the current modelling approaches, as used in the context of the safety case.

The objective with this first state-of-the-art report is to underline what are the key uncertainties on the transport of gas in clays at the beginning of the project and how some of these uncertainties will be treated in the WP GAS. It gives a general overview of the state of knowledge with respect to main WP

---

[3] Building safety cases is best left to national programmes, accounting for their different, specific context. RD&D work packages in EURAD essentially aim to widen the supporting scientific databases, provide insights about processes that are of relevance to geological disposal and in some cases, test methodologies for evaluating the consequences of these processes. It is essential for R&D work packages to be transparent about what is known, where there is consensus and what are the uncertainties. Uncertainties, in particular, have to be communicated in such a way their relevance to different national programmes can be assessed within these programmes. To support this, the work package GAS collaborates in EURAD with the Strategic Study UMAN on the management of uncertainties and how these can be communicated to a variety of actors/groups.

EURAD (Deliverable n° 6.1) – Initial State of the Art on Gas Transport in Clayey Materials
Dissemination level: PU
Date of issue of this report: 17/11/2021

Page 5

European Joint Programme
on Radioactive Waste Management

RD&D (research, development and demonstration) topics, with sufficient context so that it can be used by a lay audience, early-stage programmes and RD&D managers. In addition, it provides a baseline against which the WP progress can be measured.

In the final stage of the project, a new state-of-the-art report will be issued (Deliverable D6.2), integrating the findings of all RD&D tasks in this WP, the relevant findings from other WPs and knowledge on gas transport in clay that could emerge between 2019 and 2024 outside EURAD. The main objective will be to highlight the significance and consequences of the findings of tasks on the phenomenological descriptions of gas transport in clayey materials (Tasks 2 and 3) for the conceptualisation of gas transport through geological disposal systems (Task 4). The ambition is to make clear statements on scientific consensus that can support a shared vision on gas management, recognising differences between national programmes, *in varietate concordia*, but also to clearly identify and formulate, with all participants to this WP (REs, WMOs and TSOs), the uncertainties of all types with sufficient context and full transparency in order to make it as practical as possible for the end-users to later assess which of those uncertainties are the most relevant within their national programme and to devise the best ways to handle these.

1.3 Outline of this initial state-of-the-art report on gas transport

The organisation of this state-of-the-art report on gas transport through clayey materials is broadly aligned with the structure of the WP GAS of EURAD, which is schematised in Figure 1-1. More information is given on the WP GAS and how it plans to improve the current knowledge and its integration in Chapter 5.
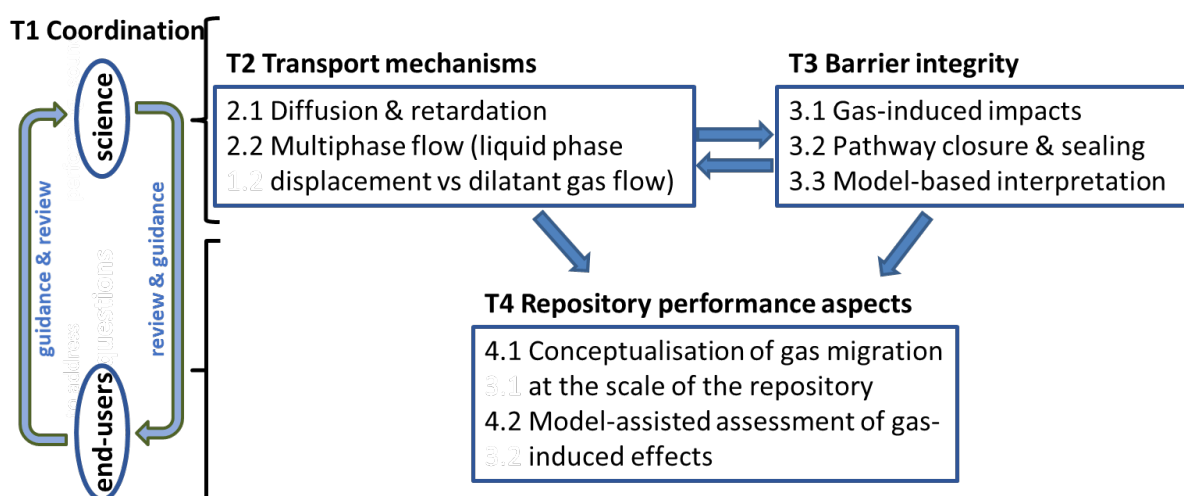
Figure 1-1 – Structure and organisation of the WP GAS in EURAD.

Chapter 2 focusses on the main gas transport mechanisms which are expected to take place in a disposal system in the post-closure phase:

- Gas produced within the system can dissolve in the pore water and can then be transported by diffusion. The diffusion of dissolved gas may be retarded by physico-sorption on the solid phase. Drawing the state of knowledge on the mechanistic understanding of diffusive transport of dissolved gas and gas sorption mechanisms are the objectives of Sections 2.2 and 2.3 respectively.

- If the gas production rate exceeds the rate at which gas can be dissolved and evacuated by diffusion, a free gas phase will develop. As gas pressure increases, two primary modes for

EURAD (Deliverable n° 6.1) – Initial State of the Art on Gas Transport in Clayey Materials
Dissemination level: PU
Date of issue of this report: 17/11/2021

Page 6

gas transport can be activated: (i) visco-capillary flow and (ii) the formation of discrete gas-filled pathways. Describing which transport mechanisms prevail under which range of conditions, what are the hydro-mechanical couplings associated and how can they be modelled are the objectives of Sections 2.4 and 2.5.

Although couplings with the mechanical behaviour of the porous media are briefly discussed, Chapter 2 essentially presents gas transport 'from the perspective of the gas'. Mostly laboratory work, multiphase flow concept and models are discussed in that chapter. Models are sometimes extended through representation of mechanical couplings via stress/strain dependent parameters.

Gas transport modes which depend on a strong mechanical coupling between the fluid and the solid phase, such as pathway dilation and the creation of discrete, additional pathways through the material are mainly discussed in Chapter 3, which also covers the consequences of gas transport in terms of temporary or permanent perturbations of the porous media. Hence, the focus of Chapter 3 is on the mechanistic understanding of the hydro-mechanical processes associated with:

- The gas-induced failure of clay barriers, i.e. within the engineering barrier system, within the excavation damaged zone (EDZ) and within the host rock (Section 3.1).
- The effectiveness of self-sealing along gas-induced pathways in the clay barriers of a geological repository (Section 3.2).

It is completed in Section 3.3 with an overview of process-level models and modelling tools.

Chapter 4 provides phenomenological descriptions of gas transport and likely consequences on barrier integrity and radionuclides transport at repository scale, in the form of storyboards for different national repository concepts (Section 4.1). It is completed in Section 4.2 with an overview of approaches that can be used for evaluating the impact of gas on repository performance.

Chapter 5 builds upon the state of the art presented in this report to explain the rationale of the WP GAS of EURAD and to present how it proposes to improve upon the available scientific bases, how these can be integrated in a stepwise and traceable fashion, fill knowledge gaps and answer the key end-users' questions.

To set the stage for Chapters 2 to 4, the next section of this introductory Chapter 1 draws a broad picture of gas transport in the specific context of geological disposal and provides an overview of the main clayey materials which are used in the experimental and modelling programme of the WP GAS of EURAD. These materials are representative of a broad range of natural and engineered clay barriers for geological disposal systems.

EURAD (Deliverable n° 6.1) – Initial State of the Art on Gas Transport in Clayey Materials
Dissemination level: PU
Date of issue of this report: 17/11/2021
Page 7

1.4 Overview of gas transport modes through clayey materials in the context of geological disposal facilities

1.4.1 Processes relevant to gas transport

There are a number of processes associated with the transport of gas from a geological disposal facility (GDF), whatever the type of host rock. First, the rate and amount of gas generated within the GDF is important in determining the subsequent gas transport behaviour. In addition, some chemical or biochemical interactions can occur and reduce the volume of gas in the repository (e.g. carbonation of cementitious materials and conversion of hydrogen gas to methane by microbes).

The focus of the WP GAS is on post-closure GDF evolution, once initial transients linked to repository construction and exploitation are over. From that time on, the repository will be at least partially saturated by pore water coming from the host rock. The gases produced in the GDF will first dissolve and be transported by diffusion in, and advection with, pore water. Dissolved gas may also sorb onto some materials or mineral phases. As the solubility of gas in the pore water is limited, a separate gas phase may form, depending on the production rate. If a gas phase forms, there are several processes by which it may be transported (see Figure 1-2). Whether and how a gas phase is transported through an engineered barrier system (EBS), host rock or overlying rock material depends on the properties of that material.

The processes relevant to gas transport from a GDF can be summarised as follows:

- **Gas generation processes**. There are a number of processes that can generate gas from waste packages and other materials in a GDF. The type, rate and amount of gas generated can affect its subsequent transport behaviour. Gas generation will depend on the gas generating materials and the conditions, including the presence of water, oxygen and some ions (e.g. chloride (Cl^-), sulphate (SO_4^2) that may promote metal corrosion), pH and temperature.

- **Gas consuming reactions**. Some reactions can reduce the net quantity of gaseous molecules. **Gas sorption** may occur on engineered barrier materials, on their degradation products and on specific mineral phases (e.g. pyrite).

- **Dissolution of gaseous molecules**[4]. Where water is present, gaseous species will dissolve in the water until their solubility limits at the in situ temperature and pressure are reached. If the quantities of gas are sufficiently small (i.e. so that the solubility limits are not reached) this would prevent the formation of a gas phase. Gases may also come out of solution as conditions change (e.g. due to the reduction in pressure when gases in solution are transported upwards towards the ground surface).

- **Advection and diffusion in solution**. Advection with groundwater and aqueous-phase diffusion in groundwater may both be important in some scenarios. Diffusion of gases in solution may be particularly important through materials where transport of gas phase is inhibited and there is little or no water flow.

- **Visco-capillary two-phase flow**. Two-phase flow conditions are encountered when gas can invade a water-filled porous medium as a separate phase. To enter the porosity, gas has to displace water, overcoming viscous and capillary effects. This process is likely to be important for a number of scenarios. Visco-capillary two-phase flow properties of EBS and geosphere

---

[4] In this document, dissolution of gaseous molecules is treated in sections about advection and diffusion in solution.

EURAD (Deliverable n° 6.1) – Initial State of the Art on Gas Transport in Clayey Materials
Dissemination level: PU
Date of issue of this report: **17/11/2021**

Page 8

materials are wide-ranging, so visco-capillary two-phase flow may occur readily or may be very difficult depending on the materials through which the gas must be transported. Careful consideration is required to ensure properties are defined on a suitable scale, taking into account material heterogeneity.

- **Pathway dilation**. In deformable materials where visco-capillary two-phase flow is difficult, gas transport may occur preferentially by pathway dilation, or dilatancy-controlled gas flow. In such case, displacements of the liquid phase are limited.

- **Gas fracturing**. In deformable materials where pathway dilation is not able to prevent continued gas build-up (this is likely for very high gas generation rates), the gas pressure may eventually become sufficient that macroscopic fracturing of the material occurs. Such fractures would provide a substantial local increase in the permeability. Once the gas pressure is released, fractures are however expected to close and seal, reducing the permeability. The efficiency of this depends on the self-sealing capacity of the clayey materials.

The basic principles of the processes related to the transport of gas are introduced in the following sections (Sections 1.4.1.1to 1.4.1.5). These processes are further detailed in Chapters 2 and 3 for clayey materials of interest within the WP GAS. The processes of sorption, diffusion and visco-capillary two-phase flow are included in Chapter 2, whereas the concepts of pathway dilation and gas fracturing are explained in Chapter 3. Gas generation processes and gas consuming reactions being out of the scope of the WP GAS, these processes are not discussed further in this state-of-the-art report except briefly in Chapter 4. For more information, reader can refer to Wareing et al. (2008), Norris (2013), Leupin et al. (2016a), Nagra (2016a), Poller et al. (2016), Neeft (2018), Small (2019) and the WP ACED of EURAD.
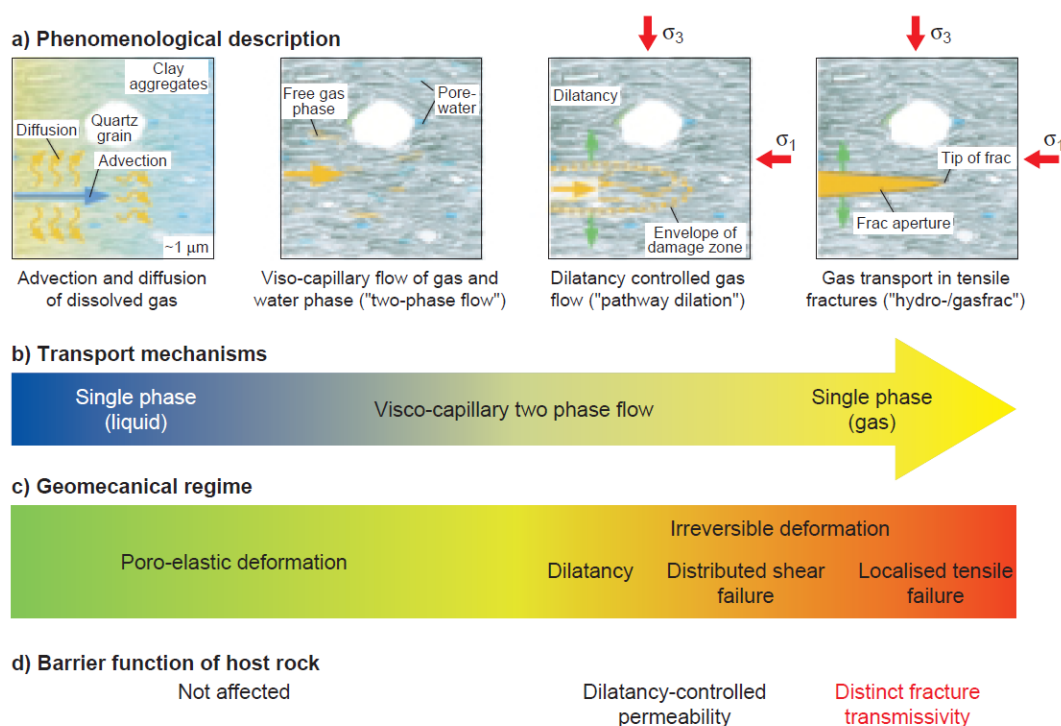
Figure 1-2 – Classification and analysis of gas transport processes in all clayey materials (Marschall et al. 2005). (a) phenomenological description based on the microstructural model concept (σ_1: horizontal total stress, σ_3: vertical total stress); (b) basic transport mechanisms; (c) geomechanical regime; (d) effect of gas transport on the barrier function of the host rock.

EURAD (Deliverable n° 6.1) – Initial State of the Art on Gas Transport in Clayey Materials
Dissemination level: PU
Date of issue of this report: **17/11/2021**
Page 9

1.4.1.1 Dissolution of gaseous molecules

Dissolution of gaseous molecules is potentially important to gas transport from, or build up within, a GDF, because it will reduce the total amount of gas existing as a gas phase. If, in combination, gas generation is sufficiently slow, and transport of the dissolved gas is sufficiently rapid, then all the generated gas could potentially dissolve, preventing a gas phase from forming at all.

Provided there is some water in a GDF, the gases generated within the GDF will dissolve in the water according to Henry's law (Henry W. 1803) until the solubility limits of the gases are reached. The solubility limits depend on the partial gas pressure in the GDF. Gas will continue to dissolve in the water if there is a flow of water through the GDF that allows additional water that is not saturated with gas to flow into the GDF and as gas diffuses away in solution.

The solubility of gases in the groundwater may also be important to gas transport within the geosphere. Since gas solubility is approximately proportional to the pressure, if groundwater migrates from a GDF towards the surface and remains saturated with gas, then as the pressure reduces, gas will come out of solution, so that a gas phase may form in the geosphere at some distance from a GDF. However, this is not certain, since the dissolved gas may also disperse as the groundwater migrates, so that the water is no longer saturated with the gas, even where the pressure is lower.

So, the parameters that are important for describing dissolution of gases in groundwater are the solubilities of the gases (at GDF and geosphere pressures), the rate of diffusion of the gases in the pore water and the rate of flow of groundwater through the GDF and overlying rocks. Gas solubilities in water are reasonably well-defined parameters. Therefore, the main parameters required to understand dissolution of gases generated in a GDF are the diffusion of the gases in the pore water and the rates of groundwater flow through the GDF (i.e. the parameters that describe gas transport in solution, as discussed hereafter). The groundwater flow rate could vary widely depending on the host rock, and could be essentially zero in some cases, especially for a repository in a clay host rock.

1.4.1.2 Gas transport in solution

Transport of gases in solution is a basic gas transport process in fully saturated porous media, which is controlled by the solubility of the gas in the pore water. Gas transport in solution involves two major gas transport mechanisms, diffusion of the dissolved species and advection in the liquid phase (pore water). Diffusion is driven by a concentration gradient in the pore water, whereas advective transport is caused by a pressure gradient in the pore water. The relative importance of these processes will vary depending on the properties of both the medium that the water is in and the properties of the dissolved gas in the water. For example, where the water is flowing through a material with a relatively high permeability, there is likely to be a significant water flow, so advection of the dissolved gas will be relatively rapid and diffusion may not be important. Conversely, if the material has a low permeability, there will be very little water flow, so transport of the gas in solution will be mainly due to diffusion.

The key parameters to describe gas transport in solution are therefore:

- the solubility of the gaseous species,
- the aqueous diffusion coefficient of each gas,
- the porosity of the porous media,
- the tortuosity and constrictivity of the porous media,
- the permeability of the porous media.

EURAD (Deliverable n° 6.1) – Initial State of the Art on Gas Transport in Clayey Materials
Dissemination level: PU
Date of issue of this report: **17/11/2021**

Page 10

1.4.1.3 Visco-capillary two-phase flow

Flow of immiscible fluids in porous media is often denoted as 'two-phase flow' when the fluids are water and gas. Two-phase flow conditions occur when gas invades as a separate phase a water-saturated porous medium. This process is called invasion or drainage, because the non-wetting fluid (gas) displaces a wetting fluid (pore water, 'defending' fluid). The propagation of the gas front is controlled by the complex interaction of gravity, viscous forces and capillary forces, giving rise to viscous or capillary fingering (instable displacement). Immiscible displacement of a non-wetting fluid by the wetting fluid is called imbibition (pore water displaces the air in an initially dry porous medium). In this case the propagation of the pore waterfront in the porous medium is smoother; the process is called stable displacement. The potential for visco-capillary two-phase flow will depend on the micro-fabric of the porous medium, in particular the characteristic pore throat radius and its distribution. The deformation behaviour of the porous medium in response to gas invasion processes remains reversible in the two-phase flow regime. However, when the prevailing gas pressure exceeds the strength of the porous medium, the solid skeleton will fail and gas transport may alternatively occur by opening additional porosity within the material (such pathway dilation is discussed in the next subsection).

Visco-capillary two-phase flow in a (porous) material can be defined in a similar way to single-phase flow, but taking account of the saturations of (i.e. the fractions of the porosity occupied by) each phase in the material. The permeability of the material that defines single-phase flow is modified by a relative permeability for each phase that depends on the saturation. In addition, there is a difference in pressure between the phases, the capillary pressure, which a gas must exceed for it to be transported into a water-saturated material. The capillary pressure increases with the gas saturation, so that the gas pressure must increase to increase the gas saturation. This is important since in many materials the relative permeability becomes greater than zero, so allowing the transport of gas, only once the saturation rises above a given value.

So, transport of gas by visco-capillary two-phase flow depends on the following parameters of the porous material that the gas is to be transport through:

- the porosity of the porous media,
- the permeability of the porous media,
- the parameters defining the relative permeabilities to gas and water,
- the parameters defining the variation of capillary pressure with saturation.

EBS materials, host rocks and overlying rocks can have a wide range of permeabilities and 'gas entry pressures' (a parameter that defines the threshold capillary pressure necessary to displace the wetting phase). As a result, gas transport by visco-capillary two-phase flow will occur readily in materials with relatively high permeabilities and low gas entry pressures. However, for materials with very low permeabilities and high gas entry pressures, gas transport will occur by visco-capillary two-phase flow only after substantial pressure build-up, and then will occur only slowly. Given this, gas transport may preferentially occur by a mechanism other than visco-capillary two-phase flow in such materials.

1.4.1.4 Pathway dilation

Gas transport by pathway dilation may be important in low-strength materials for which visco-capillary two-phase flow is difficult (see previous subsection). In such materials no transport of gas phase will occur until a significant gas pressure has built up. Such pressures may allow localised consolidation of the material, such that additional porosity is created in the material (i.e. micro-fractures), allowing pathways to form, along which the gas can be transported. This behaviour can occur in preference to the displacement of water by gas from the existing porosity, which would be required for visco-capillary

EURAD (Deliverable n° 6.1) – Initial State of the Art on Gas Transport in Clayey Materials
Dissemination level: PU
Date of issue of this report: 17/11/2021

Page 11

two-phase flow. If, as a result of the gas transport along the additional pathways, the gas pressure is reduced (i.e. the gas transport is more rapid than any continued gas generation), then, for some materials at least, it is likely that the pathways will close. So gas transport by pathway dilation may be intermittent.

In the terminology of multiphase flow concepts, gas flow by pathway dilation is still controlled by visco-capillary forces; the main difference with respect to conventional two-phase flow is that the transport properties of the solid phase (permeability, relative permeability, capillary pressure relationship) can no longer be viewed as invariants, since they depend on the state of deformation of the material (Marschall et al. 2005), thus the mechanical properties of the material are important. Therefore, key parameters to describe gas transport by pathway dilation are:

- the parameters defining the permeability and its variation with deformation,
- the parameters defining the porosity and its variation with deformation,
- the parameters defining the relative permeabilities to gas and water and their variation with deformation,
- the parameters defining the variation of capillary pressure with saturation and deformation,
- the parameters defining the deformation (i.e. the mechanical properties) of the porous media.

However, given the complex couplings between hydraulic and mechanical properties in relevant materials, the understanding of pathway dilation that has been developed so far is not sufficiently detailed that this process can be modelled directly to predict gas transport behaviour. Therefore, in materials where gas transport is expected to occur by pathway dilation, the transport behaviour is often approximated by modelling it using a visco-capillary two-phase flow approach with suitably chosen parameters (for instance, considering a gas entry pressure value that accounts for a deformed state of the material).

1.4.1.5 Gas fracturing

Gas fracturing may happen if gas generation rates occur in low-strength materials in which transport by pathway dilation is not able to keep up with gas build-up and the gas pressure increase rate. Given the likely implications for GDF performance of the large change in material properties associated with gas fracturing, the GDF design process would need to ensure that such a scenario is avoided. Therefore, it is important to recognise the circumstances under which it could occur. Given this, the key parameters relating to gas fracturing are generally:

- the minimum principal stress on the material,
- the tensile strength of the material.

As it has been observed that gas fracturing could also happen below the principal minimum stress at low gas injection rate (e.g. as shown in the Callovo-Oxfordian claystone by de la Vaissière et al. (2019, 2020)), an additional key parameter is the gas generation rate.

Once the gas pressure is released, these fractures are expected to close and seal. The efficiency of these processes depends on the self-sealing capacity of the clayey materials (discussed in Section 3.2).

EURAD (Deliverable n° 6.1) – Initial State of the Art on Gas Transport in Clayey Materials
Dissemination level: PU
Date of issue of this report: 17/11/2021

Page 12

1.4.2 Natural and engineered clayey materials considered in this WP

The previous section summarises the potential key processes affecting gas transport from a GDF. However, not all of these processes will be important for gas transport through all components of a GDF (EBS materials and host rocks). As information needs will differ between materials, it is important to understand the specific information needs relating to gas transport through each material to ensure these needs are appropriately tackled.

The materials through which gas transport is to be considered within the WP GAS are clayey potential host rocks (Boom Clay, Callovo-Oxfordian claystone and Opalinus Clay) and engineered clayey materials (granular Wyoming sodium bentonite (MX-80), FEBEX bentonite, Czech bentonite BCV and their mixtures with sand).

The information needs for each material will depend on the safety functions to be fulfilled by that material, which in turn may vary depending on the disposal concept and between different uses of a material within a disposal concept.

A wide range of disposal concepts are considered in the WP GAS as described in Section 4.1. This range of concepts includes a number of layout options for each waste group, but in each case the potential uses and associated functions of each material are similar. The potential uses of engineered clayey materials for disposal concepts for each host rock and waste group considered in the WP GAS are summarised in Table 1-1.

Table 1-1 – Engineered barrier component options for disposal concepts for each host rock and waste group (clayey materials are in bold).

Host rock	Waste group *	Parts of the engineered barrier system			
		Container	**Buffer/local backfill**	**Mass backfill**	**Seals**
Boom Clay	ILW	Cementitious materials	Cementitious materials	Cementitious materials	Concrete, **Bentonite**
	HLW/SF	Carbon steel for overpack, Cementitious materials	Cementitious materials	Cementitious materials	Concrete, **Bentonite**
Callovo-Oxfordian claystone (COx)	HLW	Stainless steel and carbon steel for overpacks	None	Crushed excavated COx with additives (**bentonite**, sand)	**Bentonite, Sand/bentonite mixture**
	ILW	Cementitious materials	Cementitious materials	Crushed excavated COx with additives (**bentonite**, sand)	**Bentonite, Sand/bentonite mixture**
Opalinus Clay	SF/HLW/ILW		**Granular bentonite, pellets and blocks**	**Granular bentonite**	**Bentonite blocks**
	L/ILW		Waste fixation concrete	High porosity mortar	**Sand/bentonite mixture**

* HLW: high-level waste, ILW long-lived intermediate-level waste, L/ILW: low and intermediate-level waste, SF: spent fuel

EURAD (Deliverable n° 6.1) – Initial State of the Art on Gas Transport in Clayey Materials
Dissemination level: PU
Date of issue of this report: **17/11/2021**

Page 13

The engineered barrier component choices for each host rock are used as the basis for determining the information needs for each material in this WP. The information needs will depend on the function of the relevant barrier components directly in relation to gas transport. The function of the seals will be either to contain gas to prevent (or minimise) the release of radionuclides from the GDF, or to provide a controlled release of gas (to other parts of the GDF) to prevent excessive pressurisation. The backfill may be required to provide the same functions as the seals, but in addition it (particularly the mass backfill) may need to provide storage capacity for the gas so that gas can be contained while also preventing excessive pressurisation.

Two key properties that differ between these studied clayey materials are the gas entry pressure and the permeability. These are linked to the connectivity of the pore space and determine the ease with which a gas phase can enter and be transported through the porous material. Considering the likely ranges of values for these properties, the considered materials can be classified in two groups:

- For intact clay host rocks and pure bentonite, permeabilities are generally extremely low and gas entry pressures are high, so gas transport is difficult.

- For damaged/fractured clay host rocks and/or sand/bentonite mixtures with high sand content, permeabilities are higher and gas entry pressures are low, so transport of gas occurs relatively easily.

For the materials in which the transport of gas is relatively easy, transport is likely to occur predominantly by visco-capillary two-phase flow, provided that the gas generation rate or gas flow rate to the material is substantial (i.e. it is sufficient to maintain a significant gas phase). Where the rate of gas supply is lower, gas transport by dissolution and advection with the water and/or aqueous diffusion through the water will become more important.

For materials in which the transport of gas is more difficult, transport is likely to occur predominantly by pathway dilation, again provided that the gas generation rate or gas flow to the material is substantial (i.e. it is sufficient to build up a significant pressure in a gas phase).

1.4.3 Influence of burial depth

The hydro-mechanical properties of host formations are intrinsically linked with their void ratio/porosity. In particular, the void ratio and transport properties of clays are highly sensitive to the effective stress state (Neuzil 1994; Katsube et al. 1996a, 1996b; Dewhurst et al. 1999; Katsube 2000; Kwon et al. 2001), which is a function of the burial depth. Changes in the effective stress may be caused by an alteration in the confining pressure (i.e. a change in burial depth through exhumation or burial) or by a change in the pore fluid pressure (pressure build-up or release). For a clayey rock, burial and exhumation history can have a profound influence on the hydro-mechanical properties of the material (Bjerrum 1967).

Consolidation of a clayey material can be considered as a time-dependent loss of both volume and porosity during burial, resulting from the associated increase in total stress. The consolidation rate depends on the initial porosity and permeability of the material and on the applied stresses. A standard approach to describe the consolidation state of a clay is to quote the over-consolidation ratio (OCR), which is the ratio between the maximum stress experienced by the rock and its present stress state. It then follows that a clay with an OCR = 1 is considered normally consolidated, while under consolidated clays and over-consolidated clays have respectively OCR values of less than one and greater than one.

Considerable effort has been devoted to examining the relationship between porosity and the depth of burial in clayey materials (Gibson and Henkel 1954; Skempton 1970; Been and Sills 1981; Burland 1990; Leddra et al. 1992; Olgaard et al. 1995). These early datasets provide a large resource on which to summarise this relationship and examine trends across various materials and conditions (Rieke and

EURAD (Deliverable n° 6.1) – Initial State of the Art on Gas Transport in Clayey Materials
Dissemination level: PU
Date of issue of this report: 17/11/2021

Page 14

Chilingarian 1974; Dzevanshir et al. 1986; Novello 1988). A number of empirically derived functions have been proposed for specific lithologies, where there is sufficient available porosity data and the diagenetic history is well understood. It should also be noted that secondary mineralisation can have a significant influence on the consolidation properties of clay and this effect (particularly in older sediments) can lead to a pseudo consolidation state.

The relationship between void ratio and effective stress can be examined in the laboratory, often using a standard oedometer set-up with a saturated sample of specified geometry. The sample is constrained radially while axially loaded and unloaded in increments. Volumetric changes and/or net pore fluid loss are measured in order to ascertain the material response to a specified loading/unloading path. In soil mechanics testing, sample response to compression is typically described in a *e-log(p')* space (where *e* is the material void ratio and *p'* is its mean effective stress). Examination of the transition to the material virgin yield is then used to estimate the maximum previous burial pressure (and, hence, OCR) that it has experienced.

A similar experimental approach is usually adopted to examine the influence of the effective stress on the water permeability. Comparatively, relatively few studies have examined the influence of the effective stress on the gas entry/breakthrough pressures or the resulting gas permeabilities. Typically, gas entry pressures are determined, along with water retention curves, in absence of external stress on the samples. The coefficient of diffusion of dissolved gas is generally determined from experiments in which the sample is confined within a constant volume, hence without control of its stress state. Consequently, the role of the effective stress on the dominance of one gas transport mode over another is not always clear. When comparing measured gas properties from one study to another, or when attempting to transfer understanding from one clay host rock to another, it is therefore essential to consider the influence of both the effective stress conditions of the experiment and the consolidation state of the test material.

1.4.4 Influence of existing discontinuities in clay host formations

A limited body of evidence is related to gas transport in existing[5] fractures or faults in clay formations comparable to those considered as potential host rocks for a GDF. This most likely results from the assumption that the self-sealing characteristics of clays will diminish any potential effects of discontinuities on gas transport. Nevertheless, the relevance of damage generation in a geological disposal facility will be particularly dependent upon the specific self-sealing characteristics of the host formation. It is well-established that an excavation damaged zone (EDZ) will be created during the excavation of a GDF, but there is very little laboratory evidence to provide information of the effect on gas flow behaviour. This may be due to the belief that self-sealing is likely to occur before significant gas is generated. Although the self-sealing behaviour of clays is well documented (e.g. Bernier et al. 2007b), there are only few studies assessing the longevity of this behaviour in relation to gas.

Laboratory examination of gas transport properties in fractured clayey host rock is complicated by the selection of an appropriate loading regime. Several studies focus on changes in bulk properties in response to differential loading, while others examine changes in transmissivity across an individual fracture in response to shear and normal loading, though these are primarily conducted with water. Key

[5] Existing, in the sense that these discontinuities can exist before the passage of gas and are therefore not created by gas transport. Evidence about the effect of such discontinuities come, for instance, from the oil and gas industry.

EURAD (Deliverable n° 6.1) – Initial State of the Art on Gas Transport in Clayey Materials
Dissemination level: PU
Date of issue of this report: 17/11/2021　　　　Page 15

controls on flow behaviour include: (i) the degree and rate of swelling, (ii) the stress conditions and (iii) the prior burial history.

A number of studies are available within the literature that examine two-phase flow properties of samples with manufactured/simulated fractures (Fourar et al. 1993; Merrill 1994; Nicholl et al. 1994; Reitsma and Kueper 1994). Where earlier studies were conducted on natural fractures, the initial focus was on crystalline rocks, perhaps because these represented simpler systems to study. More recently, a few experiments (e.g. Zhang and Rothfuchs 2004; Billiotte et al. 2008; M'Jahad et al. 2017) have been reported considering the influence of microfracturing/fracturing/faulting on gas transport properties in clays. There is some cross-over between these studies and those considering the transport properties of intact rock, whose samples may contain damage occurred either during excavation or sample preparation.

1.4.5   Required properties for understanding gas transport behaviour

Using the information presented in the previous sections, the properties required to adequately describe gas transport in each of the EBS materials and host rocks can be determined. In identifying these properties, it is important to consider the level of understanding required to support the development of a GDF. Ultimately gas transport understanding is required to address challenges that gas may pose to the safety case, namely (RWM 2016c):

- gaseous release of radionuclides in the biosphere,

- detrimental effects on the EBS/host rock properties (i.e. changes that impact the groundwater pathway) due to pressurisation.

However, these challenges may be removed or minimised through features of the engineering design. In this case, understanding of specific aspects of gas transport through such features will be required to facilitate their design. For example:

- If gas pressurisation is to be managed by allowing its transport between different areas of a GDF, designing relevant seals to ensure gas is transported through them at a sufficient rate at appropriate pressures (while minimising water flow) will be important.

- Where the EDZ has the potential to play an important role in gas transport, it may be necessary to understand the impact of the GDF construction method on the gas transport behaviour through the EDZ.

In addition, some understanding is required to provide underlying confidence in the approach to the development of a GDF and its subsequent operation. Therefore, there are three drivers for understanding gas transport behaviour:

- generic understanding of the processes,

- understanding to facilitate engineering design,

- understanding to support the safety case.

The understanding and properties required for each material are given in turn in the following subsections.

EURAD (Deliverable n° 6.1) – Initial State of the Art on Gas Transport in Clayey Materials
Dissemination level: PU
Date of issue of this report: 17/11/2021   Page 16

1.4.5.1 Bentonite

Bentonite may be used both as a backfill/buffer of a GDF and as seals in all areas of a GDF. Gas transport in bentonite is complex because of:

- submicroscopic dimensions of the interparticle spacing (Romero and Simms 2008),

- strong physico-chemical interactions between pore water and substrate (Abdullah et al. 1999),

- low permeability (e.g. Neuzil 1994),

- deformable matrix and low tensile strength (Wang et al. 2017).

These factors can result in a significant hydro-mechanical coupling in bentonite. They also highlight the importance of hydraulic saturation state and initial compaction state on fluid flow properties.

For near-saturated bentonite, the key gas transport process is diffusion in solution or pathway dilation. The key process will depend on the gas generation rate. Therefore, the key properties that are required to describe gas transport through near-saturated bentonite are:

- the solubility of each gas,

- the aqueous diffusion coefficient of each gas and the geometric factors that account for the topology of the pore network (e.g. tortuosity and constrictivity),

- the properties defining the permeability and porosity of the bentonite and their variation with deformation,

- the properties defining the relative permeabilities of the bentonite to gas and water and their variation with deformation,

- the properties defining the variation of capillary pressure of the bentonite with saturation and deformation.

However, it is not currently possible to model pathway dilation directly. Therefore, consideration needs to be given to the level of understanding required to adequately represent gas transport behaviour through bentonite in this case. In some instances, it may be sufficient to make bounding assumptions regarding this behaviour, while in others it may be sufficient to use other representations of the transport (such as visco-capillary two-phase flow) to approximate the behaviour, provided appropriate property values can be determined. In particular, whereas seals are specifically required to control fluid flows through a GDF, this may be less of a requirement for backfills/buffers in some cases.

In some GDF concepts, a mixture of bentonite and sand may be used as an EBS material. If the sand content is sufficient, gas transport through the material is expected to occur more easily, so the gas transport processes for such materials may be more aligned with those expected for cementitious materials. This will also be the case for pure bentonite at lower saturations. Therefore, the key properties that may be required to describe gas transport through pure bentonite at lower saturations, at lower density or through a bentonite-sand mixture (above a critical sand content) will be those given above. In addition, for pure bentonite, understanding the evolution of the saturation will be important in determining the key gas transport process.

EURAD (Deliverable n° 6.1) – Initial State of the Art on Gas Transport in Clayey Materials
Dissemination level: PU
Date of issue of this report: 17/11/2021

Page 17

1.4.5.2 Clay host formations

Clay host formations considered in the WP GAS are defined as sedimentary rocks with a fine grain size, a low to moderate mechanical strength, a high clay content and a low permeability. As with bentonite, gas transport through such clays is a complex process characterised by

- submicroscopic dimensions of the interparticle spacing (Nelson 2009),
- strong physico-chemical interactions between pore water and substrate (Derjaguin et al. 1987; Abdullah et al. 1999),
- low permeability (Neuzil 1994) and
- a deformable matrix and a low tensile strength (Wang et al. 2017),

which result in a very significant coupling between the hydraulic and mechanical response of these materials and highlight the importance of the state of hydraulic saturation and the consolidation state when defining fluid flow properties.

Several studies (as for instance Clayton and Hay 1994; Krooss et al. 1992; Schlömer and Krooss 1997) examining gas transport in clays have already been conducted. These have been carried out on a variety of materials, generally related to a specific subsurface activity. Many of these studies focus on the behaviour of those caprocks that are relevant to the conventional and unconventional hydrocarbons industry and carbon capture and storage projects. These are often very site-specific and well-preserved caprock is scarce. Thus, there are few materials on which a large body of experiments have been performed. In contrast, experiments conducted in the context of radioactive waste disposal often involve a few, highly characterised materials which are under consideration as host formations. Within Europe, the main clay formations currently studied in detail for the disposal of radioactive waste are:

- the Boom Clay in Belgium and the Netherlands, as potential host rock,
- the Callovo-Oxfordian claystone selected in France for the disposal of HLW and long-lived ILW,
- the Opalinus Clay selected in Switzerland for the disposal of all radioactive waste,
- the claystone formation of Boda in Hungary, as potential host rock.

Other clay formations might be added to the list in the future as many national programmes are currently somewhere along a siting programme or considering starting one.

For both intact and the EDZ around a GDF in clay host rocks, the key gas transport process may be diffusion in solution or migration as free gas in conductive pathways (generally pathway dilation). The key process will depend on the gas generation rate, so may differ between waste types, and on the gas transport process through the EBS materials. Therefore, the key properties that are required to describe gas transport through clay host formations are:

- the solubility of each gas,
- the aqueous diffusion coefficient of each gas and the geometric factors that account for the topology of the pore network (e.g. tortuosity and constrictivity),
- the properties defining the permeability and porosity of the clay and their variation with deformation,
- the properties defining the relative permeabilities of the clay to gas and water and their variation with deformation,
- the properties defining the variation of capillary pressure of the clay with saturation and deformation.

EURAD (Deliverable n° 6.1) – Initial State of the Art on Gas Transport in Clayey Materials
Dissemination level: PU
Date of issue of this report: 17/11/2021

Page 18

In addition, it is expected that an EDZ in clay host formations will evolve over time, with its properties returning towards those of the undisturbed rock. Therefore, to describe gas transport through the EDZ, variation of the properties with time is also required.

1.5 Overview of the clayey materials studied in the WP GAS

The following subsections summarise, for the three host clays selected for the WP GAS (Boom Clay, Callovo-Oxfordian claystone and Opalinus Clay), aspects of the geology of the formation, mineralogy, pore water composition, as well as basic properties and parameters at the formation level. These are complemented by a description of bentonites (granular Wyoming sodium bentonite MX-80, FEBEX bentonite and Czech bentonite BCV) and sand/bentonite mixtures selected as clay-based engineered barriers. Most of the information gathered comes from research projects financed by or with participation of the waste management organisations (WMOs).

1.5.1 Boom Clay

The Boom Clay formation (Tertiary clay formation) is one of the potential clay formations studied for the geological disposal of high-level and/or long-lived radioactive waste in Belgium. This clay is a detrital marine deposit from the Oligocene and more specifically from the Rupelian stage, between 33.9 and 28.4 Ma. The Boom Clay dips gently towards the northeast, is located in the north part of Belgium and covers a surface of almost 5 000 km² (Figure 1-3). The thickness of the formation increases from a few decametres at outcrop to more than 150 metres in the deeper part of the basin. This sedimentary formation has been deposited in layers according to the climate and geological conditions change. The formation is composed of rhythmically alternating clay-rich and silt-rich materials with variations in organic matter content resulting in a grey-tone banding (Vandenberghe et al. 2014).
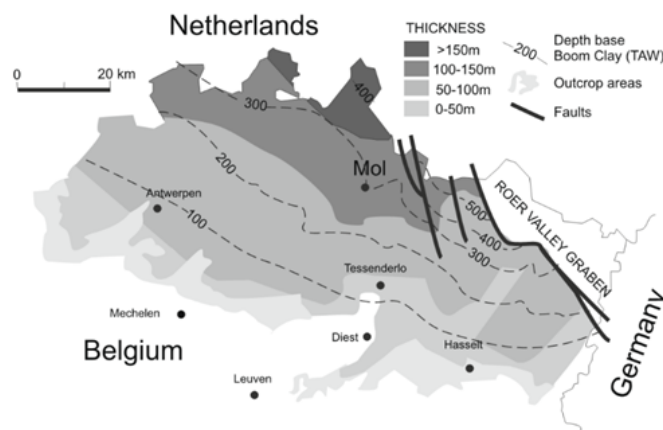
Figure 1-3 – Extension of the Boom Clay formation in northern Belgium. The formation dips towards the northeast. The underground research laboratory is located in Mol (ONDRAF/NIRAS 2001).

At the level of the HADES URL in Mol (Belgium), the Boom Clay has a thickness of about 100 metres and is located at depths between 185 and 287 metres below the surface with the underground laboratory at a depth of 223 metres below the surface (Mertens et al. 2004).

The Boom Clay is an uncemented fine-grained compacted clay with a well-developed particle alignment according to the bedding plane and high porosity. Moreover, the microstructure shows porosity of larger

EURAD (Deliverable n° 6.1) – Initial State of the Art on Gas Transport in Clayey Materials
Dissemination level: PU
Date of issue of this report: **17/11/2021**

Page 19

pores caused by the presence of silt particles. The clay can be considered as an open structure with a high porosity (Dehandschutter et al. 2004). Figure 1-4(1) shows an image of the microstructure of the clay taken with scanning electron microscopy (SEM) technique where it is possible to observe the preferential alignment of the clay particles in relation with the bedding plane. The microscopically well-developed arrangements are the results of the geological history of the clay. Indeed, this one has been deposited in a marine environment and has been submitted to different vertical loads during its history (Mertens et al. 2003). Consequently, this microstructure results from the post-sedimentation history. Broad Ion Beam cross-sectioning methods are used to produce high quality polished surfaces suitable for high-resolution SEM imaging, allowing the determination of the distribution, orientation and shape of pores (Figure 1-4(2)) (Desbois et al. 2010).

(1)
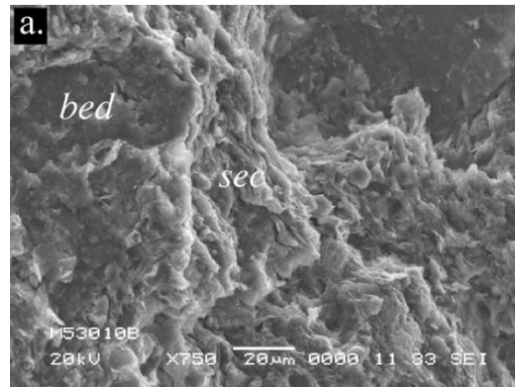
(2)
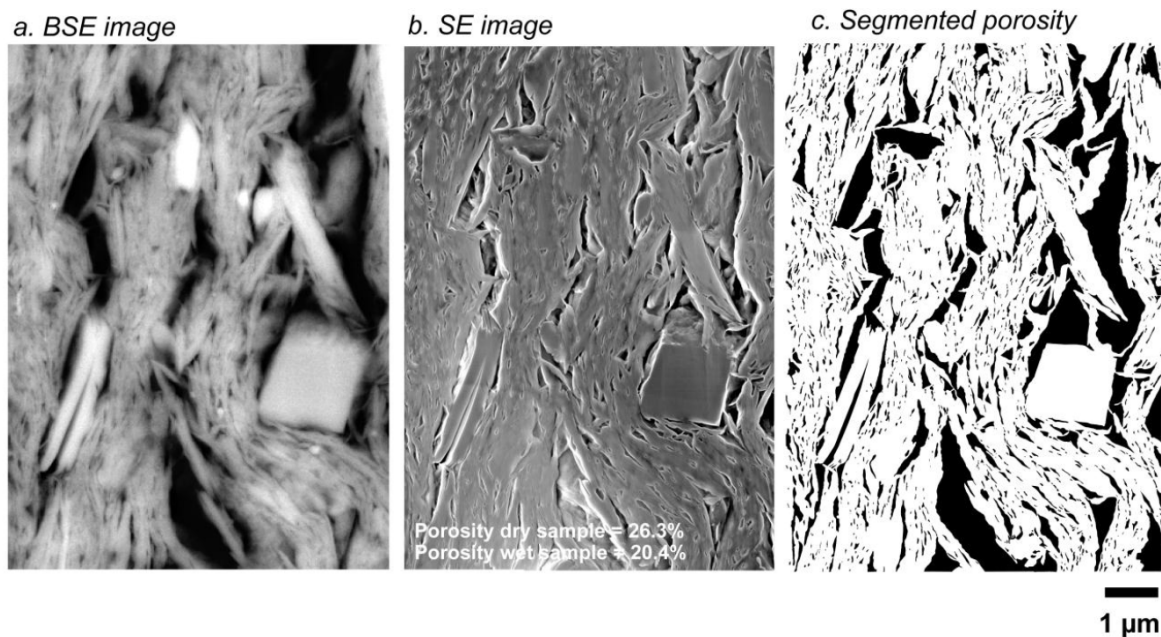
Figure 1-4 – (1) Boom Clay microstructure with the preferential alignment according to the bedding plane (bed) (sec: section perpendicular to the bedding plane) (Dehandschutter et al. 2004). (2) SEM micrographs of a cross-section cut perpendicular to the bedding of dried Boom Clay. (a) Back Scattered Electrons micrograph allowing relative identification of minerals phases by density contrast. (b) SE micrograph showing the 2D pore space. (c) Segmented porosity from (b) used for quantification of porosity. In all images, the bedding is vertical. (Desbois et al. 2010).

The granulometry of the Boom Clay reveals that it is composed of more than 60% of fine silt and clay-size particles. Lima et al. (2011) provide a compilation of several granulometric curves for the Boom Clay (Figure 1-5) and several results of mercury intrusion porosimetry (MIP) tests (Figure 1-6 and

EURAD (Deliverable n° 6.1) – Initial State of the Art on Gas Transport in Clayey Materials
Dissemination level: PU
Date of issue of this report: 17/11/2021

Page 20

Figure 1-7). The analysis of these curves shows that the majority of the pores have a radius of from 0.001 µm to 0.1 µm with a peak of the unimodal distribution around 0.01 µm.
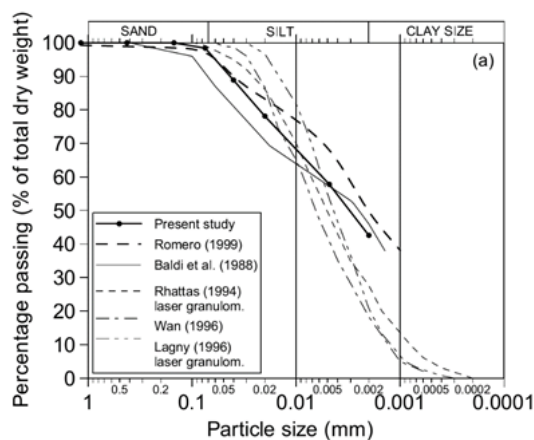
Figure 1-5 – Particle size distribution of Boom Clay from granulometric curves compiled by Lima (2011).
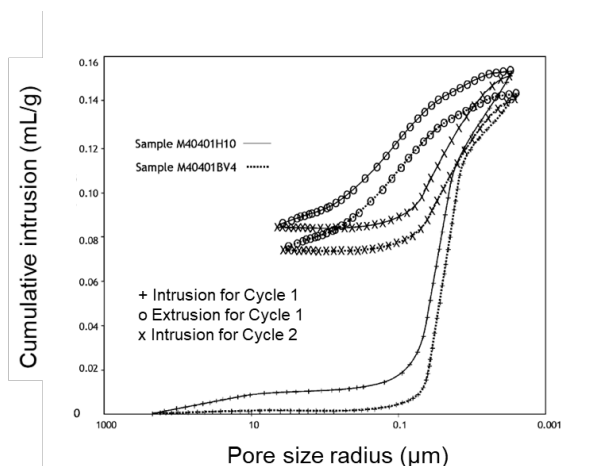
Figure 1-6 – Cumulative mercury intrusion versus pore size for undisturbed Boom Clay (Dehandschutter et al. 2004).
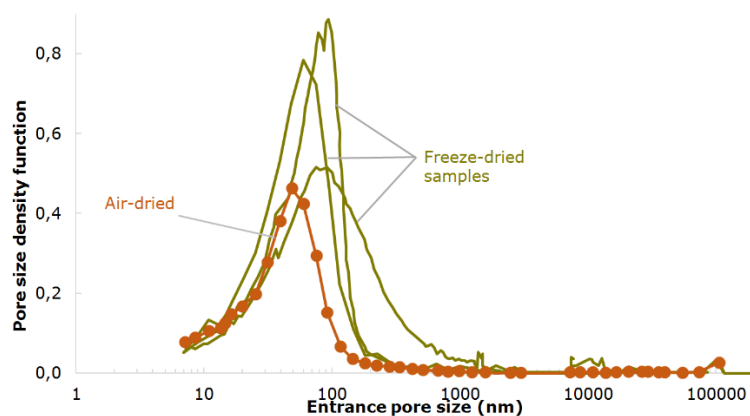
Figure 1-7 – Pore size density function for Boom Clay for different samples (Lima 2011).

EURAD (Deliverable n° 6.1) – Initial State of the Art on Gas Transport in Clayey Materials
Dissemination level: PU
Date of issue of this report: **17/11/2021**

Page 21

The mineralogical composition of Boom Clay consists of clay minerals (up to 60 wt%), quartz, feldspars, and minor amounts of muscovite, biotite, and some heavy minerals. The clay mineralogy is dominated by illite, smectite, illite/smectite interstratifications, and kaolinite. Chlorite, degraded chlorite and illite/chlorite interstratifications are present. Organic matter is found in the clay. Table 1-2 presents the main mineralogical composition of Boom Clay compiled by De Craen et al. (2004) and updated by Zeelmaekers et al. (2015) and Frederickx (2019).

Based on the differences in granulometry and mineralogical content, the Boom Formation is subdivided in three members: the Belsele-Waas Member, the Terhagen Member and the Putte Member (Figure 1-9).

Table 1-2 – Mineralogical composition of the Boom Clay at the Mol site (Mol-1 borehole) and in the Campine basin (based on data compilation from the boreholes Mol-1, Zoersel-1, Doel-2b and the outcrop area (southern border of the Campine basin) (compiled by Frederickx (2019) and Honty and De Craen (2012)).

Mineralogical composition	[% weight] (min–max)	
	Mol-1 borehole	**Campine basin**
Quartz	19–71	20–66
Na-plagioclase	0–7	0–7
K-Feldspar	4–12	0–8
Siderite	0–4	0–6
Calcite	0–6	0–5
Dolomite	0–1	0–1
Apatite	0.1–0.5	0–1
Pyrite	0.2–4	0–5
Illite/muscovite	3–19	4–37
Smectite and illite-smectite	10–44	6–43
Kaolinite	0.8–16	1–20
Chlorite	0.1–4	0–4
Organic matter	0.4–5	

The pore water composition of Boom Clay at the reference location for RD&D (HADES URL, Mol) is presented in Table 1-3. Pore water sampling was done in situ from various piezometers, or by the squeezing or leaching of clay cores in the surface laboratory. Piezometer water is considered to be the most representative for the in situ pore water since piezometer water samples experience minimum laboratory manipulations and therefore suffer minimum artefacts. The reference pore water composition was based on experimental data from the HADES URL, combined with supplemental chemical constraints, via a geochemical model. The composition of the synthetic clay water which is typically used in laboratory experiments is also given in the table.

EURAD (Deliverable n° 6.1) – Initial State of the Art on Gas Transport in Clayey Materials
Dissemination level: PU
Date of issue of this report: **17/11/2021**

Page 22

Table 1-3 – The reference compositions of Boom Clay pore water and synthetic clay water as compiled by De Craen et al. (2004).

Dissolved constituent	Boom Clay pore water		Synthetic clay water
	[mg/L]	[mmol/L]	[mg/L]
Na	359	15.6	330
K	7.2	0.2	13
Ca	2.0	0.05	saturated
Mg	1.6	0.06	2.6
Fe	0.2	0.003	1.3
Si	3.4	0.1	-
Al	0.6×10^{-3}	2.4×10^{-5}	-
B	-	-	7.5
HCO_3^-	878.9	14.4	848
Total Inorganic Carbon	181.3	15.1	-
Alkalinity [meq/L]	15.12	-	-
Cl	26	0.7	27.3
Total S	0.77	0.02	-
SO_4^{2-}	2.2	0.02	0.2
F	-	-	4.9

The Boom Clay is categorised as plastic clay, stiff, over-consolidated with a very low permeability and a relatively high swelling pressure. Table 1-4 gives an overview of the basic geotechnical properties with their ranges. This table was obtained by lumping together several sources (Horseman et al. 1987; Baldi et al. 1988; Sultan 1997; Mertens et al. 2003; Mertens et al. 2004; Dehandschutter et al. 2004; Bernier et al. 2007a).

Table 1-4 – Basic geotechnical properties of Boom Clay compiled by a review of several studies (Horseman et al. 1987; Baldi et al. 1988; Sultan 1997; Mertens et al. 2003, Mertens et al. 2004; Dehandschutter et al. 2004; Bernier et al. 2007a).

Parameter [unit]	Value (or range of values)
Bulk density [kg/m³]	1 900–2 100
Grain density [kg/m³]	2 682
Dry density [kg/m³]	1 490–1 648
Water content [wt%]	20–30 (close to 40% in volume)
Porosity [%]	35–40
Plastic limit [%]	13–29
Liquid limit [%]	55–80
Over-consolidation ratio (OCR) [–]	2.4

The total vertical stress and pore water pressure at the level of the HADES URL (depth = 223 metres) are respectively 4.5 MPa and 2.2 MPa. The vertical stress is the major principal stress. A value of the coefficient of earth pressure at rest, K_0, was determined by laboratory methods and in situ investigations (pressuremeter, dilatometer, self-boring pressuremeter, hydrofracturing tests, borehole breakouts and back-analysis of the stresses in the segmental concrete lining) (Bernier et al. 2007a). The value of K_0 ranges from 0.7 to 0.8 (ONDRAF/NIRAS 2013a), hence the total horizontal stress at the level of HADES

EURAD (Deliverable n° 6.1) – Initial State of the Art on Gas Transport in Clayey Materials
Dissemination level: PU
Date of issue of this report: 17/11/2021

Page 23

URL is expected to be about 3.9 MPa which is the minor principal stress. There is no indication of stress anisotropy in the horizontal plane.

The Boom Formation is characterised by a very low permeability with limited hydraulic gradient over the formation. Consequently, the main mechanism of transport is via diffusion; the water flow by advection being negligible. Figure 1-8 presents a geological cross-section (northern Belgium) (modified from Steurbaut et al. (2003) (Lima 2011). The Boom Formation is surrounded by two sandy aquifers (the Neogene aquifer, which includes the Eigenbilzen Sand, and the Lower Rupelian aquifer). Aertsens et al. (2004) studied with cores the value of the hydraulic conductivity parallel and perpendicular to the bedding plane in the whole formation. The horizontal and vertical values are different with a ratio (K_H/K_V) more or less equal to two. Note the different values of the hydraulic conductivity in relation with the granulometry of the studied material. For instance, the values in the Belsele-Waas member are higher than those of the other members of the formation because of its higher sand content. Aertsens et al. (2004) proposed an average value of 2.3×10^{-12} m/s for the vertical hydraulic conductivity, which corresponds to an intrinsic vertical permeability of 2.3×10^{-19} m^2. This value has been confirmed since then (Lima 2011; Yu L. et al. 2011). Figure 1-9 presents the vertical profile of horizontal (K_h) and vertical (K_v) hydraulic conductivities measured in laboratory on cores of the ONDRAF/NIRAS-Mol-1 borehole. Spatial analysis of K values across the Boom Clay at the Mol site reveals a typical profile with a very homogenous 61-metres thick central part, i.e. the Putte and Terhagen Members, which is also the least permeable part of the Boom Clay. According to Yu L. et al. (2013), the geometric mean of the vertical (K_v) and horizontal (K_h) hydraulic conductivities for the Putte and Terhagen Members at the Mol site are 1.7×10^{-12} and 4.4×10^{-12} m/s, respectively, with a vertical anisotropy K_h/K_v of about 2.5. Higher hydraulic conductivities values, but still low (10^{-12} to 10^{-10} m/s), are observed in the more silty zones above and below the Putte and Terhagen Members, i.e. the Belsele-Waas Member and the Boeretang Member, as well as in the double band of the lower Putte Member.

Table 1-5 presents some values of the hydraulic conductivity and their order of magnitude from Bernier et al. (2007a), Aertsens et al. (2004), Wemaere et al. (2008), Horseman et al. (1987) and Lima (2011). It has to be indicated that the measurements done by Aerstens et al. (2004) using the pulse injection method did not involve any mechanical coupling. Indeed, no confining pressure was used to perform these tests whereas the effect of a mechanical load can reduce the value of the permeability due to change in the size of voids and hence in porosity. Knowing the different consolidation parameters obtained by oedometer tests, Horseman et al. (1987) found similar values to those observed by the other authors, considering an effective stress of 2.5 MPa similar to the in situ stress. Lima (2011) estimated the permeability of the Boom Clay from MIP results following the approach developed in Romero (1999). The values found by this back-analysis were in the order of magnitude of the previous method. The water permeability was also determined experimentally in this study with the controlled-gradient permeability test and the measurement of vertical and horizontal water permeability in the purpose of verifying the anisotropy at sample scale. Once again, the values found were compatible with values determined in the previous studies.

The storage coefficient is the volume of water that an aquifer releases from or takes into storage per unit surface area per unit change in head. This value was determined by Horseman et al. (1987) from the consolidation parameters. Coll (2005) performed pulse tests on Boom Clay samples and found similar values.

EURAD (Deliverable n° 6.1) – Initial State of the Art on Gas Transport in Clayey Materials
Dissemination level: PU
Date of issue of this report: **17/11/2021**

Page 24

Table 1-5 – Hydraulic properties of Boom Clay (from laboratory and in situ measurements).

Parameter, symbol [unit]	Horseman et al. 1987	Aertsens et al. 2004	Bernier et al. 2007a	Wemaere et al. 2008	Lima 2011
Hydraulic conductivity, K [m/s]	-	-	$2.0–4.0 \times 10^{-12}$	-	$1.5–1.8 \times 10^{-12}$
Vertical hydraulic conductivity, K_V [m/s]	$2.0–3.5 \times 10^{-12}$	2.3×10^{-12}	-	3×10^{-12}	2.3×10^{-12}
Horizontal hydraulic conductivity, K_H [m/s]	5.5×10^{-12}	4.6×10^{-12}	-	-	$4.0–4.5 \times 10^{-12}$
Specific storage coefficient [m^{-1}]	1.2×10^{-4}	-	-	-	-
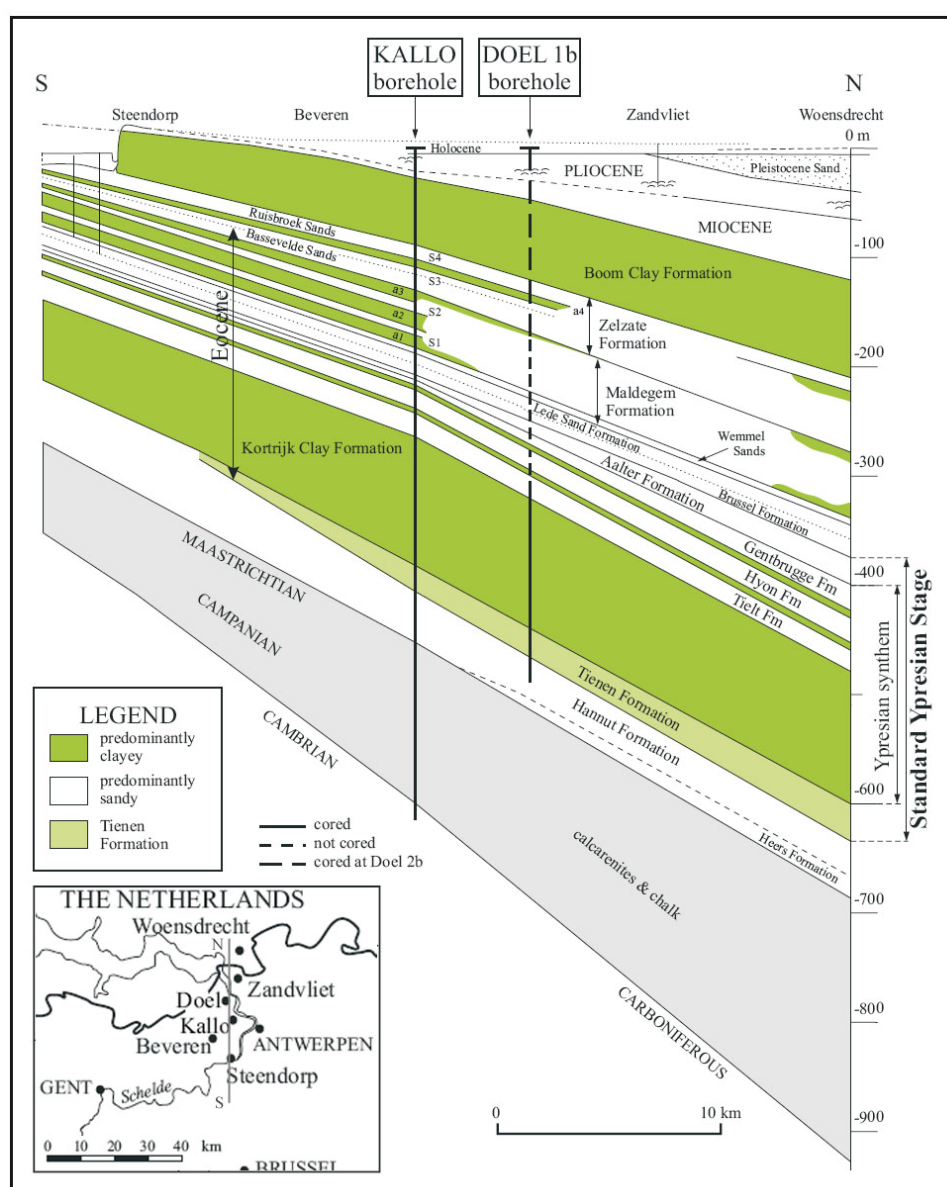
Figure 1-8 – Geological cross-section (northern Belgium) (Lima 2011) (after Steurbaut et al. 2003).

EURAD (Deliverable n° 6.1) – Initial State of the Art on Gas Transport in Clayey Materials
Dissemination level: PU
Date of issue of this report: **17/11/2021**

Page 25
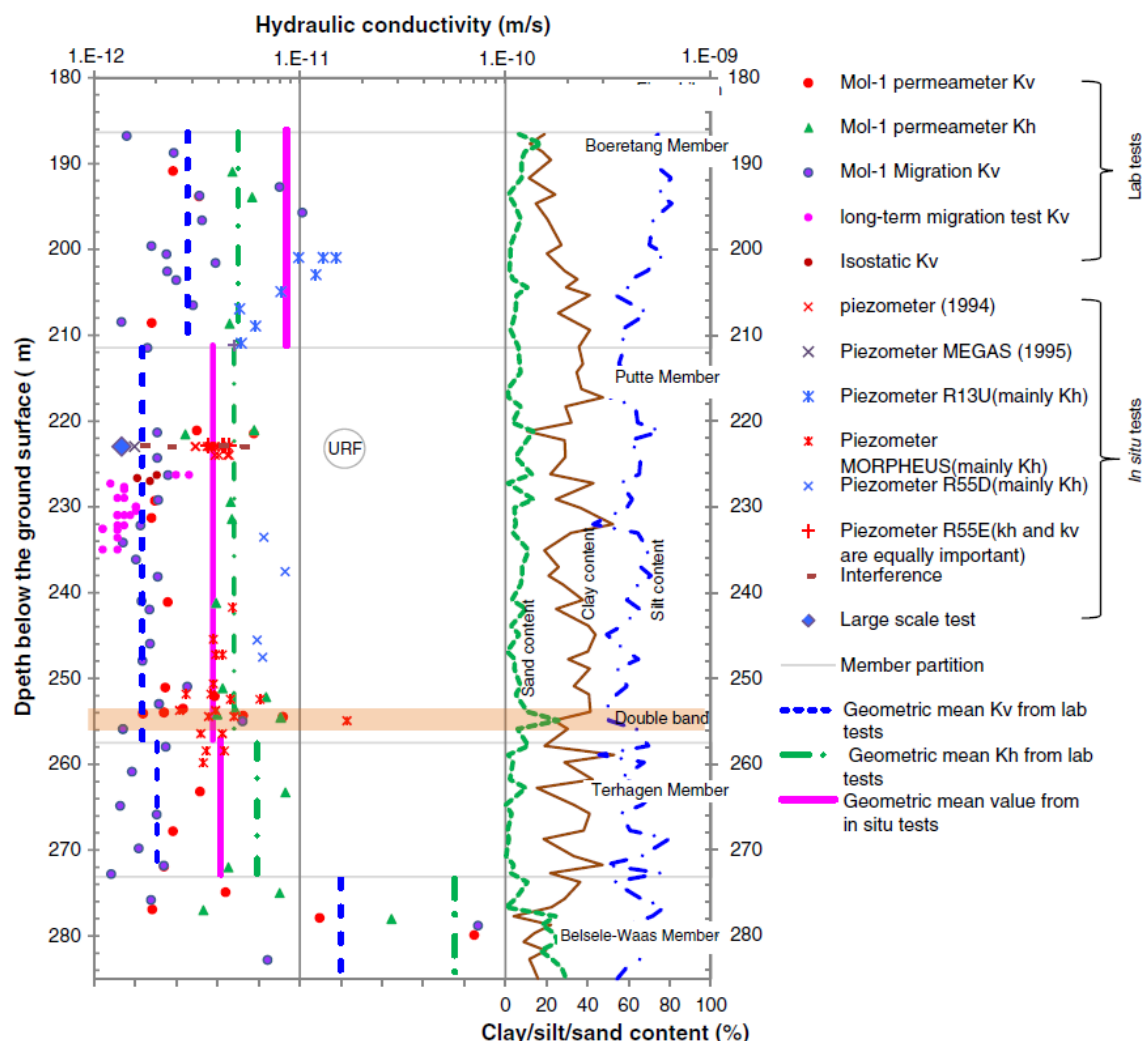
Figure 1-9 – Hydraulic conductivity profile of Boom Clay at the Mol site based on laboratory tests and in situ tests at the HADES URL (clay: <2 µm, 2 µm ≤ silt <62.5 µm, sand: ≥62.5 µm) (Yu L. et al. 2013).

Since the operational start of HADES URL early in the 80s, many laboratory and in situ tests have been performed to understand the Boom Clay behaviour, and in particular its hydro-mechanical behaviour, among which are triaxial and oedometer tests. Triaxial tests allow the determination of deviatoric behaviour and then the strength parameters while oedometer tests are more focused on the volume change behaviour. Clay samples have been studied in conditions as close as possible to their natural state around the HADES URL. As resaturating Boom Clay samples at low confining pressure induces an important swelling which affects the microstructure and thus modifies clay properties (Rousset 1988; Coll 2005; Sultan 1997), Le (2008) suggested saturating Boom Clay at a confining pressure close to the in situ state of stress to minimise this swelling and disturbance of the clay. These laboratory test protocols are detailed in the initial state-of-the-art report of the WP HITEC (Villar et al. 2020a).

The Boom Clay behaviour is characterised by a non-linear stress-strain response. The description of this behaviour as well as the associated hydro-mechanical parameters and properties are provided in the initial state-of-the-art report of the WP HITEC (Villar et al. 2020a).

EURAD (Deliverable n° 6.1) – Initial State of the Art on Gas Transport in Clayey Materials
Dissemination level: PU
Date of issue of this report: **17/11/2021**
Page 26

1.5.2 Callovo-Oxfordian claystone

The Callovo-Oxfordian (COx) claystone was deposited 160 million years ago over a period of approximately five million years, in an open and calm marine environment. The formation is surrounded above and below by the Dogger and the Oxfordian limestones. Three major geological units are defined (Figure 1-10):

- The argillaceous unit (UA) at the base is the thickest (thickening from 100 to 120 metres from the southwest to the northeast in the zone of interest), the most homogeneous and the richest in argillaceous minerals (more than 40% on average) of the three. It is subdivided into three subunits (UA1, UA2 and UA3) with small and progressive variations. Subunit UA2 corresponds to the stratigraphic level where the clay content is higher and in which the Meuse/Haute-Marne underground research laboratory (MHM URL) is located;

- The transition unit (UT) forms a transition between the mainly argillaceous rocks of the UA and the rocks of the silty-carbonated unit (USC) with the highest carbonate contents (40% to 90%);

- The silty-carbonated unit (USC), 29 metres thick, shows considerable vertical petrophysical variability linked with the lithological alternations (marls and calcareous siltstones). It comprises levels with more contrasted and heterogeneous mineralogical composition.

The interval of interest is the argillaceous unit, that is the level of the URL and the planned repository. Only this unit will therefore be described in detail in this document. The formation dips gently (average 1°) towards the northwest, the bedding plane can therefore be considered horizontal. The main level of the URL is located at a depth of 490 metres.

The main mineralogical phases of COx are shown in Figure 1-11. The clay phase consists mainly of illite and interstratified illite/smectite. The tectosilicates are primarily quartz and feldspar, and the carbonates are primarily calcite and dolomite. The RIO (*Repère Inférieur Oolithique*) layer in the middle of the UA is a 3 to 10-metres thick calcareous claystone.

The porosity varies between 14% in the carbonate-rich intervals to 19.5% in the more argillaceous levels; in the UA, the average porosity is 18%. The characterisation of this porosity, performed using several techniques (mercury intrusion porosimetry, helium pycnometer, nitrogen adsorption, water content), indicates that the network of pores mainly comprises meso- and micropores with a predominant pore size of approximately 10 to 30 nm, and that this network has an extremely low connectivity for pore sizes greater than 40 µm (Figure 1-12). For pores of less than 3–4 nm, the water is influenced by the electrostatic field on the outer surface of the clay minerals, and is therefore relatively immobile. For larger pores, the pore water (free) is not affected by electrostatic interactions and will be mobile for flow.

For levels in which the proportion of clay minerals is greater than 45% (UA), COx shows a relatively uniform structure beyond a few hundred µm. The texture is finely divided and is an assembly of tectosilicate and carbonate grains, connected by a fine matrix formed of clay minerals and calcite microcrystals (Figure 1-13). Both the tectosilicate and the carbonate grains show a preferential orientation of their long axis parallel to the sedimentation plane. The anisotropy of magnetic susceptibility of the clay minerals shows a magnetic foliation in the sedimentation plane, indicating a similar orientation of the clay minerals. However, the anisotropy is less pronounced than in other undeformed marine claystone.

The water permeability in the UA was measured both in laboratory (over 200 samples) and through in situ testing on a scale of several decimetres to several metres. It is very low and ranges from 1.0×10^{-21} m^2 to 2.0×10^{-20} m^2, with a relatively low anisotropy (2 to 3 ratio) (Armand et al. 2017). The

EURAD (Deliverable n° 6.1) – Initial State of the Art on Gas Transport in Clayey Materials
Dissemination level: PU
Date of issue of this report: **17/11/2021**
Page 27

reference value of 4×10^{-21} m^2 corresponds to the median value of the measurements obtained in steady-state tests.

The stress regime in the area is anisotropic and has the following characteristics (Figure 1-14):

- The major principal stress is horizontal and oriented N155°E (±10°). The vertical stress and the minor principal horizontal stress are more or less equal,

- The vertical stress is equal to the weight of the overburden formations,

- The ratio between the major horizontal stress and the minor horizontal stress (σ_H/σ_h) is at most 1.3.

For the calculations, at the URL level at 490 metres, the major principal horizontal stress σ_H is set at 16.1 MPa, the vertical stress σ_v = 12.7 MPa and the minor principal horizontal stress σ_h = 12.4 MPa.

The pore pressure measurements performed for the past 15 years at the level of the URL show that the pressure in the COx is 0.45 MPa higher than the pressure in the surrounding carbonates. At 490 metres, the pore pressure is 4.7 MPa.

The composition of the COx pore water is given in Table 1-6. The reference chemical composition for the pore water of the COx calculated with the ThermoAr model (Gaucher et al. 2006) and calibrated with all the data acquired in the area is applicable to the Meuse/Haute-Marne underground research laboratory (MHM URL).

EURAD (Deliverable n° 6.1) – Initial State of the Art on Gas Transport in Clayey Materials
Dissemination level: PU
Date of issue of this report: **17/11/2021**

Page 28
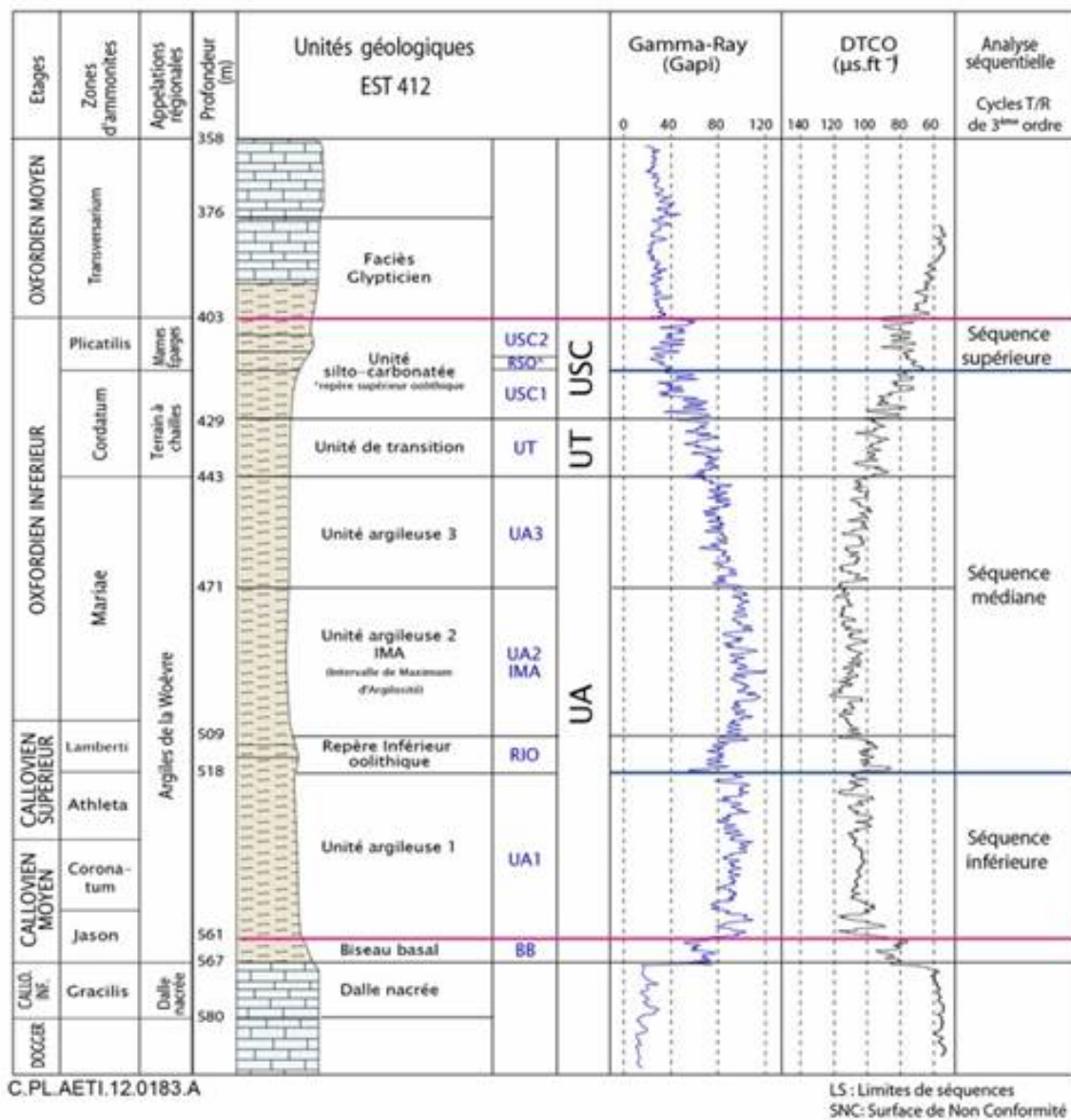
Figure 1-10 – Main geological units of the Callovo-Oxfordian claystone: argillaceous unit (UA), transition unit (UT) and silty-carbonated unit (USC).

EURAD (Deliverable n° 6.1) – Initial State of the Art on Gas Transport in Clayey Materials
Dissemination level: PU
Date of issue of this report: 17/11/2021

Page 29
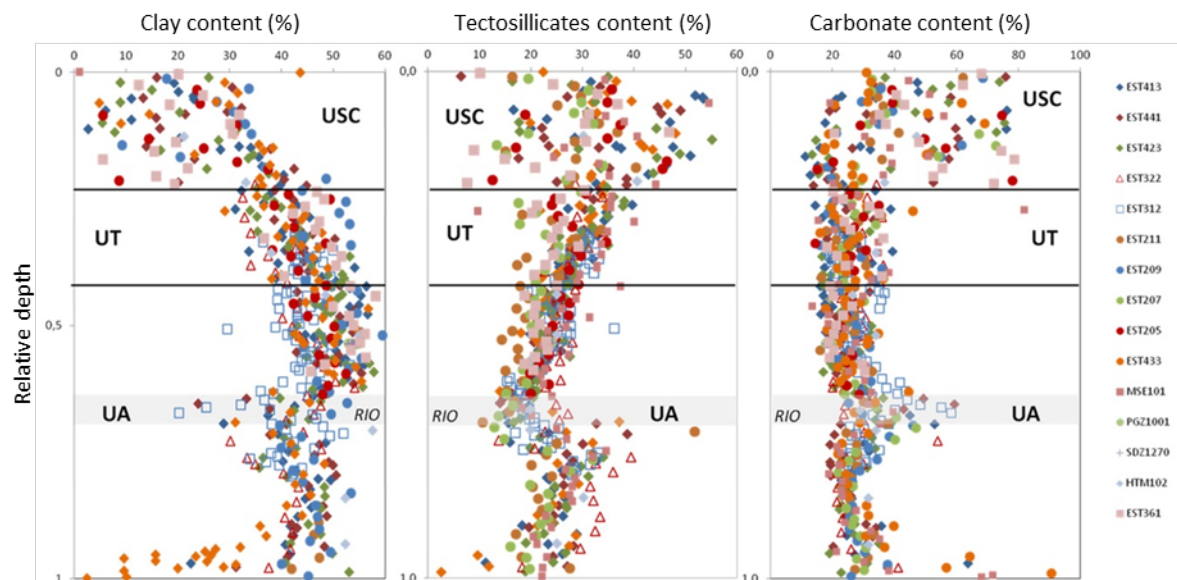
Figure 1-11 – Vertical variations in primary mineralogical phases (phyllosilicates, tectosilicates and carbonates) of the Callovo-Oxfordian claystone in different boreholes (Conil et al. 2018).
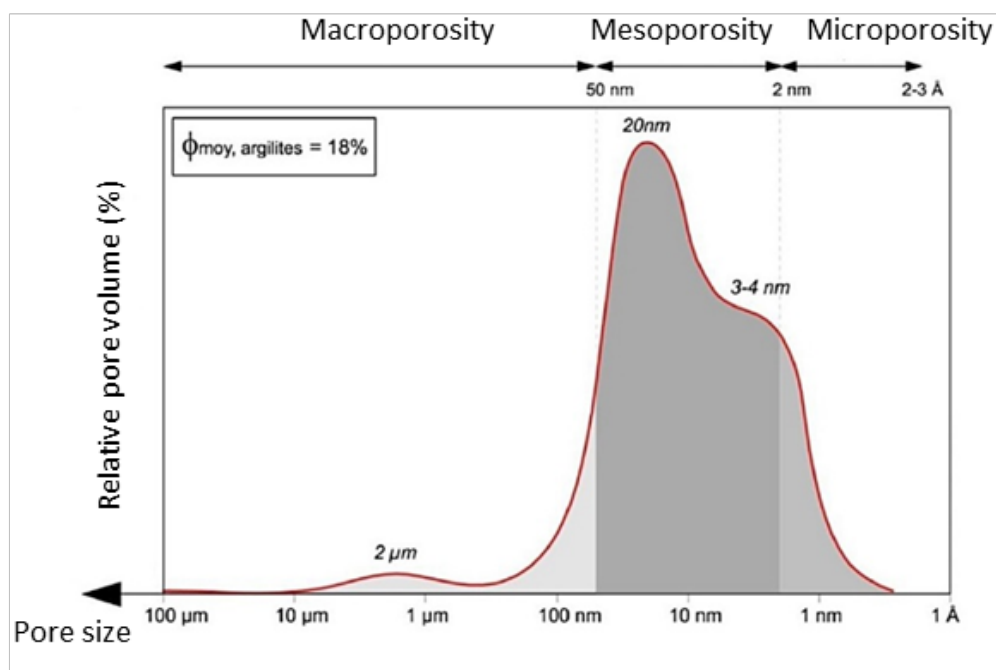
Figure 1-12 – Conceptual model of the pore size distribution for the UA2 claystone, based on mercury intrusion porosimetry, NMR and gas adsorption measurements (COx).

EURAD (Deliverable n° 6.1) – Initial State of the Art on Gas Transport in Clayey Materials
Dissemination level: PU
Date of issue of this report: 17/11/2021

Page 30
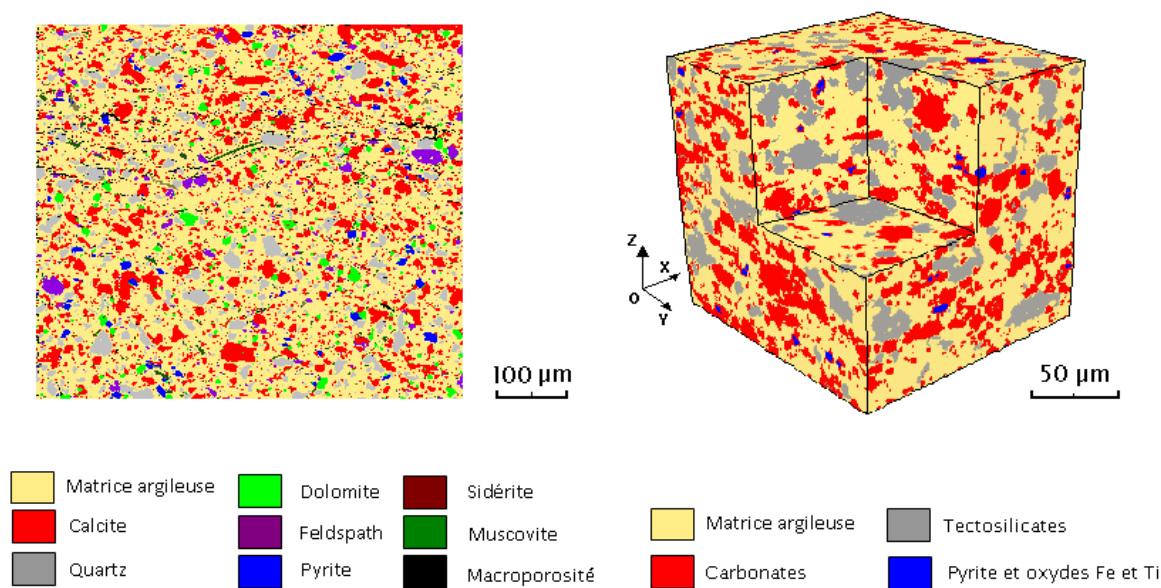
Figure 1-13 – Two-dimensional and three-dimensional distribution of minerals in the Callovo-Oxfordian (Robinet et al. 2012a).
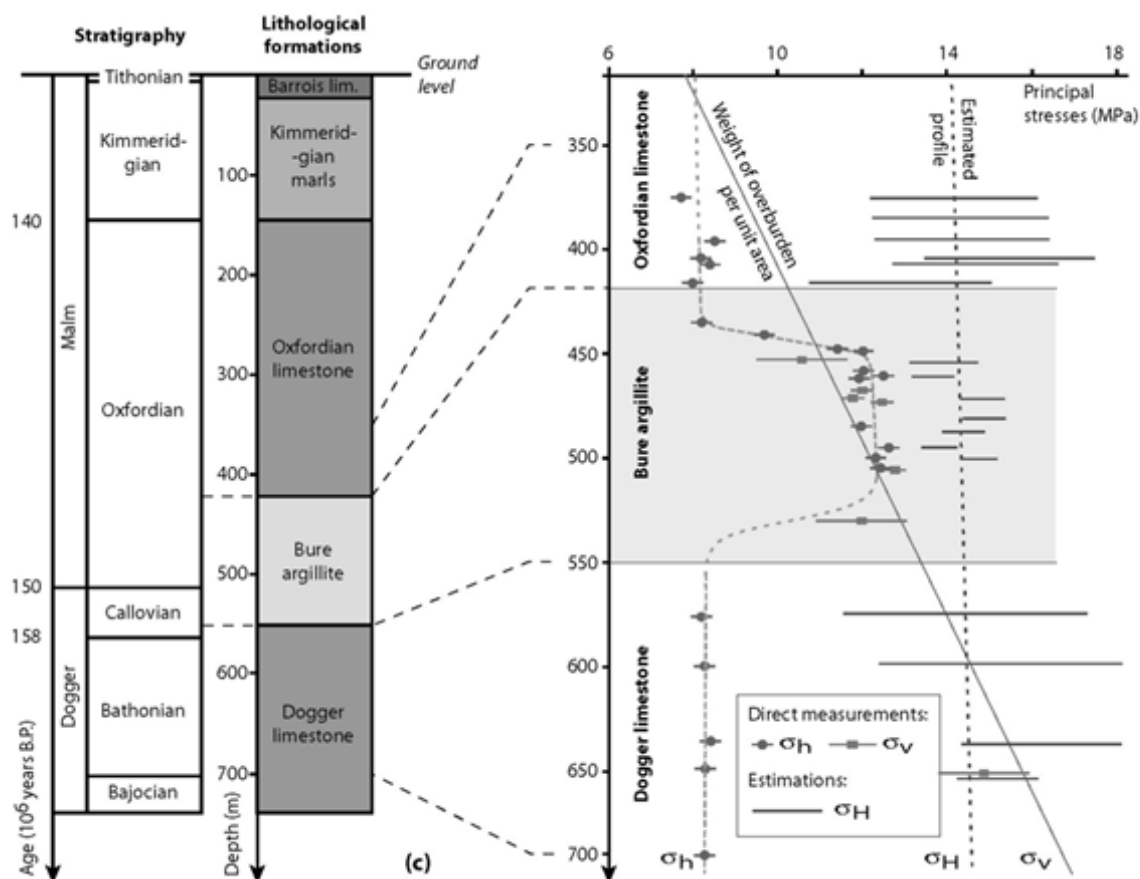
Figure 1-14 – Stress profile in the Dogger, Callovo-Oxfordian and Oxfordian layers in the MHM URL (Gunzburger and Cornet 2007; Wileveau et al. 2007).

EURAD (Deliverable n° 6.1) – Initial State of the Art on Gas Transport in Clayey Materials
Dissemination level: PU
Date of issue of this report: **17/11/2021**

Page 31

Table 1-6 – Callovo-Oxfordian claystone pore water composition predicted from the ThermoAr model and measured in the PAC1002 and POX1201 boreholes (Gaucher et al. 2006).

Parameter [unit]	Geochemical model	Experimental data (± 5%)	
	'ThermoAr'	PAC1002	POX1201
pH	7.2	7.1 ± 0.1	7.1 ± 0.1
Ionic strength [mol/L]	0.08	-	0.08
Redox potential [pE]	-3.0	-	-
Concentration [mmol/L]			
Chloride	37.0	36.6	38.8
Sulphate	12.8	12.8	12.9
Total Inorganic Carbon	2.1	2.7	2.4
Sodium	47.0	46.9	46.7
Calcium	8.0	5.0	5.0
Magnesium	5.0	4.2	4.3
Potassium	1.0	0.6	0.5
Strontium	0.2	0.2	0.2
Iron (II+III)	0.002	0.008	0.02
Silica	0.2		0.2

1.5.3 Opalinus Clay

The Opalinus Clay formation in the Molasse Basin and in the Jura Fold and Thrust Belt of northern Switzerland is a moderately over-consolidated claystone of Jurassic age, that has been formed by a complex burial and compaction history with two distinct periods of subsidence. The formation was deposited by the sedimentation of fine clay, quartz and carbonate particles in a shallow marine environment. It is part of a thick sequence of Mesozoic and Tertiary sediments in the Molasse Basin (Figure 1-15), which overly Palaeozoic sediments and crystalline basement rocks. The overlying Tertiary sediments thicken considerably into the Molasse Basin to the south.

The Opalinus Clay at the candidate siting regions in northern Switzerland has been explored by several 3D seismic surveys and a number of deep investigation boreholes. Figure 1-16 displays interpreted clay logs and drillcore material from the borehole Benken, illustrating the mineralogical and structural features of the Opalinus Clay in the Zürcher Weinland on various scales.

Geotechnical characterisation of core samples from Benken and other deep investigation boreholes in northern Switzerland reveals a moderately to heavily over-consolidated claystone (1.5 ≤ OCR ≤ 5) with a clay mineral content between 40 and 75%, quartz content between 10 and 30% and a carbonate content between 5 and 35% (Figure 1-16a). Porosity displays moderate depth-dependence with typical values of 11–16% (corresponding to an overburden of several hundred metres). Hydraulic conductivity derived from laboratory and in situ testing exhibits typical values between 10^{-12} and 10^{-14} m/s and conforms well to empirical permeability correlations, drawing on measurements of porosity and clay mineral content (Yang and Aplin 2010). Based on grain size distribution, the Opalinus Clay classifies as a clayey (and sandy) siltstone (Figure 1-16b). The consistency behaviour (Atterberg limits) provides additional insight to the intrinsic geomechanical properties of the (destructured) geomaterial, representing a qualitative indicator for the friction angle. As shown in Figure 1-17c the plasticity index plots broadly along the A-line of the plasticity chart, which separates clayey from silty soils. The reported

EURAD (Deliverable n° 6.1) – Initial State of the Art on Gas Transport in Clayey Materials
Dissemination level: PU
Date of issue of this report: **17/11/2021**

Page 32

values for liquid limit (w_L) and plasticity index (PI) range from approximately 30 to 50% and approximately 10 to 25%, respectively. Drawing on empirical correlations by Terzaghi et al. (1996) and Stark and Eid (1994), the friction angle of the Opalinus Clay can be bracketed in the range between 20 and 35°, which is in good agreement with findings from geomechanical testing. Table 1-7 gives an overview of the basic geotechnical properties with their ranges (see also Nagra 2014a).
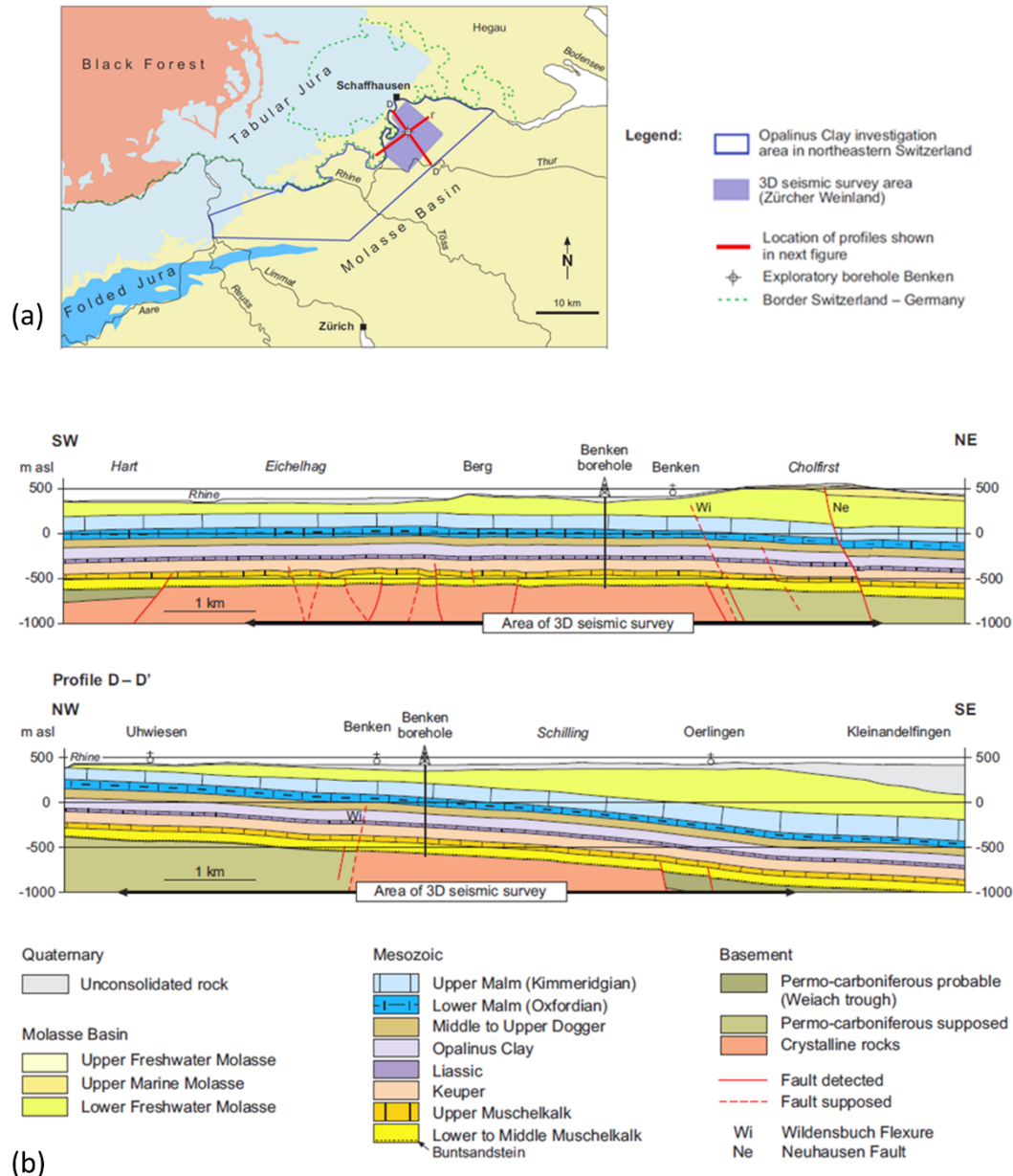
Figure 1-15 – Candidate siting area 'Zürcher Weinland' in northern Switzerland: (a) principal tectonic units and (b) schematic geological profiles from SW to NE (top) and NW to SE (bottom) through the sedimentary rocks in the vicinity of the borehole at Benken (Nagra 2002a).

EURAD (Deliverable n° 6.1) – Initial State of the Art on Gas Transport in Clayey Materials
Dissemination level: PU
Date of issue of this report: 17/11/2021

Page 33
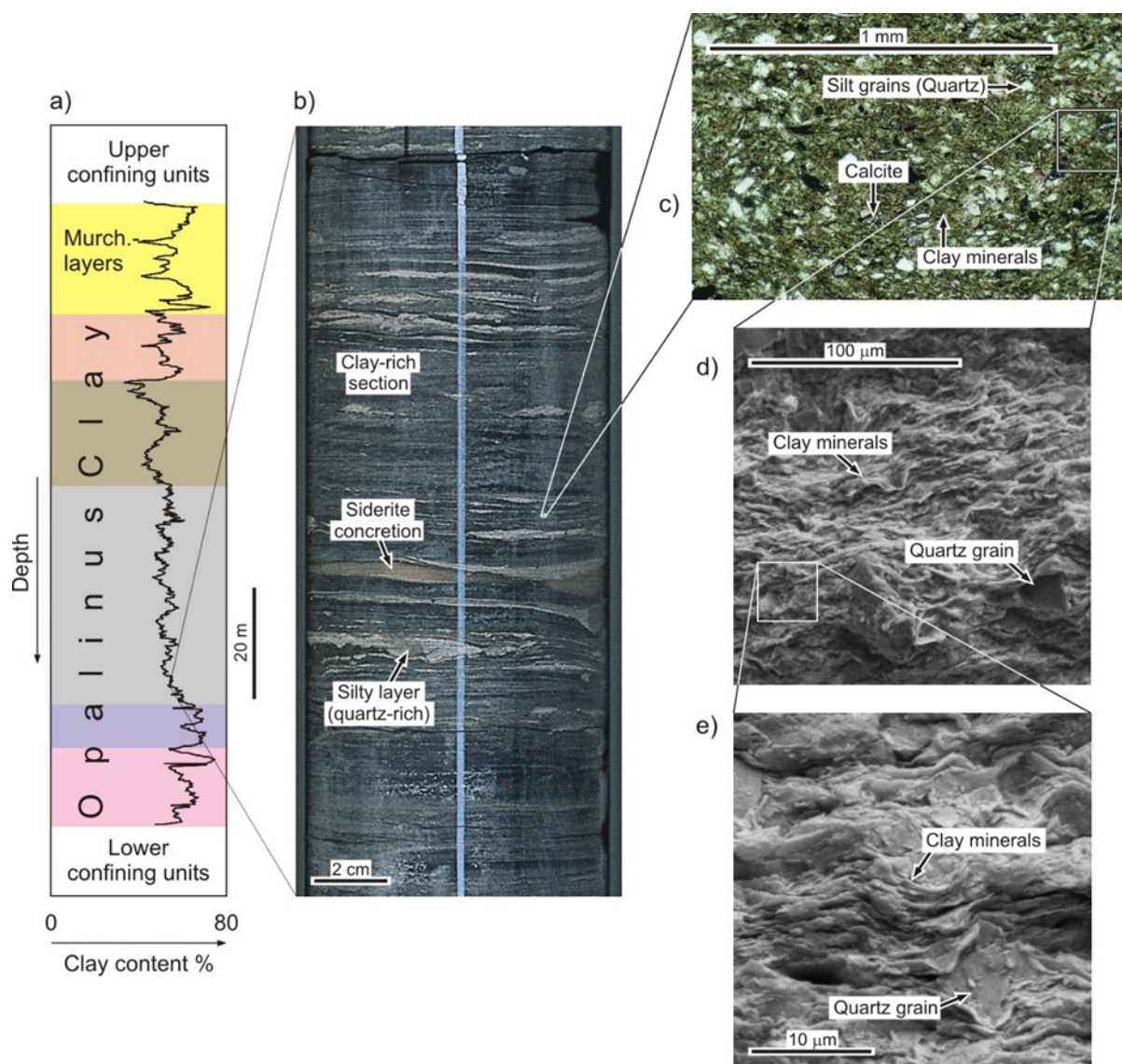
Figure 1-16 – Illustration of the mineralogy and structure of the Opalinus Clay at different scales, based on data from the Benken borehole in the Zürcher Weinland: (a) vertical profile of clay content determined by petrophysical logging, (b) core sample, (c) thin sections and (d+e) SEM images (Nagra 2002b).

EURAD (Deliverable n° 6.1) – Initial State of the Art on Gas Transport in Clayey Materials
Dissemination level: PU
Date of issue of this report: **17/11/2021**

Page 34
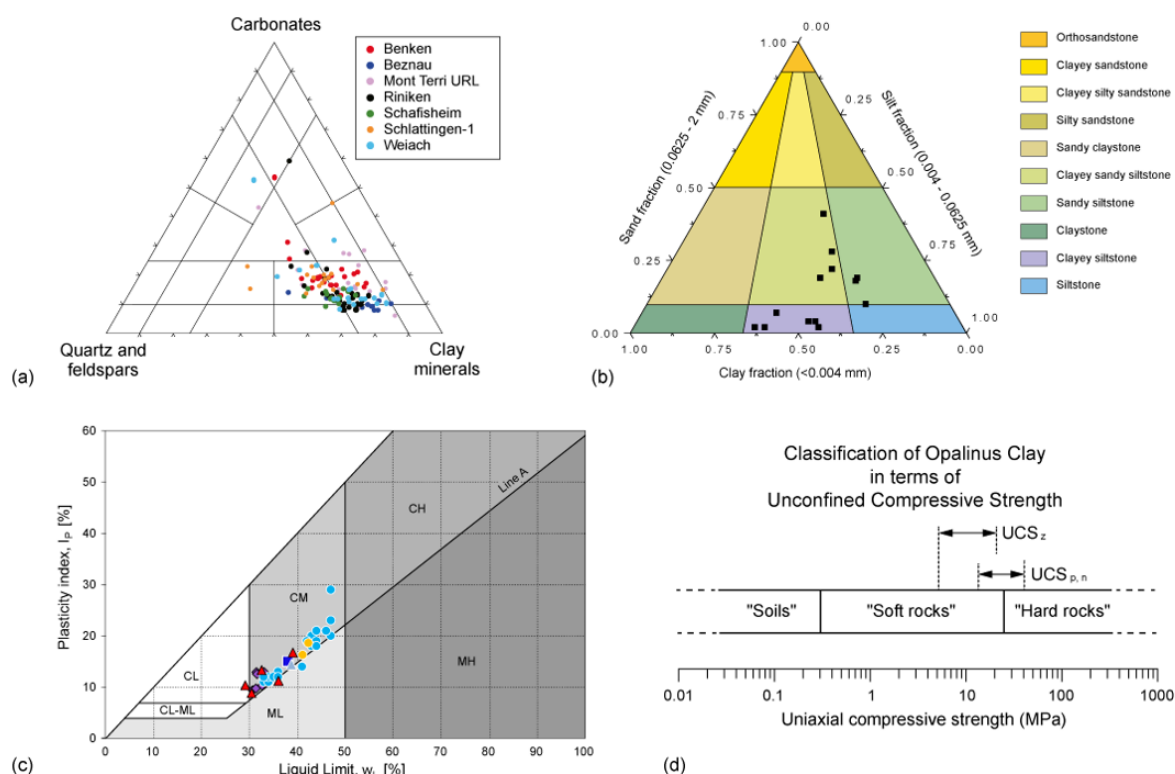
Figure 1-17 – Classification of the Opalinus Clay in terms of mineralogy, grain size and consistency (Marschall et al. 2016): (a) ternary diagram of principal mineralogical components, (b) unified soil classification system (USCS) classification of fine-grained sedimentary rocks, (c) Plasticity chart (SN 670 004-2a) and (d) unconfined compressive strength after Gens (2013).

Table 1-7 – Basic geotechnical properties of the Opalinus Clay from Mont Terri URL and from borehole investigations in the candidate siting regions in northern Switzerland (Nagra 2014a).

Parameter [unit]	Value (or range of values)
Dry density [kg/m³]	2 330–2 430
Grain density [kg/m³]	2 710
Water content [wt%]	4.5–6.4
Porosity [%]	11–16
Plastic limit [%]	10–30
Liquid limit [%]	30–50
Over-consolidation ratio (OCR) [–]	1.5–5.0

Microstructural investigations of Opalinus Clay samples from a deep geothermal well in northeastern Switzerland (located near the village of Schlattingen) and from the Mont Terri underground research laboratory (located in the Jura Fold and Thrust Belt) have been conducted by Keller et al. (2013a, 2013b). The investigations comprise the multi-scale characterisation of the samples by X-ray computed tomography (XCT), focused ion beam nano-tomography (FIB-nt) and scanning transmission electron microscopy (TEM), followed by segmentation and reconstruction of the rock fabric (Figure 1-18). The reconstructed digital representation of the microstructure with a maximum size in the order of 10 003 voxels was then subjected to quantitative data analyses and model simulations. The analyses include estimations of the pore size distribution, water retention behaviour and grain size distribution,

EURAD (Deliverable n° 6.1) – Initial State of the Art on Gas Transport in Clayey Materials
Dissemination level: PU
Date of issue of this report: 17/11/2021

Page 35

the derivation of representative elementary volumes (REV) of porosity (Keller et al. 2013a), clay content (Keller 2015) and connectivity, capillary properties and permeability on the basis of numerical channel network simulations (Keller et al. 2013a), impact of sand fraction on solute diffusion (Keller et al. 2015).
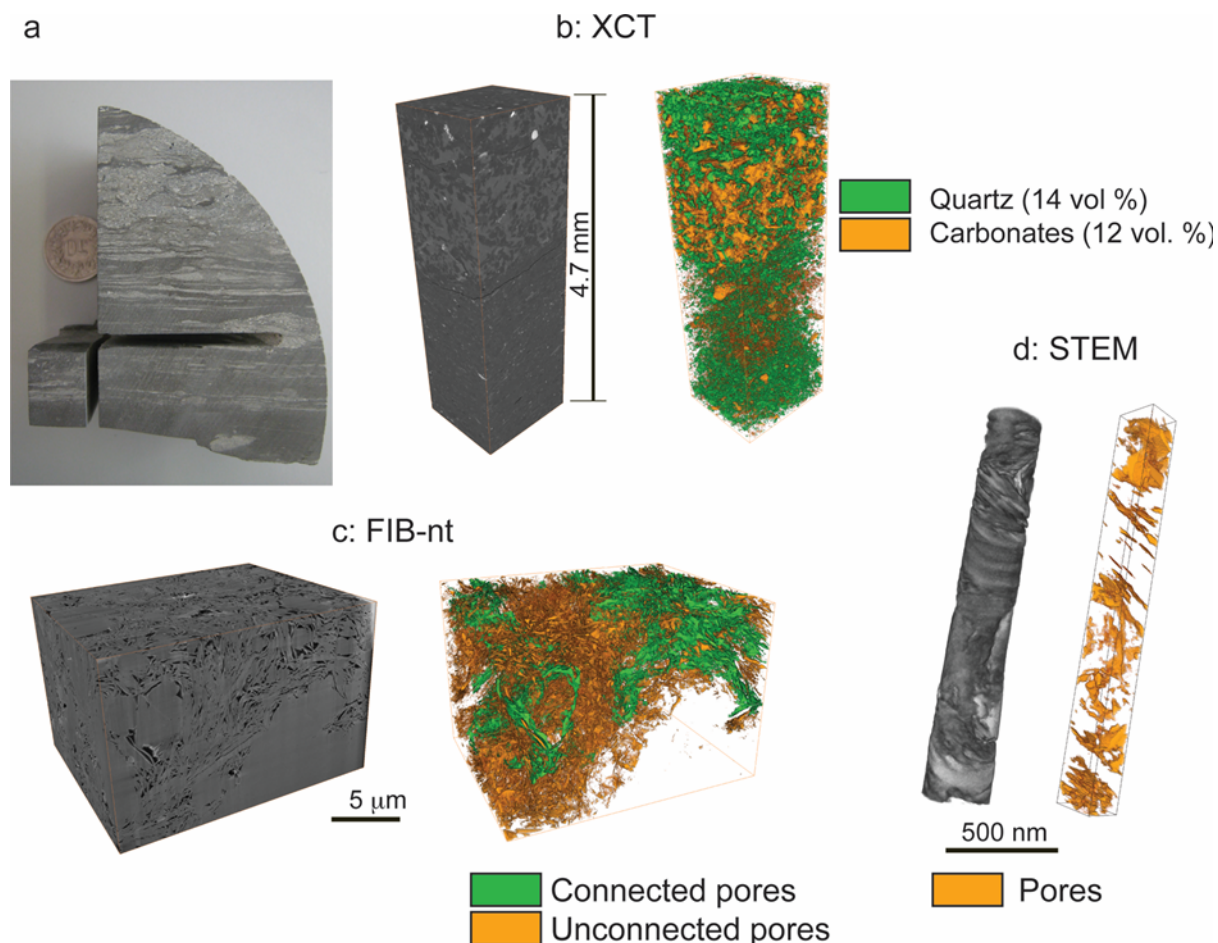
Figure 1-18 – Microstructural characterisation of Opalinus Clay (Marschall et al. 2016): (a) photograph of a core sample which contains carbonate/quartz-rich and clay-rich layers on various scales. (b) X-ray tomography data of a thin slab from the sample and 3D reconstruction of the mineral components (green: quartz; orange: carbonates). (c) FIB-nt and visualisation of connected/unconnected pore space (green: connected pore space; orange: unconnected pores). (d) Scanning transmission electron microscopy (TEM) and visualisation of pore space.

The reference pore water composition of the Opalinus Clay is presented in Table 1-8. The pore water composition was derived based on a large body of experimental data on aqueous extracts from the Mont Terri URL and from the deep borehole near Benken (see Figure 1-15), combined with supplemental chemical constraints. For instance, the Ca and Mg concentrations were fixed by imposing calcite and dolomite saturation, respectively. Si, Fe(II) and S(-II) were constrained via quartz, siderite and pyrite saturation. Chloride concentrations were determined based on squeezed aqueous extracts and Na, K, Sr were controlled by measured occupancies in the exchangeable clay combined with selectivity coefficients. Finally, the carbonate system and pH were constrained by fixing the pCO_2 ($10^{-2.2}$ bar in the reference case) and applying charge balance (Bradbury et al. 2014).

EURAD (Deliverable n° 6.1) – Initial State of the Art on Gas Transport in Clayey Materials
Dissemination level: PU
Date of issue of this report: **17/11/2021**

Page 36

Table 1-8 – 'Initial state' reference pore water chemistry of Opalinus Clay (Bradbury et al. 2014).

Opalinus Clay 'Initial state'			
Temperature [°C]		25	
pH		7.203	
log P-CO$_2$ [bar]		-2.20	
Ionic strength [mol/kg]		0.2299	
Dissolved constituent [mol/L]			
Na	1.644×10^{-1}	Fe^{II}	5.24×10^{-5}
K	2.604×10^{-3}	Fe^{III}	3.31×10^{-9}
Mg	9.625×10^{-3}	Si	1.779×10^{-4}
Ca	1.251×10^{-2}	Cl	1.600×10^{-1}
Sr	2.106×10^{-4}	S^{IV}	2.472×10^{-2}
Ba	–	S^{-II}	1.24×10^{-8}
Al	–	C^{IV}	2.506×10^{-3}

1.5.4   Bentonite

Bentonite and sand/bentonite mixtures are favoured options for clay-based engineered barriers for nuclear waste repositories due to their inherently low hydraulic conductivity at full saturation (e.g. Leupin et al. 2016b; Jenni et al. 2019). This ensures that diffusion of solutes such as radionuclides will be the dominating mechanism for transport through the engineered barriers. Another advantageous property of bentonite is that it swells in contact with water, ensuring the closure of gaps or openings and the development of a swelling pressure when it is mechanically confined. Owing to its good sealing properties, the use of compacted bentonite is foreseen under different forms (powder, granular, pellets, blocks and also mixed with sand) for different functions (buffer surrounding the waste containers, sealing structure, backfill) in the repository concepts of many waste management organisations (see Box 2 and Table 1-1). Next to its sealing properties, other aspects are involved in the selection of a bentonite. For instance, its general quality, availability and production techniques, its dry grain size, exchangeable ions and accessory minerals are considered at the design stage depending on the intended application.

The gas transport capacity of bentonite and sand/bentonite mixtures depends strongly on the hydro-mechanical conditions but also on the barrier emplacement procedures. Aspects to consider are the form (bentonite blocks, pelletised/granular bentonite, sand/bentonite mixtures), the applied emplacement and compaction methods (placement of blocks, treatment of gaps, in situ compaction technique for pelletised/granular materials, dry density of the emplaced material). The initial dry density is generally a key design parameter as it conditions the swelling and swelling pressure upon hydration.

After emplacement, the hydro-mechanical properties – including those that can affect gas transport – will evolve throughout the hydration process. Hydration will depend on the availability of water, the mobility of the water in the bentonite and on the mechanical conditions as well as the material swells and exerts a pressure on its surroundings. The early phase of hydration is often heterogeneous.

EURAD (Deliverable n° 6.1) – Initial State of the Art on Gas Transport in Clayey Materials
Dissemination level: PU
Date of issue of this report: 17/11/2021   Page 37

In this document, emphasis is on materials considered by organisations involved in the WP GAS:

- granular Wyoming sodium bentonite (MX-80). The use of this type of bentonite is foreseen in the Swiss concept for a HLW repository as a buffer material for the emplacement of the spent fuel canisters. In the French concept, MX-80 would be used for sealing galleries and shafts. The target emplacement dry density of the bentonite in these concepts is of 1 500 kg/m^3.

- FEBEX bentonite. This type of bentonite is considered in the Spanish concept for a radioactive waste repository in crystalline rock (AGP Granito): the waste canisters are placed horizontally in drifts and surrounded by a clay barrier constructed with pre-compacted bentonite blocks of 1 700 kg/m^3 dry density (ENRESA 2006).

- Czech bentonite BCV. The Czech buffer concept involves a combination of compacted bentonite blocks and pellets, and the reference backfill concept is based on the use of bentonite only; however, the option of using a mixture of bentonite and crushed rock has not been rejected.

- Sand/bentonite (S/B) mixtures of quartz sand and granular Wyoming sodium bentonite (MX-80) in proportion 80/20 and 60/40 in dry mass. The use of 80/20 S/B mixtures is foreseen in the Swiss concept for a L/ILW repository as barrier materials for cavern seals with high barrier efficiency for dissolved radionuclides, combined with a significant gas transport capacity. The use of mixtures with proportions 60/40 S/B is foreseen to seal horizontal tunnels in the French concept while fulfilling the specifications in terms of swelling pressure, water permeability and gas transport capacity.

1.5.4.1 Granular Wyoming sodium bentonite (MX-80)

The main batch of granular Wyoming sodium bentonite considered in the WP GAS contains more than 85% Na-smectite clay. Its mineralogical composition was reported by Plötze and Weber (2007) with 84.9% smectite (montmorillonite), 4.8% muscovite, 3.7% quartz, 5.2% feldspar and 1.3% calcite. A total specific surface area of 523 m^2/g was derived from adsorbed water content and an external specific surface area of 33.1 m^2/g was determined by nitrogen adsorption. High values of liquid limit (w_L = 420%) and plastic limit (w_p = 65%) reveal its high water activity. The reference value of specific gravity, or relative density, is reported as 2.74. Furthermore, a cation exchange capacity of 74 meq/100 g including 52.4 meq/100 g sodium, 13.2 meq/100 g magnesium and 1.4 meq/100 g potassium were measured for the smectite mineral in Wyoming bentonite.

A comprehensive geotechnical characterisation programme of this granular Wyoming bentonite was accomplished by several research groups (Seiphoori 2015; Molinero Guerra et al. 2017, 2018; Bernachy-Barbe et al. 2020). The experimental work concerns a range of grains and pellet sizes from few mm to 32 mm and different kinds of mixtures (pellets/powder with variation of percentages for each component, pellets assembly). Most of this work concentrated on the unsaturated behaviour of the material under different thermo-hydro-mechanical conditions and developing insights into the microstructural evolution. In this context, constant and free volume swelling tests were performed to evaluate the swelling properties of the granular Wyoming bentonite. The experimental observations on the behavioural features of the material at the macroscopic and microscopic level provided a sound basis for the development of a water retention model that accounts for the hydro-mechanical coupling and microstructural evolutions (see also Section 2.4.2.5).

Pellets are considered for use in repositories because of their relative simplicity of installation and their ability to be homogenised after wetting. Figure 1-19 presents the evolution of a pellet (7 mm cylindrical)/powder mixture with a proportion 80-pellet/20-powder in dry mass. The initial structure loses its granular nature on wetting. After 100 days of hydration, an apparent overall homogenous state is observed (Molinero Guerra et al. 2018).

EURAD (Deliverable n° 6.1) – Initial State of the Art on Gas Transport in Clayey Materials
Dissemination level: PU
Date of issue of this report: 17/11/2021

Page 38

Figure 1-20a presents the swelling pressure developed under constant volume conditions with respect to time for different dry densities for granular bentonite using an optimised Fuller granulometry. The results of the constant volume swelling pressure measurement versus dry density are presented in Figure 1-20b. The results are similar to the ones previously reported by Bucher and Müller-Vonmoos (1989) and Karnland et al. (2008) and therefore are consistent with results obtained on compacted blocks.

The swelling capacity of the bentonite material can be significantly influenced by the salinity of the pore water (Zhu et al. 2013; Navarro et al. 2017; Shehata et al. 2020). The swelling pressure of bentonite exposed to a NaCl or a $CaCl_2$ solution is significantly less than that exposed to distilled water (Zhu et al. 2013; Shehata et al. 2020). Therefore, gas transport in saturated bentonite is expected to be influenced by the geochemical environment of the repository (Guo and Fall 2021).
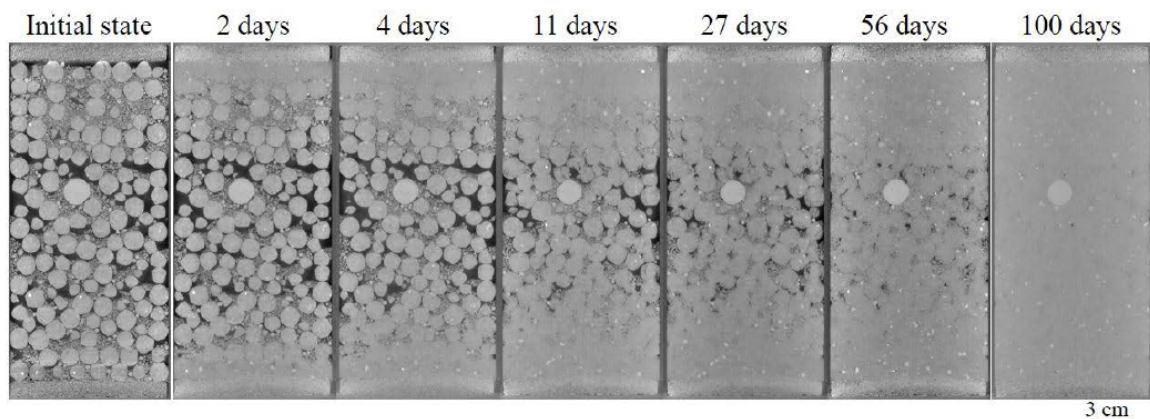
Figure 1-19 – Pellet/powder mixture while wetting. under µ-CT observations (Molinero Guerra et al. 2018).
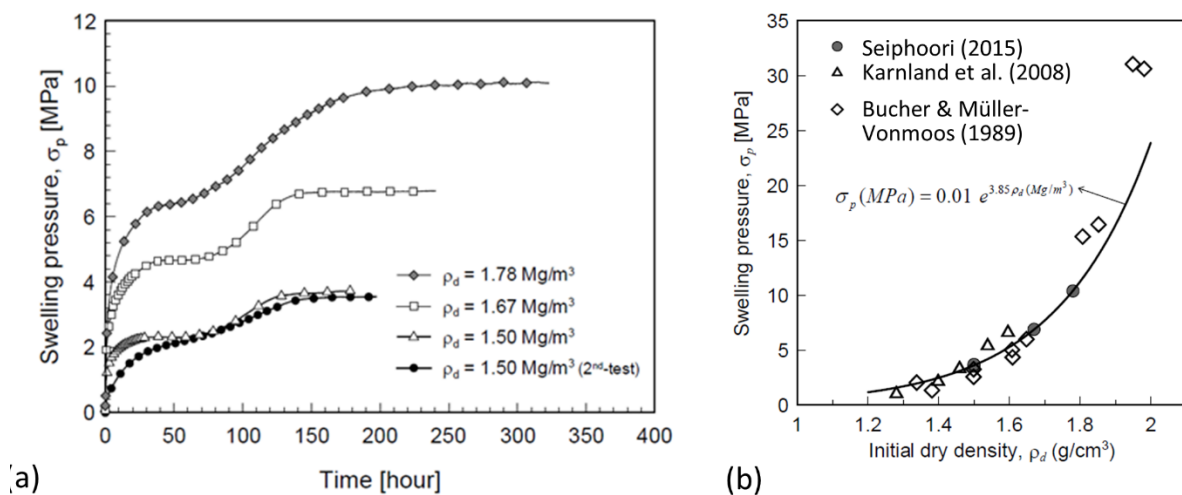
Figure 1-20 – Swelling behaviour of Wyoming granular bentonite (modified after Seiphoori 2015): (a) swelling pressure developed under constant volume conditions at different dry densities for Wyoming granular bentonite; (b) constant volume swelling pressure.

EURAD (Deliverable n° 6.1) – Initial State of the Art on Gas Transport in Clayey Materials
Dissemination level: PU
Date of issue of this report: **17/11/2021**

Page 39

1.5.4.2 FEBEX bentonite

The FEBEX bentonite is a 900-tonnes batch of bentonite that was extracted from the Cortijo de Archidona deposit in Spain and processed in 1996 for the Full-scale Engineered Barrier Experiment (FEBEX) project (Huertas et al. 2000). The processing consisted in homogenisation, air-drying and manual removal of volcanic pebbles on site and, at the factory, crumbling, drying in a rotary oven at temperatures between 50 and 60°C and sieving through a 5-mm mesh. This bentonite was initially used as homogeneous blocks for the FEBEX in situ test at the Grimsel test site and was characterised over the years in various laboratories during the FEBEX and FEBEX II projects (ENRESA 2006) and in Villar (2002) and Fernández (2004) and during the NF-PRO, the PEBS, the ABM[6] and the ESDRED projects (Alonso J. et al. 2008; Villar and Gómez-Espina 2009; Svensson et al. 2011).

The smectite content of the FEBEX bentonite is above 90 wt% (92 ± 3 wt%). The smectitic phases are actually made up of a montmorillonite-illite mixed layer, with 10-15 wt% of illite layers. Besides, the bentonite contains variable quantities of quartz (2 ± 1 wt%), plagioclase (3 ± 1 wt%), K-felspar (traces), calcite (1 ± 1 wt%), and cristobalite-tridymite (2 ± 1 wt%). The cation exchange capacity of the smectite is 98 ± 2 meq/100g, the main exchangeable cations being calcium (33 meq/100g), magnesium (33 meq/100g) and sodium (28 meq/100g). The predominant soluble ions are chloride, sulphate, bicarbonate and sodium.

The liquid limit of the bentonite is 102 ± 4%, the plastic limit 53 ± 3%, the density of the solid particles 2.70 ± 0.04 g/cm^3. 67 ± 3% of particles are smaller than 2 µm. The hygroscopic water content in equilibrium with the laboratory atmosphere (relative humidity 50 ± 10 %, temperature 21 ± 3°C, total suction about 100 MPa) is 13.7 ± 1.3 %. The external specific surface area is 32 ± 3 m^2/g and the total specific surface area is around 725 m^2/g.

The saturated hydraulic conductivity of compacted bentonite samples is exponentially related to their dry density (Equations 1-1 and 1-2). For a dry density of 1.6 g/cm^3, the saturated permeability of the bentonite is approximately 5·10^{-14} m/s at room temperature, either with diluted granitic or deionised water used as percolating fluid.

For dry densities lower than 1.47 g/cm^3,

$$log\ k_w = -6.00\ \rho_d - 4.09 \tag{1-1}$$

For dry densities higher than 1.47 g/cm^3:

$$log\ k_w = -2.96\ \rho_d - 8.57 \tag{1-2}$$

where k_w is the water permeability [m^2] and ρ_d the dry density [g/cm^3].

A few isothermal infiltration tests and heat flow tests at constant overall water content were performed during the FEBEX I project and were back analysed using CODE_BRIGHT (Pintado et al. 2002). It is possible to fit the experimental data using a cubic law for the relative permeability as a function of saturation ($k_r = S_r^3$) and a value of 0.8 for the tortuosity factor (τ).

---

[6] The 'alternative buffer material test' (ABM) performed by SKB in the Äspö HRL is an upscaled experiment in which different bentonites are compared. 11 different materials were compared in different setups with different running times.

EURAD (Deliverable n° 6.1) – Initial State of the Art on Gas Transport in Clayey Materials
Dissemination level: PU
Date of issue of this report: 17/11/2021

Page 40

The swelling pressure of compacted samples is also exponentially related to the bentonite dry density (Equation 1-3). The bentonite compacted at dry density of 1.6 g/cm³ and saturated with deionised water at room temperature develops a swelling pressure of about 6 MPa.

$$ln\,P_s = 6.77\;\rho_d - 9.07 \tag{1-3}$$

where P_s is the swelling pressure [Pa].

1.5.4.3 Czech bentonite BCV

Czech bentonite BCV is a typical bentonite that formed via the in situ alteration of Fe-rich tuffs and augite-biotite-type tuffites in the northwestern region of the Czech Republic (Černý vrch deposit). The contribution of Fe to the system occurred as a consequence of the activity of the Krušnohorsko-ohárecká tectonic zone (Franče 1992). And, since Fe erosion did not take place during the argillisation phase, the smectites in these bentonites remained enriched with iron (especially in the octahedral positions). Moreover, the accessory minerals also contain a significant proportion of Fe, i.e. Fe carbonates and oxyhydroxides.

The montmorillonite content of the Czech bentonite BCV is between 58 and 72 wt% (Červinka and Vašíček 2018) (montmorillonite is a member of the smectite group). In addition, the bentonite contains variable quantities of quartz (11 wt%), calcite (4 wt%), kaolinite (4 wt%), illite (3 wt%), goethite (3 wt%), anatase (3 wt%), ankerite and siderite (determined by means of the Rietveld method). Moreover, the Czech bentonite BCV is rich in amorphous phases, the content of which can be as high as 10 wt% (Červinka and Vašíček 2018). The cation exchange capacity of this bentonite is 63.7 ± 2.2 meq/100g and the major exchangeable cations consist of magnesium (42.0 ± 0.6 meq/100g) and calcium (15.1 ± 1.8 meq/100g). The liquid limit of the bentonite is 140 ± 2% and the density of the solid particles 2.76 ± 0.02 g/cm³. The total specific surface area of this bentonite (employing the ethylene glycol monoethyl ether (EGME) method) is 438 ± 6 m²/g.

The saturated hydraulic conductivity of compacted Czech bentonite BCV samples decreases exponentially with the dry density (see Figure 1-21). For a dry density of 1.6 g/cm³, the saturated hydraulic conductivity of the bentonite is approximately 1.14 × 10⁻¹³ m/s at room temperature with deionised water as the percolating fluid.

The swelling pressure of compacted samples is also related exponentially to the dry density of the Czech bentonite BCV (see Figure 1-21). The material develops a swelling pressure of around 8 MPa when compacted at a dry density of 1.6 g/cm³ and saturated with deionised water at room temperature.
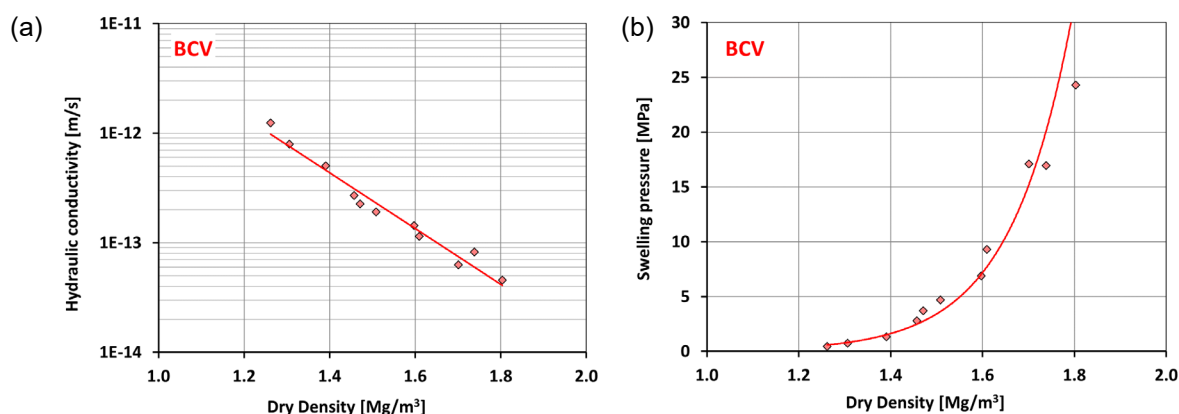
Figure 1-21 – (a) saturated hydraulic conductivity and (b) swelling pressure in relation to dry density – Czech bentonite BCV (Hausmannová et al. 2018).

EURAD (Deliverable n° 6.1) – Initial State of the Art on Gas Transport in Clayey Materials
Dissemination level: PU
Date of issue of this report: **17/11/2021**

Page 41

1.5.4.4 Sand/bentonite (S/B) mixtures

Different kinds of sand/bentonite (S/B) mixtures are studied for mainly two reasons: adding sand to bentonite tends (i) improve the mechanical stability and thermal conductivity and (ii) increase the capacity of gas transport without a large reduction of water permeability or swelling pressure.

In the Swiss concept of deep geological disposal, S/B mixtures at low bentonite content (i.e. 20 to 30% of bentonite) are considered as appropriate sealing and backfilling materials for the underground structures, forming the main component of the so-called 'engineered gas transport system' (EGTS) of the L/ILW repository (Nagra 2008). The EGTS is aimed at increasing the gas transport capacity of the backfilled underground structures without compromising the radionuclide retention capacity of the EBS.

Understanding and quantifying the hydro-mechanical and -chemical (HMC) phenomena governing water and gas transport through an 80/20 S/B mixture is crucial for ensuring the safety of the L/ILW repository at both short- and long-term. The need for in-depth investigations of the gas transport capacity of S/B seal sections gave rise to a comprehensive research programme dedicated to experimental characterisation of S/B mixtures at macroscopic and microscopic level, following a well-established soil-mechanical workflow (Manca 2016).

The investigated material is a mixture of grey quartz sand and MX-80 bentonite in proportion 80/20 in dry mass. The mineralogical composition and the geotechnical characteristics of the bentonite are given in Section 1.5.4.1. The quartz sand was selected due to its high chemical and mechanical stability. The specific gravity of the pure quartz sand is 2.65. The mineralogical composition comprises mainly silicon dioxide (97.40%), alumina (1.35%), potassium and sodium oxides (0.8%), small amounts of titanium dioxide, periclase and lime. The presence of sand in mixtures prepared with a low bentonite content provides a load support enhancing the macroscopic mechanical stability (Kenney et al. 1992). It also reduces the shrinkage of the mixture when the water content decreases and thus reduces the risk of cracking (Dixon et al. 1985). This risk is much more present in a pure bentonite (Graham J. et al. 2002).

The index tests of the 80/20 S/B mixture by Manca (2016) revealed strong dependence of the index properties on the water composition. The liquid limit and the plastic limit were determined with four different water types (deionised water, synthetic pore water, 1-molar NaCl solution, 4-molar NaCl solution). The liquid limit has a maximum value of 89% with distilled water and it decreases with the increasing of the osmotic suction of water implemented for testing (Figure 1-22a) whereas the plastic limit is only slightly altered by the composition of the pore water (Figure 1-22b). The obtained values of the Atterberg limits for the different pore waters are indicated in the plasticity chart in Figure 1-22c. Substantial reduction of the mixture activity is observed with increasing pore water salinity, providing an initial indication of the swelling capacity reduction of the bentonite fraction. This result is explained with the reduction of the swelling capacity of the smectite minerals at the particle level. The relatively low values of liquid and plastic limits as compared to those of the pure bentonite (see Section 1.5.4.1) are attributed to the presence of the sand grains in the mixture.

EURAD (Deliverable n° 6.1) – Initial State of the Art on Gas Transport in Clayey Materials
Dissemination level: PU
Date of issue of this report: **17/11/2021**

Page 42
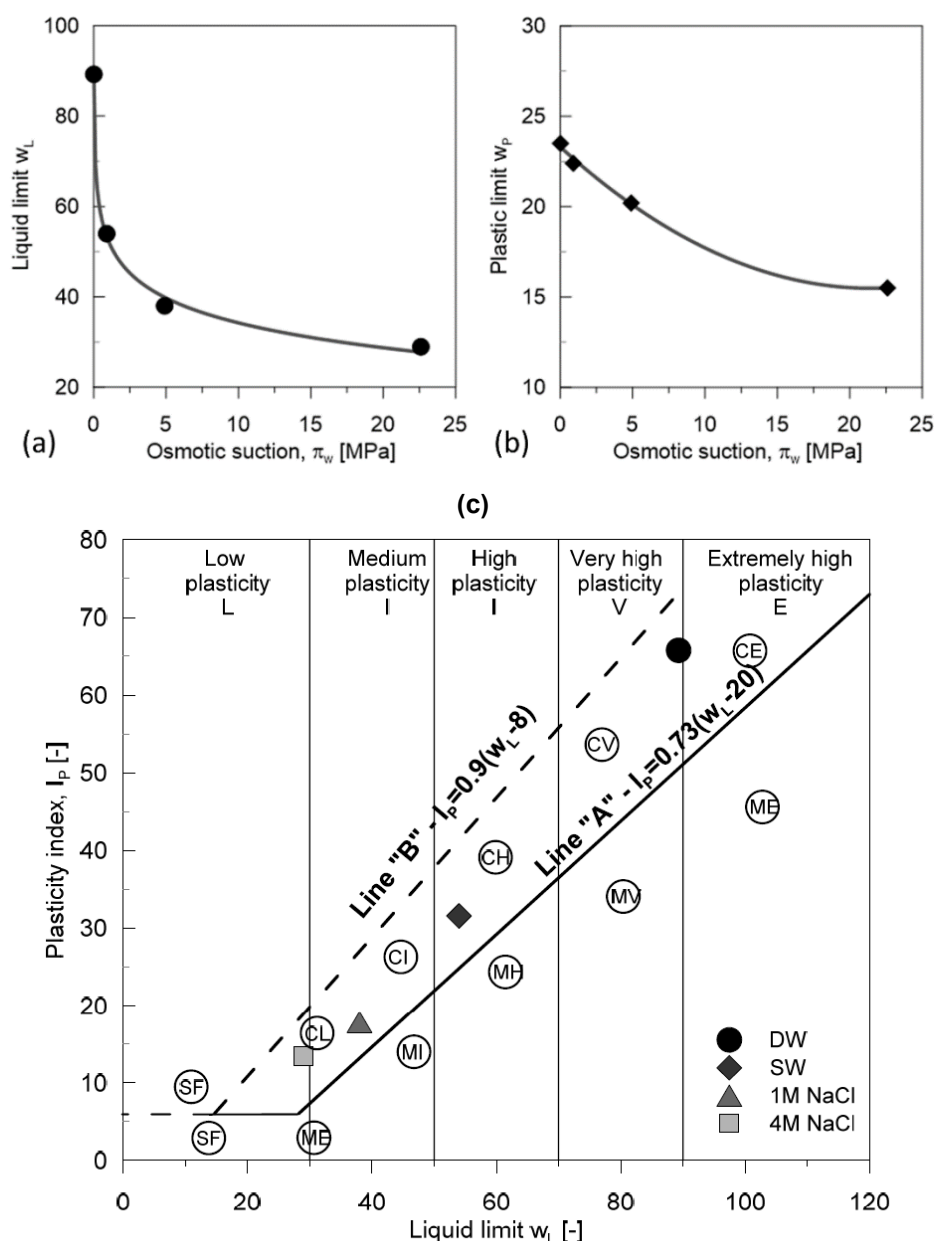
Figure 1-22 – Dependence of the Atterberg limits of 80/20 sand/bentonite mixture on water composition (modified after Manca 2016): (a) decrease of liquid limit and (b) decrease of plastic limit with the increase of osmotic suction of the pore water; (c) plasticity chart. The four different water types are deionised water (DW), synthetic pore water (SW), 1-molar NaCl solution and 4-molar NaCl solution.

Further index properties reported by Manca (2016) are the specific area of 105 m^2/g and the specific gravity of 2.67. The grain size distributions of the tested materials are presented in Figure 1-23.

EURAD (Deliverable n° 6.1) – Initial State of the Art on Gas Transport in Clayey Materials
Dissemination level: PU
Date of issue of this report: **17/11/2021**
Page 43
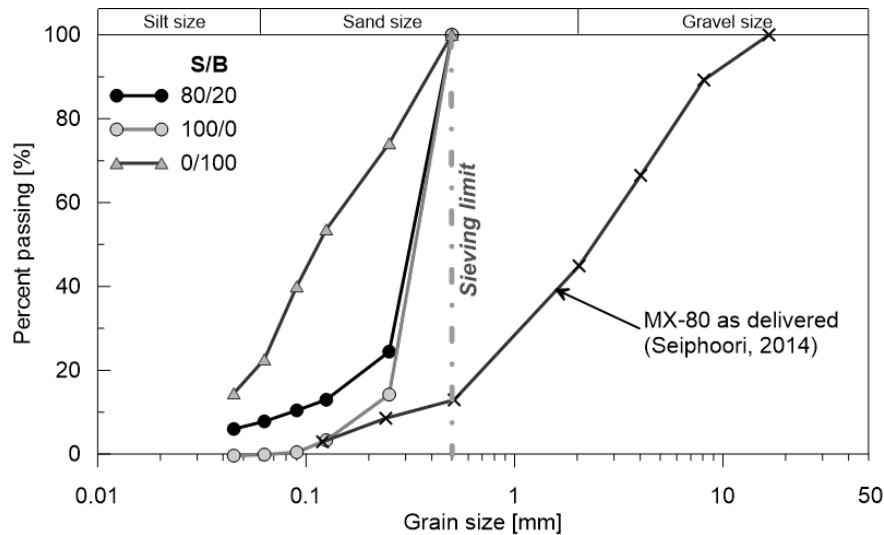
Figure 1-23 – Apparent grains size distribution of the tested 80/20 sand/bentonite mixture and its two solid components (pure sand and pure bentonite, after sieving to remove the coarse grains).

Dynamic compaction tests were performed to determine the maximum achievable compaction density that can be obtained for a specific compaction energy. The results of the test are presented in Figure 1-24a. An optimum water content of 0.12 and a corresponding maximum dry density of 1.88 g/cm^3 were determined for a compaction energy of 3.4 J/cm^3. These results are referring to a S/B mixture wetted with distilled water. The volumetric behaviour of the material was tested in an oedometer cell. The compression index (C_c) at the as-compacted state is equal to 0.45 and the swelling index (C_s) is equal to 0.01 (Figure 1-24b).

(a)

(b)
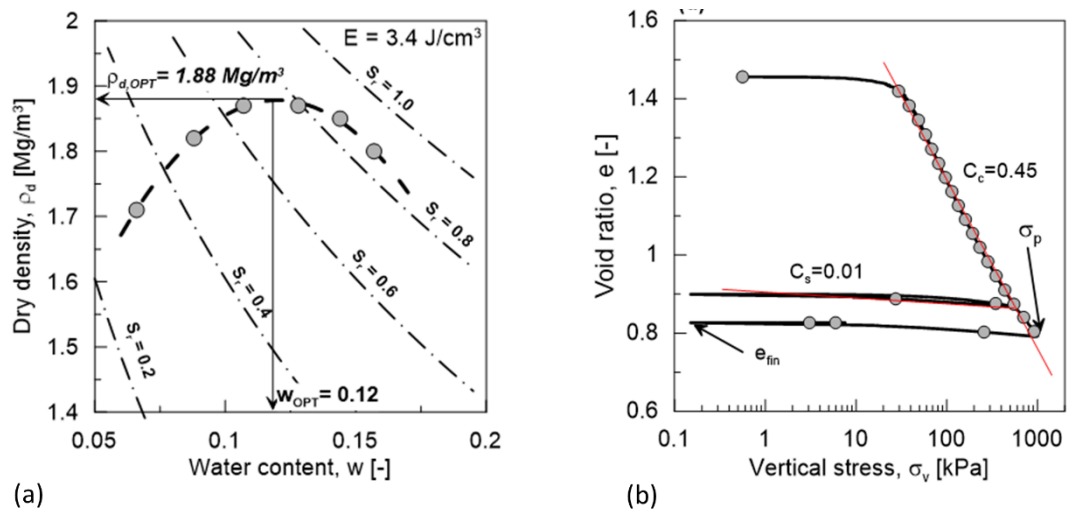
Figure 1-24 – Volumetric behaviour of the 80/20 sand/bentonite mixture: (a) dynamic compaction test for determining the optimum compaction density, with isolines for saturation degrees (b) determination of compression and swelling indexes in oedometric configuration.

Free and constrained swelling tests were conducted in a thick-walled oedometric cell, using S/B mixtures with dry densities between 1 300 and 1 800 kg/m^3. The tests were performed with deionised water. The swelling strains under free swelling conditions ranged between 0.4 and 0.8. The swelling pressure under constant volume conditions exhibit a distinct spread between 35 kPa (ρ_d = 1 300 kg/m^3) and 205 kPa (ρ_d = 1 800 kg/m^3). The transients of swelling strain and swelling pressure are shown in Figure 1-25.

EURAD (Deliverable n° 6.1) – Initial State of the Art on Gas Transport in Clayey Materials
Dissemination level: PU
Date of issue of this report: **17/11/2021**
Page 44
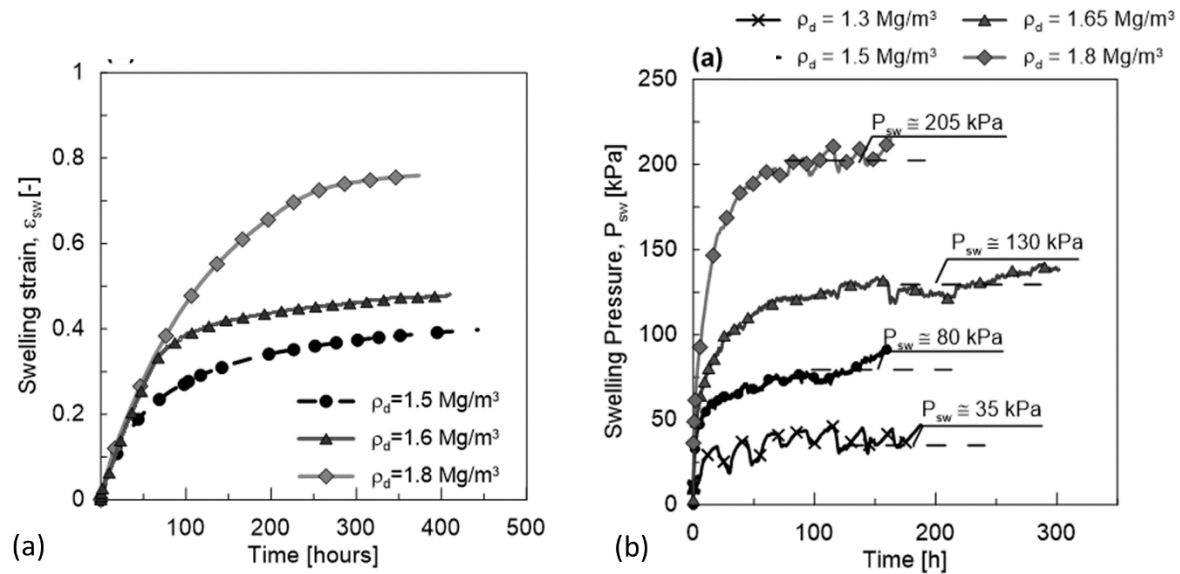
Figure 1-25 – Swelling behaviour of the 80/20 sand/bentonite mixture with dry densities between 1 300 and 1 800 kg/m³: (a) free swelling strains under oedometric conditions, (b) swelling pressure under constant volume conditions.

In the French concept of deep geological disposal, S/B mixtures with different bentonite contents have been considered as materials that can be used for gallery sealing. The effect of sand content on the main properties such as water permeability or swelling pressure have been explored. Figure 1-26 shows a set of measures that can be used to define the most suitable mixture according to the expected specifications. Based on this type of analysis, a mixture (60% sand / 40% bentonite) has been selected for a large scale experiment – NSC – performed in Meuse/Haute-Marne URL (de la Vaissière et al. 2014a) and is being considered for use in underground repository seals. Further investigations have been made and especially the consequences of water chemical composition used for hydrating on the hydro-mechanical properties when decreasing the bentonite content.
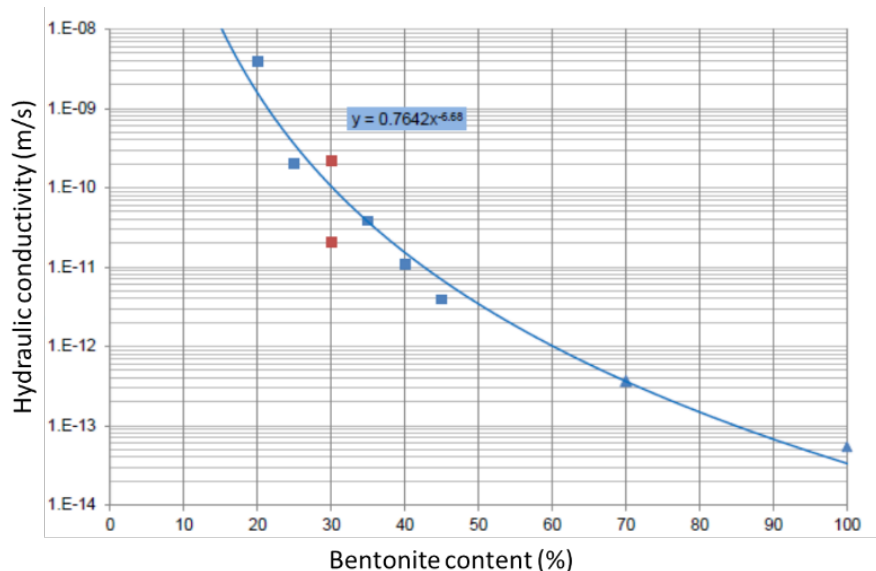
Figure 1-26 – Hydraulic conductivity for sand/bentonite mixtures compacted at 1.3 g/cm³.

EURAD (Deliverable n° 6.1) – Initial State of the Art on Gas Transport in Clayey Materials
Dissemination level: PU
Date of issue of this report: **17/11/2021**

Page 45

1.5.5 Synthesis: compared characteristics of the studied clayey materials

In brief, Tables 1-9 and 1-10 provide a few basic properties and mineralogical composition of the 3 host formations and the 3 bentonites studied in the WP GAS. The comparison between clayey host formations already highlights some differences between poorly indurated clays like the Boom Clay and indurated clays like the Callovo-Oxfordian claystone and the Opalinus Clay. These differences may affect the characteristics of gas transport in these different materials (see next chapters).

Table 1-9 – A few basic properties and mineralogical composition of the 3 host formations studied in the WP GAS.

Property / composition [unit]	Host formation		
	Boom Clay	**COx**	**Opalinus Clay**
Dry density [kg/m^3]	1 490–1 648	2 290–2 340	2 330–2 430
Grain density [kg/m^3]	2 682	2 710	2 710
Porosity [%]	35–40	18	11–16
Water content [wt%]	20–30	6.2–8.0	4.5–6.4
Plastic limit [%]	13–29	15–25	10–30
Liquid limit [%]	55–80	30–40	30–50
Over-consolidation ratio [–]	2.4		1.5–5
Clay mineral content [wt%]	up to 60	25–55	40–75
Quartz content [wt%]	19–71	15–30	10–30
Hydraulic conductivity [m/s]	vertical: 1.7×10^{-12} horizontal: 4.4×10^{-12}	vertical: 1×10^{-13} horizontal: 3×10^{-13}	10^{-12}–10^{-14}

Table 1-10 – A few basic properties and mineralogical composition of the 3 bentonites studied in the WP GAS.

Property / composition [unit]	Granular Wyoming sodium bentonite (MX-80)	Czech bentonite BCV	FEBEX bentonite
Dry density [kg/m^3]	1 450 (granular) 1 800 (blocks)		1 600
Grain density [kg/m^3]	2 740–2 800	2 760 ± 20	2 700 ± 40
Porosity [%]	45–50 (granular) 35 (blocks)		
Water content [wt%]	20–30		13.7 ± 1.3
Plastic limit [%]	65		53 ± 3
Liquid limit [%]	420	140 ± 2%	102 ± 4
Clay mineral content [wt%]	80–85 montmorillonite 0.1–0.8 illite	58–72 montmorillonite 4.1 kaolinite 2.7 illite	92 ± 3 smectite
Quartz content [wt%]	2.5–4.0	10.8	2 ± 1
Hydraulic conductivity [m/s]	1×10^{-13}–2×10^{-12} *	~1.14×10^{-13} **	~5×10^{-14} **

* depending on dry density, compaction, hydration, etc.
** for a dry density of 1.6 g/cm^3, saturated hydraulic conductivity at room temperature with deionised water as the percolating fluid

EURAD (Deliverable n° 6.1) – Initial State of the Art on Gas Transport in Clayey Materials
Dissemination level: PU
Date of issue of this report: **17/11/2021**

Page 46

2.   Gas transport processes

This chapter presents and discusses key results from previous experimental programmes on the transport of gas in the clayey materials of interest in this WP GAS of EURAD and insights gained alongside these experiments through modelling activities. Although couplings with the mechanical behaviour of the porous media are briefly discussed, this chapter essentially presents gas transport 'from the perspective of the gas'. Mostly laboratory work, multiphase flow concept and models are discussed in this chapter. Models are sometimes extended through representation of mechanical couplings via stress/strain dependent parameters. Gas transport modes that depend on a strong mechanical coupling between the fluid and the solid phase, such as pathway dilation and the creation of discrete, additional pathways through the material, are mainly discussed in Chapter 3. Based on literature review, relevant experimentations are described and the key findings on each gas transport process in and around a GDF are summarised. Particular attention is given to shared understanding and knowledge gaps for the characterisation of each gas transport process.

It is useful to keep in mind the context in which the knowledge on gas transport will be used. To that aim, this context – what end-users are interested in and what they need are – is briefly recalled hereafter. End-users include the waste management organisations (WMOs) in charge of the development and implementation of GDFs, the regulatory bodies and their technical support organisations (TSOs). Beyond these organisations, the knowledge on gas can be of interest to third parties involved in the stepwise decisional process towards implementation of a GDF and possibly industrial actors from unrelated sectors[7].

2.1   Interests and needs of end-users in the context of geological disposal

In a deep geological repository, gases are generated as a result of anaerobic corrosion of metals (which produces H_2), microbial and chemical degradation of organic matter (which may produce gaseous compounds CO_2, CH_4, potentially incorporating ^{14}C and other volatile radionuclides) and radiolysis of water (which principally produces H_2). If the production rate of gas is higher than what can be removed by dissolution and diffusion, a free gas phase will form and accumulate, building up gas pressures, which will eventually lead to gas release along the backfilled underground structures and/or through the host rock. Figure 2-1 shows a generic and schematic representation of potential gas paths along the backfilled repository structures and through the host rock.

---

[7] Technology transfer can go both ways. For instance, knowledge originating from the oil and gas industry can sometimes provide further evidence on gas transport mechanisms and their consequences in geological media. However, the transposition of this knowledge to the typical setting of a GDF should be done with care.

EURAD (Deliverable n° 6.1) – Initial State of the Art on Gas Transport in Clayey Materials
Dissemination level: PU
Date of issue of this report: 17/11/2021

Page 47
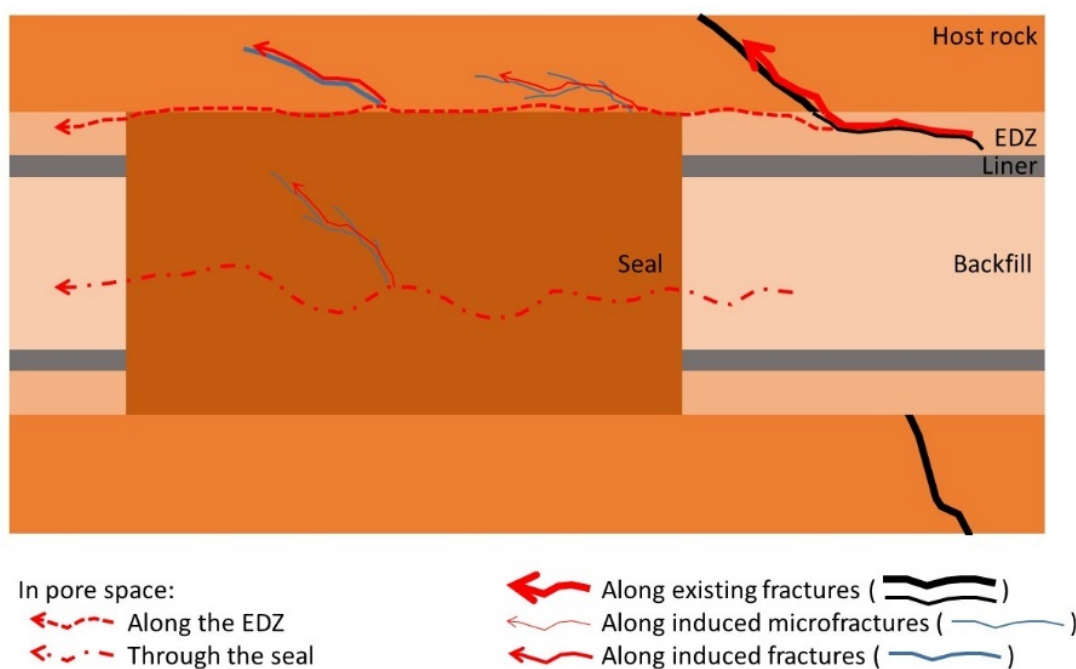
Figure 2-1 – Generic and schematic representation of potential gas paths along the backfilled repository structures and through the host rock (not linked to a specific repository design).

From a performance assessment (PA) perspective, the following gas-related impacts need to be addressed:

- The **expulsion of radionuclides dissolved in the pore water** due to the build-up of gas overpressures acting as driving force for displacing contaminated water.

- The **rapid release of volatile radionuclides** along the unsaturated engineered barrier system and through discrete pathways in the host rock.

- The partial desaturation of the multi-barrier system, giving rise to **modifications of the effective flow and transport properties of the barriers** (dependence of diffusion coefficient and water permeability on the water saturation of the porous medium). Conversely, gas production can retard the saturation of engineered barrier components.

- Beyond a certain gas pressure that depends on the stress state, on the strength of the clayey material and also on the rate of gas pressure increase and the presence of local heterogeneities, generation of new pathways by modifications of the host rock structures, either by **microfracturing** or eventually by **macrofracturing** (see also Section 3.1). The loss of mechanical integrity may result in a reduced barrier performance leading to enhanced release of dissolved/volatile radionuclides.

- Conversely, the development and fate of gas pathways along the seals and access structures such as shafts and ramps are of interest as these pathways may eventually reach aquifers above the repository. Pathway closure and **sealing processes** after gas release are discussed in Chapter 3.

The issues to be addressed in a safety case depend on the repository concepts developed by each waste management organisation (WMO) in the specific context of its national programme. While these contexts may significantly differ (in programme stage, repository concept, regulatory context, wastes to be disposed of, etc.), an area of shared interests and needs in all programmes is the fundamentals of gas transport in saturated clayey materials to adequately understand the relevant phenomena and

EURAD (Deliverable n° 6.1) – Initial State of the Art on Gas Transport in Clayey Materials
Dissemination level: PU
Date of issue of this report: 17/11/2021

Page 48

processes so that gas transport can be appropriately represented or bound in performance and safety assessments. Further aspects of common interest are the characterisation of gas-related properties and solute/gas transport behaviour of the partially saturated clay barriers before and after gas invasion (hysteresis). Gas retention and conversion[8] processes are also of interest. Table 2-1 displays a survey of relevant needs of national programmes for evaluating how gas can be transported throughout a disposal system. As presented in that table, gas transport through the components of a disposal system is usually considered from a Darcian perspective, i.e. via two-phase flow, possibly extended through the use of stress/stain dependent or 'effective' parameters to account for mechanical aspects such as pathway dilation.

Table 2-1 – Survey of gas-induced impacts on repository performance and relevant needs of the end-users in the national programmes.

Barrier component	Category of gas-induced impacts	Relevant needs with respect to the evaluation of gas transport at repository scale
Host rock	Expulsion of radio-nuclides dissolved in the pore water	- Threshold gradient for linear pore water flow and validity of the generalised Darcy law in partially saturated rock
	Effective flow and transport behaviour in unsaturated host rock	- Two-phase flow properties of the host rock along drying/wetting paths (capillary pressure-saturation relationship, relative permeabilities to water/gas, residual water/gas saturation) - Dependence of effective diffusion coefficient of gaseous components on water saturation
	Enhanced expulsion of dissolved/volatile radio-nuclides associated with induced fracturing	- Induced transport behaviour, for gas and water, in the generated discontinuities including dilation pathways
EDZ	Rapid release of volatile radionuclides	- Gas transport regimes in invaded pores/discontinuities/fault zones (capillary- vs. viscous fingering)
	Effective flow and transport behaviour of unsaturated EDZ	- Gas transport regimes in invaded discontinuities/fault zones (capillary- vs. viscous fingering) - Homogenised two-phase flow properties of the EDZ along drying/wetting paths (capillary pressure-saturation relationship, relative permeabilities to water/gas, residual water/gas saturation)
	Enhanced expulsion of dissolved/volatile radio-nuclides associated with induced fracturing	- Gas transport regimes in re-activated EDZ fractures (capillary- vs. viscous fingering) - Homogenisation of gas invasion front along the gas pathway (homogenised two-phase flow properties)
Bentonite seals	Effective flow and transport behaviour of unsaturated seals	- Two-phase flow properties of the EDZ along drying/wetting paths (capillary pressure-saturation relationship, relative permeabilities to water/gas, residual water/gas saturation) in contact with the swelling material of the seal core (i.e. recompression of the EDZ) - Two-phase flow properties of the swelling clayey material (i.e. bentonite possibly mixed with other porous media)
	Gas transport in initially saturated seals	- Two-phase flow initiation (displacement flow) - Dilation pathways initiation

---

[8] Experimental characterisation and modelling of conversion processes, e.g. conversion of hydrogen to methane by microbes, falls outside the scope of the WP GAS of EURAD and are not discussed in detail in this state-of-the-art report. The interested reader can find more information over microbial processes in the deliverables of the MIND EC project (https://www.mind15.eu/).

EURAD (Deliverable n° 6.1) – Initial State of the Art on Gas Transport in Clayey Materials
Dissemination level: PU
Date of issue of this report: 17/11/2021

Page 49

Barrier component	Category of gas-induced impacts	Relevant needs with respect to the evaluation of gas transport at repository scale
Bentonite buffer	Effective flow and transport behaviour of unsaturated buffer	- Two-phase flow properties of the EDZ along drying/wetting paths (capillary pressure-saturation relationship, relative permeabilities to water/gas, residual water/gas saturation) in contact with the swelling clay core of the buffer (i.e. recompression of the EDZ) - Two-phase flow properties of the swelling clayey material (i.e. bentonite possibly mixed with other porous media)
	Gas transport in initially saturated seals	- Two-phase flow initiation - Dilation pathways initiation

![eurad logo] European Joint Programme on Radioactive Waste Management

EURAD (Deliverable n° 6.1) – Initial State of the Art on Gas Transport in Clayey Materials
Dissemination level: PU
Date of issue of this report: **17/11/2021**

Page 50

2.2 Diffusion of dissolved gas through clayey materials

2.2.1 Diffusion of dissolved gas through low-permeability materials close to saturation: processes and terminology

Gas can dissolve in the pore water of (partially) saturated clayey materials. The **process of dissolution** of a gas in a liquid is described by Henry's law which states that the amount of gas that dissolves in a volume of liquid is directly proportional to the partial pressure p_i [Pa] of the gas in equilibrium with the liquid: $p_i = H \, C_{i\_liquid}$, where C_{i_liquid} [mol/m³] is the concentration of the dissolved gas in the liquid and H [Pa.m³.mol⁻¹] is the coefficient of Henry for that gas. Henry's coefficient is temperature-dependent. At high pressures, the relationship between the gas partial pressure and the concentration of the dissolved gas is no longer linear (Prausnitz et al. 1999). Henry's coefficient is also dependent on salinity. In general, the solubility of a gas decreases with increasing salinity ('salting out'). Users should be aware that there are several forms of Henry's law, written as a function of the mole fraction of the solute, its molar concentration or its molality. One should hence be careful to note which form of the Henry's law equation is used.

The underlying process behind **diffusion** is the random thermal motion of particles – here, gas molecules dissolved in clay pore water – also known as the Brownian motion. The random motion of particles results in increasing entropy (Grathwohl 1998). Diffusion results in a net movement of dissolved gas from regions of high concentration to regions of low concentration, in absence of bulk transport. According to Fick's laws, the diffusion flux is proportional to the negative gradient of concentrations. The diffusion coefficient (D) is the proportionality constant between flux and concentration gradient and is defined as the ratio of flux density to the negative of the concentration gradient in the direction of diffusion. It is usually expressed in the units $m^2 \, s^{-1}$.

The processes related to diffusion are described within the literature using many terms and definitions. All terms that are used in this work are clarified in the next section and an overview is given in Table 2-2.

Table 2-2 – Overview of diffusion and other parameters.

Symbol	Parameter	Unit	Formula
D_0	Diffusion coefficient in free water	m²/s	
D_{app}	Apparent diffusion coefficient	m²/s	$D_{app} = D_{eff}/\eta R$
D_{eff}	Effective diffusion coefficient	m²/s	$D_{eff} = \eta R \, D_{app}$
D_p	Pore diffusion coefficient	m²/s	$D_p = D_{app} \, R = D_{eff}/\eta$
ηR	Capacity factor	–	$\eta R = C_b/C$
G	Geometric factor or G-factor	–	$G = \eta \, D_0/D_{eff} = \tau/\delta$
F	Formation factor	–	$F = \dfrac{G}{\eta} = \dfrac{D_0}{D_{eff}}$
τ	Tortuosity	–	
δ	Constrictivity	–	
ϕ	Accessible porosity	–	
ϕ_{tot}	Total porosity	–	
AF	Anisotropy factor	–	$AF = D_{eff,//} / D_{eff,\perp}$
K	Hydraulic conductivity	m/s	

EURAD (Deliverable n° 6.1) – Initial State of the Art on Gas Transport in Clayey Materials
Dissemination level: PU
Date of issue of this report: **17/11/2021**

Page 51

In general, two transport parameters can be obtained from diffusion experiments: the apparent diffusion coefficient D_{app} [m²/s] and the capacity factor ϕR, being the product of the accessible porosity ϕ (dimensionless) and the retardation factor R (dimensionless) which accounts for retention of the diffusing species by chemo-physical interactions with the solid phase, e.g. gas sorption processes. The capacity factor is the ratio of the tracer concentration C_b [mol/L] in the bulk sample and the corresponding tracer concentration C [mol/L] in the pore fluid (solution): $\phi R = C_b/C$.

From these two basic parameters, one can calculate the effective diffusion coefficient D_{eff} [m²/s]:

$$D_{eff} = \phi\, R\, D_{app} \tag{2-1}$$

and, assuming the accessible porosity equals the total porosity η_{tot}, the pore diffusion coefficient D_p [m²/s]:

$$D_p = R\, D_{app} \tag{2-2}$$

For unretarded species without ion exclusion (e.g. HTO), the retardation factor is generally put equal to one ($R = 1$), leading to $D_{app} = D_p$ and a capacity factor equal to the total porosity η_{tot}, which is measured independently.

Chemo-physical interactions between the studied gases (noble gases, light hydrocarbons and H_2) and the discussed with the studied material, which would lead to $R > 1$ have not yet been studied in detail under relevant disposal conditions (saturation, pressure and temperature) and are therefore considered as a knowledge gap. Based on the observations of (Jacops et al. 2017a; Jacops et al. 2016; Jacops et al. 2015), no interaction was considered for the gases of interest[9] and the retardation factor was set one ($R = 1$).

The diffusion coefficient of dissolved gas in bulk water or bulk aqueous solution is denoted as D_0. Experimental values for D_0 are available in the literature, e.g. Boudreau (1996).

The geometric factor G (dimensionless) relates the diffusion coefficient in a porous medium to the corresponding diffusion coefficient D_0 [m²/s] in water and is defined by

$$G = \frac{D_0}{D_p} = \frac{D_0}{R\, D_{app}} = \frac{\phi\, D_0}{D_{eff}} \tag{2-3}$$

It is often split in two factors: tortuosity τ and constrictivity δ:

$$G = \frac{\tau}{\delta} \tag{2-4}$$

In this equation, used by Grathwohl (1998) and by Jacops et al. (2017b), tortuosity (dimensionless) is defined as the square of the ratio of the effective path length (along the path) of a diffusing component to the shortest distance (end-to-end straight line distance) of that path. Constrictivity (dimensionless) takes into account the reduction of the effective diffusion coefficient due to a drag by the pore wall, and depends on the ratio of the solute diameter to the pore diameter. In case of large pores, the constrictivity

---

[9] Should CO_2 gas be produced in the repository, that gas will interact with EBS (carbonation of cement-based materials) and the host rock (presence of carbonates).

EURAD (Deliverable n° 6.1) – Initial State of the Art on Gas Transport in Clayey Materials
Dissemination level: PU
Date of issue of this report: **17/11/2021**

Page 52

factor δ is one. Constrictivity becomes important (much smaller than one) if the solute diameter has the same order of magnitude as the pore diameter.

Analogous to the electrical conductivity of water-saturated rocks, the diffusion coefficient in free water and the effective diffusion coefficient can be used to define a 'formation factor' *F* (dimensionless), defined by:

$$F = \frac{G}{\phi} = \frac{D_0}{D_{eff}}$$

(2-5)

Three types of methods are described in literature to determine gas diffusion coefficients: (i) outgassing of clay samples or from boreholes, (ii) calculating diffusion coefficients from natural tracer profiles and (iii) in/through-diffusion experiments.

The first method consists of the outgassing of clay samples or from boreholes, taking advantage of the natural presence of dissolved gases (e.g. helium from alpha decay of naturally-occurring radioactive elements such as uranium and thorium in the clay). In the first case, freshly drilled clay samples are immediately transferred into vacuum containers and the evolution of the *gas releases* as a function of time from the sample is measured (Bigler et al. 2005). For boreholes, gas released by the formation into the borehole as a function of time is measured (Gómez-Hernández 2000). Based on these measurements, the diffusion coefficient is determined. The main disadvantage of core outgassing is the preservation of the cores: sample treatment after coring has to be done very carefully because cores will degas immediately after sampling, or they can take up gas from the atmosphere. Therefore, these experimental results always have to be interpreted with care. Also for boreholes, outgassing starts immediately upon drilling.

The second method is calculating the diffusion coefficient of gases naturally present in the clay (e.g. He, Ar and CH$_4$) based on the measurement of vertical concentration profile of these natural tracers, in combination with assumptions about their production rate and environmental boundary conditions. The *total gas concentration* at different depths is obtained by outgassing (Rubel et al. 2002; Bensenouci et al. 2011). Calculating diffusion coefficients for naturally present gases, based on their concentration profile is an interesting method, but it has two major disadvantages. Firstly, the method is only applicable for natural tracers and cannot be used for direct determination of the diffusion coefficient for e.g. hydrogen. The second disadvantage is that, similar to the method of the outgassing of cores, experimental results have to be interpreted with care. The uncertainty on the initial state of the system and on the in situ boundary conditions increases the uncertainty of the obtained diffusion coefficient. Mazurek et al. (2011) stated that the core outgassing of noble gases requires sophisticated equipment and there is a possibility of gas leakage at several stages.

The third method to determine diffusion coefficients for gases is by performing laboratory experiments based on the in- or through-diffusion technique (Krooss and Schaefer 1987; Rebour et al. 1997). In through-diffusion experiments, the clay sample is placed between two water reservoirs. The water of one of these reservoirs, connected to the inlet of the diffusion cell, initially contains a high concentration of dissolved gas. The other reservoir, the low-concentration reservoir connected to the outlet of the diffusion cell, does not initially contain dissolved gas. By measuring the time evolution of the dissolved gas concentration in the low-concentration and/or the high-concentration reservoir, the diffusion parameters can be estimated by fitting to the experimental data the solution of a transport model based on Fick's law with the appropriate boundary conditions and formalisms. In in-diffusion experiments, clay is placed in contact with a reservoir containing water with a known initial concentration of dissolved gas. It can be considered as the first stage of a through-diffusion experiment; only the decrease of the dissolved gas concentration in the high-concentration reservoir is used to calculate the diffusion parameters. We consider the in- and through-diffusion technique to be the most reliable, provided that the set-up is well designed, and sample conditions are still representative. Alternatively, through- or in-

EURAD (Deliverable n° 6.1) – Initial State of the Art on Gas Transport in Clayey Materials
Dissemination level: PU
Date of issue of this report: 17/11/2021

Page 53

diffusion experiment can be performed by directly exposing the sample to gas instead of water containing dissolved gas. In that case, dissolution/exsolution of gas occur at the sample boundaries. One has to check, however, that no significant desiccation of the sample occurs as it could affect the measurement of the diffusion coefficient.

2.2.2   State of knowledge for Boom Clay

The first set of gas diffusion parameters for hydrogen in Boom Clay were obtained from the MEGAS project (Modelling and Experiments on Gas Migration in Repository Host Rocks) (Volckaert et al. 1995). During this project, two types of diffusion experiments with H_2 (pure gas phase) were performed: in-diffusion experiments and through-diffusion experiments. The in-diffusion experiments suffered from H_2 leakages, and the through-diffusion experiments were disturbed by CO_2-outgassing of the clay samples. These experimental problems led to an uncertainty of up to two orders of magnitude (diffusion coefficient expressed as D_{app}) (4.2×10^{-12} m²/s $< D_{app} < 1.6 \times 10^{-10}$ m²/s). Re-evaluation of these MEGAS experiments by Aertsens (2009) showed that the applied technique did indeed not allow a more precise determination of the diffusion coefficient. The lumped parameter $\eta R D_{app}$ could be fitted but due to different experimental problems like outgassing of the clay, occurrence of a H_2 leak and a too short duration of the experiment compared to the length of the samples, only estimations of D_{app} could be made. Finally, this re-evaluation led to an estimated D_{app} between 5×10^{-12} m²/s and 4×10^{-10} m²/s (Aertsens 2009).

Experimental methodology

SCK CEN (Belgian Nuclear Research Centre), being supported by ONDRAF/NIRAS, developed a new technique to measure diffusion coefficients of dissolved gases in Boom Clay with high precision and accuracy. The basis is the double through-diffusion technique, using water dissolved gases (Figure 2-2).

First, the sample is embedded in a constant volume cell. Next, it is saturated with water and hydraulic conductivity is obtained from Darcy's law by application of constant water pressure difference and measurement of the flow rate (Wemaere et al. 2008). The sample is considered to be saturated when water outflow and inflow rates are in equilibrium. Then, both sides of a test core are connected to a water vessel filled with circa 500 mL oxygen-free synthetic Boom Clay pore water (0.014 M NaHCO₃, (De Craen et al. 2004)) and pressurised with a specific gas (circa 500 mL gas at 1 MPa). Both vessels are filled with a different gas, but the total pressure is the same. In this way, no advective flux can occur and the clay sample remains fully water saturated. According to Henry's law, equilibrium is obtained between the free gas in the gas phase and the dissolved gas in the water. The water at both sides is then circulated over the filters, which are in contact with the clay sample, allowing the dissolved gases to diffuse through the clay sample, towards the reservoir on the opposing side. The change in gas composition in both reservoirs is measured as a function of time by gas chromatography. Sampling of the gas phase is performed on a regular basis (generally once per week) until 10 data points are

EURAD (Deliverable n° 6.1) – Initial State of the Art on Gas Transport in Clayey Materials
Dissemination level: PU
Date of issue of this report: **17/11/2021**   Page 54

obtained in the regime of approximately constant outlet flux of the diffusion process. The experiment is performed in a temperature-controlled room (21 ± 2°C).
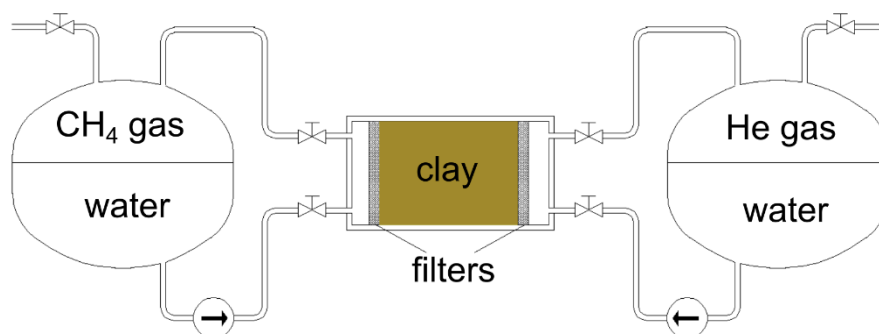
Figure 2-2 – Schematic overview of the double through-diffusion technique set-up developed by SCK CEN to measure diffusion of dissolved gases.

Experiments with hydrogen often suffer from experimental problems such as leakage and microbial activity. In order to obtain reliable diffusion coefficients for hydrogen in Boom Clay, a dedicated protocol which combines different sterilisation techniques such as heat sterilisation, gamma irradiation, gas filtration and the use of a specific inhibitor has been designed by Jacops et al. (2015).

Determination of diffusion coefficients

A through-diffusion experiment allows, based on the curve of the flux, fitting both the apparent diffusion coefficient D_{app} and the capacity factor ϕR, which are in general both unknown. Besides, also the initial concentration, which is known but prone to measurement errors, is fitted and this is described as the 3-parameter fit. An alternative fitting strategy is also possible: assuming $R = 1$ (Jacops et al. 2017a), only D_{app} is fitted and ϕR is a constant equal to ϕ_{tot} (independently measured or average value from literature). In some gas through-diffusion experiments, the (quasi) stationary state is reached very fast, leading to a nearly total correlation between the capacity factor, the apparent diffusion coefficient and the initial concentration. In this case, the one-parameter fit is the only option and only the effective diffusion coefficient can be determined. To ensure consistency, all reported diffusion coefficients for dissolved gases which are measured with the set-up of Jacops et al. (2013) are obtained from a one-parameter fit. The diffusion equation is solved by COMSOL coupled with MATLAB for optimisation. Note that porosity is calculated from the water content of each sample, which is measured at the end of the diffusion experiments.

Available diffusion coefficients

Diffusion coefficients for a series of gases (He, Ne, H_2, Ar, CH_4, Xe, C_2H_6) have been obtained for several samples of the Boom Clay and its overlying formation, called Eigenbilzen Sand (Table 2-3). Diffusion was measured parallel as well as perpendicular to the (subhorizontal) bedding planes. Results are shown in Table 2-4.

Diffusion in Boom Clay is known to be anisotropic for HTO (Aertsens et al. 2009): the diffusion in the horizontal direction is higher than in the vertical direction. The average anisotropy factor for HTO for the Boom Clay samples is 1.5, while for the Eigenbilzen Sand samples it is 1.3 (Table 2-5). For the diffusion experiments with dissolved gases, the average anisotropy factor for the Boom Clay samples is 1.5 while it is 1.1 for the Eigenbilzen Sand samples. Please note that in the calculations, only the data for the commonly measured gases (He, Ne, CH_4 and C_2H_6) were taken into account. For both dissolved gases and HTO, the anisotropy factor is lower for the clayey sand samples compared to the clayey samples. As anisotropy is mainly caused by the typical layering of clay platelets, it is expected to decrease when

EURAD (Deliverable n° 6.1) – Initial State of the Art on Gas Transport in Clayey Materials
Dissemination level: PU
Date of issue of this report: **17/11/2021**

Page 55

EURAD Deliverable 6.1 – Initial State of the Art on Gas Transport in Clayey Materials

the clay content decreases (and hence the silt/sand content increases). This is clearly observed for the samples of the Eigenbilzen Sand. Likely, the decrease starts only at a certain threshold value which is currently unknown.

Table 2-3 – Overview of the samples from the ON-Mol-1 core, their origin and orientation with respect to the bedding plane (Jacops et al. 2020b).

Core reference	Formation (member)	Orientation [2]	Depth [m TAW] [1]
35b	Eigenbilzen Sand	⊥	154.91–155.01
36a	Eigenbilzen Sand	//	155.99–156.19
37b	Eigenbilzen Sand	//	156.89–156.99
39b	Eigenbilzen Sand	⊥	158.89–158.99
48a	Boom Clay (Boeretang)	⊥	167.92–168.02
48a	Boom Clay (Boeretang)	⊥	168.02–168.12
84b	Boom Clay (Putte)	⊥	203.29–203.39
112a	Boom Clay (Putte)	⊥	231.11–231.31
127b	Boom Clay (Terhagen)	//	245.89–245.99

[1] TAW: Tweede Algemene Waterpassing (Second General Levelling).
[2] of the sample with respect to the bedding plane, respectively parallel (//) and perpendicular (⊥).

EURAD (Deliverable n° 6.1) – Initial State of the Art on Gas Transport in Clayey Materials
Dissemination level: PU
Date of issue of this report: 17/11/2021

Page 56

Table 2-4 – Measured hydraulic conductivities (K), porosities (ϕ_{tot}) and effective diffusion coefficients (D_{eff}) (including the 95% confidence interval of the fit) from samples from the ON-Mol-1 core (BC: Boom Clay samples, EZ: Eigenbilzen Sand samples).

			He	HTO	Ne	H$_2$	Ar	CH$_4$	Xe	C$_2$H$_6$
Kinetic diameter *d* [× 10⁻¹⁰ m] ****			2.58	2.75	2.79	2.97	3.42	3.82	4.06	4.42
D$_0$ [× 10⁻⁹ m] ****			7.28	2.20	4.03	5.11	2.44	1.84	1.47	1.38
Core reference (formation, orientation *)	**K [m/s]**	**ϕ_{tot} [–]**	**D_{eff} [× 10⁻¹¹ m²/s]**							
84b (BC, ⊥)	3.3 ± 0.1 × 10⁻¹²	0.40	46.8 ± 1.7	18.7 ± 0.6	17.5 ± 0.3	n.m. **	6.9 ± 0.2	9.7 ± 0.3	6.1 ± 0.2	4.6 ± 0.2
127b (BC, //)	3.4 ± 0.1 × 10⁻¹²	0.38	74.7 ± 2.0	27.8 ± 0.9	22.9 ± 1.0	51.2 ± 1.1	14.5 ± 0.2	15.5 ± 0.5	6.6 ± 0.9	5.9 ± 0.1
112a (BC, ⊥)	2.4 ± 0.1 × 10⁻¹²	0.42	45.0 ± 1.0	16.0 ± 0.5	n.m.	n.m.	n.m.	8.8 ± 0.3	n.m.	n.m.
48a (BC, ⊥)	1.5 ± 0.1 × 10⁻¹¹	0.39	50.0 ± 0.6	20.6 ± 0.6	n.m.	n.m.	n.m.	11.0 ± 0.1	n.m.	n.m.
48a (BC, ⊥)	1.0 ± 0.1 × 10⁻¹¹	0.34	51.0 ± 2.0	17.6 ± 0.9	n.m.	n.m.	n.m.	8.4 ± 0.2	n.m.	n.m.
36a (EZ, //)	4.4 ± 0.2 × 10⁻¹⁰	0.37	67.9 ± 0.7	32.1 ± 3.0	33.6 ± 1.1	n.m.	n.m.	23.1 ± 0.6	n.m.	14.3 ± 0.1
37b (EZ, //)	1.1 ± 0.3 × 10⁻¹⁰	0.40	82.3 ± 2.1	43.9 ± 2.3	40.0 ± 2.1	n.m.	n.m.	27.8 ± 0.5	n.m.	15.2 ± 0.2
35b (EZ, ⊥)	1.2 ± 0.8 × 10⁻⁸	0.41	74.5 ± 2.1	33.1 ± 1.8	35.4 ± 1.3	n.m.	n.m.	37.2 ± 0.5	n.m.	13.7 ± 0.4
39b (EZ, ⊥)	4.2 ± 0.2 × 10⁻¹⁰	0.40	58.8 ± 1.1	29.9 ± 2.7	30.6 ± 0.6	n.m.	n.m.	24.4 ± 0.5	n.m.	8.9 ± 0.3

* of the core with respect to the bedding planes, respectively parallel (//) and perpendicular (⊥).

** n.m.: not measured.

*** D$_0$ values are taken from Boudreau (1997).

**** kinetic diameters from Hirschfelder et al. (1964).

EURAD (Deliverable n° 6.1) – Initial State of the Art on Gas Transport in Clayey Materials
Dissemination level: PU
Date of issue of this report: **17/11/2021**

Page 57

Table 2-5 – Estimated diffusion coefficients for dissolved gases (He, Ne, CH$_4$ and C$_2$H$_6$) and for HTO, measured in Boom Clay and Eigenbilzen Sand samples and the corresponding anisotropy factors.

Estimated diffusion coefficient [m^2/s] and calculated anisotropy factor	Boom Clay	Eigenbilzen Sand
$D_{eff\,//}$ (He, Ne, CH$_4$, C$_2$H$_6$)	3.0×10^{-10}	3.8×10^{-10}
$D_{eff\,\perp}$ (He, Ne, CH$_4$, C$_2$H$_6$)	2.0×10^{-10}	3.4×10^{-10}
→ calculated anisotropy factor	*1.5*	*1.1*
$D_{eff\,//}$ (HTO)	2.8×10^{-10}	3.8×10^{-10}
$D_{eff\,\perp}$ (HTO)	1.9×10^{-10}	3.0×10^{-10}
→ calculated anisotropy factor	*1.5*	*1.3*

Correlation between diffusion coefficients and size of the diffusing molecule

Table 2-4 also shows for the studied gases the diffusion coefficients in free water (D_0). Plotting now in Figure 2-3 these D_0 values versus the kinetic diameters of the gases shows that D_0 decreases as a function of the kinetic diameter d.
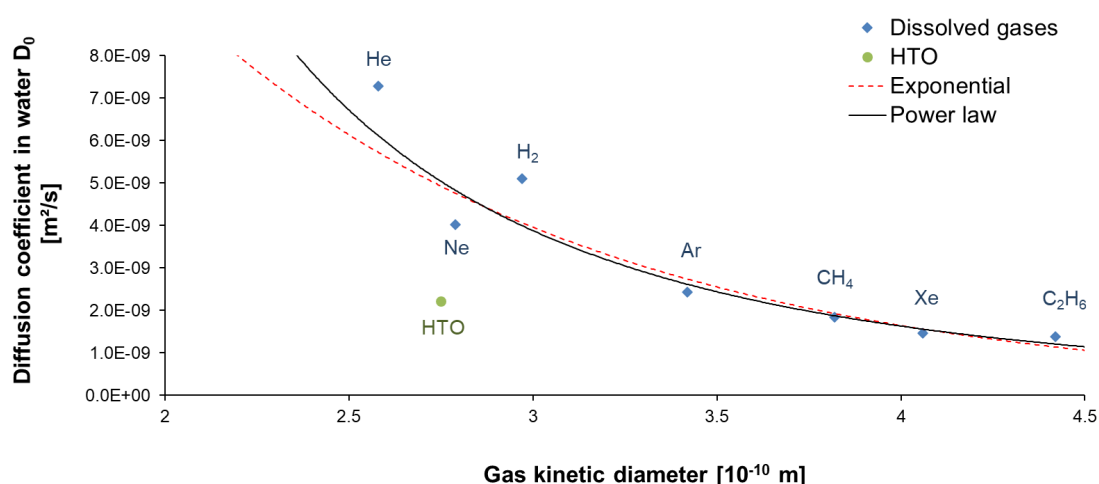
Figure 2-3 – The relation between the diffusion coefficient D_0 in free water and the kinetic diameter for dissolved gases fitted with an exponential fit and a power law fit (He: helium, Ne: neon, H$_2$: hydrogen, Ar: argon, CH$_4$: methane, Xe: xenon, C$_2$H$_6$: ethane). The HTO value is not included in the fit and given only for comparison with dissolved gases.

Empirically, this can be fitted by, for instance, an exponential equation:

$$D_0 = D_{0,exp} \times \exp(-A_{0,exp}\, d)$$

(2-6)

leading to $D_{0,exp} = 5.5 \pm 2.3 \times 10^{-8}$ m^2/s and $A_{0,exp} = 8.8 \pm 1.2 \times 10^9$ m^{-1} (see Figure 2-3) with $R^2 = 0.93$.

EURAD (Deliverable n° 6.1) – Initial State of the Art on Gas Transport in Clayey Materials
Dissemination level: PU
Date of issue of this report: **17/11/2021**

Page 58

Note that a better fit ($R^2 = 0.96$) was obtained by a power law:

$$D_0 = D_{0,pow} \times d^{-A_{0,pow}}$$ (2-7)

where the kinetic diameter (d) is expressed in 10^{-10} m, $D_{0pow} = 1.1 \pm 0.45 \times 10^{-7}$ m^2/s and $A_{0,pow} = 3.0 \pm 0.4$.

Due to its polar nature, water (HTO) might interact with the aqueous solution in a different way than noble gases and light hydrocarbons. Therefore, it is not included in the fits of Equations 2-6 and 2-7. To allow a comparison with gases, the data point is included in Figure 2-3.

The effective diffusion coefficient D_{eff} of all samples of Boom Clay and Eigenbilzen Sand decreases with increasing size of the diffusing molecule (Figure 2-4). This means that despite some deviations, a larger molecule exhibits a smaller effective diffusion coefficient. As for the diffusion coefficient D_0 in free water and assuming expressions similar to Equations 2-6 and 2-7, trend lines for the dependency of the effective diffusion coefficient on the size of the diffusing molecule d were inferred (Equations 2-8 and 2-9).

$$D_{eff} = D_{eff,exp} \times \exp\left(-A_{exp}\, d\right)$$ (2-8)

and

$$D_{eff} = D_{eff,pow} \times d^{-A_{pow}}$$ (2-9)

As these relations between diffusivity and size of the diffusing molecule seem to exist for each sample, using Equation 2-8 could be a possible and new way to estimate diffusion coefficients. This equation has two parameters, meaning that a first effective diffusion coefficient can be estimated experimentally from experiments with two gases[10]. Evidently, it is best to do this for a large molecule (e.g. C_2H_6) and a small one (e.g. Ne). An example of such a prediction was performed by Jacops et al. (2017a). By using this approach, the diffusion coefficient of for instance H_2 (which is difficult to measure due to microbial activity (Jacops et al. 2015)) can be estimated based on its molecular size (Figure 2-5).

---

[10] This could be improved upon through a least-square fitting procedure as more test results become available.

EURAD (Deliverable n° 6.1) – Initial State of the Art on Gas Transport in Clayey Materials
Dissemination level: PU
Date of issue of this report: **17/11/2021**

Page 59
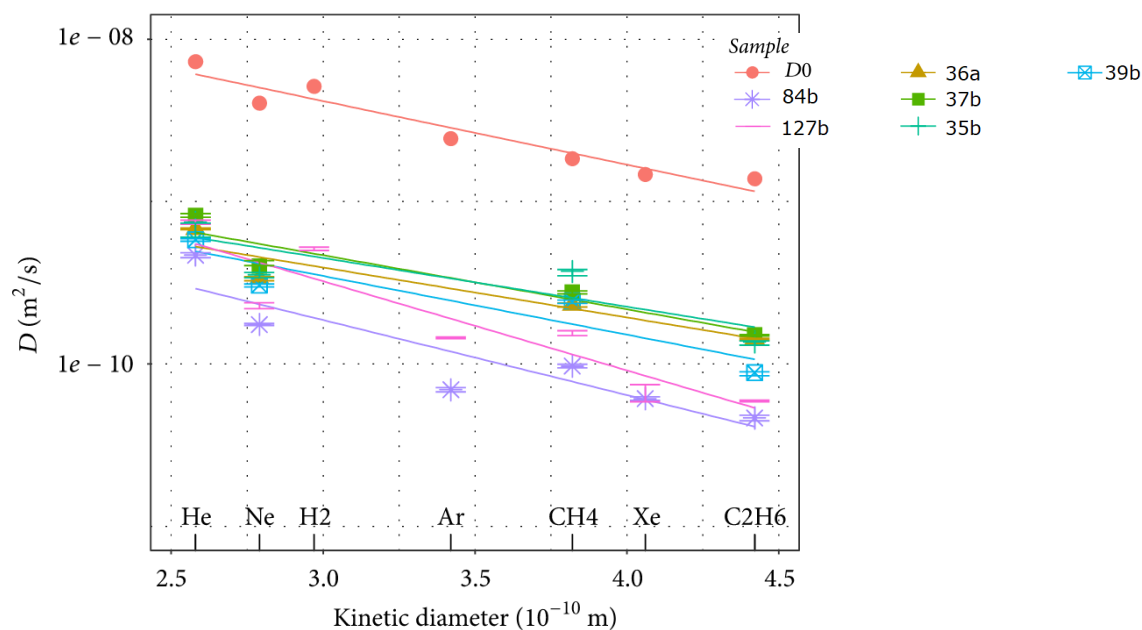
Figure 2-4 – Effective diffusion coefficients for dissolved gases in Boom Clay, fitted with Equation 2-8. The diffusion coefficient D is either the diffusion coefficient D_0 in pure water or the effective diffusion coefficient D_{eff} in a porous medium (Jacops et al. 2017a).

$$D_{eff} = 5.7E^{-9} \; x \; e^{-1.1E^{10}\sigma}$$
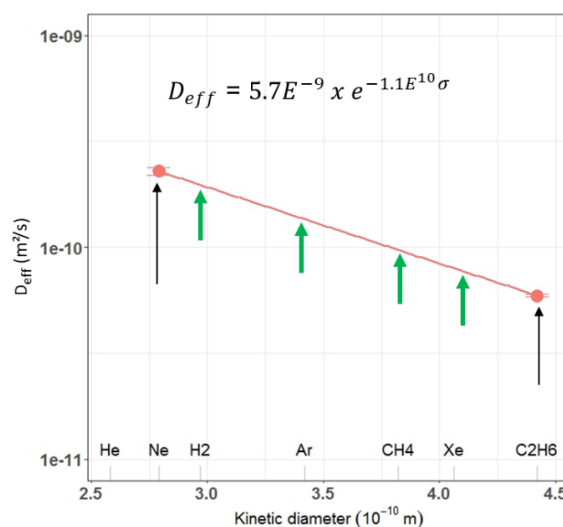
Figure 2-5 – Example of estimating diffusion coefficients for sample Boom Clay 127b, based on the exponential relationship (Equation 2-8) between D_{eff} and the kinetic diameter of the used gases (Jacops et al. 2017a).

Correlation between transport parameters and petrophysical properties

One of the objectives of the research on diffusion of dissolved gases was to assess the impact of lithological variations in the Boom Clay (mainly variations in clay/silt/sand content) on its transport properties. Therefore, samples from different layers have been selected: 'clayey' samples from the clayey middle part (Putte and Terhagen Member), 'silty' samples from the top part (Boeretang Member) and 'sandy' samples from the Eigenbilzen Sand, the formation overlying the Boom Clay one.

The hydraulic conductivity in the Boom Clay formation is not homogeneous, with values in the range of 10^{-12} m/s for samples from the Putte and Terhagen Members and 10^{-11} m/s for samples from the

EURAD (Deliverable n° 6.1) – Initial State of the Art on Gas Transport in Clayey Materials
Dissemination level: PU
Date of issue of this report: **17/11/2021**

Page 60

Boeretang Member (Table 2-4). The samples from the Eigenbilzen Sand present a higher hydraulic conductivity, in the range of 10^{-10} m/s.

Total porosity values have been obtained by drying the samples and following their weight till mass stabilisation. All porosity values are very similar, with an average of 39% and a standard deviation of 2%.

When comparing the measured diffusion coefficients for the Boom Clay and Eigenbilzen Sand samples, one can observe that despite similar porosity values, the diffusion coefficients in the Eigenbilzen Sand are slightly higher than in Boom Clay. On the other hand, there is no significant difference in diffusivity between the samples of Putte and Terhagen and those of Boeretang Member.

After finishing diffusion experiments with dissolved gases, a detailed petrophysical analysis was performed on all used samples of the Boom Clay and Eigenbilzen Sand. The results of the characterisation are available in Jacops et al. (2020a). In a next step, an attempt was made to correlate transport parameters and petrophysical properties.

To explore the multivariate relationships between all measured parameters of the full dataset, a principal component analysis biplot (PCA-biplot) is provided in Figure 2-6, including all transport properties (log-transformed), all petrophysical properties, and all interactions with the molecule size (labelled in Figure 2-6 with '.int').

We can clearly see two major axes of variation within the data on this PCA-biplot:

1. The first one describes the porous medium properties, and summarises the characteristics of *log(K)*, most minerals, the cumulative pore volumes, specific surface area, and the cumulative grain size percentages.
2. The second axis, perpendicular to this first one, relates to the size of the gas molecules, which is not related to *log(K)*. However, the logarithm of the effective diffusion coefficient, *log(D$_{eff}$)*, and the logarithm of the geometrical factor, *log(G)*, depend on the interactions between the gas and the pore network and thus on the petrophysical properties and the molecule size. Therefore, their loadings shifted to this direction, which makes e.g. the molecule size interactions with the lower cumulative pore volumes correlate negatively with *log(D$_{eff}$)*. It is also very clear that *log(D$_{eff}$)* displays a larger correlation with the molecule size than *log(G)* for instance.

The intermediate pore volume fraction, chlorite, gypsum and ankerite-dolomite contents clearly show there is only very weak to no relation with the porous medium properties, nor with the effect of gas molecule size. More information on the correlation between transport and petrophysical properties in the Boom Clay and Eigenbilzen Sand can be found in Jacops et al. (2020a).

EURAD (Deliverable n° 6.1) – Initial State of the Art on Gas Transport in Clayey Materials
Dissemination level: PU
Date of issue of this report: 17/11/2021

Page 61
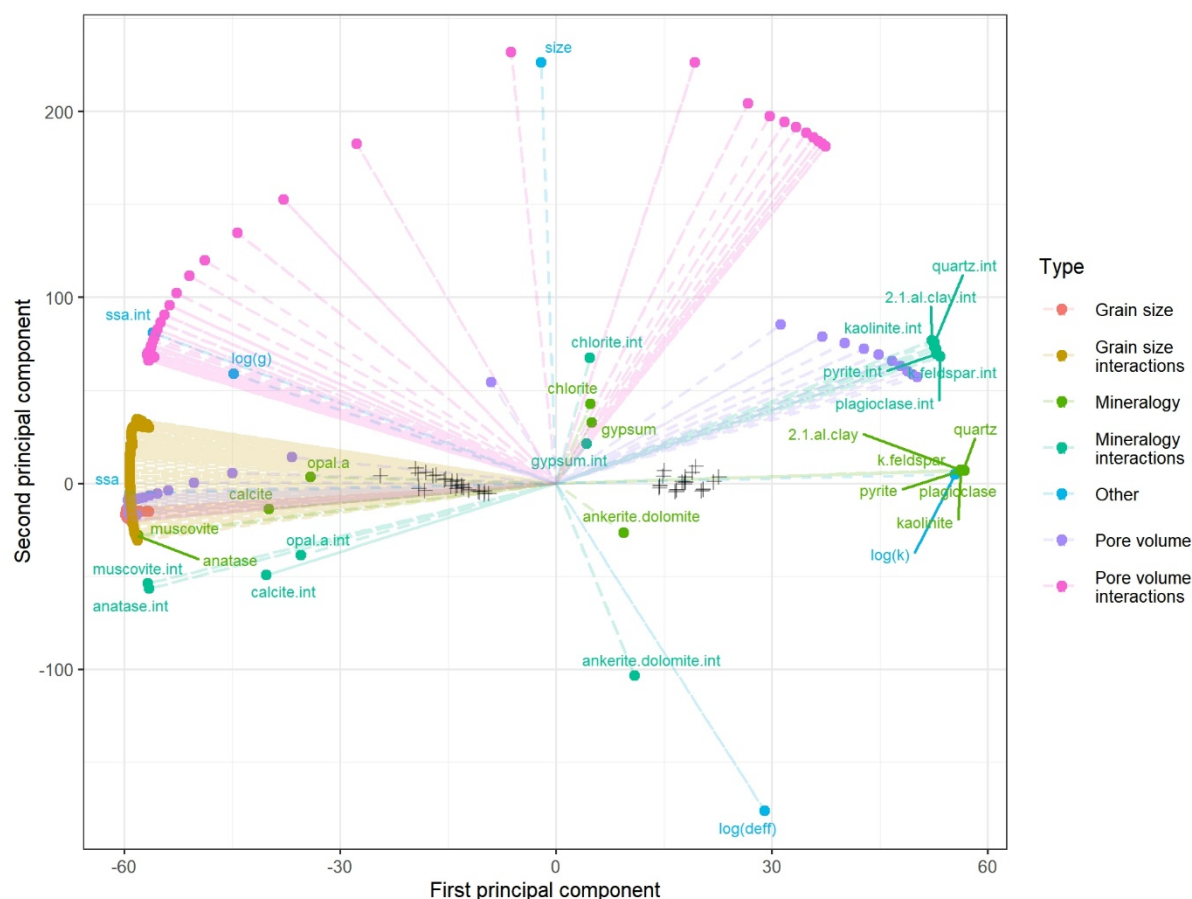
Figure 2-6 – Biplot of the variable loadings (coloured lines) and sample scores (points indicated with + symbols) of the full joined data set, including all transport properties and interactions with size (labels ending on '.int') (Jacops et al. 2020a)[11].

Note that a difference of one order of magnitude was observed between the hydraulic conductivity of the samples of Putte and Terhagen and those of Boeretang Member. Most likely, this could have been explained by a difference in composition, but both the mineralogical composition and the grain size distribution show similar results. So, no clear explanation could be found. As transport is related to the microstructure of the studied material, the petrophysical characterisation was followed by a petrographical analysis in order to reveal the microstructure of the involved samples.

A detailed petrographical study, including medical computed tomography, μ-CT and light microscopy of thin sections was performed on the samples of the Boom Clay and Eigenbilzen Sand (Figure 2-7) (Jacops et al. 2020b). Cumulative pore size distributions were obtained from low pressure N_2 physisorption measurements and omnidirectional mercury intrusion porosimetry (MIP) (Figure 2-8).

---

[11] In Figure 2-6, '*log(g)*' should be replaced by '*log(G)*'.

EURAD (Deliverable n° 6.1) – Initial State of the Art on Gas Transport in Clayey Materials
Dissemination level: PU
Date of issue of this report: **17/11/2021**

Page 62
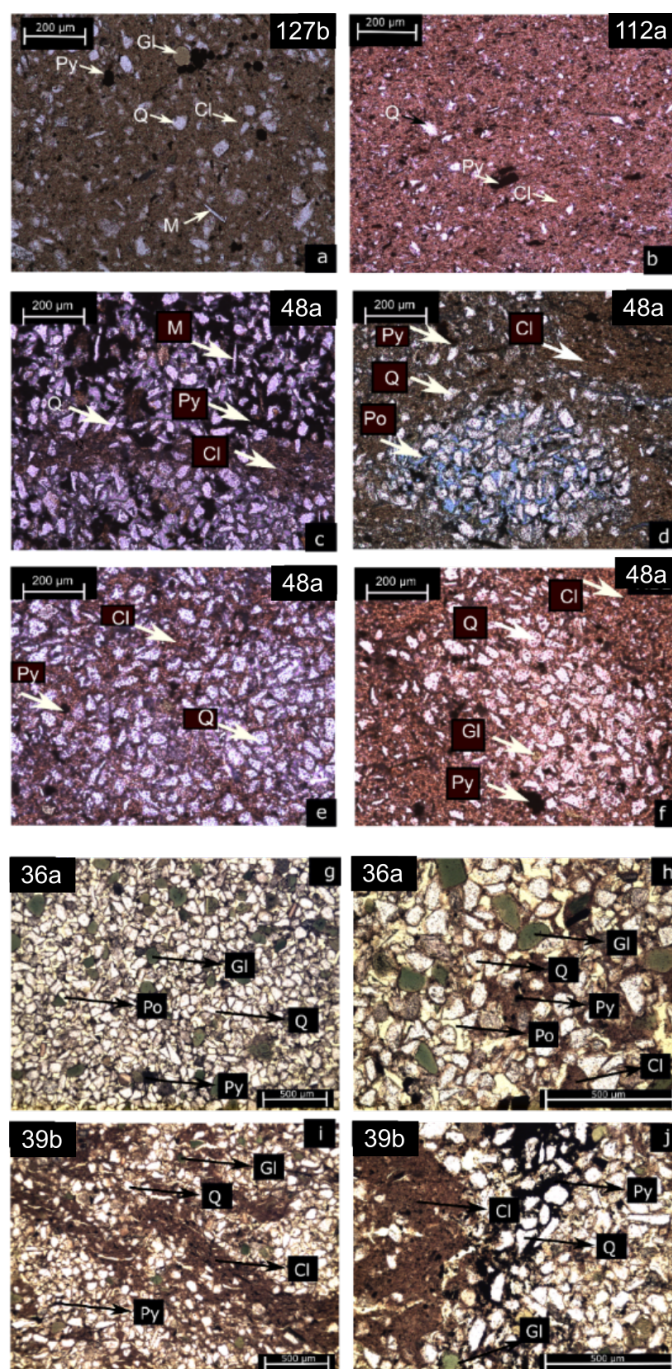
Figure 2-7 – Transmitted light microscopy images of thin sections of samples from different members of Boom Clay. These members differ, among other things, by their silt/clay content. Pictures from samples 127b (Terhagen Member) (a) and 112a (Putte Member) (b) show transparent quartz grains (Q) floating in a clay matrix (Cl), with local mica platelets (M) and glauconite grains (Gl). Black spots correspond to framboidal pyrite (Py). Pictures from samples 48a (Boeretang Member) (c, d, e, f) show the grouping of quartz grains and often these quartz clusters are accentuated by the presence of pyrite. The blue epoxy between the quartz grains indicates intergranular porosity. In samples 36a (Eigenbilzen Sand) (g, h) and 39b (Eigenbilzen Sand) (i, j), quartz grains (Q) are abundant, but sample 39b contains considerably more clay (Cl) and framboidal pyrite (Py) compared to sample 36a, whereas sample 36a contains more interparticle porosity (Po). Glauconite grains (Gl) are omnipresent. Porosity is shown in yellow because of impregnation with a fluorescent yellow resin (Jacops et al. 2020b).

EURAD (Deliverable n° 6.1) – Initial State of the Art on Gas Transport in Clayey Materials
Dissemination level: PU
Date of issue of this report: **17/11/2021**

Page 63
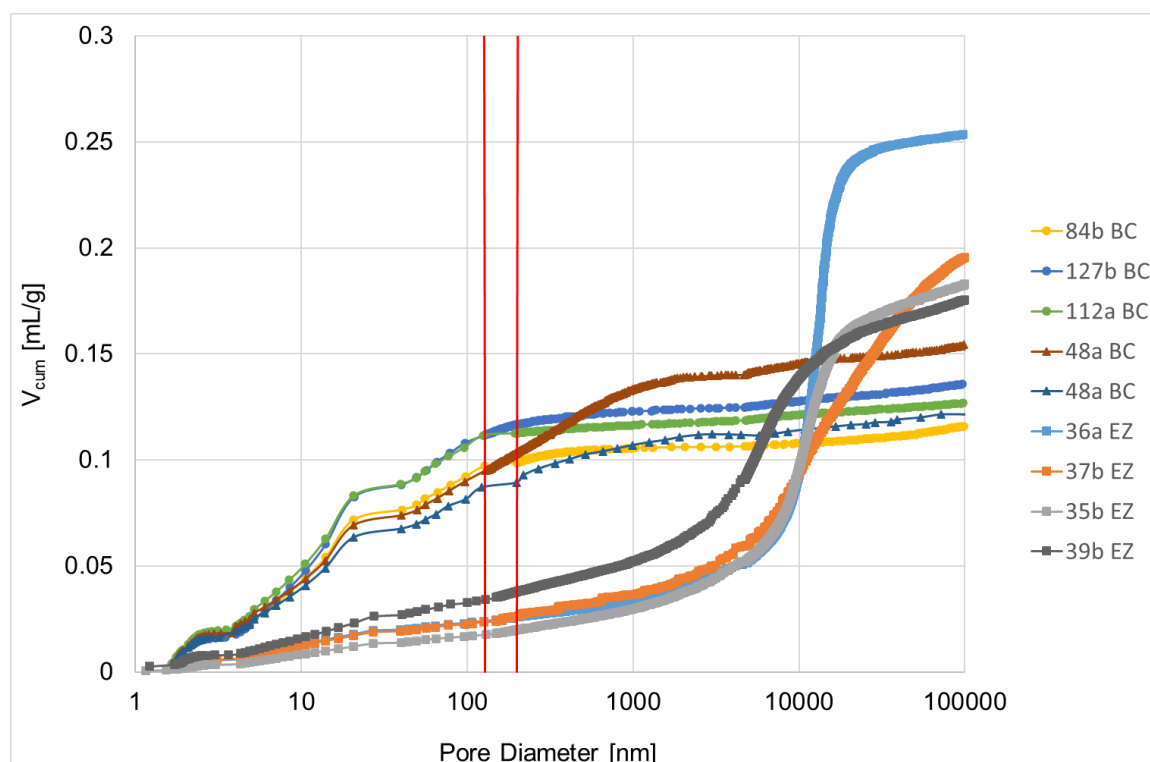
Figure 2-8 – Pore size distribution, based on N₂-adsorption and MIP measurements. Note that the MIP data are scaled to the N₂-adsorption data and merged between 128 and 200 nm (zone between the two red lines) (Jacops et al. 2020b).

It is clear from Figure 2-8 that the origin and composition of the samples strongly affect pore size distributions. For both diffusivity and hydraulic conductivity, a significant difference can be observed between Boom Clay and samples from the Eigenbilzen Sand at the top of the Boom Clay. More specifically, hydraulic conductivity is about two orders of magnitude larger and effective diffusivity (D_{eff}) is a factor 1.7 larger in the Eigenbilzen Sand. For most of the investigated petrophysical and petrographical properties, significant differences between both groups are identified. The Eigenbilzen Sand samples contain more quartz particles and less 2:1 clay minerals. This difference in composition is reflected in the microstructure. Samples from the Putte and Terhagen Members of the Boom Clay formation are characterised by a clay matrix in which quartz grains are homogeneously distributed and by locally increased porosity. The Boeretang Member samples reveal a heterogeneous distribution of quartz grains and interparticle pores (as deduced from thin sections analysis) and zones of increased porosity (based on μ-CT). By contrast, the Eigenbilzen Sand samples have more quartz grains, with heterogeneously distributed clay phases and increased porosity adjacent to quartz grains. The way these different mineral phases are distributed leads to changes in pore size distribution, which influences transport properties. From the combined results of nitrogen adsorption and mercury intrusion porosimetry experiments, the Boom Clay contains mainly pores <2 μm, with the majority <500 nm, while the Eigenbilzen Sand samples contain only a small number of pores <500 nm and a very large amount between 4 and 40 μm.

As water and solutes transport is less hindered when larger pores are available, the values of the transport parameters in the Eigenbilzen Sand are higher than those of Boom Clay.

Two different types of Boom Clay were investigated, representing different lithologies: 'clayey' samples from the Putte and Terhagen Members, and 'silty' samples from the Boeretang Member. Due to similarities in mineralogical composition and grain size distribution, the 'silty' nature is not confirmed. However, when comparing transport parameters of the Boeretang Member, higher hydraulic conductivity by a factor 5 to 10 is observed, while diffusivity remains similar. This elevated hydraulic

EURAD (Deliverable n° 6.1) – Initial State of the Art on Gas Transport in Clayey Materials
Dissemination level: PU
Date of issue of this report: 17/11/2021

Page 64

conductivity can be explained by a difference in the microstructure as outlined in the previous sections. Quartz grains are often grouped into clusters and interparticle porosity can be observed on 3D μ-CT images (Jacops et al. 2020b). Some of these clusters are elongated and connected and can be found throughout the sample. This leads to the conclusion that these quartz clusters are mostly remainders of burrows that have been filled during sedimentation. The cumulative pore volume is similar for all samples, but the samples of Putte and Terhagen Members mainly contain pores smaller than 250 nm whereas the samples from Boeretang Member also contain a considerable portion of pores between 250 nm and 3 μm. Probably, only water transport, under a pressure gradient, benefits from locally increased pores sizes forming a preferential flow path, whereas diffusive transport of solutes (including dissolved gas) is dominated by the micro- and mesopores located in the clay phase.

2.2.3   State of knowledge for Callovo-Oxfordian claystone

When looking in literature, mainly diffusion coefficients for He have been obtained for Callovo-Oxfordian claystone. In a chronological order, results were reported by Rebour et al. (1997), Bigler et al. (2005) and Jacops et al. (2016). An overview of available diffusion coefficients for He is shown in Table 2-6.

Table 2-6 – Diffusion coefficients for He in Callovo-Oxfordian claystone.

Orientation*	Technique	Type	Measured D [m²/s]	η [%]	T [°C]	Reference
sphere	outgassing core	D_p	$7.5 \times 10^{-10} \pm 20\%$	16.3	20	Bigler et al. 2005
$\perp$	natural He profile	D_p	2.41×10^{-10}	15.4	20	Bigler et al. 2005
$\perp$	through-diffusion	D_{app}	$5 \pm 1 \times 10^{-11}$	23	50	Rebour et al. 1997
$\perp$	through-diffusion	D_{eff} D_p	$8.1 \pm 0.2 \times 10^{-11}$ $4.5 \pm 0.09 \times 10^{-10}$	18	21 ± 2	Jacops et al. 2016
//	through-diffusion	D_{eff}	$10 \pm 0.2 \times 10^{-11}$	18	21 ± 2	Jacops and Maes 2015

* of the sample with respect to the bedding plane, respectively parallel (//) and perpendicular ($\perp$)

Rebour et al. (1997) performed diffusion experiments with helium as pure gas phase, using a through-diffusion set-up. Despite the fact that this set-up could be used for different gases, only data for He diffusion on COx were reported ($D_{app} = 5 \pm 1 \times 10^{-11}$ m²/s).

Bigler et al. (2005) performed a He-4 outgassing experiment with a spherical sample of Callovo-Oxfordian claystone. With the best fit between the experimental results and the analytical solution, a pore diffusion coefficient (D_p) of 7.5×10^{-10} m²/s was obtained with an uncertainty of 20%. They also obtained an in situ pore diffusion coefficient based on the natural He profile in the Callovo-Oxfordian claystone:

$D_p = 2.41 \times 10^{-10}$ m²/s with a range of uncertainty from 0.8×10^{-10} to 7.2×10^{-10} m²/s.

Jacops et al. (2016) reported diffusion coefficients for He, Ne, Ar and C_2H_6, using the through-diffusion set-up for dissolved gases as described in the previous section and in Jacops et al. (2013). Results are shown in Table 2-7. The used sample (COX1 EST 49109; depth 478.52 metres) was taken from the OHZ6560 borehole that was drilled from a technical gallery at the MHM URL. The sample axis is oriented perpendicular to the bedding plane. Sample COX2 (EST51008) was also drilled in the MHM URL (depth of 490 metres, distance: 10.85–11.15 metres), and the sample axis is oriented parallel to the bedding plane. Diffusion coefficients for He and Ar are reported in Jacops and Maes (2015). The

EURAD (Deliverable n° 6.1) – Initial State of the Art on Gas Transport in Clayey Materials
Dissemination level: PU
Date of issue of this report: 17/11/2021

Page 65

measured anisotropy ratios for He and Ar are respectively 1.23 and 1.74, leading to an average anisotropy ratio of 1.5.

Table 2-7 – Measured hydraulic conductivities (K), porosities (ϕ_{tot}) and effective diffusion coefficients (D_{eff}) (including the 95% confidence interval of the fit) for Callovo-Oxfordian claystone.

Core and orientation *	K [m/s]	ϕ_{tot} [–]	D_{eff} [× 10^{-11} m²/s]						
			He	HTO	Ne	Ar	CH$_4$	Xe	C$_2$H$_6$
COx 1, ⊥	3.4× 10^{-13}	0.18	8.1 ± 0.2	n.m.	2.1 ± 0.1	0.7 ± 0.0	n.m. **	n.m.	0.2 ± 0.01
COx 2, //	1.3× 10^{-13}	0.18	10.0 ± 0.2	n.m.	n.m.	1.3 ± 0.3	n.m.	n.m.	n.m.

* of the sample with respect to the bedding plane, respectively parallel (//) and perpendicular (⊥)
** n.m.: not measured

When looking at the data of Bigler et al. (2005), one can consider that the diffusion coefficient obtained for the spherical sample is actually a mixed diffusion coefficient with respect to bedding plane orientation. In addition, the sample was not a perfect sphere and might have been disturbed by cutting. Therefore, it is reported that this value has to be considered as a maximum value, affected by experimental artefacts (Bigler et al. 2005). The calculated in situ pore diffusion coefficient (based on the natural He profile in the Callovo-Oxfordian claystone), shows a large uncertainty of almost one order of magnitude. The experimentally obtained value from the spherical sample does not fall within this range. This discrepancy could be explained by the disturbed nature of the spherical sample, leading to an increased and mixed (with respect to bedding plane) diffusion coefficient. The value $D_p = 7 \times 10^{-10}$ m²/s has, as discussed above, to be considered as a maximum value.

Bigler et al. (2005) reviewed the work of Rebour et al. (1997) and commented that (i) the interpretation of the data suffered from complications such as anisotropy effects and (ii) that the measured porosity (23%) did not correspond to the porosity value needed to obtain a good fit (16%).

Jacops et al. (2016) used the through-diffusion technique for dissolved gases developed for Boom Clay which has proven to provide consistent results. The measured diffusion coefficients for Callovo-Oxfordian claystone show small uncertainties. Though, the measured diffusion coefficient for He differs about one order of magnitude from the diffusion coefficients obtained by Rebour et al. (1997), who used also a through-diffusion technique. A possible explanation for this difference can be the origin of the sample: the only information given by Rebour et al. (1997) is that the sample was cored from the Callovo-Oxfordian sediments from the northeast of the Paris basin at a depth of about 400 metres. Given the lithostratigraphy of the Oxfordian (Gaucher et al. 2004), the sample of Rebour et al. (1997) can be located in the calcareous Oxfordian, whereas the sample used in Jacops et al. (2016) is located in the Argillaceous Callovian-Oxfordian. Descostes et al. (2008) indicated that transport (and thus diffusion) properties are different for the different lithofacies of the Oxfordian, leading to for instance differences in the diffusion coefficient for HTO. For samples cored at a depth of 400 metres, Descostes et al. (2008) reports an average $D_{eff}(HTO) = 3.3 \times 10^{-12}$ m²/s with an average porosity of 3.8%. This differs considerably from the data obtained from a sample at a depth of 376 metres: the average $D_{eff}(HTO)$ is 22 × 10^{-12} m²/s with an average porosity of 19.5%. In that context, no direct comparison can be made between the experimental results of Rebour et al. (1997) and those of Jacops et al. (2016). The value obtained by Jacops et al. (2016) corresponds best to the values reported by Bigler et al. (2005); it is in between the maximum value which is obtained from outgassing of the spherical sample and the value obtained from the natural tracer profile.

EURAD (Deliverable n° 6.1) – Initial State of the Art on Gas Transport in Clayey Materials
Dissemination level: PU
Date of issue of this report: 17/11/2021

Page 66

Then, the diffusion coefficient for hydrogen in Callovo-Oxfordian claystone is $D_p = 4 \times 10^{-10}$ m²/s (assuming a porosity of 15%), or $D_{eff} = 6 \times 10^{-11}$ m²/s. This value deduced by Boulin (2008) is in good agreement with the D_p obtained for He by Jacops et al. (2016) and Rebour et al. (1997).

Similar to data for Boom Clay, diffusion coefficients in Callovo-Oxfordian claystone decrease with increasing size of the diffusing molecule and this relation can also be described with an exponential relation, based on Equation 2-8 (see Figure 2-9).
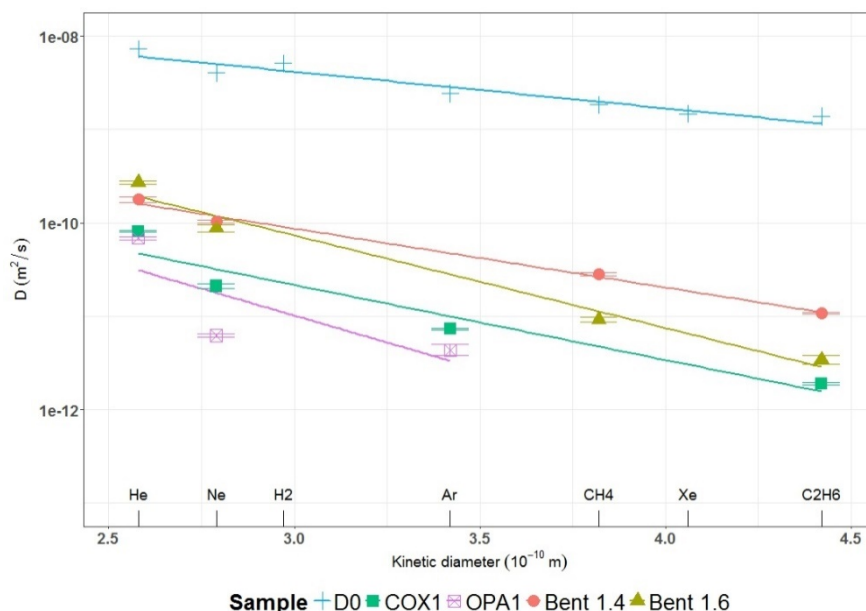
Figure 2-9 – Effective diffusion coefficients for dissolved gases in Callovo-Oxfordian claystone, Opalinus Clay and bentonite, fitted with Equation 2-8. The diffusion coefficient D is either the diffusion coefficient D_0 in pure water or the effective diffusion coefficient D_{eff} in a porous medium (Jacops et al. 2017a).

Based on the measured diffusion coefficients and the measured porosity, the geometric factor can be calculated. For Callovo-Oxfordian claystone, the geometric factor is not a constant value but clearly increases with the size of the diffusing molecule (Figure 2-10), as for bentonite.
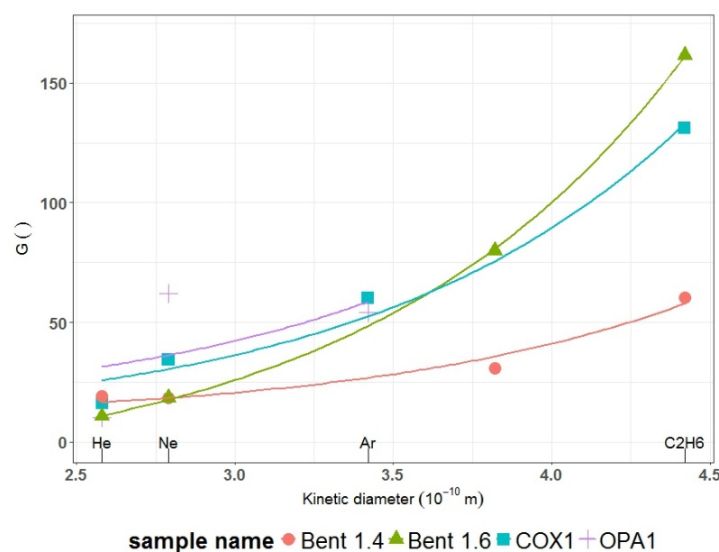
Figure 2-10 – Evolution of the geometric factor with the size of the diffusing molecule for Callovo-Oxfordian claystone (COx), Opalinus Clay (OPA) and bentonite (Bent) (Jacops et al. 2017a).

EURAD (Deliverable n° 6.1) – Initial State of the Art on Gas Transport in Clayey Materials
Dissemination level: PU
Date of issue of this report: **17/11/2021**

Page 67

2.2.4   State of knowledge for Opalinus Clay

Gómez-Hernández (2000) performed an in situ in- and out-diffusion experiment with He parallel to the bedding plane in Opalinus Clay in the Mont Terri underground research laboratory. The best fit for the apparent diffusion coefficient $D_{app}(He)$ = 7.0 × 10^{-10} m²/s was obtained from an out-diffusion experiment but a porosity of 30% was used, which is twice the typical porosity value of 12–18% reported for Opalinus Clay (Mazurek et al. 2011).

Rubel et al. (2002) fitted D_{app} for He ($D_{app}(He)$ = about 3.5 × 10^{-11} m²/s) in Opalinus Clay, based on the natural He concentration profile measured at Mont Terri URL, Switzerland.

Krooss and Alles (2006) performed gas injection experiments on initially fully saturated Opalinus Clay samples from Mont Terri URL using He and Ar as test gases. The experimental data were analysed by Poller et al. (2008) using a two-phase flow code. The model-supported analyses revealed that diffusion of dissolved gas is a non-negligible gas transport mechanism even when the two-phase flow regime prevails. Inverse modelling of several experiments resulted in best-guess parameter ranges $D_{eff}(Ar)$ = 3.6–3.8 10^{-12} m²/s and $D_{eff}(He)$ = 2.8–3.6 × 10^{-11} m²/s.

Vinsot et al. (2014) performed an in situ in-diffusion experiment in the Opalinus Clay. A mixture of Ar, H_2, He and Ne was injected in a borehole in Mont Terri URL, and the concentration evolution (influenced by dissolution and diffusion) was followed over time. Diffusion coefficients are calculated based on D_0, porosity (0.16) and tortuosity (7.5). Using these calculated values ($D_{eff}(He)$ = 11.5 × 10^{-11} m²/s and $D_{eff}(Ne)$ = 6.4 × 10^{-11} m²/s), the modelled concentration decrease over time corresponds for a limited time frame to the measured pressure decrease. For H_2 the results of this in situ tests were not exploitable. Analysis of pore water samples suggest that measurements were perturbed by biological processes involving hydrogen oxidation, sulphate reduction and Fe(III) reduction.

Jacops et al. (2016) reported diffusion coefficients for He, Ne, Ar and HTO, using the through-diffusion set-up with dissolved gases as described in Jacops et al. (2013). Results are shown in Table 2-8 and Table 2-9. The studied sample was taken from the Schlattingen borehole (northeast of Switzerland, canton Thurgau), at a depth of 860.32 metres below surface. Note that the burial history for the Mont Terri site and Schlattingen is different, with deeper burial in Schlattingen (Mazurek et al. 2006) and therefore the physical properties of the Opalinus Clay are different at both locations. The sample axis is oriented perpendicular to the bedding plane. Anisotropy of diffusion of dissolved gases was not studied.

Table 2-8 – Diffusion coefficients for He in Opalinus Clay.

Orientation *	Technique	Type	Measured D [m²/s]	η [%]	T [°C]	Reference
//	in situ in- and out-diffusion	D_{app}	7.0 × 10^{-10}	30		Gómez-Hernández 2000
⊥	natural He profile	D_{app}	3.5 ± 1.3 × 10^{-11}		RT **	Rubel et al. 2002
⊥	gas injection/in- and out-diffusion	D_{eff}	2.8–3.6 × 10^{-11}	12	RT	Poller et al. 2008
–	in-diffusion	D_{eff}	11.5 × 10^{-11}	16	15–16	Vinsot et al. 2014
⊥	through-diffusion	D_{eff} D_p	6.8 ± 0.3 × 10^{-11} 7.1·± 0.3 × 10^{-10}	9.6	21 ± 2	Jacops et al. 2016

* of the sample with respect to the bedding plane, respectively parallel (//) and perpendicular (⊥)
** RT: room temperature

EURAD (Deliverable n° 6.1) – Initial State of the Art on Gas Transport in Clayey Materials
Dissemination level: PU
Date of issue of this report: 17/11/2021

Page 68

Table 2-9 – Measured hydraulic conductivity (K), porosity (ϕ_{tot}) and effective diffusion coefficients (D_{eff}) (including the 95% confidence interval of the fit) for Opalinus Clay.

Core and orientation *	K [m/s]	ϕ_{tot} [–]	D_{eff} [× 10^{-11} m²/s]						
			He	HTO	Ne	Ar	CH$_4$	Xe	C$_2$H$_6$
OPA 1, ⊥	1.2× 10^{-13}	0.096	6.8 ± 0.3	1.2 ± 0.04	0.6 ± 0.03	0.4 ± 0.1	F **	F	F

* of the sample with respect to the bedding plane, perpendicular (⊥)
** F: failed

When looking at the data of Gómez-Hernández (2000), the necessity to use a high porosity of 30% might be explained by the fact that during the drilling of the experimental borehole an excavation damaged zone (EDZ) was created, leading to a higher permeability and increased porosity – as discussed by Gómez-Hernández (2000). If the higher porosity is indeed related to the creation of an EDZ, the measured diffusion coefficient might not be relevant for diffusion under undisturbed conditions. The other out- and in-diffusion experiments performed by Gómez-Hernández (2000) could not confirm this value for D_{app} without adapting parameters like the circulation volume or the initial concentration of He-4.

The data of Rubel et al. (2002) are commented by Mazurek et al. (2011) who state that this D_{app} value is likely too low because of the use of an overly simplified model – in particular, of the unsubstantiated assumption of a steady-state situation in which out-diffusion of He is balanced by in situ production.

The data of Poller et al. (2008) and Krooss and Alles (2006) are obtained from gas injection experiments and not all boundary conditions (e.g. volumes of the up- and downstream reservoirs) are well constrained to allow an accurate calculation of diffusion coefficients. Diffusion of gas, through the sleeve into the containing fluid could partly explain the sometime high inlet fluxes, but is not taken into account. Hence, the presented diffusion coefficients should be put into a correct perspective for future data processing.

The data of Jacops et al. (2016) have been obtained using a reliable technique and set-up which provided also a large, consistent data set for Boom Clay. As indicated in Table 2-9, some of the experiments on the Opalinus Clay failed: no diffusion coefficient could be obtained for gases larger than argon (CH$_4$, Xe and C$_2$H$_6$).

As discussed in Jacops (2018), hypotheses such as degassing of the sample or interaction of the gases with the clay were investigated, but considered to be unlikely. Opalinus Clay has a very low porosity (9.6%) and very small pores (mainly <10 nm, with peaks at 0.6 and 4 nm (Gimmi and Fernández 2017)). Likely, from a certain gas size on, only very few connected pores are left for diffusive transport through the sample. This is also described as 'percolation threshold problem'. Percolation threshold is reached when the pores become so small (compared to the size of the diffusing molecule), so that the number of connected paths diminishes drastically. Finally, there is no longer a connected path of pores available for transport. Based on the currently available information, Jacops et al. (2017) and Jacops (2018) believe that this phenomenon occurred in the Opalinus Clay for all gases larger than argon. The occurrence of the percolation threshold in Opalinus Clay has also been discussed by Keller et al. (2013a), whose observations are based on the analyses of the connected pore space that was derived from FIB-SEM (focused ion beam scanning electron microscopy) images. However, the effect of the size of the diffusing molecule has not been considered. Percolation threshold was also observed in concrete and cement-based samples. Jacops et al. (2021) observed a percolation threshold for CH$_4$ and C$_2$H$_6$ in concrete samples of the gallery lining of HADES URL and in samples of a mock-up of the supercontainer. Phung et al. (2019) observed for cement paste samples a strong correlation between

![eurad logo] European Joint Programme on Radioactive Waste Management

EURAD (Deliverable n° 6.1) – Initial State of the Art on Gas Transport in Clayey Materials
Dissemination level: PU
Date of issue of this report: 17/11/2021

Page 69

diffusivity and the size of the diffusing molecule, and a percolation threshold for Xe in some samples. Hence, we can conclude that percolation threshold problems can occur in different materials, in which their pore size distribution is a determining factor.

Similar to the results for Boom Clay and Callovo-Oxfordian claystone, diffusion coefficients in Opalinus Clay decrease when the size of the diffusing molecule increases and an exponential relation can be found (Figure 2-9). The geometric factor increases with increasing size of the diffusing molecule (Figure 2-10). The variability of the geometric factor with the size of the diffusing molecule was not observed in the in situ experiment described by Vinsot et al. (2017).

2.2.5   State of knowledge for bentonite

The availability of diffusion coefficients of gases in bentonite-based materials is comparatively limited.

During the FORGE EC project, gas injection experiments with hydrogen were performed on Rokle bentonite[12] and Volclay KWK[13] by ÚJV Řež (Sellin 2014). Based on the flux of hydrogen, measured at the downstream side, diffusion coefficients were calculated, and results are shown in Table 2-10. As mentioned by Sellin (2014), the reported estimates of the diffusion coefficients are affected by neglecting an advective component of the transport of hydrogen, which is caused by an evolving, non-zero pressure gradient.

Table 2-10 – Calculated diffusion coefficients for H_2, based on the flux measured in the downstream compartment.

Bentonite type	Dry density [g/cm³]	Hydraulic conductivity K [m/s]	$D_{eff}(H_2)$ [m²/s]
Volclay KWK	1.6	3.0×10^{-14}	2.9×10^{-11}
Rokle bentonite	1.6	10.4×10^{-13}	3.7×10^{-10}

Jacops et al. (2017) measured diffusion coefficients for dissolved He, Ne, CH_4 and C_2H_6 in water-saturated compacted Volclay KWK with dry densities of 1.4 and 1.6 g/cm³ in absence of hydraulic gradient. The corresponding values are found in Table 2-11.

An increase in compaction from 1.4 to 1.6 g/cm³ in Volclay KWK seems to have little impact on the diffusion coefficient of He, while for other gases (Ne, CH4 and C2H6) and HTO the diffusion coefficients clearly decrease. Only for HTO, a comparison can be made with other data available in literature: Glaus et al. (2017) obtained for Volclay KWK samples with dry densities of 1.3 and 1.6 g/cm³ D_{eff} values of respectively 1.4×10^{-10} and 8.2×10^{-11} m²/s, which are very similar to the results of Jacops et al. (2017).

Also for Volclay KWK, diffusivity decreases with increasing size of the diffusing molecule, while the geometric factor increases (Figure 2-9 and Figure 2-10). For the bentonite with the highest dry density (1.6 g/cm³), the geometric factor of C_2H_6 is 16 times larger than the one of He. This clearly indicates that the geometric factor is not an intrinsic property of the studied material, but strongly depends on the diffusing gas. The geometric factor is higher for gas with larger molecular size.

---

[12] The Rokle bentonite is a Czech bentonite from Rokle deposit. It is a complex mixture of (Ca, Mg)-Fe-rich montmorillonite, micas, kaolinite and other mineral admixtures (mainly Ca, Mg, Fe carbonates, feldspars and iron oxides).

[13] The Volclay KWK (a Wyoming type bentonite, USA) is a fine-grained sodium bentonite with montmorillonite as the main component.

EURAD (Deliverable n° 6.1) – Initial State of the Art on Gas Transport in Clayey Materials
Dissemination level: PU
Date of issue of this report: **17/11/2021**

Page 70

Table 2-11 – Measured hydraulic conductivities (K), porosities (ϕtot) and effective diffusion coefficients (D_eff) (including the 95% confidence interval of the fit) for Volclay KWK.

Bentonite density [g/cm³]	K [m/s]	ϕ_tot [–]	D_{eff} [× 10^{-11} m²/s]						
			He	HTO	Ne	Ar	CH_4	Xe	C_2H_6
1.4	1.5× 10^{-13}	0.47	17.7 ± 1.1	16 ± 1.2	10.3 ± 0.4	n.m.*	2.8 ± 0.1	n.m.	1.1 ± 0.02
1.6	5.8× 10^{-14}	0.40	27.0 ± 0.9	8.1 ± 0.5	8.7 ± 0.7	n.m.	0.9 ± 0.1	n.m.	0.3 ± 0.04

* n.m.: not measured

Given the very similar size of H_2 and Ne, the diffusion coefficient of Ne measured in Volclay KWK with a dry density of 1.6 g/cm³ obtained by Jacops et al. (2017) can be compared with the data reported in Sellin (2014). The values are of the same order of magnitude ($D_{eff}(H_2)$ = 2.9 × 10^{-11} m²/s and $D_{eff}(Ne)$ = 8.7 × 10^{-11} m²/s). Also the measured hydraulic conductivities for both Volclay KWK samples (dry density 1.6 g/cm³) are in the same order of magnitude, but do differ a factor of 2 (3.0 × 10^{-14} and 5.8 × 10^{-14} m/s from respectively Sellin (2014) and Jacops et al. (2017)). The difference in D_{eff} can be explained in several ways. A first explanation is variability between samples, e.g. local changes in degree of compaction. A second explanation is the used methodology: contrary to the through-diffusion technique of Jacops et al. (2013) in which the sample is put in contact with water containing dissolved gas, in the experiment reported in Sellin (2014), the sample is directly in contact with pressurised gas at the inlet and the flux at the outlet is determined by the accumulated volume of gas released under a constant pressure condition. A third explanation could be some dehydration of the sample in the test reported in Sellin (2014), due to the high applied pressure (up to 10 MPa). But dehydration would increase the diffusive flux, leading to an overestimation of the diffusion coefficient. A last explanation could be defects in the experimental set-up. Experiments with hydrogen are known to be prone to leakages, and a potential leak could lead to the underestimation of D_{eff}. Despite some uncertainties in the work reported by Sellin (2014), the presented results give a good indication of the magnitude of diffusion coefficients of H_2 in bentonite buffer materials.

2.2.6 Shared understanding of gas diffusion

During the last ten years, the availability of reliable diffusion coefficients for different dissolved gases, measured in a broad range of materials, has increased. Currently, comprehensive data sets are available for different lithologies of the Boom Clay (He, Ne, Ar, Xe, H_2, CH_4, C_2H_6). For Callovo-Oxfordian clay, diffusion coefficients are available for He, Ne, Ar and C_2H_6. For Opalinus Clay, diffusion coefficients are available for He, Ne and Ar. For Volclay KWK at dry density 1.4 and 1.6 g/cm³, data for He, Ne, CH_4 and C_2H_6 are available. Also for two types of bentonite, considered in the Czech disposal concept (Rokle bentonite and Volclay KWK – both dry density 1.6 g/cm³), diffusion coefficients for H_2 are available. Unfortunately, most of the other diffusion data available in literature suffer from large uncertainties and experimental problems and a comparison with the data of Jacops (2018) is not straightforward. In order to assess the correctness of obtained gas diffusion coefficients, a comparison is made with diffusion data for HTO, which are more widely available. Most gas diffusion coefficients are in line with the measured diffusion coefficients for HTO. Unfortunately, diffusion coefficients for hydrogen, which is the most relevant gas in a geological repository, are still lacking for almost all materials. As described by Jacops et al. (2015), measuring diffusion coefficients of hydrogen in clay-based materials is experimentally challenging because of microbial conversion of H_2 into CH_4. Only by using a complicated protocol, including heat sterilisation, gamma irradiation, gas filtration and using a microbial inhibitor, Jacops et al. (2015) were able to measure the diffusion coefficient of hydrogen in Boom Clay.

EURAD (Deliverable n° 6.1) – Initial State of the Art on Gas Transport in Clayey Materials
Dissemination level: PU
Date of issue of this report: 17/11/2021

Page 71

For all discussed materials, an exponential relationship, describing the decrease in diffusivity with an increase in the size of the diffusing molecule can be found. For the geometric factor, the observed relationship depends on the material. For the Boom Clay, the geometric factor increases only slightly when the diffusing molecule becomes larger: the difference in geometric factors between the smallest (He) and largest (C_2H_6) molecules is not more than a factor of two. For the other materials (Callovo-Oxfordian claystone, Opalinus Clay and Volclay KWK (density 1.4 and 1.6 g/cm³)), the geometric factor clearly increases with an increasing molecule size. The ratio in geometric factors between the smallest (He) and largest (C_2H_6) molecule is about 16 for the Volclay KWK sample with density 1.6 g/cm³. This implies that the geometric factor is not an intrinsic property of the studied material, but also strongly depends on the size of the studied diffusing molecule.

2.2.7 Uncertainties and knowledge gaps

From the results of Jacops (2018), it is clear that diffusion is influenced by parameters such as the mineralogical composition and density. Though, the impact of the presence of individual minerals has not been assessed so far, and only two different densities were investigated for bentonite. Knowing the dependency of gas diffusion to these parameters would provide relevant information for generic disposal concepts and would make the existing data more widely usable by different end-users. Hence, a dedicated set of experiments is included in the WP GAS of EURAD to understand variations in the diffusion coefficient as a function of mineralogy and density. Complementary to this work, the relationship between diffusive transport and the pore network of the studied materials will be investigated in more detail. Building pore network models also allows to theoretically calculate diffusion coefficients under different conditions such as variable density and variable degree of saturation. Theoretical data should be validated by experimental results.

All diffusion coefficients for gases reported above were obtained for samples close to full saturation. Solute diffusion experiments on desaturated samples have been performed on Callovo-Oxfordian claystone for HTO, Cs-134, Na-22 and I-125 (Savoye et al. 2012; Savoye et al. 2017; Savoye et al. 2010). Results show that, for a decrease in saturation from 100 to 80%, D_{eff} drops with a factor 60, 50 and 7 for respectively Cs-134, I-125 and HTO. Unlike these solutes, diffusing gases can also enter the vapour phase in the desaturated sample, the impact of desaturation on their effective diffusion coefficient D_{eff} might thus be fundamentally different than the impact on e.g. HTO. However, the effect of desaturation on the diffusivity of gases has not yet been studied and is therefore considered as a knowledge gap.

At an even lower level of detail, the pore scale level, it is still unclear which interactions play a role in the diffusive process, and how these interactions would be influenced by desaturation. Therefore, pore network models have to be created for relevant samples, and transport simulations under different conditions have to be performed. The models can be applied to evaluate the saturation state of the individual micro pores and to derive pore scale diffusion coefficients for relevant gaseous species as a function of relative humidity (RH) and pore size (Churakov 2013). These simulations can also provide information about the distribution of the gaseous species between pores with different pore sizes. Data can also be used to evaluate the effect of heterogeneities and pore network connectivity, based on a model structure of clay rocks (Churakov et al. 2014).

Finally, the potential effects of sample size and mechanical conditions on diffusion process have not been discussed here. For the moment, they are considered as knowledge gaps that will be investigated in the course of the WP GAS.

EURAD (Deliverable n° 6.1) – Initial State of the Art on Gas Transport in Clayey Materials
Dissemination level: PU
Date of issue of this report: **17/11/2021**

Page 72

2.3   Gas sorption

2.3.1   Hydrogen adsorption: lessons learned from solid-state H$_2$ storage

Hydrogen adsorption (physisorption) on various materials has been primarily studied in the context of solid-state hydrogen storage. To date, several materials have been tested (Table 2-12), but those presented below, are among the most thoroughly investigated for hydrogen sorption (Voskuilen et al. 2012):

- Metal Organic Frameworks (MOFs) are by far the most studied and promising materials for hydrogen storage (Dinca and Long 2006; Lee et al. 2007; Vitillo et al. 2008; Hirscher et al. 2010). Some MOFs can store up to 7.5 wt% at 77 K (Wong-Foy et al. 2006). These crystalline compounds consist of a metal ion coordinated to a rigid structure of organic molecules forming a microporous structure whose cavity diameter varies from 90 to 130 nm.

- Zeolites (crystallised aluminosilicates characterised by a microporous structure) have pore volumes close to the kinetic diameter of molecular hydrogen (2.89 Å) and therefore an increased trapping capacity (up to 1.5 wt% H$_2$ at 77 K) (Palomino et al. 2006; Ramirez-Cuesta and Mitchell 2007).

- Nanotubes (Kadono et al. 2003; Patchkovskii et al. 2005) and carbon nanofibers (Marella and Tomaselli 2006) have the advantage of their low densities, high chemical stabilities and good sorption capacities ranging from 1.4 to 6.8 wt% H$_2$ at 77 K depending on the manufacturing processes.

In addition, most of these materials can be functionalised for a better H$_2$ storage capacity: by modifying the nature of some of their components, their concentration, and localisation in the crystallographic structure, the involved creation of pores or sites leads to more suitable structures for H$_2$ adsorption or absorption. One example is a type of MOFs materials called 'open metal sites' MOFs, which are designed for having transition metal ions in their frameworks, leading to a most effective capture of hydrogen molecules inside cavities (Langmi et al. 2014; Gygi et al. 2016).

Note that hydrogen may also be stored through chemisorption. Metal hydrides (LaNi5, MgH$_2$, LiH, NaAlH4) offer a high-volume capacity and good compactness (Freni et al. 2009; Sakintuna et al. 2007). Mostly known for their application in batteries, metal hydrides are also promising material for hydrogen storage (de Rango et al. 2016). Contrarily to the three previous class of hydrogen storage material, metal hydrides store hydrogen directly into their crystal structure (chemo-sorption), and the absorption process requires high temperature (>300°C). Some hydrides such as NaAlH4 have favourable storage decomposition conditions: at 1 bar and at 100°C they release up to 5.5 wt% of hydrogen (Schüth et al. 2004). However, the enthalpy of absorption is rather high (*ΔHabs* = -30 to -75 kJ/mol H$_2$) which guarantee a good stability of the hydride phase, but requires an efficient thermal management, even when the absorption reaction is reversible at room temperature (for example LaNi5 or Ti-V-Cr alloys). In addition, the amount of heat to be supplied during desorption reduces the energy efficiency of the storage system.

However, all these materials have many disadvantages, such as their high production costs (Table 2-12), their complex manufacturing process, their low stability (MOFs decompose in the presence of water), their ability to release easily and rapidly physisorbed hydrogen (i.e. reversibility of storage), or their toxicity (nano particles, heavy metals). In addition, hydrogen storage material based on physisorption process (e.g. MOFs, zeolites, carbon nanotubes) suffer from a drastic loss of storage capacity as temperature increases from 77 K (the temperature usually used in the laboratory for adsorption isotherm measurements) due to the low enthalpy of H$_2$ sorption (i.e. binding energy) on these materials (typically 5–8 kJ/mol).

EURAD (Deliverable n° 6.1) – Initial State of the Art on Gas Transport in Clayey Materials
Dissemination level: PU
Date of issue of this report: 17/11/2021

Page 73

Table 2-12 – Comparison of gravimetric and volumetric storage capacity of various H₂ storage technologies. Charge/discharge conditions and cost in $/kgH₂ are also indicated. Reference material in each category, and associated storage conditions are highlighted in blue.

	Amount H$_2$ [wt%]	Amount H$_2$ [kg/m^3]	Charge condition (*T, P*)	Discharge condition (*T, P*) ***	Cost ** [$/kg$_{H2}$]	Reference
Established technologies						
Compressed 350 bar	~6*	~18	20°C, 350 bar	P decrease		DOE 2020
Compressed 700 bar	~4*	~28	20°C, 700 bar	P decrease		DOE 2020
Cryo-compressed	~5.5*	~30	-93°C, 350 bar	T increase		DOE 2020
Liquid	~4.8*	~70	-252.8°C, 1 bar	T increase		DOE 2020
Chemical storage						
Metal hydrides (NaAlH$_4$)	5.5	94	300°C, 5 bar	100°C, 1 bar	1 430	Schüth et al. 2004
Liquid organic H$_2$ carriers (dibenzyltolu.)	6	40	150°C, 50 bar catalyst required	300°C, 1 bar	550	DOE 2020
Amine borane	19	80	Irreversible (complex synt.)	160°C, 1 bar	120	Keaton et al. 2007
Physical storage						
MOF-177 @77 K	3.8	17	-196°C, 70 bar		6 500	Thomas 2007
MOF-177 @room T	0.6	3.3	25°C, 100 bar		40 000	Li and Yang 2007
Zeolite-CAX	2.2	15	-196°C, 15 bar		560	Langmi et al. 2005
Carbon nanotubes	1.5	25	20°C, 77 bar		55 000	Marella and Tomaselli 2006
Physical storage: clayey material						
Cigar Lake's natural clays	0.05	1.2	20°C, 1 bar (?)	250°C, 1 bar	~0 (raw natural sample)	Truche et al. 2018
Callovo-Oxfordian claystone	0.15	3.75	90°C, 30 bar	P decrease	~0 (raw natural sample)	Didier 2012
Synthetic Montmorillonite	0.2	5	90°C, 30 bar	P decrease	20	Didier 2012
Laponite	0.45	11	-196°C, 1 bar	P decrease	10	Edge et al. 2014

* The values are estimated and include the volume and mass of the tank.
** Energy costs for charge and discharge not included in this estimation. Material prices available from Sigma- Aldrich online catalogue.
*** *T*: temperature [°C]; *P*: pressure [bar]

EURAD (Deliverable n° 6.1) – Initial State of the Art on Gas Transport in Clayey Materials
Dissemination level: PU
Date of issue of this report: 17/11/2021
Page 74

2.3.2　Hydrogen uptake by clay minerals

Surprisingly, clay minerals have not been the subject of a dedicated study for the storage of hydrogen. Their ease of mass production, their availability in the natural environment, their large surface area and their very good sorption capacities make them potentially promising materials. The intercalation of H_2 in the interlayer space, on the basal and edge sites, and in the micropores between stacks of clay particles is favoured by:

    i)   the presence of a very strong electrostatic field inside the interlayer cavities due to the presence of exchangeable cations (this electrostatic field induces a dipolar moment to the molecule of H_2 – normally apolar – and thus promotes its physisorption),

    ii)   the geometry of the interlayer space which is homogeneous and does not present bottleneck likely to prevent H_2 diffusion,

    iii)   the size of the micropore network which is close to the kinetic diameter of H_2 (2.89 Å).

The interactions of hydrogen gas with clay rock have been principally investigated within the context of high-level radioactive waste disposal. Molecular hydrogen is a product from the anoxic corrosion of metallic components of waste containers and from water radiolysis reactions caused by alpha decay (Rodwell et al. 2003b). If H_2 gas cannot escape from clay-rich media faster than it is generated, and exceeds the sorption capacity of the clays, pressure build-up may have effect on repository barrier integrity. In addition, certain proposals for geologic storage of H_2 generated by excess renewable energy also require clay rock to serve as an impermeable and inert cap rock for H_2. Detailed studies for relevant formations are currently lacking, however, in part because performing diffusion and sorption experiments with H_2 on natural clays and clay rock is difficult. Set-ups are prone to leakage and microbial processes can interfere (transforming CO_2 to CH_4 or nitrate to N_2) (Vinsot et al. 2014; Jacops et al. 2015; Bagnoud et al. 2016).

A series of pioneering studies of hydrogen sorption on Callovo-Oxfordian claystone (mixture of illite/smectite, quartz, and carbonates) and montmorillonite was carried out at CNRS (UGrenoble) in the framework of investigations on hydrogen mobility in deep geological disposal of radioactive waste (Didier 2012, Didier et al. 2012, Bardelli et al. 2014, Mondelli et al. 2015). The results of these studies show that dry montmorillonite can adsorb up to 0.2 wt% H_2 (or 5 kgH_2/m^3 – density of mont-morillonite = 2.4) at 30 bar H_2 pressure and at 90°C (Figure 1-11). Having in mind that temperature increase drastically decreases the amount of hydrogen adsorbed, one may expect a better storage capacity at room temperature or below. These measurements reveal hydrogen sorption isotherm comparable to what is obtained with MOFs under similar pressure-temperature conditions (e.g. Collins and Zhou 2007). Despite being far less studied than MOFs, clay minerals seem to be very promising materials for hydrogen storage as they display similar sorption capacity as MOFs albeit being 1 000 times less expensive (Edge et al. 2014).

Hydrogen sorption onto dry clay rock can reach ~0.1% in weight (Bardelli et al. 2014), a similar value to methane and CO_2 sorption onto clay-rich media (Didier et al. 2012) (Figure 2-12). However, water competes strongly with H_2 for adsorption on hydrophilic clay surfaces, and in water fully saturated conditions, H_2 diffusion measured in undisturbed Boom Clay and COx cores showed no sorption effects (Didier et al. 2012; Jacops et al. 2015). Neutron scattering has revealed the structure and dynamics of molecular hydrogen physisorbed in the interlayer space of montmorillonite and laponite (Bardelli et al. 2014; Mondelli et al. 2015; Edge et al. 2014). Up to four hydrogen molecules coordinate directly to partially solvated interlayer Ca^{2+} cations. Hydrogen transport occurs via a jump diffusion mechanism leading to a H_2 diffusion coefficient an order of magnitude slower than in bulk liquid water (Edge et al. 2014).

EURAD (Deliverable n° 6.1) – Initial State of the Art on Gas Transport in Clayey Materials
Dissemination level: PU
Date of issue of this report: 17/11/2021

Page 75
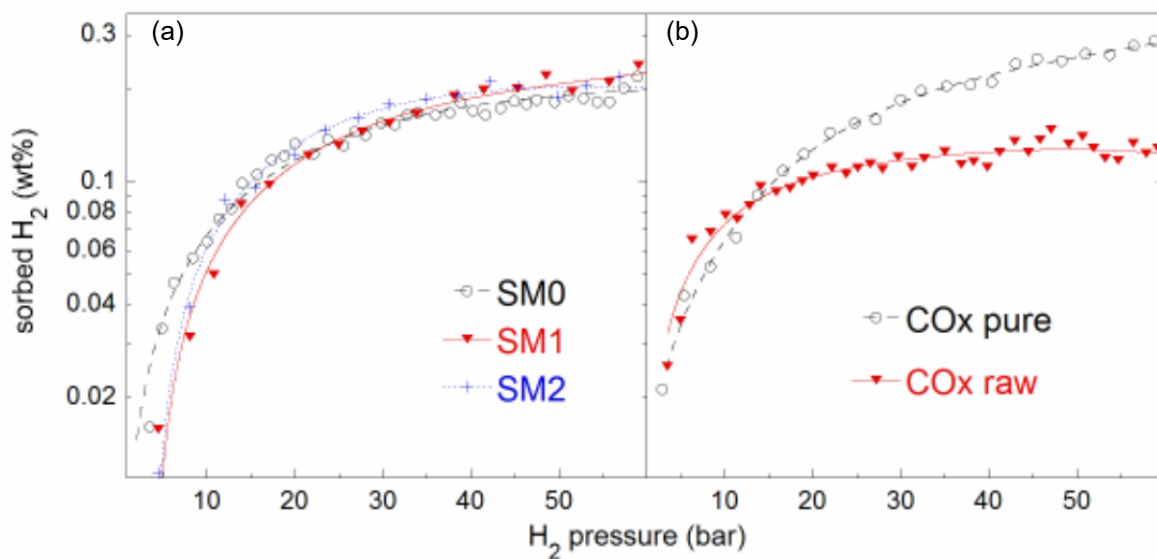
Figure 2-11 – High pressure volumetric measurements of hydrogen adsorption performed (a) on synthetic montmorillonite (SM0, SM1 and SM2) and (b) on natural Callovo-Oxfordian claystone (COx) as raw bulk rock, and on purified clay component of COx (Didier 2012; Didier et al. 2012).
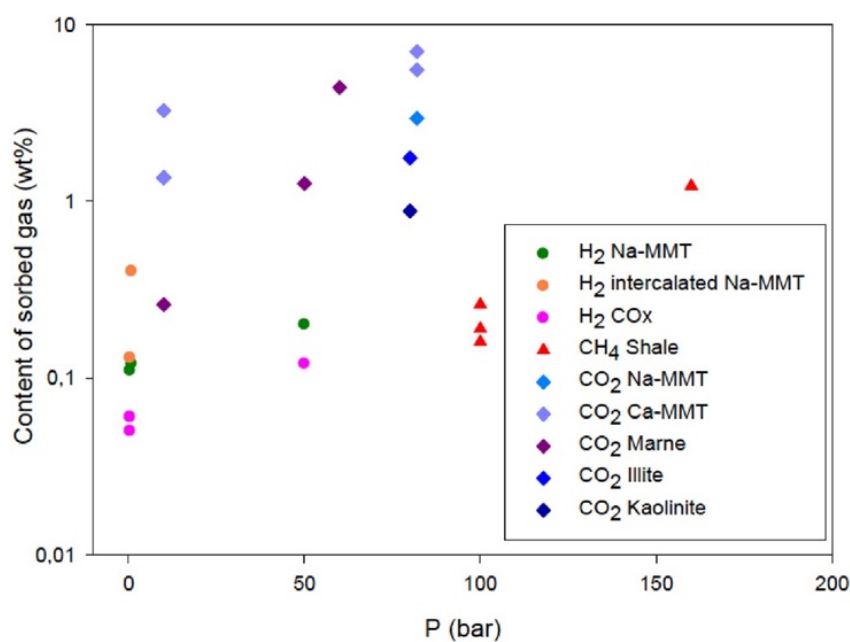
Figure 2-12 – Adsorption isotherms of hydrogen, methane and carbon dioxide on clays and clay rock. MMT: montmorillonite. COx: Callovo-Oxfordian. Data from Didier et al. (2012).

EURAD (Deliverable n° 6.1) – Initial State of the Art on Gas Transport in Clayey Materials
Dissemination level: PU
Date of issue of this report: **17/11/2021**

Page 76

Recently, a natural enrichment in hydrogen was revealed in the clay alteration halo surrounding the Cigar Lake uranium deposit, located in the Athabasca province, Canada (Truche et al. 2018). This study was initially motivated by an industrial issue at the production site related to a release of hydrogen in the plant during the processing of the ore. It was demonstrated that hydrogen, produced by water radiolysis at the contact of the massif and focus uranium ore body, is naturally trapped in the surrounding rocks at a concentration reaching up to 0.05 wt% (Figure 1-13). The acidic dissolution of the rocks during ore processing causes the release of hydrogen. At first glance, these levels remain rather low, but three important facts have to be taken into account:

- First, the rocks surrounding the deposit are not made of 100% clay. The measured H_2 sorption rates (up to 0.05 wt%) is an average value that applies to the total rock and not to a given purified clay phase. The alteration halo surrounding the deposit contains between 50 and 80% of a mixture of clay composed of illite and sudoite (magnesium di-trioctahedral chlorite), the remaining part being mainly composed of uraninite (uranium oxide), tourmaline, iron oxide, and micas. At present, we do not know exactly where hydrogen is adsorbed, even if the clay phases (illite and/or sudoite) are the main candidates with regard to their abundance and their sorption properties. Anyway, we can logically assume that the rate of H_2 sorption on a pure phase will be greater than on the bulk rock. Figure 2-11(right graph) shows, for example, that the clay component (interstratified illite/smectite) of a claystone adsorbs three times more H_2 than the bulk claystone itself (composed of interstratified illite/smectite, quartz and calcite in similar proportion). Illite and sudoite, have very different morphologies than montmorillonite hitherto investigated for H_2 sorption. Indeed, these two clay phases have no or few interlayer sites, but have large basal areas and contrasting morphologies, particularly regarding their border sites. In addition, the sudoite is a di-trioctahedral type of clay, thus it presents vacancies in its octahedral sites. The presence of these vacancies may represent favourable sites for H_2 trapping. It is also important to note that the formation of the argillaceous alteration halo (dated at 1.3 Ga) is synchronous with the emplacement of the deposit at the unconformity between the crystalline basement and the sedimentary cover. Clays have therefore undergone numerous disturbances over the different geological events that have affected the region. These disturbances (tectonic, geochemical, mechanical) may have contributed to the release of some of the hydrogen produced outside the mineralised zones. Much higher hydrogen contents are expected in the presence of pure clay phases (e.g. illite, sudoite) having well-constrained morphological and crystallographic characteristics.

- Second, the clays present in the deposit are totally saturated with water. It is clearly established that the presence of water is an unfavourable factor for H_2 sorption. The effect of relative humidity or water saturation is expected to decrease this sorption effect. Although, the few available data (Didier 2012) have been collected on apparatus with leakages, we can figure out that dry Cigar Lake's clays can adsorb at least 0.5 wt% H_2, which brings us closer to the values of interest for hydrogen storage. Note that the current temperature at the deposit is around 20°C, and that hydrogen partial pressure is probably around one bar based on dissolved hydrogen measurements made in the aquifer.

- The clays of the deposits contain other gases (e.g. CO_2, CH_4, H_2S) that occupy some sorption sites and thus reduce the amount of potentially adsorbable hydrogen at saturation.

EURAD (Deliverable n° 6.1) – Initial State of the Art on Gas Transport in Clayey Materials
Dissemination level: PU
Date of issue of this report: 17/11/2021

Page 77
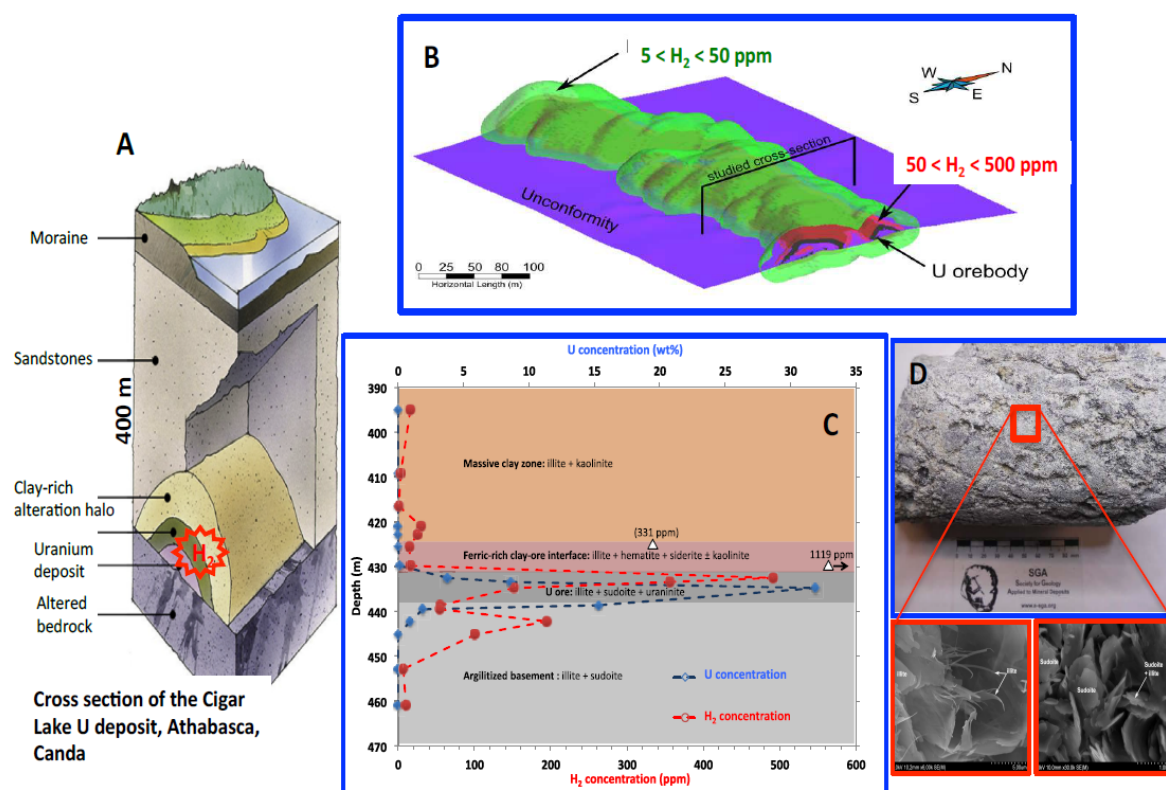
Figure 2-13 – (a) schematic 3D view of the Cigar Lake uranium deposit (Athabasca, Canada) displaying the different surrounding lithologies. (b) 3D map of the hydrogen (H_2) content around the deposit. (c) adsorbed hydrogen (red dots) and U (blue dots) concentrations as a function of depth along one borehole crosscutting the U orebody. (d) In blue: photo of a rock core sample (few centimetres) from the altered bedrock on which the hydrogen desorption measurements have been carried out; in red, scanning electron micrographs showing the texture, at a scale of a few microns, of the clay minerals (illite and sudoite) present in the rocks surrounding the deposit on which the hydrogen is adsorbed (Truche et al. 2018).

2.3.3   Shared understanding of gas sorption

Molecular sorption of H_2 onto clay aggregates is recognised as a retardation mechanism, which could contribute as a favourable feature to the long-term safety functions of clayey barrier materials. Thus, gas pressure build-up could be reduced and the transport of volatile radionuclides in the free gas phase would be retarded.

2.3.4   Uncertainties and knowledge gaps

Hydrogen adsorption on claystone at room temperature and few tens of bars does not seem to be negligible as it may reach up to 0.1 wt% under such conditions (Didier 2012; Bardelli et al. 2014). However, these measurements display surprisingly high value when compared to MOFs, activated carbon or zeolite materials under the same conditions (Voskuilen et al. 2012). In addition, H_2 uptake by COx claystone seems to be slightly enhanced at 90°C when compared to 25°C (Bardelli et al. 2014). This latter observation is in contradiction with the plethora of measures available on gas adsorption on porous material. The effect of relative humidity or water saturation is expected to decrease this sorption effect, but again the few available data (Didier 2012) have been collected on apparatus where leakages were manifest. Currently, the quality and quantity of the available data on H_2 adsorption on natural claystone is insufficient for a robust assessment of this phenomenon. There is a need to develop robust

EURAD (Deliverable n° 6.1) – Initial State of the Art on Gas Transport in Clayey Materials
Dissemination level: PU
Date of issue of this report: 17/11/2021

Page 78

protocol for H_2 isotherm measurements as a function of temperature, pressure and relative humidity. In addition, the contribution of the claystone organic content to H_2 uptake has not been evaluated either.

In the past, limited experimental data bases and the complexity of the associated phenomena and processes have been the reason for neglecting molecular sorption in the assessment of repository performance. From the perspective of long-term safety this can be seen as a conservative approach. However, for repository concepts, which are particularly vulnerable with regard to gas pressure build scenarios, it might be worth evaluating the scientific basis of H_2 sorption and the associated consequences in repository evolution scenarios.

EURAD (Deliverable n° 6.1) – Initial State of the Art on Gas Transport in Clayey Materials
Dissemination level: PU
Date of issue of this report: 17/11/2021

Page 79

2.4 Gas flow through clayey materials

This section presents gas transport 'from the perspective of the gas'.

2.4.1 Visco-capillary two-phase flow

2.4.1.1 Two-phase flow concept

In its conventional form, visco-capillary two-phase flow[14] is described as a transport process whereby pore water in the pore volume of a rock formation is displaced by gas under the influence of viscous and capillary forces (e.g. Bear 1972). As stated briefly in Section 1.4.1.3, the propagation of the gas front in an initially fully saturated porous medium is controlled by the complex interaction of viscous forces, capillary forces and gravity. Intensive research activities have been undertaken in the fields of oil and gas industry and subsurface science and engineering, with the aim to analyse and classify the governing processes of immiscible fluid flow in porous media (see for example Lenormand et al. 1988; Méheust et al. 2002; Glass et al. 2001). Lenormand et al. (1988) conducted two-phase flow experiments for a wide range of capillary numbers *Ca* and viscosity ratios *M* defined as:

$$Ca = \frac{viscous \rightleftarrows forces}{capillary \rightleftarrows forces} = \frac{\mu_{wf} \cdot v_f}{\gamma_{wf,\rightleftarrows nwf}}$$

$$M = \frac{\mu_{defending}}{\mu_{invading}}$$

(2-10)

where μ_{wf} and μ_{nwf} represent the viscosities of the wetting and non-wetting fluid [Pa.s], v_f is the characteristic (Darcy) velocity in the medium [m/s], $\gamma_{wf,\rightleftarrows nwf}$ is the surface tension between the two fluids [N/m], $\mu_{defending}$ is the viscosity of the defending fluid and $\mu_{invading}$ is the viscosity of the invading fluid [Pa.s]. Lenormand et al. (1988) identified three major flow regimes in the *Ca-M*-space, which they coined stable displacement, viscous fingering and capillary fingering (Figure 2-14) (Lenormand et al. 1988):

- Stable displacement: the viscosity of invading fluid, higher than the one of the defending fluid, controls the invasion process. The invasion pattern is rather flat, with some irregularities.

- Viscous fingering: the viscosity of the defending fluid, higher than the one of the invading fluid, controls the invasion process. The invasion pattern contains 'fingers' with side branches but without loops, growing towards the exit.

- Capillary fingering: the capillary forces control the invasion process, as at low capillary numbers, the viscous forces are negligible. The invasion pattern also contains 'fingers' but growing in all directions, forming loops.

The regime of stable displacement applies for the special case where the invading fluid has a higher viscosity than the defending fluid as for example water imbibition in a gas-filled porous medium[15]. Viscous and capillary fingering are associated with instable displacement of a wetting fluid by the non-wetting fluid, giving rise to phenomena such as migration, fragmentation and coalescence of the non-wetting fluid (Wagner et al. 1997). When a gas front invades the initially saturated matrix of a low-

---

[14] Note, the more general term "flow of immiscible fluids in porous media" is often used in fluid mechanics and in reservoir engineering.

[15] Relevant for resaturation processes in the repository near-field (out of scope of this document)

EURAD (Deliverable n° 6.1) – Initial State of the Art on Gas Transport in Clayey Materials
Dissemination level: PU
Date of issue of this report: **17/11/2021**

Page 80

permeability host rock, capillary fingering can be assumed as the prevailing regime. On the other hand, gas release through a re-activated fault or along the EDZ and the backfilled underground structures may be associated with viscous fingering, a process which creates a distinct precursor flux (early gas breakthrough). This phenomenon is of potential relevance for the transport of volatile radionuclides.
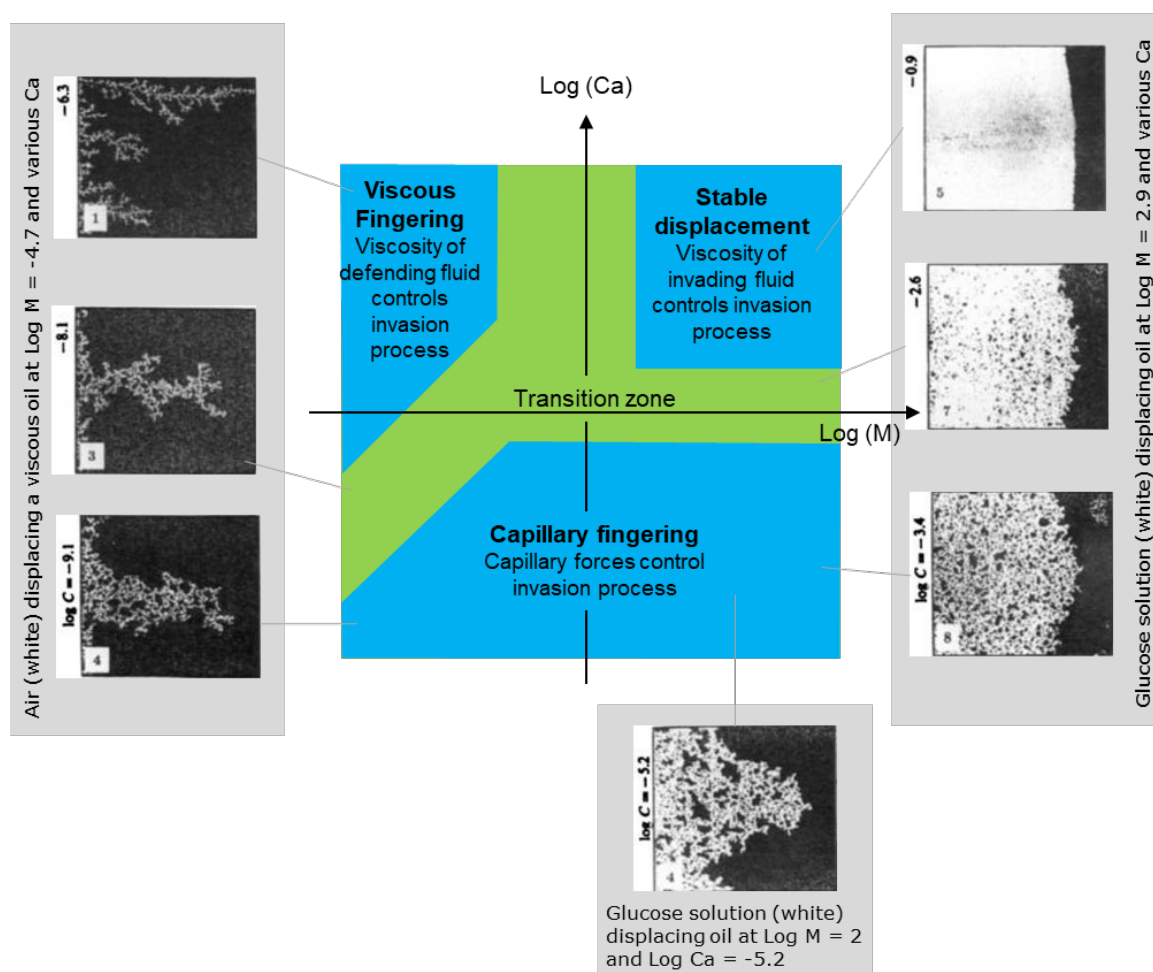
Figure 2-14 – Schematic representation of the three major flow regimes in the Ca-M-space after Lenormand et al. (1988): viscous fingering, capillary fingering and stable displacement.

Two-phase flow conditions are then encountered when gas can invade a water-filled rigid porous medium as a separate phase. To enter the porosity, gas has to displace water, overcoming capillary effects. The pressure required for this, called the *gas entry pressure,* is the difference between the pressure in the non-wetting phase (here the gas), and the pressure in the wetting phase (here the pore water). It represents thus the difference between gas pressure and water pressure ($P_g - P_w$) needed to displace the pore water from the initially fully saturated medium. This displacement of water leads to (partial) desaturation of the rock matrix. The gas entry pressure corresponds to the matric suction above which actual desaturation begins and the water content starts to decrease. This two-phase flow is often called 'visco-capillary two-phase flow'.

The gas entry pressure strongly depends on the connected pore size: the smaller the connected pores, the higher the capillary effects and the gas entry pressure.

EURAD (Deliverable n° 6.1) – Initial State of the Art on Gas Transport in Clayey Materials
Dissemination level: PU
Date of issue of this report: **17/11/2021**

Page 81

Busch and Amann-Hildenbrand (2013) conceptualised the purely capillary-controlled invasion of a non-wetting (gas) phase into a fully water-saturated medium as illustrated in Figure 2-15:

- Once the gas pressure increases up to the gas entry pressure, the gas phase starts to displace water from the pore system.

- Upon further gas pressure increase, the gas phase displaces the water out of larger pores first.

- When a continuous non-wetting phase has developed throughout the pore network, viscous gas flow is initiated (breakthrough pressure (not illustrated)).

- Higher capillary pressures lead to further desaturation and correspondingly higher gas flow rates until maximum desaturation is reached. Upon desaturation, the porous medium contains two immiscible fluids, water and gas, each at a different saturation. The extent to which the fluids are in contact with the pore walls is determined by the interfacial tension, between the fluid phases (water, gas) and the wetting angle (measured in the denser fluid phase). Generally, water, which is the wetting fluid, occupies the smallest pores and is in direct contact with the pore walls while the non-wetting fluid (gas) tends to minimise its contact area with the pore walls.

- A decrease in pressure leads to the resaturation of water, reducing the interconnected flow pathways of the gas until flow stops (shut-in pressure). Trapped amounts of the gas within the pore network lead to a saturation hysteresis between the first drainage and resaturation process as well as after successive drainage/resaturation cycles (repetitive gas pressure build-up, gas pressure release, and decrease).

The hysteresis phenomenon is related to two different processes: water retention within the pore network by capillary forces and adsorption (Daïan 2010; M'Jahad 2012). The first desaturation cycle (drainage) can be described by (1) the initial viscous water displacement, and (2) by desorption down to (theoretically) full drying. Upon resaturation, natural porous materials do not regain the same water saturation. This phenomenon is independent of the type of resaturation, i.e. change of capillary pressure or relative humidity and is a consequence of the complex arrangement of small pore throats and larger pore bodies (Romero et al. 1999; Diamond 2000; Hildenbrand et al. 2002; Espinosa and Franke 2006; Ishida et al. 2007; Ma et al. 2020). During resaturation, gas bubbles are trapped within the pore space due to the existence of small pore throats, the so-called bottle neck effect (shut-in) (Kleppe et al. 1997; Diamond 2000; Luo et al. 2008). Therefore, water saturation at a given pressure is higher during first desaturation than along any subsequent drainage/resaturation process.

EURAD (Deliverable n° 6.1) – Initial State of the Art on Gas Transport in Clayey Materials
Dissemination level: PU
Date of issue of this report: **17/11/2021**

Page 82
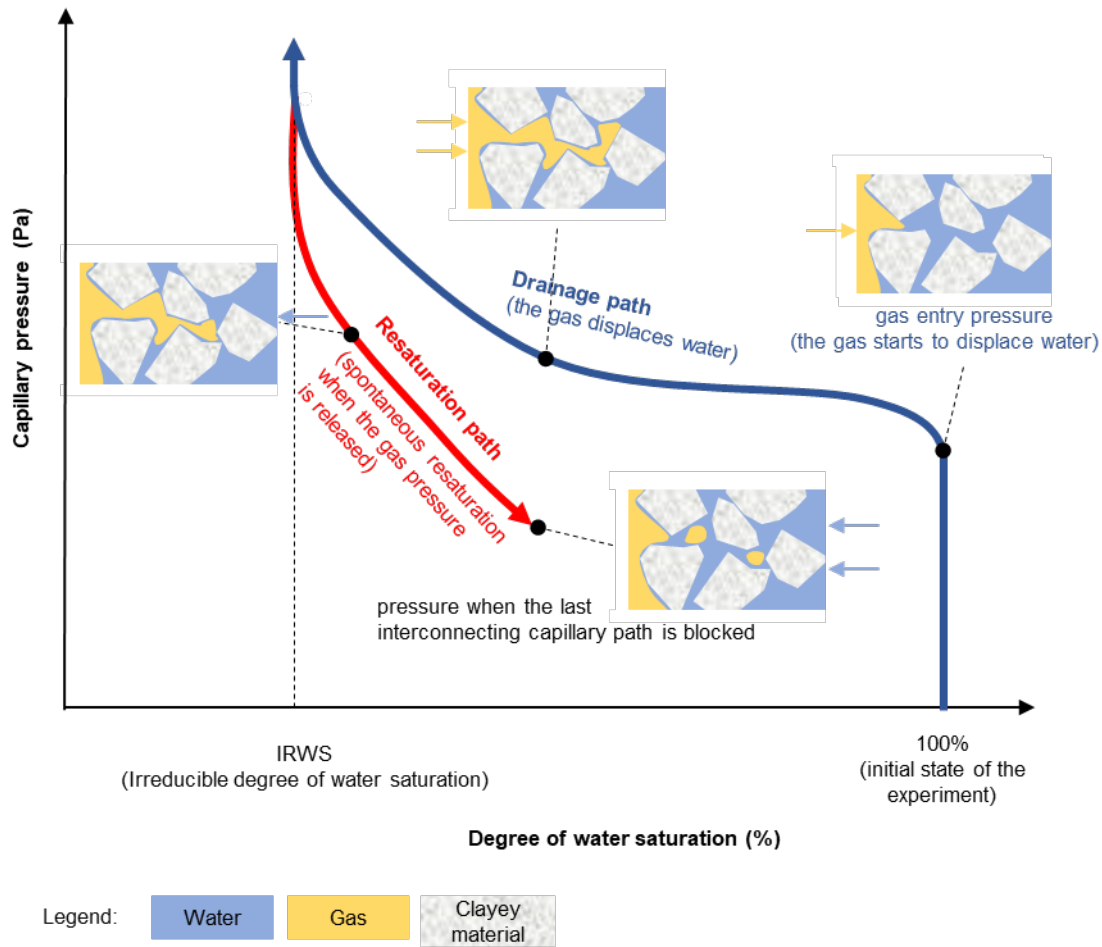
Figure 2-15 – Conceptual sketch of capillary processes in clayey materials. The graph shows the evolution of the capillary pressure as a function of water saturation in a stepwise desaturation and resaturation experiment starting with a fully saturated sample. The blue line marks the drainage path, where the gas displaces the water (increasing capillary pressures). The red line describes the resaturation path (decreasing capillary pressures).

Gas entry pressure can be estimated from water retention curve (obtained through stepwise desaturation and resaturation experiments), corresponding to the relation between the amount of water present in soil pore space (quantified by the degree of saturation of liquid $S_{r,w}$ or the water content w) and the soil suction s (linked to capillary pressure). Water retention functions ('suction' curves) describe the capacity of a porous medium to retain water at a given suction. The matrix suction s is defined by the difference between the gas and water pressures in the pore. This water retention curve can be fitted by for instance a van Genuchten-type relationship defined as a relation between the degree of saturation and the soil suction (van Genuchten 1980):

$$S_{r,we} = \frac{S_{r,w} - S_{res}}{S_{max} - S_{res}} = \left(1 + \left(\frac{s}{P_r}\right)^{\frac{1}{1-m}}\right)^m \tag{2-11}$$

where $S_{r,w}$ is the water saturation, $S_{r,we}$ is the effective saturation of porous media, S_{res} is the residual degree of saturation, S_{max} is the maximum degree of saturation, s the suction, P_r is the gas entry pressure and m is a shape parameter. Hence, gas entry pressure corresponds to the suction for which the desaturation becomes significant. It represents the difference between gas pressure and water pressure ($P_g - P_w$) needed to displace the pore water from the initially fully saturated medium.

EURAD (Deliverable n° 6.1) – Initial State of the Art on Gas Transport in Clayey Materials
Dissemination level: PU
Date of issue of this report: **17/11/2021**

Page 83

Such water retention curve linking saturation and suction is very important to model water flow in unsaturated media. However, a large number of experiments provide instead the evolution of the matrix suction with volumetric water content, i.e. the soil water characteristic curve (SWCC), that can also be fitted by a van Genuchten-type relationship defined as a relation between the soil matrix suction and volumetric water content such as:

$$S_{r,we} = \frac{\theta - \theta_r}{\theta_s - \theta_r} = \left(\frac{1}{1 + (\alpha\, s)^n}\right)^{1-n^{-1}} \qquad (2\text{-}12)$$

where θ_s is the saturated volumetric water content, θ_r the residual volumetric water content, $S_{r,we}$ the effective saturation, s is the suction and α and n are the van Genuchten parameters (Benson et al. 2014).

The parameters α, n, and θ_r are generally obtained by non-linear regression of Equation 2-12 on the soil water characteristic curve, whereas the saturated volumetric water content θ_s is obtained by weight-volume relationships. The α parameter is related inversely to the air entry suction for drying (s_a, suction at which soil begins to de-saturate) or the water entry suction for wetting (s_w), the n parameter describes the slope of the SWCC for $s > s_a$ or s_w, and θ_r describes the lowest practically attainable water content (as defined on Figure 2-16).
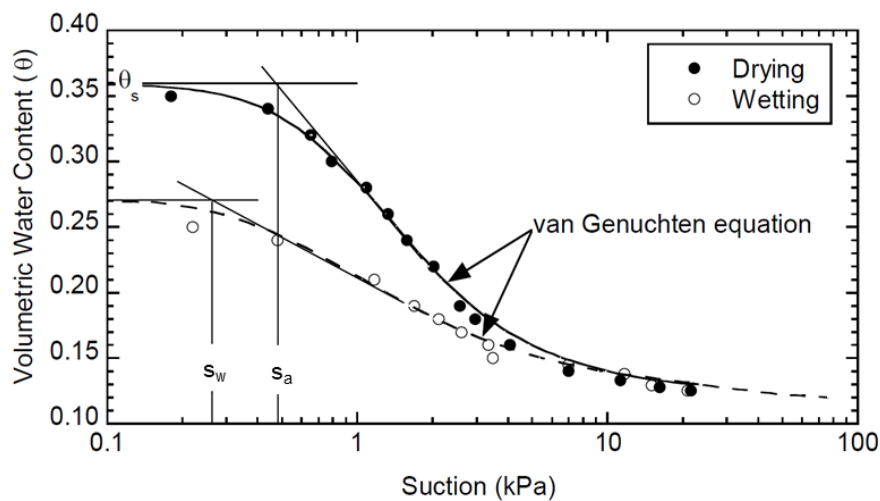
Figure 2-16 – Example of soil water characteristic curve (SWCC) showing fit of van Genuchten equation and air entry suction (s_a), water entry suction (s_w), and saturated water content (θ_s) (Benson et al. 2014).

The transition from Equation 2-11 to Equation 2-12 can be done by assuming a fixed porosity value (Equation 2-13. However, this assumption may sometimes lead to saturation higher than 100%.

$$\phi = \frac{\rho_d}{\rho_w} \frac{w}{S_{r,w}} \qquad (2\text{-}13)$$

where ϕ is the porosity [–], w the water content [-], ρ_d and ρ_w are respectively the density of the dry and wet porous media [kg/m³], and $S_{r,w}$ the saturation degree.

EURAD (Deliverable n° 6.1) – Initial State of the Art on Gas Transport in Clayey Materials
Dissemination level: PU
Date of issue of this report: 17/11/2021

Page 84

A special form of the Young Laplace equation for cylindrical capillaries describes the relationship between the capillary pressure (P_c) and the (equivalent) capillary radius (r) invaded by the gas phase at this particular pressure:

$$P_c = P_g - P_w = 2\,\gamma\,\frac{\cos\theta}{r} \tag{2-14}$$

with γ the water/gas interfacial tension [N/m], θ the wetting angle, and r the radius [m] of a cylindrical pore.

This equation can be used to describe the purely capillary-controlled invasion of a non-wetting (gas) phase into a fully water-saturated medium.

Once the gas entry pressure has been exceeded, the gas mobility is controlled mostly by the effective gas permeability which is defined as the intrinsic permeability of the formation multiplied by the relative permeability. The notion of intrinsic permeability in clayey materials has to be used with caution as it depends on the microstructure of the clay which varies between saturated and unsaturated state (Tindall and Kunkel 1999; Villar and Lloret 2001). Here, it refers to the permeability of the saturated medium. The relative permeability is a dimensionless term devised to adapt the Darcy equation to multiphase flow conditions. It is expressed, for instance, by a van Genuchten-type permeability-saturation relationship such as:

$$k_{rw} = \sqrt{S_{r,w}} \cdot \left[1 - \left(1 - S_{r,w}^{\frac{1}{m}} \right)^{m} \right]^{2} \tag{2-15}$$

where k_{rw} is the relative permeability [–], $S_{r,w}$ the degree of saturation of the porous media [–] and m a shape parameter.

The multiphase fluid flow is generally modelled by combining the continuity equation for each phase with the generalised form of Darcy's law and the constitutive equations for relative permeabilities and capillary pressures between phases (Parker 1989). The continuity equation for each phase is given by:

$$\frac{\partial}{\partial t} (\phi\, \rho_i\, S_i) + \nabla\,(\rho_i\, q_i) = \gamma_i \tag{2-16}$$

where ϕ is the medium porosity [–], ρ_i is the phase density for phase i [kg/m³], S_i is the saturation of phase i [–], q_i is the Darcy velocity vector for phase i [m/s], and γ_i is a source-sink term for mass transfer between the phases and any external sources.

Darcy's law for phase i is expressed as

$$q_i = -\,\frac{k_{ri}\, k}{\mu_i}\, \nabla\,(P_i + \rho_i\, g\, z) \tag{2-17}$$

where q_i is the Darcy velocity vector for phase i [m/s], k_{ri} is the relative permeability of phase i [–], k is the intrinsic permeability tensor, μ_i is the dynamic viscosity of phase i [Pa s], P_i is the pressure in phase i [Pa], and g is the acceleration due to gravity [m/s²].

EURAD (Deliverable n° 6.1) – Initial State of the Art on Gas Transport in Clayey Materials
Dissemination level: PU
Date of issue of this report: **17/11/2021**

Page 85

2.4.1.2 State of knowledge for Boom Clay

2.4.1.2.1   Pore size distribution

The Boom Clay pore network has been characterised by Gonzalez-Blanco (2017), among others, by mercury intrusion porosimetry (MIP) tests complemented by nitrogen adsorption tests (in this last, the pore size distribution is estimated following the Barrett, Joyner and Halenda (BJH) method using the desorption information). Figure 2-17 shows the cumulative intrusion pore volume normalised by solid volume (intrusion void ratio) plotted against the entrance pore size for Boom Clay intact samples.

From the MIP and BJH methods, the pore size density function (PSD) can be estimated as:

$$PSD = f(logx) = -\frac{de}{d(logx)} \tag{2-18}$$

where *x* represents the entrance pore size. The PSD function obtained from MIP displays one dominant pore size at intra-aggregate scale, as expected for a matrix type microstructure, being around 70 nm. Regarding BJH data, a less important smaller peak is observed around 3 nm (Figure 2-18).
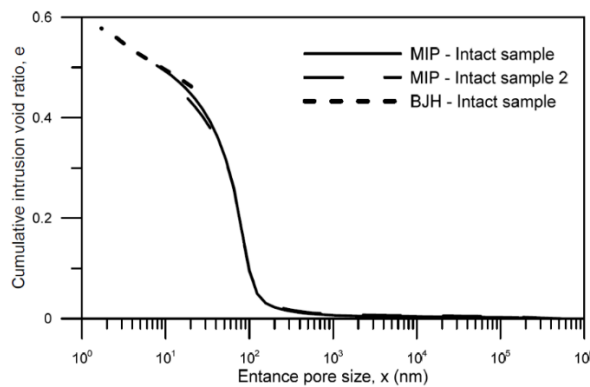

Figure 2-17 – Cumulative intrusion void ratio obtained with MIP and BJH methods (Gonzalez-Blanco 2017).

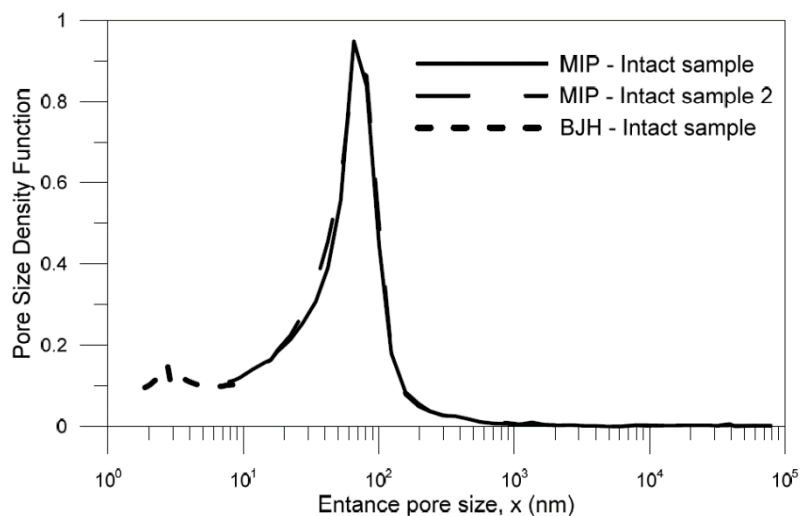*Figure 2-18 – Pore size density function of intact Boom Clay samples (Gonzalez-Blanco 2017).*

EURAD (Deliverable n° 6.1) – Initial State of the Art on Gas Transport in Clayey Materials
Dissemination level: PU
Date of issue of this report: **17/11/2021**

Page 86

2.4.1.2.2　Water retention curve

Water retention curves or 'suction' curves describe the capacity of a porous medium to retain water at a given suction. Water retention properties of Boom Clay, covering a wide suction range and using different complementary techniques for both drying and wetting paths, have been investigated intensively at the Polytechnic University of Cataluña, Spain (Lima et al. 2011; Gonzalez-Blanco 2017) and at the Ecole Nationale des Ponts et Chaussées (ENPC) in France (Le 2008). The results obtained by the two laboratories are generally consistent.

The Boom Clay water retention curve has been estimated by Gonzalez-Blanco (2017) and Le et al. (2008) from a dew-point psychrometer on specimens first dried in steps and then wetted in steps following identical procedure until saturation. Pore size distribution results from MIP tests were used to determine the relationship between matric suction and degree of saturation, as well as the air entry value corresponding to the dominant pore mode.

Figure 2-19 shows the estimated water retention curve which includes curves based on MIP data together with psychrometer measurements and the fitted van Genuchten's equation. The air entry value, corresponding to the dominant pore mode detected from MIP data, was determined using Laplace's equation. Gonzalez-Blanco (2017) estimated the air entry value to be around 4.8 MPa.
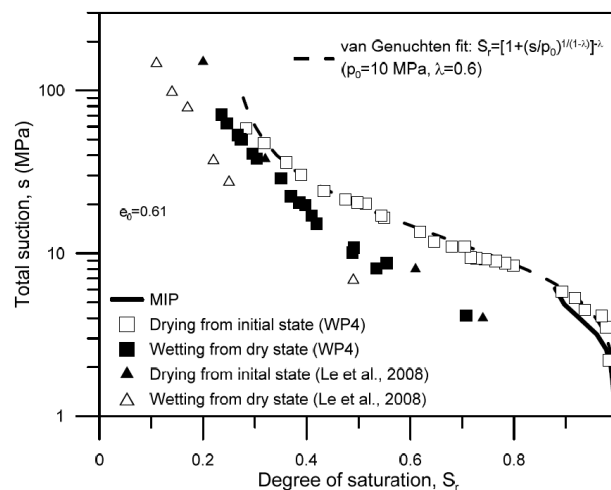
Figure 2-19 – Boom Clay water retention curve (Gonzalez-Blanco 2017).

2.4.1.2.3　Intrinsic and relative permeabilities

The mobility of the liquid/gas phase in the intact Boom Clay (expressed in terms of relative permeability relationships for both phases) has be determined by water and gas permeameter experiments in the laboratory. The intrinsic permeability tensor depends on the pore structure of the porous medium. The value of relative permeability controls the variation of permeability in the unsaturated regime.

The intrinsic permeability of the matrix k_{matrix} can be written in terms of the porosity ϕ through Kozeny's law

$$k_{matrix}(\phi) = k_0 \frac{\phi^3}{(1-\phi)^2} \frac{(1-\phi_0)^2}{\phi_0^{\,3}} \tag{2-19}$$

where k_0 = 4.2 10^{-19} m^2 is the intrinsic permeability for the reference porosity ϕ_0 = 0.363.

EURAD (Deliverable n° 6.1) – Initial State of the Art on Gas Transport in Clayey Materials
Dissemination level: PU
Date of issue of this report: **17/11/2021**

Page 87

By comparing the mean values of air and water intrinsic permeabilities versus the average void ratio for all tests performed by Gonzalez-Blanco (2017) on samples with bedding planes parallel and perpendicular to water flow (Figure 2-20), it can be observed that water intrinsic permeability consistently displayed lower values than air intrinsic permeability values, for both sample orientations. This suggests that air flow takes place along preferential pathways and depends on the volume of this pathway. Higher water intrinsic permeability values were observed when bedding planes were parallel to flow. This was not the case of the air intrinsic permeability values. This highlights the main role played by the deformation of the material along the injection and dissipation stages. Boom Clay intrinsic permeability and its retention curve depend then on strains through pathway aperture changes.
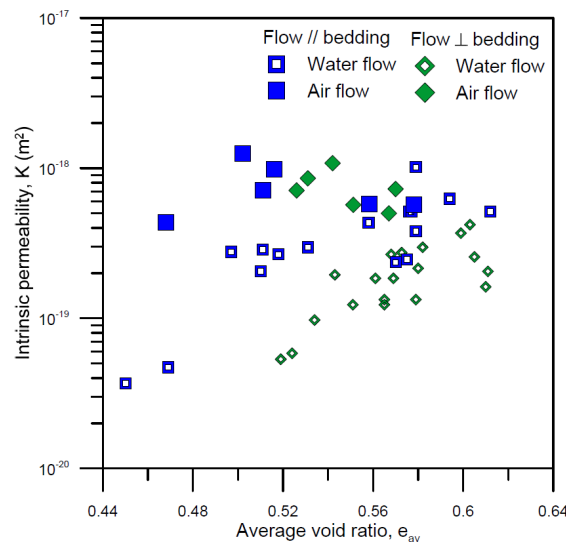
Figure 2-20 – Intrinsic permeability after injection of air or water in direction parallel or perpendicular to the bedding plane (Gonzalez-Blanco 2017).

The relative permeability of liquid and gaseous phases is made dependent on degree of saturation using empirical relationships. According to Delahaye and Alonso (2002), the gas relative permeability of the Boom Clay can be expressed as a generalised power law fitted on Volckaert et al. (1995) experimental data:

$$k_{rg} = A \, (1 - S_{r,w})^{\beta} \qquad\qquad (2\text{-}20)$$

where k_{rg} is the gas relative permeability [–], $S_{r,w}$ is the degree of saturation and A and β are material parameters respectively equal to 1 and 2.8 (see Figure 2-21).

In the terminology of multiphase flow concepts, gas flow is controlled by visco-capillary forces (phase interference between wetting and non-wetting fluid). In case of gas-driven microfracturing, an increase of the pore space is accompanied by a detectable increase in intrinsic permeability and a change in the capillary pressure-saturation relationship. The main difference compared to conventional two-phase flow is that the transport properties of the solid phase (rock permeability, relative permeability, capillary pressure) can no longer be viewed as invariants since they depend on the state of deformation of the rock. The consequences on barrier integrity are developed in Section 3.1.4.1.

EURAD (Deliverable n° 6.1) – Initial State of the Art on Gas Transport in Clayey Materials
Dissemination level: PU
Date of issue of this report: **17/11/2021**

Page 88
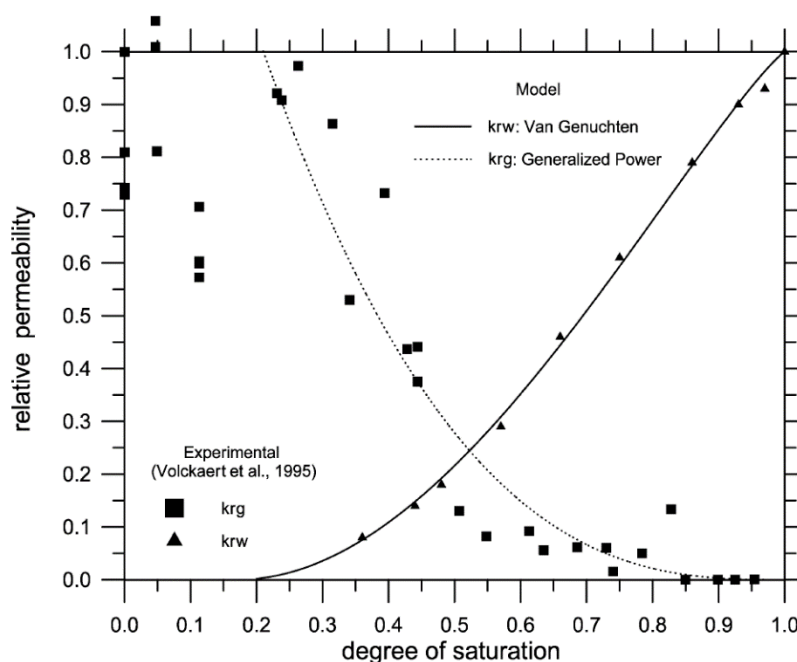
Figure 2-21 – Experimental data for relative permeability in Boom Clay (Volckaert et al. 1995) together with model fitting (Delahaye and Alonso 2002) (k_{rw}: relative permeability of water/liquid phase, k_{rg}: relative permeability of gas).

2.4.1.3 State of knowledge for Callovo-Oxfordian claystone

2.4.1.3.1 Pore size distribution

A good knowledge of the microstructure is needed to well understand gas transfer through Callovo-Oxfordian claystone. The transport of gas through the Callovo-Oxfordian claystone is assumed to only take place within the clay matrix, the other minerals (mainly carbonates and tectosilicates) being considered as nonporous. Within the clay matrix, the pore network is composed of interparticle and inter-aggregate pores with diameters ranging between 1 nm and a few hundreds of nanometres, and the interlayer porosity inside swelling clays (smectite in interstratified illite/smectite) (Sammartino et al. 2003; Yven et al. 2007). Interlayer porosity represents less than 15% of the total porosity in agreement with the relative low content of swelling clay minerals in the Callovo-Oxfordian claystone. At the macroscopic scale, the Callovo-Oxfordian claystone exhibits anisotropy relative to the bedding plane. The thermo-hydro-mechanical (THM) properties such as permeability or diffusion coefficients measured parallel to the bedding plane are in general 1.5 to 3 times higher than those measured perpendicular to the plane. Porosity is studied with different complementary experimental techniques in terms of investigation and resolution scales (Figure 2-22). At field scale, logging techniques such as nuclear magnetic resonance (NMR) have been used to assess the in situ porosity of the host rock. At sample scale, several methods are used to have a quantitative description of the pore network structure such as mercury intrusion porosimetry (MIP), gas/water adsorption or X-ray micro-tomography (µ-CT) that could provide access to 3D pore space organisation. More recently, higher resolutions are available with focused ion beam scanning electron microscopy (FIB-SEM) and transmission electron microscopy (TEM) or scanning transmission electron microscopy (STEM) techniques (Song et al. 2015).

EURAD (Deliverable n° 6.1) – Initial State of the Art on Gas Transport in Clayey Materials
Dissemination level: PU
Date of issue of this report: **17/11/2021**

Page 89
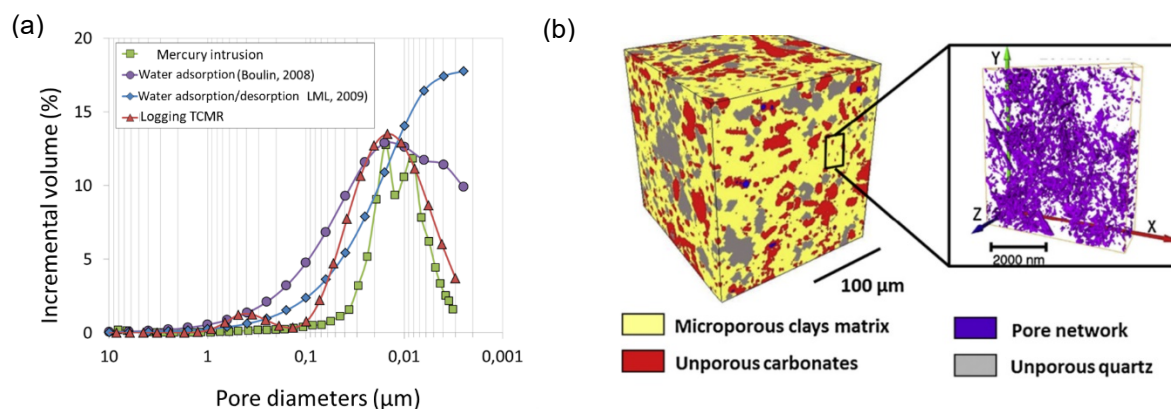
Figure 2-22 – (a) comparison of pore size distributions obtained by different methods for the MHM URL level (Robinet et al. 2012b). (b) observation in synchrotron X-ray micro-tomography, of the clay matrix (yellow) and the quartz (grey) and carbonate (red) inclusions according to Robinet et al. (2012a); 3D reconstruction of the pore network from SEM and FIB images from Song et al. (2015).

Mercury intrusion and extrusion curves representative of the COx claystone at MHM URL level are shown in Figure 2-23.
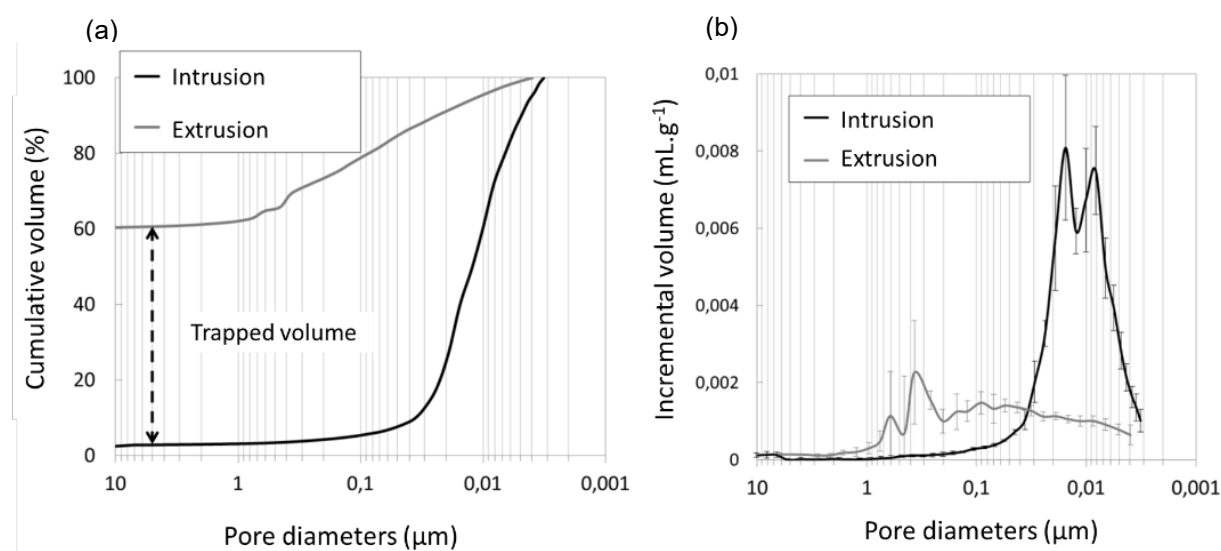
Figure 2-23 – Pore size distribution: average mercury intrusion and extrusion curves for 10 samples from borehole SDZ1270 and 10 samples from hole PGZ 1001. (a) cumulative volume. (b) incremental volume with standard deviation calculations (Robinet et al. 2012b).

2.4.1.3.2   Water retention curve

Gas entry pressure measurements have been performed on samples of different thicknesses (between 10 and 80 mm), under variable confining conditions, for various gas and with different injection rates. The main method used for Callovo-Oxfordian claystone consists in subjecting a water-saturated sample to several levels of gas pressure until a flow rate is detected on the downstream side. Some tests have also been carried out by the residual method following the experimental protocols described in Hildenbrand et al. (2002).

The analysis of the gas breakthrough pressure reveals two groups of values. Pressures between 0.3 and 3 MPa which are representative of damaged material and values of the order of or greater than 5 MPa (Figure 2-24) that can be considered as values approaching the gas entry pressure in sound

EURAD (Deliverable n° 6.1) – Initial State of the Art on Gas Transport in Clayey Materials
Dissemination level: PU
Date of issue of this report: 17/11/2021

Page 90

COx claystone. The knowledge acquired on the microstructure and connectivity of the porous network (Robinet 2008; Song et al. 2015), indicates that these values are probably a minimum for the breakthrough pressure in COx which would be between 6 and 10 MPa. The lower values are representative of a damaged materiel and illustrate the difficulty of conditioning and preparing the COx samples without damaging them (Conil et al. 2018). The gas is very sensitive to the potential presence of micro-cracks and a rigorous protocol is needed to avoid measurements artefacts that could lead to underestimate the gas entry pressure.
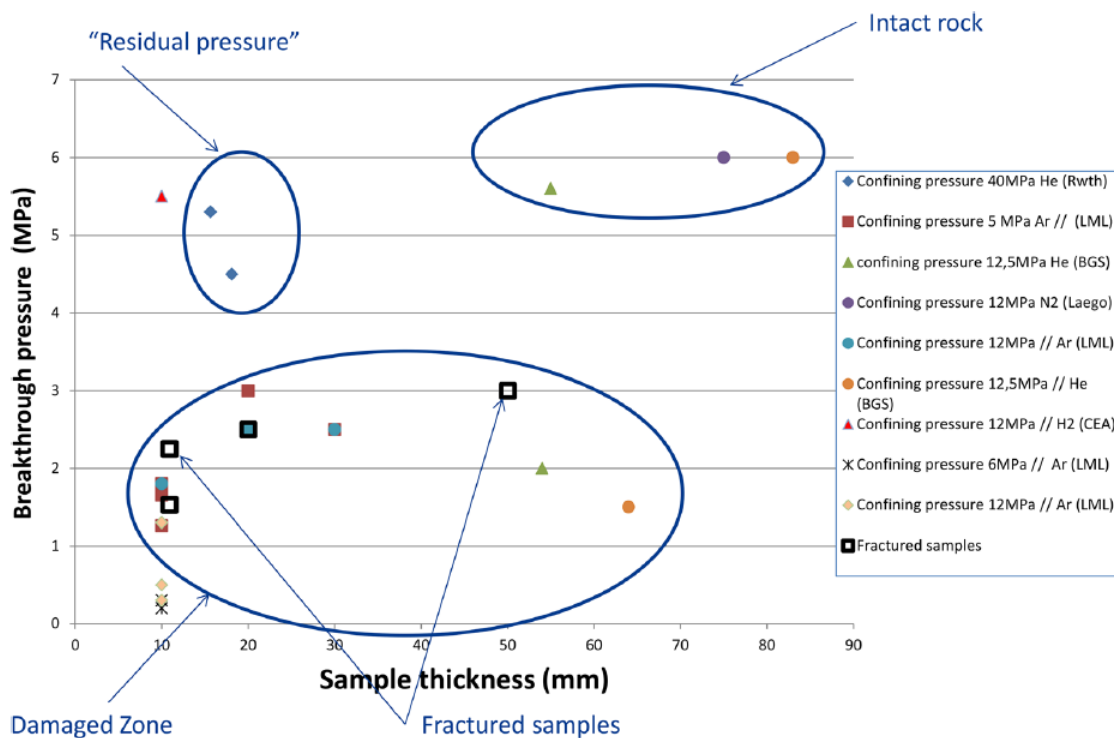
Figure 2-24 – Compilation of gas breakthrough data plotted against sample thickness (Krooss and Alles 2008; Didier 2012; M'Jahad 2012; Cuss et al. 2014; Song et al. 2016).

Many measurements were carried out to define the relationship between suction and water saturation with different technics (Homand et al 2004; Zhang and Rothfuchs 2007; Boulin 2008; Guillon 2011; M'Jahad 2012; Wan et al. 2014; etc.).

The main method used to obtain a relationship between suction and water saturation for COx consists of following the mass evolution of a sample submitted to a controlled relative humidity atmosphere. The monitoring of the mass of the sample gives the progress of the wetting/drying process till an equilibrium state is reached. The measurements are done either at free volume, in which case variations in volume can disturb the measurement at high saturation values due to swelling, or at constrained volume, a situation more representative of in situ conditions. The relationship between relative water permeability and water saturation can be also estimated by monitoring the evolution of mass as a function of relative humidity by inverse numerical calculations.

From the available data, water retention curves for COx in the clay-rich unit are estimated and are fitted with a van Genuchten equation on a wetting path and on a drying path as shown in Figure 2-25. Hysteresis effects depending on the hydration path followed can be observed.

EURAD (Deliverable n° 6.1) – Initial State of the Art on Gas Transport in Clayey Materials
Dissemination level: PU
Date of issue of this report: 17/11/2021
Page 91
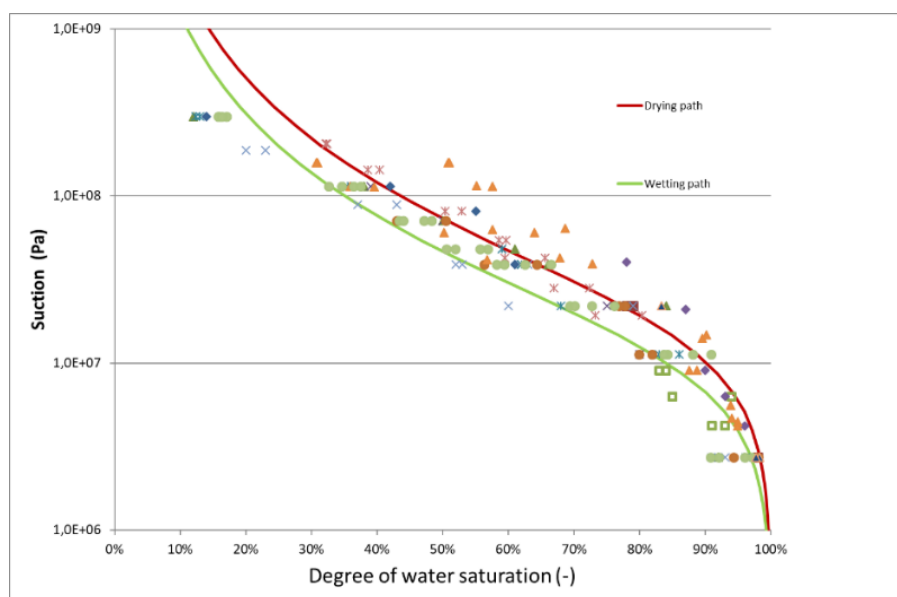
Figure 2-25 – Relation between water saturation and suction: measurements obtained on several samples and fitted by a van Genuchten model on a drying path and wetting path for Callovo-Oxfordian claystone (Armand et al. 2017).

2.4.1.3.3   Intrinsic and relative permeabilities

Many data are available on the effective gas permeability in COx (Zhang et al. 2002; Yang 2008; Boulin 2008; Gerard 2011; Didier 2012). Some of them are shown in Figure 2-26, samples coming from boreholes taken between 404 and 505 metres in the COx layer and whose permeability was measured either perpendicular or parallel to the bedding. It is difficult on these measurements to identify an anisotropy of gas permeability. A part of dispersion in the presented results is mainly due to the sensitivity of the gas measurement to local damages in the samples. Thus, even a small amount of cracking can lead to a significant increase in gas permeability.

A calibration of the permeability curves is done by retaining only the values measured on samples between -480 and -500 metres, with a confinement of 12 MPa which limits the effect of cracking on the permeability. In Figure 2-26b, the selected data and the fitting curves for relative permeability are given using a power law function.

When measuring gas permeability, a correction should be applied considering the Klinkenberg effect. This is induced by collisions between gas molecules and the pore walls in a porous medium. This effect is more important for materials with pores of small sizes compared to the free mean path. The main consequence is a sliding effect on the wall and an overestimation of gas permeability. For low pressures, the correction to be made to the permeability can be significant. To avoid this phenomenon, measurements are generally made at gas pressures of the order of 2 to 3 MPa.

The expression of effective gas permeability k_g [m/s] including the Klinkenberg correction (b = Klinkenberg coefficient in Pa) can be expressed as a function of the gas pressure P_g [Pa] as follow:

$$k_g(P_g) = k_g\left(1 + \frac{b}{P_g}\right)$$

(2-21)

Measurements of the Klinkenberg coefficient as a function of water saturation indicate that the correction to be made to effective gas permeability becomes very small as saturation increases as it was observed by Boulin et al. (2008a) and Didier (2012), see Figure 2-27.

EURAD (Deliverable n° 6.1) – Initial State of the Art on Gas Transport in Clayey Materials
Dissemination level: PU
Date of issue of this report: **17/11/2021**

Page 92

Figure 2-26 – Effective gas permeability as a function of water saturation – (a) compilation of the data set, (b) relative gas permeability fitting with power law and Parker approach.

EURAD (Deliverable n° 6.1) – Initial State of the Art on Gas Transport in Clayey Materials
Dissemination level: PU
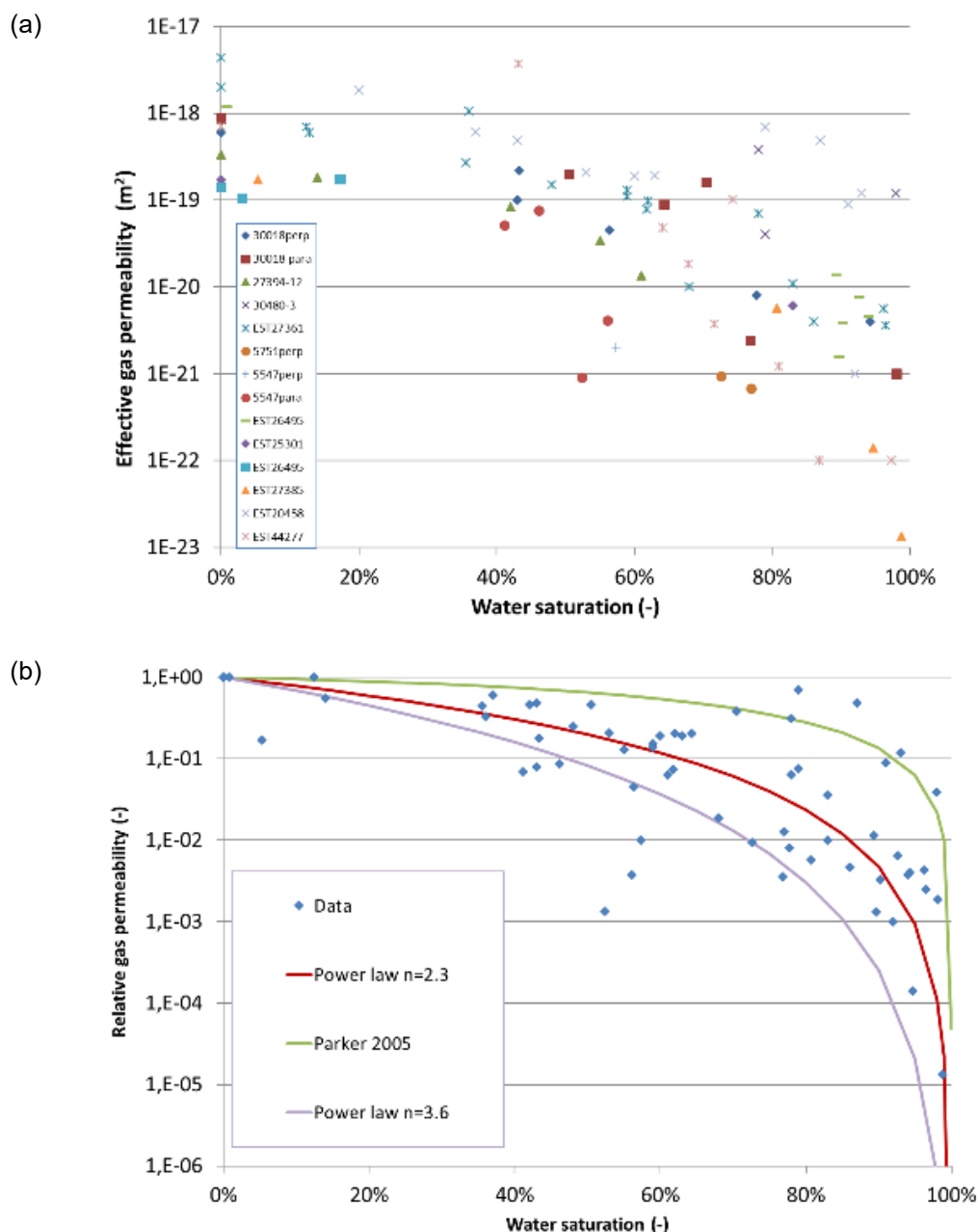Date of issue of this report: **17/11/2021**

Page 93
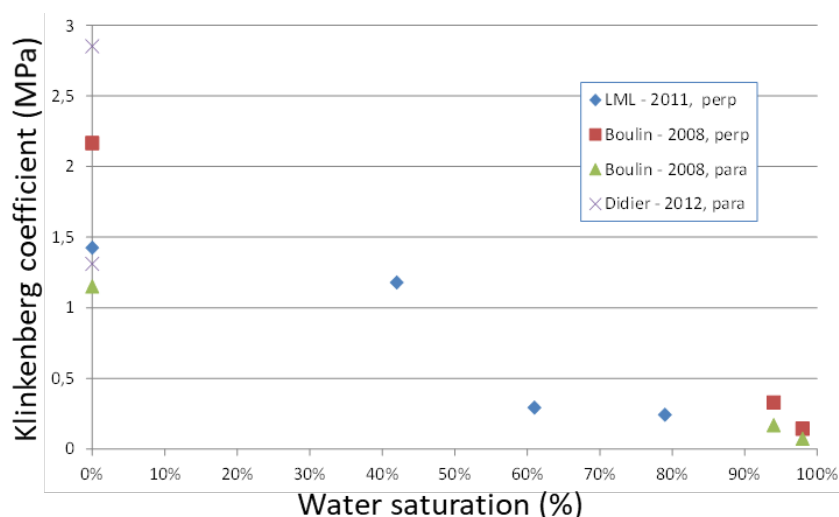
Figure 2-27 – Klinkenberg coefficient for argon as a function of water saturation (COx).

2.4.1.4 State of knowledge for Opalinus Clay

2.4.1.4.1 Pore size distribution

Gas transport in the Opalinus Clay is largely controlled by the microstructure of the rock matrix. A balanced assessment of gas transport processes in the intact rock matrix requires careful consideration of both structure and texture of the rock ranging from the repository scale to the nanometre-scale (see Figure 1-16). Microstructural investigations of the Opalinus Clay have been conducted for all relevant lithostratigraphic sequences ('facies') using complementary methods such as microstructural imaging techniques (X-ray micro-computed tomography (µ-CT), focused ion beam nano-tomography (FIB-nt), transmission electron microscopy (TEM)), water/nitrogen adsorption (BET) and mercury intrusion techniques (MIP).

Microstructural imaging with µ-CT and SEM reveals that the size of the mineralogical components (10^{-7}–10^{-3} m) determines the fabric of the solid skeleton (see also Figure 1-18). Quartz minerals may exhibit grain sizes in the range 0.01–1 mm, whereas the clay minerals form flake-like packages with typical sizes in the order of 100 nm–10 µm. The pore space of the rock is formed by a network of micro/meso- and macropores, which is too small (in the order 1–100 nm) to be shown by FIB-nt and TEM methods. This network of pores actually dominates the flow and transport properties of the rock. Complementary experimental evidence suggests that at least 20% of the total pore water can be attributed to the interlayer water.

Complementary methods were used to characterise the pore space of the Opalinus Clay, such as the measurement of the adsorption/desorption isotherms and mercury porosimetry. To obtain nitrogen and water isotherms, the powder samples were dried at temperatures of at least 120°C and degassed under vacuum. Nitrogen isotherms were measured at 77 K, water isotherms at 303 K by gravimetry in quasi-equilibrium mode, where water vapour was introduced at a constant, low flow rate. The pore size distributions were obtained by incremental saturation of the sample. Table 2-13 depicts the volume fractions of the different pore classes (definition according to IUPAC 1997), indicating that the majority of pores can be classified as mesopores (1–25 nm). The inferred macropore fraction in the order of 20–30% represents the pore space that is relevant for gas transport, because these pores are accessible to gases at moderate gas pressures.

EURAD (Deliverable n° 6.1) – Initial State of the Art on Gas Transport in Clayey Materials
Dissemination level: PU
Date of issue of this report: **17/11/2021**

Page 94

Table 2-13 – Volume fractions of the different pore classes, determined by adsorption and desorption isotherms (H₂O, N₂), after Nagra (2002a).

Class (equivalent radius [nm])	Fraction of pores per class (%)		
	Micropores (<1)	Mesopores (1–25)	Macropores (>25)
N₂-Isotherm	20 (assumed *)	46–56	24–35
H₂O-Isotherm	20 (assumed *)	54–63	17–26
* Assumption: fraction of micropores is 20% (interlayers)			

For mercury porosimetry, Hg was injected at increasing pressures into crushed, dried and degassed samples. Two core samples from Benken and Mont Terri were tested – the equivalent pore size distributions are shown in Figure 2-28b. UPC complemented the MIP analyses by the BJH method using the desorption information from the nitrogen adsorption tests. This provides a wider range of pore size, whereby the spike around 0.004 micron is an artefact due to evaporation of metastable pore fluid (Romero et al. 2012).
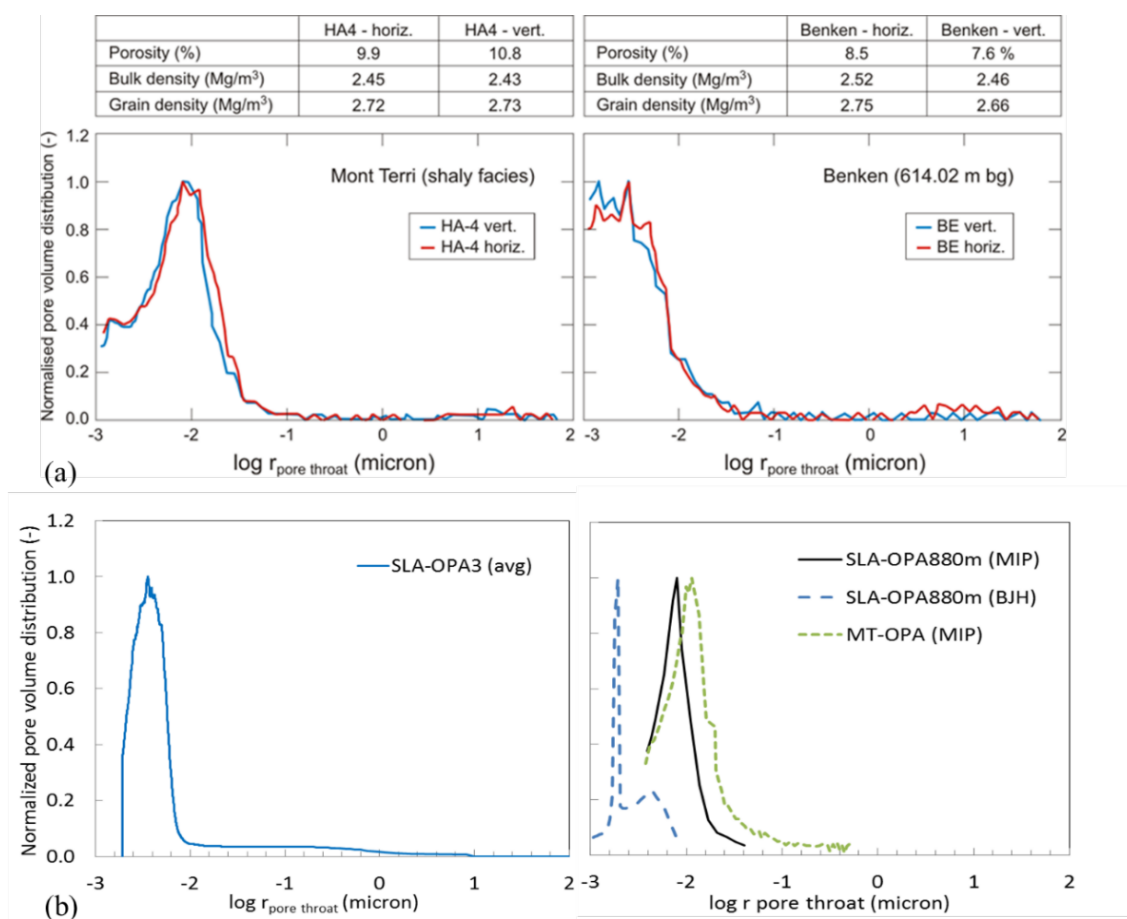
Figure 2-28 – Equivalent pore size distributions of drill core samples: (a) from Benken (sampling depth 614.82 metres below ground) and Mont Terri (shaly facies), determined by mercury intrusion methods at Chevron's laboratories in Houston (by courtesy of Philip Mariotti); (b) from Schlattingen (sampling depth 880 metres below ground), determined by mercury intrusion methods at EPFL (left) and UPC (right), that was complemented by BJH method.

EURAD (Deliverable n° 6.1) – Initial State of the Art on Gas Transport in Clayey Materials
Dissemination level: PU
Date of issue of this report: **17/11/2021**

Page 95

2.4.1.4.2   Water retention curve

Water retention functions ('suction' curves) describe the capacity of a porous medium to retain water at a given suction. Thus, the water retention function represents the water adsorption isotherm. A variety of experimental procedures have been applied for characterising the water retention behaviour of Opalinus Clay. Water retention curves were determined at the geotechnical laboratories of UPC (Universitat Politècnica de Catalunya, Barcelona, Spain), by stepwise desaturation and resaturation of core samples under controlled humidity (Nagra 2002a; Muñoz et al. 2003). A comprehensive experimental programme was accomplished by the laboratories of GRS (Braunschweig), aimed at comparing the capillary pressure – saturation relationships of different clay formations. More recently, the Laboratory for Soil Mechanics at EPFL (Ecole Polytechnique Fédérale de Lausanne) and the Department of Geotechnical Engineering and Geosciences at UPC determined water retention curves as well hydraulic and geomechanical properties of core samples from Mont Terri and from a deep borehole (Ferrari and Laloui 2012; Ferrari et al. 2013; Romero and Gomez 2013). Figure 2-29a depicts a compilation of water retention curves of Opalinus Clay samples from Mont Terri, determined by GRS (Zhang and Rothfuchs 2007), by UPC (Muñoz et al. 2003; Romero and Gomez 2013), and by EPFL (Ferrari et al. 2013). Water retention curves of deep Opalinus core samples (880 metres depth in Schlattingen borehole) are shown in Figure 2-29b using the FDT (Fluid Displacement Technique with Kerdane) for the volumetric determination of the specimen and for the determination of the suction as a function of water content and void ratio. The water retention curves in Figure 2-29c were based on the progressive method (Ferrari et al. 2013), where the wetting and drying paths of the retention curve are obtained on a single specimen from a core. This method better reproduces the hysteretic behaviour compared to the FDT method where the data points are from different specimens, resulting in greater scatter (Figure 2-29c).

Characteristic features of the Opalinus Clay are the high capillary pressures in the order of 10 MPa and the marked hysteresis between wetting and drying path. The water retention measurements are fitted with the van Genuchten model according to Equation 2-12. The fitted parameters in terms of the capillary strength parameter P_0 and the shape parameter n and the corresponding water retention curve, shown in Figure 2-29c, represent the characteristic of the Opalinus Clay at low/moderate depth (e.g. Mont Terri). The corresponding van Genuchten parameters for the deep Opalinus Clay (600–900 metres below ground) are shown in Figure 2-29b&c.

EURAD (Deliverable n° 6.1) – Initial State of the Art on Gas Transport in Clayey Materials
Dissemination level: PU
Date of issue of this report: **17/11/2021**

Page 96
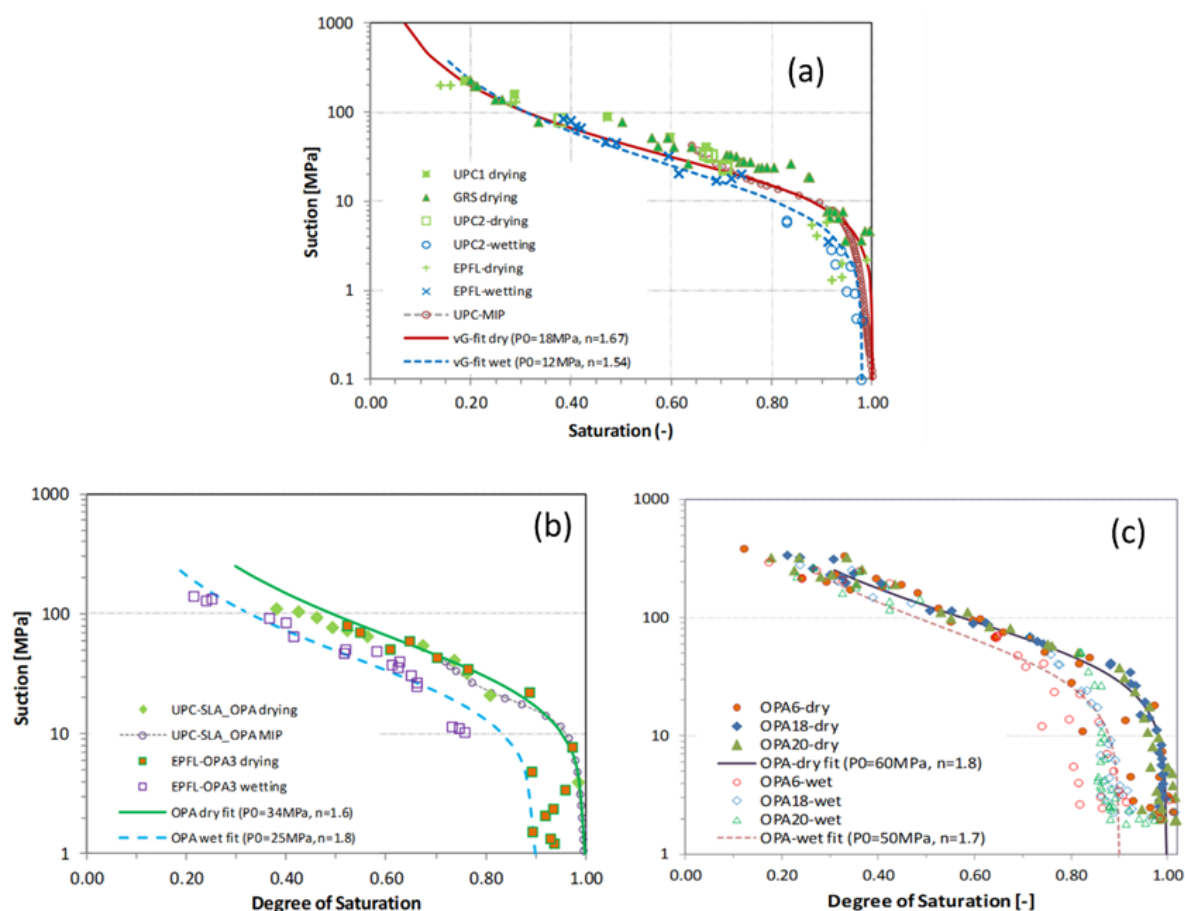
Figure 2-29 – Capillary pressure measurements (water retention curves) by stepwise desaturation and resaturation: (a) experiments by GRS (Zhang and Rothfuchs 2007), UPC (Muñoz et al. 2003; Romero and Gomez 2013) and EPFL (Ferrari and Laloui 2012) using a desiccator for sample equilibration; (b) experiments by Ferrari et al. (2013) and Romero and Gomez (2013) using a WP4c dew-point psychrometer and volumetric measurements with the Kerdane method on deep core samples from the Schlattingen borehole; (c) experiments by Ferrari et al. (2013) using a WP4c dew-point psychrometer and volumetric measurements using the progressive method on a deep core sample from the Schlattingen borehole.

EURAD (Deliverable n° 6.1) – Initial State of the Art on Gas Transport in Clayey Materials
Dissemination level: PU
Date of issue of this report: **17/11/2021**

Page 97

2.4.1.4.3   Intrinsic and relative permeabilities

The mobility of the liquid/gas phase in the intact Opalinus Clay (expressed in terms of relative permeability relationships for both phases) can be determined by water and gas permeameter experiments in the laboratory and by in situ gas injection tests in boreholes. An experimental data base for the derivation of relative permeabilities of the intact Opalinus Clay was elaborated in previous research programmes; the key references of previous experiments are given in Nagra (2002a) and in Marschall et al. (2005). Further experiments and data analyses have been conducted since then as part of the Mont Terri project (Croisé et al. 2006; Poller et al. 2007) and in the context of the NF-PRO and FORGE EC projects (Villar and Romero 2012; Villar et al. 2015, 2019).

Nine gas permeability tests were performed by Villar et al. (2015) in triaxial cells with Opalinus Clay samples. The cores were recovered from borehole BDR-1 in the shaly facies of the Opalinus Clay at Mont Terri with drilling direction perpendicular to bedding. The average dry density of the samples was 2.31 ± 0.04 g/cm^3 and water content of $4.5 \pm 1.8\%$ (i.e. a degree of saturation Sr = $69 \pm 22\%$). The gas injection tests reported showed that the breakthrough pressure in the sense perpendicular to bedding was higher than 18 MPa (effective pressure of 11.5 MPa); gas flow occurred only in a few instances. When this happened, the effective gas permeability measured (intrinsic permeability x relative gas permeability) was in the range from $8 \cdot 10^{-21}$ to $4 \cdot 10^{-23}$ m^2 (average k_g of $1.8 \cdot 10^{-22}$ m²), decreasing very slightly with confining pressure.

New gas permeameter experiments have been initiated in recent years using triaxial test configurations (Romero and Gomez 2013; Minardi 2018). The tests by Romero and Gomez (2013) were conducted with core samples from Mont Terri (overburden around 300 metres) and with Opalinus Clay from a deep investigation borehole in northern Switzerland (Schlattingen borehole; core sample from 880 metres below ground). The tests were conducted in a triaxial cell with flow direction parallel (shallow samples only) and perpendicular to bedding at isotropic stress levels of 15 and 19 MPa, respectively (Romero and Gomez 2013). An example of the gas injection phase with flow parallel and normal to bedding is shown in Figure 2-30. The diagrams display the transient of gas pressure on the injection and outflow side (dotted lines). The gas tests on both, the sample from the shallow and the deep site were subjected to detailed numerical analyses by Romero et al. (2012) and Senger et al. (2014) using a conventional numerical two-phase flow simulator. The numerical simulations successfully reproduced the observed injection/outflow pressure responses for both the test with flow parallel to bedding and for the test with flow normal to bedding (Figure 2-30). The experiments for flow normal to bedding indicated a significant delay on the outflow response after full injection of air volume from the injection chamber as compared to the experiment with flow parallel to bedding that indicated a relatively rapid outflow pressure response. This delay in the outflow pressure response is also observed in core samples from a deep borehole in the Opalinus Clay, on which similar laboratory experiments have been conducted (Romero et al. 2012). The best fitting two-phase flow parameters together with corresponding capillary pressure – saturation relationship and the relative permeability functions are given in Table 2-14.

![eurad logo] European Joint Programme on Radioactive Waste Management

EURAD (Deliverable n° 6.1) – Initial State of the Art on Gas Transport in Clayey Materials
Dissemination level: PU
Date of issue of this report: **17/11/2021**

Page 98
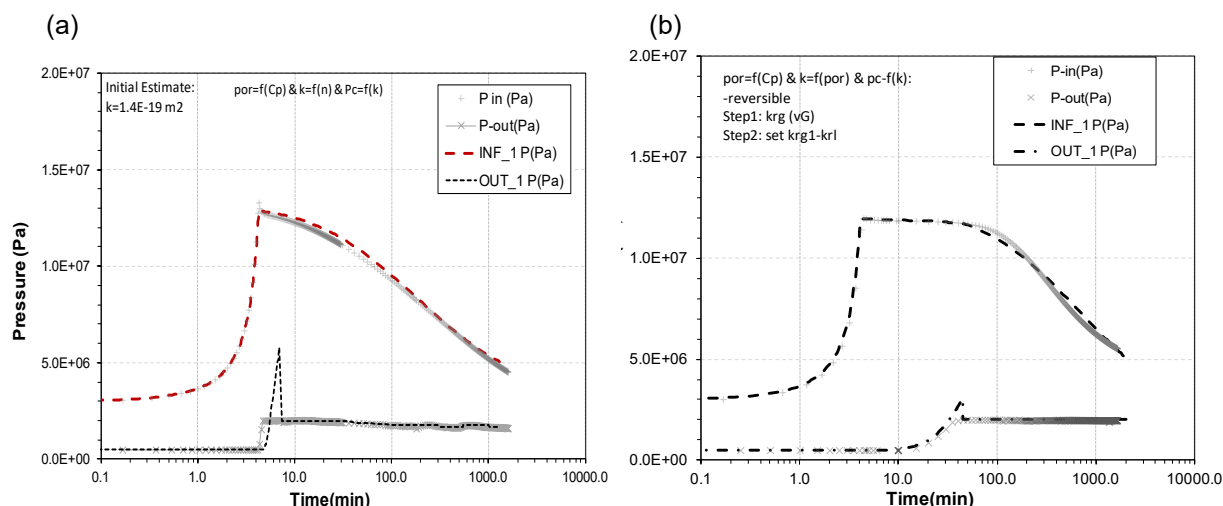
Figure 2-30 – Simulated and measured pressures for air-pulse injection tests on core samples from Mont Terri for flow parallel (a) and perpendicular (b) to bedding after Senger et al. (2014).

Table 2-14 – Model input parameters (Opalinus Clay, Mont Terri; 'shallow OPA').

Parameter	Symbol [unit]	Test 1a parallel	Test 1 normal
Permeability	k [m^2]	1.4×10^{-19}	4.3×10^{-20}
Porosity	ϕ [–] [a]	0.20	0.18
Pore compressibility	C_p [1/Pa] [a]	2.0×10^{-08}	1.5×10^{-08}
van Genuchten capillary strength parameter	P_0 [Pa] [b]	$18.0 \times 10^{+6}$	$18.0 \times 10^{+6}$
van Genuchten shape parameter	n (with $n = 1/(1-m)$)	1.67	1.67
Residual water saturation [c]	S_{lr} [–]	0.01	0.01
Residual gas saturation [c]	S_{gr} [–]	0	0
Initial saturation [c]		1	1

[a] Measured

[b] Fitted to the water retention curve using van Genuchten/Mualem model:

$$P_c = P_0 \left(S_{el}^{-\frac{1}{m}} - 1\right)^{1-m}; \quad S_{el} = \frac{S_l - S_{lr}}{1 - S_{lr}}$$

$$k_{rl} = S_{el}^{1/2} \left[1 - \left(1 - S_{el}^{\frac{1}{m}}\right)^m\right]^2; \quad S_{el} = \frac{S_l - S_{lr}}{1 - S_{lr}}$$

$$k_{rg} = (1 - S_{eg})^{\frac{1}{3}} \left(1 - S_{eg}^{\frac{1}{m}}\right)^{2m}; \quad S_{eg} = \frac{1}{1 - S_{gr}}$$

[c] Assumed

In petroleum engineering, the gas transport capacity of rock formations is often expressed in terms of empirical gas entry pressure – permeability relationships. The gas entry pressure is derived from mercury intrusion porosimetry, from gas invasion experiments on core samples or from water retention curves and in rare occasions from in situ gas threshold pressure testing in boreholes. The permeabilities are derived from water/gas permeation experiments on core samples or from in situ packer testing. A survey of data bases from different lithologies is given in the following section. A compilation of correlations from various sources representing empirical entry pressure – permeability relationships for clay-rich lithologies is given in Figure 2-31a (modified after Marschall et al. 2005). The cross were fitted with different power laws, referenced in Leverett (1941), Davies (1991) and Marschall et al. (2005).

EURAD (Deliverable n° 6.1) – Initial State of the Art on Gas Transport in Clayey Materials
Dissemination level: PU
Date of issue of this report: 17/11/2021

Page 99

Ferrari et al. (2014) derived another empirical relationship for Opalinus Clay, which is based on cross-plots of void ratio vs. gas entry pressure (Figure 2-31b). The gas entry pressure was determined from water retention curves on Opalinus Clay samples from the Schlattingen borehole in northern Switzerland.

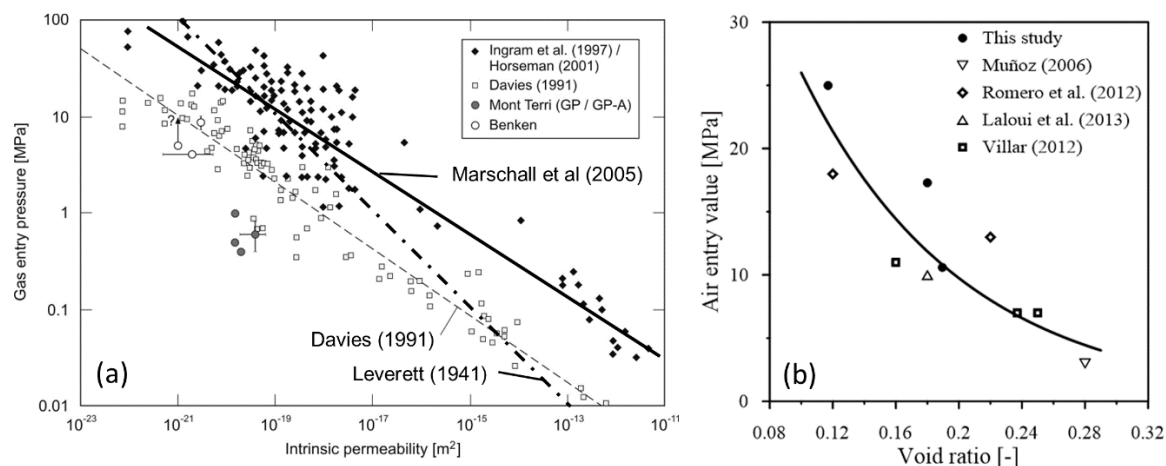*Figure 2-31 – Empirical relationships of entry pressure vs. permeability and entry pressure vs. void ratio: (a) compilation by Marschall et al. (2005) from clay-rich lithologies worldwide; (b) compilation by Ferrari et al. (2014), representing data from a deep investigation borehole in the Opalinus Clay formation of northern Switzerland.*

2.4.1.5 State of knowledge for bentonite

The hydro-mechanical properties of a bentonite sample highly depend on the amount of montmorillonite it contains. According to Villar (2005), Seiphoori et al. (2014), Villar et al. (2014), Xu L. et al. (2017) and Xu L. et al. (2020), some key hydro-mechanical properties of saturated samples, including intrinsic permeability, gas entry value and swelling pressure, are directly controlled by the dry density of the bentonite sample. As discussed in detail in Section 1.5.4, for the bentonite sample with high dry density, there are more expansive clay minerals per unit volume of the sample that can adsorb water molecules. Thus, a high swelling pressure is expected to develop when the sample reaches a fully saturated state under constant volume condition. As the adsorbed water film is relatively immobile, the porous space available for fluid flow will significantly decrease with the increase of dry density. As a result, the saturated bentonite sample with high dry density has a very low intrinsic permeability and a high gas entry value.

Unsaturated bentonite having double pore structures, i.e. inter-aggregate pores and intra-aggregate pores, it presents a bimodal pore size distribution (Gens and Alonso, 1992; Alonso E. et al. 1999; Sánchez et al. 2016; Dieudonné et al. 2017). When a bentonite is progressively hydrated under constant volume conditions, the inter-aggregate pores gradually reduce due to the swelling of clay particles (Gens and Alonso, 1992). This suggests that, at saturated state, the bentonite primarily presents an unimodal pore size distribution. However, recent mercury intrusion porosimetry (MIP) results showed that the saturated bentonite can also exhibit a bimodal pore size distribution which, nevertheless, is less significant than that of the (as-compacted) unsaturated bentonite (Madaschi and Laloui (2018), Figure 2-32).

The µ-CT images obtained by Gonzalez-Blanco et al. (2018) also show that the saturated bentonite has a double pore structure, i.e. fissures between clay grains and pores in grains. Under high gas pressure, these fissures may be activated and then serve as the preferential pathways for gas flow (see Figure 2-33 and more details in Section 3.1.4.4). The existence of wider passages in highly compacted

EURAD (Deliverable n° 6.1) – Initial State of the Art on Gas Transport in Clayey Materials
Dissemination level: PU
Date of issue of this report: 17/11/2021

Page 100

bentonite was also confirmed in Pusch and Forsberg (1983), Pusch and Hökmark (1990) and Xu L. et al. (2017).
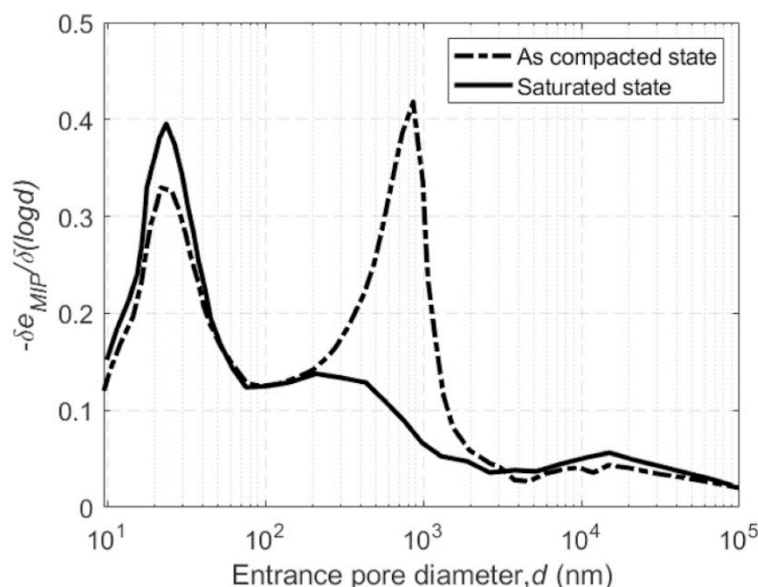
Figure 2-32 – Pore size distribution of as-compacted and saturated bentonite (Guo and Fall 2021) (after Madaschi and Laloui 2018).
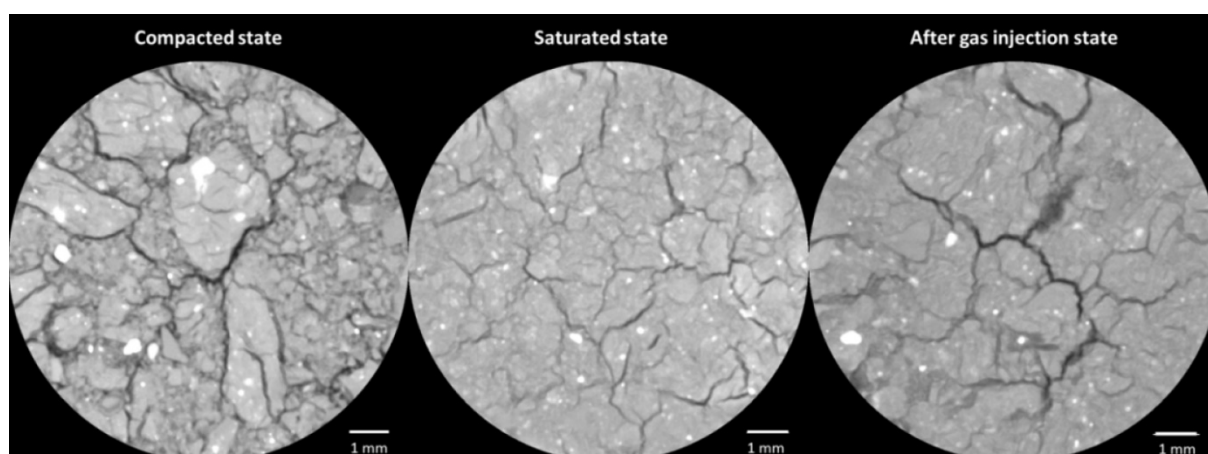
Figure 2-33 – µ-CT images of samples at compacted, saturated and after gas injection states (Gonzalez-Blanco et al. 2018).

According to Guo and Fall (2021), it is worth noting that whether the saturated bentonite can be considered as a porous medium having double pore structures depends on the context. For applications that focus on the overall mechanical behaviour, it may be appropriate to consider the saturated bentonite as a single-porosity medium, since the small number of larger pores may have no significant influence on the mechanical behaviour. In contrast, for the research and applications in which the saturated bentonite is subjected to a highly pressurised gas, the larger connected pores, even if these account for only a small fraction of the total porosity, will significantly influence the gas transport process. Indeed, the larger connected pores may be utilised by the highly pressurised gas as the preferential flow pathways. In this case, it is reasonable to consider the saturated bentonite as a double porosity media in which the larger connected pores serve as the potential flow pathways while the smaller pores in the matrix remain saturated.

The transport of gas though bentonite and barrier materials containing bentonite and its effect on these materials is investigated in the WP GAS of EURAD. Some specific results are given hereafter for each

EURAD (Deliverable n° 6.1) – Initial State of the Art on Gas Transport in Clayey Materials
Dissemination level: PU
Date of issue of this report: **17/11/2021**

Page 101

of these materials. One of the key properties that needs to be first evaluated when studying gas flow through bentonite is the water retention behaviour. The time needed to reach equilibrium and the final distribution of dry density being dependent on the water retention curve, a precise determination of the water retention behaviour is a prerequisite in order to assess of the evolution of the state of the barrier.

2.4.1.5.1   Granular Wyoming sodium bentonite (MX-80)

Seiphoori (2015) determined the water retention curves of Wyoming granular bentonite with dry densities between 1 500 kg/m³ and 1 800 kg/m³ under a constant void ratio along successive wetting and drying cycles (Figure 2-34b). Gas entry pressures were derived from the water retention curves, indicating a marked increase of the gas entry pressure with increasing dry density/decreasing void ratio (Figure 2-34b). Additional tests were carried out with the aim of investigating the water retention behaviour in wetting and drying cycles. Tests were performed on samples compacted at the void ratio e = 0.53 (ρ_d = 1.80 g/cm³). The results in Figure 2-35 suggest that during the first wetting stage (A-D) the material experienced a significant and irreversible modification in the retention behaviour. In particular, after the first saturation (point D), the retention capacity of the material increased in the sense that more water can be stored in the bentonite for a given suction in a wetting path. According to Laloui et al. (2020), these findings were related to the modification of the fabric after saturation. Indeed, MIP results showed that a significant change of the pore size distribution took place due to the apparent homogenisation of the initial structure formed by the highly compacted grains.
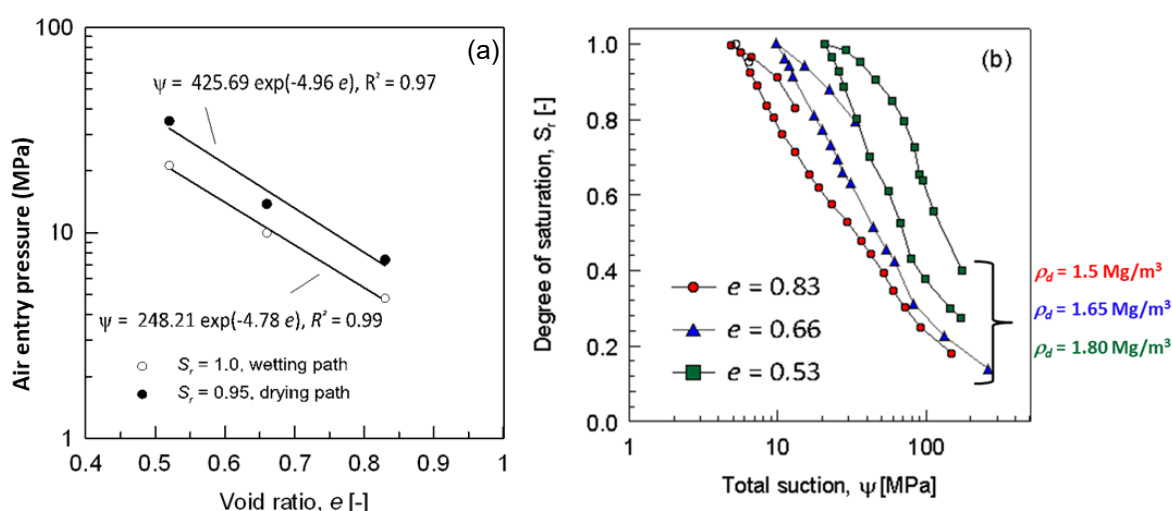
Figure 2-34 – Water retention behaviour of Wyoming granular bentonite with dry densities between 1 500 kg/m³ and 1 800 kg/m³ under a constant void ratio: (a) empirical correlation between gas entry pressure and void ratio (derived from water retention curves); (b) water retention curve along a wetting path, followed by a single drying path (Seiphoori 2015).

The water retention capacity of MX-80 bentonite and the effect on the water retention curve of dry density have also been analysed by Jacinto et al. (2009) and Pintado et al. 2013 (Figure 2-36). According to them, the influence of dry density on the water retention capacity depends on the suction range, the limiting value being around 30 MPa. For suctions above this threshold value, the retention capacity in terms of water content is slightly higher when the dry density is higher, whereas for lower suctions, the lower the dry density of the bentonite the higher its water content.

EURAD (Deliverable n° 6.1) – Initial State of the Art on Gas Transport in Clayey Materials
Dissemination level: PU
Date of issue of this report: **17/11/2021**

Page 102
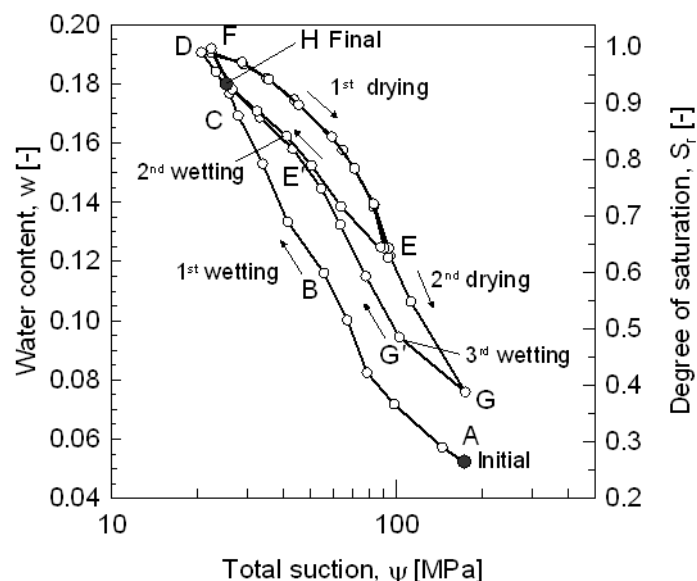
Figure 2-35 – Hysteresis of water retention behaviour in wetting and drying cycles (Seiphoori 2015): the compacted sample is wetted in steps (path A – B – C – D) until full saturation is reached (point D). The main drying path ends at a maximum suction value of 95 MPa (path D – E). A second wetting path (E – F) is imposed reaching again full saturation. Drying is then initiated once more until a suction of 174.5 MPa (point G), succeeded by a final wetting stage until a degree of saturation of 0.95 is reached (point H).
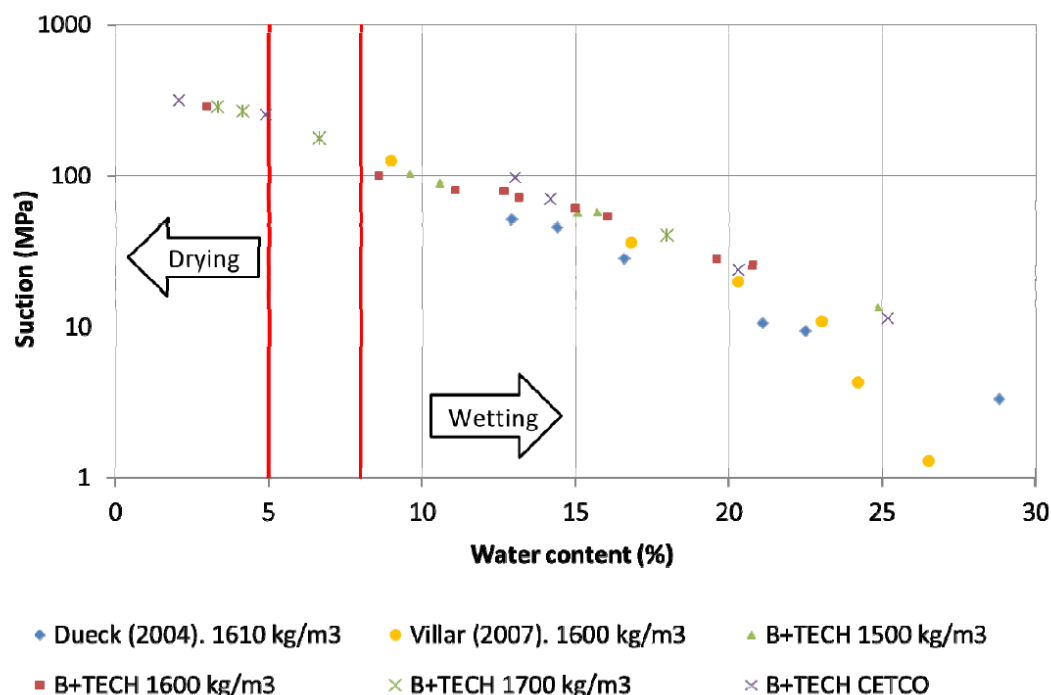
Figure 2-36 – Water retention curve in terms of water content vs suction of MX-80 samples for different dry density values. The suction values considered are the average of the psychrometer measurements between the vacuum and the pressure face. The initial water content was between 5 and 8% (between the red lines). The experiments were conducted by B+Tech for both Volclay KWK (B+TECH 1 500, 1 600 and 1 700 kg/m³) and Cetco MX-80 bentonites (B+TECH CETCO), and by Dueck (2004) (1 610 kg/m³) and Villar (2007) (1 600 kg/m³) (Pintado et al. 2013).

EURAD (Deliverable n° 6.1) – Initial State of the Art on Gas Transport in Clayey Materials
Dissemination level: PU
Date of issue of this report: **17/11/2021**

Page 103

Gonzalez-Blanco and Romero (2019) complemented the geotechnical data base in compacted granular Wyoming bentonite by performing multiple gas invasion experiments in oedometric and triaxial set-ups with dry densities in the range 1.45–1.55 g/cm³. Key issues addressed in their study were the impact of (i) the grain size distribution of the raw material, (ii) the sample preparation procedure and (iii) the stress path during hydration on the results of water/gas permeation. Numerous test specimen were prepared using different grain size distributions (see Figure 2-37a). The sample preparation procedure and the stress path followed during hydration was similar in all cases (Figure 2-37b/c). Water permeability of the fully saturated specimen was determined under controlled-gradient conditions (hydraulic gradient $i \approx 770$) at constant vertical stress (compaction stress) and steady-state inflow/outflow water rates. The tests revealed a significant scatter of the measured water permeabilities in the order of one magnitude (Figure 2-37d).

Numerous gas injection tests were also conducted by Gonzalez-Blanco and Romero (2019) to investigate the hydro-mechanical behaviour of bentonite in response to gas invasion. The tests were conducted with nitrogen and helium with gas injection rates between 0.04 mL/min and 100 mL/min (volumetric rate). These experiments revealed that gas transport processes in compacted bentonite are affected by numerous factors, such as the dry density, the grain size distribution of the raw material, the compaction and hydration process and the gas injection regime (fast and slow injection rates). Results of these tests are discussed in Section 3.1.4.4.
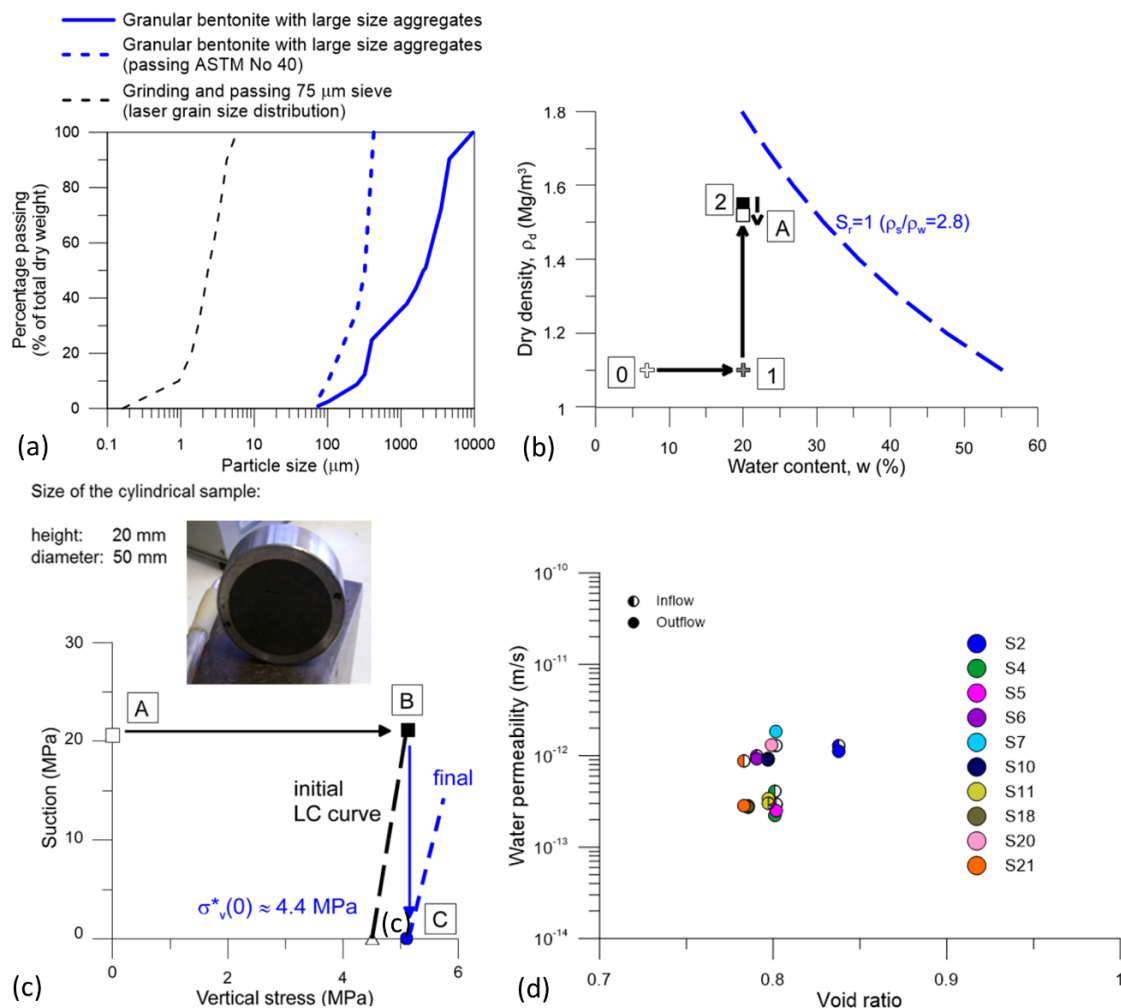
Figure 2-37 – Investigations on the impact of the sample preparation procedure on the results of water/gas injection tests with compacted granular bentonite (Gonzalez-Blanco and Romero 2019): (a) grain size distributions of the tested materials, (b) sample preparation paths to reach a dry density of 1.55 g/cm³; (c) stress paths followed under oedometer conditions, (d) water permeability results (inflow and outflow data) as a function of the void ratio.

EURAD (Deliverable n° 6.1) – Initial State of the Art on Gas Transport in Clayey Materials
Dissemination level: PU
Date of issue of this report: 17/11/2021

Page 104

2.4.1.5.2   FEBEX bentonite

Mercury intrusion porosimetry (MIP) tests have been performed by Lloret et al. (2003) to examine the pore size distribution of the statically compacted FEBEX bentonite. Figure 2-38 shows the measured incremental pore volume for two samples compacted to very different values of dry density (ρ_d), 1.5 Mg/m^3 and 1.8 Mg/m^3. It can be observed that the pore size distribution is clearly bimodal, which is very characteristic of this type of material after dry compaction. The dominant values are 10 nm, which would correspond to the pores inside clay aggregates, and a larger pore size that depends on the compaction dry density and ranges from 10 μm (for ρ_d = 1.8 Mg/m^3) to 40 μm (for ρ_d = 1.5 Mg/m^3). These larger voids would correspond to the inter-aggregate pores. The boundary between the two pore size families can be seen to be around 130 nm, as pores smaller than this magnitude do not appear to be affected by the magnitude of the compaction load. As Figure 2-38 clearly shows, compaction affects mainly the pore structure of the larger inter-aggregate pores.
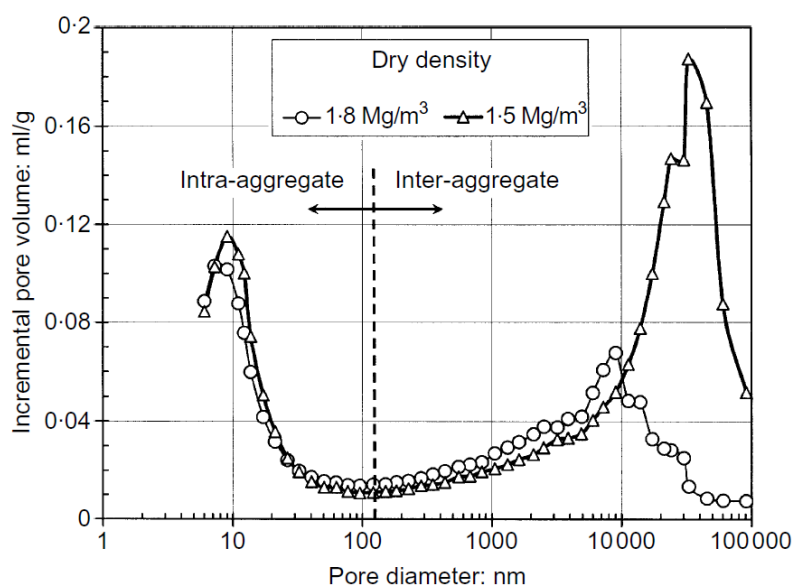
Figure 2-38 – Distribution of incremental pore volume for two compacted bentonite samples at different dry densities. Mercury intrusion porosimeter test (Lloret et al. 2003).

The retention curve of the FEBEX bentonite determined by Lloret et al. (2003) in samples compacted to different dry densities is presented in Figure 2-39. The volume of the samples remained constant during the determinations, since they were confined in constant volume cells. It can be observed that the water retained at suctions higher than about 15 MPa is independent of the total void ratio (or dry density). It seems plausible that the water retained at those high suctions belongs to the intra-aggregate pores where the total porosity plays no relevant role (Romero et al. 1999). The fact that the water content corresponding to the intra-aggregate pores appears to be somewhat higher than their pore volume (as measured in the MIP tests) may be due to a density of the water tightly bound to the clay particles higher than that of free water (Villar 2002). It is also likely that part of the water is retained on the surface of the aggregates.

The saturated permeability of the bentonite compacted to a dry density of 1.7 Mg/m^3 is of the order of 10^{-14} m/s (Villar and Lloret 2001). Consequently, testing times of stages requiring water content changes and hydraulic equilibration are very long, usually taking several weeks. This places important time constraints on the laboratory testing programme.

The gas permeability of the FEBEX bentonite was compared by Gutiérrez-Rodrigo et al. (2014) to the gas permeability of the MX-80 bentonite, for dry densities between 1.4 and 1.8 g/cm^3. As expected, it

EURAD (Deliverable n° 6.1) – Initial State of the Art on Gas Transport in Clayey Materials
Dissemination level: PU
Date of issue of this report: 17/11/2021
Page 105

was observed for all densities that an increase of water content causes a clear decrease in gas permeability in both bentonites. They also showed that, for similar water contents, gas permeability was strongly affected by dry densities, decreasing by about three orders of magnitude when dry density is increased from approximately 1.5 to 1.8 g/cm^3. Gas permeability is mainly related to the accessible porosity which is itself inversely related to the degree of saturation. The decrease of accessible porosity with saturation follows a potential law with exponent close to 3. For similar dry densities after compaction and water content, the gas permeability values obtained for the FEBEX bentonite were higher than those obtained for MX-80 because of the finer grain size of the latter.

Gas permeability was also measured in a triaxial apparatus in isotropic conditions for different confining pressures, injection pressures and backpressures. For confining pressures in the range 0.6 – 1.2 MPa, no significant effect of the injection or confining pressures on the values of permeability was detected. However, gas permeability tended to be slightly lower as the effective pressure increased, either by the increase in confining pressure or by the decrease in backpressure or injection pressure, particularly for the MX-80 bentonite.

According to Gutiérrez-Rodrigo et al. (2014), the Klinkenberg effect was not significant for these two materials in the range of pressures applied in the tests. Furthermore, with the pressures applied, it was not possible to measure gas permeability for degree of saturation higher than 97%, which could be considered the limit above which no two-phase flow (without significant deformation of the pore space) takes place.
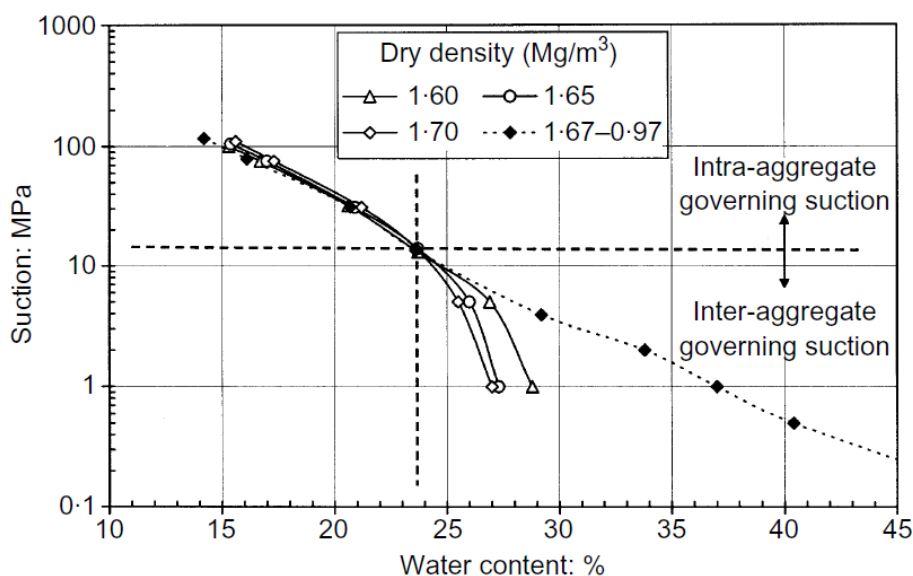
Figure 2-39 – Retention curves for compacted bentonite obtained under constant volume conditions (1.60, 1.65 and 1.70 Mg/m^3 dry density) and free swelling conditions (variable density) (Lloret et al. 2003).

2.4.1.5.3   Czech bentonite BCV

Water retention curves of the Czech bentonite BCV (see also Section 1.5.4.2) were determined for samples compacted to various dry densities employing a method which has been described by e.g. Villar (2007) and Večerník et al. (2014). All tests were performed in constant volume cells. The samples were compacted directly into the cells, which are equipped with relative humidity and temperature sensors. The retention curves for various dry densities (1.4, 1.6 and 1.8 g/cm^3) were evaluated at ambient temperature. No differences of retention curves were observed between the samples compacted to different dry densities (Figure 2-40).

EURAD (Deliverable n° 6.1) – Initial State of the Art on Gas Transport in Clayey Materials
Dissemination level: PU
Date of issue of this report: 17/11/2021

Page 106

Additional tests have been performed for three other samples with different initial dry densities. Figure 2-41(a) from Baryla et al. (2019) compares the water retention curves for both wetting and drying paths for dry densities of 1.27, 1.60 and 1.90 g/cm^3. For suctions between 3 and 300 MPa, the relationship between water content and suction is almost linear in this semi-logarithmic plot. There is only a narrow hysteretic loop between wetting and drying paths. With the assumption that most water is contained in the micropores at high suctions, these results suggest that micropores sizes are almost independent of the compaction pressures. Indeed, if the micropore size would have been affected by the degree of compaction, the water retention (which is porosity dependant) should have changed. Figure 2-41(b) and Figure 2-41(c) show that, unlike water content, the void ratio and the water saturation depend on the initial dry density. The degree of saturation under a given suction hence increases with dry density.

Mercury intrusion porosimetry of these later samples was made during the BEACON EC project (Baryla et al. 2019). Figure 2-42 compares the MIP results under different suctions levels, to evidence the effect of the dry density after compaction. The comparison demonstrates that compaction has big influence on the predominant pore radius represented by the highest peak. An increase of dry density leads to the reduction of the peak and of a shift of the predominant pore size towards smaller pores. This trend is observed for all applied suction values.

Figure 2-43 shows the same results, this time replotted to evidence the effect of suction on pore size distribution. It shows that the peaks representing predominant pore radius are slightly affected by applied suction. With increase of suction, the peak is shifted towards smaller pore radius. This effect is more obvious for high dry density samples. Compared to the effect of dry density, the suction has a significantly smaller influence on the predominant pore size.

Romero et al. (2011) proposed a criterion to discriminate the macro- and micropore. According to them, the transition pore radius boundary between macropores and micropores is around 0.05–0.07 µm. Consequently, pore size distribution curves such as those shown above indicate that the compacted bentonites have a double structure pore network, which consists of macropores (represented by pore radius around 1–2 µm) and micropores (represented by a peak at approximately 5–6 nm). The comparison of pore size distribution curves shows that suction and especially compaction have a significant influence on the macropores and much less influence on the micropores.

This is important in the context of visco-capillary two-phase flow as gas will predominantly flow through the macropores while most of the pore water, which is present in the micropores, will not be displaced.

EURAD (Deliverable n° 6.1) – Initial State of the Art on Gas Transport in Clayey Materials
Dissemination level: PU
Date of issue of this report: 17/11/2021

Page 107
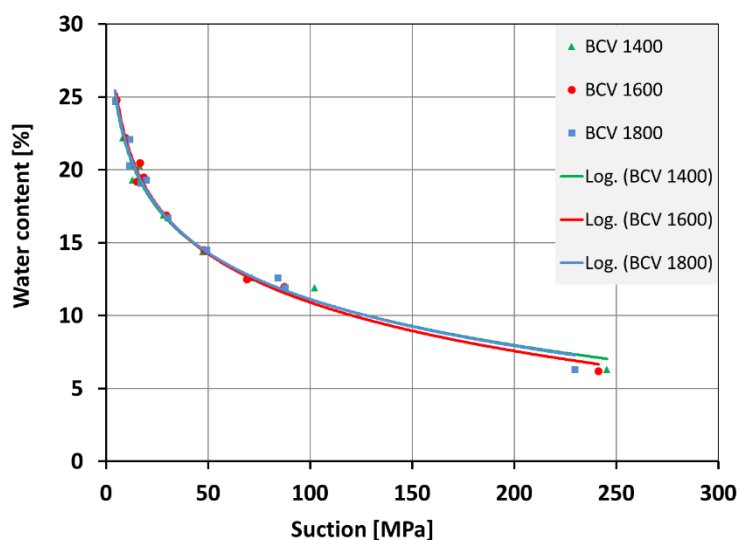
Figure 2-40 – Retention curves (gravimetric water content related to suction) of compacted Czech bentonite BCV samples with dry densities of around 1.4, 1.6 and 1.8 g/cm³ (data from Červinka and Vašíček 2018).
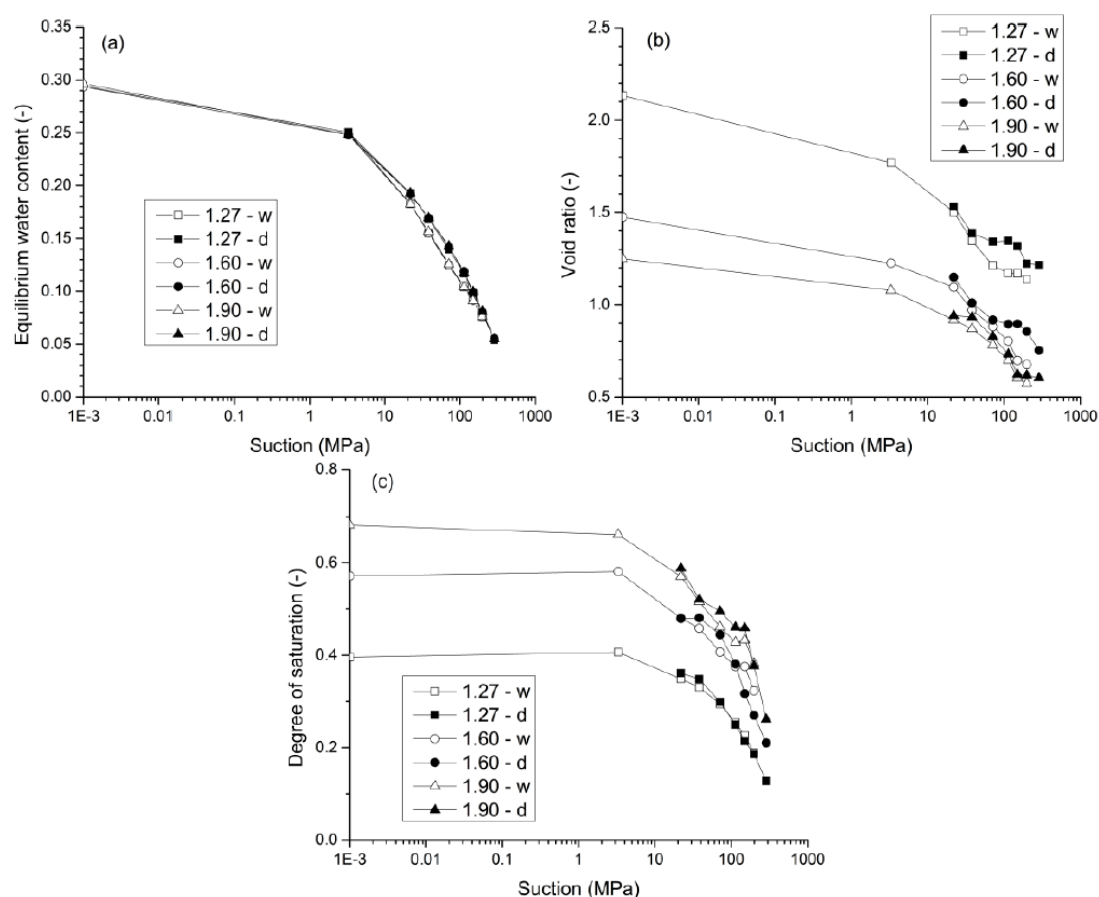
Figure 2-41 – (a) water content, (b) void ratio and (c) degree of saturation with respect to suction along wetting and drying path at dry densities of 1.27, 1.60 and 1.90 g/cm³ (Baryla et al. 2019).

EURAD (Deliverable n° 6.1) – Initial State of the Art on Gas Transport in Clayey Materials
Dissemination level: PU
Date of issue of this report: **17/11/2021**

Page 108
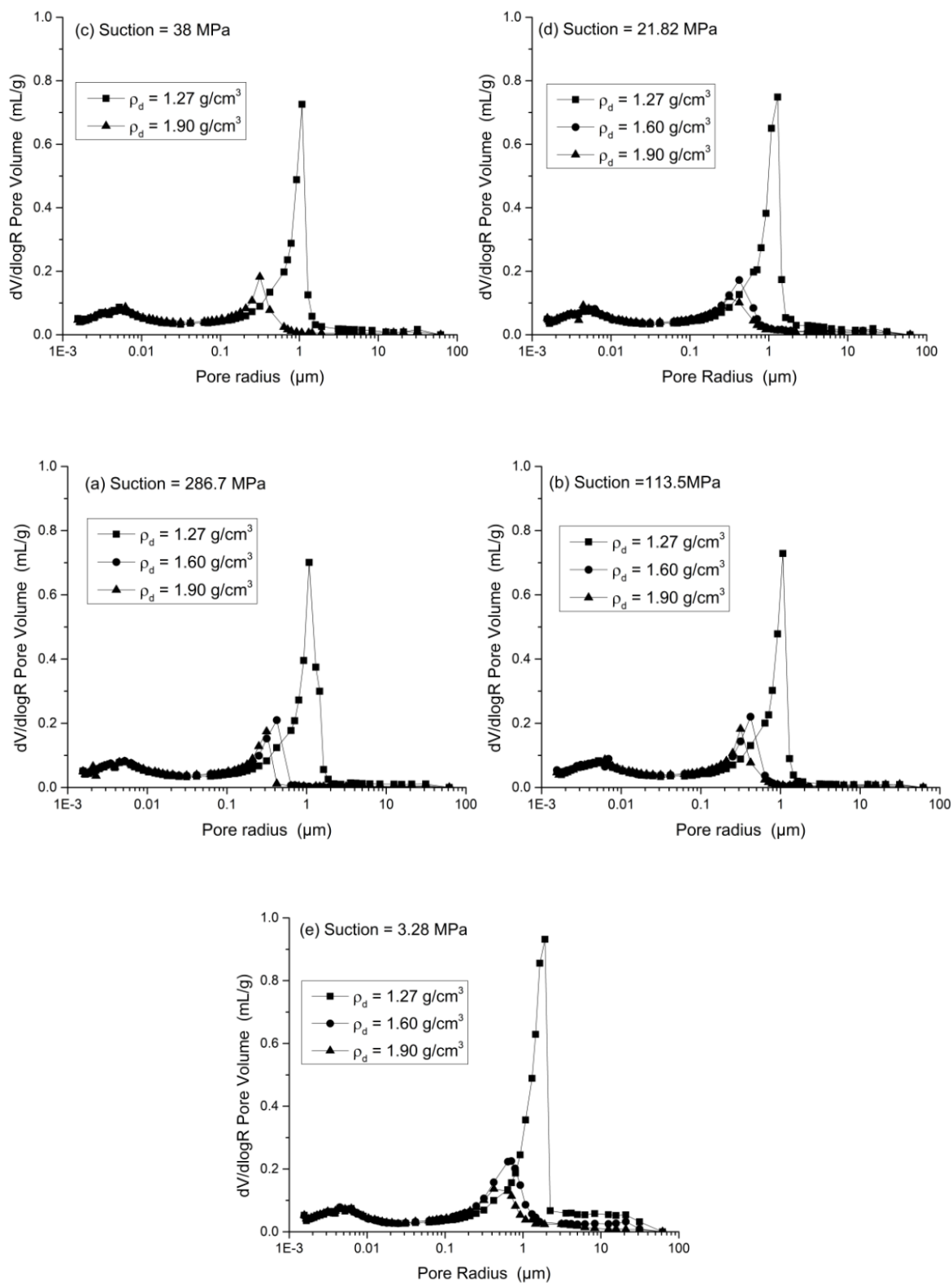
Figure 2-42 – Pore size distribution curves of samples with different dry densities at constant suction (Baryla et al. 2019).

EURAD (Deliverable n° 6.1) – Initial State of the Art on Gas Transport in Clayey Materials
Dissemination level: PU
Date of issue of this report: **17/11/2021**

Page 109
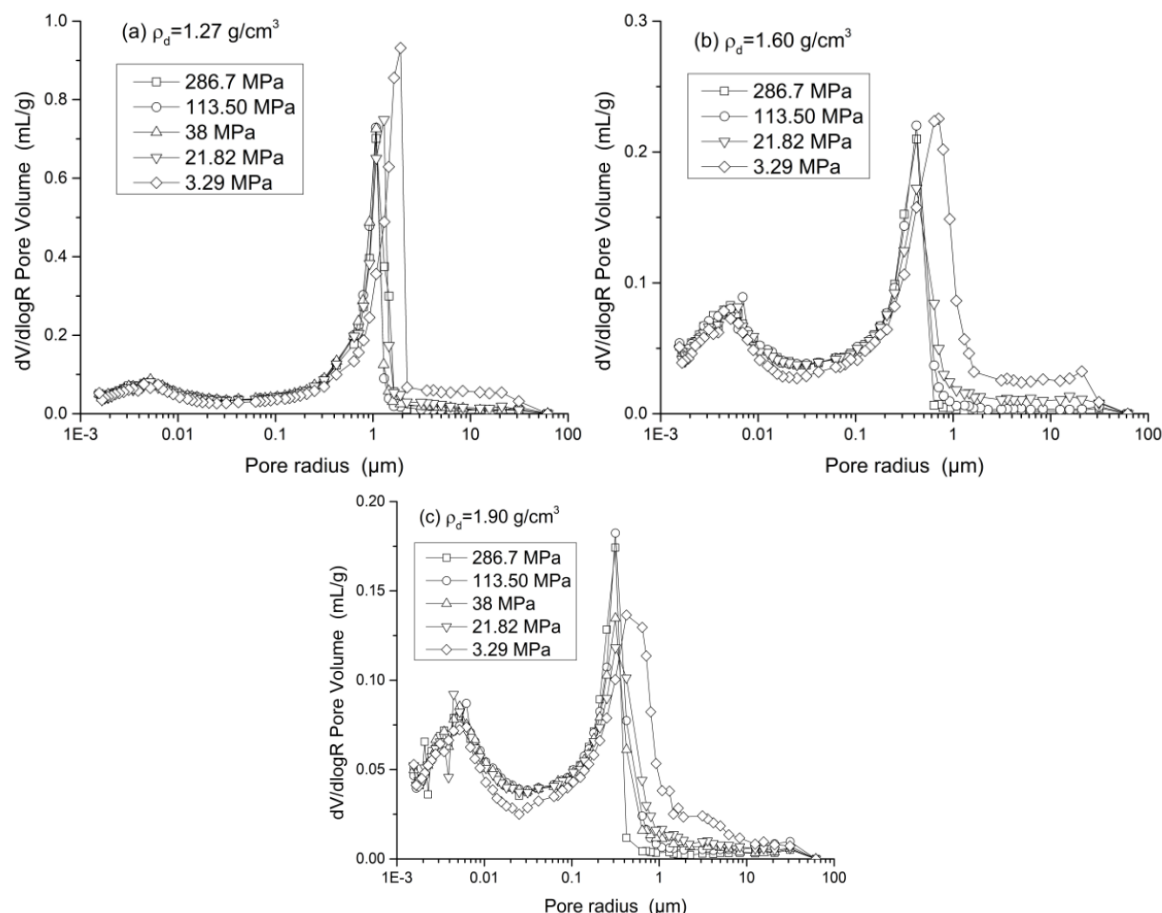
Figure 2-43 – Pore size density distribution curves of three different initial dry densities with different suctions (Baryla et al. 2019).

2.4.1.5.4 Sand/bentonite (S/B) mixtures

The research programme by Manca (2016) on the geotechnical characterisation of granular S/B mixtures (see also Section 1.5.4.4) comprised comprehensive measurements of the water retention behaviour of S/B mixture compacted to the target dry densities of 1.50 and 1.80 g/cm^3. The water retention curves were obtained by combining three well-established techniques for suction measurements (filter paper method (FPM), axis translation technique (ATT) and micro cell technique (MCT)). The acquired retention curves shown in Figure 2-44 indicate that the S/B mixture has a relatively low retention capacity when compared to pure bentonite. This characteristic is attributed to the large amount of sand in the mixture and to the microstructural features of the bentonite fraction. For total suctions higher than 3 MPa, the experimental data is following a similar curve for densities of 1.5 and 1.8 g/cm^3, respectively, showing that the effect of compaction density on the water retention behaviour of the 80/20 S/B mixture is low. This result suggests that the water is mainly stored in the pores belonging to the bentonite fraction, that are not affected by the compaction process, and that the dominant retention mechanism is adsorption. In the suction range between 3 and 0.5 MPa, the water retention shows a sort of transitional zone where the mechanisms of adsorption and of capillary retention contribute in the same order of magnitude to the total suction. This explains the modest dependency of the initial matrix and total suctions of the mixture on the dry density variations. A distinct effect of the dry density variation of the shape of the water retention curve is observed for suctions lower than 0.5 MPa. Below this threshold, the specimen compacted at lower dry density tends to retain less water as the volume of the pores is larger.

EURAD (Deliverable n° 6.1) – Initial State of the Art on Gas Transport in Clayey Materials
Dissemination level: PU
Date of issue of this report: 17/11/2021

Page 110
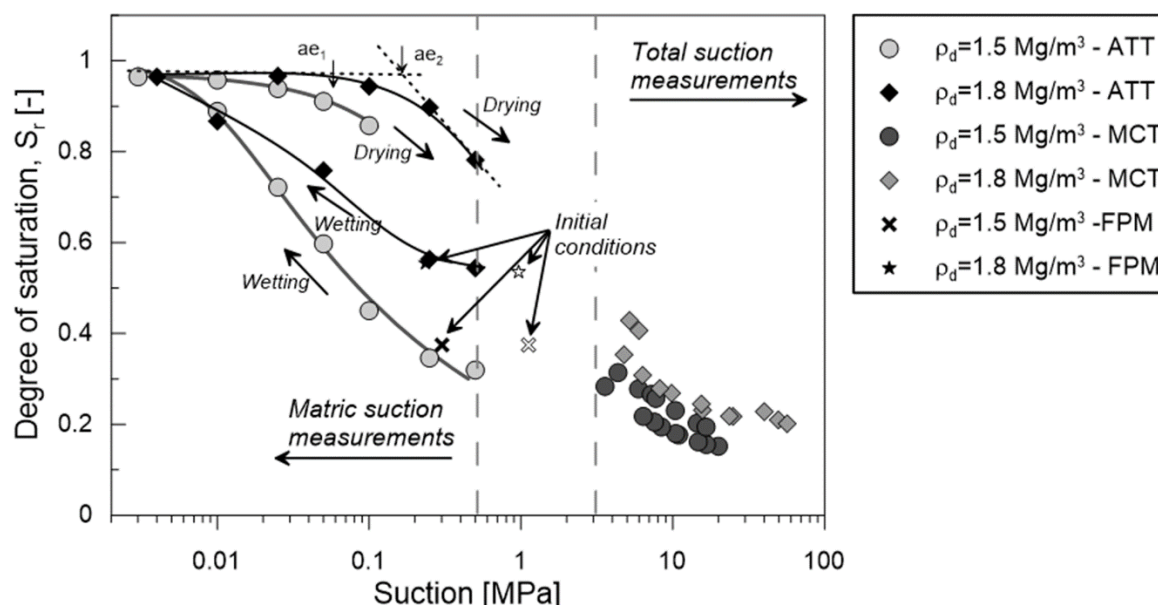
Figure 2-44 – Full range water retention curve of the 80/20 S/B mixture at two different dry densities using well-established techniques for suction measurements (filter paper method – FPM, axis translation technique – ATT, micro cell technique – MCT). Further details are given in Manca (2016).

The evolution of water permeability under conditions of partial saturation is presented in Figure 2-45 (Manca 2016), for two specimens compacted to an initial dry density of 1.5 Mg/m³ and 1.79 Mg/m³. Regardless of the initial dry density, the effective permeability of the mixture to the water phase increases monotonically with the degree of saturation. This behaviour is a consequence of the increase of the fraction of the pore volume devoted to the water flow and the enlargement of the bentonite pores due to the internal swelling of the bentonite aggregates. At low degrees of saturation, the effective permeability become very small because the water occupies the smallest pores belonging to the bentonite, where adsorption forces are the greatest. This saturation state is called irreducible or connate-water saturation. In this state, the water is quasi-immobile. In the plane hydraulic conductivity versus degree of saturation, the unsaturated hydraulic conductivity curve obtained with the applied wetting-drying path shows hysteresis for the two dry densities. However, the higher hysteresis is detected for the specimen compacted to the higher dry density and lower void ratio. In the plane hydraulic conductivity versus suction, the curve also shows hysteresis along a wetting and drying cycle. This hysteresis is related to the irreversible deformation of the internal structure of the bentonite along this cycle.

Hence, in the context of visco-capillary flow, sand/bentonite mixtures allow gas passage at lower pressures while still providing good retention of the pore water.

EURAD (Deliverable n° 6.1) – Initial State of the Art on Gas Transport in Clayey Materials
Dissemination level: PU
Date of issue of this report: 17/11/2021

Page 111
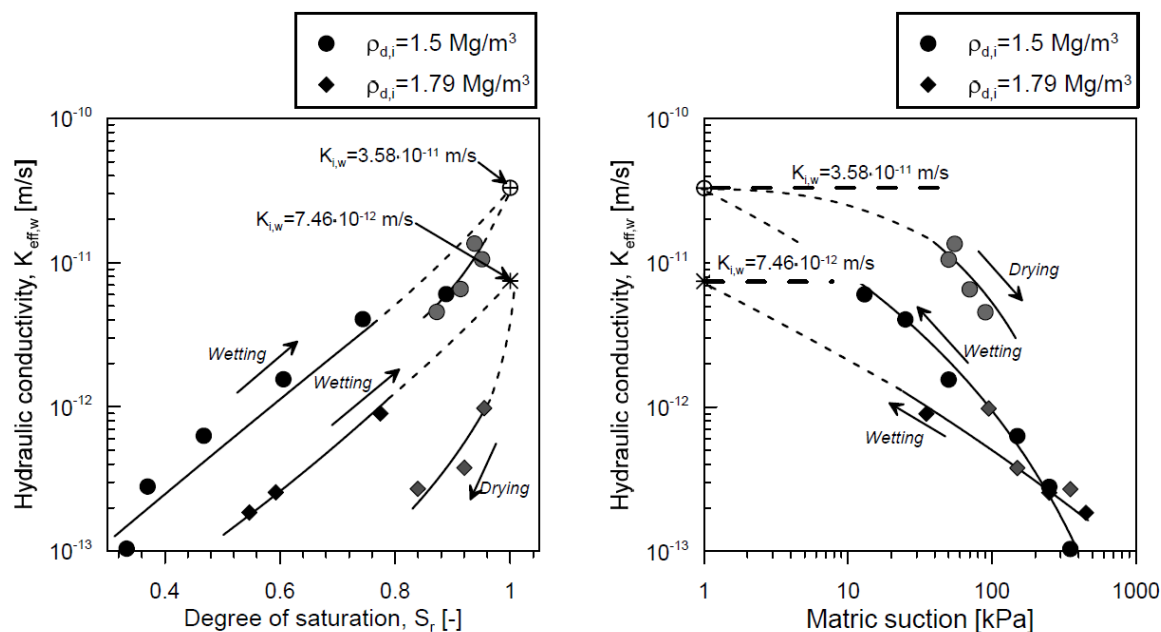
Figure 2-45 – Unsaturated hydraulic conductivity of the S/B mixture compacted to two different dry densities (Manca 2016).

2.4.2 Gas conducting pathways

2.4.2.1 Two-phase flow concept in materials with pre-existing discontinuities

Separation planes such as fractures (which divide a solid body into two or more pieces) or interfaces between two porous materials represent preferred gas transport paths. They are characterised by abrupt changes in stiffness and material strength together with localised modifications of microstructure across the discontinuity. Separation planes in a porous barrier material may exhibit a very small, but well-connected fraction of the total pore volume. When gas invades such a discontinuity of an initially fully water-saturated porous material, the water saturation of the material does not change significantly even though a distinct gas transport capacity of the feature may be seen due to its high connectivity. Further hydro-mechanical interactions (pathway dilation, gas fracturing) may enhance gas transport along discrete features.

When the gas entry pressure of the clayey material is higher than the in situ mechanical constrains or if the gas generation rate exceeds the capacity for pore water displacement by visco-capillary flow the gas will create additional pathways through the porous media. These pathways could be either pathway dilation or gas fracturing. As the formation of these pathways can impact barrier integrity, the generation of these gas transport processes are described in Chapter 3. This section only describes how the gas is transported by existing open pathways, regardless of how these pathways were formed and opened.

To enter the fracture/interface, gas has to displace water, overcoming capillary effects. This latter depends on fracture/interface transmissivity and connectivity which are functions of fracture/interface normal loads. In these conditions, when gas invades a water-filled fracture and/or interface, two-phase flow conditions are encountered locally like in continuous porous media.

EURAD (Deliverable n° 6.1) – Initial State of the Art on Gas Transport in Clayey Materials
Dissemination level: PU
Date of issue of this report: **17/11/2021**

Page 112

2.4.2.2 State of knowledge for Boom Clay

Harrington et al. (2017a) conducted experiments to examine the shear and normal load dependency of fracture transmissivity in Boom Clay. Fractures were formed by shearing three cylindrical samples of clay, before investigating the hydro-mechanical properties of the resulting fractures. In general, shearing was found to reduce flow, but in one test additional brittle deformation occurred, thereby enhancing fluid transport, suggesting that shear can result in opening of new fluid pathways. Whether flow is reduced or enhanced will depend on connectivity of new pathways, as well as the degree of dilatancy versus compaction in the (brittle versus ductile) deformation response of the clay. As with the Opalinus Clay and Callovo-Oxfordian claystone, normal loading was seen to result in a significant reduction in flow rate and transmissivity values were found to be generally lower in this plastic clay than the other two clays (10^{-14}–10^{-15} m^2/s).

2.4.2.3 State of knowledge for Callovo-Oxfordian claystone

In a pre-fractured COx sample, only a low gas pressure is necessary to initiate flow (M'Jahad 2012). This highlights the potential impacts of sample damage on measured gas entry pressures. The measured bulk effective gas permeability of the sample in some cases is found to be entirely controlled by the initial presence of the fracture. Changes in confining pressure during tests have a direct consequence on the effective gas permeability of the material. Theses effective gas permeability evolutions are linked to the reduction of the fracture aperture due to the loading but also to self-sealing processes observed in COx (see Section 3.2.4.2). This is confirmed by Cuss et al. (2017) that used a shear-rig apparatus to examine the transport behaviour of fractures in COx, taken from the MHM URL in France, as a function of normal and shear stresses. Despite the complexity of the loading/unloading history applied on the sample and the orientation of the fracture in relation to the bedding, sensitivity of fracture transmissivity to normal load has been highlighted. Fracture flow was observed to reduce with normal load, as had been seen with Opalinus Clay. A power law relationship produced a good fit to experimental data relating fracture transmissivity to normal load. The initially flow rates reduced on increased normal load and were partially, but not fully, recovered on unloading. In M'Jahad (2012), the author notes a hysteresis effect during fracture loading-unloading with lower effective gas permeability after loading-unloading sequence. Several processes are involved in these hysteresis effects. The loading/unloading history is an important factor leading to a decrease of asperities of fracture surface but also the swelling of the clays (depending on the level of saturation) and the changes in the microstructure of the material in and around the fracture.

2.4.2.4 State of knowledge for Opalinus Clay

Cuss et al. (2011a, 2014) investigated the fracture transmissivity of OPA as a function of normal and shear stress. As with Gutiérrez et al. (2000) a clear relationship between effective stress and transmissivity was observed (between normal stresses of 1 and 5 MPa), with transmissivity decreasing at higher effective stresses. During all stages of this test phase, the very low transmissivities measured were close to the bulk permeability of the OPA, implying that the fracture made no significant contribution to the measured values and indicating that the fracture was, essentially, closed. It should be noted that these measurements were made over significant timescales (weeks). Swelling of the sample was also observed, leading to a sample dilation of 700 μm (or 1.7% axial strain). A further test, doubling the applied pore pressure saw transmissivity more than double, demonstrating that fracture transmissivity is also a function of pore pressure. While this effect should be accounted for when determining the fracture transmissivity, the calculation neglects the difference in compressibility between pore and matrix, which evidently needs to be allowed for in OPA.

The evolution of fracture transmissivity was also examined during active shear (resulting from a constant applied displacement, under a constant normal load). During the initial stages of shear testing

EURAD (Deliverable n° 6.1) – Initial State of the Art on Gas Transport in Clayey Materials
Dissemination level: PU
Date of issue of this report: 17/11/2021

Page 113

a slight drop in fracture transmissivity was observed, which was interpreted as being the result of clay smearing. This was followed by a series of flux events, leading to an increase in peak transmissivity to four times the initial level. Cuss et al. (2011a) report that while a number of these flux events can be correlated with dilation behaviour, this is not always the case, indicating that the opening of flow pathways may have been a localised phenomenon with limited impact on bulk dilatancy of the material. Over the duration of the shear test, a new series of fractures were formed along the initial fracture surface, resulting in a complex evolution of deformation and flow behaviour. Fluorescein was used to trace the flow of fluid and post-test analyses indicated that flow was not uniformly radial and occurred predominantly in the direction of shear, exploiting both the original fracture surface and a newly formed shear surface. Findings from this study demonstrate the complexity of fracture transmissivity and the potential to exhibit dynamic behaviour under certain conditions.

2.4.2.5 State of knowledge for bentonite

2.4.2.5.1   The role of interfaces

Gas transport experiments in which bentonite is put in contact with other materials suggest that interfaces between bentonite and other repository components, such as cementitious structural components or barriers, metal containers or the host rock may serve as preferential pathways for the gas flow (Davy et al. 2009; Liu J. et al. 2014a; Popp et al. 2013; Xu L. et al. 2017). The gas pressure required to trigger the formation of a pathway varies from case to case. This gas pressure is distinctly less than the swelling pressure in Davy et al. (2009), while it is equal to or slightly higher than the swelling pressure in Liu J. et al. (2014a). According to Guo and Fall (2021), and as detailed in the following paragraphs, interfaces may significantly control the gas flow when present.

From the FORGE EC project (Sellin 2014), experimental findings relating to the role of interfaces are as follows:

- Interfaces between unsaturated bentonite blocks act as preferential flow pathways.

- Interfaces between bentonite blocks will seal upon saturation and will not act as preferential flow pathways for gas.

- Interfaces between bentonite and another material offer a preferential flow pathway, even at full saturation. The conditions necessary for gas transport remain the same, however.

- Interfaces are inevitably present in experiments, even those in which only the behaviour of bentonite is investigated, e.g. cell/sample interface. This makes experiment design challenging but it is possible to design gas injection experiments where gas is 'forced' to enter and be transported through the bulk bentonite.

Davy et al. (2009) examined the transport properties of a laboratory scale bentonite-claystone (MX-80 and Callovo-Oxfordian claystone) interface under isotropic conditions, appropriate for the MHM URL. Samples were first hydrated for 21–28 days and before gas testing, an interfacial water permeability was measured that was found to be of the same order of magnitude as that of bulk Callovo-Oxfordian claystone. Incrementally increasing gas pressures were then applied to the interface and the downstream end was monitored for gas bubbles. After measuring swelling pressures during an independent test programme, the authors argue that the resulting gas flow measurements are indicative of transport occurring at gas pressures of around half that of the swelling pressure. This suggests that the presence of the interface reduces the gas entry pressure. Comparisons between testing on a control sample and testing using metal 'obturators' to limit the area of contact with gas indicated that flow occurred through the interface rather than the bulk of the bentonite or the claystone.

EURAD (Deliverable n° 6.1) – Initial State of the Art on Gas Transport in Clayey Materials
Dissemination level: PU
Date of issue of this report: 17/11/2021

Page 114

More recently, Shimura et al. (2017) presented laboratory experiments examining the role of bentonite/bentonite interfaces on gas transport. Testing was conducted on two samples of Na bentonite (Kunigel VI [16]), prepared one with and one without an interface. The samples (60 mm diameter × 25 mm length) were compression moulded to a required dry density of 1.36 g/cm^3 and initial saturation of 90%. A 1 mm thick plate was used to create an interface in the second sample and removed before testing. Each sample was put in a constant volume cell and hydrated before nitrogen gas was then injected through the base of the cell by applying constant pressure increments (increasing every two days from 0.1 MPa until breakthrough), while a backpressure of 0.1 MPa was maintained at the other end of the sample. Gas breakthrough was assessed by detection of a sudden increase in gas flow rate. Despite being hydrated for about 3 times longer, the hydraulic conductivity across the sample in which an interface had been created was found to be two orders of magnitude higher than that of the intact clay sample (~10^{-13} m/s rather than ~10^{-15} m/s) and a reduced swelling pressure was also observed (0.33 MPa, as opposed to 0.47 MPa). In addition, gas breakthrough was detected at a slightly lower pressure for the sample with an interface (1.3 MPa rather than 1.6 MPa). Nevertheless, the authors state that this difference is well within the range of variation noted in previous studies and, in contrast to the previous work of Sellin (2014) and Davy et al. (2009), the influence of the interface on gas flow is not significant. Post-test water content measurements indicated no detectable differences between clay in the vicinity of the interface and the bulk of the sample. This was also taken as evidence that the interface did not act as a conduit for preferential flow, although it must be acknowledged that the spatial resolution of these measurements, in relation to the interface aperture, may limit detection of any such differences. The authors suggest that further testing using interfaces of various initial openings would be beneficial to understanding of these features.

2.4.2.5.2   Gas injection in a dual density bentonite

In several engineered barrier systems (EBS) concepts, the waste canister is surrounded by rings of pre-compacted bentonite and the void space between the blocks and the deposition wall is filled with bentonite pellets in order to reduce voidage. As a result, this arrangement will initially generate a dual density bentonite/bentonite interface with the potential to persist for significant timescales. The degree of maturity of the buffer is likely to impact on this interaction and will depend on the ability of the bentonite to homogenise over the long term[17]. As part of the FORGE EC project, an experiment was designed to investigate the influence of such an interface (Graham C. et al. 2014) on (i) the hydration phase and associated stress development, (ii) the gas entry pressure and associated flow behaviour, and (iii) the longer term system evolution and the transience/degree of permanency of such an interface.

Using a similar set-up to Harrington and Horseman (2003), Graham C. et al. (2014) performed two tests on compact MX-80 bentonite. In each, two compacted blocks were each used to fill 1/3 of the cell, then the remaining 1/3 internal volume was filled with bentonite powder. This arrangement was chosen so the interface between two compacted blocks could be analysed on decommissioning, while the top 1/3 of the clay would consist of a low density slurry on hydration. In the first test, the authors report a long hydration phase (>200 days) stemming from a substantial inhomogeneity in the stress field of the clay. However, results from gas injection into the bentonite slurry indicate that, in spite of the heterogeneity of the hydration process, once the sample is saturated the gas entry behaviour appears remarkably similar to that observed for samples prepared entirely from pre-compacted bentonite blocks. In particular, gas entry only occurred once the applied gas pressure exceeded the local stresses measured in the top of the clay, in this instance ~3–3.5 MPa. This experimental programme continued at the end

---

[16] Kunigel VI is a commercial sodium type bentonite from Japan, containing nearly 48% montmorillonite (IAEA 2014).

[17] Understanding bentonite properties and fundamental processes that lead to material homogenisation with time is one of the main objectives of the BEACON EC Project (https://www.beacon-h2020.eu/).

EURAD (Deliverable n° 6.1) – Initial State of the Art on Gas Transport in Clayey Materials
Dissemination level: PU
Date of issue of this report: 17/11/2021

Page 115

of FORGE and remains ongoing, with gas injection tests that are planned and will be reported in the future.

2.4.2.5.3   Detailed studies of gas entry process

More recently, Harrington et al. (2017b) conducted a gas flow experiment on pure, fully saturated, MX-80 bentonite, using a constant volume apparatus with a similar configuration to that of Horseman et al. (2004). This experiment was undertaken to examine the gas entry process and associated hydro-mechanical coupling in detail. A complex experimental history was reported of more than 1 400 days, during which time the authors examined: (i) the onset of gas entry, (ii) the evolution of a gas flow network capable of quasi-steady-state flow and the associated changes in outflow/ local stress field (Harrington et al. 2017b), (iii) the ongoing development and stability of a gas transport network and (iv) the influence of applied gas boundary conditions and the impact of stimulation of the flow network (Harrington et al. 2018). In particular, they used a new approach to detect perturbations in the stress field to provide insight into the micromechanical deformation of the clay resulting from gas flow. Some key observations include:

- Strong hydro-mechanical coupling during the establishment of a gas flow network.

- Spatial evolution of the gas flow network in the initial stages after gas entry.

- Significant perturbation of the stress field in advance of all major gas outflow events, which is attributed to the propagation of gas flow pathways.

- No major outflows in the absence of stress field disturbance.

- Changes in gas pathways to outflow, indicating instability of flow and the potential for self-sealing.

- A reduction in stress field disturbance as 'quasi'-steady-state flow is approached.

- The cessation of gas flow is shown to result in crack closure and self-sealing.

- Network meta-stability is relatively well-maintained, despite change the applied injection pressure/flow rate.

- A strong destabilisation of the flow network by removal of the primary drainage route, resulting in a rapid redevelopment of the gas flow network was observed.

The authors, therefore, argue that availability of drainage pathways will represent a key control on the generation of peak gas pressures and distribution of gas within the engineered barrier. They also suggest that characterisation of the gas network distribution is, therefore, of fundamental importance in predicting gas dissipation rates.

EURAD (Deliverable n° 6.1) – Initial State of the Art on Gas Transport in Clayey Materials
Dissemination level: PU
Date of issue of this report: **17/11/2021**

Page 116

2.4.3   Shared understanding of gas flow through clayey materials

There is a consensus that visco-capillary two-phase flow of gas and water is possible through the porous media and/or through discontinuities.

It is shared understanding that the transport mode that will prevail in a given material is largely controlled by the fabric of the material, either undisturbed or locally disturbed by discontinuities. A balanced assessment of gas transport processes therefore requires careful consideration of structure and texture of the solid skeleton and, even more important, of the spatial connectedness of pore network which fills the space between the mineral aggregates forming the solid skeleton. The displacement of pore water by a gas phase is mainly restricted to the sparse network of macropores (pores >25 nm), because micro- and mesopores are hardly invaded by the gas phase due to their high gas entry pressure. High-resolution microstructural investigations provide most valuable information towards robust conceptualisations of gas transport. Advanced microstructural imaging workflows have been developed and tested successfully which allow to resolve 3D pore networks in clayey material with dominant pore sizes below 1 µm. The techniques have been extended to image not only static pore networks but also to visualise dynamic gas invasion and water imbibition processes in porous media at the µm-scale (Nagra 2020).

Multiple empirical and experimental evidence has been collected, confirming that high gas entry pressures are needed to invade a fully water-saturated clay sample. Gas invasion is not associated with major desaturation of the material. Consequently, characterisation of the water retention behaviour requires advanced laboratory methods, comprising precise measurements of (gravimetric) water content and adequate control of the volumetric behaviour of the clayey material in response to the applied suction. In this context, the axis translation techniques have been proposed as promising methods to complement the classical suction-controlled technique by exploring the suction range close to the gas entry pressure (Marinho et al. 2009). Several research teams have gained evidence for a hysteretic water retention behaviour, when the material is subjected to successive wetting/drying paths. Another phenomenon associated with cyclic wetting/drying has been particularly observed in granular bentonite. After several cycles of wetting/drying, the macroporosity of the material disappears, leading to increasing gas entry pressures and a general homogenisation of the material under fully saturated conditions. This observation coincides with experience in other research projects in the EURATOM framework (e.g. BEACON EC project).

While gas flow rates are generally low during the initial water displacement phase, many experimentalists report a high gas transport capacity of the clayey materials when gas breakthrough has been reached. Experiments suggest that the gas transport capacity during the initial water displacement phase is not only controlled by the magnitude of gas pressure but also by the gas pressure build-up rate, which may be attributed to the so-called 'dynamic effect'. Furthermore, clear evidence for distinct localisation of gas flow is found. Measurements of gas permeability in the dry state and water permeability in the fully saturated state suggest, that the concept of an intrinsic permeability is not fully applicable to clayey materials, especially to more expansive ones such as bentonite.

The invaded material may undergo irreversible deformation in response to gas pressure build-up, depending on the mechanical confinement and the tensile / shear strength of the test sample. Well-controlled gas injection tests under oedometric, isotropic and triaxial conditions have been performed in recent years with focus on the deformation behaviour of clayey materials in response to gas transport. These tests suggest that a distinct volumetric response ('dilatancy') may correlate with an enhancement of gas transport capacity of the material. These statements on indurated/soft clays being not yet fully supported by experimental evidence, they still need to be confirmed.

EURAD (Deliverable n° 6.1) – Initial State of the Art on Gas Transport in Clayey Materials
Dissemination level: PU
Date of issue of this report: 17/11/2021

Page 117

2.4.4   Uncertainties and knowledge gaps

The compilation of gas-related investigations with clayey materials reveals a great diversity of experimental results in terms of observed phenomena and processes. Comparison of results (and experiments) is not trivial and differing interpretations are sometimes possible to explain observations from a single experiment. A key source of uncertainty is a lack of experiment reproducibility and/or replication. With respect to flow through gas-specific pathways, a considerable source of uncertainty is that beyond the passage of gas, the actual transport mechanism is only observed indirectly, through its effect in terms of permeability of the material or transmissivity of a discontinuity.

This calls for a structured review of the existing knowledge base on gas transport in clayey materials, aimed at identifying the origin of ambiguous observations and inconclusive interpretations. As a step forward, a strategy is required which facilitates:

- a rigorous assessment of the acquired empirical observations and experimental data,

- a traceable workflow for identification and validation of existing conceptual frameworks,

- the development of sensible new modelling approaches (see Section 2.5).

The subsequent paragraphs address the knowledge gaps associated with the quality of the experimental data bases and the validity of the conceptual frameworks.

Empirical observations and experimental data bases: Compilations of laboratory investigations on water retention behaviour, gas and liquid permeability, volumetric and shear behaviour of clay-rich barrier materials tend to reveal a significant scatter. Agreed geotechnical workflows are required to gain confidence with regards to adequate sample preparation techniques and reliable basic characterisation of material properties (index properties). Furthermore, benchmark exercises are needed to confirm the reliability and comparability of various techniques for water retention measurements (e.g. static vs. dynamic; axis translation vs. vapour transfer techniques) and effective gas permeability testing along well-established loading paths. It is expected that the origin of the data scatter can be bracketed significantly by specifying an agreed technical guidance for gas testing (reference test protocols).

Identification and validation of the appropriate conceptual frameworks: Many interpretations of gas-related experiments on clayey barrier material, both, at the laboratory- and the field-scale reveal a wide spectrum of speculations on the governing transport mechanisms and the associated constitutive relationships, characterising the state of deformation of the tested material before and after gas transfer. Controversial discussions have been launched with regards to the appropriate representative elementary volume (REV) for gas transport in clay barriers and the associated scaling laws. Worth mentioning in the context of process upscaling, that some phenomena of potential relevance for repository safety, such as capillary and viscous fingering of volatile radionuclides in the backfilled repository structures have not gained major attendance. The validity of the well-established conceptual framework called *flow of immiscible fluids in deformable media* has been questioned for soft clays. Furthermore, the transferability of classical two-phase flow concepts from common soil physics applications ('vadose zone') towards gas transport in clay barriers has been challenged by various researchers. This includes the empirical van Genuchten relationships for water retention behaviour and Mualem relative liquid/gas permeability. Further issues addressed are the validity of the generalised Darcy law and the suitability of the concept of intrinsic permeability. Volumetric strain measurements are useful to support the classification of observed gas transport processes in clay barriers as *two-phase flow* or *pathway dilation*. Such measurements can provide conclusive evidence with regards to the postulated deformation behaviour but are not always performed or reported.

EURAD (Deliverable n° 6.1) – Initial State of the Art on Gas Transport in Clayey Materials
Dissemination level: PU
Date of issue of this report: 17/11/2021

Page 118

2.5   Modelling of gas transport

This section presents the fundamental basics of macroscopic theory for multiphase porous media, equivalent (multiple) continua, theory of mixtures, fluid mechanics (including multiphase flow), equations of state and phase-related general balance equations. The perspective adopted here is the description of typical, advanced tools that are currently used for the interpretation of experimental gas tests results. Section 3.3 will continue the state-of-the-art description of modelling gas processes in clayey material in particular with respect to barrier integrity, i.e. mechanical and coupled processes.

2.5.1   Introduction

Gas transport processes in natural or recompacted clay rocks are complex. Laboratory tests show the dependence of the flow dynamics on the experimental conditions, whether that is the injection conditions, mechanical loading, or interfaces between materials. In addition, the transfer of these observations to the scale of the underground structures raises questions about the scale effect of such methods. In situ tests thus highlight the influence of the damaged zone or interfaces between the different materials on the gas transport.

In order to achieve a synthesis of the gas transfer mechanisms to be taken into account in the models, four main processes can be identified (Figure 1-2). These develop gradually in clayey rocks with increasing gas pressure:

1. Advection and diffusion of the dissolved gas within the liquid phase when the quantities of injected gas are small.

2. The formation of a gas phase when the gas production is too large to be dissolved in the liquid phase and a two-phase water-gas transfer when the injection pressure is higher than the gas entry pressure.

3. The development of preferential flow paths (usually referred as 'Dilatant pathways' (Horseman and Harrington 1994; Marschall et al. 2005)) when the injection pressure becomes greater than a pressure threshold. The opening of these preferential paths is controlled by the gas pressure and is accompanied by a net increase in intrinsic permeability and a probable modification of the pore's volume. A two-phase water-gas flow still takes place within these micro-fractures, but the transfer properties are not constant and vary depending on the deformation state of the clay rock. The origin of these preferential paths can be:

   o the heterogeneity of the material which favours flows along the largest interconnected pores because they are the ones with the lowest capillary resistance forces,

   o the presence of fractures prior to gas transport, which are closed by confinement and then reopened given the increased pressure of gas.

4. Under certain conditions (e.g. mechanical loading favouring the fracturing), the formation of macroscopic fractures following the strong and rapid increased gas pressure, in a process similar to hydraulic fracking. A single gas phase then flows in these macro-fractures.

This classification of gas transport processes clearly highlights the importance of the mechanical behaviour of clay rocks to reproduce the development of preferential flow paths or macro-fractures. For gas pressure lower than a threshold pressure, it is essential to have a two-phase (water-gas) flow model in a numerical code to reproduce the transport of gas in porous media. This type of model takes into account the presence of water, water vapour, but also 'dry' gas and dissolved gas. These multiphase models generally exist in geomechanics (Thomas and Ye 1995; Olivella et al. 1996; Collin et al. 2002a; Gawin and Sanavia 2010 and in commercial codes like TOUGH2). The 'classical' hydro-mechanical two-phase flow models and their equations are first presented in the next section.

EURAD (Deliverable n° 6.1) – Initial State of the Art on Gas Transport in Clayey Materials
Dissemination level: PU
Date of issue of this report: 17/11/2021

Page 119

However, when the gas pressure is above the threshold value, other additional constitutive models are needed to be able to reproduce the development of preferential flow paths for gas in clay rocks. Alternative numerical approaches exist and are introduced in Section 2.5.3.

2.5.2   Classical hydro-mechanical models

The objective of this section is to present hydro-mechanical models of a porous medium in partially saturated conditions. We particularly pay attention to the description of the flow model. A two-phase flow model of water and gas is thus considered. Such flow models are common in the modelling codes for geomaterials. They take into account the presence of water and dissolved gases within the liquid phase and a mixture of 'dry' gas and water vapour within the gaseous phase. During excavation of a gallery, the two fluids to be considered in a two-phase flow model are water and air. In the case of gas (produced by corrosion among others) transport, the two fluids to be considered are water and hydrogen. Nitrogen and helium are also used in some laboratory and in situ experiments. In the following, only the case of one gas species is considered.

In this section, the balance equations of the hydro-mechanical model are first introduced. Then, the different constituent equations and equilibrium equations necessary to reproduce the behaviour of geomaterials in partially saturated conditions are presented. Different gases (air, hydrogen, nitrogen, helium, etc.) must be considered in the hydro-mechanical model in order to be able to simulate the different examples of interest. It is shown how the two-phase flow equations remain identical regardless of the gas envisaged, so that only certain specific parameters are modified according to the gas species envisaged. While the applicability of this hypothesis to all stages of radioactive waste disposal is arguable, the model presented in this section is developed under isothermal conditions.

The presentation of the hydro-mechanical model provides few details on some specific mechanical constitutive laws. The idea is rather to introduce the main concepts used to develop a mechanical law under unsaturated conditions. The objective of this section is to evidence the coupling sources between the multiphase flow of fluids and the mechanical behaviour of clayey materials.

2.5.2.1   Balance equations

Geomaterials, such as clayey materials, are generally considered to be porous materials filled by one or more fluids. Interactions between the solid skeleton and the different fluid phases are very important in many engineering problems. It is therefore necessary to develop numerical tools capable of modelling the multiphase behaviours of these materials. Three main approaches exist to describe porous media and build the idealised homogeneous continua:

Macroscopic theories

Macroscopic theories are based on the consolidation theory proposed by Terzaghi (1943), and later extended by Biot (1941, 1956, 1962, 1972). In these theories, the porous medium is studied at the macroscopic scale. Accordingly, stresses and other related concepts are macroscopic concepts. In addition, the different phases are not treated separately, and the balance equations are written for the whole porous medium, without any distinction between the different phases and species (or constituents). Further extensions of Biot's work include the contributions of Coussy (1995) and Dormieux et al. (1995).

EURAD (Deliverable n° 6.1) – Initial State of the Art on Gas Transport in Clayey Materials
Dissemination level: PU
Date of issue of this report: 17/11/2021

Page 120

Theory of mixtures

In the theory of mixtures, the porous medium is also studied at the macroscopic scale but the different phases are treated separately. All phases are assumed to occupy the same region of space simultaneously, and consequently, every point of the idealised system consists of a mixture of phases (Figure 2-46). The theory of mixtures was initially developed to solve multi-components gas mixtures. Bowen (1980, 1982) used the concept of volume fractions to extend the theory to multiphase porous media. The concept of volume fractions is used to create homogenised continua of reduced densities, so that the methods of continuum mechanics can be applied.
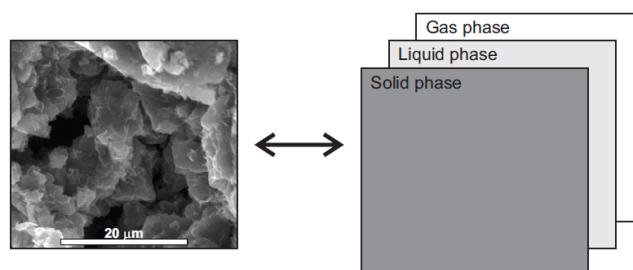
Figure 2-46 – Definition of equivalent continua. Example for theories of mixtures.

In the mixture theory, balance equations are expressed at the macroscopic scale (for each phase or species), and constitutive models are also introduced at this scale.

Averaging theory (or hybrid mixture theory)

In the averaging theory (Hassanizadeh and Gray 1979a, 1979b, 1980), two structural levels are defined, namely a microscopic scale, corresponding to the pore level, and a macroscopic scale, which corresponds to the representative elementary volume (REV). At the microscopic level, the system is viewed as the superposition of interpenetrating continua. In opposition to the mixture theory, each continuum occupies only a part of the space. The different continua are separated by interfaces which have their own thermodynamic properties. Balance equations (and sometimes constitutive laws) are introduced at this scale.

Averaging techniques are then used to obtain averaged (over the REV) macroscopic field equations. Different averaging methods may be used, ranging from analytical to numerical (e.g. Finite Element Square method). Special care should be taken to select the size of the REV (see Bear 1972; Hassanizadeh and Gray 1979a; Bachmat and Bear 1986; De Marsily 1986).

Although attractive, averaging theory requires the description of phenomena at a microscopic scale, typically the size of few aggregates. Because, in practice, this scale is difficult to investigate and very few experimental data are available, Dieudonné (2016) adopted instead a hybrid mixture approach that enables the description of fluid flow and deformation of the porous medium, and thus enables to easily tackle coupled phenomena.

The balance equations are obtained for a mixture composed of three species, namely mineral, water and air, distributed in three phases, namely solid, liquid and gas (Figure 2-47). Accordingly, the kinematics of the porous medium is described by its displacement field u [m], liquid pressure field u_l [Pa] and gas pressure field u_g [Pa] (one field for each homogenised continuum). Unless otherwise specified, the subscripts s, l and g refer to the solid, liquid and gas phase properties, while the superscripts w and a refer to the properties of water and air. In the formulation of Dieudonné (2016), it is assumed that the mineral species and the solid phase coincide. The liquid phase contains both water and dissolved air in concentration x_a^l [–]. However, it is assumed that the liquid phase properties are not

EURAD (Deliverable n° 6.1) – Initial State of the Art on Gas Transport in Clayey Materials
Dissemination level: PU
Date of issue of this report: **17/11/2021**

Page 121

affected by the amount of dissolved air and they therefore correspond to the ones of liquid water. Consequently, the liquid pressure u_l is equal the water pressure u_w [Pa], whose symbol is preferred in the following. Finally, the gas phase is a perfect mixture of dry air and water vapour. The partial pressure of dry air is denoted as u_a [Pa] and the partial pressure of water vapour, u_v [Pa]. According to Dalton's law, the total pressure of the gas phase u_g is equal to the sum of the partial pressures.

As already stated, the hybrid mixture approach (further developed in the following) holds for water and air and can be applied for any pair of water and gas species (hydrogen, natrium, helium …).
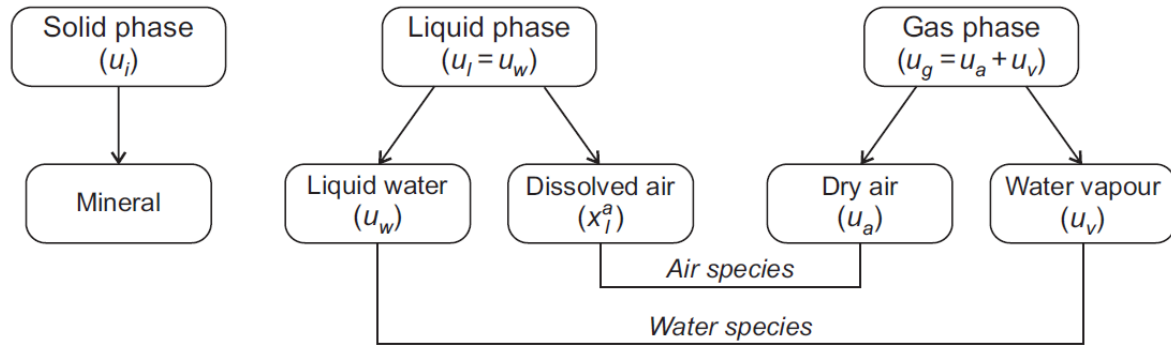
Figure 2-47 – Definition of phases (solid, liquid and gas) and species (mineral, water and air). The mineral species and the solid phase are assumed to coincide.

In the following, the different balance equations, namely the mass balance equations and the momentum balance equation, are expressed in local form. As presented in Dieudonné (2016), the balance equations are written in an updated Lagrangian framework, namely in the current solid configuration. This latter framework thus takes implicitly into account the contribution of the porous medium deformation in the balance equation. Under small strain hypothesis, the contribution of these deformations has to be included in the derivatives of the considered quantities.

2.5.2.1.1 Mass balance equation

The compositional approach (Panday and Corapcioglu 1989; Olivella et al. 1994; Collin 2003) is adopted to establish the mass balance equations. It consists of balancing species rather than phases. This approach has the advantage that phase exchange terms cancel out, which is particularly useful when equilibrium is assumed.

Solid mass balance equation

For a given volume of mixture Ω [m³], the mass balance of the solid phase reads:

$$\frac{\partial (\rho_s (1 - \phi)\Omega)}{\partial t} = 0 \tag{2-22}$$

where ρ_s [kg/m³] is the density of the solid and ϕ [–] is the porosity. If the solid particles are assumed to be incompressible (i.e. ρ_s is a constant), then Equation 2-22 reduces to

$$\frac{\dot{\Omega}}{\Omega} = \frac{\dot{\phi}}{1 - \phi} \qquad \text{where the superior dot denotes time derivative.} \tag{2-23}$$

EURAD (Deliverable n° 6.1) – Initial State of the Art on Gas Transport in Clayey Materials
Dissemination level: PU
Date of issue of this report: **17/11/2021**

Page 122

Fluid mass balance equations

The water and air mass balance equations are expressed as

$$\dot{m}_l^w + \boldsymbol{\nabla} \cdot \boldsymbol{f}_l^w + \dot{m}_g^w + \boldsymbol{\nabla} \cdot \boldsymbol{f}_g^w = Q^w \tag{2-24}$$

$$\dot{m}_g^a + \boldsymbol{\nabla} \cdot \boldsymbol{f}_g^a + \dot{m}_l^a + \boldsymbol{\nabla} \cdot \boldsymbol{f}_l^a = Q^a \tag{2-25}$$

where $m_l{}^w$, $m_g{}^w$, $m_g{}^a$ and $m_l{}^a$ are respectively the masses [kg] of liquid water, water vapour, dry air and dissolved air inside the porous volume Ω, $\boldsymbol{f}_l{}^w$, $\boldsymbol{f}_g{}^w$, $\boldsymbol{f}_g{}^a$ and $\boldsymbol{f}_l{}^a$ are the mass fluxes [kg/m³/s] of liquid water, water vapour, dry air and dissolved air, and Q^w [kg/m³/s] and Q^a [kg/m³/s] are water and air source terms. In these equations, the terms for the partial derivatives of time correspond to the change in fluid storage in the porous medium, while the divergence of fluxes express the difference between the input and output fluxes of a given volume of mixture Ω. These terms express that porous media, unlike classic continua, are thermodynamically open (Coussy 1995).

The different terms of Equations 2-24 and 2-25 corresponding to the change in fluid storage per unit volume are expressed as:

$$\dot{m}_l^w = \frac{\partial}{\partial t}(\rho_w \, S_l \, \phi) \tag{2-26}$$

$$\dot{m}_g^w = \frac{\partial}{\partial t}(\rho_v (1 - S_l)\phi) \tag{2-27}$$

$$\dot{m}_g^a = \frac{\partial}{\partial t}(\rho_a (1 - S_l)\phi) \tag{2-28}$$

$$\dot{m}_l^a = \frac{\partial}{\partial t}(\rho_l^a \, S_l \, \phi) \tag{2-29}$$

where ρ_w, ρ_v, ρ_a and $\rho_l{}^a$ are the densities [kg/m³] of liquid water, water vapour, dry air and dissolved air respectively. The liquid saturation degree S_l [–] corresponds to the ratio between the liquid phase volume and the porous volume. The gas saturation degree S_g [–] corresponds to the ratio between the gaseous phase volume and the porous volume. It is assumed that the sum of these two quantities (S_l and S_g) is equal to one. These relationships introduce coupling between the mechanical and hydraulic problems. Indeed, changes in porosity directly affect the fluids storage capacity. For a unit porous volume ($\Omega = 1$), Equations 2-24 and 2-25 become

$$\frac{\partial}{\partial t}(\rho_w \, S_l \, \phi) + \boldsymbol{\nabla} \cdot \boldsymbol{f}_l^w + \frac{\partial}{\partial t}(\rho_v (1 - S_l)\phi) + \boldsymbol{\nabla} \cdot \boldsymbol{f}_g^w = Q^w \tag{2-30}$$

$$\frac{\partial}{\partial t}(\rho_a (1 - S_l)\phi) + \boldsymbol{\nabla} \cdot \boldsymbol{f}_g^a + \frac{\partial}{\partial t}(\rho_l^a \, S_l \, \phi) + \boldsymbol{\nabla} \cdot \boldsymbol{f}_l^a = Q^a \tag{2-31}$$

2.5.2.1.2   Linear momentum balance equation

The balance of momentum is expressed for the entire mixture. For quasi-static loading, the equation reduces to the equilibrium of stresses

$$\boldsymbol{\nabla} \cdot \boldsymbol{\sigma}_t + \boldsymbol{b} = 0 \tag{2-32}$$

where $\boldsymbol{\sigma}_t$ [Pa] is the total Cauchy stress tensor (with compressive stress taken as positive), and $\boldsymbol{b}$ [N/m³] is the body force vector.

![eurad logo] European Joint Programme on Radioactive Waste Management

EURAD (Deliverable n° 6.1) – Initial State of the Art on Gas Transport in Clayey Materials
Dissemination level: PU
Date of issue of this report: **17/11/2021**

Page 123

If the only body force is gravity $\boldsymbol{g}$ [N/kg], $\boldsymbol{b}$ is equal to $\rho\boldsymbol{g}$, where ρ is the density of the mixture

$$\rho = \rho_s(1 - \phi) + \rho_w S_l \phi + \rho_g(1 - S_l)\phi \qquad (2\text{-}33)$$

where ρ_g [kg/m³] is the density of the gas phase (defined later by Equation 2-50.

The total stress tensor includes a contribution of the effective stress (supported by the solid skeleton) and of the fluid pressure (see Section 2.5.2.3). The effective stress tensor is computed through the mechanical constitutive model from the strain increment tensor. In this way, the two-phase flow models are coupled to deformation processes.

2.5.2.2 Multiphase flow model

The fluid mass balance Equations 2-30 and 2-31 involve mass fluxes of water and air which should be related to the displacement, water pressure and gas pressure fields. In this section, the equations for multiphase flow in porous media are developed with particular emphasis placed on the hydro-mechanical coupling relationships.

2.5.2.2.1 Fluid transfer equations

In both liquid and gas phases, water and air fluxes are a combination of advective and non-advective fluxes. Advective fluxes are associated with the phase movements, while non-advective fluxes are associated with the motion of species within phases. The mass fluxes of liquid water, water vapour, dry gas and dissolved gas are given by

$$\boldsymbol{f}_l^w = \rho_w \boldsymbol{q}_l \qquad (2\text{-}34)$$

$$\boldsymbol{f}_g^w = \rho_v \boldsymbol{q}_g + \boldsymbol{i}_g^w \qquad (2\text{-}35)$$

$$\boldsymbol{f}_g^a = \rho_a \boldsymbol{q}_g + \boldsymbol{i}_g^a \qquad (2\text{-}36)$$

$$\boldsymbol{f}_l^a = \rho_l^a \boldsymbol{q}_l + \boldsymbol{i}_l^a \qquad (2\text{-}37)$$

respectively, where $\boldsymbol{q}_l$ [and $\boldsymbol{q}_g$ are the advective fluxes [m/s] of the liquid and gas phases, and $\boldsymbol{i}_g^w$, $\boldsymbol{i}_g^a$ and $\boldsymbol{i}_l^a$ are the diffusive fluxes [kg/m³.m/s] of water vapour, dry air and dissolved air. Note that, in Equation 2-34, water diffusion in the liquid phase is neglected due to the small amount of dissolved air.

Advective fluxes

Advective fluxes of both liquid and gas phases are described by the generalised Darcy's law for partially saturated porous media. The mass fluxes of the liquid and gas phases are given by

$$\boldsymbol{q}_l = -\frac{k_w}{\mu_w}(\nabla u_w + \rho_w \boldsymbol{g}) \qquad (2\text{-}38)$$

$$\boldsymbol{q}_g = -\frac{k_g}{\mu_g}(\nabla u_g + \rho_g \boldsymbol{g}) \qquad (2\text{-}39)$$

where k_w and k_g are the water and gas permeabilities [m²] of the partially saturated medium, and μ_w and μ_g are the dynamic viscosities [Pa.s] of liquid water and the gas phase respectively. In non-reactive

![eurad logo] European Joint Programme on Radioactive Waste Management

EURAD (Deliverable n° 6.1) – Initial State of the Art on Gas Transport in Clayey Materials
Dissemination level: PU
Date of issue of this report: 17/11/2021

Page 124

porous media, the water and gas permeabilities strongly depend on the degree of saturation. Accordingly, the water and gas permeabilities are generally expressed as

$$\boldsymbol{k}_w = \boldsymbol{K}_w k_{rw}(S_r) \tag{2-40}$$

$$\boldsymbol{k}_g = \boldsymbol{K}_g k_{rg}(S_r) \tag{2-41}$$

where K_w and K_g are the water permeability tensor [m²] in fully saturated conditions and the gas permeability tensor in totally dry conditions respectively. k_{rw} and k_{rg} [–] are the water and gas relative permeabilities, which are functions of the degree of saturation. For a given degree of saturation, the water relative permeability is defined as the ratio between the unsaturated water permeability and the saturated water permeability. This ratio takes a value of 0 for theoretically completely dry conditions and 1 for saturated conditions. Accordingly, the gas relative permeability is the ratio between the unsaturated gas permeability and the gas permeability for totally dry conditions. In non-reactive porous materials, the relative permeability takes into account the change in cross-section responsible for water flow with the amount of water in the porous material.

While the generalised Darcy's law is treated here as a constitutive law, it has been obtained from balance equations and thermodynamic principles in averaging theories (see Hassanizadeh and Gray 1980; Lewis and Schrefler 1998, for instance). The generalised Darcy's law may indeed be derived from the equation of linear momentum balance for the liquid phase, assuming that inertial, viscous and phase change effects are negligible. One can show that these assumptions are valid if water flow is sufficiently slow (Lewis and Schrefler 1998), as is the case in clay-based materials, and hence providing a theoretical background for the use of Darcy's law in low-permeability porous media.

Diffusive fluxes

Diffusive fluxes are described by Fick's law. According to Fick's law, the diffusive flux is proportional to the gradient of mass fraction of species, with the proportionality coefficient being the hydrodynamic dispersion coefficient. The diffusive fluxes of water vapour and dissolved air read

$$\boldsymbol{i}_g^w = -D_g^{w*} \rho_g \boldsymbol{\nabla}\left(\frac{\rho_v}{\rho_g}\right) = -\boldsymbol{i}_g^a \tag{2-42}$$

$$\boldsymbol{i}_l^a = -D_l^{a*} \rho_w \boldsymbol{\nabla}\left(\frac{\rho_l^a}{\rho_w}\right) \tag{2-43}$$

where D_g^{w*} and D_l^{a*} are the effective diffusion coefficients [m²/s] of water vapour and dissolved air in the porous medium respectively. These coefficients depend on the porous volume of the material, its structure and its water content. Philip and de Vries (1957) suggested that the diffusion coefficients should be expressed as

$$D_g^{w*} = \phi \, S_g \, \tau \, D_g^w \tag{2-44}$$

and

$$D_l^{a*} = \phi \, S_l \, \tau \, D_l^a \tag{2-45}$$

where S_l *and* $S_g = (1 - S_l)$ are the liquid and the gas degree of saturation respectively, τ [–] is the tortuosity, ϕ is the porosity and D_g^w and D_l^a are the diffusion coefficients [m²/s] of water vapour in air

EURAD (Deliverable n° 6.1) – Initial State of the Art on Gas Transport in Clayey Materials
Dissemination level: PU
Date of issue of this report: **17/11/2021**

Page 125

and dissolved air in water, which are independent of the porous medium. In Equation 2-44, the product $\phi (1 - S_l)$ expresses the fact that vapour diffusion occurs through the gas phase of a porous medium, assuming that the total porosity contributes to vapour diffusion.

On the other hand, the tortuosity takes into account the fact that the path of a water molecule is not rectilinear, but that vapour flow occurs in a tortuous porous medium (Figure 2-48). Accordingly, the effective length covered by a water molecule (L_e) is larger than the straight line distance (L), meaning that $\tau = L_e/L$.
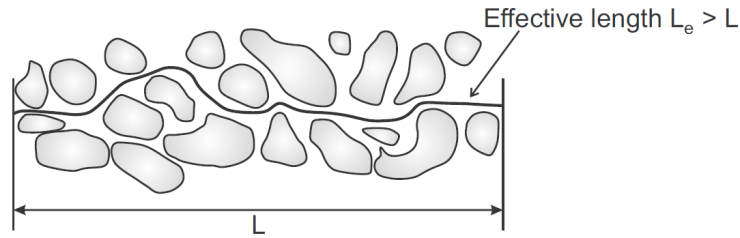
Figure 2-48 – Concept of tortuosity in granular porous media (Shackelford et al. 1989).

According to Millington and Quirk (1961) who developed a solute diffusion tortuosity factor model, tortuosity is a function of the volumetric soil water content θ and the total porosity ϕ:

$$\tau = \gamma \frac{\theta^n}{\phi^m} \tag{2-46}$$

where γ, n, and m are empirical constants.

The diffusion coefficient D_g^w depends on the gas pressure and temperature, but it is independent of the porous medium. For a mixture of water vapour with any gas species, the diffusion coefficient can be expressed as

$$D_g^w = D_{g0}^w \left(\frac{u_{g0}}{u_g}\right)\left(\frac{T}{T_0}\right)^{1.75} \tag{2-47}$$

where D_{g0}^w [m²/s] is the diffusion coefficient of the gas mixture at T_0 = 273.15 K, u_g is the gas pressure and u_{g0} = 0.1 MPa. The diffusion coefficient of water vapour in air D_l^a is equal to 5.03 × 10⁻⁹ m²/s.

Liquid density variation

The liquid water bulk density ρ_w is a function of the water pressure u_w. Its evolution might be described by an exponential function or linearised as:

$$\rho_w = \rho_{w0}\left(1 + \frac{u_w - u_{w0}}{\chi_w}\right) \tag{2-48}$$

where ρ_{w0} [kg/m³] is the liquid water density at the reference water pressure u_{w0} [Pa], and χ_w [Pa] is the water compressibility (= 2 10⁹ Pa at 20°C). The strong physico-chemical interactions between water and clay minerals in compacted bentonites are likely to lead to values of water density higher than 1 g/cm³ for saturated conditions. Accordingly, values of ρ_{w0} higher than 1 g/cm³ might be assumed for u_w = 0.1 MPa.

EURAD (Deliverable n° 6.1) – Initial State of the Art on Gas Transport in Clayey Materials
Dissemination level: PU
Date of issue of this report: **17/11/2021**

Page 126

Gas density variation

The gas phase is considered as an ideal mixture of ideal gases, namely dry air (or any other gas species) and water vapour, that is

$$u_g = u_a + u_v \qquad\qquad (2\text{-}49)$$

The density of the gas phase is obtained using Dalton's law. It yields

$$\rho_g = \rho_a + \rho_v \qquad\qquad (2\text{-}50)$$

with ρ_a and ρ_v the densities of dry air and water vapour respectively, and

$$\rho_a = \frac{M_a}{RT} u_a \qquad\qquad (2\text{-}51)$$

$$\rho_v = \frac{M_w}{RT} u_v \qquad\qquad (2\text{-}52)$$

where R is the universal gas constant (= 8.3143 J/mol K), T is the absolute temperature (°K), and M_a and M_w are respectively the molecular mass of dry air (= 0.029 kg/mol) and water (= 0.018 kg/mol).

2.5.2.2.2 Equilibrium restrictions

Equilibrium restrictions relate dependent variables with kinematics variables. They are obtained assuming thermodynamic equilibrium between the different phases of the species. This hypothesis is justified by the fast kinetics of the dissolution processes compared to the transport phenomena in clay-based materials.

Kelvin's law

It is assumed that water vapour is always in thermodynamic equilibrium with liquid water. Kelvin's law expresses the pressure of water vapour u_v as a function of suction s [Pa] according to

$$u_v = u_v^0 \exp\left(\frac{-s\,M_w}{RT\rho_w}\right) \qquad\qquad (2\text{-}53)$$

where u_v^0 [Pa] is the saturated pressure of water vapour. For a given temperature, the saturated pressure of water vapour is a constant. It may be calculated from the Clausius-Clapeyron equation or obtained from empirical relationships (see Garrels and Christ 1965; Ewen and Thomas 1989).

Henry's law

Henry's law expresses the equilibrium between dissolved air in the liquid phase and dry air in the gas phase. Under constant temperature, the amount of dissolved air is proportional to the air partial pressure u_a:

$$u_a = K_l^a x_l^a \qquad\qquad (2\text{-}54)$$

where K_l^a [Pa] is a constant and x_l^a [–] is the dissolved air mass fraction. This law may be written in terms of densities, so that

EURAD (Deliverable n° 6.1) – Initial State of the Art on Gas Transport in Clayey Materials
Dissemination level: PU
Date of issue of this report: **17/11/2021**

Page 127

$$\rho_l^a = H_a \, \rho_a \tag{2-55}$$

where H_a [–] is called the Henry's coefficient and is equal to 0.0234 for air at 20°C (Henry W. 1803).

2.5.2.3 Mechanical constitutive model

The momentum balance Equation 2-32 introduces the total Cauchy stress tensor which should be related to the main unknowns of the problem. Yet, contrary to classic continuous media, the mechanical behaviour of porous media is not only controlled by the total stress, but it is also influenced by the fluids occupying the pore space. Therefore, alternative stress variable(s) should be defined. In the case of saturated porous media, the concept of effective stress was early introduced by Terzaghi (1936). In this section, the concept of effective stress in saturated soils is first presented. Then, the definition of adequate stress variables in unsaturated porous media is considered. Finally, important aspects of constitutive models for unsaturated soils are discussed. Further reviews of constitutive modelling of unsaturated soils can be found in Wheeler and Karube (1995), in Gens (1996), Gens et al. (2006), Sheng et al. (2008a) and Sheng (2011).

2.5.2.3.1 Effective stress in saturated porous media

Terzaghi (1936) introduced the concept of effective stress to describe the mechanical behaviour of fully saturated porous media. The effective stress transforms a real multiphase porous medium into a mechanically equivalent single-phase continuum. It is defined as

$$\boldsymbol{\sigma}' = \boldsymbol{\sigma}_t - u_w \, \boldsymbol{I} \tag{2-56}$$

where σ' [Pa] is the effective stress tensor (defined as positive in compression) and $\boldsymbol{I}$ is the identity tensor. Note that this definition assumes that the solid minerals and water are incompressible and that the contact between minerals is punctual.

The validity of Terzaghi's effective stress to describe the behaviour of expansive clays has been the subject of debate for several years (Graham J. et al. 1992; Hueckel 1992a; Masin and Khalili 2016). According to Terzaghi, the load is indeed supported by the effective stress and the fluid pore pressure only, so that physico-chemical interactions between clay particles are not considered. However, these are likely to contribute to load support. Attempts to incorporate physico-chemical effects in the definition of effective stress include the works of Sridharan and Venkatappa (1973), Hueckel (1992a, 1992b), Bennethum et al. (1997) and Mainka et al. (2014), among others.

A constitutive model for saturated geomaterials relates the effective stress increments (regardless of its definition) to the strain increments. It reads

$$d\boldsymbol{\sigma}' = \boldsymbol{D} : d\boldsymbol{\varepsilon} \tag{2-57}$$

where $\boldsymbol{D}$ [Pa] is a constitutive tensor and $\boldsymbol{\varepsilon}$ [–] is the strain tensor. Alternatively, the previous relationship can be expressed in terms of effective stress and strain rates

$$\dot{\boldsymbol{\sigma}}' = \boldsymbol{D} : \dot{\boldsymbol{\varepsilon}} \tag{2-58}$$

The definition of the effective stress yields a first-order important hydro-mechanical coupling. Indeed, changes in water pressure u_w directly affect the mechanical behaviour of the porous medium.

![eurad logo] European Joint Programme on Radioactive Waste Management

EURAD (Deliverable n° 6.1) – Initial State of the Art on Gas Transport in Clayey Materials
Dissemination level: PU
Date of issue of this report: **17/11/2021**

Page 128

2.5.2.3.2   Stress variables in unsaturated porous media

The choice of constitutive variables is an inevitable issue in modelling unsaturated soils. Over the years, the choice of appropriate stress variables to model the behaviour of unsaturated soils has indeed been an intensively debated issue. Two main approaches are generally distinguished:

- the extension of the effective stress definition for saturated porous media towards unsaturated states,

- the definition of two independent stress variables (while only one, the effective stress, is used for saturated media).

Each of these two approaches has advantages and drawbacks. They are briefly described in the next two sections. Further discussion and historical review can be found in Khalili et al. (2004) and Nuth and Laloui (2008).

Effective stress approach

In the effective stress approach, Terzaghi's definition of the effective stress (Equation 2-56 is extended to the partial saturation domain. One of the most famous definitions was proposed by Bishop (1959). It is given by

$$\boldsymbol{\sigma'} = \left(\boldsymbol{\sigma}_t - u_g \, \boldsymbol{I}\right) + \chi\left(u_g - u_w\right)\boldsymbol{I} \tag{2-59}$$

where χ [–] is a material parameter, called Bishop's parameter, which depends on the degree of saturation. It takes the value of 1 for fully saturated states and 0 for totally dry states. Experimental results on unsaturated soils evidence the relationship between χ and the degree of saturation (Jennings and Burland 1962; Fredlund and Rahardjo 1993). Note that, since Bishop's stress σ' depends on the material properties, it is not strictly speaking an effective stress (Sheng et al. 2008a). Indeed, in this case, the effective stress space depends on the material behaviour and changes with its state. Accordingly, the constitutive behaviour of the material results from both constitutive relations and the stress space in which the constitutive model is defined.

When working with constitutive models for unsaturated soils, the main advantage of the effective stress approach is that the models previously developed for saturated soils are straightforwardly extended to the unsaturated domain. In addition, there is a continuous and smooth transition from saturated to unsaturated states. However, the determination of the different model parameters from laboratory tests is often complex. Indeed, during testing on unsaturated samples, the controlled variables are usually total stress (or displacement) and suction (or water content). In order to use the test results for the parameters' determination (of a model in effective stress), the saturation needs to be introduced. It means also that a constant total stress wetting stress path corresponds to a path with varying effective stress and suction.

In addition, the effective stress approach has shown limitations in representing the important swelling of compacted clays and bentonites. The approach is also incapable of reproducing the collapse phenomenon upon wetting paths under high stress levels. Indeed, upon hydration, the fluid pressure increases, producing a decrease in the effective stress. Accordingly, the material swells, while compaction is observed experimentally. In order to overcome this issue, constitutive models written in terms of a generalised effective stress generally introduce suction as a variable and define a Loading-Collapse curve, similar to the Barcelona Basic Model (Alonso E. et al. 1990), (see for instance Jommi and di Prisco 1994; Bolzon et al. 1996; Loret and Khalili 2000; Wheeler et al. 2003; Sheng et al. 2004; Laloui and Nuth 2005; Della Vecchia et al. 2013, among many others).

EURAD (Deliverable n° 6.1) – Initial State of the Art on Gas Transport in Clayey Materials
Dissemination level: PU
Date of issue of this report: 17/11/2021
Page 129

Independent variables approach

According to Fredlund and Rahardjo (1993), the number of independent variables is directly linked to the number of phases. For a saturated porous material, only one variable is required: the effective stress. For partially saturated soils, Coleman (1962), Bishop and Blight (1963), Fredlund and Morgenstern (1977) and Alonso E. et al. (1990), among others, show that two independent variables enable the limitations of the single effective stress to be overcome. In particular, Fredlund and Morgenstern (1977) demonstrated that any pair of $\boldsymbol{\sigma} = \boldsymbol{\sigma}_t - u_g \boldsymbol{I}$, $\boldsymbol{\sigma}^t = \boldsymbol{\sigma}_t - u_w \boldsymbol{I}$ and suction $s = u_g - u_w$ could be used to describe the behaviour of unsaturated soils. The so-called net stress tensor $\boldsymbol{\sigma}$ is defined as follows:

$$\boldsymbol{\sigma} = \boldsymbol{\sigma}_t - u_g \boldsymbol{I} \tag{2-60}$$

In most cases, the net stress and suction are selected to work in the unsaturated domain. This couple of variables is primarily justified by the fact that the variables are directly accessible during experimental tests. Once the material is saturated, the effective stress (Equation 2-56 is often used instead of the net stress. Null test can be performed to verify the applicability of the coupling of variables. Indeed, if the components of the variables are changed identically so that the variables do not change ($\Delta\boldsymbol{\sigma}_{t,ij} = \Delta u_g = \Delta u_w$), no volume change nor distortion should be observed.

The main drawback of the independent variables approach is that the extension of constitutive models for saturated materials is not straightforward. Specific constitutive models, accounting for the different independent variables, should be developed. In addition, there might be a lack of continuity in the transition between saturated and unsaturated states.

The first and most famous complete constitutive model for unsaturated soils is the Barcelona Basic Model (BBM) developed by Alonso E. et al. (1990). The model uses suction and net stress as independent variables. As an extension of the Modified Cam-Clay model (Roscoe and Burland 1968), BBM is formulated in the framework of elasto-plasticity theory and critical state models. An important contribution of the BBM is the definition of the Loading-Collapse (LC) curve. This yield surface represents the evolution of the preconsolidation pressure with suction, and allows the easy reproduction of the collapse phenomenon upon wetting under high stress levels. The three-dimensional yield surface of the model is presented in Figure 2-49.

The BBM pioneered the development of almost all advanced constitutive models for unsaturated soils, being formulated with independent stress variables or an effective stress. Examples of models written in terms of independent variables (net stress and suction) include the ones of Cui et al. (1995), Wheeler and Sivakumar (1995), Cui and Delage (1996), Alonso E. et al. (1999), Collin et al. (2002b), Sánchez et al. (2005) and Sheng et al. (2008b).
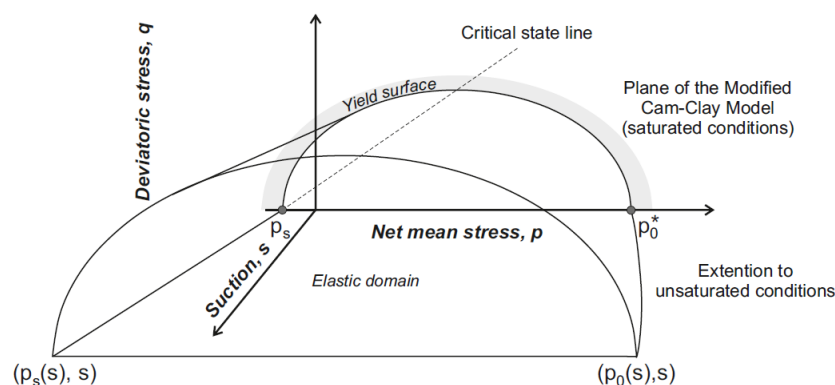
EURAD (Deliverable n° 6.1) – Initial State of the Art on Gas Transport in Clayey Materials
Dissemination level: PU
Date of issue of this report: **17/11/2021**

Page 130

Figure 2-49 – Three-dimensional yield surface of the Barcelona Basic Model (Alonso E. et al. 1990).

2.5.3   Advanced hydro-mechanical models

In classical hydro-mechanical models, the coupling between fluid flow and mechanical behaviour is twofold: the evolution of pore pressure affects the effective stress distribution (H→M coupling) and the storage of fluid is a function of the mechanical deformation (M→H coupling). The intrinsic permeability is usually considered as constant but formulations with modified intrinsic permeability exist in the literature (see Section 3.3.5). These classical models are not able as such to reproduce all the features of the gas flow processes.

Gas flow in clay rocks is a complex process because it strongly depends on the heterogeneity and microstructure of the material, as well as chosen experimental conditions. In the previous section, a hydro-mechanical model for partially saturated media was presented and was able to reproduce the experimental observations under these saturation conditions. But experimental results have highlighted how some parameters such as mechanical loading or gas injection kinetics can influence the observed behaviour. They highlight the development of paths of preferential flow beyond a certain injection pressure, called the 'fracturing pressure'. Such behaviour cannot be reproduced by conventional two-phase flow models that include constant flow parameters such as permeabilities and retention curves. It is therefore necessary to improve our models to be able to reproduce such phenomena.

Different numerical methods are used to improve the modelling response. The fundamental idea is to introduce stronger couplings between the gas flow and the mechanical behaviour of the clayey material. A first approach is the following: stress-dependent porosity and permeability are one of the options to better reproduce a rapid increase of gas flow above a threshold injection pressure (Senger et al. 2014). Fall et al. (2014) and Yamamoto et al. (2015) used a fully coupled poro-mechanical model to couple explicitly two-phase flow transport models with the evolving stress field. The latter models are claimed to better reproduce the effect of pathway dilation on gas transport at the relevant scale of the system, but they do not model explicitly the dilatation pathway.

In a finite element code, in order to model the localised gas flow, different approaches can be adopted as detailed hereafter in Section 2.5.3.1. In addition to these finite element approaches based on continuous models, discrete approaches have been also used in the literature referring to so-called lattice models (Pazdniakou et al. 2018), pore scale approaches (smoothed-particle-hydrodynamics, Pazdniakou and Dymitrowska 2018) or distinct element method (DEM, Caulk et al. 2020). Lattice models are briefly discussed in Section 2.5.3.2.

EURAD (Deliverable n° 6.1) – Initial State of the Art on Gas Transport in Clayey Materials
Dissemination level: PU
Date of issue of this report: 17/11/2021

Page 131

2.5.3.1 Finite element approach

Finite element codes rely on the continuum mechanics hypothesis (assuming averaged properties of the porous medium) operating on a representative elementary volume. Three options are presented in this section:

- assuming an initial and natural heterogeneity of the transfer parameters of the material,

- taking into account the presence of discontinuities in the rock by averaging the permeability within the elements of the mesh as a function of the assumed density of fractures,

- inserting explicit fractures in the mesh.

2.5.3.1.1 Natural heterogeneity

In this approach, the development of preferential paths is explained by the natural and initial heterogeneity of the material. Heterogeneous distribution of porosity or of the permeability explains why the gas is transported preferentially in certain directions.

Delahaye and Alonso (2002) proposed that the non-uniform distributions of the permeability could create preferential flow paths for gas. This approach is used with a continuous two-phase flow model, so that the gas transport is favoured along certain paths with a higher initial permeability. The choice of the spatial distribution of the permeability remains a parameter that strongly influences the results obtained. On the other hand, Olivella and Alonso (2008) used the same approach with heterogeneous distributions of porosity (Figure 2-50). According to the Kozeny-Karman law that couples the permeability to the porosity, they also reproduce some experimental gas transport observations made on samples of clay.

This numerical approach has certain disadvantages:

- The high CPU cost, because many initial statistical distributions must be tested numerically in order to find a distribution satisfactorily reproducing the experimental results.

- The initial heterogeneity fixed by the user does not rely on direct measurements made on the tested sample.

- Strongly coupled hydro-mechanical behaviours such as gas fracturing or the generation of an excavated damaged zone after gallery construction is difficult to be taken into account in such an approach. Indeed, the heterogeneity must be defined initially.

EURAD (Deliverable n° 6.1) – Initial State of the Art on Gas Transport in Clayey Materials
Dissemination level: PU
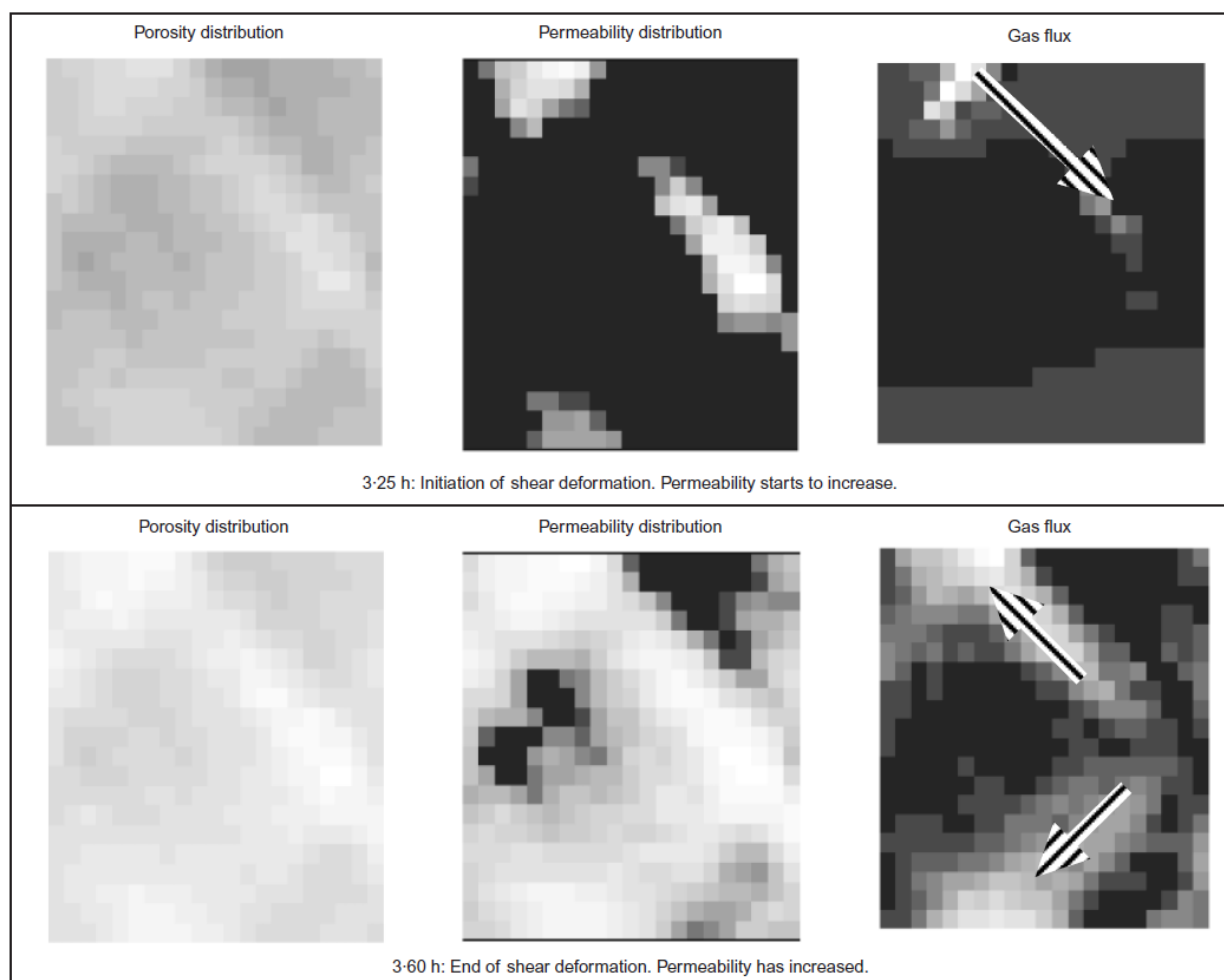Date of issue of this report: **17/11/2021**

Page 132

Figure 2-50 – Evolution of several variables during distributed fracture induced by deviatoric stress application (white zones are zones of higher porosity, ranges from 0.105 to 0.116), permeability (ranges from 10^{-19} to 10^{-15} m^2) and gas flux. Analysis considering a random strength (Case B) (Olivella and Alonso 2008).

2.5.3.1.2   Embedded fracture model

The Two-Part Hooke's Model (TPHM) is not an embedded fracture model but relies on the same ideas. It assumes that sedimentary rocks can be considered as a layered structure made of a superposition of 'soft' parts undergoing relatively large strains (and consequently larger permeability increase) and 'hard' parts, which undergo small strains (Liu H. et al. 2009; Liu H. et al. 2011; Senger et al. 2015).

The embedded fracture model assumes that fractures created by traction are inducing the development of preferential flow paths within the sample. The opening of these fractures therefore causes a significant increase in permeability in the direction of the fractures (Alonso E. et al. 2006; Olivella and Alonso 2008). With the embedded fracture model, permeability is related to the state of deformation within the sample. The flow properties of the rock matrix and the fractures created by traction are averaged within a representative volume.

To take into account material anisotropy and the possible presence of preferential gas transport pathways along a given orientation, some authors used embedded fracture permeability models or added joint elements to a continuum model (Arnedo et al. 2013; Gerard et al. 2014; Gonzalez-Blanco et al. 2016a). In this approach, the discontinuities are assumed to be tensile fractures with two flat parallel surfaces (Figure 2-51). Therefore, if assuming laminar flows within these fractures, the intrinsic

EURAD (Deliverable n° 6.1) – Initial State of the Art on Gas Transport in Clayey Materials
Dissemination level: PU
Date of issue of this report: 17/11/2021

Page 133

permeability $K_{fracture}$ in the direction of the discontinuities is a function of the opening of this fracture and is given by the Poiseuille solution:

$$K_{fracture} = \frac{b^2}{12}$$

(2-61)

with b [m] equal to the opening of the fracture.
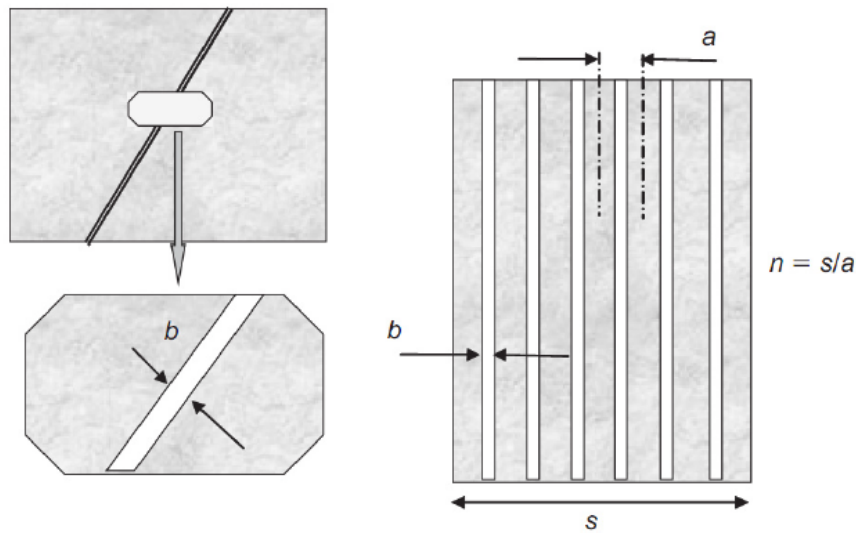
Figure 2-51 – Idealised sketch of one fracture (with an opening b) and of a representative elementary volume containing n parallel fractures – Embedded fracture model (Olivella and Alonso 2008).

From the density of fractures within an element, it is possible to average the permeability of the rock matrix and fractures within a representative volume. The global permeability K of a volume composed of a rock matrix (with a permeability K_{matrix} [m²]) and a-spaced fractures is expressed as:

$$K = K_{matrix} + \frac{b^3}{12\,a}$$

(2-62)

It is then possible to link the opening of the fracture to the tensile deformation in the direction normal to the fracture. This is a more easily identifiable variable during simulations with finite elements:

$$K = K_{matrix} + \frac{(b_0 + a\,\varepsilon^T)^3}{12\,a}$$

(2-63)

where ε^T is the tensile strain [–] within the element, a [m] is the distance between two fractures and b_0 [m] is the initial opening of the fractures.

On the other hand, in addition to this significant increase in permeability, Olivella and Alonso (2008) suggest taking into account a change in the retention behaviour in the volume where traction discontinuities develop. They consider that modifications of the pore volume will influence the characteristics of material retention. In this approach, it is assumed that the pore radii increase following the opening of discontinuities, so that a decrease in the gas entry pressure is observed. From Jurin's law, it is possible to write:

EURAD (Deliverable n° 6.1) – Initial State of the Art on Gas Transport in Clayey Materials
Dissemination level: PU
Date of issue of this report: 17/11/2021

Page 134

$$P_r = P_{r,0} \sqrt[3]{\frac{K_0}{K}}$$

(2-64)

where P_r [Pa] is the current gas entry pressure, $P_{r,0}$ [Pa] is the initial gas entry pressure, K is the current permeability and K_0 is the initial permeability.

Alonso E. et al. (2006) and Olivella and Alonso (2008) used this model coupling the mechanical behaviour and fluid flow to reproduce experimental observations of gas transport tests carried out on clay samples. This model was afterwards applied to some experimental results on sand/bentonite (Arnedo et al. 2008) and claystone (Gerard 2011; Arnedo et al. 2013). They showed the great sensitivity of the results to certain parameters of the model that are difficult to identify, such as the density of fractures or their initial opening. But these data are more and more accessible through advanced experimental techniques (Gonzalez-Blanco et al. 2016a). On the other hand, Levasseur et al. (2010) showed that this model allows the reproduction of the results of the SELFRAC in situ test in Opalinus Clay, consisting of measurements of a dilatometer in saturated conditions.

This model has the advantage of:

- proposing a coupled hydro-mechanical evolution of the permeability as a function of tensile deformations, which highlights the contribution of the mechanical behaviour of clayey materials to reproduce the development of preferential paths.

- linking the mechanical damage of the material to a modification of the retention curves, via the proposed simple relationship between gas entry pressure and tensile deformations.

However, this model also has some drawbacks, such as:

- a simplified representation of the geometry of a tensile fracture, assuming that a fracture is made up of two flat and parallel surfaces and therefore disregards factors such as the roughness of the walls;

- the damage is only induced as a consequence of tensile deformations, even if rupture mode can occur for other mechanical loadings;

- the model parameters are difficult to identify experimentally, like the density or the initial opening of the fractures.

2.5.3.1.3   Explicit fracture in the mesh

In order to numerically reproduce the development of preferential paths in a clayey material, it is possible to explicitly define fractures in the finite element mesh. These fractures are modelled by interface elements, which manage the opening and contact between the two walls. Hydro-mechanical interface elements in saturated conditions have been developed (Guiducci et al. 2002a, 2002b; Segura and Carol 2008). A discontinuity (Figure 2-52) between two bodies $\mathcal{B}^1$ and $\mathcal{B}^2$ creates a preferential pathway for longitudinal fluid flow and a volume for fluid storage. Moreover, there is also a transversal fluid flow between the material and the discontinuity.
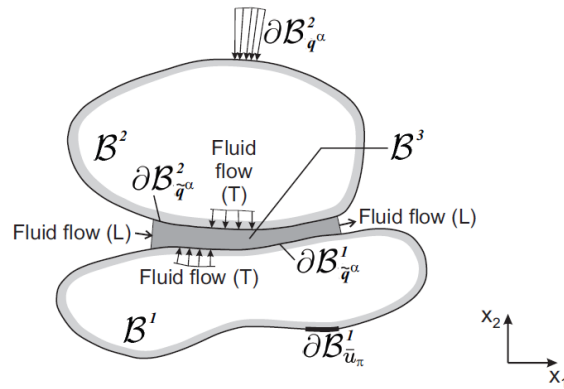
EURAD (Deliverable n° 6.1) – Initial State of the Art on Gas Transport in Clayey Materials
Dissemination level: PU
Date of issue of this report: **17/11/2021**

Page 135

Figure 2-52 – Statement of the multiphase flow problem. u_π denotes the water or gas pressure and q^α, the total water or air mass flux.

There is a conceptual difference between the treatment of the mechanical and flow contact problems. On the one hand, the mechanical contact constraint consists of a non-zero contact pressure applied along the contact zone between two solids. On the other hand, the opening of the discontinuity creates a gap g_N filled with water and air. This gap creates a new volume $\mathcal{B}^3$ in which fluid flow takes place. It is bounded by the two porous media. Their boundaries are termed $\mathcal{B}^1_{q\alpha}$ and $\mathcal{B}^2_{q\alpha}$ with q^α denoting the total water or air mass flux on the boundary. Therefore $\mathcal{B}_{q\alpha}$ represents a boundary where the solids are close enough, fluid interaction holds and mechanical contact is likely to happen. $\mathcal{B}^3$ is modelled as an equivalent porous medium. Flows of water and air exist both longitudinally (L) and transversally (T) between the inner volume $\mathcal{B}^3$ and both adjacent porous media $\mathcal{B}^1$ and $\mathcal{B}^2$ (Figure 2-53). This transversal flow is a function of the difference in pressure between them. It introduces a non-classic boundary condition on $\mathcal{B}_{q\alpha}$ since neither the pressure nor the flux is imposed.

The extension of such a formulation to partially saturated conditions can be found in the work of Cerfontaine et al. (2015).
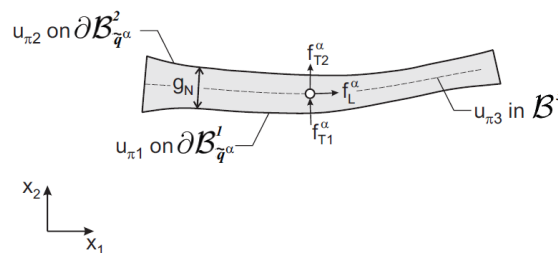
Figure 2-53 – Definition of the longitudinal and transversal water and air fluxes.

Beside the explicit introduction of fracture into the mesh, there exist also numerical methods that do not require any modification of the mesh. In the embedded crack models, the displacement jump inside the fracture is introduced inside the finite element through additional degree of freedom (Dvorkin et al. 1990; Jirásek and Zimmermann 2001). A comparative study of the finite elements with embedded discontinuities can be found in Jirásek (2000).

The extended finite element method (X-FEM) allows (among others) to treat the propagation of discontinuity independently of the mesh by generalising the shape functions of the finite element discretisation according to the partition of unity method (Melenk and Babuška 1996). The idea is to incorporate in the interpolation of the fields, functions allowing a good approximation of the solution for the problem being treated. The finite element interpolation is enriched by additional functions in the parts of the domain where they are relevant. The X-FEM method was first used for crack propagation

EURAD (Deliverable n° 6.1) – Initial State of the Art on Gas Transport in Clayey Materials
Dissemination level: PU
Date of issue of this report: 17/11/2021

Page 136

in Griffith models (Dolbow et al. 2000; Moës et al. 1999). In this case, the enrichment functions must be able to describe the discontinuity and the field of displacement at a crack point. The X-FEM method was then applied for models of cohesive zones (Moës and Belytschko 2002; Wells and Sluys 2001; Mariani and Perego 2003). In this case, the main difference with a crack propagation for a Griffith model is the description of the crack point fields, which no longer shows infinite stresses.

2.5.3.2 Lattice model

In the lattice models, the porous medium is supposed to be composed of a set of capillaries or tubes forming a 'lattice'. Fluids (water, gas) flow within these tubes according to a two-phase model controlled by capillary forces. The geometric characteristics of these tubes (section, length, etc.) are fixed by the user. Different models have been developed, gradually taking into account the complexity of the microstructure of clay rocks.

2.5.3.2.1 Capillary bundle

In the 'capillary bundle' approach (Rodwell and Nash 1992; Grindrod et al. 1994), the porous medium is assumed to be composed of a series of tubes (Figure 2-54):

- which do not intersect;
- with a constant radius over the length of the sample;
- whose distribution of the radius is not uniform;
- of length equal to τL, where L is the length of the modelled sample and τ the tortuosity of the porous medium.

Capillary radii control the respective gas entry pressures of each flow path via Jurin's law. From a generalised Darcy law for unsaturated media, this model has been used to simulate the development of preferential flow paths by Ortiz et al. (1998) as part of the MEGAS EC project (Volckaert et al. 1995).
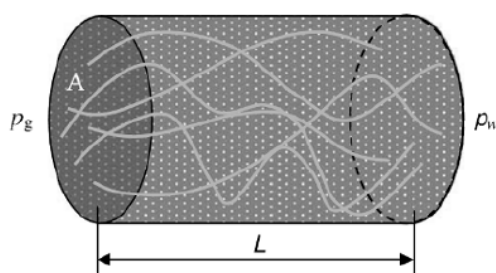
Figure 2-54 – Schematic view of the capillary bundle model (Ortiz et al. 1998).

2.5.3.2.2 Capillary network

The 'capillary network model' is an extension of the 'capillary bundle model', allowing a more realistic, but still simplified approach to a porous clay medium. In this model, the porous medium is represented by the superimposition of a lattice of capillaries with different radii. Within each lattice, the following conditions are met:

- The capillaries have a uniform and constant radius, but which is different for each lattice.
- The length of the capillaries is constant within each lattice, but varies for each lattice.
- The density of capillaries within a lattice is set by the user.

EURAD (Deliverable n° 6.1) – Initial State of the Art on Gas Transport in Clayey Materials
Dissemination level: PU
Date of issue of this report: **17/11/2021**

Page 137

- The distribution of the capillaries within a lattice is random.

Figure 2-55 thus represents a 2D network of capillaries based on the superposition of three lattices. Each of them is formed by meshes of different sizes, corresponding to the length of the capillaries. The density of the capillaries changes with the considered lattice. The radius of these capillaries is proportional to the mesh dimensions, so that in the example presented in Figure 2-55, the radii of class 1 capillaries are larger than those of class 3.

Once the different lattices are superimposed, a network of capillaries representing the porous medium is obtained. This model allows the representation of capillaries which cross or which are interrupted within the sample. This representation was not possible in the case of the 'capillary bundle model'.

From a generalised Darcy's law and a gas entry pressure depending on the radius of the capillaries (Jurin's law), such a structure allows the reproduction of (Impey et al. 1997):

- the development of preferential flow paths,
- the complex dynamics of flows in the preferential channels during the post-peak phase, thanks to crossing and interrupting paths of flows.

In order to find the best capillary network reproducing the microstructure of the studied material, a method has been proposed by Xu K. et al. (1997a, 1997b) and then applied by Boulin et al. (2008b) on clayey materials to link the density functions of capillaries within each lattice to experimental observations on the microstructure of the material obtained during mercury intrusion tests.

The advantage of these lattice models is that they allow the representation of post-breakthrough cyclic phenomena observed on samples in the laboratory, that other models fail to reproduce. However, they also present certain disadvantages, such as:

- the general absence of coupling between the mechanical behaviour of the rock matrix and the evolution of gas flows, which seems necessary to reproduce experimental observations such as gas fracturing or the increase in permeability around the galleries following the damage caused by excavation;
- strong freedom left to the user in the definition of capillary networks, which is actually a fitting variable to reproduce the experimental observations. Although, Boulin et al. (2008b) did attempt to link information from mercury intrusions to the definition of the capillary network.

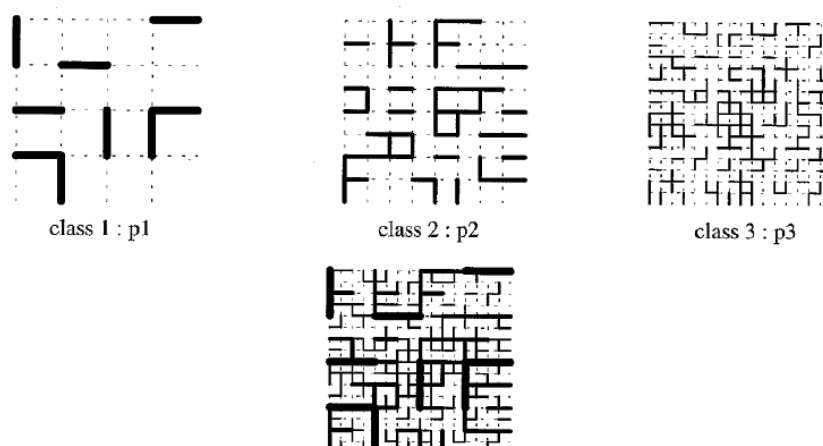*Figure 2-55 – 2D network of capillaries from the superposition of three grids of capillaries with a given radius (Xu K. et al. 1997a).*

EURAD (Deliverable n° 6.1) – Initial State of the Art on Gas Transport in Clayey Materials
Dissemination level: PU
Date of issue of this report: **17/11/2021**

Page 138

2.5.4 Shared understanding on the modelling of gas transport

Gas transport processes in natural or recompacted clay rocks are complex. Laboratory tests show the dependence of the flow dynamics on experimental conditions including the injection conditions, mechanical loading and interfaces between materials. The modelling of laboratory and in situ experiments generally shows that a continuous two-phase flow model is able to reproduce gas transport in clay rocks before preferential pathway development. In this case, the hydro-mechanical coupling is generally weak. The major contribution to gas flows in the unsaturated region comes from advection of the gas phase, while the diffusion of dissolved gas is predominant in the saturated zone. Regarding this two-phase flow model, experimental data on the retention curve and on the effective gas permeability are necessary in the almost saturated zone, which is relevant for gas transfer.

When the gas injection pressure increases, tests in clayey rocks indicate instabilities in the flows, which are certainly associated with path openings and closures. The introduction of an additional hydro-mechanical coupling linking the permeability and the retention curve to deformations is necessary to improve the modelling response and enable reproducing (a posteriori) the development of preferential pathways. These numerical models are still not able to predict in advance the material response. There is clearly a need for a better mechanistic understanding of the gas flow processes.

2.5.5 Uncertainties and knowledge gaps

The modelling of gas transfer in saturated clayey materials is still a challenging task. Some models have been proposed but they fail in being predictive. The main reasons are the following:

- *Gas transfer in a water-saturated clay sample is controlled by the microstructure, the connectivity of the macropores and the heterogeneity*. These features are poorly taken into account in classical two-phase flow model. Clear progresses have been made by introducing these aspects in the advanced hydro-mechanical models but a model describing the full complexity of the physical processes is still missing.

- *Lack of model predictability*: some advanced hydro-mechanical models have been proposed and are able to reproduce qualitatively the experimental response. However, some model parameters are still tuned in order to mimic the laboratory data. The consequence is that it is still difficult to predict the experimental behaviour. This issue comes from the fact that gas transfer processes are influenced by some microstructure features of the material that are not completely captured by the models.

- *Upscaling*: while classical two-phase flow models are not able to reproduce the experimental data at the laboratory scale, the situation is not the same for in situ tests (see Chapter 3). In this latter case, the classical two-phase flow models appear to reproduce reasonably well the observed rock mass response, at least below the fracturation pressure. This suggests that the scale of the REV influences the type of model one needs to use. The transition between the laboratory scale (cm scale) and in situ test (m scale) is still an open key question that is to be addressed by the WP GAS.

- *Experimental understanding of the gas transfer mechanism*: even if experimental data on gas transport are available, a clear mechanistic understanding of the gas flow processes is still desirable to properly bound the effects of these processes using simple and robust descriptions. One the one hand, the progress of the numerical models remains tributary of a correct characterisation and understanding of the processes. On the other hand, to the extent that process-level models allow to test hypotheses, these models can contribute to the understanding; hence the need of continuous interactions between modellers and experimentalists.

EURAD (Deliverable n° 6.1) – Initial State of the Art on Gas Transport in Clayey Materials
Dissemination level: PU
Date of issue of this report: 17/11/2021

Page 139

3. Impact of gas transport on the material properties of natural and engineered clayey barriers

Gas accumulation in a deep geological repository associated with the build-up of excessive gas pressures in the backfilled and sealed underground structures may impair the long-term safety functions and/or safety principles of the engineered barrier system (EBS) and the geological barriers, namely by:

- **Affecting the mechanical integrity** of one or more components of the multi-barrier system. The associated safety functions and/or safety principles are *physical isolation* of the wastes from the human environment, the *robustness* of the barrier system with regard to internal processes involving the barrier elements with each other and other materials (*compatibility*) and *long-term stability* of the elements that contribute to post-closure safety, considering the relevant repository-induced effects and external long-term evolution processes.

- **Reducing their performance as a barrier against fluid and solute transport**. Clayey components of the multi-barrier system contribute to the safety functions and/or safety principles *immobilisation, retention and slow release of radionuclides*.

When subjected to excessive gas pressures, clayey rocks and bentonite EBS components are particularly prone to mechanical failure[18] due to their low strength. The impacts of gas accumulation, gas pressure build-up and gas transport processes on the performance of the clay barriers depend not only on the hydro-mechanical properties of the barrier materials but also on the environmental conditions at repository depth (pore pressure, rock stress, temperature), on the repository design and on various other aspects such as waste-related source terms (gas and heat generation, radionuclide release). Consequently, an in-depth understanding of the gas-related failure mechanisms is required for a balanced assessment of the safety-related impacts on barrier performance, together with a broad evaluation of the radiological consequences. Section 3.1 provides a compilation of the existing scientific basis associated with the gas-induced failure of clay-based geomaterials as part of the engineered barriers and geological barrier system, respectively.

Clayey materials exhibit the favourable feature of self-sealing after sustaining mechanical failure. In the context of performance assessments (PA), the distinct self-sealing capacity of clay-based barriers is associated with the safety functions and/or safety principles '*robustness*' and '*long-term stability*' of the barrier system which must be substantiated for the full range of expected hydro-mechanical and hydro-chemical conditions at repository level and their evolution with time. The state of knowledge associated with the self-sealing capacity of clay-based EBS and clay-rich host rocks is addressed in Section 3.2.

Models play an important role for performance assessment in general as they allow e.g. for parameter identification based on experiments and for prediction of repository evolution in future. Modelling is essential for the entire systems analysis, fundamental process understanding, transferability and upscaling as a basis for building safe repositories in future, just to mention a few points. Process-level modelling and tools are discussed in Section 3.3.

---

[18] It should be noted that mechanical failure of a clay component does not necessarily imply a failure with respect to the fulfilment of safety functions and/or safety principles. For example, a local gas path opening might not lead to the failure of the entire bentonite buffer and might, in fact, have negligible or no impact on the performance of that component.

EURAD (Deliverable n° 6.1) – Initial State of the Art on Gas Transport in Clayey Materials
Dissemination level: PU
Date of issue of this report: **17/11/2021**   Page 141

3.1   Impact of gas transport on barrier integrity

3.1.1   Interests and needs of end-users in the context of geological disposal

Gas accumulation, gas pressure build-up and gas transport processes along the considered release paths (see Figure 2-1) may impair the long-term safety functions of the EBS and the host rock formation. From a performance assessment perspective, the impacts belong to the category of the 'Repository-Induced Effects' and can be classified in the light of the designated safety functions of the considered barrier components:

- The **loss of mechanical integrity** of the engineered and geological barriers. Relevant for long-term safety is the reliable inference of related phenomena and processes, comprising the temporal evolution, spatial extent and magnitude of (irreversible) deformation of the affected barrier system.

- The **consequences of failure** of the barrier materials on barrier performance. Emphasis is on the change of the release paths and the transport properties of the barrier materials after having been subjected to irreversible deformation.

The associated phenomena and processes depend not only on the type of barrier material and its fabric (granular/compacted bentonite, soft clays, indurated clay), but also on the general repository design and the site-specific conditions which control the THM evolution of the repository near field. Thus, in repository concepts which are based on a bentonite near field, gas-induced impacts in the bentonite buffer may become manifest in the mobilisation of bentonite colloids, leading to a loss of swelling pressure and an increase in buffer permeability. In poorly indurated clays and indurated claystone formations, the re-activation of existing fractures or development of micro-fractures may be expected when gas invades the host rock, giving rise to enhanced transport of dissolved and volatile radionuclides along the newly created release paths.

Consequently, the issues to be addressed in a safety case depend strongly on the repository concepts at the level of national programmes. A common area of importance in all programmes is the in-depth understanding of the fundamentals of gas transport in clayey materials through the identification of the associated phenomena and processes, as exposed in Chapter 2. Further aspects of common interest and needs are the characterisation of (T-)HM properties and solute/gas transport behaviour of the clay barriers before and after gas invasion. Table 3-1 displays a survey of typical needs of the end-users in the national programmes with respect to barrier performance.

Table 3-1 – Survey of gas-induced impacts on barrier performance and relevant needs of the end-users in the national programmes.

Barrier component	Category of gas-induced impacts	Relevant needs with respect to barrier performance
Host rock	Irreversible deformation of intact rock (pathway dilation/gas fracturing)	Phenomena and processes associated with damage initiation and damage propagation (onset of pathway dilation; sub-/ supercritical growth of damage zones) Shape and extend of gas-induced damage zones (T)HM properties of gas-induced damage zones (residual strength, …)
	Fault re-activation	Fracture opening/closure laws Spatial extent and localisation of fracture re-activation processes (T)HM properties of re-activated fractures (fracture stiffness, …)

EURAD (Deliverable n° 6.1) – Initial State of the Art on Gas Transport in Clayey Materials
Dissemination level: PU
Date of issue of this report: 17/11/2021
Page 142

Barrier component	Category of gas-induced impacts	Relevant needs with respect to barrier performance
	Gas/solute transport behaviour of failed host rock	Water retention behaviour and relative permeability relationships (gas/water) of the host rock in the dilatant regime Gas transport regimes in dilated/fractured host rock and in re-activated fault zones (capillary- vs. viscous fingering) Self-sealing capacity of the failed rock
EDZ	Gas-induced EDZ re-activation	Phenomena and processes associated with gas-induced EDZ re-activation
	Gas/solute transport behaviour after gas-Induced EDZ re-activation	Gas transport regimes in re-activated EDZ (capillary- vs. viscous fingering) Self-sealing capacity of the re-activated EDZ at the end of the gas release phase
Bentonite seals	Irreversible impacts on seal structure	Phenomena and processes associated with gas-induced mobilisation of bentonite colloids (loss of mechanical support)
	Transport characteristics of seal after gas transfer	Phenomena and processes associated with gas-induced mobilisation of bentonite colloids (loss of radionuclide retention capacity)
Bentonite buffer	Irreversible deformation of intact rock	Phenomena and processes associated with gas-induced mobilisation of bentonite colloids Mass fraction of mobilised bentonite / reduction of density / swelling pressure
	Gas/solute transport behaviour of buffer (gas invasion phase/water imbibition phase)	Water retention behaviour and relative permeability relationships (gas/water) of the buffer along wetting /drying paths Impact of compaction/hydration history on water retention behaviour

3.1.2 Fundamentals of gas transport in deformable media – phenomenology

From a phenomenological perspective, multiple evidence has been collected, indicating that clayey materials exhibit generally a high water retention capacity, inherently associated with a high gas entry pressure value. This characteristic feature originates from their special microstructure, consisting of (i) a fine-grained solid skeleton predominantly composed of clay minerals with typical grain sizes in the micrometre range and lower and (ii) a poorly connected pore network, mainly comprising meso- and micropores[19].

The mechanical characteristics of clay-rich materials cover a wide property range in terms of strength and stiffness, representing the full spectrum of deformation behaviour in the transition between soft soils and weak rocks (Gens 2013). The distinct differences in deformation behaviour contrast the obvious similarities in mineralogical composition. They can be explained by the experienced history of the geomaterials, such as complex subsidence and uplift histories, diagenetic processes, and weathering effects. All these effects become manifest in the peculiar structure of the considered

---

[19] Pore size classes according to definition for catalysis of IUPAC (1997): micropores (half width <1 nm), mesopores (1 – 25 nm) and macropores (>25 nm).

EURAD (Deliverable n° 6.1) – Initial State of the Art on Gas Transport in Clayey Materials
Dissemination level: PU
Date of issue of this report: 17/11/2021

Page 143

geomaterial and affect its hydro-mechanical behaviour. In this context, the term 'structure' is used according to Lambe and Whitman (1969), characterising the combined effect of fabric (geometric arrangement of soil particles) and bonding (interparticle forces, chemico-physical bonds). Bonding is usually dominant in rocks while fabric controls the strength in soils.

Gas-induced failure of clay-rich barrier materials is controlled by the interplay between water retention behaviour and deformation behaviour. When an initially water-saturated clay barrier with a high water retention capacity is invaded by a gas phase, the gas entry pressure may exceed the strength of the material at the locus of gas entry, giving rise to local failure. Gas-induced failure initiation and propagation depend strongly on the deformation behaviour of the clay barrier as well as on the evolution of gas pressure build-up (loading history). Thus, claystone and shales exhibit a moderate to low plasticity and a well-marked bedding plane fissility, giving rise to brittle failure when subjected to excessive gas pressure build-up. Depending on the speed of pressure build-up, the propagation of the damage front may take place by subcritical crack growth ('pathway dilatancy'), if the gas production rate is balanced steadily by the newly created pore volume at the crack tip. Supercritical crack growth ('gas fracturing') with fracture propagation velocities up to the shear velocity of the material may be expected for high gas production rates associated with rapid gas pressure build-up (Valkó and Economides 1995). In contrast to the low plasticity claystone and shales, a high-plasticity clay barrier such as granular bentonite with moderate emplacement density is expected to yield in a ductile manner when the applied gas pressure exceeds the local swelling pressure. The prevailing failure propagation mode is subcritical, the occurrence of supercritical damage growth in high-plasticity clays is very unlikely. The shear strength of saturated bentonite is controlled by its micro-fabric, largely limited to the interlocking of the clay aggregates and bonding of the adsorbed water layer on the particle surfaces (e.g. Schmertmann 2012). The resulting low shear strength makes bentonite prone to particle mobilisation (colloid transport) in case of high gas flow rates.

3.1.3 Conceptual models of gas-induced deformation in clay barriers

The *classical formulation* of flow of immiscible fluids in porous media (referred as 'two-phase flow' in the previous chapter) describes the combined flow of a wetting fluid (water) and a non-wetting fluid (gas) in the connected pore system of *a rigid/elastic*[20] *porous medium* on the action of viscous and capillary forces. A capillary pressure – water saturation relationship[21] and two relative permeability – saturation relationships of the liquid and the gas phase, respectively, are forming the key constitutive relationships of classical two-phase flow concepts. The conceptual model of gas transport *in deformable porous media* is essentially an extension thereof, assuming, that the porous medium can undergo irreversible deformation. As a consequence, capillary pressure and relative permeability do no longer represent an intrinsic behaviour of the porous medium in response to wetting/drying processes, but, depend on the state of deformation of the material. Complementary measurements of the volumetric behaviour of the porous medium are required to couple the equations of state of the solid phase with the two fluid phases. This can be achieved by expressing capillary pressure and relative permeabilities in terms of gravimetric water content of the medium and by establishing complementary relationships between water content and volumetric behaviour (e.g. void ratio). An extended formulation of the constitutive stress is required to account for the interaction of the internal pressures of the two liquid phases with the total stress, which acts on the solid skeleton.

---

[20] The deformation behaviour of the porous medium in response to internal / external forces is reversible.
[21] in geomechanics referred as "water retention" or "suction".

EURAD (Deliverable n° 6.1) – Initial State of the Art on Gas Transport in Clayey Materials
Dissemination level: PU
Date of issue of this report: 17/11/2021

Page 144

3.1.4 Gas-induced failure of clayey materials – state of knowledge

The mechanical impacts associated with the flow of immiscible fluids in low-permeability porous media are inevitably controlled by the microstructural features of the porous material. Therefore, careful consideration of both structure and texture is required for a balanced assessment of gas transport processes in engineered clay barriers and argillaceous host rocks. This includes the analysis of the mineralogical composition, basic geotechnical property tests such as granulometry, water content, porosity and plasticity parameters and measurement of the water retention behaviour, aimed at determining the state of water in the porous medium. High-resolution visualisation techniques such as µ-CT, FIB-nt and TEM allow for quantitative assessment of both the micro-fabric of the solid skeleton and the connectivity of the pore network of the porous medium using advance image processing techniques.

The investigation of dynamic processes associated with the gas-induced deformation behaviour of clay barriers calls for high performance experimental set-ups, allowing well-controlled execution of gas invasion experiments at the laboratory scale by monitoring the (T-)HM response of the test specimen along representative loading paths.

Mock-up and long-term in situ experiments are aimed at transferring mechanistic understanding and property measurements from the laboratory scale to larger scales. Process models derived from lab-scale experiments can be validated by extending the validation ranges in time and scale.

In the past two decades, comprehensive knowledge has been collected concerning deformation behaviour of clay barriers in response to gas invasion processes. Gas-related data bases exist for argillaceous host rocks, namely Boom Clay, Callovo-Oxfordian claystone and Opalinus Clay and for clay-based EBS, such as granular bentonite, compacted bentonite (blocks) and sand/bentonite mixtures. In the following paragraphs, the state of knowledge on gas transport in clay barriers is compiled in a structured manner:

- Experimental evidence for gas-induced modifications of fabric of the material (post-mortem analyses of micro-fabric, imaging while testing, etc.),
- Dedicated laboratory investigations on the impact of gas transport on mechanical integrity,
- Mock-up experiments and in situ experiments for process/parameter upscaling, validation.

3.1.4.1 State of knowledge for Boom Clay

Experimental evidence for gas-induced modifications of fabric

A significant body of gas experimentation was conducted in the 1990s, particularly within the frameworks of the MEGAS (under the umbrella of the PEGASUS EC project) and PROGRESS EC projects. Findings from these projects are presented in a variety of documents, both in the literature and through project reporting (Volckaert et al. 1995; Harrington and Horseman 1999; Rodwell et al. 2000). Many of the experimental studies involved were conducted on Boom Clay.

Primary experimental findings from the PEGASUS and MEGAS EC projects are described within several project reports (Haijtink and McMenamin 1993; Haijtink and McMenamin 1994; Haijtink 1996; Horseman and Harrington 1994; Ortiz et al. 1994; Volckaert et al. 1995; Ortiz et al. 1997). Work performed on Boom Clay included both laboratory (at centimetre-scale) and field (at decametre-scale) studies. Laboratory testing reported as part of the MEGAS EC project (Volckaert et al. 1995; Ortiz et al. 1997) included gas injection testing in oedometer (SCK CEN) and isotropic (BGS) cells.

EURAD (Deliverable n° 6.1) – Initial State of the Art on Gas Transport in Clayey Materials
Dissemination level: PU
Date of issue of this report: 17/11/2021

Page 145

The British Geological Survey's (BGS) experiments showed that gas advection was occurring by dilatant pathway formation. The resulting dataset was published by Horseman and Harrington (1994) and Harrington and Horseman (1999) and it was expanded upon during MEGAS Phase II and the PROGRESS EC projects. Several empirical relationships were derived from testing. Horseman and Harrington (1994) and Volckaert et al. (1995) demonstrated that, specifically for Boom Clay, gas breakthrough pressure could be directly related to the hydraulic conductivity or the intrinsic permeability, as had earlier been postulated by Davies (1991) for salt. A first relationship

$$P_b = 4.71 \times 10^{-4} K^{-0.312} \qquad \text{(3-1)}$$

relating the gas breakthrough pressure P_b [MPa] to the hydraulic conductivity K [m/s] was derived for situations involving a constant pressure head. A second relationship was also established for gas injection at a constant flow rate, relating gas breakthrough pressure to the intrinsic permeability, k_i [m²], such that

$$P_b = 1.694 \times \left(\frac{1}{k_i}\right)^{0.357} \qquad \text{(3-2)}$$

Given that the influence of anisotropy is allowed for by the inclusion of hydraulic conductivity or intrinsic permeability, these values were proposed to be effective for gas flow both perpendicular and parallel to bedding. Horseman and Harrington (1994) also derived an empirical relationship for the influence of the effective stress upon peak gas pressure. Based on data from a gas injection test, where gas was injected into a Boom Clay sample consolidated to increasing values of effective stress, σ' [MPa], the peak excess gas pressure P_{pg} [MPa] was found to be estimated as

$$P_{pg} \approx 0.85\,\sigma' \qquad \text{(3-3)}$$

It should be noted that this relationship is based on data from a single test. Hence, although the influence of the effective stress on gas transport behaviour was clearly established with this dataset, it should be taken with caution. There have been limited studies examining this effect and the influence of lithological controls has not been examined in significant detail.

Experiments performed as part of the PEGASUS and MEGAS EC projects were continued, as part of the PROGRESS EC project and are reported by Rodwell (2000). This work included experiments performed on Boom Clay by BGS and SCK CEN. The observation of a threshold pressure for gas entry is not specific to the process and should not be considered as evidence of one form of gas advection mechanism over another. The BGS conducted a gas injection test under a constant applied hydraulic backpressure (Rodwell 2000). Gas breakthrough pressures were measured for samples under external boundary conditions and under flow both perpendicular and parallel to bedding. The resulting values for a virgin clay ranged from 0.48–3.57 MPa. Given the variation in sample orientation and applied effective stress, trends in peak and breakthrough pressures are made clear by plotting reported values (Figure 3-1). Measured gas permeabilities were found to vary from 6.6×10^{-19} to 0.5×10^{-20} m². As with earlier findings from the MEGAS EC project, this dataset demonstrates the sensitivity of gas transport in Boom Clay on the effective stress conditions. The influence of anisotropy is also apparent with larger gas breakthrough and peak pressures for flow perpendicular to bedding.

Observations from all tests demonstrated that gas breakthrough only occurred above a conspicuous threshold pressure and a post-peak negative transient leading to steady-state gas flow. Examination of flow rate dependence after breakthrough also indicated a non-linear relationship. The authors argue that these observations were consistent with gas flow by dilatant pathway formation and that measured gas permeabilities must be a stress-dependent variable. They also hypothesised that these flow pathways must open and close as gas pressures vary, explaining the observed nonlinearity in the flow

EURAD (Deliverable n° 6.1) – Initial State of the Art on Gas Transport in Clayey Materials
Dissemination level: PU
Date of issue of this report: 17/11/2021

Page 146

dependence. It was also noted that some tests provide evidence of an intermittent or burst-type flow response, which was also explained by pathway propagation/collapse.
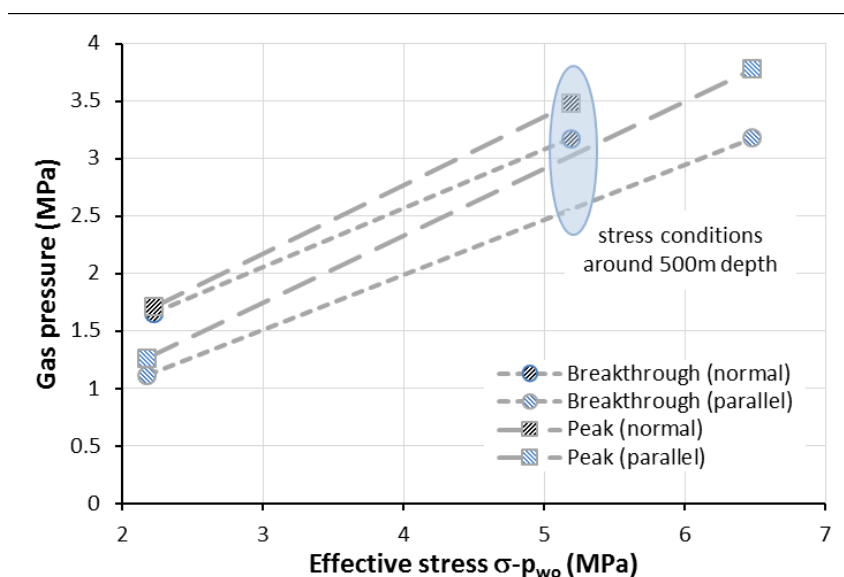

Figure 3-1 – The relationship between gas entry behaviour and effective stress, based on data presented by Rodwell (2000). The blue ellipse represents the effective stress conditions for a repository in Boom Clay at a depth of 500 metres (after Wiseall et al. 2015).

When comparing the influence of flow rate on gas pressure between tests performed on isotropically-consolidated samples and on K_0-consolidated samples (i.e. radially-constrained[22] samples), a clear difference was apparent with higher gas pressures occurring at lower flow rates for the radially-constrained samples (Figure 3-2). By reducing the potential for radial strain, higher gas pressures were necessary to achieve gas flow. These observations were presented as evidence that the stress field and boundary conditions applied to a sample were primary controls on gas transport processes in Boom Clay. Based on their observations, Rodwell (2000) suggested that conventional two-phase flow theory may not fully emulate the gas transport processes that occur in initially saturated compact clays (such as the Boom Clay) and are distinct from those in classical porous media.

During shut-in, gas pressure was observed to decline to a finite lower threshold, below which gas flow ceased. This was described as the capillary threshold pressure and was found to be around 1 MPa for the majority of test samples. On reinitiating gas injection, the pressure required to instigate breakthrough was observed to be substantially lower than for the virgin clay. This behaviour was thought to relate to the presence of residual gas within the clay. Moreover, residual gas was found to double the value of the specific storage after gas testing. The authors attribute this effect to compressibility of the clay and highlight that it provides direct evidence of gas entry during testing. Despite the residual presence of gas after injection, it was also found that the original peak pressure could be re-established by either: (i) reconsolidating the clay to higher confining stress or, (ii) allowing a phase of hydraulic resaturation. This behaviour was seen to be evidence for the capacity of gas pathways to self-seal.

---

[22] In this configuration the sample is only able to strain axially i.e. radial stress is prevented.

EURAD (Deliverable n° 6.1) – Initial State of the Art on Gas Transport in Clayey Materials
Dissemination level: PU
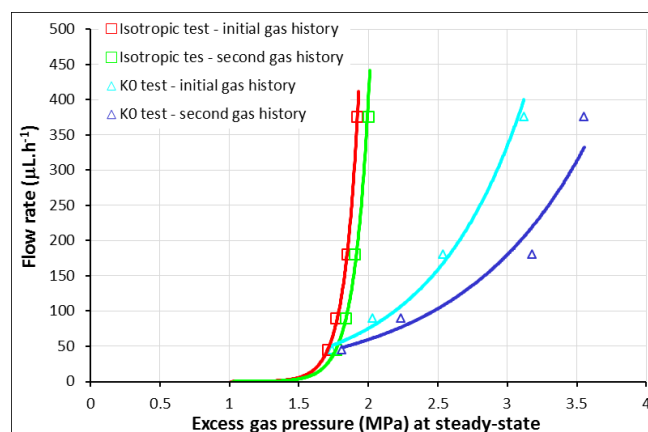Date of issue of this report: **17/11/2021**

Page 147

Figure 3-2 – Cross-plot of steady-state gas flow data from Rodwell (2000) for comparable flow rates from tests on isotropically-consolidated samples and on K_0-consolidated samples (i.e. radially-constrained).

Geotechnical analysis of test samples showed that all samples (except one) remained saturated to greater than 99%, after gas testing, despite the potential for degassing on depressurisation. Furthermore, mass balance calculations demonstrated that all samples were saturated to 98% while under test stress conditions. These observations demonstrate that substantial volumes of gas can pass through Boom Clay with minimal desaturation occurring.

Gas injection experiments were also performed in the PROGRESS EC project by SCK CEN (Ortiz et al. 2002). As with the BGS experiments, these gas injection tests also indicated that gas pressure has to overcome a threshold to become advectively mobile for the gas. Gas flow then ceases if pressure is allowed to fall below this threshold again. The authors argue that this demonstrates hydro-mechanical coupling of gas flow and, combined with evidence for heterogeneity in the gas flow distribution, indicates flow by pathway dilatancy. Desaturation of samples after gas breakthrough was also found to be no more than 2%. Gas breakthrough and peak gas pressures were found to vary from 0.47–2.25 MPa and from 0.49–2.25 MPa, respectively. Effective gas permeability measurements ranged from 0.7×10^{-20} to 9.5×10^{-20} m^2. It should be noted that samples were hydraulically tested using tap water, which may have slightly impacted the swelling state of the clay, although despite this, the findings are within a similar range to those reported by the BGS. The permeability decreased by a factor of 2 when the confining pressure was released from 5.7 MPa to 4.5 MPa. Outflow was found to begin above the pressure necessary to overcome the surface tension of water in the largest apertures of the clay porous network. The authors estimate this value to be around 0.05 MPa, based on their observations, which is consistent with a radius of 2–3 µm for the largest connected pores in the Boom Clay. Under these conditions, outflow was found to be constant and proportional to the excess gas pressure. When a given quantity of expelled water was reached (around 2% of the total porosity), the water expulsion rate decreased sharply. The authors suggest that this quantity relates to the degree of mobile water contained within the clay. An inflow of gas was detected from the injection system in advance of gas breakthrough at the downstream end. This is interpreted as occurring at the moment of gas entry into the clay, potentially marking the beginning of pathway propagation within the specimen. Observations also indicated that the greater the gas breakthrough pressure is, the higher the resulting effective gas permeability becomes. The authors argue that this evinces that gas flow under these conditions is not Darcian in nature.

A primary difficulty in assessing the size and distribution of dilatant pathways during gas flow is capturing this information while the sample is subjected to pressurised conditions. One approach, taken by Harrington et al. (2012a), was to use nanoparticle tracers during gas injection testing of a cylindrical

EURAD (Deliverable n° 6.1) – Initial State of the Art on Gas Transport in Clayey Materials
Dissemination level: PU
Date of issue of this report: 17/11/2021

Page 148

sample of Boom Clay (cut perpendicular to bedding, 50 mm diameter, 25 mm length), recovered from the HADES URL. Gas injection was conducted using an isotropic permeameter apparatus, similar to that described by Harrington and Horseman (1999). A 50:50 mixture (by volume) of gold (<100 nm) and hydrophobic coated TiO_2 (<50 nm) was used as a tracer during gas injection testing.

After testing, the sample was split and visually examined (Figure 3-3). The freshly-fractured core surface displayed a very diffuse, pale bluish white 'bloom', extending from immediately beneath the nanoparticle injection cake to a distance of up to 20 mm into the sample, as a 'tongue-like' plume with a generally narrowing tail, running approximately parallel to the core axis. Small diffuse lobes were also observed to spread laterally from the margins of the main plume, parallel to the bedding lamination. These visual observations were found to match with areas of high TiO_2 concentration found by elemental mapping, using a scanning electron microscope (SEM).

Nanoparticle aggregates and isolated nanoparticles of gold were also seen to be trapped and enclosed within the clay matrix of the rock (Figure 3-3). The aggregate diameter generally decreased with increasing distance from the gas injection interface, but traces of the gold nanoparticles could be found up to 20 mm from the point of gas injection. The size of the nanoparticle aggregates, typically between 0.5 and 4 µm (though up to 10 µm diameter), point to a minimum aperture of the pathways generated during gas transport. Observations indicated that the nanoparticles had been transported along transient pathways, through the clay matrix and around grain boundaries of coarser detrital siliciclastic silt and sand grains, during gas injection. It would appear that these features then sealed, trapping any nanoparticles that were being transported in the gas stream.
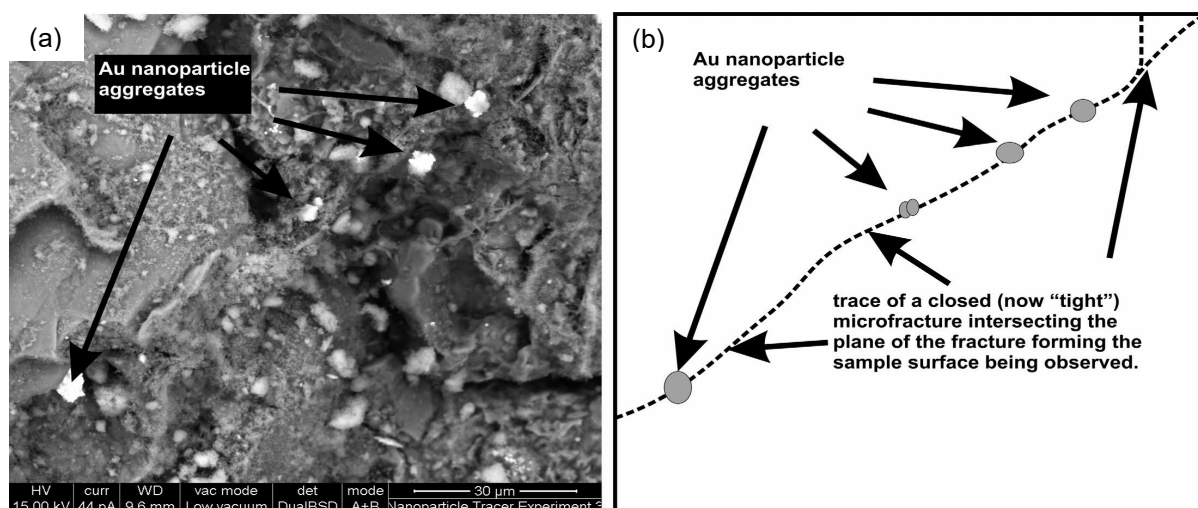
Figure 3-3 – (a) a combined scanning electron and backscatter electron image showing a trail of aggregated gold nanoparticles (Au) trapped within the trace of a now closed pathway. The Au particles are trapped along what appears to be a sealed pathway that is suborthogonal to the plane of the fracture surface imaged in (b).

The passage of gas causes some mechanical disturbances in clay. The evaluation of microstructural changes induced by the transport of air performed by Gonzalez-Blanco (2017), suggests that gas flow may mainly take advantage of natural discontinuities. In particular, Gonzalez-Blanco (2017) clearly put in evidence the fundamental role of bedding planes in the transport of gas. Under oedometric conditions, samples with bedding planes normal to the direction of flow underwent higher expansions on gas equalisation and larger compression on the gas dissipation stage (less constrained) than samples with bedding planes parallel to the direction of gas flow (Figure 3-4). She then concluded that gas pathways more easily develop along bedding planes in these oedometric conditions.

EURAD (Deliverable n° 6.1) – Initial State of the Art on Gas Transport in Clayey Materials
Dissemination level: PU
Date of issue of this report: 17/11/2021

Page 149

This effect is enhanced by gas injection rate. Under oedometric conditions, faster injections induced higher expansions while the pressure front propagated (Figure 3-4). In case of slow injection rate, no pressure front propagates after shut-off. According to (Gonzalez-Blanco 2017), during slow air injection, pore pressure was nearly equilibrated and the volume change response is quasi-reversible along dissipation stage. Consequently, when gas flow is slow the formation of gas pathway is easier and the consequences of pathways on the volumetric strain are more limited than when gas flow is fast.
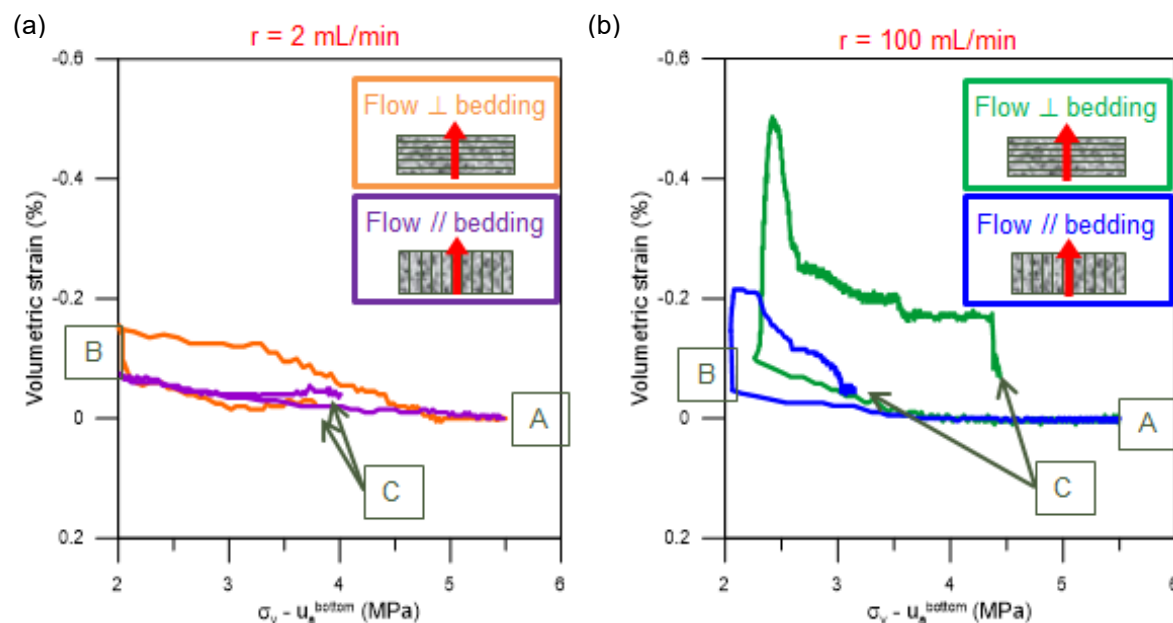

Figure 3-4 – Evolution of volumetric strains with vertical stresses during air injection/dissipation stages in slow (a) and fast (b) injection experiments (Gonzalez-Blanco 2017).

Observations of pathway desaturations after sample dismantling performed by Gonzalez-Blanco (2017) confirm a low desaturation degree and even suggest that clay matrix remains saturated. Opening of gas pathways is at the origin of new pore size without significantly modifying matrix porosity. In consequence, as already discussed by Hildenbrand et al. (2002, 2004), only very small additional classes of (large) pore radii would become accessible for gas transport and changes in intrinsic permeability of Boom Clay should be very limited.

A series of scoping gas tests were recently performed on Boom Clay, in the context of the OPERA concept for a Dutch GDF. Detailed reporting of these experiments is given in Harrington et al. (2017a). Most transport studies on the Boom Clay relate to depths relevant to the Belgian national disposal programme. The primary focus of this work was, therefore, to make an initial assessment of the influence of consolidation on gas transport properties with a view to assessing the impact of the greater repository depths that may be expected in the Netherlands.

Two gas injection experiments were performed using a triaxial permeameter apparatus, each involving one hydraulic test and two gas injection tests. Testing first involved assessing the water permeability and gas injection behaviour of the clay at stress conditions comparable to those at the HADES URL. The sample was then consolidated to higher stress conditions representative of those proposed in the OPERA concept and gas injection testing was then repeated under these conditions. No evidence was observed for gas transport until pressures exceeded the value of the minimum principal stress (confining pressure). Gas entry occurred at a pressure of 4.3 MPa (2.1 MPa excess gas pressure) for both samples at the lower effective stress conditions. Peak pressures were measured as 4.51 MPa (2.3 MPa excess gas pressure) and 4.59 MPa (2.4 MPa excess gas pressure) under the lower stress conditions. At higher effective stresses, gas entry occurred at 9.99 MPa (5.1 MPa excess gas pressure) and peak gas

EURAD (Deliverable n° 6.1) – Initial State of the Art on Gas Transport in Clayey Materials
Dissemination level: PU
Date of issue of this report: **17/11/2021**

Page 150

pressure reached 10.68 MPa and an excess gas pressure of 5.78 MPa. These findings highlight the influence of effective stress (and consolidation history) upon gas entry properties of the clay. The impact of consolidation on the capillary threshold pressure was not examined. Breakthrough pressure was assumed to occur at peak gas pressure, at which time dilatant deformation of the clay was observed (by three linear variable differential transformers (LVDT's) which were in direct contact with the sample). The clay increased in volume and reduced in weight, indicating considerable amounts of trapped gas within the sample. Once major gas outflow was established, an effective gas permeability of 2.3×10^{-20} m^2 was measured.

Further gas testing was also performed under constant volume boundary conditions, so as to investigate the degree of the hydro-mechanical coupling between gas pressure, total stress and pore water pressure in Boom Clay (Harrington et al. 2017a). Gas entry was detected at a pressure just greater than the local total stress measured near the point of injection. This was significantly lower than for the triaxially-constrained samples and was attributed to the test boundary conditions by the authors. A strong coupling was observed between gas flow, total stress and pore water pressure, once gas entry was established. The stress and pore water pressure distributions measured within the sample were found to be anisotropic and their distribution evolved with time. In advance of major breakthrough, a substantial stress gradient was generated within the clay. At the same time, small outflows were detected, which were attributed to outflow of water resulting from localised consolidation of the clay. The stress gradient along the sample was observed to reduce at major breakthrough, at which time its peak value was reached. Test data demonstrated that, on the laboratory length-scale, a minimal drop in gas pressure was apparent along the conductive pathways, which appeared to be reasonably stable, once formed. This is consistent with the observation shortly after breakthrough that in- and outflow were approximately equal, indicating minimal variation in the volume (saturation) of gas pathways with time. The authors suggest that this points towards a relatively stable gas flow network.

Gas injection using nanoparticle tracers (Harrington et al. 2012a) was also reused on Boom Clay that was first consolidated to a higher effective stress (equivalent to 500 metres depth in the Netherlands). Gas breakthrough was only detected at a pressure just below that of the confining pressure. After decommissioning, the post-test sample and an untested control sample were imaged using a X-ray computed tomography (CT). This method highlighted some regions of high nanoparticle concentration, although nanoparticles could not be detected throughout the bulk of the sample. A few scarce nanoparticle aggregates were located in the interior of the sample, though only within the top couple of millimetres. However, this imaging methodology has a resolution that is limited to dimensions around an order of magnitude larger than those of the individual nanoparticles used. Therefore, it is possible that constraints of the technique only allow the visualisation of larger nanoparticle aggregates. Further comment on the likely distribution of gas flow in the sample could, therefore, not be made.

As with the previous study, mapping using an environmental scanning electron microscope and energy dispersion X-ray analysis was performed to assess the distribution of nanoparticles within the sample. Only a few nanoparticles could be found within the sample using this technique. Based on these post-test observations, it seems likely that the tracer nanoparticles aggregated to the extent that they could not pass through these pathways into the sample. It is unclear whether this was because particle aggregation was more extensive than in previous tests or because the higher effective stress conditions resulted in a narrower aperture of the pathways. The authors suggest that the use of improved imaging methodologies, such as high-resolution synchrotron methods, would be beneficial to developing this gas tracing methodology further.

EURAD (Deliverable n° 6.1) – Initial State of the Art on Gas Transport in Clayey Materials
Dissemination level: PU
Date of issue of this report: 17/11/2021

Page 151

Laboratory investigations of the impact of gas transport on mechanical integrity

The impact of gas transport on mechanical integrity of Boom Clay was investigated by UPC under oedometer conditions on initially saturated samples with bedding planes oriented parallel and normal to the direction of water and gas flows (Gonzalez-Blanco 2017).

Selected results of the air injection and dissipation stages at constant vertical stress of 6 MPa and with bedding planes parallel to water flow are presented in Figure 3-5 and are explained in detail by Gonzalez-Blanco et al. (2016a). The figure shows the time evolution of the air injection pressure at the upstream boundary and the outflow pressure and volume at the downstream boundary, jointly with the average axial strain, calculated based on recorded axial displacement. The tests were performed on two samples with bedding planes parallel to air flow, at different injection rates, 100 mL/min and 2 mL/min. The time evolutions of the relevant variables follow a similar pattern. The air pressure at the upstream boundary was increased in time (A–B in the figure), followed by shut-off (point B) and dissipation at closed air injection line (B–C). The time of breakthrough was clearly visible through a rapid increase of the flow rate at the downstream end of the sample and an increase of the outflow pressure in the downstream reservoir. Increase in injection pressure was accompanied by expansion (negative axial strains). At a pre-set inlet pressure, injection was stopped (shut-off). From that point on, the system enters a dissipation stage and the pressure progressively starts to decrease at the upstream end. Expansion can continue for some time at a reduced rate at this stage, then compression strains are observed. The time of air outflow breakthrough depended on the injection rate. In samples tested at 100 mL/min, the first outflow was detected during the dissipation stage, whereas in samples tested at 2 mL/min it already occurred during the last phase of the injection stage.

Figure 3-6 presents the evolution of the average axial strain with a measure of the net stress at the bottom boundary, defined as the vertical stress, σ_v, minus the air pressure at the bottom injection boundary, p_a. The net stress at the bottom boundary, $\sigma_v - p_a^{bottom}$, is used as a "constitutive stress variable" to provide an initial interpretation of the deformation response of the material. The evolution of this constitutive stress and the axial strain during the air injection and dissipation stages of the two selected tests at two gas injection rates are presented. The samples, kept at constant vertical stress (6 MPa) displayed some expansion during the early air injection stage (A–B in Figure 3-6), which was slightly larger at the slower air injection rate. After shut-off (point B in the figure), expansion continued in the sample subjected to faster air injection (B–B′ in the figure) as the air pressure front propagated into the sample, inducing the fluid pressure to increase and the constitutive stress to decrease. After shut-off, no expansion was observed on the sample subjected to the slower air injection rate, since the pore pressure was nearly equilibrated during air injection. Some time after shut-off, the air injection pressure started to decline along the dissipation stage towards point C. Consequently, the constitutive stress increased inducing compression on the material. The sample subjected to the slower injection rate showed a quasi-reversible volume change response along the dissipation stage. So, the slower the injection rate, the more limited the consequences of gas pathways on Boom Clay are.

These results suggested also that some changes in the pore size distribution of the samples could take place during injection. Figure 3-7 presents the pore size density functions obtained from MIP tests for the intact material and after the air tests. A new family of large pores, which was not detected on intact samples, was observed. According to Gonzalez-Blanco et al. (2016a), this new family of pores with entrance sizes larger than 2 μm is associated with the expansion undergone by the material during the air injection stage. This new family of pore can be interpreted in term of permeability and water retention properties of the Boom Clay. Figure 3-8 presents the fitted Kozeny's model for the intrinsic permeability increases of the matrix as a function of void ratio together with the experimental measurements for samples with bedding planes parallel to water flow. Figure 3-9 presents the water retention curve estimated from MIP data by Gonzalez-Blanco (2017). From the theoretical variation of the intrinsic permeability and the capillary pressure, the water retention curves are significantly modified: the highest the proportion of gas pathways is, the highest the gas entry pressure drops. These results confirm that

EURAD (Deliverable n° 6.1) – Initial State of the Art on Gas Transport in Clayey Materials
Dissemination level: PU
Date of issue of this report: 17/11/2021

Page 152

deformation history should play a role on gas transport properties which are then stress-dependent properties rather than material properties.
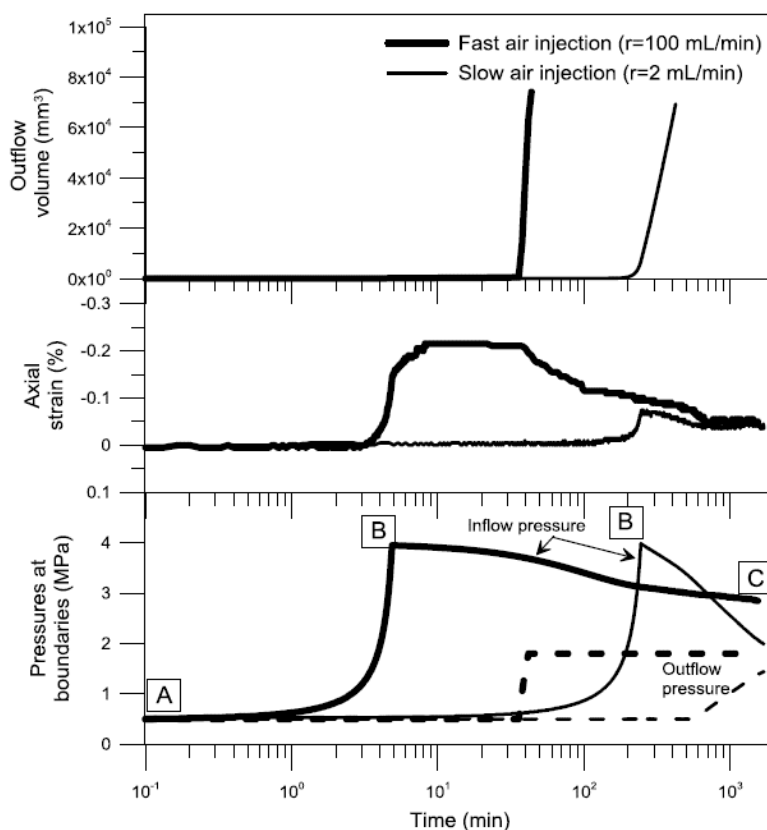
Figure 3-5 – Time evolution of outflow volume, axial strain and pressures at the injection (inflow) and recovery (outflow) boundaries, for the two injection rates. A – B: air injection stage; B: shut-off; B – C: dissipation stage (Gonzalez-Blanco et al. 2016a).
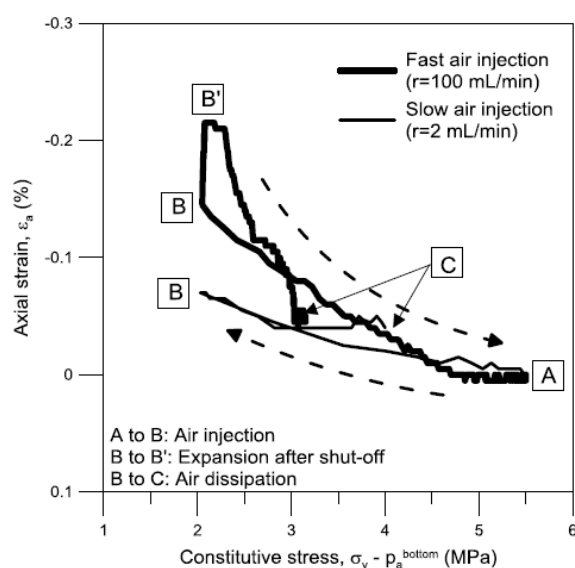
Figure 3-6 – Axial strains against constitutive stress (vertical stress minus air pressure at the upstream boundary) for tests at two injection rates (Gonzalez-Blanco et al. 2016a).

EURAD (Deliverable n° 6.1) – Initial State of the Art on Gas Transport in Clayey Materials
Dissemination level: PU
Date of issue of this report: **17/11/2021**

Page 153
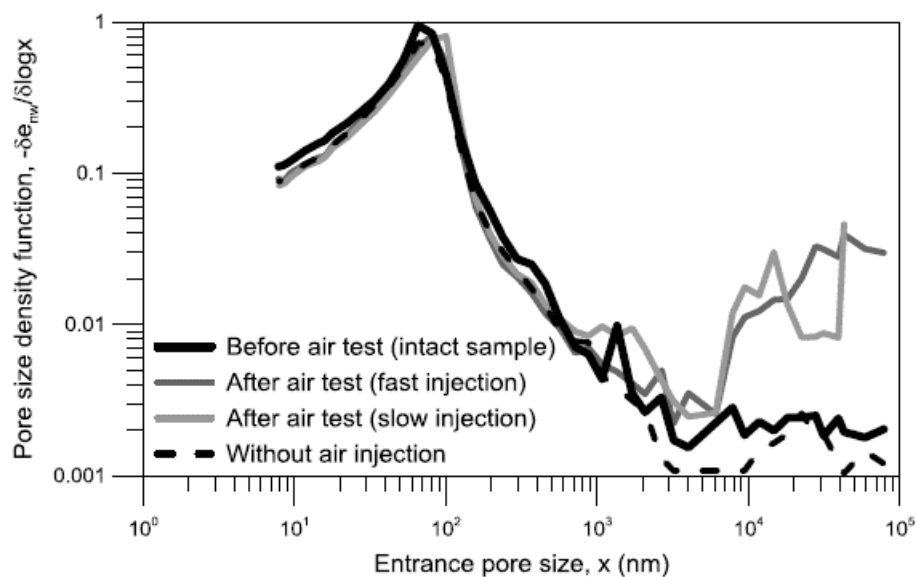
Figure 3-7 – Pore size distribution changes before and after air injection tests (Gonzalez-Blanco et al. 2016a).
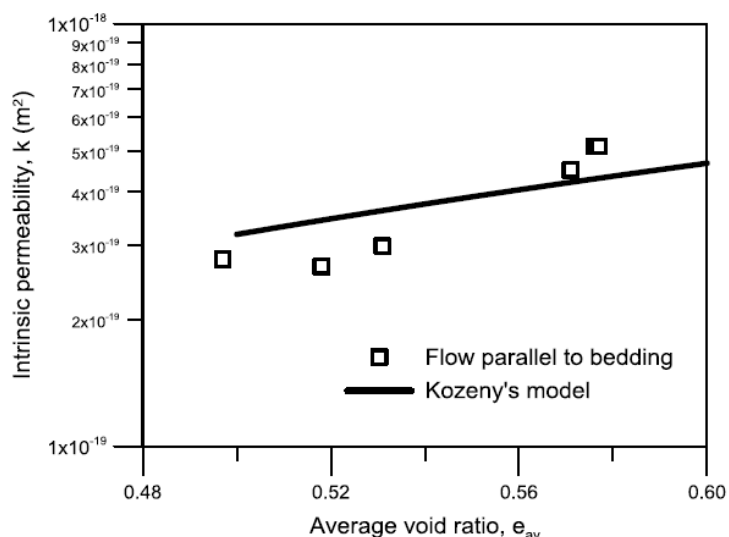
Figure 3-8 – Intrinsic permeability as a function of void ratio together with fitted Kozeny's model (Gonzalez-Blanco et al. 2016a).

EURAD (Deliverable n° 6.1) – Initial State of the Art on Gas Transport in Clayey Materials
Dissemination level: PU
Date of issue of this report: **17/11/2021**

Page 154
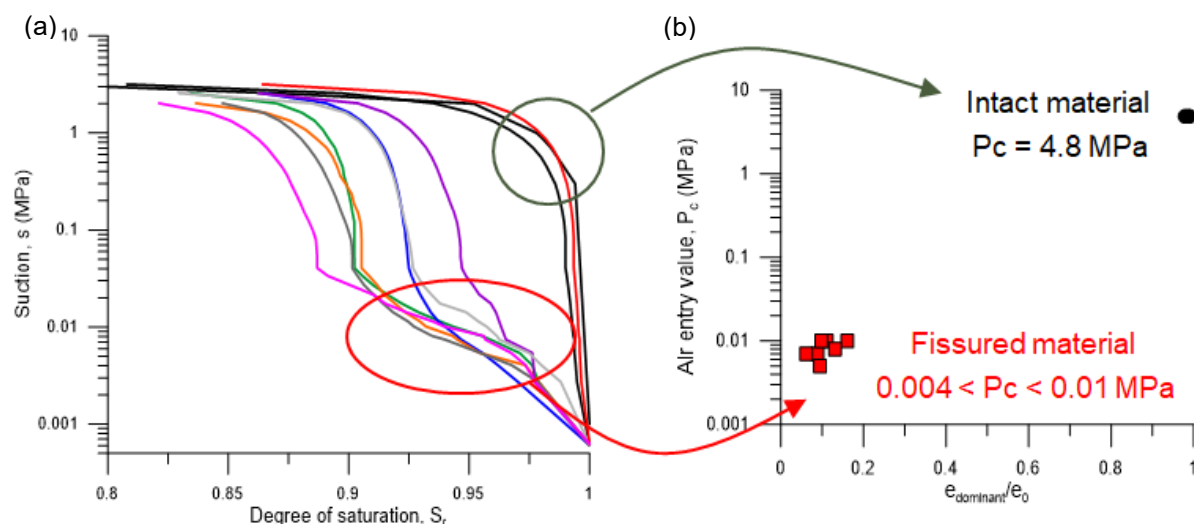
Figure 3-9 – (a) water retention curves of intact samples and after air injection tests; (b) air entry value determined with the dominant entrance pore size (adapted from Gonzalez-Blanco 2017).

In situ experiments

Field-scale gas injection testing was conducted using helium at the HADES URL, in Belgium, as part of the MEGAS EC project. These experiments are described in detail in the project report (Volckaert et al. 1995).

The E4 gas injection experiment was performed at the bottom of the shaft at HADES URL, where a vertical piezometer containing several injection filters was installed within a borehole into the formation (Figure 3-10). After pore water pressures were observed to equilibrate, gas injection was performed in two separate tests (through different filters) while pressures were monitored at filters located above the injection filter.

A number of key observations were reported, including a lower gas breakthrough pressure than expected (0.6 to 0.65 MPa instead of a predicted value of 1.25 MPa, on the basis of the total stress at the location of the filter). At least one preferential pathway was generated along the length of the piezometer and testing was halted as a result, since gas was entering the access shaft of HADES URL. The low entry pressure was explained as a result of damage resulting from drilling of the borehole, though it was suggested that convergence over the long-term would minimise this behaviour.

EURAD (Deliverable n° 6.1) – Initial State of the Art on Gas Transport in Clayey Materials
Dissemination level: PU
Date of issue of this report: **17/11/2021**

Page 155
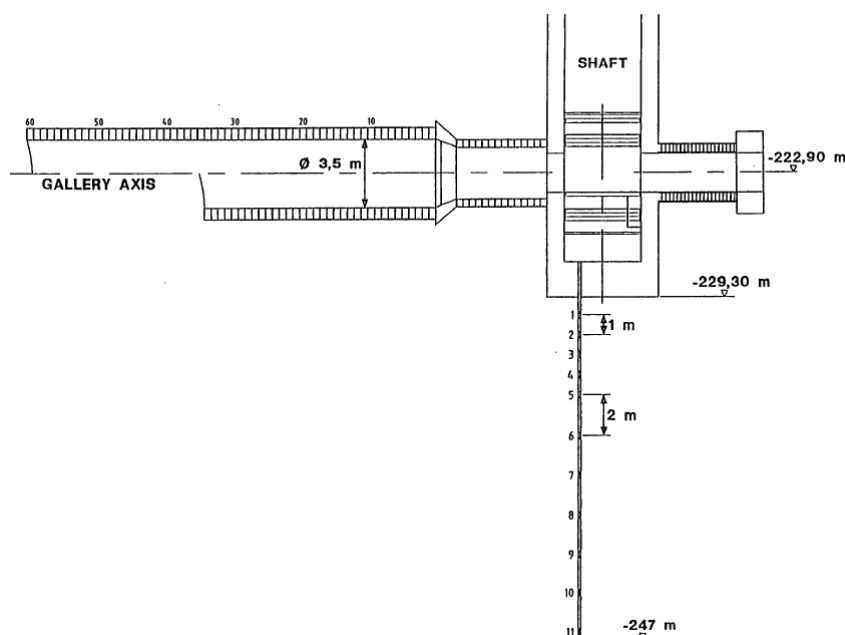
Figure 3-10 – Vertical piezometer installed under the shaft in the HADES URL for the MEGAS E4 gas injection experiment (Volckaert et al. 1995).

The E5 gas injection experiment was performed from the test drift at HADES URL. Four horizontally oriented piezometers were installed within the formation; one central piezometer for gas injection (Figure 3-11) and three additional monitoring piezometers. Pore pressures were monitored at 29 filters in total, as well as the injection pressure. Hydraulic testing was first conducted to determine baseline parameters (pore water pressure, total stress and water permeability). This was followed by injection of helium, of which the pressure was increased by increments of 0.1 MPa above the local pore water pressure on a weekly basis until breakthrough occurred. A preferential pathway was detected between the injection filter and a neighbouring filter on the same multipiezometer, in which gas inflow observed. This was followed by observations of increasing pore water pressure in some, but not all, of the surrounding filters. Measured gas fluxes once flow was established were of a similar magnitude to those encountered in laboratory testing. Observations from gas testing indicate that gas transport in Boom Clay is strongly dependent of the hydro-mechanical behaviour of Boom Clay.
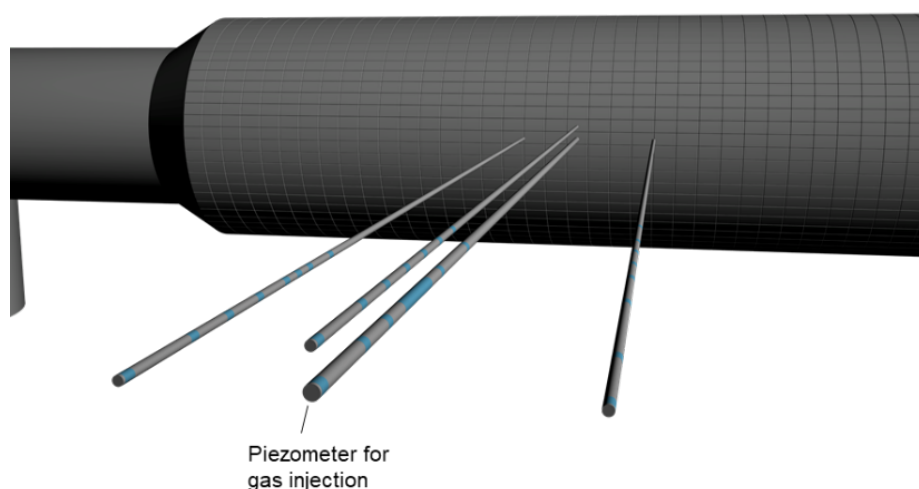

Figure 3-11 – Horizontal piezometers installed in the HADES URL for the E5 gas injection experiment (EURIDICE 2020).

EURAD (Deliverable n° 6.1) – Initial State of the Art on Gas Transport in Clayey Materials
Dissemination level: PU
Date of issue of this report: **17/11/2021**

Page 156

The in situ test programme conducted at the HADES URL during the MEGAS EC project was followed with additional field testing, as part of the PROGRESS EC project. The primary purpose of the 3D-multipiezometer test was to examine the self-sealing properties of the formation. Testing was conducted using the pre-existing 3D-multipiezometer system that was used for the E5 gas injection test in the MEGAS EC project. Gas injection was conducted at a constant flow rate and breakthrough occurred at an excess gas pressure of 0.23 MPa above the initial pore water pressure. Activity concentration measurements from the subsequent radioactive tracer migration test matched simulated predictions and indicate that in the case of short term gas flow, a depressurised pathway does not represent a preferential flow path for subsequent transport of radionuclides in groundwater. The authors suggest this behaviour is the result of effective self-sealing behaviour in the clay (Rodwell 2000; Ortiz et al. 2002).

3.1.4.2 State of knowledge for Callovo-Oxfordian claystone

Experimental evidence for gas-induced modifications of fabric

Many tests have been conducted to explore the consequences of gas breakthrough on the hydro-mechanical behaviour of COx and to detect possible modifications of fabric. Gas breakthrough tests performed on samples suggest that gas transport could be associated with pathway dilatancy. The conceptual model deduced from these tests and presented Figure 3-12 highlights the strong dependency between gas flow and stress state. However, it was difficult to know from those tests if the localised flow pathways were due to initial micro-cracks that could appear during sample preparation or if they are link with local natural heterogeneities at the microstructure scales. The consequences of the creation of such localised pathways could be assimilated at a very diffuse damage and may induce weaknesses in the material. In fact, hydro-mechanical tests performed on these samples after the gas breakthrough event did not show any significant changes on the hydro-mechanical properties and certainly not a global failure of the material.

Charlier et al. (2013) developed a hydro-mechanical model and used it in the modelling of two in situ experiments from MHM URL. In that context, they collated data from a number of gas injection studies (Zhang and Rothfuchs 2004; Boulin et al. 2008a; Yang 2008 and Andra 2009) in the Callovo-Oxfordian claystone (COx). Data compiled from these tests shows a decreasing trend in effective gas permeability between saturations of 40% and 100%, resulting in a reduction by more than 2 orders of magnitude close to full saturation. Zhang and Rothfuchs (2004) examined the evolution of effective gas permeability during the progress of microfracturing of samples and this study is described in more detail within the context of fractured COx.

Boulin et al. (2008a) conducted gas flow tests on COx samples, using a triaxial cell to provide isotropic confinement at stress conditions below those found in situ at the Meuse/Haute-Marne (MHM) URL. Analysis of test observations resulted in estimated values for dry gas permeability and effective diffusion coefficients for gas of the order of 10^{-18} m^2 and 10^{-8} to 10^{-9} m^2/s, respectively. Despite the fact that before gas testing, samples were subjected to a week of oven drying at 70°C and could lead to changes in the pore structure, these values are in the range of dry gas permeability reported by Charlier et al. (2013) (10^{-19} to 10^{-17} m^2). The variability observed in the measures is related to the modification of clay materials when submitted to drying processes.

A series of experiments examining the gas transport samples of COx claystone were performed and reported in Cuss and Harrington (2011), Harrington et al. (2012b), Cuss et al. (2014), Harrington et al. (2013) and Jacops et al. (2014). Samples were tested using either an isotropic loading arrangement or a triaxial permeameter cell (with volumetric strain monitoring). A detailed description of the isotropic testing is given by Harrington et al. (2012b) and Jacops et al. (2014), while the triaxial testing is presented in Cuss et al. (2014) and Harrington et al. (2013). Measured excess gas entry pressures

EURAD (Deliverable n° 6.1) – Initial State of the Art on Gas Transport in Clayey Materials
Dissemination level: PU
Date of issue of this report: 17/11/2021

Page 157

were found to be markedly different for the two test specimens, with unexpectedly low values (2 MPa) being estimated in one case and a more conventional value in excess of 6.0 MPa in the second. The authors suggest the low entry pressures may relate to localised features within the claystone and use evidence of downstream pore pressure evolution to demonstrate that, at this stage of testing, major gas penetration had only occurred in the case of the second sample. In this case, combined with no measurable desaturation of the sample, gas transport was attributed to pathway dilatancy. Sensitivity to applied gas pressure was also examined and resulted in a hysteresis in observed outflow rates during pressure reduction. The authors argue that this hysteresis points towards a non-recoverability (on the short-timescale) of the experiments, which may result from incomplete resaturation and/or local plastic strains in the vicinity of gas pathways with permanent changes to the fabric of the claystone. These findings do not, however, exclude the possibility of recoverability in the long-term.

Cuss and Harrington (2010, 2011) and Cuss et al. (2012, 2014) describe the experimental approach and findings from triaxial testing of COx samples in two different apparatuses (one at BGS and one at CNRS (ULorraine)). Gas breakthrough was estimated to occur at 10.5 MPa and 6 MPa for the BGS and Université de Lorraine tests, respectively. It was suggested that the deviation between these values may be explained by differences in sample preparation technique. Because of the experimental geometry used at the BGS, secondary evidence of gas entry was identified, whereas CNRS (ULorraine) could not identify the pressure at which gas entry occurred. For both experimental set-ups, a clear dilatational deformation was detected at the onset of gas flow. These observations were also seen to correlate with changes in flow and pressure. The authors attribute this behaviour to a hydro-mechanical process linked to gas transport and an associated perturbation of the pore water pressure field. This is interpreted as being the result of the formation of dilatant pathways and is consistent to the post-test geotechnical observation made by BGS that no discernible sample desaturation occurred. Based on their own and previous observations, the authors describe a three-stage conceptual model of the onset and establishment of a gas flow network in COx claystone (Figure 3-12).
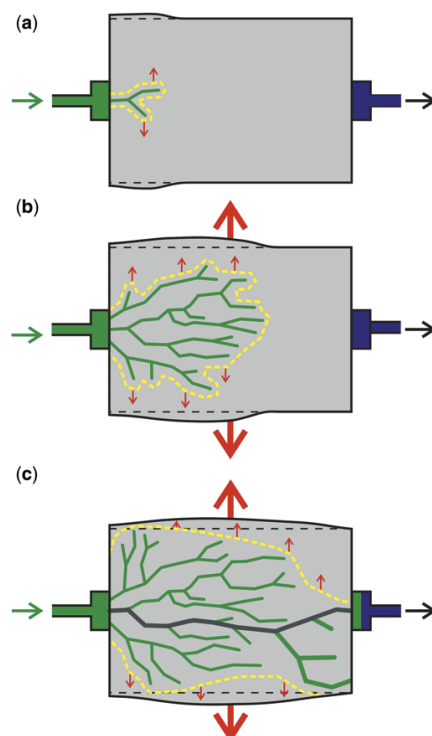
Figure 3-12 – Conceptual model of the onset of gas flow in COx. (a) Initial gas entry. Localised compaction around the pathway, causing bulk sample dilation. (b) Gas pathway network slowly propagates through the sample, resulting in substantial dilation at the mid. (c) Gas pathways reach the downstream end of the sample, resulting in greater outflow and continued dilation (Cuss et al. 2014).

EURAD (Deliverable n° 6.1) – Initial State of the Art on Gas Transport in Clayey Materials
Dissemination level: PU
Date of issue of this report: 17/11/2021

Page 158

Harrington et al. (2017c) compiled test data from the BGS triaxial permeameter (Cuss et al. 2014) and isotropic tests (Harrington et al. 2012b), and combined it with observations from three further experiments using the same apparatus (two isotropic tests and one measuring volumetric strain in a triaxial cell). By comparing reported gas breakthrough pressures with sample thicknesses (Figure 2-24), several 'domains' of behaviour were apparent. Shorter samples generally resulted in lower breakthrough pressures and it was suggested that this resulted from the greater proportion of damaged versus intact claystone constituting the bulk of smaller samples. However, when subjected to higher confining pressures, this effect is reduced, possibly due to microfracture closure. These observations indicate that sample damage may be one possible explanation for the discrepancy between observations of both low and high entry pressures in COx. However, given the likely influence of sample heterogeneity on gas entry values, further explanation of the dataset may be required to fully demonstrate this. Nevertheless, these observations indicate that gas entry pressures reported in excess of 5 MPa may well reflect the properties of 'intact' COx at in situ conditions.

The authors also used observations of long-timescale evolution in sample pore pressures as evidence for the time-dependent development of gas flow pathways, which can take >200 days to occur. They also point to the detection of hysteresis during drainage and imbibition as evidence of non-recoverability in gas flow behaviour. Geotechnical analysis also showed minimal desaturation of test samples despite gas transport, indicating negligible transport of interstitial fluid from the original porosity of the claystone. These findings indicate that gas transport could occur by pathway dilation. This is consistent with findings when a post-test sample was gently heated while submerged in glycerol as done for OPA (see Figure 3-17). Gas was observed to escape from both ends of the sample as a result. Visual inspection highlighted a greater proportion of gas pathways at the upstream end than the downstream end. It was suggested that this indicates a 'fanning out' of gas pathways, as they propagate through the sample. In contrast, a 'control' COx sample, discharged no gas when also heated in glycerol. Scanning electron microscopy was used to qualitatively analyse regions of the sample where gas escape had been detected or absent. Microcracking was found to have occurred in those areas where outflow had been observed, but not in areas where it was absent. While these features could be related to shrinkage of the clay after testing, it seems a noteworthy observation.

A strong link between gas flow and the mechanical state of the clay is highlighted by findings from the triaxial permeameter experiment. As with Cuss et al. (2014), fluid outflow was shown to be associated with a small, but well-defined, volumetric strain, which could not be explained by compressibility/poroelasticity of the material alone (Cuss et al. 2012). Volumetric outflow from the sample was also shown to increase as dilation increased. This provides evidence that the aperture of gas flow pathways influences gas flow permeability. The observation of non-uniformity in the strain field also points to localised gas flow, which evolves over a substantial period of time.

In situ experiments

Several in situ experiments dedicated to the study of gas injection and gas fracturing in the Callovo-Oxfordian claystone were carried out in the Meuse/Haute-Marne URL and from the surface. Several rates of gas injection have been used for these tests to evaluate the influence of this parameter on the threshold gas fracturing pressure. The consequences of gas injection below this threshold pressure and after gas fracturing events on the water permeability was also one of the objectives of the tests.

A rapid gas injection (1 L/min, TPN – normal temperature and pressure conditions) in a vertical borehole in a 5-metre interval from the surface (EST363) leaded to a dynamic stressing of the rock (Figure 3-13). Gas fracturing was observed at a gas pressure in the chamber of about 11.9 MPa.

EURAD (Deliverable n° 6.1) – Initial State of the Art on Gas Transport in Clayey Materials
Dissemination level: PU
Date of issue of this report: 17/11/2021

Page 159
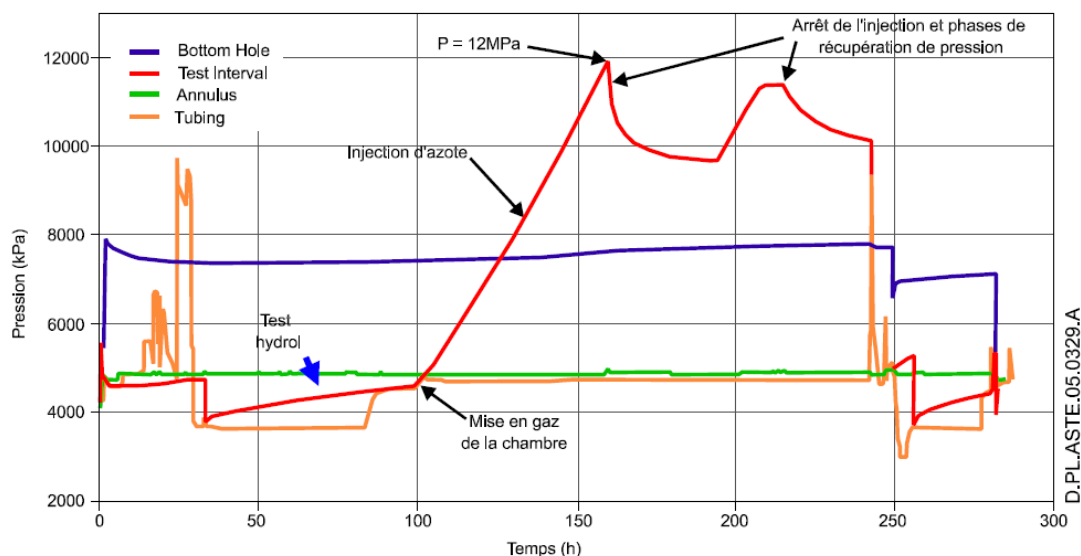
Figure 3-13 – Gas fracturing test of COx performed in a borehole from the surface (EST363): measurements of the pressure in the borehole during the gas injection phases (Senger et al. 2006).

A gas injection was carried out in an inclined borehole (PGZ1202) from a URL gallery in a 1-metre interval with a high injection rate of 500 mL/min. Gas fracturing was detected at a pressure of 14.1 MPa (Figure 3-14).
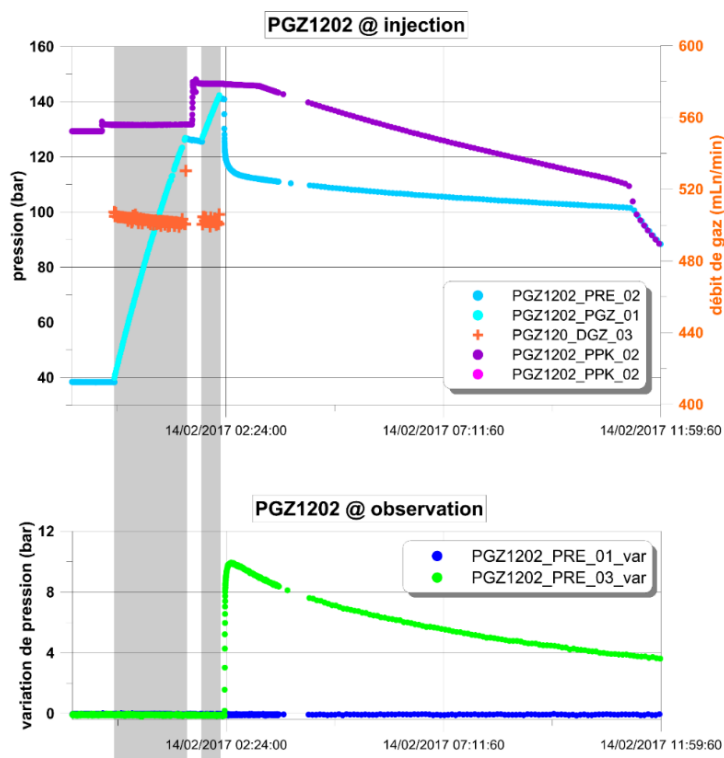
Figure 3-14 – Evolution of gas pressures and flow rate during the gas fracturing test carried out in well PGZ1202 (interval 2) in MHM URL.

EURAD (Deliverable n° 6.1) – Initial State of the Art on Gas Transport in Clayey Materials
Dissemination level: PU
Date of issue of this report: 17/11/2021

Page 160

Several gas injection sequences were carried out in an inclined borehole (PGZ1201) from the GED gallery (de la Vaissière et al. 2014b). The gas pressure build-up history is more complex due to the multiple objectives of the test (Figure 3-15). The first objective was to identify the regimes of gas transfer in the saturated claystone while remaining under fracturing pressure. Thus, it was shown a gas pressure of the order of 9.1 MPa (GAS1) or 9.8 MPa (GAS2) did not induce the initiation of a fracture. Creation of dilatant pathways at such levels of gas pressure could not be demonstrated on these tests.
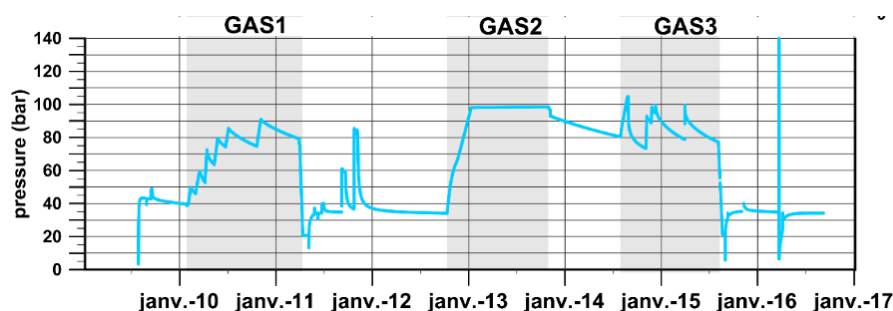
Figure 3-15 – Evolution of the gas pressure measured in borehole PGZ1201 drilled in the MHM URL according to the 3 test sequences.

It has been shown that continuous models based on a generalised Darcy law were able to give a good representation of the experimental results (Gerard 2011).

This is illustrated in Figure 3-16 with modelling of the PGZ1 experiment conducted in the Meuse Haute-Marne URL: in this test, a sequence comprising two gas tests separated by a hydraulic test was carried out. The gas pressure is controlled so as to remain below the fracturing pressure. Modelling of this test using parameters consistent with the characterisations obtained on samples enables the experimental observations to be reproduced.
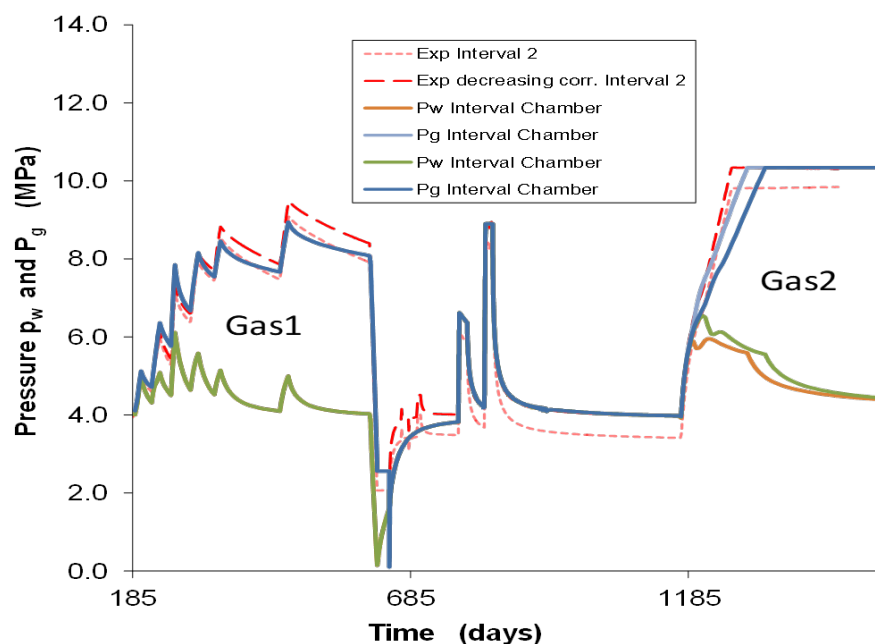
Figure 3-16 – PGZ1 experiment in the MHM URL: comparison between measurements and numerical simulation (Gerard 2011).

EURAD (Deliverable n° 6.1) – Initial State of the Art on Gas Transport in Clayey Materials
Dissemination level: PU
Date of issue of this report: **17/11/2021**

Page 161

In a second stage, a relatively slow gas injection (less than 1 mL/min (TPN)) was used and led to fracturing at a pressure of 10.45 MPa (GAS3), below the minimum principal stress.

The gas fracturing tests confirmed that the fracturing pressure depends on the stress field around the injection zone but may also depend on the gas injection rate and certainly on the geometry of the damaged zone around the drift. The orientation of the borehole in the direction of the major stress induced an elliptical damaged zone developed laterally with respect to the borehole axis.

When gas injection rate is high (gas fracturing pressure reached in few hours), the gas fracturing pressure is consistent with the natural minor principal stress and the estimated level of tensile strength for COx. The situation is very close to what is observed on classical hydraulic tests where gas fracturing can be deduced from the total pressure applied on the walls of the cavity.

When the gas injection rate is low, gas starts to penetrate the surrounding media before gas fracturing initiation and in particular the damaged zone which is a more accessible to gas due to low gas entry pressure (Figure 2-24). This implies some modification in pore pressure around the injection zone with consequences on the effective stress. During a slow gas injection, this variation in effective stress and the geometry of the damaged zone (elliptic in this experiment) may explain lower value of fracture pressure obtained (de la Vaissière et al. 2020).

3.1.4.3 State of knowledge for Opalinus Clay

Experimental evidence for gas-induced modifications of fabric

Several researchers carried out post-mortem analyses of drillcore samples from Opalinus Clay, which had been subjected to gas invasion experiments.

An early study of water and gas flow through a specimen of Opalinus Clay from the Benken borehole (Figure 1-15) was performed by Horseman and Harrington (2002). Two samples OPA-1 and OPA-2 were subject to an isotropic confining stress in a novel permeameter, featuring the so-called guard-ring technique. Flow direction was normal and parallel to bedding, respectively. The results of the gas invasion stages of the tests on specimens OPA-1 (flow normal to bedding) and OPA-2 (flow parallel to bedding) show conspicuous differences. In OPA-1, the outflow at elevated gas pressures comprised a mixture of both water and gas. Measurements during decommissioning of this test show that water was the dominant phase flowing from the downstream filter, with only very minor amounts (circa 0.13 mL at 5.0 MPa) of entrained gas. This contrasts greatly with OPA-2, where the simple calculations show that the outflow to the downstream filter at higher pressures was predominantly gas. The post-test measurements suggest that gas penetration of the specimens resulted in a measurable amount of desaturation (up to 7% gas).

In order to provide some confidence that gas actually penetrated the rock during the gas test stages on OPA-1, the specimen was taken from the apparatus and immersed in a Pyrex vessel containing liquid paraffin. The vessel was then gently warmed on an electrical hotplate to expand any gas trapped in the pore space of the rock. A series of photographs were taken of the surfaces of the specimen. Two of these photographs are reproduced in Figure 3-17. Gas trapped in the rock during testing can be seen emerging from the specimen, predominantly in the region of the upstream filter. Gas also emerged from the downstream surface of the specimen, with the bubbles more dispersed over the full area. Additionally, there were local signs of gas around the cylindrical surface of the specimen, with small pools of gas evident under the Epimac epoxy ester coating. Visual inspection of the outflow point did not reveal any damage of the rock fabric, such as micro-fractures or mobilisation of mineral grains.

EURAD (Deliverable n° 6.1) – Initial State of the Art on Gas Transport in Clayey Materials
Dissemination level: PU
Date of issue of this report: 17/11/2021

Page 162
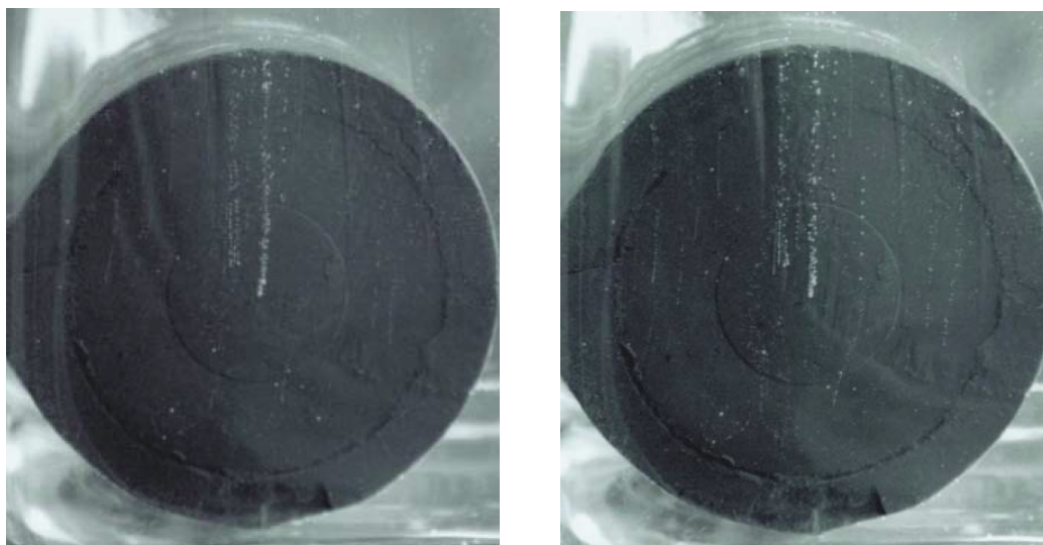
Figure 3-17 – Photographs of specimen OPA-1 after gas testing, immersion in liquid paraffin and gently warming using an electrical hot plate. The former positions of the upstream filter (central area) and the upstream guard-ring filter (periphery) can be identified from the impressions left on the rock surface. Gas trapped in the rock during testing can be seen emerging from the rock, predominantly in the region of the injection filter. The streams of gas bubbles emerge from discrete points on the rock surface, suggesting highly non-uniform gas penetration of the specimen (Horseman and Harrington 2002).

Water and air permeability tests in a triaxial cell on Opalinus Clay drill cores from the deep geothermal well SLA-1 at Schlattingen in northern Switzerland were initiated by Romero and Gomez (2013) and complemented by Romero and Gonzalez-Blanco (2015). At the end of the isotropic test on drill core OED 1/1 (Opalinus Clay from a depth of 936.26–936.49 metres below ground), the sample was cut at the proper size and freeze-dried to performed mercury intrusion tests (MIP). A comparison of the pore size density (PSD) functions with those obtained at initial state shows some reduction of the micro-porosity as well as an aperture which is indicated by the change of the dominant pore mode, slightly higher after water and air injections (Figure 3-18). Moreover, some macroporosity was detected after the injection tests, which could be developed during the expansion produced at the early stage of injection experiments. The observed volume changes may suggest some degradation of the material due to the air passage. However, it cannot be excluded that the volume increase is caused at least partly by the freeze-drying procedure.

EURAD (Deliverable n° 6.1) – Initial State of the Art on Gas Transport in Clayey Materials
Dissemination level: PU
Date of issue of this report: **17/11/2021**

Page 163

(b)
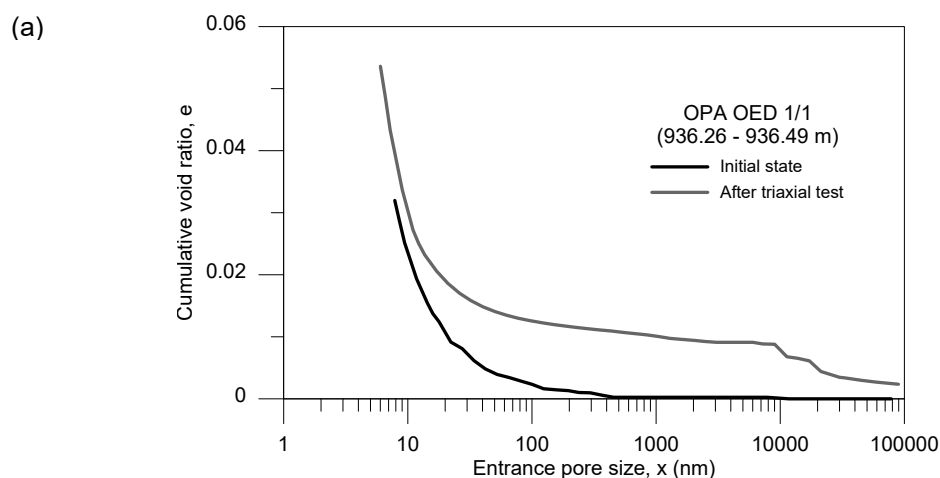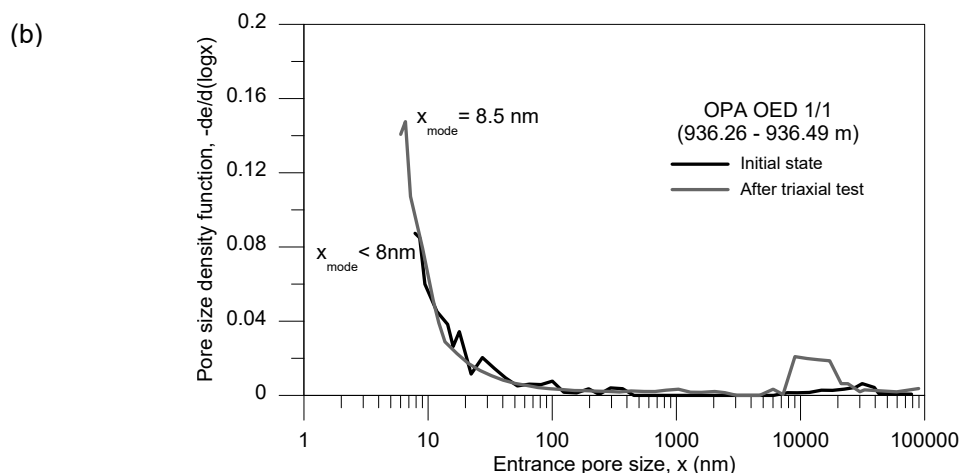
Figure 3-18 – Comparison of (a) cumulative void ratio and (b) PSD function between initial and final state after triaxial test of OED 1/1 Opalinus Clay.

Laboratory investigations of the impact of gas transport on mechanical integrity

The impact of gas transport on mechanical integrity of Opalinus Clay was investigated by UPC and EPFL using triaxial cells. Gas injection tests were conducted by UPC in a triaxial cell with flow direction parallel (shallow samples only) and perpendicular to bedding at isotropic stress levels of 15 and 19 MPa, respectively (Romero and Gomez 2013). The corresponding gas injection pressures (14 and 18 MPa, respectively) remained below the confining stress. Figure 3-19 presents the results of gas injection tests on the core sample from the deep geothermal well SLA-1 in terms of gas pressures at the injection and outflow sides together with outflow volume and axial displacements.

The water/gas injection experiments on the Opalinus Clay sample show clear evidence for the dependency of water permeability on void ratio and thus on constitutive stress (estimated as the isotropic stress minus the air pressure at the injection point). Furthermore, a marked dependency of gas dissipation was observed on the direction of gas flow with respect to bedding orientation. Significantly higher gas flow rates were observed for the flow direction parallel to bedding. Another important observation is the marked dependency of volumetric strain on the constitutive stress changes during air injection/dissipation tests. The samples displayed expansion at the early fast air injection stage in response to constitutive stress decrease, and dominant compression on air pressure dissipation. During the early period after shut-in, the axial strain continued to expand despite the slight increase in constitutive stress due to gas dissipation (Figure 3-20). Higher bulk moduli were consistently obtained in the air dissipation phases compared to bulk moduli from loading and unloading stages.

EURAD (Deliverable n° 6.1) – Initial State of the Art on Gas Transport in Clayey Materials
Dissemination level: PU
Date of issue of this report: 17/11/2021

Page 164
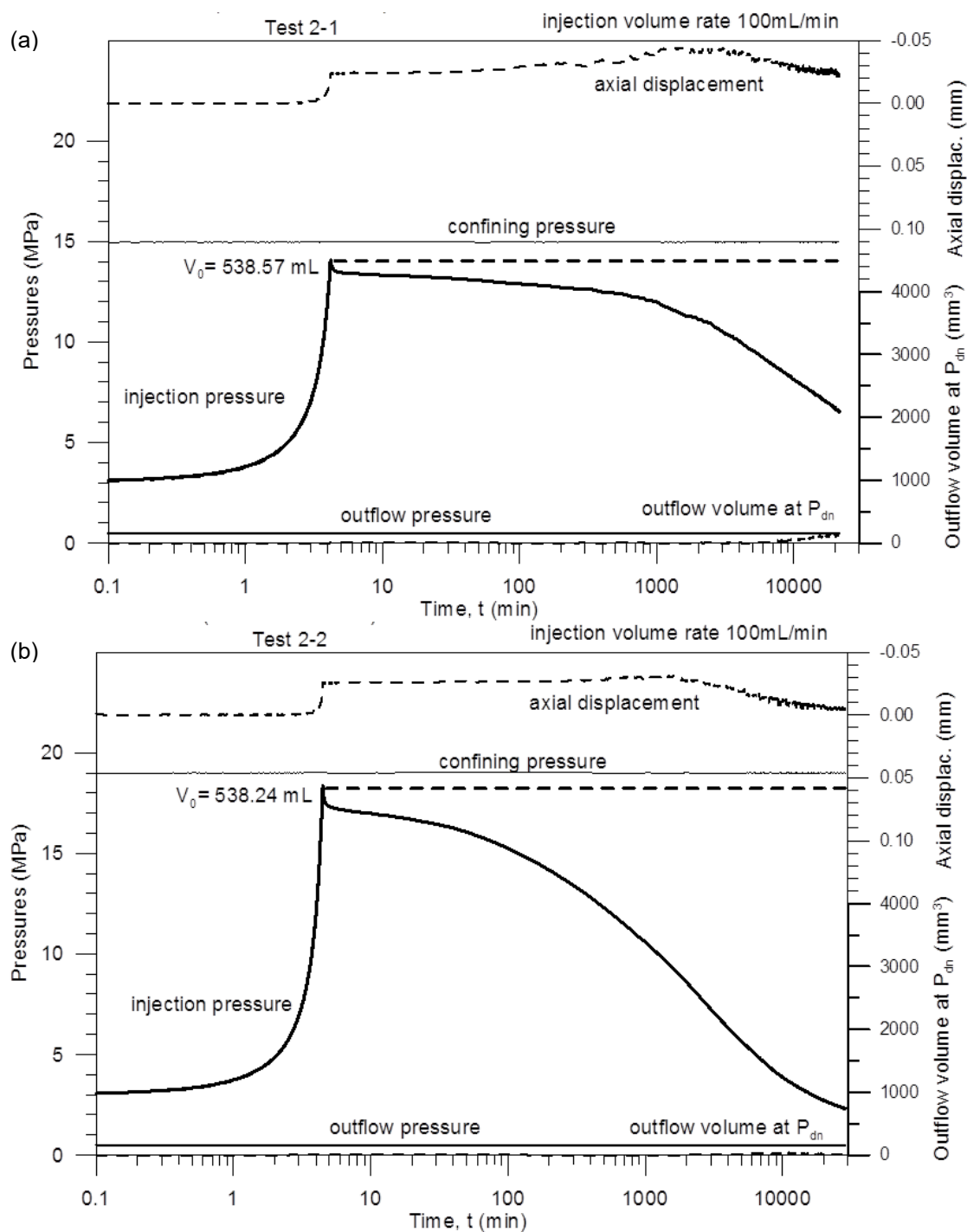
Figure 3-19 – Gas injection experiments on core sample OED/Opalinus Clay (879.79–880.01 m) from the SLA-1 borehole with isostatic stress conditions and flow orthogonal to bedding (Romero and Gomez 2013). Measured time evolution of pressures at the injection and outflow sides together with outflow volume and axial displacements at confining pressures of (a) p = 15 MPa and (b) p = 19 MPa.

EURAD (Deliverable n° 6.1) – Initial State of the Art on Gas Transport in Clayey Materials
Dissemination level: PU
Date of issue of this report: **17/11/2021**

Page 165
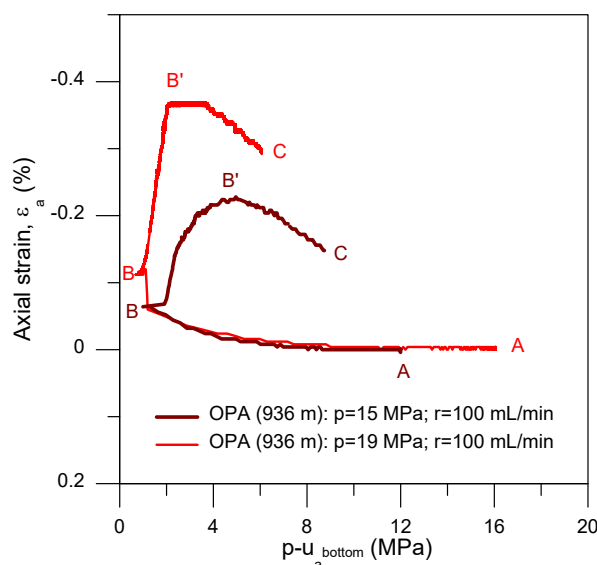
Figure 3-20 – Axial strain changes associated with constitutive stress changes during gas injection/dissipation stages (OPA).

A comprehensive experimental programme on the water retention behaviour of shales with particular focus on the Opalinus Clay was launched by Ferrari and Laloui (2012) and Ferrari et al. (2014). Focus of the early investigations was on the volumetric behaviour of unsaturated shales along wetting and drying paths in the unconfined state and at oedometric conditions. Follow-up experiments by Minardi (2018) and Minardi et al. (2019) included gas injection experiments in a triaxial cell, aimed at analysing the volumetric response of fully saturated samples of Opalinus Clay on gas invasion. It was concluded that the overall hydro-mechanical response experienced by the material during the gas injection phase can be considered reversible under triaxial conditions. In terms of strain, the overall volumetric expansion accumulated during the gas injection steps 2, 3, and 4 (-0.580%) is almost completely recovered in the final shut-in last step (Figure 3-21), where a volumetric compaction of +0.558% is experienced by the specimen. The observed reversibility supports the hypothesis that the injection of gas at different pressures was not able to create new pathways in the material, which are usually associated to a plastic deformation mechanism. The conclusion was drawn that the penetration and propagation of gas in the specimen occurs in its original pore space.

EURAD (Deliverable n° 6.1) – Initial State of the Art on Gas Transport in Clayey Materials
Dissemination level: PU
Date of issue of this report: **17/11/2021**

Page 166
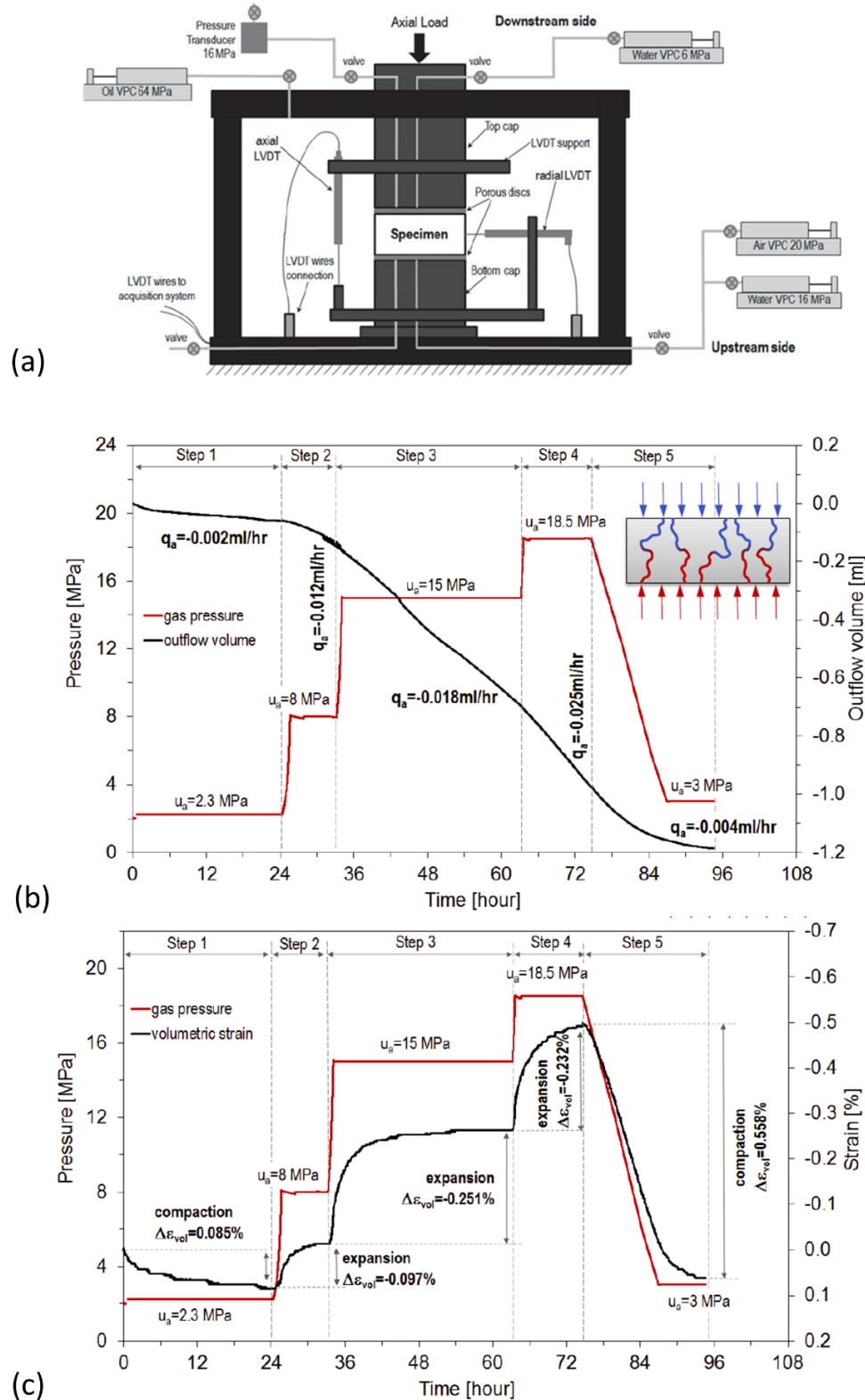
Figure 3-21 – Gas invasion experiments on a drill core from the shaly facies of the Opalinus Clay at the Mont Terri URL; (a) experimental set-up for water/gas testing with radial and axial strain measurements; (b) transients of the gas pressure and outflow volume at the downstream side during the different steps of gas injection phase; (c) transients of gas pressure and volumetric strain (Minardi 2018).

EURAD (Deliverable n° 6.1) – Initial State of the Art on Gas Transport in Clayey Materials
Dissemination level: PU
Date of issue of this report: 17/11/2021

Page 167

Mock-up experiments and in situ experiments

Process models of gas-related failure mechanisms can be developed at the laboratory scale by dedicated experiments with adequate instrumentation, which permit a full control of initial and boundary conditions during the test execution. The transferability of such process understanding requires confirmation by complementary experiments at larger scales. In the past two decades several gas-related in situ experiments were conducted in the Opalinus Clay at the Mont Terri URL and in the deep investigation borehole in Benken (e.g. Daneshy et al. 2004; Marschall et al. 2005; Marschall et al. 2013). Combined hydro- and gas tests at the GS-site in the Mont Terri URL are representative for gas testing at elevated gas injection pressures.

The multi-step gas test GS-2 was explicitly designed for monitoring hydro-mechanical responses of the rock formation to a gas injection event (Marschall et al. 2005). The experimental layout comprised a total of 4 boreholes at a distance of less than 2 metres from each other, two of them equipped with triple-packer systems and the others instrumented with multiple extensometers for observations of the axial deformation (Figure 3-22). The test lasted for a total of 30 days and incorporated a testing sequence with three pressure levels. Before testing commenced in the injection borehole, the borehole fluid in the test interval was replaced with nitrogen gas. The main gas injection sequence consisted of stepwise increase gas pressure in the test interval to 1175 kPa (PI1), 1916 kPa (PI2) and 2776 kPa (PI3), followed by a shut-in and recovery stage. Figure 3-22b shows the development of the interval pressure in the gas injection borehole, as well as the deformation in the observation borehole at a distance of 0.8 m. For the pressure step PI1, the formation appears practically impermeable to gas as the gas entry pressure has not yet been reached.

Low leak-off rates are observed during PI2 without any significant deformation in the adjacent extensometer boreholes. Finally, the highest pressure level PI3 is characterised by a distinct gas leak-off. The extensometer, placed in the mid-interval of the observation borehole, shows significant extension of about 20 µm/m which is not reversible during the pressure release phase PW1. Correspondingly, during PI3 the two adjacent extensometer intervals exhibit a tendency for contraction.

Several campaigns of complementary gas injection experiments were conducted in the same borehole array, aimed at re-opening the previous gas-frac and at determining pressure dependent fracture transmissivities (Marschall et al. 2013). Another series of gas injections was aimed at monitoring the gas invasion process with a passive and active seismic survey (Maurer and Spillmann 2014). Results from four comprehensive seismic monitoring campaigns allowed to image the (re-)activation of separate two fracture planes around the gas injection borehole. A first fracture (R1) opened immediately after the onset of gas leak-off ('gas breakthrough'), while the second fracture (R2) started to open several tens of days later. Interestingly, the opening of R2 temporally coincided with the closure of R1. Passive seismic monitoring demonstrated that the acoustic emission (AE) activity was very low. Only two AE events could be detected and located. They occurred immediately after the 'gas breakthrough' and they lie on R1 at a distance of about 1.4 metre away from the injection interval. Continuous active monitoring using a single source and 8 receiver positions allowed significant changes of the recorded waveforms to be identified. The most pronounced changes were associated with the gas breakthrough, but also at later stages the continuous measurements indicated changes within the volume of interest.

EURAD (Deliverable n° 6.1) – Initial State of the Art on Gas Transport in Clayey Materials
Dissemination level: PU
Date of issue of this report: 17/11/2021

Page 168
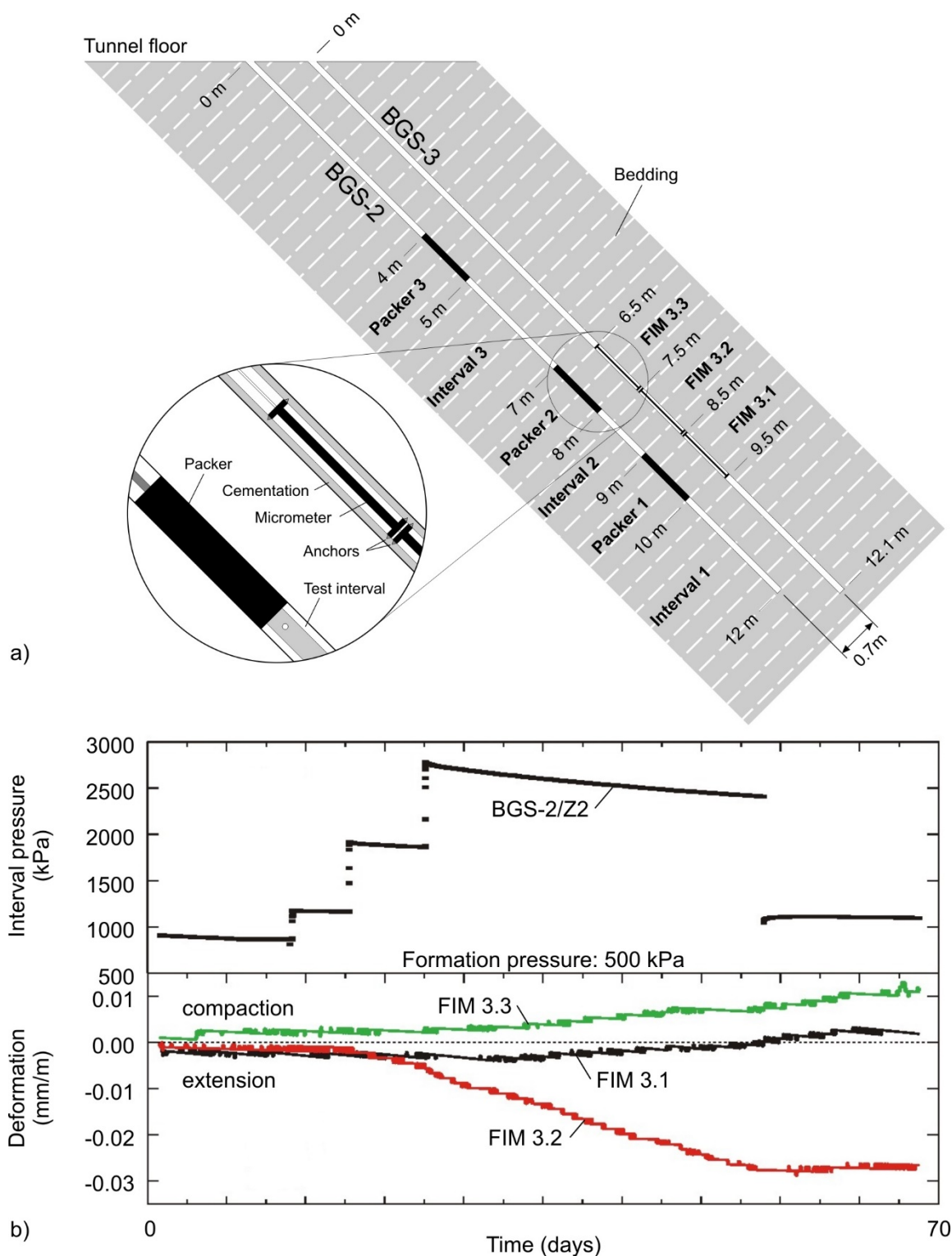
Figure 3-22 – Multi-step gas injection test GS-2 at Mont Terri: (a) hydro-mechanical instrumentation of the injection and monitoring boreholes, (b) transients of interval pressure in the injection borehole and axial deformation in the adjacent monitoring borehole (Marschall et al. 2005).

EURAD (Deliverable n° 6.1) – Initial State of the Art on Gas Transport in Clayey Materials
Dissemination level: PU
Date of issue of this report: **17/11/2021**

Page 169

3.1.4.4 State of knowledge for bentonite

Bentonite clay and bentonite clay mixtures are used as buffers, seals, or backfills in many geological disposal programmes worldwide (Box 2). The development of the concepts started in the late 1970s and extensive research and technology development has been going on since then (Sellin and Leupin 2013). Early laboratory experiments on MX-80, French Fo-Ca clay, Japanese Kunigel VI and Canadian Avonlea bentonite[23] were performed by Pusch and co-workers who published some of the earliest studies on the gas transport behaviour of compact bentonite.

According to Sellin and Leupin (2013), a linear dependence is observed between the gas flow rate and pressure gradient in an unsaturated or partially saturated bentonite. This means that two-phase flow is the dominant transport mechanism (Villar et al. 2012). This may also be the case for saturated sand/bentonite mixtures if the sand content is sufficiently high. However, for bentonite materials close to saturation, Sellin (2014) indicates that no advective gas transport will take place, until the applied gas pressure is equal to or above the total stress experienced by the clay. In such instances, significant mechanical deformations do occur, which results in either (i) consolidation of the bentonite, and/or (ii) formation of dilatant pathways. In the case of the former, a gas volume will be formed within the clay and the clay is consolidated within the vicinity of the gas volume, resulting in a local increase in the swelling pressure to balance the gas pressure. The degree to which this consolidation can occur is, however, limited.

Pusch and Forsberg (1983) measured gas permeability values in pre-saturated MX-80 bentonite following gas breakthrough. They noted sample saturations remained close to 100%, after gas had passed through the clay, suggesting gas transport had occurred in a highly localised fashion. Additional tests were performed on saturated MX-80 specimens by Pusch et al. (1985). Gas advection was encouraged by incrementally increasing the applied gas pressure at one- to five-day intervals, until outflow was seen at the downstream end of the sample. This outflow occurred at some 'critical pressure', which was noted to be related to the swelling pressure of the bentonite. This critical threshold is now generally known as the 'gas breakthrough pressure' and provided an indication of the coupling between advection and the mechanical properties of the clay.

Later work by Gallé (1998) and Gallé and Tanai (1998) on Fo-Ca clay, compacted to a range of dry densities (from 1 600–1 900 kg/m³), observed two distinct pressure thresholds. The lower threshold related to the gas pressure at which the first downstream appearance of gas was observed. They termed this the 'gas entry pressure', though it would now more likely be described as the 'gas breakthrough pressure'. In contrast, the 'gas entry pressure' is generally taken to be the critical value above which gas is first observed to enter the clay, though it is difficult to measure experimentally. The upper threshold they termed 'gas breakthrough pressure' and was characterised by a sharp increase in measured flow rate, indicating the onset of major outflow of gas. While the latter threshold pressure was always greater than the former, these two pressures were observed to be very close in fully saturated clay. Effective gas permeability values measured for the Fo-Ca clay were shown to decrease systematically for both increasing dry density and saturation state.

Tanai et al. (1997) examined the relationship between dry density (1 600, 1 700 and 1 800 kg/m³), swelling pressure and breakthrough pressure for samples of saturated Japanese Kunigel VI and French Fo-Ca clay in an oedometer cell. For both clay types, the authors noted that the observed gas breakthrough pressures were similar in value to the measured swelling pressures. The importance of sand content on the gas transport behaviour of bentonite was illustrated by Hokari et al. (1997), who performed a series of experiments on Kunigel VI bentonite, mixed with a high sand content (~15%

---

[23] also known as Saskatchewan bentonite

EURAD (Deliverable n° 6.1) – Initial State of the Art on Gas Transport in Clayey Materials
Dissemination level: PU
Date of issue of this report: **17/11/2021**

Page 170

bentonite). Exceptionally low gas entry pressures were noted, ranging between 10 and 60 kPa and consequential gas conductivities of between values of the order of 10^{-10} and 10^{-12} m/s.

In contrast, a series of controlled flow rate gas injection experiments on pure pre-compacted MX-80 bentonite was reported by Horseman et al. (1997, 1999) and Harrington and Horseman (1999). To ensure samples were fully saturated (>99%), they were first equilibrated under an isotropically applied confining stress, with an external water pressure of 1.0 MPa applied at both ends. Helium gas was then injected at a constant flow rate. Findings from these experiments again highlighted the importance of swelling pressure on the gas transport process, for initially saturated bentonite.

In all tests, gas breakthrough occurred at an excess gas pressure just fractionally greater than the calculated swelling pressure of the clay. As with Pusch and Forsberg (1983), desaturation of the test samples was found to be negligible after gas injection. The authors suggest this can be explained by gas flow not through the original pore space of the water-saturated bentonite, but via a number of localised pathways. As such, Harrington and Horseman (1999) argued that effective gas permeability measured in these tests must therefore be a dependent variable, rather than a material property. This would imply that effective gas permeability is directly related to the number of pressure-induced pathways allowing gas transport from the upstream to downstream filter, together with the width, aperture and distribution of these features.

Harrington and Horseman (1999) reported a series of tests which included the immersion of samples in a beaker of glycerol following gas injection. The beaker was then heated gently to cause trapped gas to expand. Streams of gas bubbles were observed emerging at discrete points on all surfaces of the clay. As helium solubility in clay pore water is extremely low, it was argued that this represented further evidence for the movement of gas through the clay as a discrete phase, following multiple localised pathways. No emergent gas bubbles were observed in a previous control experiment on fresh bentonite not used for gas testing.

Hume (1999) conducted gas injection experiments on Canadian Avonlea bentonite in both an oedometer cell and a constant volume cell. In the case of the oedometer experiments, the influence of initial dry density and of varying degrees of saturation on breakthrough pressure were investigated by applying five-minute pressure increments until the passage of gas was observed. Gas breakthrough pressures were reported to range from 0.3 MPa to 19.8 MPa, for dry densities of between 0.8 Mg/m^3 and 1.4 Mg/m^3. It was noted that gas breakthrough pressures increased significantly for samples close to full saturation. Breakthrough pressures were also shown to be minimal for unsaturated clay, while reaching high values (exceeding 10 MPa) when fully saturated. Constant volume testing of saturated samples was also conducted at constant gas pressure and highlighted the dependence of breakthrough time to pressure and dry density. However, in this case, the test duration was substantially longer, higher pressures could be achieved and breakthrough was also observed to occur for the higher dry densities (up to 1.4 Mg/m^3). The authors argued that the time to breakthrough was, therefore, controlled by the time required for sufficient water to be expelled, allowing the transport of gas. However, this behaviour could be equally explained by the rapid pressurisation at the start of these constant pressure tests, leading to insufficient time for gas pathways to develop.

Tanai and Yamamoto presented a series of gas transport tests, performed in an oedometer cell, at a GAMBIT club[24] meeting later reported in Rodwell et al. (2003a). Samples of bentonite and sand/bentonite mixtures were placed within the cell, uniaxially compacted to chosen dry densities and then saturated under a constant head. A stepwise increase in hydrogen gas pressure was applied to

---

[24] The GAMBIT club is a consortium of radioactive waste management organisations: SKB, Andra, ENRESA, JNC (Japanese organisation), Nagra and Posiva.

EURAD (Deliverable n° 6.1) – Initial State of the Art on Gas Transport in Clayey Materials
Dissemination level: PU
Date of issue of this report: 17/11/2021

Page 171

the one end of the sample and the downstream flow rate monitored. Gas breakthrough pressure was then determined as the onset of detectable downstream outflow and the resulting effective gas permeability measured. Tanai and Yamamoto noted a correlation between the experimentally-determined swelling pressure and the measured gas breakthrough pressure. Nevertheless, a strong correlation was also found between breakthrough pressure and sample length (twice as high for 10 cm than 5 cm). This was interpreted as resulting from the time necessary for gas pathways to propagate the necessary sample length before gas pressure was relieved. It was also shown that gas breakthrough pressures were restored to similar values, where samples were resaturated before re-injection. Effective gas permeability was also found to reduce for higher clay densities. Measured gas permeabilities ranged from 10^{-17} m^2 for mixtures with a 30% sand mass fraction (at a dry density of 1.6 Mg/m^3) to 10^{-20} to 10^{-21} m^2 for pure bentonite (at a dry density of 1.8 Mg/m^3).

Further testing conducted on an isotropically confined bentonite sample was also presented by Tanai and Yamamoto (see Rodwell et al. (2003a)). The aim of this test programme was to use X-ray CT to image the distribution of liquid/ gas during experimentation. Gas breakthrough occurred at a pressure of 2.6 MPa (higher than the 1 MPa swelling pressure of the bentonite), at which time major downstream outflow was detected. Applied gas pressure fell as outflow continued, but rapid transient increase in outflow was observed after gas upstream pressure fell to ~1.8 MPa. They attributed this behaviour to the generation of a preferential pathway through the specimen. CT scans were conducted before gas injection, at gas breakthrough and after the second peak in gas outflow. The results suggest a small change in the measured bulk density of the sample after gas breakthrough, but it was not possible to determine if this was the result of gas present at the centre of the core. Changes were not pronounced, and it was not possible to detect any discrete gas channels, which are probably out of the resolution range of the technique.

Finally, gas testing was conducted on a Kunigel VI/sand mixture (70/30). For this mixture, gas injection resulted in water displacement. Primary conclusions of Tanai and Yamamoto (see Rodwell et al. (2003a)) were as follows:

- Early gas transport experiments indicate a correlation between gas breakthrough pressure and swelling pressure. Later experiments (at moderate densities) led to breakthrough pressures significantly above the swelling pressure.

- Gas pathways were effectively sealed by resaturation.

- Some instability was apparent in gas pathways after breakthrough.

- X-ray tomography was not found capable of imaging gas pathways, which may be smaller than the technique can resolve.

At the end of the FORGE EC project, Sellin (2014) reports of local gas injection experiments by BGS that show that above some critical pressure, dilatant pathways form, resulting in the movement of gas through the bentonite. The pathways are characterised by a strong coupling between (local fluctuations in) the total stress, swelling pressure and pore pressure, as well as unstable flow, exhibiting spatio-temporal evolution, localised outflows during gas breakthrough and no measurable desaturation in any test samples. The transition between bulk consolidation and pathway dilatancy is unclear. For some experiments, pathways were observed to form as soon as gas pressure reached (average) total stress in the sample, but in other cases breakthrough only occurred at pressures 2–3 times higher than this. It is thought that the sample geometry strongly controls this behaviour, though there may be other influences.

The impact of gas transport on the integrity of several bentonite-bearing barrier materials and their ability to perform the intended safety functions is investigated in the WP GAS of EURAD (see also Sections 1.5.4, 2.4.1.5 and 2.4.2.5). The state of knowledge on gas-induced deformation and failure of the MX-80 bentonite, the FEBEX bentonite and the sand/bentonite mixtures under study in the WP

EURAD (Deliverable n° 6.1) – Initial State of the Art on Gas Transport in Clayey Materials
Dissemination level: PU
Date of issue of this report: 17/11/2021

Page 172

GAS, is presented hereafter as derived from the results of the laboratory tests. Thereafter, the results of the Lasgit and FEBEX in situ tests are presented.

Granular Wyoming sodium bentonite (MX-80)

Seiphoori (2015) determined the coupled thermo-hydro-mechanical (THM) behaviour of granular Wyoming sodium bentonite in triaxial conditions as part of a comprehensive geotechnical characterisation programme. Volumetric and shear behaviour was investigated at saturated and unsaturated conditions, using a vapour transfer technique for controlled suction tests in the range of total suction between 0 and 100 MPa. Gonzalez-Blanco and Romero (2019) performed multiple gas invasion experiments in an oedometric cell with emphasis on the evolution of volumetric strains of the test samples in response to the prevailing constitutive stresses. After testing, the bentonite samples were dismantled and imaged by μ-CT to identify possible sample damage associated with the gas invasion process. Furthermore, one of the gas injection tests was combined with colloid sampling, aimed at quantifying the amount of mobilised bentonite particles as a result of gas percolation through the bentonite.

Understanding the mechanical behaviour of the material in unsaturated conditions is a prerequisite to the understanding of interactions with gas. The isotropic behaviour of granular Wyoming sodium bentonite in the saturated state and at different suctions is presented in Figure 3-23 (Seiphoori 2015). The compressibility of the material in unsaturated tests increases when the total suction decreases (Figure 3-23a). In case of the saturated sample, no volume change was allowed until the pressure level p_s = 1 MPa was reached which is basically referring to the swelling equilibrium phase where the volume of the sample is kept constant. The pore volume change monitored during this step (Figure 3-23b) is associated to the uptake of water by the sample and the lateral drainage (filter paper and geotextile layer). Due to the fact that the sample could become slightly desaturated after extraction from the saturation mould and during the installation inside the triaxial cell, the saturated sample starts to be consolidated for mean total stresses higher than 1 MPa.

The change of the degree of saturation for unsaturated tests upon a constant water content is due to the reduction of the void ratio as depicted in Figure 3-23b. In this range of total suction, the water content of the material is associated with the retention of water in micropores including the interlayer porosity.

The corresponding stress path in the water retention plane is presented in Figure 3-23c. For unsaturated samples, under a typical stress path like A → B, the void ratio decreases at constant water conditions, while the total suction remains constant. Such a stress path, called iso-suction path can be shown between two successive retention curves of two void ratios of 0.83 and 0.66.
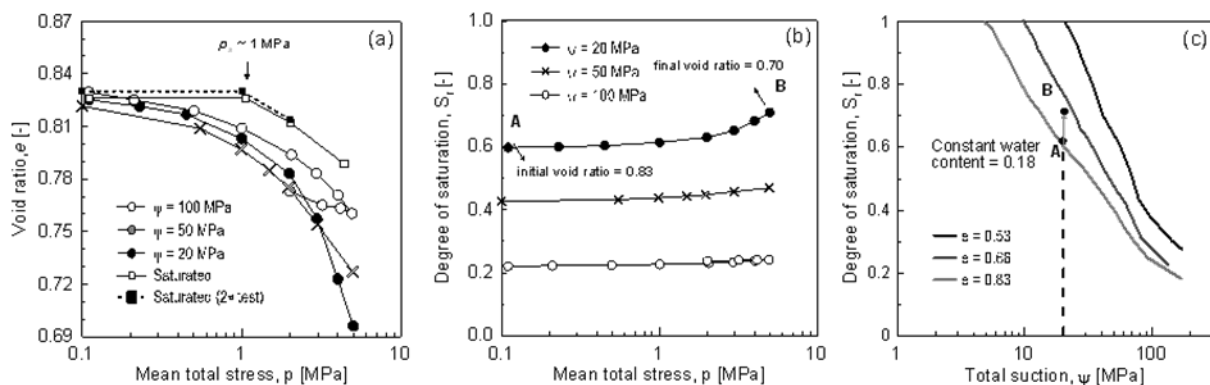
Figure 3-23 – (a) influence of the total suction on the isotropic behaviour of granular Wyoming sodium bentonite, (b) variation of degree of saturation in unsaturated tests, and (c) corresponding path for unsaturated tests in water retention plane (Seiphoori 2015).

EURAD (Deliverable n° 6.1) – Initial State of the Art on Gas Transport in Clayey Materials
Dissemination level: PU
Date of issue of this report: 17/11/2021

Page 173

The compression index C_c is defined as the slope of the normally consolidated (NC) line in the void ratio-log p plane (Figure 3-23a). Compression indexes of unsaturated samples are given in Table 3-2. The comparison with the compression index derived for the saturated sample ($C_{c,sat}$ = 0.04) shows that the compressibility of the saturated samples is lower than the unsaturated ones. This may be explained by differences in the fabric of the compacted unsaturated bentonite as compared to the initially saturated bentonite.

Table 3-2 – Compression index of unsaturated bentonite samples as a function of total suction (Seiphoori 2015).

A total suction s [MPa] of …	100	50	20	Initially fully saturated
→ results in a compression index C_c [–] of	0.05	0.07	0.20	0.04

The influence of the confining stress on the deviatoric behaviour of the material at total suctions of 100 MPa and 50 MPa is presented in Figure 3-24a&c. The decrease in the elastic domain of the over-consolidated sample at s = 100 MPa can be observed.
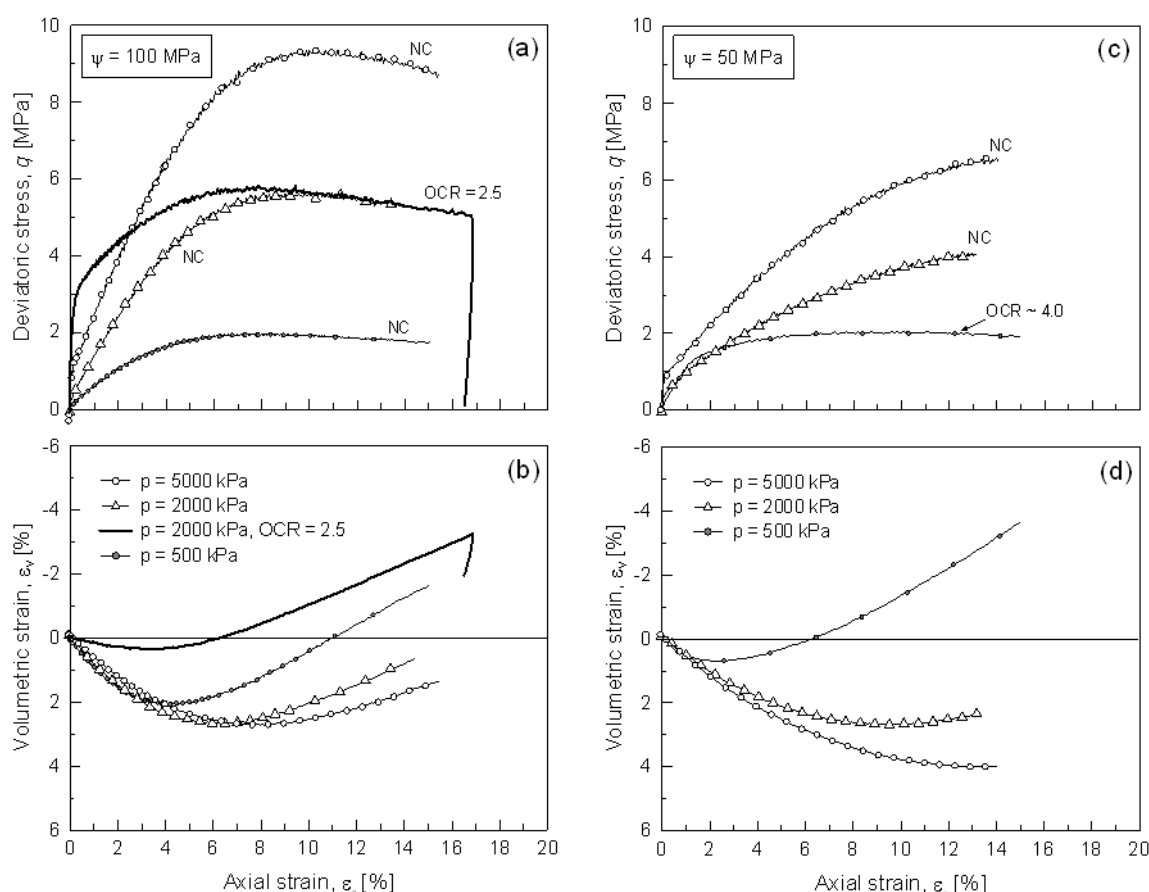
Figure 3-24 – Deviatoric behaviour of granular Wyoming bentonite: (a) and (b) influence of confining stress at s = 100 MPa; (c) and (d) influence of confining stress at s = 50 MPa (Seiphoori 2015)[25].

---

[25] The symbol for suction in the figure is ψ.

EURAD (Deliverable n° 6.1) – Initial State of the Art on Gas Transport in Clayey Materials
Dissemination level: PU
Date of issue of this report: **17/11/2021**

Page 174

Figure 3-24b&d presents the volumetric behaviour at the same suction levels, and the dilatant behaviour is seen for the over-consolidated sample starting from about 6% of the axial strain. The samples show a tendency to dilate after failure. This behaviour could be associated to the geometrical deformation of the samples after failure. Figure 3-24c indicates that the sample at confining stress p = 500 kPa exhibits ductile behaviour with deviatoric stress remaining constant after failure.

The material exhibits a ductile behaviour under saturated conditions. The deviatoric stress at the failure with respect to the mean total stress and total suction is presented in Figure 3-25a&b. Figure 3-25a exhibits the Critical State Line (CSL) at different suction values, assuming that the slope of the CSL is constant. This is valid with the assumption that the shear strength angle of the material remains constant at different total mean stress values.

In unsaturated samples, an increase in internal friction resistance can be seen with an increase in total suction. Regardless the deviatoric response of the saturated sample at swelling equilibrium, this trend can include the saturated samples as well. Figure 3-25b displays that the evolution of the peak strength of the material with a total suction increase is negligible under lower confining stress. On the other hand, clear evidence for the hardening due to the increase in total mean stress and total suction is seen. The influence of the total suction and confining stress can be explained by the hardening plasticity. The hardening associated to the movement of the yield surface is assumed to depend on the plastic volumetric strains. In the triaxial stress space, by considering deviatoric stress q, the yield surface can be represented by, for instance, the elliptic form of the Modified Cam-Clay model as shown in Figure 3-25c&d.
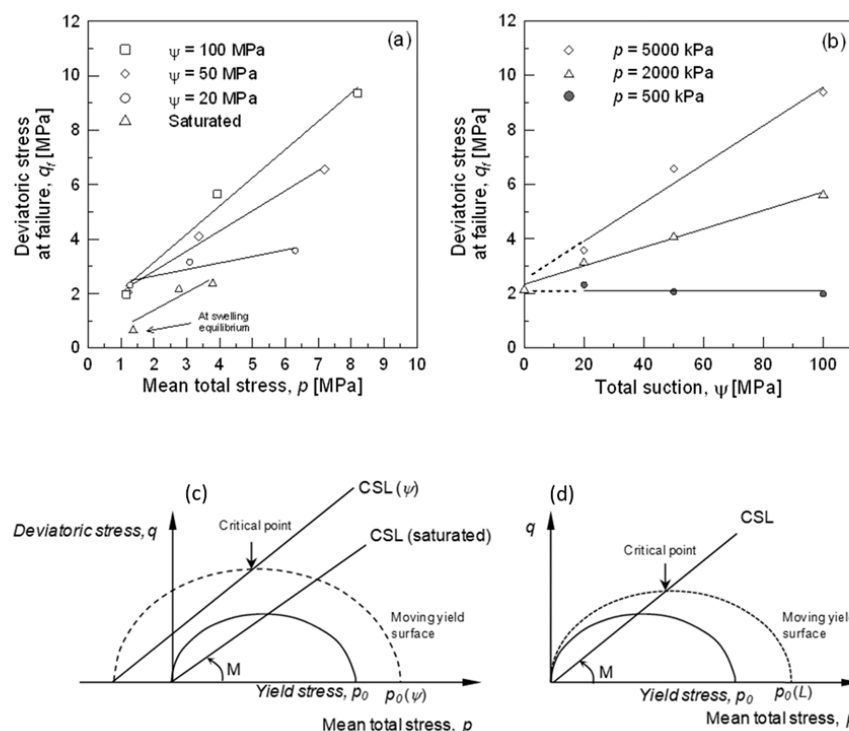
Figure 3-25 – Deformation behaviour of unsaturated Wyoming granular bentonite (modified after Seiphoori 2015)[26]. Influence of (a) suction and (b) mean total stress on the deviatoric stress at failure. Evolution of the yield surface and Critical State Line (CSL) in the hardening plasticity approach: (c) suction hardening, and (d) strain hardening.

---

[26] The symbol for suction in the figure is ψ.

EURAD (Deliverable n° 6.1) – Initial State of the Art on Gas Transport in Clayey Materials
Dissemination level: PU
Date of issue of this report: **17/11/2021**

Page 175

European Joint Programme
on Radioactive Waste Management

Gonzalez-Blanco and Romero (2019) performed a series of gas injection tests in fully water-saturated samples of compacted granular Wyoming bentonite (dry densities in the range 1.45–1.55 Mg/m³; see also Section 2.4.1.5) to investigate the hydro-mechanical behaviour of the material in response to gas invasion. The tests were conducted in an oedometer cell by invading air or helium with gas injection rates between 0.04 mL/min and 100 mL/min (volumetric rate). The applied vertical stress was around 5 MPa and the maximum gas injection rates were in most cases around 4 MPa to avoid preferential flow along the contact zone between bentonite and the steel wall of the oedometer cell.

Figure 3-26 shows the results of a helium injection test on the bentonite sample S18 (ρ_{dd} = 1.55 Mg/m³; e = 0.80; σ_v = 5.6 MPa) in terms of He injection pressure at the upstream boundary (injection point) and the outflow pressure and volume at the downstream boundary (recovery point), jointly with the average axial strain, calculated based on recorded axial displacements on the top of the sample. The gas pressure at the upstream boundary increased in time from 0.5 to 4 MPa (A to B in the figure), followed by shut-off (point B) and dissipation at closed He injection line (B to C). The initial injection piston volume was 500 mL (at 0.50 MPa) while its volume at the end of the injection was 10.77 mL.
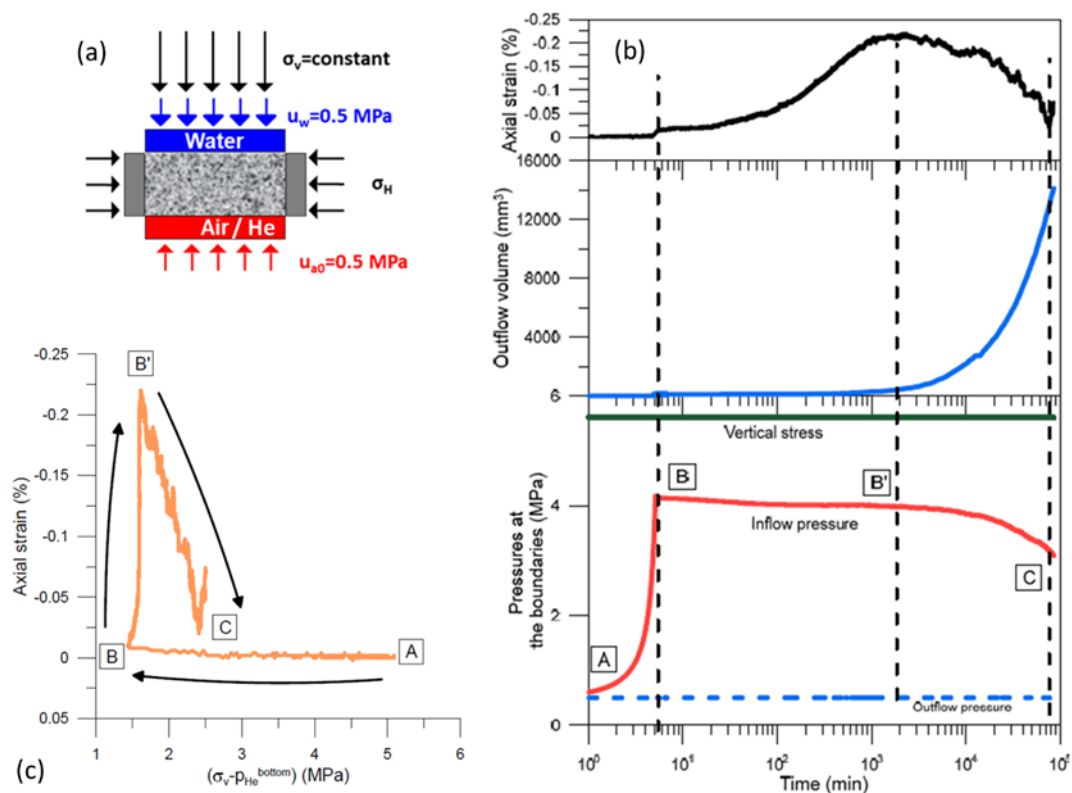
Figure 3-26 – Gas injection test on Sample S18 with helium at a volumetric flow rate of 100 mL/min (bentonite sample S18) from Gonzalez-Blanco and Romero (2019): (a) sketch with the hydraulic and mechanical initial/boundary conditions; (b) time evolution of pressures at the boundaries, outflow volume and axial deformation of the sample; (c) axial strain versus constitutive stress (vertical stress minus He pressure at the upstream boundary).

During the injection stage (A to B in Figure 3-26b), the sample expansion and outflow are insignificant. However, at the end of the injection phase (4.8 min after onset of injection), a very small outflow was detected. After shut-off (point B in the figure), the outflow volume continued increasing while the sample underwent expansion (negative axial strain). At around 1 900 min, the outflow rate speeded up and the sample started to compress (point B' in the figure).

Figure 3-26c shows the axial strain evolution during the He injection/dissipation test on sample S18. The axial strains are plotted against constitutive stresses (defined as the vertical stress σ_v minus the

EURAD (Deliverable n° 6.1) – Initial State of the Art on Gas Transport in Clayey Materials
Dissemination level: PU
Date of issue of this report: 17/11/2021

Page 176

He pressure at the injection point p_{He}). Changes in axial strain and the corresponding porosity changes are a consequence of changes in fluid pressures since tests were carried out at constant vertical stress. The examination of the axial strains revealed different deformation stages. During the air injection stage (A to B in the figure), the sample underwent a negligible expansion. After shut-off (B in the figure), expansion continued as a consequence of the gas pressure front propagation into the sample (B to B'), which induced the fluid pressure to increase and the constitutive stress to decrease. The injection pressure started to decrease along the dissipation stage towards point C, which induced sample compression during constitutive stress increase.

Gonzalez-Blanco and Romero (2019) conducted complementary microstructural investigations with test specimen of similar initial dry density (as-compacted: ρ_{dd} = 1.54–1.55 Mg/m^3) to study the evolution of porosity in response to uniaxial compaction ('as-compacted'), hydration ('fully saturated state') and gas injection. For this, cylindrical bentonite samples (10 mm in diameter, 10 mm in height) were trimmed and prepared for visualisation in a µ-CT device with a resolution of around 10 µm (Figure 3-27). Several sample preparation techniques were tested with and without freeze-drying, aimed at minimising the disturbance of the fabric by sample preparation procedure. The reconstructed 3D image of the as-compacted sample (Figure 3-27a) clearly reveals the granular structure of the compacted material with numerous well-connected pore channels, representing the intergranular porosity. After hydration of the material at constant volume conditions many of the large pore channels disappear, because the bentonite grains take up the imbibing water and swell into the intergranular pore space (Figure 3-27b). The loss of macroporosity is compensated by an increase of meso- and micro-porosity, which cannot be resolved with the µ-CT device. A similar picture is seen after gas injection (Figure 3-27c), displaying a network of distinct pore channels along the grain boundaries. Quantitative image analyses by Keller (2019) provide clear evidence, that the grain size distribution of the sample shown in Figure 3-27c is statistically similar to the as-compacted sample (Figure 3-27a), indicating a moderate increase of the mean grain size due to the swelling of the bentonite aggregates and/or the formation of grain clusters. A distinct memory of the initial grain size distribution of the as-compacted material is yet preserved after a full hydration/gas injection cycle.

(a) as compacted sample   (b) fully saturated state   (c) after gas injection
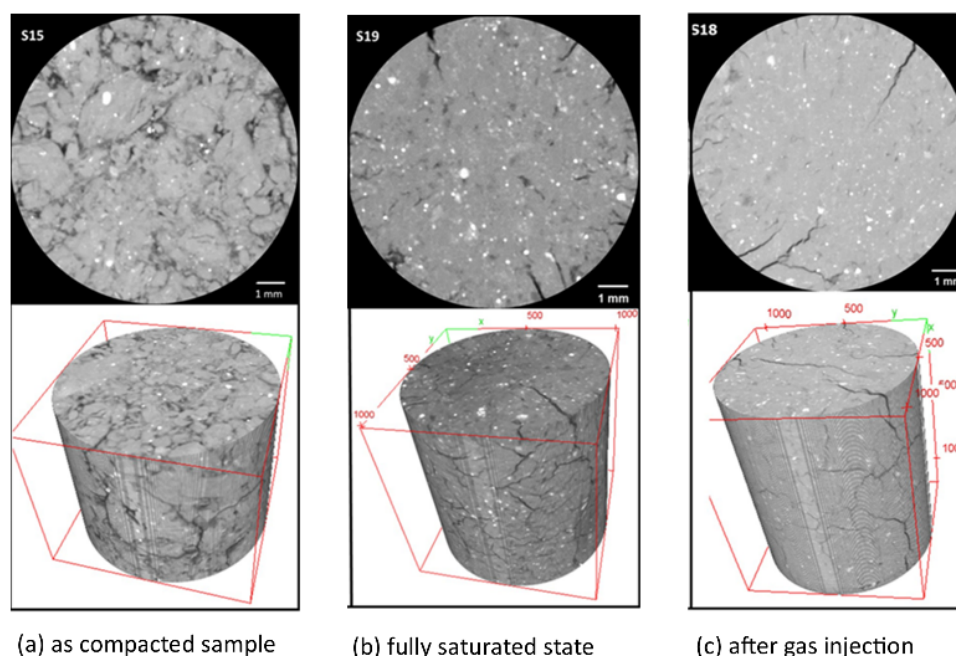
Figure 3-27 – µ-CT scans for visualising the distribution of macropores in compacted / saturated bentonite samples. Slices and 3D reconstructions of samples (a) S15 at the as-compacted state, (b) S19 at the saturated state, (c) S18 after gas injection.

EURAD (Deliverable n° 6.1) – Initial State of the Art on Gas Transport in Clayey Materials
Dissemination level: PU
Date of issue of this report: **17/11/2021**   Page 177

Gas flow in compact MX-80 bentonite was also investigated by Harrington and Horseman (2003) and Horseman et al. (2004), who performed a series of tests on volumetrically constrained samples, with dry densities around 1600 kg m^{-3}. The apparatus used in these experiments was designed to reproduce some of the main features of the repository near field, including the borehole, the corroding canister and conductive fractures in the host rock (which were simulated by using 3 independently controlled arrays of filters acting as potential sinks for migrating gas). Helium was used as permeant in place of hydrogen, due to its similar molecular diameter, and its greater suitability for laboratory testing. Harrington and Horseman (2003) reported two experiments. All samples were initially hydrated by the application of deionised water at a pore fluid pressure of 1 MPa. As a result, the bentonite was observed to swell, leading to measurable build-up of axial and radial stresses. Hydration was continued until full saturation, which was determined through mass balance and geotechnical calculations. For both test samples, gas was injected through the central rod filter, while a constant backpressure of 1 MPa was maintained through one of the large, end-closure filters. In the first test (MX-80-8) major gas entry occurred at a gas pressure of 18.9 MPa, followed by breakthrough at a gas pressure of 19.4 MPa when significant outflow of gas was observed. In the second test (MX-80-10), time-dependent effects were examined by conducting constant flow rate injection, interspersed with a number of constant gas pressure steps. Gas breakthrough resulted in detected outflow distributed non-uniformly across all three sink arrays. For both experiments, major gas entry was observed to occur close to the value of the average measured total stress. For test MX-80-10 gas entry was also associated with significant changes in local stress and pore water measurements. Gas transport was attributed to pathway dilatancy in both cases. In test MX-80-10, step-like stress responses were observed before breakthrough, despite a lack of outflow at the sink arrays. This was interpreted as resulting from the propagation of gas pathways not yet reaching a sink array. Before gas finally reached a sink, the high gas pressures mentioned above where reached as a result of the constant volume geometry. Should the same, localised pathways development mechanism occur within bentonite barriers in a repository, this suggests that the number and geometry of available sinks at the periphery of the barrier can affect the maximum gas pressure.

In both experiments, no evidence was found of a displacement of water as the result of gas pathway development and gas transport. Desaturation of the samples was not observed during post-test geotechnical analysis, despite samples MX-80-8 and MX-80-10 being exposed to gas pressures greater than 8 MPa, for 195 days and 390 days, respectively. Harrington and Horseman (2003) also calculated that 50.5 litres (for MX-80-8) and 60.4 litres (for MX-80-10) of gas (at standard temperature and pressure) had been allowed to pass through the specimens over this time, though their final saturation states were measured as approximately 100%. This strongly reinforces previous observations of the absence of desaturation in MX-80 bentonite (Pusch and Forsberg 1983; Harrington and Horseman 1999) and indicates that gas does not flow through the water-saturated pre-existing porosity but through newly developed, gas-specific pathways.

In both tests, gas pressures peaked at a value in excess of the total stress. Indeed, total stress is calculated as an average, while the development of gas-specific pathways from local gas injection induces a local stress redistribution. Thereafter, gas pressure began to decay and was observed to settle close to the measured total stress. The authors argue that the rapid pressure drop after peak results from a breakdown of the tensile strength of the bentonite and the consequent escape of gas at an outflow sink. The sustained higher gas pressures observed were interpreted as being a natural consequence of the boundary condition until gas reached an outflow sink. After breakthrough, a pronounced coupling was also noted between gas pressure, total stress and pore pressure, for both samples. Episodes of abrupt reductions in gas pressure were also noted, accompanied by similar reductions in total stress. These were interpreted by the authors as distinct fracture propagation events. In some instances, the distribution of flow was also seen to change abruptly and spontaneously during the experiments, moving from one sink array to another. It was also noted that previous pathways were not necessarily reused as conduits for future flow, indicating a capacity for pathway sealing to occur. In both tests, gas injection was stopped, and gas pressure allowed to decline to an asymptotic value as

EURAD (Deliverable n° 6.1) – Initial State of the Art on Gas Transport in Clayey Materials
Dissemination level: PU
Date of issue of this report: 17/11/2021

Page 178

outflow ceased. For both MX-80-8 and MX-80-10, the final gas pressure was seen to exceed the applied pore water pressure by an amount equal to the swelling pressure. The authors attributed this behaviour to the collapse of flow pathways due to declining pressure. The self-sealing capacity of the bentonite was invested by first rehydrating the clay and then reinjecting gas. Data showed that part of the clay's initial resistance to gas flow could be recovered and suggests that quiescent phases between gas pressure build-up events may allow the clay to recover its initial state, to some degree.

The role of swelling pressure and its impact on gas transport was further explored by the FORGE project and reported by Sellin (2014). Experiments performed by Clay Technology AB in constant volume conditions showed that once the internal (swelling) pressure of the bentonite fell as a result of flushing one end of a sample with a strong solution of NaCl, gas breakthrough occurred when the gas and swelling pressures were approximately equal. Testing was repeated for samples at different gas injection pressures, providing clear evidence of the link between swelling properties of the clay and gas transport.

Using a similar apparatus to Horseman et al. (2004), Graham C. et al. (2016) showed also that the link between the gas pressure at which entry is observed and total stress in compact MX-80 bentonite is remarkably consistent irrespective of the applied water pressure (Figure 3-28). In these experiments, gas breakthrough was induced by lowering the applied water pressure which, in turn, lowers the total stress, while maintain a constant gas pressure, mimicking an excursion in repository groundwater conditions. The resulting drop in total stress resulted in gas entry into the clay leading to episodes of 'pressure-cycling', as gas sought a stable escape pathway. The authors argue that their findings demonstrate the potential for 'phases' of pathway development and propagation within the buffer, resulting in successive transport episodes over the repository lifetime. Experiments also demonstrate the potential for gas entry into the bentonite to occur as a result of declining pore water pressure conditions. It can be seen on Figure 3-28 that at very high total stresses, entry pressure and breakthrough pressure are very close to each other. For stress states that are more representative of expected repository conditions, breakthrough pressure is significantly higher than gas entry pressure.
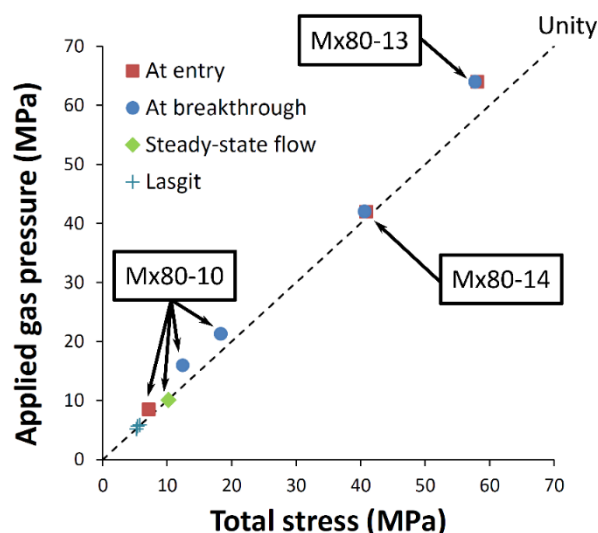
Figure 3-28 – Relationship between total stress and gas pressure in a compilation of gas injection experiments in MX-80 bentonite (Graham C. et al. 2016).

EURAD (Deliverable n° 6.1) – Initial State of the Art on Gas Transport in Clayey Materials
Dissemination level: PU
Date of issue of this report: 17/11/2021

Page 179

FEBEX bentonite

Villar et al. (2021) report that research on the gas transport properties of FEBEX bentonite started back in the 90s, when the gas permeability of samples compacted to different dry densities and water contents was measured in a falling-head permeameter, using very low injection pressures (Villar and Lloret 2001; Villar 2002). At that time, gas permeability was found to depend on the accessible void ratio, which expresses the ratio between gas accessible volume (not blocked by water) and particle volume. It was also found that the intrinsic permeability deduced from gas flow was considerably higher than the one deduced from water flow, because of the microstructural changes that take place during saturation (reduction in average pore size). However, because of the equipment limitations, it was not possible to measure the gas permeability of samples with high degrees of saturation.

New set-ups were developed in the FORGE project, which allowed to measure the gas permeability of samples with degrees of saturation up to 97% and test the effect of confining pressure and gas injection and backpressures on the gas permeability value. In these tests, the applied pressure gradient directly controlled the resulting gas flow rate, attesting conventional visco-capillary flow. The new results allowed to confirm in triaxial conditions the potential relation between accessible void ratio and gas permeability (Figure 3-29; Villar et al. 2013; Gutiérrez-Rodrigo 2018).
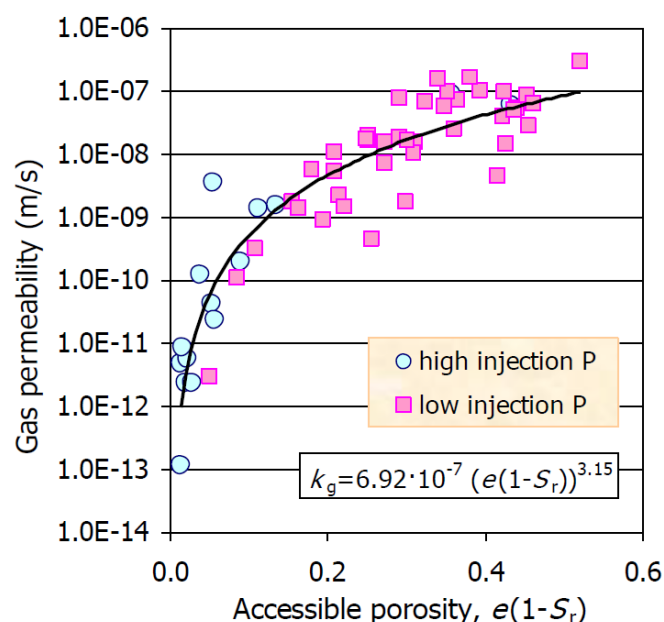
Figure 3-29 – Gas permeability as a function of the accessible porosity for FEBEX samples tested during the FEBEX (low injection pressure) and the FORGE (high injection pressure) projects (Villar et al. 2013).

Gas injection tests performed on samples fully saturated inside stainless steel cylindrical cells, where the overall volume of the bentonite could not change during the tests, showed that the gas breakthrough pressure values in saturated bentonite increased clearly with dry density, and these values were always higher than the theoretical swelling pressure of the bentonite (Figure 3-30). In addition, the permeabilities computed after breakthrough seemed to be independent of the dry density (Villar et al. 2013; Gutiérrez-Rodrigo et al. 2015; Gutiérrez-Rodrigo 2018; Gutiérrez-Rodrigo et al. 2021).

EURAD (Deliverable n° 6.1) – Initial State of the Art on Gas Transport in Clayey Materials
Dissemination level: PU
Date of issue of this report: **17/11/2021**

Page 180
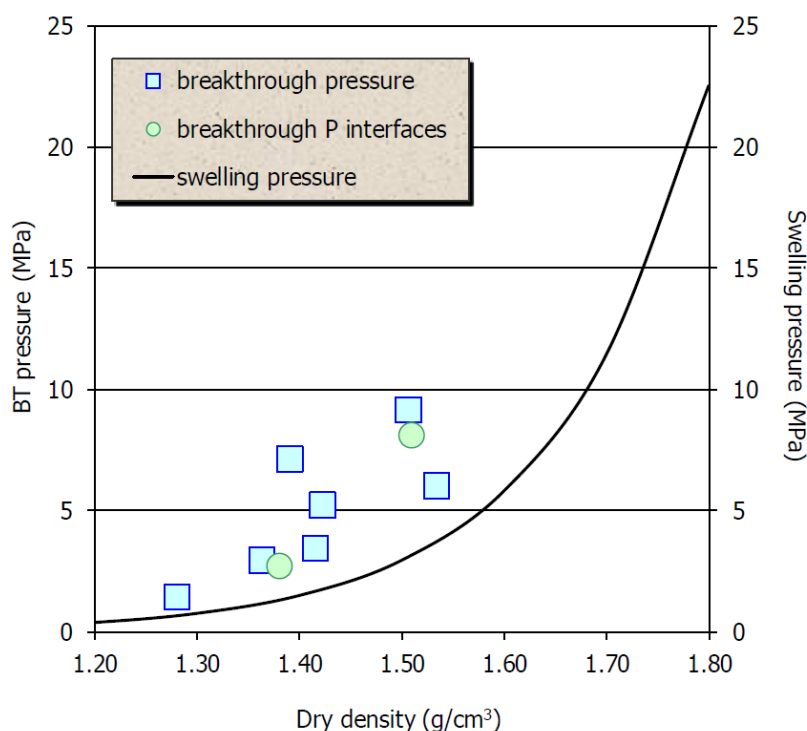
Figure 3-30 – Gas breakthrough pressure values for saturated bentonite samples compacted at different dry density and theoretical swelling pressure (Villar et al. 2013).

The tests performed in the triaxial cells and in the stainless steel cells mentioned above were designed to measure the bentonite gas permeability and the gas breakthrough pressure, respectively. The combination of both types of results allowed to conclude that in compacted bentonite two-phase flow can take place for degrees of saturation lower than about 97%. For higher degrees of saturation, the gas transport mechanism seems to be pathway dilation once the gas pressure exceeds a threshold for breakthrough. The stability of the gas pathways would depend on the degree of saturation and dry density of the samples. For partially saturated bentonite, the gas pathways seemed to be stable, since for a given pressure gradient there was a stable flow. Nevertheless, effective gas permeability was observed to drop by several orders of magnitude when approaching full saturation (Villar et al. 2013; Gutiérrez-Rodrigo et al. 2015), indicating an important restriction of the gas flow inside the bentonite. In almost completely saturated samples of bentonite, in which it was necessary to apply a high pressure to induce flow (breakthrough pressure), when the pressure gradient dropped below a given value (residual pressure), flow stopped, which was interpreted as the closing of the pathways.

Sand/bentonite (S/B) mixtures

Manca (2016) and Manca et al. (2016) investigated the fabric evolution and the related swelling behaviour of S/B mixtures upon hydro-chemo-mechanical loadings. Free and confined swelling tests were performed on specimens compacted to different dry densities and wetted with different pore fluids (see also Section 2.4.1.5).

Manca (2016) performed gas invasion tests under triaxial conditions aimed at investigating the likelihood of bentonite mobilisation associated with the gas breakthrough event. Such phenomena could reduce the performance of the S/B mixture to serve as a transport barrier for dissolved radionuclides. The gas injection test was performed on a fully saturated S/B specimen, initially compacted to 1.8 Mg/m^3. The initial confining pressure was 820 kPa. A gas pressure of 465 kPa was applied on top of the specimen for two days to check the tightness of the gas injection system. After this preliminary phase, a constant volumetric gas flux of 8.34×10^{-10} m^3/s (50 mL/min) was applied to the top of the specimen while the water pressure at the bottom was maintained constant. During the gas injection, it

EURAD (Deliverable n° 6.1) – Initial State of the Art on Gas Transport in Clayey Materials
Dissemination level: PU
Date of issue of this report: 17/11/2021

Page 181

was necessary to increase the confining pressure up to 1 150 kPa to avoid the preferential flow of the gas in the specimen/membrane interface. A special device was installed at the outflow chamber for collecting any bentonite colloids, mobilised by the gas phase.

The results of the gas injection test are presented in Figure 3-31. During the gas injection, the gas pressure increases up to a peak pressure of 1 038 kPa. A measurable outflow is detected when the gas pressure reaches 850 kPa (time t_2). The water outflow rate increases up to a value of 1.74×10^{-11} m^3/s (1.04 mL/min). This value is smaller than the volume of gas which is injected at the top of the specimen, suggesting that the gas is probably displacing water from the larger pores of the S/B mixture, but a continuous flow path towards the bottom of the sample has not yet been established. When the gas pressure reaches its maximum value (time t_3), a sudden increase of the outflow rate is observed, indicating the breakthrough of the gas phase at the bottom end of the specimen. After the breakthrough event, the gas pressure at the upstream spontaneously decreases until a stationary value of approximately 750 kPa is reached, suggesting that this gas pressure is sufficient to keep gas pathways open through the specimen when the constant gas injection rate is maintained.

Figure 3-31b shows one of the cups for collecting the water expelled from the specimen during the gas injection phase. Some fine clay is clearly visible. Approximately, 0.1739 g of bentonite particles was collected during the gas injection test, corresponding to 0.02% of the total dry mass of the specimen (equal to 816.63 g). This suggests that the transport of fine particles during the gas injection is likely to occur in S/B mixtures bentonite content and that this experimental set-up allowed collecting evidence on this issue. Further experiments are needed to investigate the relationship between the mobilised cumulative mass of bentonite and the cumulative gas flow.

The use of a sand/bentonite mixture has been investigated in the field-scale EBS experiment at the Grimsel test site (Switzerland). Significant hydro-mechanical characterisation was conducted on material from the experiment (Romero et al. 2002, 2003; Arnedo et al. 2008). Hydraulic and gas permeability testing were performed at the in situ compaction density (ranging from 1.50 to 1.85 Mg m^{-3}) on sand/bentonite (20% MX-80) mixture, using triaxial and oedometric cells. Testing was performed in a Perspex vessel and an air trap added to allow for the visual observation of gas flow. Samples were not saturated before gas testing but the initial saturation states were reported to be above 90%. Air was injected and recovered using two needles inserted into the base and top of the sample. Injection was conducted at a constant flow rate during each experiment (but varied between tests), while recovery was maintained at a constant pressure. In tests performed at higher flow rates, a horizontal fracture was generated within the clay. This was accompanied by a small drop in gas pressure which was interpreted as the moment of gas entry. Gas pressure continued to increase as the gas had yet to intersect the outflow needle. This continued until the maximum pressure of the cell (2 MPa) was reached. As such, the authors argue that the observation of a high pressure gas peak at the laboratory scale may relate to the difficulty in gas pathways intersecting the recovery needle. When gas pressure was allowed to decay, the fracture was observed to close. On re-initiation of pumping at the same injection flow rate, the same fracture was seen to reopen and propagate further, without impacting the measured gas pressure. A further 3 series of gas injection tests were conducted on sand/bentonite mixes at lower initial dry densities and similar behaviour was observed in all. Fracturing was noted to relate with compaction layers, suggesting that these may provide preferential characteristics for pathway propagation, though there is no evidence to suggest that their presence encourages this behaviour.

Liu J. et al. (2014a, 2014b) conducted gas injection experiments on plugs formed from sand/bentonite mixtures (with 70% MX-80 bentonite content). They observed that gas breakthrough pressures are more sensitive to sample saturation state than swelling pressure. Measured gas permeabilities were found to be highly sensitive to water content and applied confining pressure. The authors note that at a relative humidity of 98%, low gas permeabilities were achieved under in situ conditions, demonstrating a significant sealing capacity despite incomplete saturation. This is similar to what is observed on pure

![eurad logo] European Joint Programme on Radioactive Waste Management

EURAD (Deliverable n° 6.1) – Initial State of the Art on Gas Transport in Clayey Materials
Dissemination level: PU
Date of issue of this report: 17/11/2021

Page 182

bentonites (e.g. FEBEX bentonite, as discussed above): effective gas permeability drops rapidly when approaching full saturation.
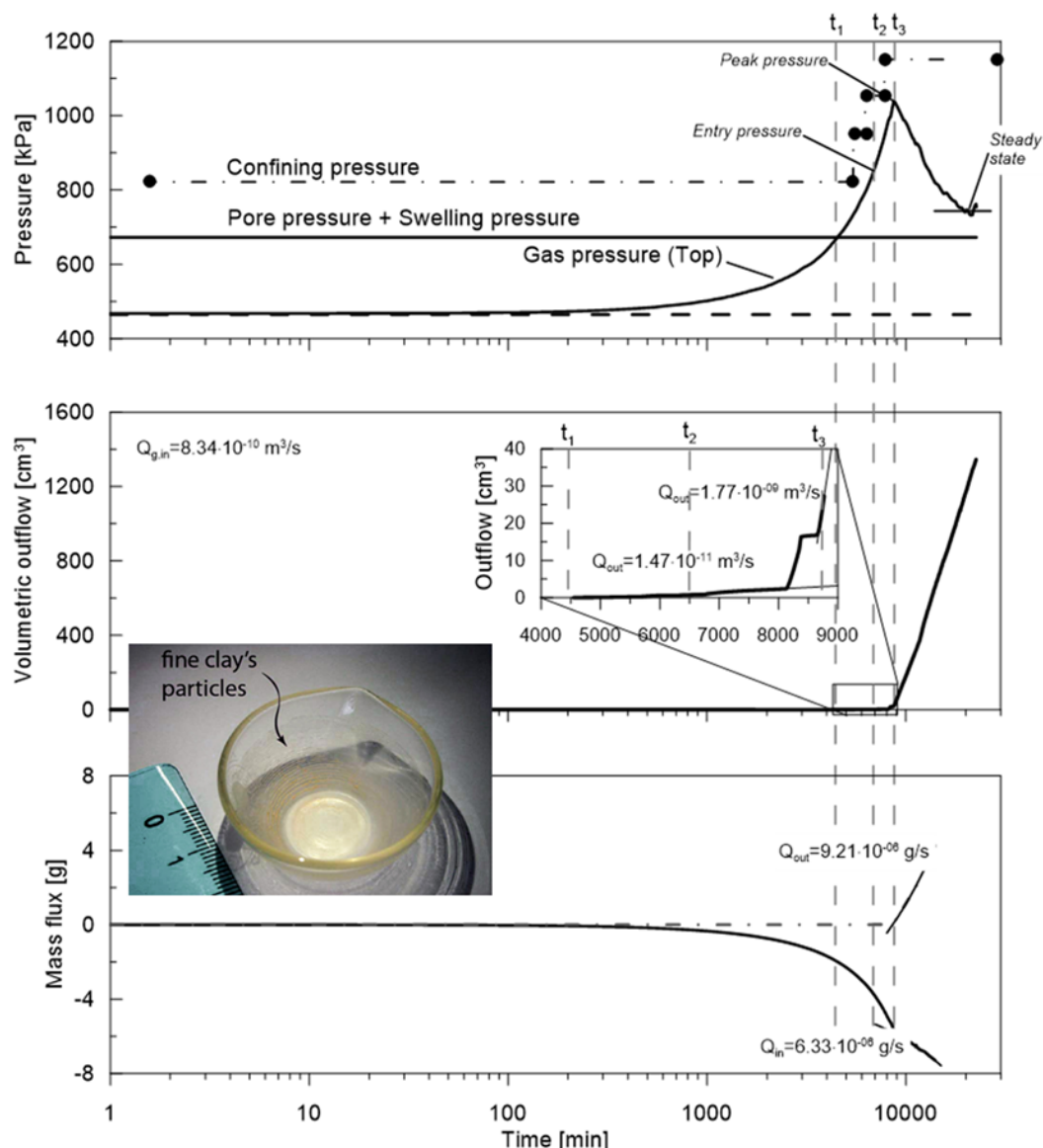
Figure 3-31 – Results of the breakthrough tests on an 80/20 S/B mixture compacted to 1.8 Mg/m³ (Manca 2016). From top to bottom: evolution of the gas pressure, confining pressure and pore water pressure, evolution of the cumulative volumetric outflow and of the cumulative mass flux. The picture shows the mobilised mass during the gas injection test under constant volume conditions.

In situ experiment: Large scale gas injection test (Lasgit) performed at the Äspö hard rock laboratory (HRL) in Sweden

Harrington et al. (2008) provide a detailed description of the LArge Scale Gas Injection Test (Lasgit) performed at the Äspö Hard Rock Laboratory (HRL) in Sweden. Lasgit is a full-scale demonstration project, designed to examine hydraulic and gaseous transport in bentonite-based EBS. It is a highly instrumented test with a large sensor array including 32 total stress sensors and 26 pore water pressure sensors distributed on the canister, in the bentonite and on the rock wall. Additional instrumentation was also included to monitor changes in relative humidity, temperature and relative displacement of the canister and the lid constraining the canister. 10 rock anchors were used to apply a pre-tension of

EURAD (Deliverable n° 6.1) – Initial State of the Art on Gas Transport in Clayey Materials
Dissemination level: PU
Date of issue of this report: **17/11/2021**

Page 183

1300 kN to simulate infill of the cavern space above the canister. For the purposes of the test programme, a full-scale KBS-3 canister was modified with thirteen circular filters of various dimensions located on its surface in three separate arrays, so as to provide point sources for gas injection (Figure 3-32). These filters were included to allow the simulation of gas release resulting from a potential canister defect. They are also suitable for injecting water and were used during the hydration stages to aid locally saturation of the buffer. Filter mats were also placed in strategic positions, both within the buffer, and on the rockwall to facilitate hydration. The canister was surrounded by specially manufactured, pure MX-80, pre-compacted bentonite blocks, with initial water saturation values above 95%.
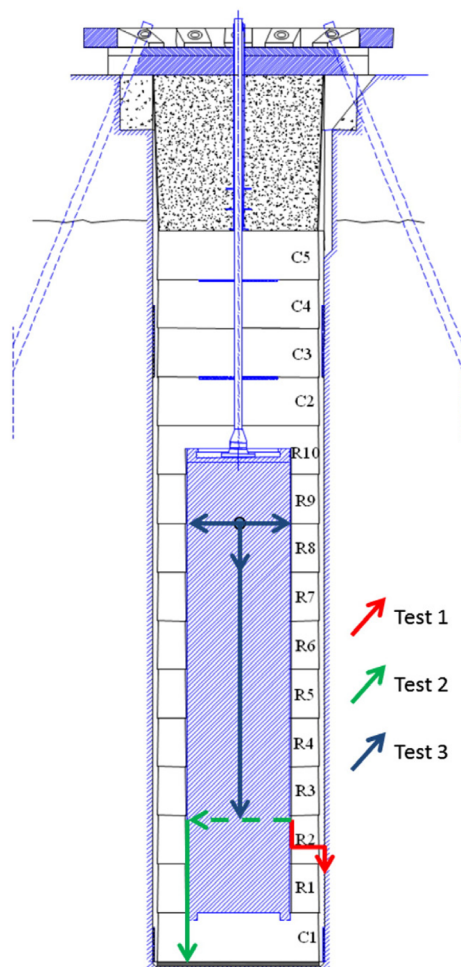
Figure 3-32 – Schematic of the layout of the Lasgit experiment showing the interpreted direction of gas transport for the first 3 injection tests (Äspö hard rock laboratory).

A full description of the test methodology is provided by Harrington et al. (2008) and detailed observations from testing are provided by Cuss et al. (2010, 2011b and 2014). Similar to previous laboratory studies (Harrington and Horseman 2003), results from a series of gas injection experiments exhibited qualitatively similar behaviour to the laboratory scale measurements including: a well-defined gas pressure peak and a spontaneous negative transient on gas breakthrough; evidence of dynamic behaviour and unstable gas pathways; asymptote close to the value of the local stress after shut-in; temporal variations in monitored stresses, pore pressures and gas inflow. These observations were interpreted as being symptomatic of the time-dependent development of pathways; gas transport was apparently localised, rather than passing in a distributed fashion through the clay. As with the laboratory scale measurements, the coupling between gas, stress and pore water pressure for flow before and

EURAD (Deliverable n° 6.1) – Initial State of the Art on Gas Transport in Clayey Materials
Dissemination level: PU
Date of issue of this report: 17/11/2021

Page 184

after major gas entry suggest mechanisms of pathway propagation and dilatancy predominate. Observations also indicate that the interface between barriers, which is a key part of the system, is exploited by migrating gas. However, this and the lack of high gas pressures and the lower stress state observed in the field may relate to non-complete hydration of the buffer (as previously noted in some laboratory tests).

Importantly, the peak gas pressures observed at Lasgit (Cuss et al. 2010, 2011b, 2014) were markedly lower than those in the laboratory. This can also be explained by the greater degree of compressibility (e.g. due to the presence of interfaces and heterogeneous hydration) within the clay (in relation to the injected gas volume), which would aid accommodation of gas within the system (Graham C. et al. 2012). The authors also highlight that, while the association between gas breakthrough pressure and local stress is clear, predicting the exact magnitude and timing is complicated by heterogeneity in the hydration state of the clay, which persisted during the first ten years of testing.

In situ experiment: FEBEX in situ test (Grimsel test site)

The aim of the FEBEX in situ test was to study the behaviour of near-field components in a repository for high-level radioactive waste in granite formations in order to:

- Demonstrate the feasibility of constructing the engineered barrier system in a horizontal configuration according to the Spanish concept for deep geological disposal and analyse the technical problems to be solved for this type of disposal method.

- Better understand the thermo-hydro-mechanical (THM) and thermo-hydro-geochemical (THC) processes in the near field, and to support the development and validation of the modelling tools required for interpretation and prediction of the evolution of such processes.

The FEBEX in situ test was performed under natural conditions and at full scale at the Grimsel test site (GTS, Switzerland), an underground laboratory managed by Nagra (ENRESA 2006). The thermal effect of the wastes was simulated by means of heaters, whereas hydration was natural. The test was monitored, thus allowing the evolution of the temperature, total pressure, water content, water pressure, displacements and other parameters to be observed continuously in different parts of the barrier and the host rock.

The clay barrier was made of FEBEX bentonite blocks arranged in vertical slices with three concentric rings (Figure 3-33). In the heater areas the interior ring was in contact with the steel liners of the heaters, whereas in the non-heater areas a core of bentonite blocks replaced the heaters. The blocks were obtained by uniaxial compaction of the FEBEX clay with its hygroscopic water content at pressures of between 40 and 45 MPa, resulting in dry densities of 1.69–1.70 g/cm^3. This initial dry density of the blocks was selected by taking into account the probable volume of the construction gaps and the need to have a barrier with an average dry density of 1.60 g/cm^3.

EURAD (Deliverable n° 6.1) – Initial State of the Art on Gas Transport in Clayey Materials
Dissemination level: PU
Date of issue of this report: 17/11/2021

Page 185
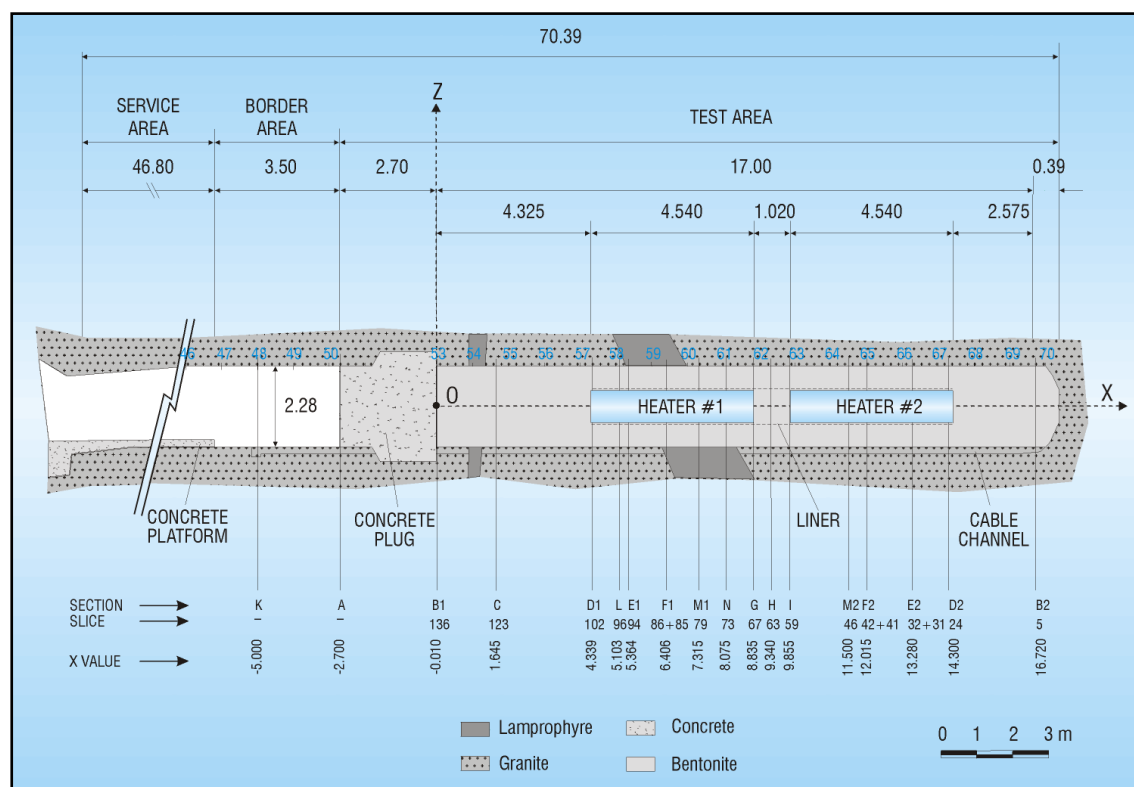
Figure 3-33 – General layout of the FEBEX in situ test during phase I, including instrumented sections (ENRESA 2006).

The heating stage of the in situ test began in February 1997. The power of the heaters was adjusted to keep the surface temperature of their liners at 100°C. After five years of uninterrupted heating at constant temperature, the heater closer to the gallery entrance (Heater #1) was switched off (February 2002). In the following months this heater and all the bentonite and instruments in front of it and surrounding it were extracted. A large number of bentonite samples were also taken for analysis in different laboratories. The remaining part of the experiment was sealed with a new sprayed concrete plug. New sensors were installed in the buffer through the concrete plug, and a second operational phase started. The test continued running until April 2015, when Heater #2 was switched off. The concrete plug started to be demolished some days earlier, and the buffer removal and sampling took place between May and August. A detailed post-mortem bentonite sampling programme was designed. Clay samples were taken to characterise the solid and liquid phases, in order to confirm predictions and validate existing models of THM and THG processes. In particular, samples were taken to determine on site their water content and dry density, with the aim of assessing the final state of the barrier and supply data to validate and check the capacity of the THM numerical codes to predict the bentonite evolution in an engineered barrier (Bárcena et al. 2006; ENRESA 2006; Villar 2006; Martínez et al. 2016; Villar et al. 2016; Villar 2017).

The investigations on the FEBEX dismantling samples (FEBEX-DP) undertaken by several laboratories confirmed the good performance and stability of the bentonite barrier over a time period of 18 years (Villar 2017). As it was observed during the partial dismantling in 2002, the swelling capacity of the bentonite was able to fill all the construction gaps after a further 13 years. It provided a continuous barrier, in which, once saturated, the interfaces between blocks did not have any role on the water content and density distribution or fluid transport. The physical state of the barrier after 18 years of operation was very much affected by the processes to which it had been subjected, namely hydration from the granite host rock and/or thermal gradient-induced moisture redistribution.

EURAD (Deliverable n° 6.1) – Initial State of the Art on Gas Transport in Clayey Materials
Dissemination level: PU
Date of issue of this report: 17/11/2021

Page 186

Villar et al. (2021) present results of the gas permeability measurements performed in samples retrieved from the FEBEX in situ tests. These results are discussed hereafter.

The water content and dry density of the bentonite changed across the barrier as a function of the distances to the heater and the granite. Consequently, the samples taken closest to the heater had lower water content and higher dry density, whereas the samples taken closest to the granite had the highest water content and lowest dry density. The effective gas permeability of the samples decreased with the increase of water content and the decrease in dry density and tended to be lower towards the granite, where the degree of saturation was higher. During the tests, the gas flow observed was steady in most cases and no effect of the injection pressure on the permeability values was detected, except for a few of the more saturated samples, for which gas permeability increased with increasing gas injection pressure (in fact this behaviour was clear only in sample BC-53-3), indicating non-Darcian flow. Additionally, it was checked that the Klinkenberg effect was not significant in the range of pressures applied (Villar et al. 2018).

However, the gas permeability was clearly affected by the stress state. It decreased noticeably with the increase in confining pressure up to 4 MPa, particularly for the wetter samples, those taken closer to the granite. Beyond a confining stress of 9 MPa no gas flow took place through any of the wetter samples, hence the breakthrough pressure for them would be higher than this value, which in turn is higher than the expected swelling pressure. In fact, gas breakthrough pressures higher than the swelling pressure were measured in the FEBEX reference bentonite compacted and tested under isochoric conditions (Gutiérrez-Rodrigo et al. 2021). In contrast, flow took place through the drier samples, even for confining pressures as high as 9 MPa. The consolidation induced by the increase in confining pressure increased the degree of saturation of the samples and reduced their suction, taking them back to a stress state closer to that in the barrier during the in situ test. At the end of operation of the FEBEX in situ test total pressures above 2 MPa were measured in the intermediate bentonite ring and higher than 5 MPa in the outer part of the barrier (Martínez et al. 2016; Villar et al. 2020b), and this could indicate that during operation the stress state in the barrier was high enough as to limit gas migration.

The confining stress reduced the size of the gas pathways, also increasing their tortuosity. In the case of the less saturated samples there was insufficient moisture to reduce or block the air-filled pore network of the specimens and minimise gas flow, and the gas found ways out until the confining pressure was enough to sufficiently reduce the air-filled pore space. In contrast, in the highly-saturated samples there was no need of applying a high confining pressure to completely block the air passages, which already were small and tortuous. This also would explain the fact that the effect of injection pressure increase was only noticeable in the samples with the highest water content, in which small changes in the size of the cross-section of the gas pathways would trigger significant changes in (very low) permeability.

The decrease in permeability that occurred during loading was not reversible, and the gas permeability of the samples after unloading was lower than the initial one. Most of the samples experienced during operation in the barrier an increase in void ratio as a result of hydration and swelling, which led to the reduction of the initial dry density of the blocks (1.7 g/cm3) to the average dry density of the barrier (1.6 g/cm3). Consequently the apparent preconsolidation stress of the bentonite decreased during in situ operation, whereas the pre-yield and post-yield compressibility values increased (Romero et al. 2017, included in Villar 2017). This would explain the fact that the samples consolidated easily during gas testing. In fact, the dry density of the samples at the end of the tests in which confining pressures higher than 2 MPa were applied was higher than the initial one.

The pore size distribution analyses carried out by mercury intrusion porosimetry showed a decrease in the macropore void ratio in all the samples on which confining pressures higher than 2 MPa had been applied during testing. This decrease was more significant as the confining pressure applied during gas testing was higher, which would mean that the compression exerted by the confining pressure was

EURAD (Deliverable n° 6.1) – Initial State of the Art on Gas Transport in Clayey Materials
Dissemination level: PU
Date of issue of this report: 17/11/2021

Page 187

mostly absorbed by the macropores. In some of the wetter samples an increase of the size of the macropores was observed after gas testing, which could correspond to the opening of pathways allowing gas flow, given the very low accessible void ratio of these nearly saturated samples. Gonzalez-Blanco et al. 2016a, 2016b) observed a new family of pores at entrance sizes larger than 2 µm after gas injection in samples of argillaceous rock formations (see Section 3.1.4.1). These pores were associated with fissure opening and would act as preferential air pathways. They were observed by micro-computed tomography, both in a clay rock (Gonzalez-Blanco et al. 2017a) and in bentonite (Gonzalez-Blanco et al. 2017b). Harrington et al. (2017b) analysed the stress field measured during a gas injection test in saturated compacted bentonite and inferred from it that the gas pathways were created by dilatancy and propagated through the clay in response to variations in applied gas pressure.

The gas permeability of the FEBEX reference bentonite is mainly related to the void ratio accessible for gas flow, which depends on water content and dry density. For the FEBEX dismantling samples (FEBEX-DP), because of the high water saturation of most of the barrier after the long operation period, the accessible void ratio was below 0.15, and decreased towards the external part of the barrier, where the degree of saturation was higher. Effective gas permeability drops of several orders of magnitude when approaching full saturation.

Comparing FEBEX and FEBX-DP data (Figure 3-34) for similar accessible void ratios, no change on the gas transport properties of the bentonite matrix seems to take place during operation. However, samples with an interface between blocks, drilled in the internal ring of the barrier, had higher permeability than samples of similar accessible void ratio with no interface and it was necessary to apply higher confining pressures to reduce or suppress gas flow in them.
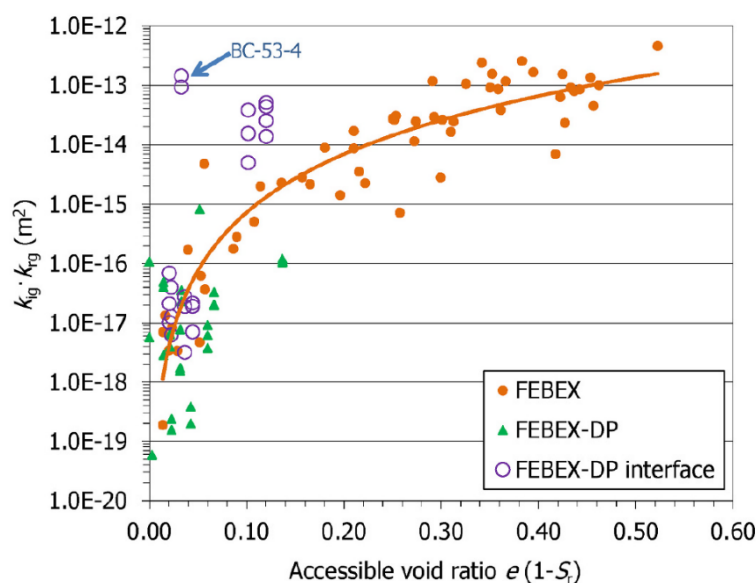
Figure 3-34 – Gas permeability as a function of the accessible porosity for the reference FEBEX bentonite and for FEBEX-DP samples with and without interface tested under confining pressures of 0.6 and 1.0 MPa (modified from Carbonell et al. 2019) (Villar et al. 2021).

In fact the presence of an interface between blocks had higher relevance than the accessible void ratio on the gas permeability, probably because the gas transport mechanisms in both kinds of samples were not the same: flow took place through the accessible porous structure, but in the samples with interface it preferentially occurred along the interface. The sudden decreases in permeability occurred in some samples when confining pressure was increased beyond a given value would correspond to the closing of the interface as a preferential pathway. In contrast, wetter samples drilled along interfaces of the intermediate and external rings of the barrier (which had very low accessible void ratio, lower than 0.08, because of the high saturation), had permeabilities closer to those corresponding to the same

EURAD (Deliverable n° 6.1) – Initial State of the Art on Gas Transport in Clayey Materials
Dissemination level: PU
Date of issue of this report: **17/11/2021**

Page 188

accessible void ratio in the reference bentonite. In fact, in these samples the interfaces were barely visible and looked like sealed before gas testing.

Popp et al. (2014) tested the interface between blocks manufactured from a bentonite/sand (60/40) mixture. Under dry conditions, gas flow along the interfaces was at least four orders of magnitude higher than through the matrix. An increase in confinement pressure significantly lowered the gas flow but the effect was more pronounced for interfaces than for the matrix. They saturated the blocks assemblages and performed gas injection and shear tests to check the behaviour of the interface. The authors concluded that the interface perfectly healed after saturation, which was physically verified by the development of cohesion after saturation. All these observations are consistent with the findings reported in Villar et al. (2021). Gas breakthrough tests performed in saturated samples of FEBEX bentonite under isochoric conditions showed that samples with an interface behaved as samples of the same dry density with no interface, finding in both cases breakthrough pressure values related to dry density (Figure 3-35). The conclusion was that after material homogenisation the interface was not a preferential pathway anymore, neither for water nor for gas (Gutiérrez-Rodrigo 2018; Gutiérrez-Rodrigo et al. 2021).
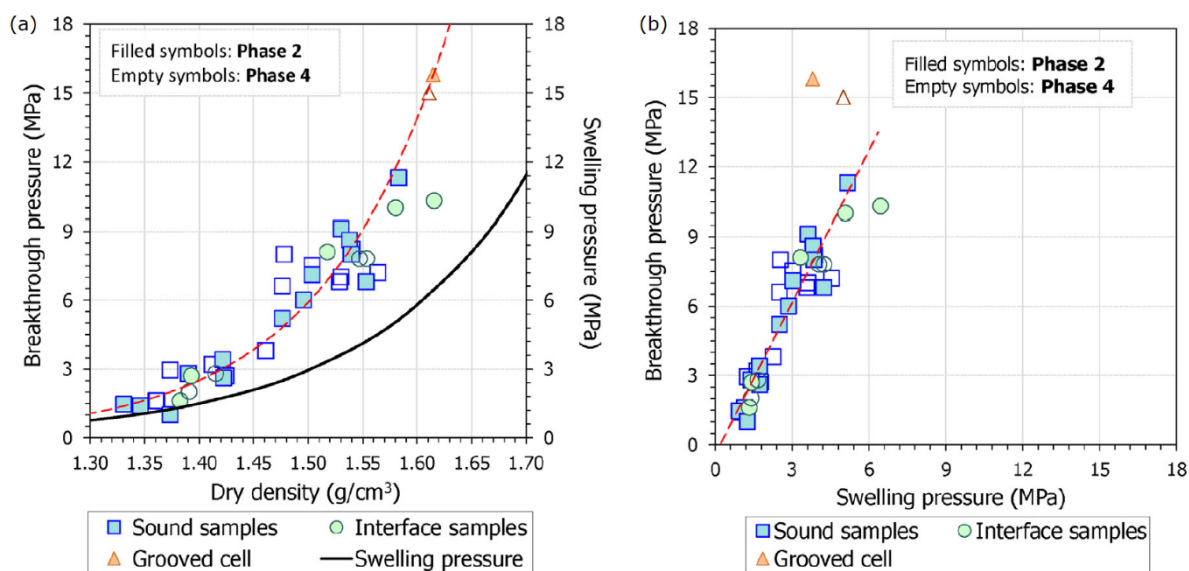
Figure 3-35 – Breakthrough pressure as a function of (a) dry density and of (b) swelling pressure. Phase 2: 1st gas injection; Phase 4: 2nd gas injection after resaturation (Gutiérrez-Rodrigo et al. 2021).

Previous laboratory studies (reported earlier in this section) showed that, in the FEBEX compacted bentonite, two-phase flow through stable pathways seemed to take place for degrees of saturation lower than about 97%, since in these samples, gas flow was stable for a given pressure gradient. For higher degrees of saturation pathway dilation could be the predominant mechanism (Villar et al. 2013; Gutiérrez-Rodrigo 2018). Graham J. et al. (2002) found that this threshold was 93% for a sodium bentonite, and that below this degree of saturation there was only small resistance to gas migration. Tests performed in compacted saturated samples under isochoric conditions showed that the threshold pressure for gas entry into the bentonite was higher than the swelling pressure and seemed to be lower than the gas pressure required for fracturing (macroscopically) the material (Gutiérrez-Rodrigo et al. 2021). In contrast, in Villar et al. (2021), two-phase flow seems to have taken place in most cases, even for samples with degree of saturation higher than 97%. The fact that these samples were tested under constant confining stress (in triaxial cells) instead of under no volume change conditions (isochoric), would have made easier the transport of gas, with opening of trajectories for gas flow that could not be opened under isochoric conditions. Hence, the testing conditions seem to have an influence on the results obtained. Graham C. et al. (2016) concluded from gas injection tests in saturated compacted

EURAD (Deliverable n° 6.1) – Initial State of the Art on Gas Transport in Clayey Materials
Dissemination level: PU
Date of issue of this report: 17/11/2021

Page 189

bentonite that the degree of compressibility of the clay and the stress conditions may be an important control on the approach to gas breakthrough in the buffer. In this line, Xu L. et al. (2015) performed laboratory tests in a saturated, low-permeability clay and showed that the failure of the sealing efficiency was closely related to the difference between the gas injection pressure and the confining pressure.

The results of the laboratory tests suggest that, once a bentonite barrier in an underground repository is saturated, gas pressures higher than the swelling pressure of the bentonite would have to build up before gas can move away and once this occurs, gas would not displace water. However, in the tests reported, the gas pressure increase took place at a high rate. In the real case, it is likely that gas could flow for lower pressures if they are sustained for longer periods of time, which would also allow for the contribution of diffusion to gas transport (negligible in these laboratory tests).

3.1.5   Shared understanding of gas-induced failure of clayey materials

The mechanical characteristics of clay-rich materials cover a wide property range in terms of strength and stiffness in the transition between soft soils and weak rocks. Despite the marked differences, these materials have in common a relatively low strength together with high gas entry pressures which makes them prone to failure when subjected to high gas pressures. When an initially water-saturated clay barrier with high water retention capacity is invaded by a gas phase, failure initiation is linked to debonding of the solid aggregates at the locus of gas entry. Micro-fabric of the material (i.e. geometric arrangement of the solid aggregates) contributes to its strength as it determines the geometric characteristics of the water-filled inter-aggregate pore space and establishes the contact forces between the solid aggregates.

In soil mechanics, well-established theoretical frameworks are used to describe the strength of soft clays at partially or fully saturated state. Without significant cementation between solid grains, bonding is attributed mainly to the electrochemical repulsive/attractive forces, exerted between the clay particles on the molecular scale. For a given spacing between adjacent clay particles, the balance of repulsive/attractive forces (and external forces) is related to the size of the diffuse double layers of water adsorbed on the clay surfaces. Notably, chemical composition of the pore water may have a non-negligible impact on the debonding process. The origin of bonding at the molecular scale explains the tendency of soft clays to deform in a ductile manner. Localisation of deformation is mainly attributed to the spatial distribution of the inter-aggregate pore space, forming discontinuities preferentially along grain boundaries, compaction planes or other small-scale variabilities of material properties.

Gas invasion experiments with engineered clay barriers such as bentonite and sand/bentonite mixtures have been conducted by many geotechnical laboratories worldwide. The experiments show consistently that high gas pressures are required to invade the fully saturated material, which close to the applied confining pressure. The typical deformation behaviour of the material in response to gas invasion exhibits first a continuous volume expansion as long as the gas front propagates through the test specimen, followed by contraction when gas breakthrough at the downstream end of the sample is reached. At the end of the gas invasion phase, when pore pressure recovers to the initial state, a minor component of irreversible strain may be observed. Several experimentalists performed post-mortem analyses of clay samples after gas invasion, indicating moderate changes in pore structure. Recent international research activities seem to reveal a strong impact of compaction and hydration procedures on the gas transport behaviour and the associated deformation behaviour of engineered clay barriers.

In hard clays, strength may be controlled by the degree of cementation of the mineral aggregates. It is generally agreed that the microstructure of natural clay barriers is a result of diagenetic evolution. After deposition as a clay-rich soil and depending on the tectonic evolution at large scale, the geomaterial undergoes diagenetic processes, forming its peculiar structure and affecting its hydro-mechanical behaviour. Indurated clays such as claystone and shales are characterised by well-marked bedding

EURAD (Deliverable n° 6.1) – Initial State of the Art on Gas Transport in Clayey Materials
Dissemination level: PU
Date of issue of this report: 17/11/2021

Page 190

plane fissility and low plasticity, i.e. they do not form a plastic mass when wet, although they may disintegrate when immersed with water. With increasing depth, effects of compaction and diagenesis cause the shale to deviate more and more from the abovementioned typical properties and behaviour of a clay-rich soil. The impact of pore water chemistry on the deformation behaviour of the material reduces gradually with decreasing porosity, because the capacity of the swelling clay aggregates to expand in contact with external water is locked-in as a consequence of partial cementation of the solid grains.

Gas invasion experiments on hard clays have been conducted not only in the field of radioactive waste disposal but also in other geoscientific disciplines like oil and gas industry, geothermal exploration and CO_2 sequestration. Similar to the experience with clay-rich soils, high gas pressures are required to invade the fully saturated material, which are close to the applied confining pressure. Experiments in triaxial cells under well-controlled mechanical boundary conditions indicated, that gas-induced failure of the material is not only controlled by the plasticity and bedding fissility of the material but depends also on the evolution of gas pressure build-up (loading history) and on the applied mechanical boundary conditions. Depending on the speed of pressure build-up, both gradual and sudden propagation of the damage front has been observed. Gradual damage evolution was predominantly observed at low pressure build-up rates and high confining stresses. This phenomenon may be attributed to the process of subcritical crack growth ('pathway dilatancy'), where the gas production rate is balanced steadily by the newly created pore volume at the crack tip. Sudden fracture initiation was observed only in a few cases; it seems to be related to high gas pressure build-up rates or it was triggered by sudden changes of the confining pressure. From a fracture mechanics perspective, this phenomenon can refer to the process of supercritical crack growth ('gas fracturing'), where the propagation of the crack tip is driven by high uniform gas pressure.

3.1.6   Uncertainties and knowledge gaps

Phenomena and features associated with gas-induced damage evolution in clayey materials are difficult to predict. This is an inherent issue with many localisation phenomena in geoscience and structural mechanics. The limited predictability of localisation phenomena in geomechanics concerns the locus of damage initiation as well as the propagation of damage in space and time. The uncertainties in predicting damage evolution have various causes, including a lack of microstructural information (e.g. small-scale variability of stiffness and strength or undetected micro-fractures), incomplete description of the prevailing boundary and initial conditions (e.g. disequilibrium in initial state) and immature mechanistic understanding of the involved hydro-mechanical processes. It is also a challenge to upscale laboratory scale results to behaviour at in situ scale. While comprehensive theoretical frameworks for modelling damage propagation in partially saturated geomaterials have been developed in soil mechanics and to lesser extent in rock mechanics, the validation of such models is a challenge due to the lack of integrated validation workflows.

For this, dedicated experimental workflows are required, which interact closely with model-supported test designs that match as much as possible the conditions (e.g. stress field) expected within a disposal system and traceable calibration procedures. Complementary information such as microstructural imaging and high-resolution measurements of stress and strain behaviour of the tested material shall be integrated in the calibration process for constraining the uncertainties of model predictions for a wide range of relevant gas invasion scenarios. Concerning gas-induced damage in engineered clay barriers special issues to address are:

- The impact of the compaction and hydration procedure as well as pore water chemistry on the onset of damage
- The impact of loading history on the onset of damage

EURAD (Deliverable n° 6.1) – Initial State of the Art on Gas Transport in Clayey Materials
Dissemination level: PU
Date of issue of this report: 17/11/2021

Page 191

- The evolution of gas transport paths when subjected to very long-term gas injections (including the aspect of colloid mobilisation)

Safety-relevant knowledge gaps associated with gas-induced damage in geological barrier materials concern:

- Damage evolution under fast / slow gas pressure build-up (subcritical vs. supercritical crack growth).

- The impact of the stress path (from tensile fracturing towards shear compaction) on damage evolution.

- The evolution of gas transport paths when subjected to very long-term gas injections (including desaturation of the intact rock matrix).

- The impact of microstructural variability on damage initiation (including the role of bedding and tectonic overprint).

EURAD (Deliverable n° 6.1) – Initial State of the Art on Gas Transport in Clayey Materials
Dissemination level: PU
Date of issue of this report: **17/11/2021**

Page 192

3.2   Self-sealing

3.2.1   Interests and needs of end-users in the context of geological disposal

The self-sealing capacity of clayey materials is a favourable feature, which makes this class of barrier materials attractive for deep geological disposal of radioactive wastes. Bock et al. (2010) state that '*Self-sealing directly addresses the functionality of the host rock as a migration barrier. When the self-sealing process proceeds in reasonable time, natural or man-induced fractures, which may have been re-activated or created by the repository construction or by the emplacement of the waste, will not persist as preferential pathways for soluble radionuclide migration, and thus the system becomes diffusion-dominated*'. In other words, from a performance assessment perspective the distinct self-sealing capacity of clayey materials can reduce significantly the safety-related consequences of failure of the barriers, when subjected to excessive gas overpressures after repository closure (see also Section 3.1.1). Thus, the safety functions of the barrier materials may be partly or even fully restored according to their design specifications as soon as the production of repository gases has stopped. For strengthening the line of arguments towards a robust safety case, convincing evidence is required, which demonstrates the efficiency of self-sealing mechanisms of the clay barriers for a wide spectrum of state conditions. This includes:

- Basic understanding of the phenomena and processes that contribute to the self-sealing of clay-based barrier components after having failed,

- Solid concepts of self-sealing mechanisms at process level, aimed at improving the predictability of the self-sealing capacity of clay barriers under the thermo-hydro-mechanical-chemical (THMC) conditions that prevail in a deep geological repository,

- Validated self-sealing models at process scale, referring to reliable experimental data bases.

In performance assessments (PA), the role of self-sealing as a favourable feature of clay-based barriers cannot be addressed without considering the overall repository concept. Nevertheless, areas of mutual interest in all national programmes have been identified, comprising the basic self-sealing mechanisms and the associated phenomena and processes. Table 3-3 displays a survey of relevant needs of the end-users in the national programmes with respect to the quantification of the magnitude of restoration of the barrier functions as compared to the undisturbed material.

Table 3-3 – Survey of the effects of self-sealing on the barrier function restoration and relevant needs of end-users in the national programmes.

Barrier component	Category of self-sealing effects	Relevant needs with respect to barrier function restoration
Host rock	Self-sealing of gas-induced fractures in the host rock (process models)	- Hydro-mechanical fracture closure mechanisms / fracture closure laws (normal closure, shear closure) - Hydro-chemical couplings (impact of pore water chemistry on sealing process)
	Gas/solute transport behaviour of re-sealed fractures	- Evolution of hydraulic properties / transport properties of fractured rock mass (as compared to intact rock) - Transport of volatile radionuclide in fractured rock (capillary vs. viscous fingering)
	Restoration of mechanical integrity in response to long-term water imbibition	- Self-healing capacity, recovery of mechanical strength (risk of fracture re-activation in the context of geological long-term evolution)
EDZ	EDZ-self-sealing (process models) response to long-term water imbibition	- Evolution of hydraulic properties / transport properties of the EDZ in the post-closure phase in response to stress/pore pressure recovery

EURAD (Deliverable n° 6.1) – Initial State of the Art on Gas Transport in Clayey Materials
Dissemination level: PU
Date of issue of this report: 17/11/2021
Page 193

Barrier component	Category of self-sealing effects	Relevant needs with respect to barrier function restoration
	Gas/solute transport behaviour in response to long-term water imbition	- Gas transport regimes in re-activated EDZ (capillary- vs. viscous fingering) - Transport of volatile radionuclides in fractured rock (capillary vs. viscous fingering)
Bentonite seals	Restoration of barrier functions in response to long-term water imbition (swelling pressure, radionuclide retention capacity)	- Phenomena and processes associated with buffer homogenisation during water imbition process - Water retention behaviour and relative permeability relationships (gas/water) of the buffer along wetting paths
Bentonite buffer	Restoration of barrier functions in response to long-term water imbition (swelling pressure, radionuclide retention capacity)	- Phenomena and processes associated with buffer homogenisation during water imbition process - Water retention behaviour and relative permeability relationships (gas/water) of the buffer along wetting paths

3.2.2   Fundamentals of self-sealing – phenomenology

According to a common definition by Bock et al. (2010), self-sealing relates to a phenomenon that fractured clayey formations tend to become, with the passage of time, less conductive to groundwater and finally hydraulically insignificant. The definition is derived from that given by Tsang et al. (2005) where 'sealing' is the reduction of fracture permeability (transmissivity) by any hydro-mechanical, hydro-chemical or hydro-biochemical processes. The prefix 'self-' implies that the sealing process is occurring spontaneously, i.e. without any consideration of or knowledge about the kinetics of the sealing process.

Tsang and Bernier (2005) distinguish between 'sealing' and 'healing' of features. Healing is used to mean '… sealing with loss of memory of the pre-healing state. Thus, for example, a healed fracture will not be a preferred site for new fracturing just because of its history'. According to Bock et al. (2010), 'healed fractures imply that the deformational and strength properties of the healed material have become identical to those of the intrinsic (i.e. non-fractured) material'.

From a phenomenological point of view, Bock et al. (2010) compiled the main mechanisms which may contribute to self-sealing of (fractured) clayey formations, referring to comprehensive laboratory investigations and field tests from several international research programmes (e.g. NF-PRO, SELFRAC, TIMODAZ as part of the EURATOM Framework):

- (Thermo-)Mechanical compaction of the intact rock body (compression of solid framework; pore space reduction),

- Mechanical closure of fractures (increased normal stress acting normal to the fracture; contractant behaviour in shear; creep of the fracture wall material),

- Physico-chemical interaction between the weakly/strongly bound pore water in the micro-, meso- and macropores and the clay platelet skeleton. Macroscopically, that interaction is evidenced as swelling and disaggregation of clay aggregates,

- Sedimentation combined with clogging of fractures by colloidal phases,

- Precipitation of solutes in the form of mineral coatings of fracture walls.

The phenomenological findings form the basis for the conceptual description of the self-sealing mechanisms in terms of process models (Section 3.2.3). Complementary empirical and experimental evidence has been collected since, which supports and extends the previous findings. A survey of the rock-specific state of knowledge is given in Section 3.2.4.

EURAD (Deliverable n° 6.1) – Initial State of the Art on Gas Transport in Clayey Materials
Dissemination level: PU
Date of issue of this report: 17/11/2021

Page 194

3.2.3   Conceptual models of self-sealing

Bock et al. (2010) considered seven mechanisms that might lead to self-sealing and reviewed the spectrum of constitutive relationships referenced in geoscientific literature for modelling self-sealing phenomena. Lanyon (2018) updated the literature review and discussed the relevance of the self-sealing mechanisms in the context of performance assessments. A survey of the seven mechanisms and their relevance to repository-induced features is given in Table 3-4. Key references of the constitutive relationships are briefly discussed in the subsequent paragraphs.

Table 3-4 – Relevance of sealing mechanisms to repository-induced features from Lanyon (2018), referring to a compilation of the key self-sealing mechanisms by Bock et al. (2010).

	Sealing mechanism		Relevance to repository-induced features
M-1	Additional compaction of the rock matrix (isotropic consolidation / shear induced pore collapse)		Undisturbed permeability is already very low and only limited increases in effective stress might be expected.
M-2	Increase of the effective normal stress σ_n' across the fracture plane		Fracture normal closure is likely to occur after any opening as the pore pressure declines.
M-3	Contraction of fracture when subjected to shear		Relevant to induced shear re-activation of features
M-4	Creep of fracture wall material		Relevant when stress differential is sufficient to result in creep
M-5	Swelling of the fracture wall material		Likely to be fast where there is significant desaturation, however swelling will still occur in open parts of any fracture.
M-6	Slaking	Body slaking / Surface slaking	Relevant to near field where cycles of drying and wetting may occur, but of limited importance in the far-field.
		Fracture surface disaggregation	Asperity damage and comminution of rock within fracture during deformation and stress change.
M-7	Mineral precipitation onto fracture walls		Potentially relevant to the repository near field regarding alkaline waters from cementitious barriers. In the very long-term might contribute to sealing. May also occur when fresh formation water flows towards the repository after thermal/gas pressurisation.

3.2.3.1 Isotropic consolidation / shear enhanced compaction

Isotropic consolidation or shear enhanced compaction of a clayey material is associated with an irreducible reduction of porosity ('pore collapse') and permeability. The critical state concept, developed by Roscoe et al. (1958), represents an idealisation of the observed patterns of behaviour of saturated clays in the normally and lightly over-consolidated state. The corresponding void ratio stress coupling is expressed by:

$$e = e_o - C_{c,s} \cdot log \frac{p'}{p_o'} \qquad (3\text{-}4)$$

where C_c / C_s are the compression / swelling index,

e, e_o are respectively the void ratio and reference void ratio and

p', p_o' are the mean effective stress and the mean effective stress at reference level.

EURAD (Deliverable n° 6.1) – Initial State of the Art on Gas Transport in Clayey Materials
Dissemination level: PU
Date of issue of this report: **17/11/2021**

Page 195

The compression index describes the irreversible volumetric behaviour of the medium along the virgin compression line whereas the swelling index characterises the reversible behaviour along the recompression/swelling line. The stress-strain behaviour can be coupled to clay-specific porosity-permeability relationships such as Kozeny-Carman (e.g. Johnson et al. 1986; Wong and Pengra 1995; Horseman et al. 1996; Valfouskaya et al. 2005).

Isotropic consolidation / shear enhanced compaction is a self-sealing mechanism of limited relevance, because undisturbed permeability of clay barriers is already very low and only limited increases in effective stress might be expected.

3.2.3.2 Self-sealing of (re-)activated features

Elevated pore water pressures due to repository-induced thermal and gas effects may result in reduced effective stresses on pre-existing features (bedding planes or sealed faults/fractures). This may result in either:

- Normal dilation/opening: where the effective normal stress on the feature is sufficiently low for the feature transmissivity to increase significantly.

- Shear re-activation and slip: where the shear stresses on the feature are sufficient to overcome friction and the feature deforms in shear.

Re-activated features may be either bedding parallel (subhorizontal) or inclined to bedding (e.g. tectonic faults). With regard to effective sealing of repository-induced re-activated features, the most important processes are likely to be M-2 to M-5 and the fracture surface damage process associated with the extended definition of M-6 (see Table 3-4). Only limited additional compaction of the rock away from the feature is expected and 'classical' surface and body slaking processes are only likely to occur where features are subject to wetting/drying cycles, while mineral precipitation will have limited effects in safety-relevant timescales. The relevant processes are M-2 to M-6 and are described in more detail in the subsequent sections.

M-2: As the induced pore pressure disturbance reduces, effective normal stress will increase and the feature close. Goodman (1974) and Bandis et al. (1983) introduce well-established fracture closure models, which can be coupled easily with aperture – transmissivity relationships such as the cubic law (e.g. Bear, 1972). The hyperbolic closure law of Bandis et al. (1983) was used within the pragmatic model of EDZ sealing by Alcolea et al. (2016). Zhang (2013, 2015) suggests that normal closure observed in laboratory tests on COx and OPA may be better modelled with an exponential relationship. A similar observation was made by Henry P. et al. (2016) regarding in situ tests at Tournemire and Mont Terri.

M-3: Shearing may result in either dilation (where normal stress is low compared to asperity/rock strength) or contraction (normal stress is high compared to asperity/rock strength). Whether dilation or contraction occur will be dependent on feature surface geometry, mineralogy, saturation and effective normal stress. Where shear results in initial dilation, subsequent shearing (at different stress or saturation) may result in self-sealing. Reduction of fracture permeability in shear is conceptualised by Makurat and Gutiérrez (1996) and Gutiérrez et al. (2000). Fang et al. (2017) describe a set of direct-shear tests on shale and tuff samples with saw-cut surfaces including two samples from the Opalinus Clay at Mont Terri. They observe that when subject to shearing, soft minerals (in clay-rich and weak-ductile fracture material) readily deform and comminute into smaller particles and fill the trough. With effect of fluid infiltration, clay swelling leads to a thin layer of clay-rich folia that seals the fracture. Similar processes are discussed by Rutter and Mecklenburgh (2017) who report that increasing shear stress causes accelerating reduction of conductivity, even before the onset of macroscopic slip. Such reduction in fluid flow rate was non-recoverable, and the combined effects of normal and shear stress

EURAD (Deliverable n° 6.1) – Initial State of the Art on Gas Transport in Clayey Materials
Dissemination level: PU
Date of issue of this report: 17/11/2021

Page 196

can reduce fracture conductivity by more than 3 orders of magnitude over the range of shale reservoir conditions. The reduction in conductivity was inferred to be due to enhanced compaction and to the formation of 'a thin smear of gouge particles containing clay and organic matter, swamping any tendency for dilatation-enhanced conduction occurring with the onset of slip'. The loss of conductivity was not recovered when the shear stress was removed.

The structure of shear-re-activated features normal and parallel to bedding are likely to be different. Carey et al. (2015) report that in laboratory tests on shales, induced fractures across bedding planes are typically more complex and pervasive than when parallel to bedding. This suggests that feature surface and void geometries may be significantly different between the two cases resulting in potentially different sealing behaviour. In complex features sealing is likely to occur more rapidly at any constrictions in the flow channels resulting in more rapid reduction in (potentially anisotropic) effective transmissivity. This is in addition to the observed preferential swelling parallel to bedding anisotropy and the influence of varying clay content within the different lithofacies (Figure 3-36).
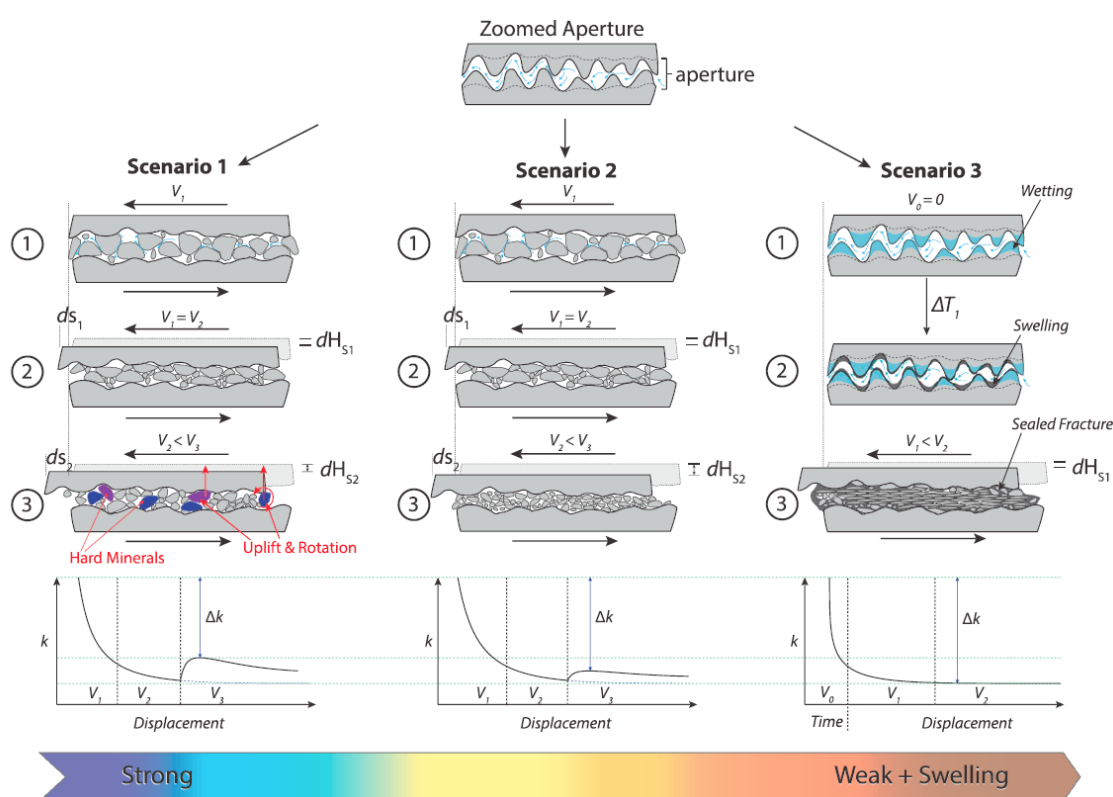
Figure 3-36 – Conceptual model of asperity and permeability evolution of planar saw-cut fractures Fang et al. (2017). Scenario 1: End-member of clay-poor, brittle-like fracture material that is composed of hard minerals. During the shearing, the hard minerals are difficult to comminute into small particles and the fracture may dilate significantly. Scenario 2: Intermediate case between clay-poor and clay-rich end-member. The fracture material is brittle and comprises weak minerals that are easier to be crushed into fine particles and compacted with shear displacement. Scenario 3: End-member of clay-rich and weak-ductile fracture material that is composed of soft minerals. When subject to shearing, the soft minerals readily deform and comminute into smaller particles and fill the trough. With effect of fluid infiltration, clay swelling leads to a thin layer of clay-rich folia that seals the fracture.

M-4: Creep in clay barriers relates to a range of processes such as diffusion, pressure dissolution, dislocation glide of minerals and subcritical crack growth through pore fluid effects. Time-dependency

EURAD (Deliverable n° 6.1) – Initial State of the Art on Gas Transport in Clayey Materials
Dissemination level: PU
Date of issue of this report: 17/11/2021

Page 197

is also due to the low hydraulic diffusivity of clay-rich geomaterials where induced pore -pressure transients may take many years to dissipate.

M-5: If the rock is initially partially saturated, the swelling process will be driven by the availability of water and will be rapid when water is freely available (as seen in laboratory and in situ tests). Once the rock is saturated, ongoing swelling will be controlled by the availability of water and to some extent by the water chemistry. Under unconstrained conditions (e.g. within the open parts of a fracture or channel) significant expansion can occur and the water content may exceed the undisturbed values. In regions of sufficiently small aperture, we can expect that swelling of the fracture wall will continue until closure. Laboratory experiments on Opalinus Clay (Seiphoori 2019) and COx samples by Auvray et al. (2015) and Auvray and Giot (2018) show closure along channels of aperture 100–800 µm. Auvray et al. (2015) suggest that swelling predominantly develops perpendicular to bedding anisotropy so that the morphology of channel-closure will vary according to feature orientation.

M-6: Swelling will also result in a loss of strength such that localised failure may occur at asperities (contact points) on the feature surface resulting in further closure and possible disaggregation of the wall-rock (potentially leading to clogging of open voids). Where normal closure tests are conducted in saturated conditions these effects will be captured within the normal stress closure relationship.

3.2.4 Self-sealing mechanisms in natural and engineered clayey barriers – state of knowledge

Processes leading to self-sealing in clay materials are well identified as presented in the previous sections. These processes have been studied at different scales from micro-scale to large scale via experiments in URL. The use of small-scale investigation and imaging techniques in recent years help to obtain a better understanding of the processes at the origin of self-sealing. In particular, the use of X-ray tomography during the tests allows to visualise at different stages the state of the clay during fracture closure, providing useful qualitative information to confirm the understanding of the processes but also quantitative data such as the evolution of fracture openings as a function of time and hydration. The quantification of the swelling processes is also accessible by using image correlation techniques in addition to macroscopic measurements.

Many laboratory tests have been performed under different kinds of experimental conditions including mechanical stress, composition of water, mode of fracture creation, fracture apertures etc. They all confirm the good capacity of self-sealing of the clay barriers with clear reduction of water permeability as a principal benefit in the context of a repository. This has been confirmed for both natural clay material such as Boom Clay, OPA or COx and bentonite type material at large scale by experiments carried out in an underground laboratory.

Many results are also available concerning gas transfer and self-sealing. It has been observed that after gas breakthrough event in intact samples or after gas fracturing in boreholes for in situ experiments, the water permeability decreased, as it was the case for other modes of fracture initiation. However, in the case of indurated rocks, the gas properties of the self-sealed materials are no longer identical. In particular, the gas entry pressure is (much) lower than in the intact material. This is understandable when one relates this to the microstructure of the material in the fracture. Depending on the state of stress around the fracture, the nature of the percolating fluid or the processes associated with self-sealing, the material in the fracture is less homogeneous with a macroporosity favourable to gas entry. This is less true in plastic clays where the gas breakthrough pressure in self-sealed material is kept at a level close to the intact one. For example, it has been showed at laboratory scale that initial interface between two bentonite blocks has a very low effect on gas breakthrough pressure, comparable to that of a compacted block.

EURAD (Deliverable n° 6.1) – Initial State of the Art on Gas Transport in Clayey Materials
Dissemination level: PU
Date of issue of this report: 17/11/2021

Page 198

3.2.4.1 State of knowledge for Boom Clay

3.2.4.1.1 Evidence of self-sealing in Boom Clay

Laboratory tests

The main laboratory tests dealing with the self-sealing capability of the Boom Clay have been performed in the framework of the SELFRAC project (Bernier et al. 2007b). The sealing process has been mostly analysed from a hydraulic point of view. In these tests, artificial fractures were initiated in Boom Clay samples. The sealing or healing properties were analysed with different pore water chemistry composition. Van Geet et al. (2008) performed permeameter tests on fractured Boom Clay samples and monitored the evolution of the hydraulic conductivity with time (Figure 3-38). They observed that the hydraulic conductivity decreases quickly with time. The evolution of a fractured Boom Clay sample before and after resaturation as presented in Figure 3-37 illustrated that, shortly after resaturation, the fracture was no more visible. According to Coll (2005) and Monfared (2011), hydraulic conductivity is not affected significantly either by shear bands. These authors concluded that it is a good indicator of the self-sealing capacity of the Boom Clay.
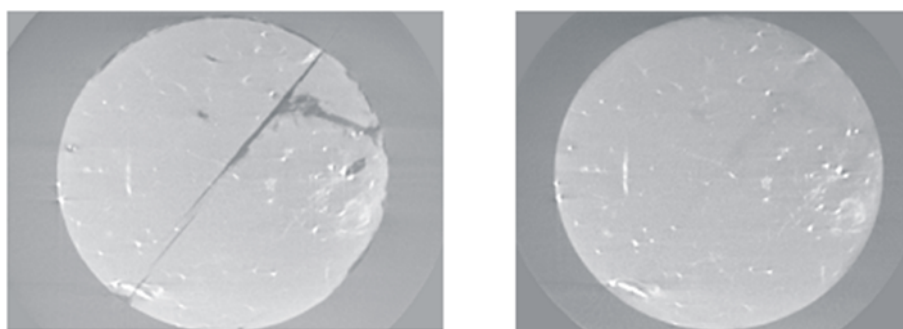
Figure 3-37 – Visualisation by µ-CT technique of the sealing process of a fracture in a Boom Clay sample after saturation (Bernier et al. 2007b).
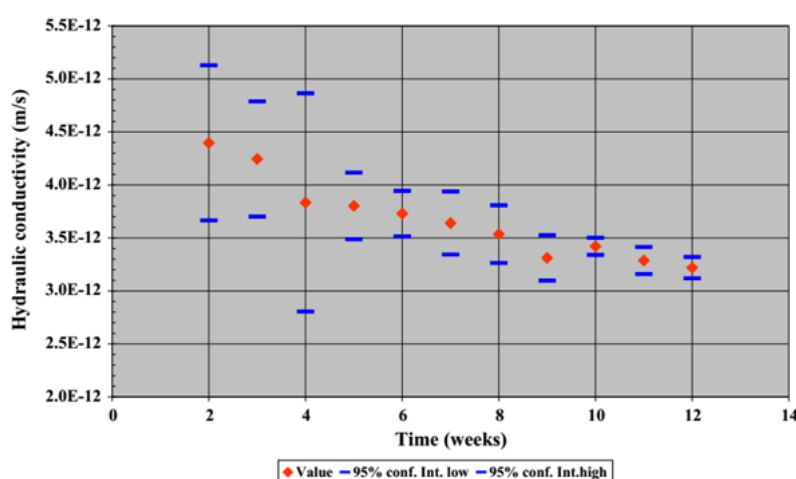
Figure 3-38 – Weekly evolution of the hydraulic conductivity in a fractured Boom Clay sample. Permeameter test with synthetic Boom Clay water as pore water solution (Van Geet et al. 2008).

Chen et al. (2014) performed similar tests in thermal loading conditions in the framework of the TIMODAZ EC project. By exposing Boom Clay samples (damaged and intact sample) to a heating cycle from 20°C to 80°C under constant volume conditions in a permeameter cell, they showed that there is no positive or negative impact of the temperature on the sealing/healing properties of the clay.

EURAD (Deliverable n° 6.1) – Initial State of the Art on Gas Transport in Clayey Materials
Dissemination level: PU
Date of issue of this report: **17/11/2021**
Page 199

Figure 3-39 presents results from the hydrostatic test on hollow cylinder of Boom Clay submitted to loading and heating cycle (from room temperature to 60°C). The initial 6-mm diameter hole was found to spontaneously close and (self-)seal, leaving no preferential flow path through the sample. The hole was not reopened by a loading-heating-cooling-unloading cycle. In addition, the intrinsic permeability was not modified during this cycle. A few days after the dismantling of the sample, the hole, which was not visible during the test, reappeared as the sample started to desiccate. This confirms what was already observed from the SELFRAC project: the original mechanical properties cannot be fully recovered, unlike sealing, healing is incomplete as disturbances of the microstructure are not reversible.

(a) Before test   (b) One day after the test   (c) One week after the test
                       (with membrane)   (without membrane)
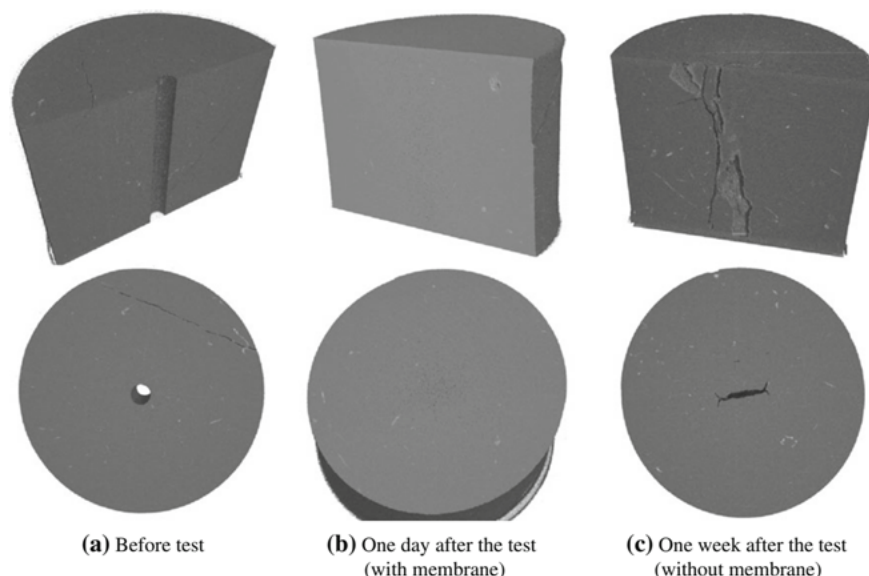
Figure 3-39 – µ-CT pictures of Boom Clay sample in hydrostatic test (Chen et al. 2014).

In situ experiment

The self-sealing capacity of the Boom Clay has been also investigated in in situ conditions around the HADES URL. Shortly after the construction of the connecting gallery, a network of radial piezometers was installed around the gallery to measure the pore water pressure distribution, hydraulic conductivity and to follow up their evolutions with time. The measurements presented on Figure 3-40 showed the influence of gallery excavation on hydraulic conductivity. The values outside the influenced zone are consistent with in situ data for 'intact' Boom Clay. The values measured a few months after excavation, close to the gallery wall, are less than one order of magnitude higher than 'intact Boom Clay' values and decrease with time. Bastiaens et al. (2007) concluded that effective stress variation alone might account for the variation of hydraulic conductivity measured around the connecting gallery by that time and that there was no more an important influence of the fractures. In the long-term, the hydraulic conductivity of the disturbed clay decreases further towards its far-field value, as pore water is drained towards the open gallery, decreasing the pore pressure and increasing the effective stress, leading to a consolidation of the clay in the near field.

EURAD (Deliverable n° 6.1) – Initial State of the Art on Gas Transport in Clayey Materials
Dissemination level: PU
Date of issue of this report: 17/11/2021   Page 200

Figure 3-40 – Results of steady-state, constant head measurements of the hydraulic conductivity around the connecting gallery (CG) performed on a horizontal (CG-55E) and a vertical (CG-55D) piezometers from 2004 to 2016 (HADES URL) (Chen 2018).

3.2.4.1.2   Gas transport and self-sealing in Boom Clay

Laboratory tests

SCK CEN investigated gas transport within discontinuities in Boom Clay samples in the frame of the FORGE EC project (Jacops et al. 2014). In a laboratory experiment, a conservative anionic tracer was used to monitor gas transport through fractured Boom Clay samples. Test cores were initially saturated with natural Boom Clay water containing a sodium iodide (NaI) tracer, which exhibits minimal sorption to clay minerals and is considered inert to organic matter. Undisturbed samples of Boom Clay were first manufactured for testing. Additionally, a disturbed Boom Clay sample was made by cutting a core in half and joining the two halves again in a permeameter cell before resaturating with natural pore water. This process was repeated for samples with resaturation over different time periods from one night to one week. Material cores were also sampled with flow perpendicular- and parallel to bedding. Samples with a bentonite-Boom Clay discontinuity were also created by splitting cores, then joining halves of each material in a permeameter cell and resaturating for one week. The bentonite used was Volclay KWK with a dry density of 1.6 g/cm³.

Test samples (undisturbed Boom Clay, Boom Clay/Boom Clay or Boom Clay/bentonite) were then positioned above a NaI-conditioned sample and confined at constant volume within a permeameter cell. A downstream filter was then flooded with natural Boom Clay pore fluid before an 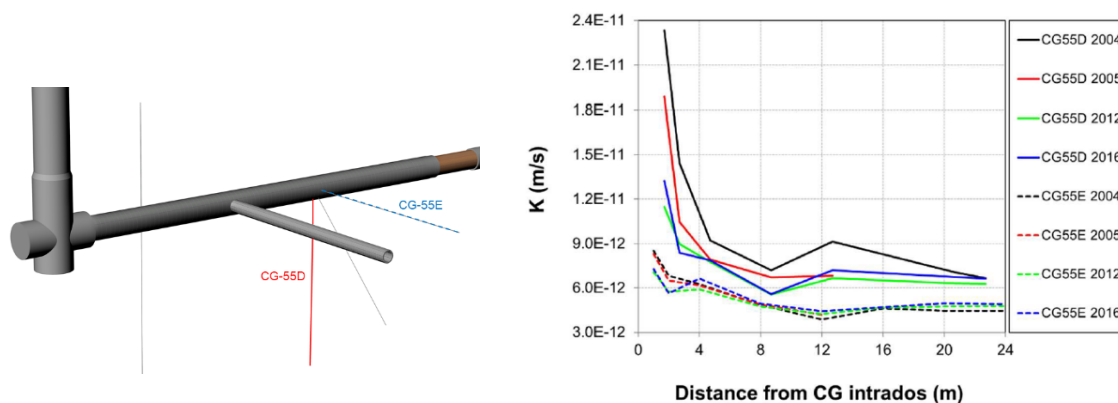excess gas pressure was applied with helium at the upstream (top) end of the sample. Finally, the applied gas pressure was increased in a stepwise fashion until breakthrough occurred, at which time the water in the downstream end of the sample was expelled. Analysis of the downstream pore fluid for iodine enrichment (by inductively coupled plasma mass spectrometry (ICP-MS)) was then determined in order to assess whether gas-driven transport of the tracer had occurred. Assuming unretarded diffusion of iodine and background concentrations in the natural Boom Clay pore water, it was possible to calculate the amount of pore water transported (and, hence, sample desaturation) as a result of gas injection. Overall, iodine transport by gas breakthrough events appears to have been low and indicates a degree of sample desaturation of less than 0.5%, indicating that no significant displacement of water occurred before and during gas breakthrough. In the case of recombined Boom Clay/Boom Clay samples, no difference in downstream iodine concentrations was found even where resaturation was only allowed for one night (desaturation of less than 0.5% was estimated). The authors also point to these observations as evidence of rapid self-sealing in Boom Clay.

Post-test observations of sample damage and degassing after testing were used in combination with measurements of iodine concentrations to assess the likely path for flow in different samples. According

EURAD (Deliverable n° 6.1) – Initial State of the Art on Gas Transport in Clayey Materials
Dissemination level: PU
Date of issue of this report: 17/11/2021

Page 201

to these findings, gas appears to have flown mostly where the fracture meets the cell wall (10 out of 19 tests). Only 3 tests provided evidence for gas pathways occurring through the clay core itself, without interference from the cell wall. These tests displayed notably lower downstream iodine concentrations than those where flow was thought to have occurred close to the cell wall. Series of tests have been performed with the bedding planes of the samples either parallel or perpendicular to the axis of the permeameter cell. Tracer concentrations indicate that a greater degree of water expulsion occurred in experiments where the flow direction was perpendicular to the bedding planes. This seems reasonably consistent with the structural properties of clays and suggests a smaller fracture surface area (and hence, degree of desaturation) is needed for gas flow parallel to the bedding planes.

In terms of Boom Clay/bentonite interface samples, no additional transport of tracer was detected, in comparison to Boom Clay/Boom Clay interfaces. Once again, the region of contact between the fracture and the wall of the cell was thought to have been the primary pathway for flow. The authors suggest an that experimental configuration where lateral confining pressure may be controlled would provide additional information in relation to the conditions over which this effect may occur, given the relatively low swelling capacity of the Boom Clay.

In situ experiment

A borehole and shaft sealing test was also performed at HADES URL, as part of the RESEAL EC project (Van Geet et al. 2009). While the main focus was on the sealing efficiency of pre-compacted bentonite pellets and powder, gas transport through and around the seal has been tested and is described here.

The RESEAL experiment involved examining the sealing behaviour of a 25 cm diameter horizontal borehole drilled in the Boom Clay (Van Geet et al. 2007, 2009). A 2.6 metres piezometer was emplaced into the formation, about 15 metres from the gallery wall at HADES URL. A borehole diameter was chosen to be slightly larger than the experimental set-up so as to allow for convergence after emplacement within the plastic host formation. Two separate compartments were filled around the central tubes, one with Fo-Ca clay (dry density of 1.6 g/cm^3) and the other with FEBEX bentonite (dry density of 1.5 g/cm^3) (Figure 3-41). The dry densities were selected to achieve a swelling pressure (at full saturation) close to the in situ lithostatic pressure at HADES URL (4.4 MPa). The test programme included artificial hydration, water permeability testing, gas breakthrough and tracer testing. Gas testing was initiated by injecting into the host formation near to the Fo-Ca seal compartment. Constant gas pressure was applied for incrementally greater pressures. Gas breakthrough occurred at an applied pressure of around 3.1 MPa and was observed to be equal to the radial total stress measured in the Fo-Ca seal. Elevated pressures in the Boom Clay and a weak pressure response in the seal led to an interpretation of either (i) gas flow along the interface between the Fo-Ca seal and the host rock or (ii) through the EDZ zone surrounding the borehole.

EURAD (Deliverable n° 6.1) – Initial State of the Art on Gas Transport in Clayey Materials
Dissemination level: PU
Date of issue of this report: 17/11/2021

Page 202
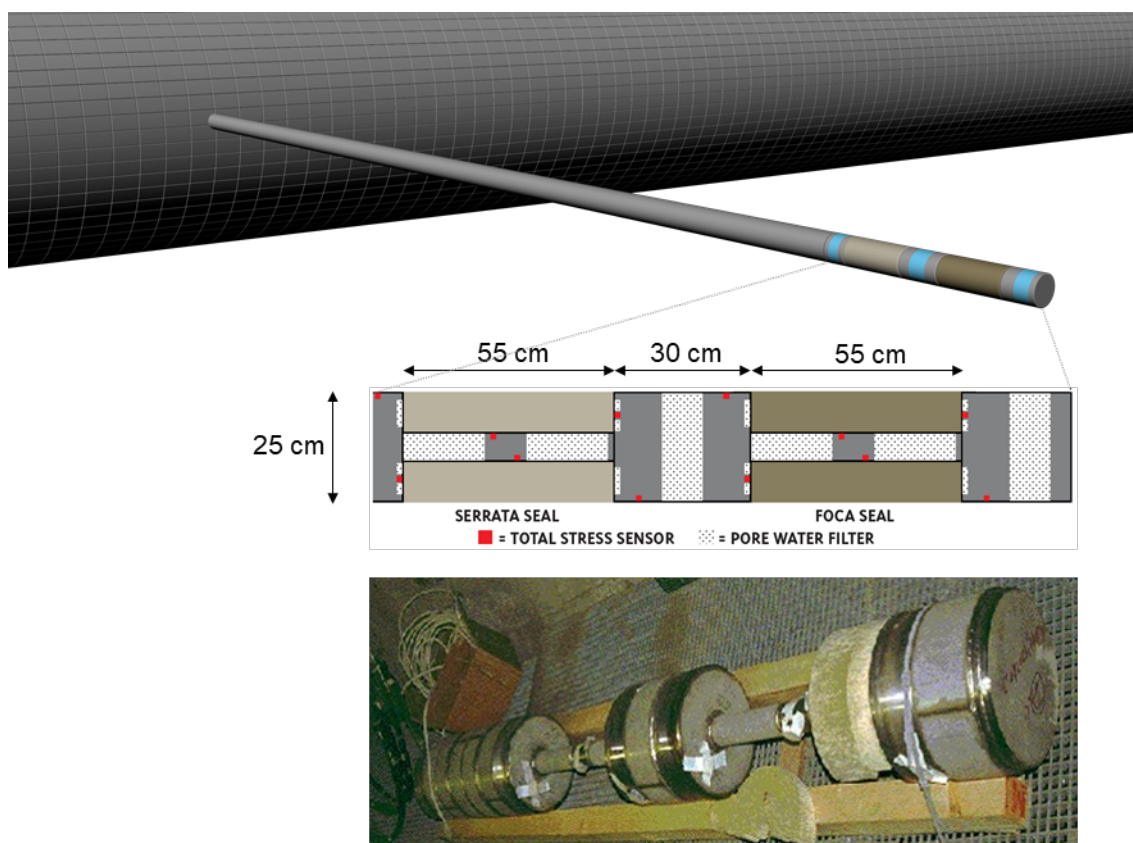
Figure 3-41 – Picture and schematic view of the piezometer used in the RESEAL borehole experiment (HADES URL).

3.2.4.2 State of knowledge for Callovo-Oxfordian claystone

Self-sealing in Callovo-Oxfordian claystone has been observed systematically in the clay-rich unit (main level of the repository) when injecting water in fractured material. This was shown at sample scale but also in several in situ experiments in the MHM URL. Self-sealing in COx seems to be independent of the mode of fracture creation. It concerns fractures created during excavation in traction close to the tunnel wall and the shear fractures of larger extension (extension about one diameter tunnel). It is also the case for fractures generated by gas pressure: large fracture due to gas fracturing event or microfracture associated to dilatant pathways.

The self-sealing in COx should be understood as a significant reduction of water permeability in fractured COx claystone when the fracture is saturated with water. Most of the time, the final water permeability after self-sealing becomes close to the one measured in intact rock. The level of permeability obtained after self-sealing is mainly dependant on the initial aperture of the fracture, the normal stress applied on it and if relevant chemical composition of the water available for the saturation.

However, even if the permeability of the rock is low after self-sealing, the history of the material is not forgotten. This means that weaknesses induced by fracturing is still present in the clay rock and mechanical properties, and potentially gas properties are much lower than those measured on intact rock are.

EURAD (Deliverable n° 6.1) – Initial State of the Art on Gas Transport in Clayey Materials
Dissemination level: PU
Date of issue of this report: **17/11/2021**

Page 203

3.2.4.2.1 Evidence of self-sealing in COx

The self-sealing behaviour of the COx claystone was investigated using several technics and methods of observations (Davy et al. 2007; Zhang 2013; Auvray et al. 2015; de la Vaissière et al. 2015; Di Donna et al. 2019).

Sample scale

For laboratory studies, samples were prepared according to several protocols, which can be divided into two categories:

- Machined samples: the fracture is created by cutting the sample. This technique allows a precise control of the fracture aperture (Figure 3-42c);

- Damaged samples: the damage is carried out under different conditions:

  o Direct shearing (Figure 3-42a) or splitting tensile test (Figure 3-42b);

  o Application of a deviator in a triaxial cell up to damage: cylindrical (solid) samples (Figure 3-42f) or hollow cylinders (Figure 3-42e);

  o Pre-treatment of samples by thermal or water cycles to generate diffuse damage (Figure 3-42d).

(a) Direct shearing (Ding et al. 2020) (b) Splitting tensile test (Davy et al. 2007) (c) Cut fractures (Auvray et al. 2015) (d) Diffuse damaged by RH cycle (M'Jahad 2012)

(e) Hollow cylinder (Menaceur et al. 2014) (f) Deviatoric stress in triaxial cell (Zhang et al. 2010)
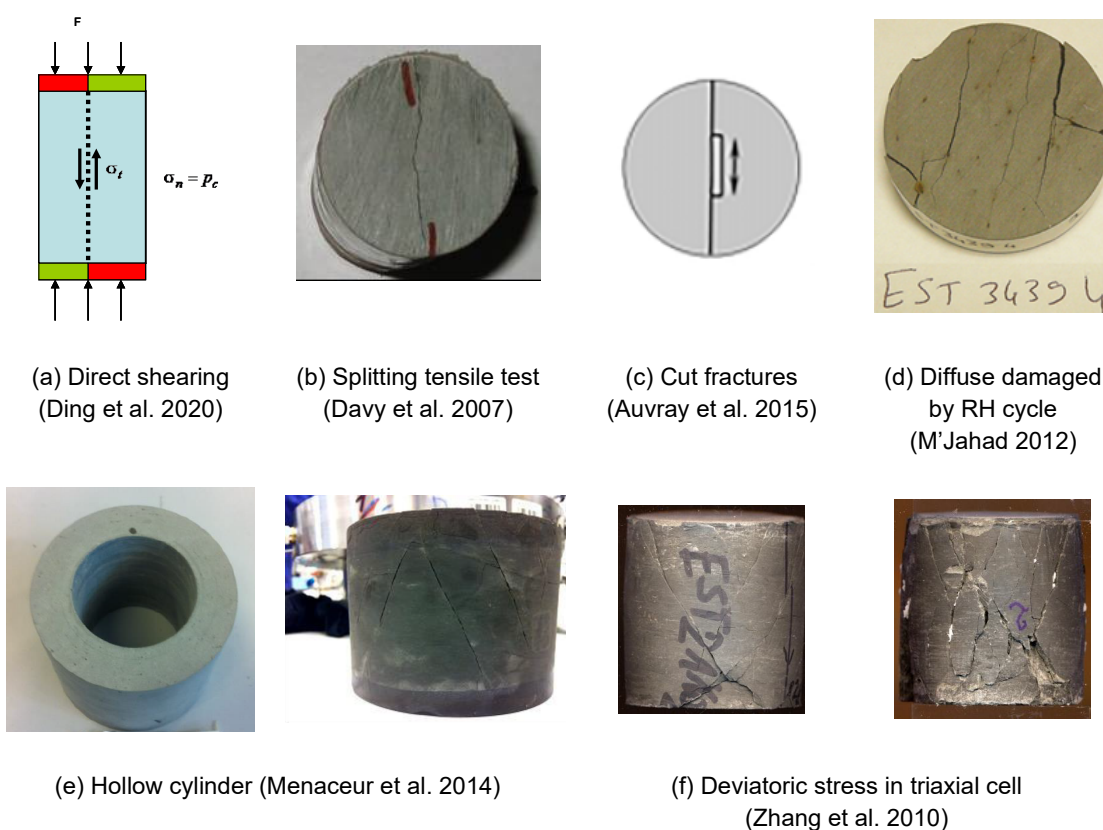
Figure 3-42 – Fractures obtained in Callovo-Oxfordian claystone samples for self-sealing tests.

Most of the tests carried out to characterise the self-sealing in COx highlighted a sequence of two phases:

1. In a first phase, a rapid decrease by several orders of magnitude of the hydraulic conductivity is observed as soon as water is injected (a few hours to a few days). The main process is the

EURAD (Deliverable n° 6.1) – Initial State of the Art on Gas Transport in Clayey Materials
Dissemination level: PU
Date of issue of this report: 17/11/2021

Page 204

swelling of smectitic clay minerals near the crack. It is illustrated on X-ray tomography tests carried out at CNRS (ULorraine) (Auvray et al. 2015). During water injection, the measurement of hydraulic conductivity and the visualisation of the evolution of the crack are performed simultaneously using an X-ray transparent triaxial cell. The cracks in the tests shown Figure 3-43 are 100 µm thick cracks. The samples are oriented parallel and perpendicular to the bedding.
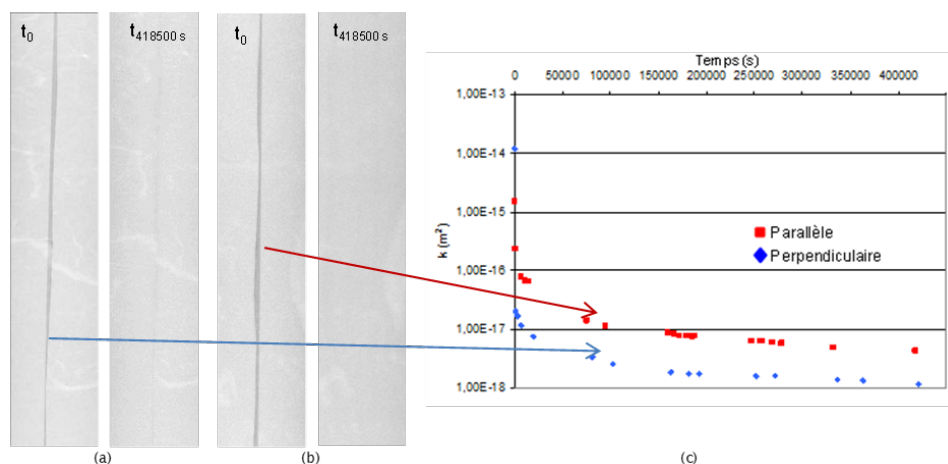
Figure 3-43 – Self-sealing of cracks with 100 µm aperture (a) perpendicular to the bedding, (b) parallel to the bedding, (c) evolution of permeability (m²) as a function of time in both directions (Auvray et al. 2015).

2. A second phase is characterised by a slow decrease of the water permeability. It gradually approaches the permeability of the intact claystone (~10^{-20} m²). This slow closure of the fracture is a consequence of rearrangements of porosity and clay minerals but is also induced by creep effects. The tests carried out by GRS (Zhang 2013) illustrate the temporal evolution of permeability. They were performed on splitting fractured samples. An isotropic confinement is applied to the samples between 2 and 3.5 MPa (low values compared to the main stresses in the Callovo-Oxfordian, between ~12 and 16 MPa). The duration of water injection was several years (>3 years). The permeability initially decreases very rapidly, and then continues to decrease gradually to values of the order of 10^{-20} m² (Figure 3-44).
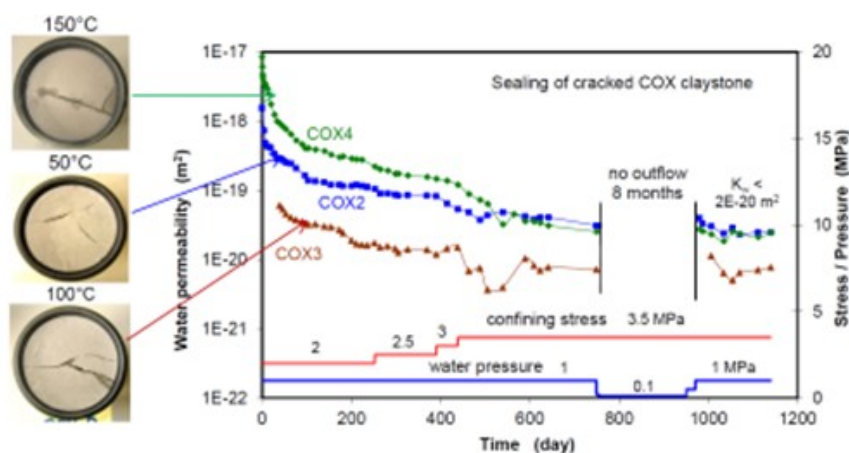
Figure 3-44 – Long-term evolution of water permeability (m²) for fractured samples (Zhang 2013).

EURAD (Deliverable n° 6.1) – Initial State of the Art on Gas Transport in Clayey Materials
Dissemination level: PU
Date of issue of this report: **17/11/2021**

Page 205

Several tests have been designed to quantify the evolution of fracture opening over time. These tests performed under X-ray tomography by the Di Donna (Di Donna et al. 2019) or Giot (Giot et al. 2019) give both quantitative and qualitative information. They give quantitative data with the monitoring of the evolution of the fracture opening or its volume (Figure 3-45). They also lead to a better analysis of the physical phenomena driving the self-sealing behaviour of the material. As an example, Figure 3-46 shows the results of a local tomography on one sample. The fracture closing is accompanied by the creation at the small scale of a factures network (peeling effect) which is often observed on clayey materials during free volume swelling tests with the appearance of fractures oriented in parallel to the bedding (see Figure 3-42d).
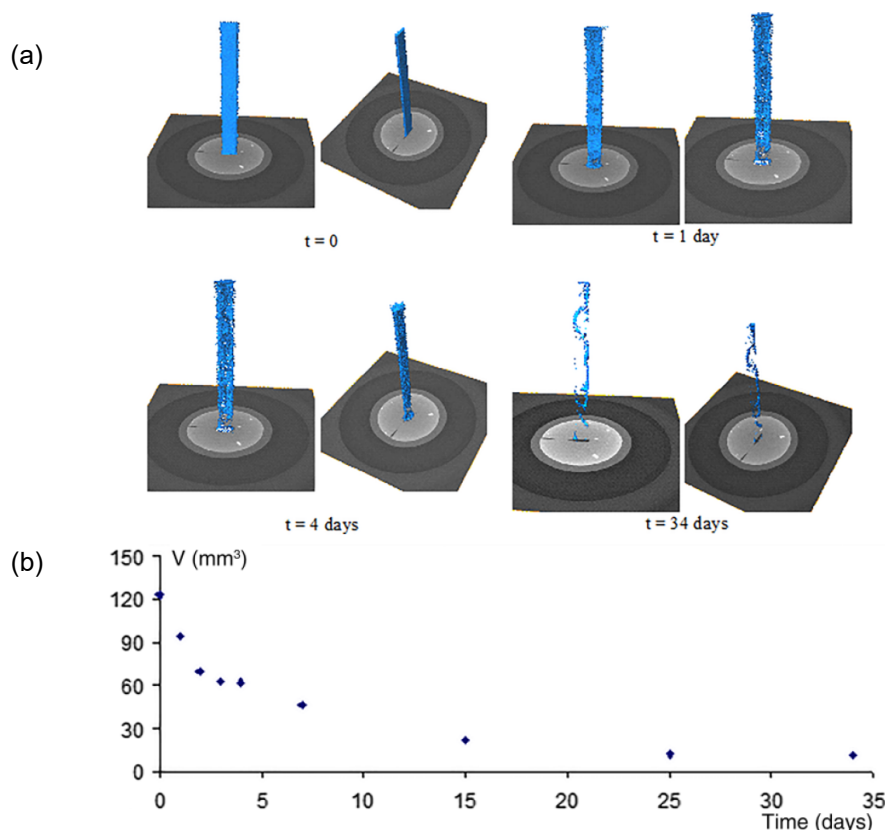
Figure 3-45 – (a) 3D tomography of the crack volume (in blue) from the beginning of the experiment (t = 0) to the end (t = 34 days). The initial aperture of the crack is 800 µm, sample 20 mm diameter, 40 mm height and crack parallel to the bedding; (b) evolution of crack volume (V) as a function of time (Giot et al. 2019).
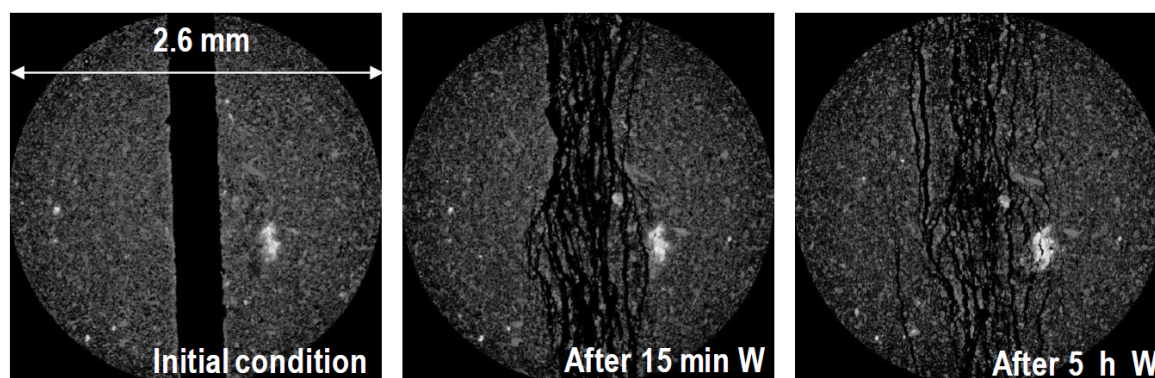
Figure 3-46 – X-ray images at different steps during water injection phase of the test, resolution 0.7 µm (bedding plane parallel to the slice) (W: start of water injection) (Di Donna et al. 2019).

EURAD (Deliverable n° 6.1) – Initial State of the Art on Gas Transport in Clayey Materials
Dissemination level: PU
Date of issue of this report: 17/11/2021

Page 206

Large scale

Specific tests to characterise self-sealing were carried out at the Meuse/Haute-Marne URL (de la Vaissière et al. 2015) in the two main stress direction (Damaged zone extension depends on the orientation of the tunnel in regards of stress field). Their principle consisted in hydrating a part of the damaged zone around a gallery, in which a high density of boreholes equipped with multiple plugs was drilled. Periodic tests are performed to monitor the evolution of hydraulic conductivity:

- The CDZ experiment (Mechanical Compression of EDZ) is a plate load test (surface area 1 m²) in a GET gallery (parallel to the main horizontal major stress H). It was equipped with 6 horizontal boreholes for hydraulic conductivity measurement (Figure 3-47);

- The OHZ experiment (Observation and monitoring of the EDZ) in the GER gallery (oriented perpendicular to the main horizontal major stress H) was equipped with 9 vertical boreholes for pressure monitoring and water injection (Figure 3-48).
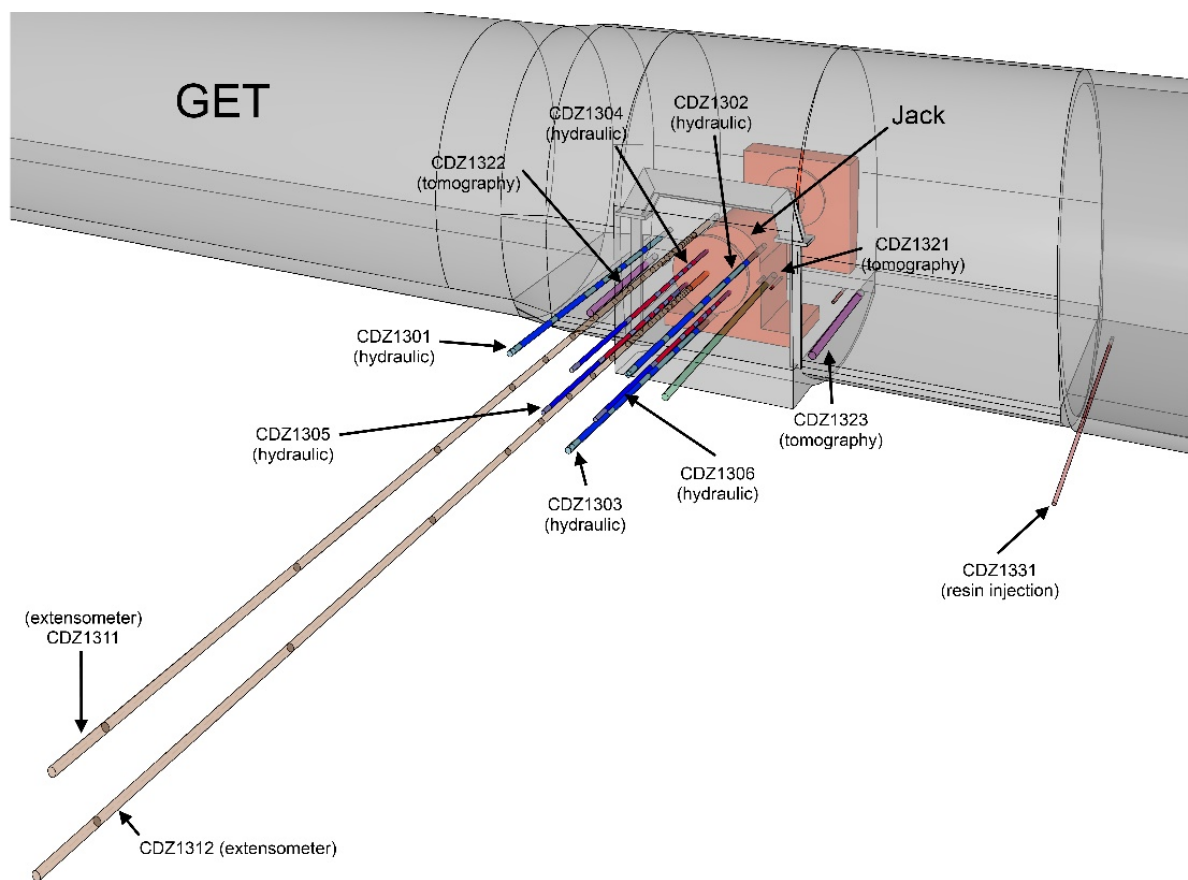
Figure 3-47 – Experiment configuration CDZ hydration experiment of EDZ in a gallery parallel to the major horizontal principal stress σ$_H$, (de la Vaissière et al. 2015).

EURAD (Deliverable n° 6.1) – Initial State of the Art on Gas Transport in Clayey Materials
Dissemination level: PU
Date of issue of this report: **17/11/2021**

Page 207
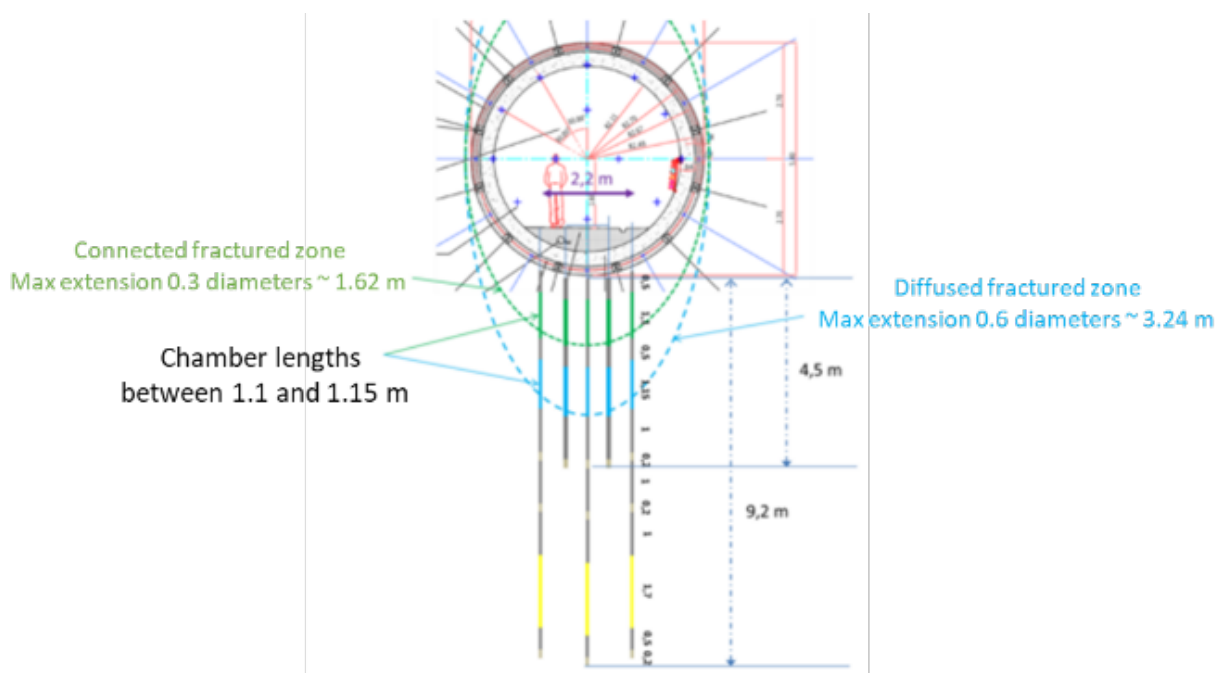
Figure 3-48 – Experiment configuration OHZ hydration experiment of EDZ in a gallery parallel to the minor horizontal principal stress σ_h.

Gas conductivity measurements were used to establish the initial value of the permeability [m²] and the connectivity of the damaged zone through interference testing. These measurements show a well-connected fracture zone with high hydraulic conductivity values (Figure 3-49) (Figure 3-50). The hydration of the damaged zone leads to a rapid decrease in hydraulic conductivity, especially at the tunnel walls where the density of tensile fractures and the initial conductivity are the highest. As soon as hydration occurs, the hydraulic conductivities decrease by several orders of magnitude. CDZ and OHZ confirm at the scale of a structure the existence of hydraulic self-sealing of the fractured zone and its rapid kinetics.
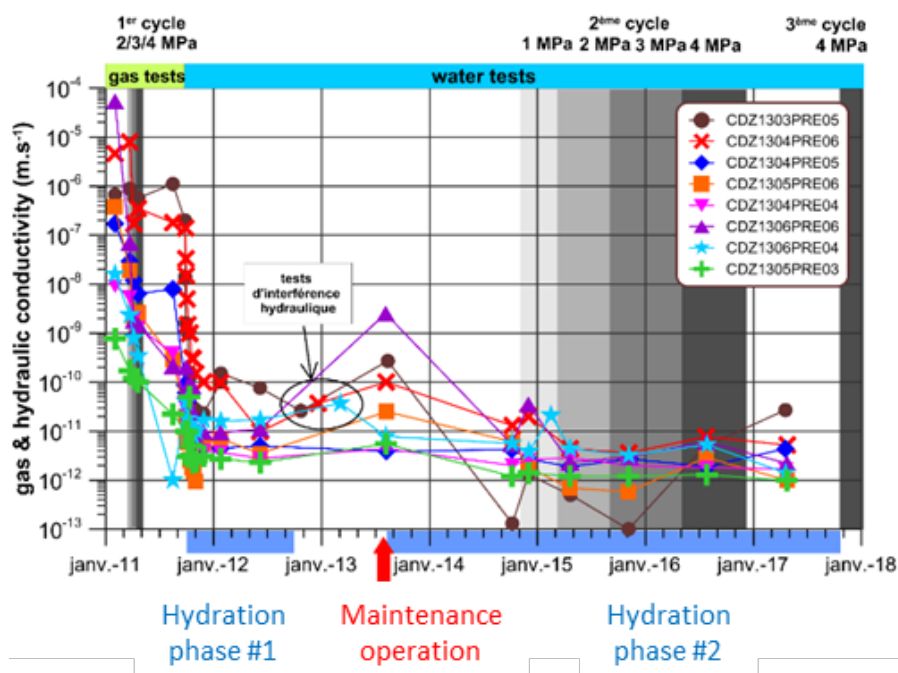
Figure 3-49 – Evolution of the hydraulic conductivity of the damaged zone in the CDZ experiment at the MHM URL.

EURAD (Deliverable n° 6.1) – Initial State of the Art on Gas Transport in Clayey Materials
Dissemination level: PU
Date of issue of this report: **17/11/2021**

Page 208
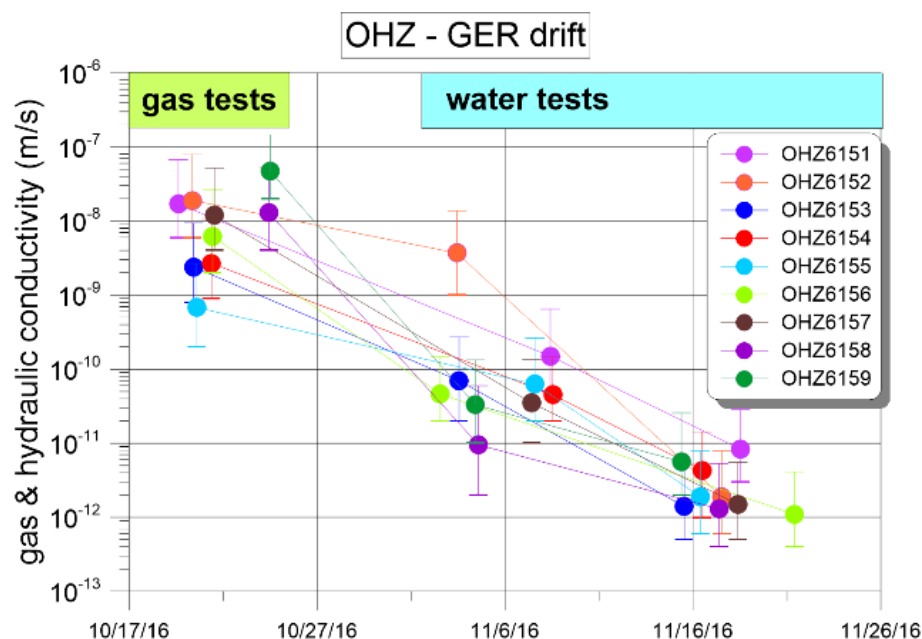
Figure 3-50 – Evolution of the hydraulic conductivity of the damaged zone in the OHZ experiment at the MHM URL.

3.2.4.2.2   Gas transport and self-sealing in Callovo-Oxfordian claystone

Several studies have been performed to characterise the gas behaviour of fractured COx, in particular the gas breakthrough pressure in an initially damaged material. The measurements carried out (M'Jahad 2012) on samples initially fractured, then saturated with water give gas breakthrough pressures between 0.3 and 1.4 MPa, very low compared to the range of values obtained for intact claystone (between 6 and 10 MPa). Despite the low entry pressure, the permeabilities measured on these same samples are between 4×10^{-21} and 6×10^{-19} m^2, indicating clearly self-sealing.

The compilation of all the gas breakthrough pressure measurements in the fractured Callovo-Oxfordian claystone (Harrington et al. 2017c) shows that the breakthrough pressures and therefore the gas entry pressures are low and between 0.3 and 3 MPa maximum (Figure 2-23). The fractured zones after self-sealing seem to keep a different microstructure from that of intact claystone, particularly in terms of higher 'equivalent pore sizes', which explains partially the low gas entry pressures observed.

The stress field has also a large impact on effective gas permeability of a fracture zone. This has been highlighted through several tests (M'Jahad 2012; Davy et al. 2007) performed on fractured samples. Tests conducted at several saturation states with confining conditions from a few MPa to 20 MPa show the consequences of stress field on effective gas permeability (Figure 3-51). A large variation of effective gas permeability as a function of the confining pressure is observed. The application of confining pressure induces a reduction of the effective gas permeability with fracture closure. The tests highlight the irreversible effect of stress on samples with lower permeability after unloading and shows that confinement is as expected a good indicator of the level of damaged in the material.

EURAD (Deliverable n° 6.1) – Initial State of the Art on Gas Transport in Clayey Materials
Dissemination level: PU
Date of issue of this report: **17/11/2021**   Page 209
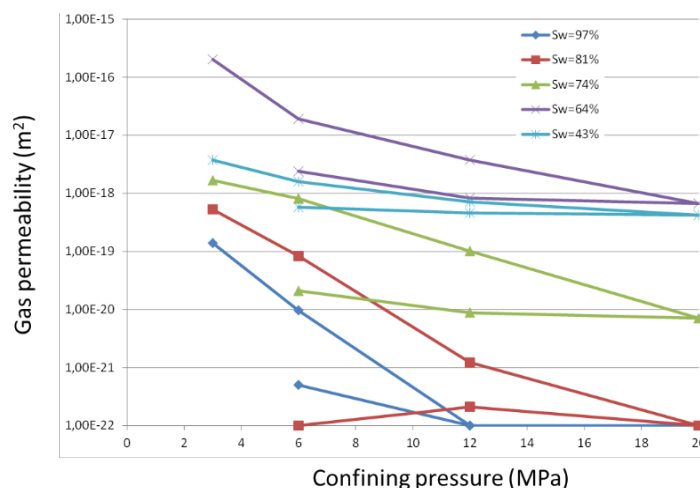
Figure 3-51 – Variation of effective gas permeability as a function of confining pressure for different degrees of liquid water saturation (COx).

The in situ experiments dedicated to study the behaviour to gas (see Section 3.1.4.2) of the COx performed in the Meuse/Haute-Marne URL and laboratory experiments confirmed the low impact of gas on hydraulic properties of the rock and did not reveal any kind of reduction on self-sealing processes efficiency.

Gas injection tests at pressure below the gas threshold fracturing pressure showed the role of EDZ in transport and the low capacity of the intact clay to be desaturated by gas for the level of pressure expected in the repository. Gas fracturing was induced in three boreholes by increasing gas pressure with rapid pressure build-up kinetics and slower kinetics. The idea in this second case was to approach the expected gas generation conditions in the repository, even if the gas pressure rise in the tests is rapid with respect to the evolution of pressures expected in the repository (pressure rise over several thousands of years at least). Alternative sequences of gas and water injection confirmed the results obtained on samples concerning the low effect of gas on self-sealing. Water permeabilities measured after gas injection are of the same order as those of intact COx even after a large gas fracturing event.

3.2.4.3 State of knowledge for Opalinus Clay

3.2.4.3.1 Evidence of self-sealing in Opalinus Clay

Bock et al. (2010) present results from recompaction and resaturation in combined triaxial and permeability tests on Opalinus Clay and COx samples (Zhang et al. 2008, Zhang and Rothfuchs 2008). More recent laboratory investigations on self-sealing of Opalinus Clay were compiled by Lanyon 2018, including results from Zhang (2015, 2017) and Cuss et al. (2011a).

Cuss et al. (2011a) report measurements of fracture transmissivity as a function of normal and shear stress for an artificial fracture in Opalinus Clay. The artificial fracture was created by machining two $60 \times 60 \times 21$ mm^3 blocks of Opalinus Clay prepared on a diamond mill. This gave smooth and parallel surfaces on both contact faces of the sample. The samples were loaded into a direct-shear-rig with a central hole drilled in the upper plate to inject fluid. Fracture transmissivity was estimated assuming radial flow within the artificial fracture.

Fracture transmissivity versus effective normal stress was investigated in five loading steps (initial loading from 3 to 5.5 MPa followed by unloading steps) lasting between 2 and 6 days. The loading steps were accompanied by dilation/swelling of ~700 µm as the sample had an initial saturation of 81.4%.

EURAD (Deliverable n° 6.1) – Initial State of the Art on Gas Transport in Clayey Materials
Dissemination level: PU
Date of issue of this report: 17/11/2021

Page 210

The artificial fracture showed a very low transmissivity 4–5 × 10^{-14} m^2/s with a roughly linear dependence on effective normal stress. The very low transmissivity may be due to the milled surfaces (no significant asperities) of the two samples giving only very small aperture. One step was performed at high injection pressure which showed a slightly higher transmissivity than might have been expected. This is thought to be due, at least in part, to differences in fracture and matrix compressibility.

Following the normal loading steps the samples were actively sheared for 70 days under constant normal stress of 2.75 MPa followed by a 35 day period without shearing. During the 70 days shearing period transmissivity initially dropped and was then relatively stable until a series of events with an initial transmissivity increase followed by decline. Peak transmissivity was ~2 × 10^{-13} m^2/s.

Examination of the sample after the test showed that during the shear test, a new fracture had formed, although there was relatively little movement on this feature. Cuss et al. (2011a) suggest that the flux increase events were the result of new fracture formation, but that subsequent shear deformation resulted in self-sealing and a reduction in transmissivity with time. Tracer injection at the end of the test demonstrated flow channelling on the fracture surfaces associated with a 'tensile' step in the fracture surface.

3.2.4.3.2   Gas transport and self-sealing in Opalinus Clay

As part of a recent laboratory programme on self-sealing core samples from the shaly facies at Mont Terri were tested by Seiphoori (2019). Detailed material characterisation included physical property determination, bulk and clay-fraction X-ray powder diffraction (XRPD), mercury intrusion porosity (MIP), N$_2$ gas sorption and high-resolution SEM (HR-SEM). Numerous triaxial experiments were conducted on both intact samples and samples with an artificial fracture (sawn or broken) to mimic the self-sealing of the fractures. The cylindrical samples were equipped with sensors for measuring gas pressure, deformation and seismic velocities. Effective gas permeability and fracture transmissivity of the respectively intact and artificially fractured samples along the bedding plane was determined for several cycles of isotropic loading/unloading, while the axial and radial strains were locally measured using high precision strain gauges installed at several locations on the periphery of the cylindrical samples. The deformation normal to the natural bedding and artificial fracture plane (aperture opening/closing) was directly measured using a radial LVDT, and the elastic wave velocities across the bedding were continuously measured during all experiments. Following the gas permeation experiments, the samples were subject to synthetic water for permeability and fracture transmissivity measurements during transient conditions. Total deformation normal to the fracture in response to effective stress changes was measured using an internal LVDT installed on the sample circumference (Figure 3-52b). The sensor readings are associated with the change in the major (artificial) aperture and the natural fracture closure. The transients of the aperture (in µm) in response to the changes of effective pressure are plotted in Figure 3-52a. The total deformation includes the elastic and accumulative inelastic (plastic) deformation behaviour. Figure 3-52c&d shows the change in effective gas permeability over multiple loading/unloading cycles for an artificially fractured and intact sample. The (apparent) permeability decreases with cyclic loading/unloading initially due to plastic deformation of the asperities along the fracture plane (effect of compaction). After second cycle, the hysteresis effect becomes negligible. A hold time of about 17 hours was considered after Cycle 4 to evaluate the effect of the creep on the permeability which resulted in a remarkable decrease as observed in Figure 3-52c. The effective gas permeability of the fractured sample is about two orders of magnitude higher than the permeability of the intact sample (Figure 3-52d).

EURAD (Deliverable n° 6.1) – Initial State of the Art on Gas Transport in Clayey Materials
Dissemination level: PU
Date of issue of this report: 17/11/2021

Page 211
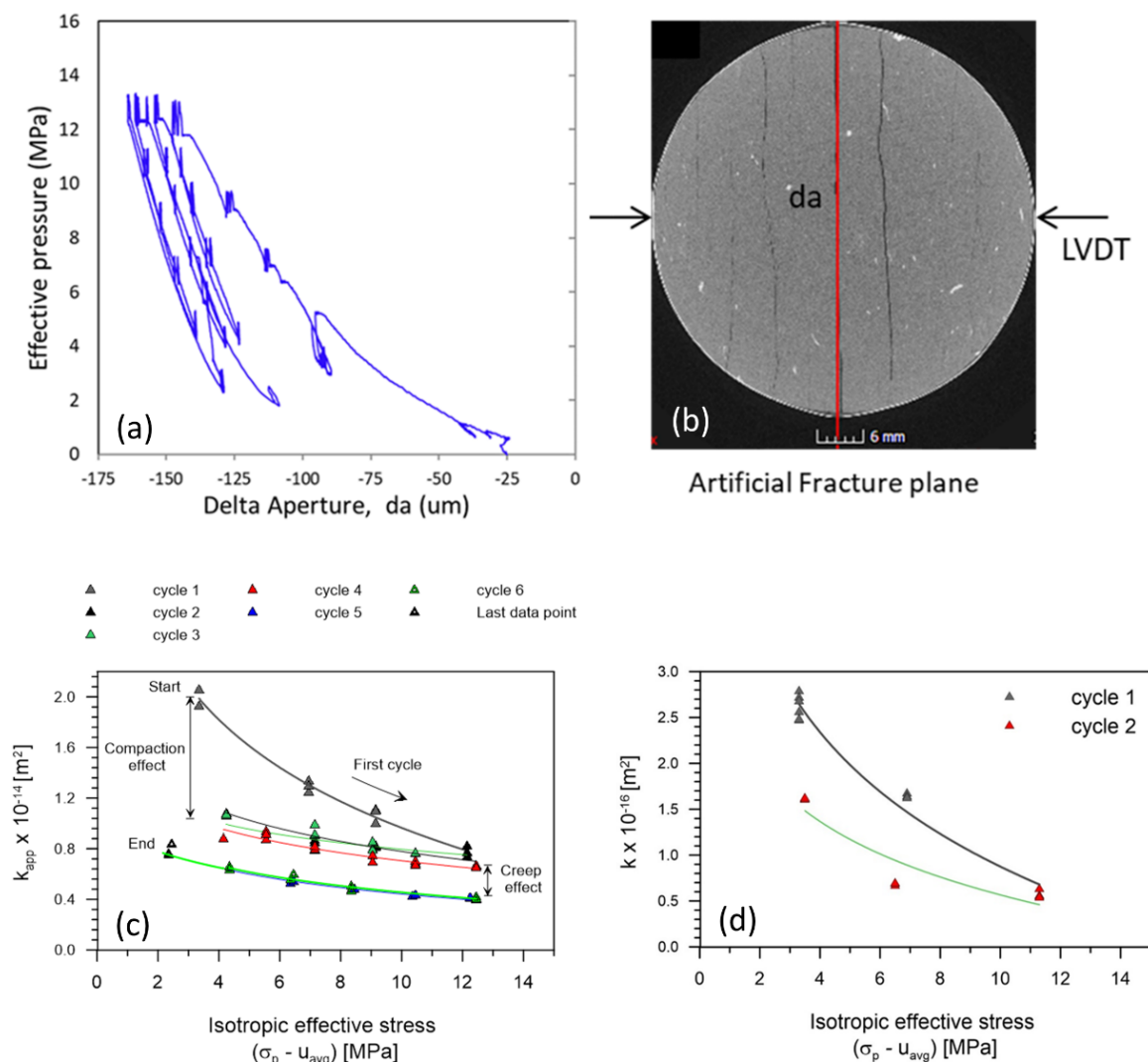
Figure 3-52 – Cyclic isotropic loading / unloading of intact / artificially fractured samples along: (a) aperture change in response to effective stress change, (b) µ-CT scan of the artificially fractured sample; (c) artificially fractured sample gas transmissivity (as permeability × thickness in m³) vs. effective stress; (d) intact sample effective gas permeability [m²].

At the end of the cyclic effective gas permeability test sequence, the artificially fractured sample was scanned with a µ-CT device. Subsequently, the self-sealing stage was initiated by hydrating the sample with synthetic pore water. A fast transition in apparent permeability for the synthetic water experiments was observed that indicates the significant self-sealing capacity of the material. The swelling behaviour of the material was monitored until a steady-state condition reached under a controlled isotropic effective stress. To determine the evolution of the internal fracture network during different stages of water imbibition process, repeated µ-CT measurements were conducted. The internal pore structure information revealed a remarkable self-sealing behaviour of fractures due to the internal hydration of clay matrix and swelling within the fracture planes. Figure 3-53 shows the µ-CT image of the core before and after hydraulic self-sealing tests (resolution 32 µm). After water injection the porosity of the minor fractures can no longer be imaged, while the major artificial fracture has undergone significant self-sealing and shows only a channelled tortuous porosity above the minimum resolution.

EURAD (Deliverable n° 6.1) – Initial State of the Art on Gas Transport in Clayey Materials
Dissemination level: PU
Date of issue of this report: **17/11/2021**

Page 212
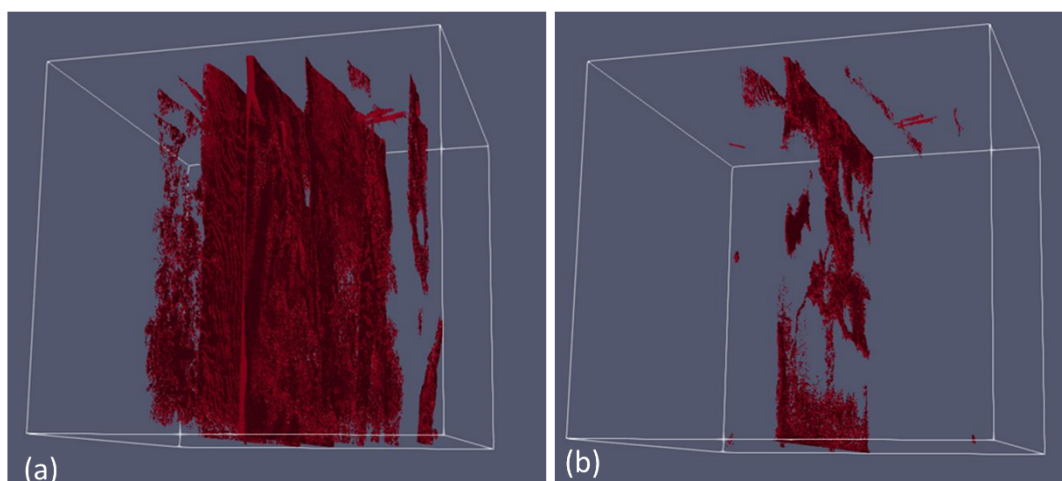
Figure 3-53 – Internal 3D pore structure of the Opalinus Clay sample (with artificial fracture plane)
(a) before and (b) after self-sealing experiment with synthetic pore water.

The experiment HG-A experiment ('Gas path through host rock and along seal sections') at the Mont Terri URL was designed as a long-term gas injection experiment in a backfilled microtunnel, to investigate the efficiency of the EDZ as a gas transport path along a sealed tunnel section in the Opalinus Clay and to demonstrate the capacity of the EDZ to self-seal after long-term gas release. For this, a 1 m-diameter, 13 m-long microtunnel was excavated parallel to the strike of bedding planes, thus replicating the expected relationship between bedding and emplacement tunnel orientation in a deep geological repository. The first 6 metres of the microtunnel were lined with a steel casing immediately after excavation to stabilise the opening. The gap behind the liner was then cement-grouted, but not sealed. A purpose-built hydraulic megapacker (diameter 940 mm and sealing section length 3 m) was installed. The sealing section was located at 6–9 metres with a 1 metre grouted zone containing the non-sealing part of the packer and retaining wall from 9–10 metres. The final 3 metres of the microtunnel from 10–13 metres are forming the test section which was instrumented and backfilled prior to megapacker emplacement. A schematical sketch of the experiment is shown in Figure 3-54a. Further information is provided in Lanyon et al. (2014).

The test section was instrumented with piezometers, extensometers, strain gauges and time domain reflectometers (TDRs) to measure pressure, deformation and water content. The seal section was instrumented with piezometers, total pressure cells and TDRs prior to the installation of the megapacker. In total, more than 100 sensors were used to monitor the hydro-mechanical conditions at the test site.

A number of long-term gas injection tests were performed in the HG-A experiment, followed by shut-in and resaturation periods. During the resaturation phases, the evolution of hydraulic conductivity in the EDZ was measured continuously. The effective hydraulic conductivity is plotted in Figure 3-54b assuming an EDZ area of 1 m^2 (equivalent to a 25 centimetres thick zone around the 1 metre diameter tunnel). Data affected by flow control problems and the post-GI4 testing are highlighted. The hydraulic conductance of the EDZ has reduced by over 2 orders of magnitude during the experimental period. The assumption of linear flow along the EDZ may result in an overestimate of the EDZ hydraulic conductivity, as at late time some part of injected flow may no longer have been dominantly along the EDZ. Two-phase flow models assuming a time-dependent permeability reduction of the EDZ showed permeability reductions of 2 orders of magnitude over the first 2 years of resaturation. The low conductivity of the EDZ to water has been shown to be largely unaffected by the gas injection with the sealing index returning to pre-gas injection levels a few months after the start of post-gas hydraulic

EURAD (Deliverable n° 6.1) – Initial State of the Art on Gas Transport in Clayey Materials
Dissemination level: PU
Date of issue of this report: 17/11/2021

Page 213

testing. After the last gas injection phase, the effective conductivity of the EDZ had reduced by 2–3 orders of magnitude, remaining about 2 orders of magnitude above the conductivity of the intact Opalinus Clay at the site.
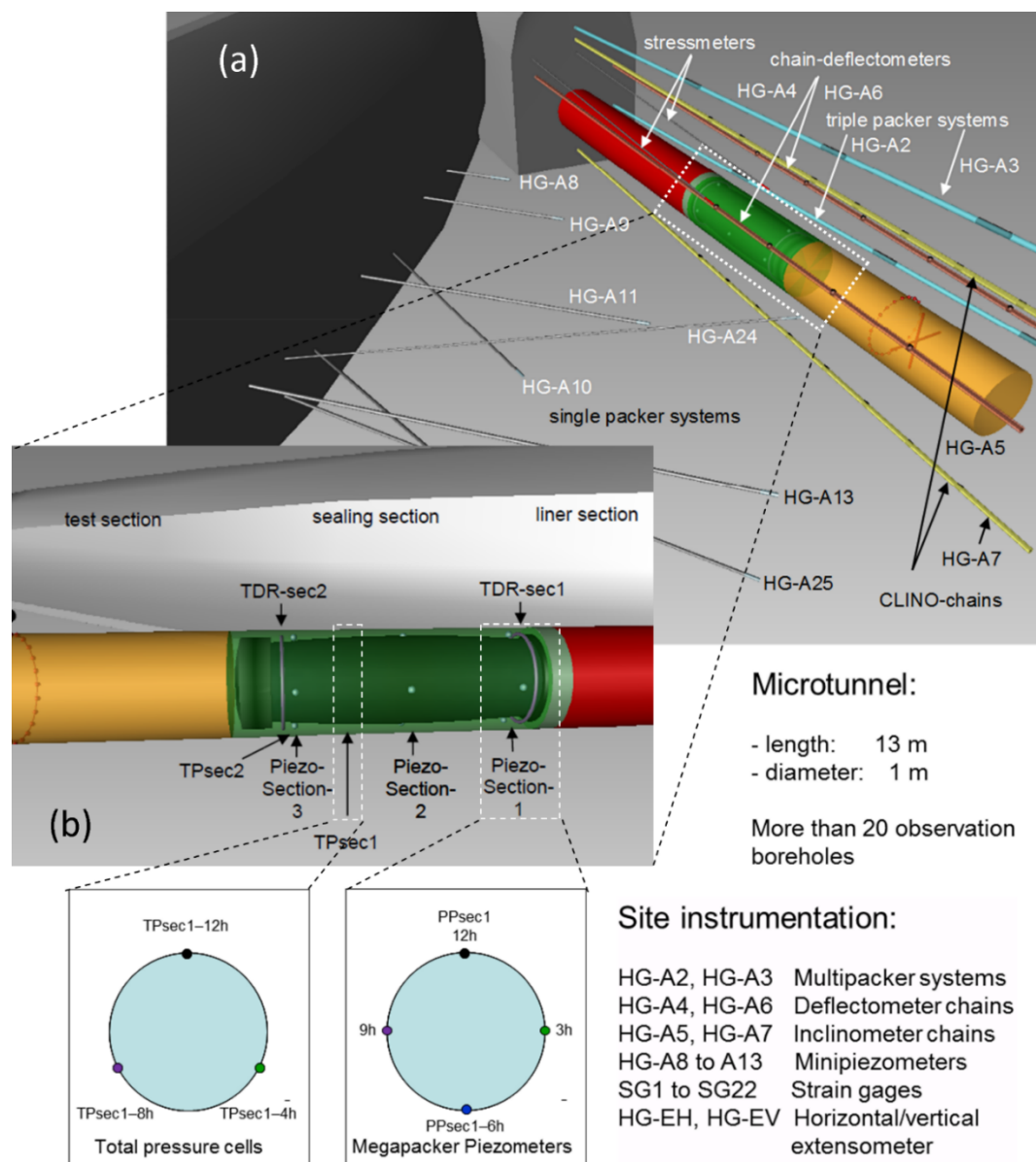
Figure 3-54 – Schematic drawing of the HG-1 A microtunnel and the site instrumentation. Colour coding refers to the steel liner (red), the seal section (green) and the backfilled test section (orange).

3.2.4.4   State of knowledge for bentonite

From the state of knowledge detailed in Section 3.1.4.4, it is clear that gas breakthrough in nearly of fully water-saturated bentonite is characterised by the formation of gas-specific pathways and that gas rapidly flows out of the sample when the developed pathways are fully connected with outlet boundaries. The gas breakthrough may also take place in subsequent injection cycles, but it is less obvious to detect because of the residual gas left by the first cycle (Harrington and Horseman 2003; Villar et al. 2013). The developed pathways may close or self-seal when gas pressure decreases below a certain value. As a result, the gas pathways developed in previous injection cycles may or may not be used again as pathways in the following cycles (Harrington and Horseman 2003).

EURAD (Deliverable n° 6.1) – Initial State of the Art on Gas Transport in Clayey Materials
Dissemination level: PU
Date of issue of this report: 17/11/2021

Page 214

The self-sealing capacity of the tested bentonite is clearly observed when the material is subjected to a rehydration process. The rehydrated sample can recover its tensile strength, permeability and gas breakthrough pressure to a certain degree (Graham C. et al. 2012; Villar et al. 2013, see also the discussion on testing FEBEX-DP samples in Section 3.1.4.4). The conclusion drawn from tests performed during the FORGE EC project is that self-sealing of bentonite always occurs after a gas migration event (Norris 2013).

The tested bentonite can keep an almost saturated state after the gas injection test (Horseman et al. 1999; Harrington and Horseman 2003; Hoch et al. 2004; Graham C. et al. 2012; Harrington et al. 2017b). As the aperture size of the developed pathways is much larger than the pore size of the clay matrix, gas preferentially flows through the fracture network, while leaving the clay matrix at a saturated state since the void space of the developed pathways only accounts for a tiny percentage of the total void space.

In case the buffer of a repository is constructed from compacted bentonite blocks of different sizes and shapes, the behaviour of the engineered barrier system will be determined not only by the matrix properties of the bentonite, but by the interfaces between the different elements of the EBS, in particular the interfaces between the bentonite blocks or between these blocks and the host rock. These interfaces may act not only as mechanical weakness planes, but also as preferential gas pathways. According to (Popp et al. 2014), there is a partial healing of the interface between blocks of a bentonite/sand (60/40) mixture after saturation. Nevertheless, these interfaces may still act as mechanical weakness planes and might be reopened during gas injection. Thus, these could still act as preferential gas pathways in that case.

Davy et al. (2009) analysed in laboratory tests the bentonite/argillite interface, and concluded that, although the assemblage formed by the two materials was highly impermeable to water (i.e. the interface sealed well after saturation), gas leakage would occur preferentially along this interface if the gas pressure was sufficiently increased (i.e. the interface did not heal). However, according to Liu J. (2013), who performed a series of similar tests, it is not possible to ascertain if the gas moved along the bentonite/argillite interface or across the argillite, whose breakthrough pressure is lower than the one of bentonite.

The experimental work carried out by Gutiérrez-Rodrigo et al. (2021) aimed to understand the gas transport in a saturated bentonite barrier. Tests were designed to determine the gas breakthrough pressure and estimate permeability value once breakthrough occurred and to test the role of interfaces inside the bentonite barrier, i.e. between compacted bentonite blocks (in the continuity of preliminary studies of Villar et al. (2013), Gutiérrez-Rodrigo et al. (2015) and Gutiérrez-Rodrigo (2018)).

Prior to the gas injection tests the samples were saturated. As a result of the full saturation, gas was not able to flow through the samples until a sufficient pressure was reached. This breakthrough pressure was found to increase with dry density in an exponential way and was in all cases higher than the swelling pressure corresponding to the dry density of the samples. The gas breakthrough could take place either in an instantaneous or in a gradual way, the difference between both modes being the flow rate, much higher in the first case. Flow went on until the residual pressure was reached, what is interpreted as the closing of the pathways. Upon again increasing the pressure gradient, a slightly lower gradient was necessary for flow to resume, likely as a consequence of the local hydro-mechanical weakening and slight local desaturation of the porous structure during the first episode. Nevertheless, the pressures needed for the second gas breakthrough episode were still much higher than the swelling pressure. The gas transport mechanism was interpreted as microscopic pathway dilation, with microfracturing in the case of the instantaneous episodes. The samples were resaturated and the breakthrough pressures found tended to be higher (but of the same order) than before resaturation, with smaller differences between the pressures needed for first and second episodes. The hydraulic

EURAD (Deliverable n° 6.1) – Initial State of the Art on Gas Transport in Clayey Materials
Dissemination level: PU
Date of issue of this report: 17/11/2021

Page 215

conductivity of samples that had been submitted to gas injection were in the order or even lower than that expected for the reference bentonite.

According to Gutiérrez-Rodrigo et al. (2021), these observations attest the healing of previous gas pathways brought about by resaturation. Once saturated, the samples with an interface between bentonite blocks behaved as samples of the same dry density with no interface. Hence, a sealed interface along the bentonite had no effect on the breakthrough pressure values and did not seem to be a preferential pathway after material homogenisation.

3.2.5   Shared understanding of self-sealing mechanisms in natural and engineered clayey barriers

Self-sealing depends on (thermo-) hydro-mechanical and chemical processes, the mineral composition of the material in link with its swelling capacity and controlled by the prevailing stress conditions. Mechanical closure of fractures (e.g. crack closure, fracture sliding), hydro-chemical interactions of the pore water with the clay-bearing solid phase of the geomaterial (e.g. swelling, disaggregation) and colloidal transport processes (e.g. sedimentation, clogging) have been identified as typical self-sealing mechanisms in clay-rich materials. Self-sealing mechanisms are well identified for both host rocks (Boom Clay, Opalinus Clay and Callovo-Oxfordian claystone) and bentonite-based materials used for engineered barriers. A summary of these mechanisms is given in Table 3-4. A large number of experiments at different scales on all the materials of interest and performed under several THMC conditions give confidence on the exhaustivity in the identification of these processes.

The contribution of small-scale imaging techniques complementary to macroscopic tests is important in confirming the physico-chemical processes relevant for self-sealing. By this means, it has been possible to visualise the closure of fractures of multiple origin and to show the rearrangements of clays in and around the fractures. For clay rocks, it highlights a difference in the microstructure of the material formed inside the fracture zone.

Gas tests in host rocks have shown that after the creation of dilatant pathways or gas fracturing, the rock always keeps a capacity for self-sealing. In contrast, changes in the structure of the material in the sealed zone usually lead to changes in gas transfer properties, in particular lower gas entry pressures than in the intact rock.

3.2.6   Uncertainties and knowledge gaps

If basic understanding and identification of the phenomena and processes that contribute to the self-sealing after gas breakthrough or gas fracturing has been acquired, a certain amount of knowledge still needs to be consolidated. An improvement of conceptualisation of self-sealing mechanisms at process level is needed to be able to model and predict the self-sealing capacity of clay barriers and the host rocks under the THM-C conditions that prevail in a deep geological repository.

Several situations have to be explored to demonstrate that self-sealing capacity is not lost due to gas breakthrough such as:

- successive opening/closing of gas pathways in particular for engineered barriers or at the interfaces between clay materials and other components of the repository.

- long-term gas flow in a fracture and possible transformations or microstructural reorganisations at the fracture wall.

EURAD (Deliverable n° 6.1) – Initial State of the Art on Gas Transport in Clayey Materials
Dissemination level: PU
Date of issue of this report: 17/11/2021

Page 216

3.3   Process-level models and modelling tools

This section continues the state-of-the-art description of modelling gas processes presented in Section 2.5 (Modelling of gas transport) in clayey material in particular with respect to barrier integrity, i.e. mechanical and coupled processes are in the focus of this section. For the fundamental basics of macroscopic theory for multiphase porous media, equivalent (multiple) continua, theory of mixtures, fluid mechanics (including multiphase flow), equations of state and phase-related general balance equations please refer to Section 2.5 as well.

3.3.1   Interests and needs of end-users in the context of geological disposal

Models play an important role for performance assessments (PA) in general as they allow e.g. for parameter identification based on experiments and for prediction of repository evolution in future. Modelling is essential for the entire systems analysis, fundamental process understanding, transferability and upscaling as a basis for building safe repositories in future, just to mention a few points.

Specific applications of modelling of gas transport in the field of radioactive waste disposal are, e.g. safety-oriented repository design and design optimisation (total system design, design and optimisation of repository components) as well as performance assessment in site selection processes and for licence applications as mentioned before.

For this, the WMOs and the TSOs of regulatory bodies need verified codes and validated models, capable to describe the complex phenomena and processes associated with gas transport in clay barriers to a sufficient level of detail for the assessment of long-term repository safety. This verification and validation process requires:

- Reliable workflows for code and calculation verification, model validation (see Figure 3-55 and explanation for it).

- Platforms for model benchmarks: A prominent example for an international benchmarking initiative is DECOVALEX (Development of coupled models and their validation against experiments, see https://decovalex.org/) which has been active for more than 25 years. The basic idea of DECOVALEX is the definition of challenging modelling task which are solved by modelling teams from different countries using different modelling concepts and codes. Most of the model challenges are directly derived from in situ experiments in underground research laboratories (URLs) all over the world. A second example is SeS Bench (Subsurface environmental simulation) which is dealing with a broad spectrum of modelling tasks from various field in environmental sciences including chemistry and biology. An overview of various benchmarking initiatives can be found in Kolditz et al. (2016).

- An important and rather new aspect in modelling is reproducibility which has impacts on the entire modelling process. Reproducibility means that complex simulations for safety assessment purposes must be repeatable even after years. This requires the implementation of modern software engineering concepts for entire workflows, i.e. version-controlled distributed code development e.g. via GitHub/GitLab platforms and version-controlled modelling (Zinner et al. 2018). This means that professional software engineering and data management become more and more important for performance and safety assessment procedures.

The WP GAS of EURAD linked to previous and ongoing related projects such as FORGE EC project (Norris, 2013) and BEACON on bentonite mechanical evolution within the framework of H2020-EURATOM (https://www.beacon-h2020.eu/). This WP GAS in continuing and complementing the model

EURAD (Deliverable n° 6.1) – Initial State of the Art on Gas Transport in Clayey Materials
Dissemination level: PU
Date of issue of this report: **17/11/2021**

Page 217

development focusses on various facets of clay rocks including gas transport (see Section 2.5) and coupled processes affecting the barrier integrity (this section).

3.3.2   Conceptual and numerical models

The present SOTA focusses on the specific requirements of the WP GAS of EURAD and briefly introduces recent developments also in related disciplines such as computer and data sciences (Section 3.3.10.1). A concise description of available process-level models of gas transport and its consequences on material properties will be given. Some guiding questions for the SOTA compilation are related to perceived strengths and weaknesses of different process-level model. Is there a scientific consensus about the applicability of these models to different materials and conditions? There is a large body of literature already available. Nagra comprehensively compiled the status on gas generation and transport processes in potential waste repositories in Opalinus Clay (Johnson et al. 2004). Within the GASTON project, modelling approaches of gas transport in clay formations have been evaluated (Alkan and Müller 2006). Research work in more recent years includes comprehensive workflows of multi-physics modelling with three main categories (i) physical modelling, (ii) numerics and implementation as well as (iii) the validation, analysis and interpretation step (Nagel et al. 2016) (Figure 3-55).
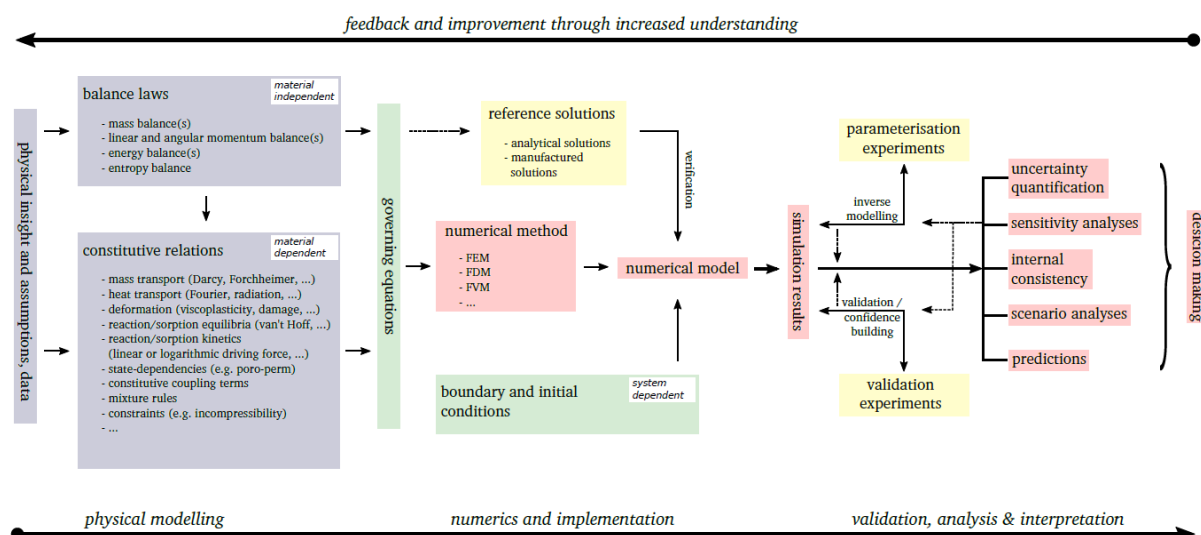
Figure 3-55 – Workflows of multi-physics modelling, after Nagel et al. (2016).

Model chains for bridging scales

Figure 3-56 serves as an explanation for building connected model chains. It starts from modelling at the process scale using methods down to the atomistic, molecular scales such as Lattice-Boltzmann, Lattice-Element approaches, Molecular Dynamics or Particle Methods. These modelling techniques are able to represent fundamental processes at very small (atomistic) scales, but computationally very expensive and difficult to upscale to measurement scales. The opposite end of the scales is represented by so-called complexity-reduced models. At this scale, questions of long-term environmental impacts of radioactive waste repositories have to be addressed. To this purpose data from various sources have to be combined including geological and geographical information as well as socio-economic aspects. For large scale analysis, stochastic approaches and network simulation are being used. Only a small portion from small-scale simulations can be used at this scale. However, fundamental process understanding will be a key for more reliable long-term predictions.

EURAD (Deliverable n° 6.1) – Initial State of the Art on Gas Transport in Clayey Materials
Dissemination level: PU
Date of issue of this report: 17/11/2021

Page 218
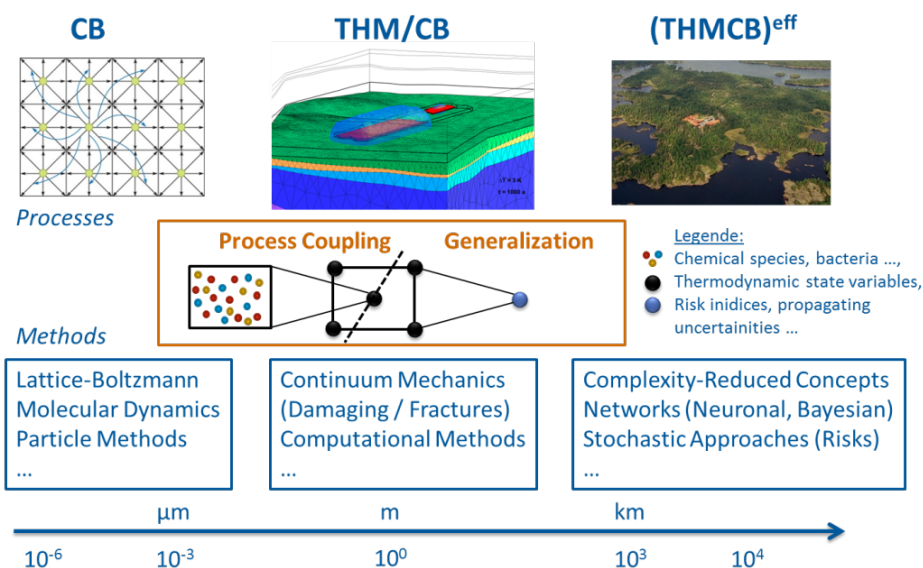
Figure 3-56 – Vision for scale transition schemes: from process to management scales (figure sources: https://developer.nvidia.com, BGR (OGS simulation), Google Earth).

A possible link between the small and large scales, in particular for multi-physics problems such as THMC (Figure 3-57), is continuum mechanics as it is based on first-order principles (conservation laws of mass, momentum and energy). On the other side continuum mechanics invoke thermodynamic consistent, constitutive laws, which may describe complex material behaviour at multiple scales (e.g. micro-mechanics). In addition to fundamental continuum mechanical approaches, numerical methods using significant computational power are available for multi-scale purposes. However, it has to be clearly stated that computational mechanics for sure can handle a certain range of process scales but not the whole required scale chain as shown in Figure 3-58. Therefore, the development of reliable and computational efficient model chains is essential for performance and safety assessment of radioactive waste management.
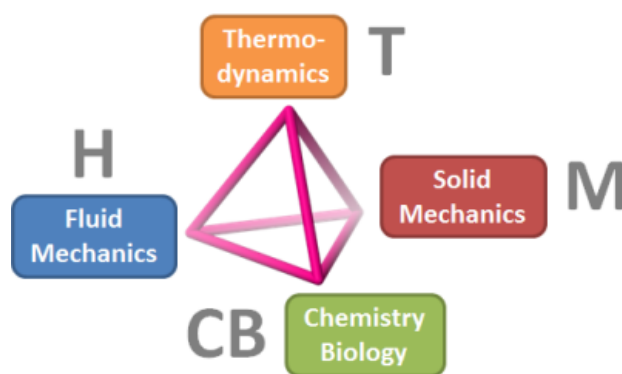
Figure 3-57 – Graphical illustration of thermo-hydro-mechanical-chemical (THMC) processes. The tetrahedron implies that all processes might be directly coupled. The B is added in order to include biogeochemical processes.

EURAD (Deliverable n° 6.1) – Initial State of the Art on Gas Transport in Clayey Materials
Dissemination level: PU
Date of issue of this report: 17/11/2021

Page 219
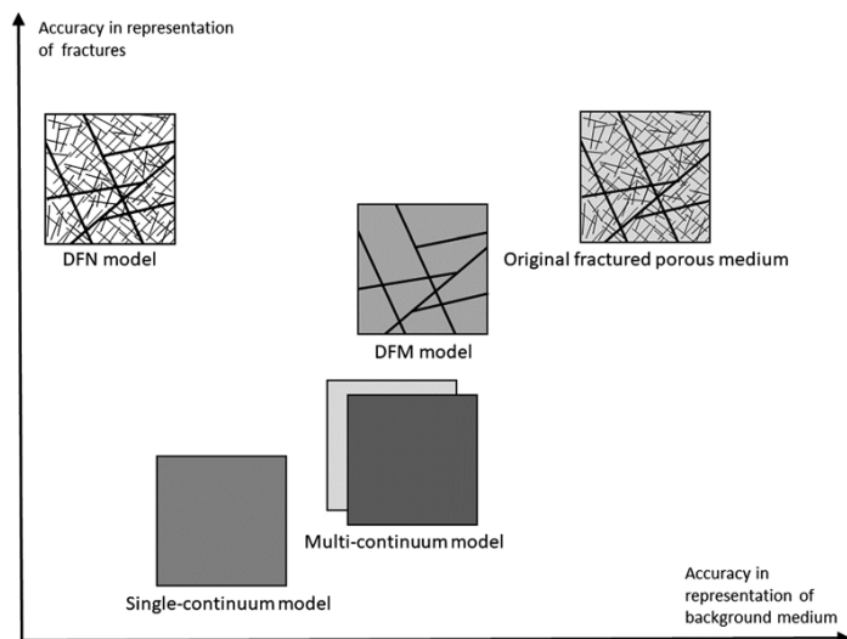
Figure 3-58 – Conceptual approach for fractured porous media (Berre et al. 2019).

In addition to building model chains over scales, as mentioned above, the second challenge for THMC modelling is the presence of discontinuities (e.g. faults, fractures, cracks). Detailed characterisation of the state of the stress (i.e. spatial stress directions and magnitudes) in a field is, if not impossible, extremely difficult. Even if the general stress field of a potential site is reasonably estimated, it is nearly impossible to map a precise description of the pre-existing or excavation-induced fractures and faults and to predict their potential evolution when temperatures, pore pressures, mechanical stresses are changing. For these reasons, characterisation of the earth model is typically combined with stochastic approaches involving multiple realisations in order to bracket the reality. For upscaling, so-called fractured porous media, different methods have been developed in past (Berre et al. 2019), Figure 3-58: (1) Discrete-Fracture-Network (DFN) models explicitly take into account the presence of discontinuities, (2) Single and Multi-Continua approaches use effective, statistically representative parameters for describing fracture behaviour (REV concept). The main idea of Multi-Continua models is to couple multiple continua via exchange functions, where every continuum is representing a typical part, i.e. fracture systems, rock matrix. (3) Discrete-Fracture-Matrix (DFM) models are combining both discrete and continual behaviours. Discrete approaches require very precise numerical methods for accurate representation of exchange processes between fracture and matrix compartments.

3.3.3   THMC processes

Theoretical background has been already given in Sections 3.1.1, 3.1.3 and 3.2.3. Concerning the theoretical background of flow, transport, deformation, and reaction processes in porous media, there is a considerable amount of monographic literature available (Cerfontaine et al. 2015; Chan and Elsheikh 2020; Collin et al. 2006; Collin et al. 2002a; Cuvilliez et al. 2017; Draper et al. 1999; Gens 2018; Eiermann et al. 2007). In the continuity of Section 2.5, the aim of the current section is to provide a concise, as brief-as-possible description (compendium-like) of governing equations for thermo-hydro-mechanical-chemical (THMC) processes in porous media. In Section 2.5, the fundamentals of the models used to reproduce gas transport experiments are described. The focus in the current section is more on the state of implementation in the existing codes and on new developments in THMC modelling including high performance-computation and aspects of data science (Sections 3.3.7, 3.3.10.1). This part will also serve as a reference point for benchmarks and examples investigated in the course of the WP GAS of EURAD. We will point to literature references rather than give detailed derivations of the

EURAD (Deliverable n° 6.1) – Initial State of the Art on Gas Transport in Clayey Materials
Dissemination level: PU
Date of issue of this report: **17/11/2021**
Page 220

governing equations. As already mentioned earlier, there is a large body of literature available (e.g. Johnson et al. 2004; Alkan and Müller 2006) that will not be repeated here.

From the mechanical point of view, we consider non-isothermal flow of multiple fluid phases (compressible and incompressible fluids) in a deformable thermo-poro-elasto-plastic porous medium based on Biot's consolidation concept. The followings steps are conducted to derive the general field equations:

- Macroscopic balance equations for mass, momentum and energy conservation of porous media,
- Constitutive relationships for non-isothermal multiphase flow and deformation processes in porous media.

Figure 3-59 shows a graphical representation of coupled THM phenomena by means of non-linear material behaviour (material properties) and processes (temporal and spatial changes) dependencies (Noorishad and Tsang 1996).

$D_{TV}(T)\nabla T$	= Vapour diffusion along thermal gradient
$\mu(T)$	= Temperature dependent fluid viscosity
$\rho(T)$	= Temperature dependent fluid density
$D_{pV}(T)$	= Temperature dependent vapour diffusion
$\lambda(S)$	= Saturation dependent thermal conductivity
$q_v(h_{pv}+L)$	= Heat convection with vapour flow
$q_l h_{pl}$	= Heat convection with liquid fluid flow
$k(\sigma)$	= Stress dependent permeability
$\beta_T \nabla T$	= Thermal strain
$b_{sw}.\nabla S$	= Moisture (saturation) induced strain
$\alpha.\nabla T$	= Effect of fluid pressure on effective strain
$\alpha \dfrac{\partial \varepsilon_v}{\partial t}$	= Poroelastic volume change

Figure 3-59 – Schematic description of THM coupling processes through material properties, from Noorishad and Tsang (1996).

A comprehensive overview on gas transport processes through low-permeability rock formations can be found in Marschall et al. (2005). Figure 1-2 shows a classification of gas transport processes in poorly permeable rocks into four main transport mechanisms: (i) advective-diffusive transport of gas dissolved in the pore water, (ii) visco-capillary two-phase flow, (iii) dilatancy-controlled gas flow, and (iv) gas transport along fractures. The specific mechanism or combination of several ones depends on both rock properties as well as the thermodynamic (e.g. gas pressure) and hydro-mechanical state (e.g. stress state). The influence of heat transport processes is a particular subject of the WP HITEC of EURAD which is closely linked to the WP GAS.

Uncertainty

The numerical modelling of physical processes is always associated with uncertainties of different origins that need to be considered in order to do a proper performance assessment. The main sources of uncertainties related to radioactive waste repositories stem from:

- Long time scales over which a model is projected. Laboratory or URL experiments prior to a disposal can only be carried out over short time periods.
- Variability of geological features. Their entire characterisation remains challenging.

EURAD (Deliverable n° 6.1) – Initial State of the Art on Gas Transport in Clayey Materials
Dissemination level: PU
Date of issue of this report: **17/11/2021**

Page 221

- Perturbation from sudden geological changes triggered by earthquakes or climate change. Changes of this kind are hard to predict and usually require hybrid modelling approaches.

- Simplification of the conceptual model. It is necessary to evaluate the applicability of a model and its ability to cover all relevant physical phenomena.

Typically, one distinguishes between aleatoric (stemming from natural variability) and epistemic uncertainties (are due to insufficient knowledge). While aleatoric uncertainties can be represented in terms of a known probability density function, the treatment of epistemic uncertainties is not as straightforward. Most of the uncertainties presented above belong to the latter class. Therefore, an important step is a further reduction of uncertainties by validating numerical modelling results against laboratory and field data.

A general overview of different uncertainty quantification and sensitivity methods can be found elsewhere (Helton 1993). Most of the outlined techniques remain pertinent and popular, while also some new methods emerged (e.g. spectral stochastic finite element method (Ghanem and Spanos 1991; Stefanou 2009; Eiermann et al. 2007), or approaches that address epistemic uncertainties specifically, like random set theory (Tonon et al. 2000; Stefanou 2009), or approaches to address global sensitivity (Sobol 2001; Saltelli et al. 2010). The choice of a particular method depends—aside from conceptual aspects—to a large extent on the specific problem, its complexity, and the available computing power. For the purpose of repository modelling, approaches that are relatively general and model-independent (like Monte-Carlo sampling) are typically better suited for treating uncertainties. However, they come with the downside of their computation burden, which is why often a combination of techniques is used.

In the context of radioactive waste repositories, past contributions were mainly concerned with parameter and model uncertainties of transport phenomena (Draper et al. 1999; Zio and Apostolakis 1996, Helton 1993; Saltelli and Tarantola 2002) of radionuclides. A future challenge remains that puts the entire coupled system (i.e. THMC processes) with all its relevant uncertainties under scrutiny.

3.3.4   Governing equations

We provide an overview of the governing equations for TH^{2}M problems (H^2 indicates two-phase flow). The equation system given below shows an example formulation for non-isothermal two-phase flow in porous media. All of the partial differential equations are developed from basic balance equations of mass, linear momentum and energy. For the hydraulic part, gas pressure p_{GR} and capillary pressure p_{cap} have been chosen to be primary variables. Temperature T and displacement $\mathbf{u}_S$ serve as primary variables for the thermodynamic and mechanical parts.

Mass balance governing equations are given by

$$
\underbrace{s_G \left(\phi \beta_{p,GR} + \frac{\alpha_B - \phi}{K_{SR}} \right) \frac{d_S p_{GR}}{dt}}_{\text{storageterm (gas pressure)}} - \underbrace{s_G \left(\phi \beta_{T,GR} + (\alpha_B - \phi)\beta_{T,SR} \right) \frac{d_S T}{dt}}_{\text{thermal expansion}} + \underbrace{s_G \alpha_B \, \text{div} \, \frac{d_S \mathbf{u}_S}{dt}}_{\text{deformation}} \tag{3-5}
$$

$$
- \underbrace{\left(s_G (\alpha_B - \phi)\beta_{p,SR} \left[s_L + p_{cap} \frac{\partial s_L}{\partial p_{cap}} \right] + \phi \frac{\partial s_L}{\partial p_{cap}} \right) \frac{d_S p_{cap}}{dt}}_{\text{storage term (capillary effects)}} + \underbrace{\text{div} \, (\widetilde{\mathbf{w}}_{GS})}_{\text{gasflow}} = 0
$$

for the gas phase and

EURAD (Deliverable n° 6.1) – Initial State of the Art on Gas Transport in Clayey Materials
Dissemination level: PU
Date of issue of this report: **17/11/2021**

Page 222

$$\underbrace{s_{\mathrm{L}}\left(\phi\beta_{p,\mathrm{LR}} + \frac{\alpha_{\mathrm{B}} - \phi}{K_{\mathrm{SR}}}\right)\frac{\mathrm{d}_{\mathrm{S}} p_{\mathrm{GR}}}{\mathrm{d}t}}_{\text{storage term (gas pressure)}} - \underbrace{s_{\mathrm{L}}\big(\phi\beta_{T,\mathrm{LR}} + (\alpha_{\mathrm{B}} - \phi)\beta_{T,\mathrm{SR}}\big)\frac{\mathrm{d}_{\mathrm{S}} T}{\mathrm{d}t}}_{\text{thermal expansion}} + \underbrace{s_{\mathrm{L}}\alpha_{\mathrm{B}}\,\mathrm{div}\,\frac{\mathrm{d}_{\mathrm{S}}\mathbf{u}_{\mathrm{S}}}{\mathrm{d}t}}_{\text{deformation}} \qquad (3\text{-}6)$$

$$-\underbrace{\left(s_{\mathrm{L}}(\alpha_{\mathrm{B}} - \phi)\beta_{p,\mathrm{SR}}\left[s_{\mathrm{L}} + p_{\mathrm{cap}}\frac{\partial s_{\mathrm{L}}}{\partial p_{\mathrm{cap}}}\right] + \phi\left[s_{\mathrm{L}}\beta_{p,\mathrm{LR}} - \frac{\partial s_{\mathrm{L}}}{\partial p_{\mathrm{cap}}}\right]\right)\frac{\mathrm{d}_{\mathrm{S}} p_{\mathrm{cap}}}{\mathrm{d}t}}_{\text{storage term (capillary effects)}} + \underbrace{\mathrm{div}\,(\widetilde{\mathbf{w}}_{\mathrm{LS}})}_{\text{liquid flow}} = 0$$

for the liquid phase.

Phase saturation s_α is the ratio of phase volume fraction ϕ_α (for $\alpha = \mathrm{L}, \mathrm{G}$) to porosity ϕ, with $s_{\mathrm{G}} = 1 - s_{\mathrm{L}}$ and where s_{L} is usually a function of capillary pressure. The volume fraction ϕ_α is the ratio of the volume occupied by phase α over the total volume ($\mathrm{d}\Omega_\alpha(\mathrm{d}\Omega^{-1})$). The *Darcy*-velocities $\widetilde{\mathbf{w}}_{\alpha\mathrm{S}}$ given by

$$\phi_\alpha \mathbf{w}_{\alpha\mathrm{S}} = \widetilde{\mathbf{w}}_{\alpha\mathrm{S}} = -\frac{k_\alpha^{\mathrm{Rel}}\mathbf{k}_{\mathrm{S}}}{\mu_{\alpha\mathrm{R}}}(\,\mathrm{grad}\,p_{\alpha\mathrm{R}} + \rho_{\alpha\mathrm{R}}\mathbf{a}_\alpha - \rho_{\alpha\mathrm{R}}\mathbf{b}_\alpha) \qquad (3\text{-}7)$$

are velocities of the fluid phases relative to the deforming solid phase. The remaining symbols are defined in Table 3-5. The Energy equation for the overall multiphase aggregate can be written as

$$\underbrace{(\rho c_p)_{\mathrm{eff}}\frac{\mathrm{d}_{\mathrm{S}} T}{\mathrm{d}t}}_{\text{thermalenergystorage}} - \underbrace{(\phi_{\mathrm{L}}\beta_{T,\mathrm{LR}} + \phi_{\mathrm{G}}\beta_{T,\mathrm{GR}} + \phi_{\mathrm{S}}\beta_{T,\mathrm{SR}})T\frac{\mathrm{d}_{\mathrm{S}} p_{\mathrm{GR}}}{\mathrm{d}t}}_{\text{pressureworkstorage(gasphase)}} + \underbrace{\beta_{T,\mathrm{LR}}T\widetilde{\mathbf{w}}_{\mathrm{LS}} \cdot \,\mathrm{grad}\,p_{\mathrm{cap}}}_{\text{advection}}$$

$$+ \underbrace{\left(\phi_{\mathrm{L}}\beta_{T,\mathrm{LR}}T + \phi_{\mathrm{S}}\beta_{T,\mathrm{SR}}T\left(s_{\mathrm{L}} + p_{\mathrm{cap}}\frac{\partial s_{\mathrm{L}}}{\partial p_{\mathrm{cap}}}\right) + \phi p_{\mathrm{cap}}\frac{\partial s_{\mathrm{L}}}{\partial p_{\mathrm{cap}}}\right)\frac{\mathrm{d}_{\mathrm{S}} p_{\mathrm{cap}}}{\mathrm{d}t}}_{\text{pressureworkstorage(gasandliquidphase)}} + \underbrace{\mathrm{div}\,\mathbf{q}}_{\text{heatconduction}}$$

$$- \underbrace{(\beta_{T,\mathrm{LR}}\widetilde{\mathbf{w}}_{\mathrm{LS}} + \beta_{T,\mathrm{GR}}\widetilde{\mathbf{w}}_{\mathrm{GS}})T \cdot \,\mathrm{grad}\,p_{\mathrm{GR}} + (\rho_{\mathrm{LR}}c_{p\mathrm{L}}\widetilde{\mathbf{w}}_{\mathrm{LS}} + \rho_{\mathrm{GR}}c_{p\mathrm{G}}\widetilde{\mathbf{w}}_{\mathrm{GS}}) \cdot \,\mathrm{grad}\,T = 0}_{\text{advection}}$$

where the assumption of local thermal equilibrium was made. This assumption follows the idea that heat transfer among the phases occurs very fast such that all phases share the same temperature at a certain point. The effective heat capacity of the overall aggregate $(\rho c_p)_{\mathrm{eff}}$ is defined as $(\rho c_p)_{\mathrm{eff}} = \sum_\alpha \phi_\alpha \rho_{\alpha\mathrm{R}} c_{p,\alpha}$ for $\alpha = \mathrm{G}, \mathrm{L}, \mathrm{S}$ with intrinsic phase mass densities $\rho_{\alpha\mathrm{R}}$. Similarly, the combined heat conductive flux $\mathbf{q} = \mathbf{q}_{\mathrm{GLS}}$ is defined as $\mathbf{q} = \sum_\alpha \mathbf{q}_\alpha$.

The mechanical part of the equation system is governed by the displacement equation given by

$$0 = \rho\mathbf{b} + \,\mathrm{div}\,\big(\boldsymbol{\sigma}_{\mathrm{S}}^{\mathrm{E}} - \alpha_{\mathrm{B}} p_{\mathrm{FR}}\mathbf{I}\big) \qquad (3\text{-}8)$$

where ρ is the bulk density of the overall multiphase aggregate defined as $\rho = \sum_\alpha \phi_\alpha \rho_{\alpha\mathrm{R}}$ for $\alpha = \mathrm{G}, \mathrm{L}, \mathrm{S}$ and $\mathbf{b}$ are body force accelerations acting equally on all phases. The total stress $\boldsymbol{\sigma}$ is given by the effective stress $\boldsymbol{\sigma}_{\mathrm{S}}^{\mathrm{E}}$, which is governed by constitutive laws, attenuated by the pore fluid pressure p_{FR}, which is given by $p_{\mathrm{FR}} = \sum_\alpha s_\alpha p_{\alpha\mathrm{R}}$. To close the above equation system, constitutive laws or material property relations are required.

European Joint Programme on Radioactive Waste Management

EURAD (Deliverable n° 6.1) – Initial State of the Art on Gas Transport in Clayey Materials
Dissemination level: PU
Date of issue of this report: **17/11/2021**

Page 223

Table 3-5 – Symbols of governing equations.

Symbol	Description
$\beta_{p,\text{GR}}$	gas phase compressibility
$\beta_{p,\text{LR}}$	liquid phase compressibility
$\beta_{T,\text{GR}}$	gas phase thermal expansivity
$\beta_{T,\text{LR}}$	liquid phase thermal expansivity
$\beta_{T,\text{SR}}$	solid phase thermal expansivity
K_{SR}	compression modulus of solid phase
$\dfrac{\mathrm{d}_\text{S}(\bullet)}{\mathrm{d}t}$	material time derivative of $\bullet$ w.r.t. solid phase

3.3.5 Material behaviour

Rock mechanical behaviour normally is investigated based on laboratory tests on related specimens. Within this context, similar stress-strain curves can be caused by different physical effects, e.g. a non-linear stress-strain curve does not necessarily suggest inelastic material behaviour. For the sake of clarity, it is possible to introduce a classification of materials based on some essential, distinctly identifiable material phenomena. For instance, comparatively simple experiments can be performed to investigate if the stress-strain curves are rate-dependent, and if hysteresis phenomena occur, indicating dissipative effects. Based on these assumptions the observable material behaviour can be divided into four different basic classes as depicted in Figure 3-60 (Haupt 2002):

- rate-independent without hysteresis,

- rate-independent with hysteresis,

- rate-dependent without hysteresis, and

- rate-dependent with hysteresis.

Even though, there exists a clear classification of constitutive material models, implementation into FEM codes is still done in separate ways which is prone to introduce new errors again when re-implementing material functions. Code generators such as MFront have been developed to overcome these difficulties. Mfront allows the development of material behaviours using a syntax very close to the mathematical description of the constitutive equations and make them available to solvers through dedicated interfaces or using a generic interface. This simplifies the numerical development of new material behaviours by minimising errors during the implementation. Using code generator like MFront facilitates the portability of constitutive equations between solvers and leads to a reproducible and efficient code. The integration of material behaviours using the generic interface provided by MFront is presented exemplary in Section 3.3.7 in the case of the solver OpenGeoSys (Helfer et al. 2020).

For the host rocks and buffer materials into investigations in this project, specific material behaviours have to be accounted for:

- strength (failure, tensile),

- anisotropy,

- effect of water content,

- effect of pore pressure,

- permeability evolution,

- effect of swelling,

EURAD (Deliverable n° 6.1) – Initial State of the Art on Gas Transport in Clayey Materials
Dissemination level: PU
Date of issue of this report: 17/11/2021

Page 224

- temperature effects,

- sealing and healing effects.

All these phenomena have some influence on the ability of clayey materials to retain gases and should be taken into considerations in the numerical treatment of gas transport mechanisms in clayey materials.

Claystone like the Callovo-Oxfordian claystone (COx) for instance are subjected to a quasi-brittle to ductile behaviour under triaxial compression and a brittle behaviour under tension loading. Under deviatoric stresses claystone show an elasto-plastic response which evolves into a quasi-brittle failure at low confining stresses. The failure is characterised by the formation of macro cracks. After the peak the stress level in the rock decrease sharply and the rock behaves thereafter as cohesion-less frictional material (Seyedi et al. 2017).
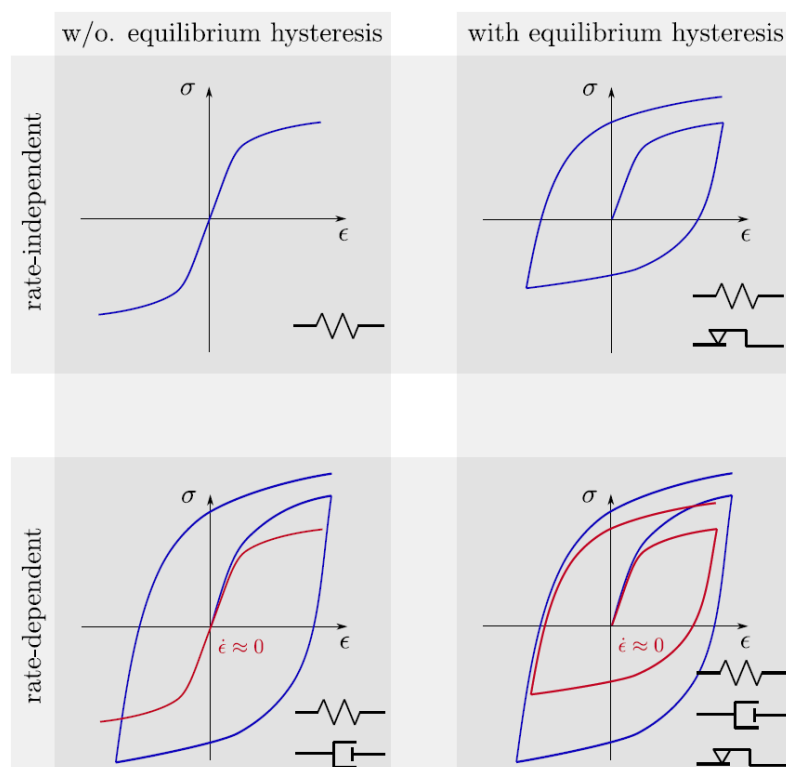
Figure 3-60 – Classification of constitutive relationship for material modelling, Top: cyclic uniaxial stress-strain curves for elastic (left) and elasto-plastic behaviour (right); bottom: cyclic uniaxial stress-strain curves for visco-elastic (left) and visco-plastic behaviour (right), after Haupt (2002).

Several constitutive material models have been developed to reproduce the hydro-mechanical behaviour of claystone. The models displayed in Table 3-6 have been used during a benchmark exercise organised by Andra and their capabilities have been tested against in situ data. These models can be categorised in four groups. Some using the framework of visco-elasto-plasticity. Others are based on damage mechanics. The rest are using relatively new numerical approaches of the rigid block spring method or the computational homogenised method. All models are capable to predict the damage of the rock. Most of them take into account the time-dependent behaviour of the rock. A good half consider the mechanical anisotropy of the rock into their formulation (Seyedi et al. 2017). The majority of the models was able to reproduce the behaviour of the rock observed in situ. This set of models can be seen as the state of the art in that matter.

EURAD (Deliverable n° 6.1) – Initial State of the Art on Gas Transport in Clayey Materials
Dissemination level: PU
Date of issue of this report: **17/11/2021**

Page 225

Table 3-6 – Overview of state-of-the-art constitutive material models for claystone (Seyedi et al. 2017).

Research teams and model used.

Team/model name	Model type	Failure criterion	Time dependent behavior	Mechanical anisotropy
EDF	Elasto-visco-plasticity	A generalized Hoek & Brown type failure criterion with hardening and softening functions	Perzyna type model with accounting for tertiary creep	No
GeoRessources	Elasto-visco-plasticity	Drucker-Prager including the effect of σ_{moy}	Lemaitre's type with creep threshold	No
INERIS	Elasto-visco-plasticity	A generalized Hoek & Brown type failure criterion with hardening and softening functions	Lemaitre's type with creep threshold and damage-dependent creep strain rates	No
PRISME	Elasto-visco-plasticity	Power type failure function with hardening/softening	The creep is governed by a kinematic hardening law accounting for *in situ* stress state	Anisotropic elasticity
ULg_1	Elasto-visco-plasticity with localization treatment	Drucker-Prager with a hardening law on friction angle/cohesion	No	No
ULg_2	Elasto-visco-plasticity with localization treatment	The same with anisotropic cohesion	No	Yes
UPC	Elasto-visco-plasticity	Mohr-Coulomb criterion for the yield and failure limits and its anisotropic extension	Modified form of the Lemaitre law for visco-plastic strains	Yes
LML_1	Elastoplasticity with isotropic damage	Strain based criterion with distinction between compression and extension damage	Creep strain modeled as a retarded elastoplastic strain	No
LML_2	Elastoplasticity with anisotropic damage	Strain based criterion with distinction between compression and extension damage and anisotropy accounted through a fabric tensor	Creep strain modeled as a retarded elastoplastic strain	Yes
LML_3	Rigid Body-Spring Model (RBSM)	Isotropic or anisotropic criterion for interface failure	No	Yes
EGC	Anisotropic damage model	Double strain based criterion in extension/compression	Time-dependent strains calculated through a creep law calibrated based on creep tests	Yes in extension
3SR	Computational homogenized model (CHM)	A double-scale finite element method (FEM2) using a representative elementary volume (REV) to model the material behavior at the micro scale. The global response of this REV serves as a homogenized numerical constitutive law for the macro scale	No	Yes

In most repository concepts under consideration in Europe, bentonites play a major role as the principal sealing material for the engineered barrier system (Table 1-1). Bentonites are used in the form of highly compacted blocks, of pellets, of granular bentonite and of sand/bentonite mixture). Each type requires different manufacturing processes leading to various kind of heterogeneity at the macro or mesoscale. This makes bentonites difficult to predict numerically. The mechanical behaviour of bentonite is strongly coupled with its hydraulic behaviour. Bentonite also exhibits complex effects such as swelling, irreversibility and stress path dependence. Due to this complexity, the European Union initiated a pan-European research project with the acronym BEACON with the aim to further develop and test available material models assessing the mechanical evolution of installed bentonite barrier. The models being developed in the scope of BEACON are described below (Gens 2018):

- **Barcelona Expansive Model – BExM** (UPC Barcelona, ES): The model presented by UPC is an improved version of the Barcelona Expansive Model (BExM) based on elasto-plasticity and a double structure formulation. The interaction between the two structure levels is expressed by means of interaction functions. Only isothermal conditions are considered. The following enhancements have been incorporated: A more consistent definition of porosity and volume fractions; the microstructure may be unsaturated; a consistent relationship for the elastic parameters of microstructure and macrostructure; no hydraulic equilibrium between microstructure and macrostructure; a linear relationship for the water exchanges between microstructure and macrostructure; a more physically based definition of the interaction functions.

- **Hypoplastic model for unsaturated expansive soils** (Charles University, CZ): The CU model is a double structure formulation developed within the framework of hypoplasticity incorporating over-consolidation ratio, water retention hysteresis, non-isothermal extension.

- **BGR Bentonite model** (BGR, DE): The model takes into account a linear elastic behaviour and it is formulated in terms of effective stresses that incorporate Biot's coefficient. To account for the

EURAD (Deliverable n° 6.1) – Initial State of the Art on Gas Transport in Clayey Materials
Dissemination level: PU
Date of issue of this report: 17/11/2021

Page 226

expansive behaviour of the bentonite, a linear swelling model component based on a linear relationship between swelling stress and water saturation.

- **Hysteresis Based Material** (Clay Technology, SE): The CU model is a double structure formulation developed within the framework of hypoplasticity incorporating over-consolidation ratio, water retention hysteresis and non-isothermal extension.

- **Advanced Constitutive Model for Environmental Geomechanics – ACMEG** (EPFL, CH): the model put forward by EPFL is a quite general constitutive model, based on elasto-plasticity, for saturated and unsaturated soils and for both isothermal and non-isothermal conditions. It belongs to the current stage of evolution of a suite of models that have progressively incorporated new phenomena and new capabilities.

- **Imperial College –Double Structure model – IC DSM** (Imperial College, UK): IC DSM model is a development of an existing single structure model of IC defined in the framework of elasto-plasticity. It shares a number of features with BExM and the Barcelona Basic Model (BBM). Some significant developments of this model are: air entry suction, flexible shape for the definition of yield surface, non-associated plasticity, Matsuoka-Nakai shape for the deviatoric plane.

- **Internal Limit Model** (Quintessa, UK): the model is empirically based and incorporates three important relationships: the swelling pressure versus dry density; suction versus water content; void ratio versus vertical stress. The full formulation of the model as a fully couple thermo-hydro-mechanical model incorporates the Modified Cam-Clay model to account for plastic deformation.

- **Teknologian tutkimuskeskus bentonite model** (VTT, FI): The adopted elasto-plastic mechanical model uses a double structure assumption. The two constitutive mechanical models BBM and BExM are adopted as modelling frameworks for the macro-and the microstructure and the coupling between them in confined conditions. The formulation of the BBM and BExM has been modified to allow for anisotropy in the stress-strain relationship. In addition, the model has been extended using a state surface approach that accounts for chemo-mechanical coupling and for free swelling processes.

- **Université de Liège bentonite model** (ULg, BE): The model developed by ULg differs from other models in the fact that a double porosity is adopted for the hydraulic component of the model whereas a single structure model is used for the mechanical component. Only isothermal conditions are addressed. Water storage and hydration mechanisms are considered in a double structure framework. The basic parameter in the hydraulic formulation is the water ratio that is considered distributed in the two levels of porosity. For the mechanical behaviour, the model uses the BBM model.

Prior to EURAD, gas transport in clay has been extensively investigated during the FORGE EC project. One of the main outcomes of this project was that a consensus emerged that the transport of free gas in such low-permeability clayey materials saturated with water or close to saturation occurs by the creation of specific gas pathways, which translate into sample dilatancy or the creation/ re-activation of discontinuities in the material that is being tested (Shaw 2013). Several teams have been trying since to incorporate these new findings into numerical modelling. Various constitutive models for gas transport in clay rocks and bentonites are briefly introduced (non-exhaustive):

- **Gas pressure dependent permeability approach** by Xu W. et al. (2011) for lower and higher gas pressures: In this model it is assumed (i) if gas pressure is lower than a critical value p_{thr} the change of gas pressure can only cause extension or compaction of pore space, which has limited effect on permeability, (ii) if gas pressure exceeds the critical threshold level, micro-cracks are generated and the permeability increases significantly due to connection and propagation of micro-cracks.

$$\mathbf{k} = f(p_g)\,\mathbf{k}_{\text{int}}^{\text{ini}} = \begin{cases} (1 + a_1 p_g)k_{\text{int}}^{\text{ini}} & p_g \leq p_{\text{thr}} \\ (a_2(p_g - p_{\text{thr}}) + 1 + a_1 p_{\text{thr}})k_{\text{int}}^{\text{ini}} & p_g > p_{\text{thr}} \end{cases} \tag{3-9}$$

![eurad logo] European Joint Programme on Radioactive Waste Management

EURAD (Deliverable n° 6.1) – Initial State of the Art on Gas Transport in Clayey Materials
Dissemination level: PU
Date of issue of this report: 17/11/2021

Page 227

- **Deformation dependent permeability approach** by Xu W. et al. (2013): This approach assumes that the permeability development is controlled by the deformation process. The model is composed of the volumetric strain ε_{vol} and the equivalent plastic strain and has been successfully applied for gas injection experiments in laboratory tests (conducted by the Institut für Gebirgsmechanik (IfG Leipzig)) and the HG-B experiment in Mont Terri (conducted by BGR Hannover).

$$\boldsymbol{k} = f(\Delta \varepsilon_{vol})\, e^{b_1 \Delta \bar{\varepsilon}^p}\, \boldsymbol{k}_{int}^{ini} \tag{3-10}$$

with

$$f(\Delta \varepsilon_{vol}) = \begin{cases} 10^{b_2 \Delta \varepsilon_{vol}} & compaction \\ 10^{b_3 \Delta \varepsilon_{vol}} & extension \end{cases} \tag{3-11}$$

- **Hydro-mechanical permeability model** (by ULg, Belgium): The model uses a two-phase flow approach to reproduce water and helium transfers in partially saturated porous media. It comprises a liquid phase, composed of liquid water and dissolved helium and a gaseous phase. It takes into account the advection of each phase using the Darcy's law and the diffusion of the components within each phase (Fick's law). The retention curve and the water relative permeability curve are given by the van Genuchten's model. The gas relative permeability curve is a cubic function. The hydro-mechanical parameters for claystone are used in the model. The model includes also a hydro-mechanical coupling between the pathways aperture, permeability and gas entry pressure.

- **Gas permeability model enhanced with 'tube-chamber' (**by GRS, Germany): In order to reproduce numerically gas and water flow through dilating pathways in claystone, the model proposed by GRS uses continuum features on the basis of TOUGH2 enhanced with so-called 'tube-chamber models' with analytic flow calculations. In the conceptual model it is assumed that micro-cracks open inside the rock if the local pore pressure exceeds a certain pressure threshold. The aperture of the cracks depends on pore pressure. The model assumes therefore a threshold pressure below which the main flow paths are closed and effective gas permeability and dilation increase linearly with the pressure. This process continues until pore pressures reach the threshold pressure thereby stopping the dilation process and microscopic tensile failure occurs.

- **Gas permeability model for gas flow through clay barrier** (by UPC Barcelona, Spain) The model proposed for the simulation of gas flow in clayey rocks and clays handles the combined phenomena of two-phase (air and liquid) flow and the generation of discrete paths. It uses for that the aperture of discrete paths as the main variable to account for permeability and capillary pressure variations. The model, which has been implemented in a general thermo-hydro-mechanical code and has been tested so far on different laboratory and field experiments.

- **Gas permeability model for saturated bentonite with double porosity and double effective stress concepts** (by Guo and Fall 2018) who developed a fully coupled hydro-mechanical model, which incorporates the concepts of double porosity and double effective stress. The model is used to simulate the gas transport process in saturated bentonite. It is able to predict the main experimental phenomena of gas transport in clay including the gas breakthrough, the volume dilation, the matrix consolidation, the build-up of water pressure and the 'shut-in' pressure. Two important processes that contribute to the development of preferential pathways, i.e. the dilation of the fractured porous media and the consolidation of the porous continuum, can be well predicted by the model.

EURAD (Deliverable n° 6.1) – Initial State of the Art on Gas Transport in Clayey Materials
Dissemination level: PU
Date of issue of this report: **17/11/2021**

Page 228

3.3.6   Numerical methods

Similar to the available literature, over the past decades a considerable diversity of numerical methods have been developed for the simulation of THMC coupled processes such as finite differences, elements, and volume methods, respectively. A list of mostly used numerical codes is compiled in the following Section 3.3.7 (not meant to be complete).

In addition to the continuum mechanical approaches, various discontinuum methods have been developed in recent times such as lattice (LEM) and distinct element methods (DEM). These discontinuum approaches have been mainly used for rather small-scale applications representing process details at atomistic or molecular levels. Other conceptual approaches, e.g. meshless methods, such as the smoothed-particle-hydrodynamics (SPH) methods came into play. SPH is based on the Lagrangian concept for solving the underlying partial differential equations for multi-field problems and has certain advantages for upscaling and computational efficiency. Thanks to the progress in computational power, those methods are entering now more and more application levels. A recent overview of numerical methods for THM coupled processes in barrier rocks can be found in Kolditz et al. (2020).

The WP GAS is focusing on the combination of experimental and modelling work to better understand gas transport processes in clayey materials and in particular mechanical effects (Section 3.3.3). For more details in model and code development please refer to the WP DONUT of EURAD.

3.3.7   Computational methods and tools

Many research areas largely benefit from new developments in information technology in many ways in particular data- and computational geosciences. Figure 3-61 shows the high-performance-computing (HPC) concept starting with development and testing methods at smaller machines (Tier 3) and then implementation of high-end infrastructure (Tier 2-0). Container technologies (e.g. Docker, Singularity) are used for standardisation and portability of HPC solutions (Bilke et al. 2019). Scalability of numerical methods for coupled THMC simulations is a particular challenge.

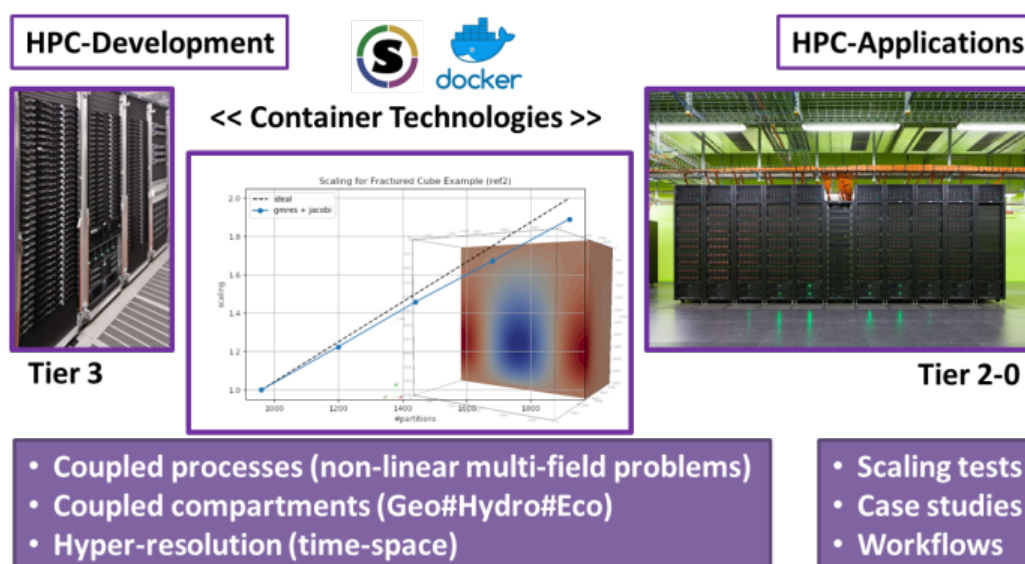*Figure 3-61 – High-performance-computing.*

Open source concepts are becoming more and more popular in geosciences. This is due to various reasons such as necessity of handling big data amounts, e.g. concerning observation and monitoring

EURAD (Deliverable n° 6.1) – Initial State of the Art on Gas Transport in Clayey Materials
Dissemination level: PU
Date of issue of this report: **17/11/2021**
Page 229

data from remote sensing, but also the progress in general software development, e.g. Python frameworks, which allows a broad use of existing components for own purposes (Bhatt et al. 2020; Yu Q. et al. 2019; Yao et al. 2019). Open source software for porous media mechanics is making progress but still lagging behind the general trend (Kolditz et al. 2012; Taron et al. 2014; Bilke et al. 2019; Baumgarten and Wieners 2020; Pastusek et al. 2019; Koch et al. 2020).

As mentioned above (Section 3.3.5) implementation of constitutive relationships is still a one-by-one repeated procedure for most existing codes. Meanwhile Code_Aster and OpenGeoSys are using generic interfaces to MFront code – a leading tool in material modelling developed by CEA and EDF (Helfer et al. 2020).

Figure 3-62 illustrates the coupling scheme between the finite element method (here OGS) and MFront via the generic interface MGIS. The numerical method feeds the state (strain estimates) for specific times to MFront and receives back the updated state and consistent tangent. The entire procedure is embedded into a global Newton method. This generic interface between numerical and constitutive modelling provides various advantages such as intuitive and unified constitutive syntax, independent testing of both modules and therefore easier development and debugging, combining quality standards etc. The code generated automatically, worthwhile to mention that all codes are open source. The biggest advantage of course is the structured and product-oriented scientific collaboration between the developer teams.
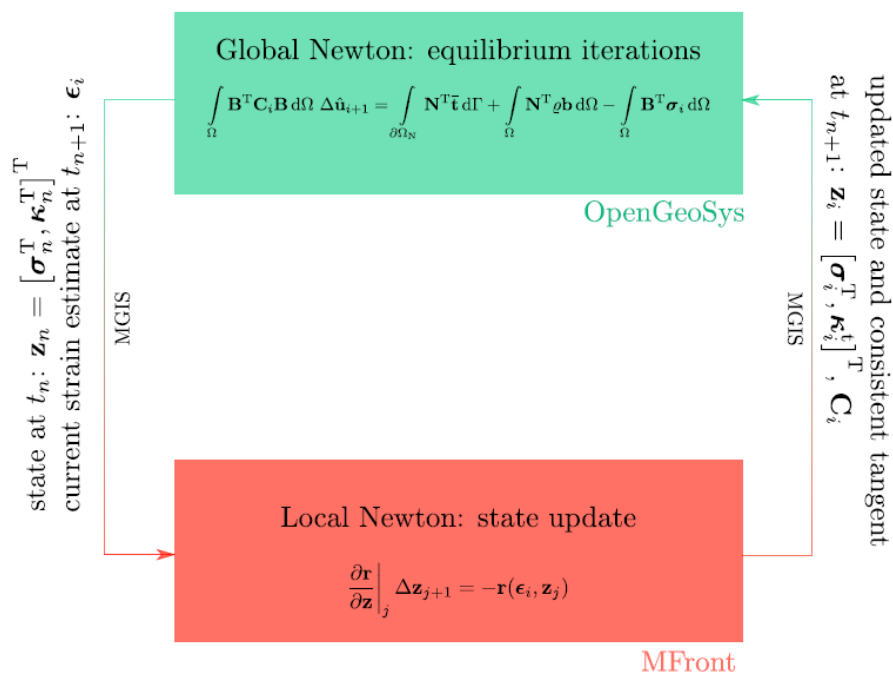
Figure 3-62 – OGS#MFront interface.

3.3.8   Benchmark definitions

For the verification of new code developments, a variety of single benchmark collections has been published and for some simplified benchmarks, analytical solutions are available. However, from code to code, there are underlying differences which lead to deviations from results obtained using different codes. Different code implementations at times make varying assumptions or even consider dissimilar physical processes altogether. Research projects such as DECOVALEX (Birkholzer et al. 2019) or

EURAD (Deliverable n° 6.1) – Initial State of the Art on Gas Transport in Clayey Materials
Dissemination level: PU
Date of issue of this report: 17/11/2021

Page 230

BenVaSim (Lux and Rutenberg 2018) focus on studying the implications of the various implementations of codes on the deviation of the results and therefore also validate models and codes.

Table 3-7 illustrates an overview of laboratory experiments planned in the WP GAS of EURAD. These systematic experimental approaches based on oedometer test, triaxial and shear box experiments will be accompanied and designed by appropriate modelling work. As a result, model-experiment-exercises (MEX) will be generated serving as benchmarks for both experiments and models equally (Kolditz et al. 2020).

Table 3-7 – Overview of laboratory experimental benchmarks (from Nagra 2020).

EXP	Type of experiment	M58	Materials	BGE	BGR	EDF IC2	UFZ	ULG	TUDe	UPC	CNRS-UPoi
	Lab tests	3.2.3									
GRS	Gas injection tests in fractured samples / hollow cylinder	HC	OPA (different facies)		green		yellow				
CIMNE	Gas injection tests oedometer cell	OED	Boom clay				green	green	green	green	
			OPA				green		green	green	
			Bentonite	green					green		
CTU	Gas breakthrough cycles oedometer cell	OE	Bentonite (BCV)		green		green				
EPFL	Gas injection tests with strain measurements in triaxial cell	TX	OPA		green		green				
	High-stress oedometer and triaxial setups	OE/TX	Bentonite	green							
BGS	Gas injection and shear fractures/fractures surfaces analysis, shear box	SB	Boom clay				yellow	green			
		SB	COx				yellow			green	
		SB	Synthetic samples (sand/silt/clay end members)				yellow				
IRSN	Gas injection tests under X Ray – CT scan, gas injection test under constant volume and effect of mixture heterogeneities	OE	MX80 bentonite pellets and powder mixture								
CNRS ULorraine	Triaxial compression tests under X-ray tomography with continuous gas permeability measurement	TX	COx					green			green
	Triaxial self-sealing tests under X-ray tomography with water/gas permeability measurement	TX						green			green

3.3.9 Overview of available process-level models and tools

Based on previous synoptic code overviews, e.g. Alkan and Müller (2006) and Steefel et al. (2015), this SOTA strives to update a code overview for modelling of THMC processes in clayey materials. Table 3-8 starts this process (not being complete). It will be continuously updated over the course of the project and will be expanded upon in the second version of the SOTA (to be issued at the end of the project). The synoptic table is followed by a short description on the EURAD GAS codes (please refer also to milestone EURAD-GAS-MS58 (Nagra 2020) for more information).

Table 3-8 – Code overview (P: processes, I: interfaces, S: software, W: websites).

Code	Origin	Features	Coupling		References
Code_Aster	EDF	3D FEM	THM	P: Fully coupled THM processes I: MUMPS and PETSc (linear solvers, parallelisation), MFront (material modelling) S: Software engineering based on continuous integration with code reviews - Integration in Salome platform – open source software W: www.code_aster.org	Raude et al. 2016 Cuvilliez et al. 2017 Mahjoub et al. 2018 Faivre et al. 2016 Paul et al. 2018
Code_BRIGHT	UPC	3D FEM	THM	P: coupled THM processes	

EURAD (Deliverable n° 6.1) – Initial State of the Art on Gas Transport in Clayey Materials
Dissemination level: PU
Date of issue of this report: 17/11/2021

Page 231

Code	Origin	Features	Coupling		References
Lagamine FE	ULiège	3D FEM	THMC	P: Partitioned and fully coupled (monolithical) THMC processes I: linear solvers and parallelised version S: Software engineering based on continuous integration with code reviews	Collin et al. 2006 Collin et al. 2002a Cerfontaine et al. 2015
OpenGeoSys	Community	3D FEM	THMC	P: Partitioned and monolithic coupling schemes for THM I: EIGEN (algebra), PETSc (parallelisation), PhreepC(chemistry), MFront (material modelling) S: Software engineering based on continuous integration with code reviews W: www.opengeosys.org, https://github.com/ufz/ogs	Bilke et al. 2019 Kolditz and Bauer 2004; Wang and Kolditz 2007; Kolditz et al. 2012
THOUGH2/3	DOE/LBNL	3D FVM	TH3	most applied multiphase code, mechanical processes are coupled via FLAC W: https://tough.lbl.gov	

Among many other THMC codes (Alkan and Müller 2006) in the WP GAS of EURAD, the following numerical platforms are used and further developed within EURAD GAS: Code_Aster, CODE_BRIGHT, Lagamine FE and OpenGeoSys. A short introduction to these codes can be found in the appendix.

3.3.10 Outlook: ongoing developments

The present state-of-the-art description provides a common ground for the activities of the WP GAS of EURAD. The large body of existing literature is briefly summarised earlier and references are given. As for future perspectives, a particular challenge for numerical simulation is an implementation or re-implementation of methodologies in modern software packages to make THMC codes fit for new computational platforms (e.g. Exascale computing). In addition, from the start of EURAD, future directions in comprehensive systems analysis are being taken into account[27]. These are outlined briefly in this section with a focus on data science, starting with seamless analysis workflows, virtualisation and machine learning concepts.

3.3.10.1 Workflows and virtualisation

Intelligent use of information technology will foster the development and implementation of seamless analysis workflows in many research areas. Figure 3-63 illustrates the concept for geotechnical applications starting with data integration from URLs, set-up of adequate models for experimental analysis and design. High-Performance-Computing (HPC) concepts for THMC simulations allow realistic analysis of process complexity and predictions. Virtual Reality makes outcomes accessible for specialists and a public audience as well.

---

[27] This goes, however, much beyond the scope of the WP GAS of EURAD. A partnership is being developed with WP DONUT to explore the possibilities in this domain and possibly initiate some developments.
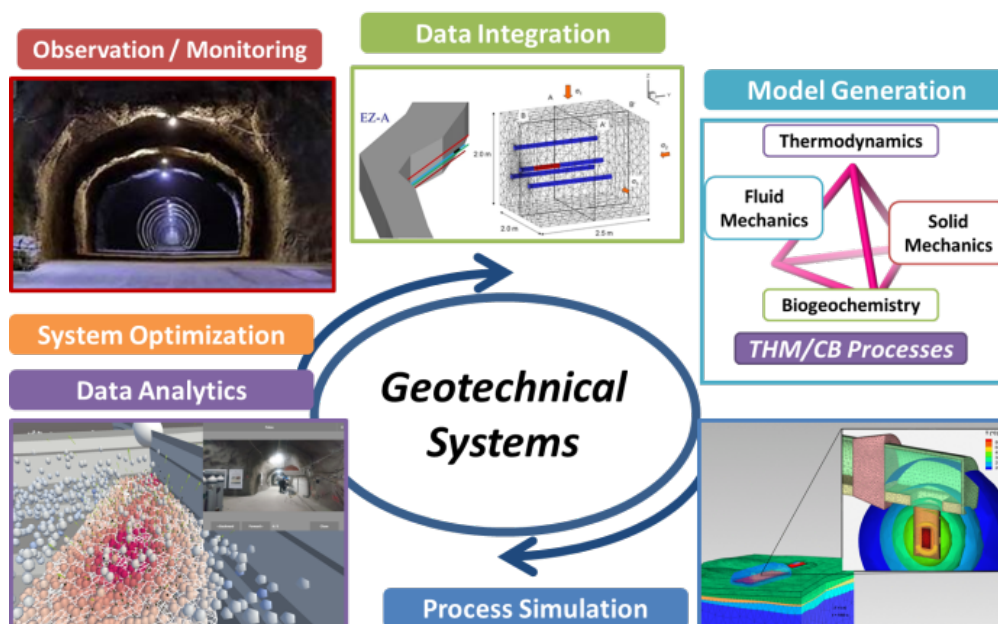
EURAD (Deliverable n° 6.1) – Initial State of the Art on Gas Transport in Clayey Materials
Dissemination level: PU
Date of issue of this report: 17/11/2021

Page 232

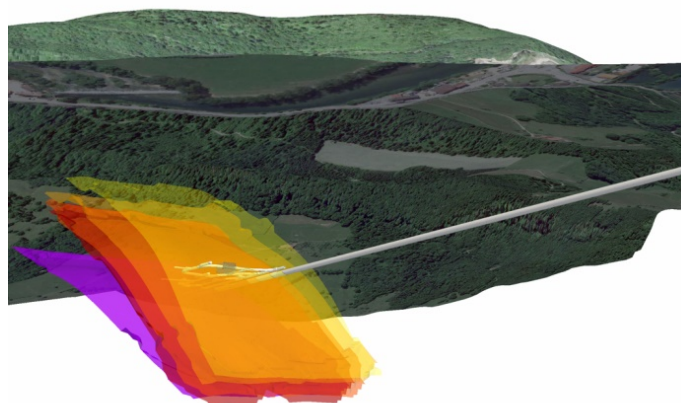*Figure 3-63 – Seamless analysis workflows (Kolditz et al. 2019).*

Figure 3-64 – Virtual reality (VR) environment for the Mont Terri URL (Rink et al. 2020).

In addition to computational efficiency, visual data analysis is promising field for many domain sciences as well. Visualisation in environmental sciences concerning terrestrial (hydrology), atmospheric (climate research), and geological systems is under intensive development. Virtual Reality concepts allow for the combination of various kind of data and models in a real geo-referenced context – making those integrated VR Labs a useful planning tool e.g. for experimental design in URLs or infrastructures for urban systems –. Figure 3-64 depicts an example from the Mont Terri underground research laboratory where numerous in situ experiments together with the respective models are combined within a virtual reality context (Virtual URL).

When upscaling models from processes to management scales (Figure 3-56) complexity-reduced approaches have to be introduced as conveying all information through all scales is neither feasible from a computational perspective nor from a practical viewpoint. Therefore, so-called surrogate models are introduced for complexity-reduced approaches. Recently, data science methods such as machine learning receive more and more attention not only to improve the computational efficiency but also to introduce new alternative parametrisation approaches, e.g. for uncertainty quantification.

EURAD (Deliverable n° 6.1) – Initial State of the Art on Gas Transport in Clayey Materials
Dissemination level: PU
Date of issue of this report: 17/11/2021

Page 233

3.3.10.2 Data science in geoscience

In recent time more and more data science concepts are entering various fields of engineering (Hegde and Rokseth 2020) including environmental (e.g. for flood forecasting) and geosciences (Morgenroth et al. 2019). Of particular interest are machine learning algorithms (MLA) in solving specific problems in geotechnical applications. As a result of a recent extended literature survey Hedge and Rokseth (2020) found that artificial neural networks (ANNs) are the most applied machine learning method in engineering risk assessment. The general limitation of ANNs is their limited capability for predictions as they very much depend on training based on existing data. Typically, MLAs are used for classification problems, upscaling observations from laboratory- to field-scale is a recent focus. Little work has been done applying MLAs to the numerical modelling methods so far. For complex processes, MLAs provide an opportunity to define the relationships between the input parameters and numerical model behaviour and therefore to conduct a more precise sensitivity analyse. A combination of data-based MLAs with process-based modelling capacities may build a way forward for complex systems analysis. For the present SOTA we conducted a small literature review on MLAs for porous media modelling:

Data-driven approach to accelerate multi-scale methods within uncertainty quantification (for elliptical problems) (Chan and Elsheikh 2020),

- Coarse grid approximation for unsaturated and two-phase flow problems in heterogeneous and fractured porous media (Vasilyeva et al. 2020),

- 3D convolutional neural network architecture that provides fast and accurate fluid flow predictions for 3D digital rock images (Santos et al. 2020),

- Linking morphology of porous media to their macroscopic permeability (Kamrava et al. 2020),

- Model reduction for fractured porous media: a machine learning approach for identifying main flow pathways, two subsets of DFN (backbone and complementary) (Srinivasan et al. 2019).

EURAD (Deliverable n° 6.1) – Initial State of the Art on Gas Transport in Clayey Materials
Dissemination level: PU
Date of issue of this report: **17/11/2021**
Page 234

4. Conceptualisation and evaluation at the scale of a repository

4.1 Conceptualisation by end-users

The current conceptualisations of gas transport through repositories as considered in Europe are presented herein by the radioactive waste management organisations working with the three clayey host formations considered in the WP GAS: RWM (UK), ONDRAF/NIRAS (Belgium), COVRA (The Netherlands), Nagra (Switzerland) and Andra (France), and by the Regulatory Technical Safety Organisation IRSN (France). Communication of the conceptualisations of gas in respective national programmes are based on 'gas storyboards' that are presented in the following sections.

4.1.1 Gas storyboard in lower strength sedimentary rock by RWM (UK context)

This section considers RWM's approach to gas generation and transport in relation to a UK GDF located within an illustrative (not site-specific) lower strength sedimentary rock, including conceptualisation and example numerical modelling.

4.1.1.1 Gas generation

Gas processes related to the UK radioactive waste inventory are shown in the below Figure 4-1.
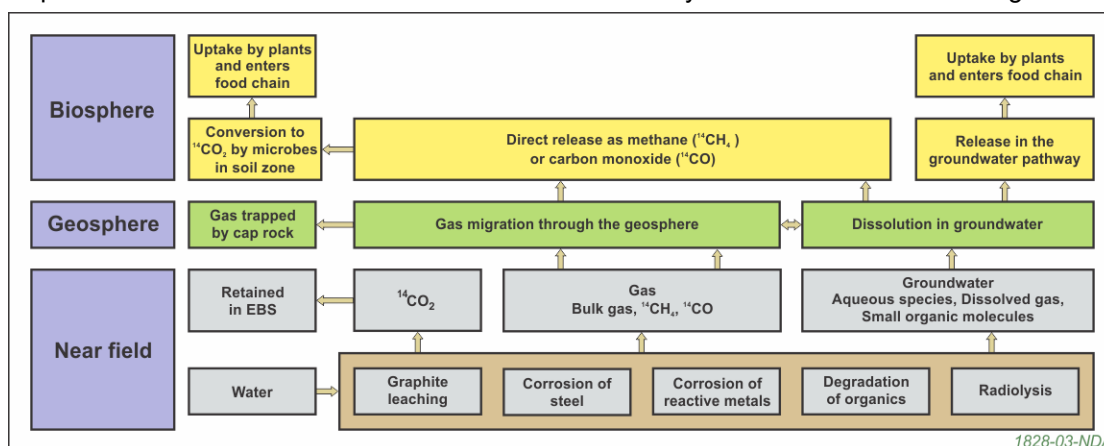
Figure 4-1 – Gas processes related to the UK radioactive waste inventory (the bulk of the gas produced by corrosion and radiolysis is hydrogen).

Gases will be formed from processes occurring in waste packages, for example corrosion of metals in the waste or the radiolysis of water, throughout their life:

- in interim surface storage at waste producers' sites,
- during transport to the geological disposal facility (GDF),
- in the operational phase of the GDF,
- after closure of the GDF.

EURAD (Deliverable n° 6.1) – Initial State of the Art on Gas Transport in Clayey Materials
Dissemination level: PU
Date of issue of this report: 17/11/2021

Page 235

In addition, components of the engineered barrier system (EBS) will contribute to gas generation after closure (for example, anaerobic corrosion of stainless waste containers and gamma radiolysis of pore water in a cementitious backfill).

Some of the gas will consist of radioactive molecules (for example, tritiated hydrogen gas, $^3H^1H$, carbon-14 bearing methane, $^{14}CH_4$); some chemotoxic gases could also form. Although these may be insignificant in terms of the volumes of gas generated, their release from waste packages can contribute to the radionuclide uptake by human and non-human biota.

Gas generation and release of gases during interim surface storage at waste producers' sites will reduce the inventory of materials with the potential to generate gas in the GDF (as will the aerobic corrosion of steels, although this produces no hydrogen). Similarly, gas generation and release during the operational phase of the GDF will reduce the inventory of gas generating material after closure (the transport duration will be too short to be of significance in this respect).

4.1.1.2 Gas transport

The range of geological environments potentially suitable for hosting the GDF for higher activity wastes in the UK is wide and diverse. Currently no site is selected in the UK for the GDF, and a range of potential host rocks (higher strength rocks, lower strength sedimentary rocks and halite) and surrounding geology is considered in RWM's generic (i.e. not site-specific) work.

This section describes the knowledge base for the behaviour of gas in different geological environments, and identifies the post-closure considerations that may need to be investigated as part of a site selection process.

The properties of the host rock and the geosphere will control the migration of gas from the facility. Thus, the combined properties of the EBS and the host rock should provide passive protection against significant over-pressurisation. In addition, the system should have properties that ensure that transport of radioactive, flammable and toxic gases to the biosphere does not result in the relevant regulatory guidance or limits being exceeded.

After closure of the GDF, any gas that is formed may dissolve in water, may undergo chemical reactions or form a free gas phase. The volume of any free gas phase, its effect on the EBS and the geological barrier, and its migration through the EBS and the geological barrier, depend strongly on the illustrative geological disposal concept and on the properties of the geological environment, in particular the host rock. These issues have been a focus of investigation for many years in the UK and internationally.

The generation and transport of gas after closure of the GDF will depend on the combination of waste, EBS and geology. Water availability is a key issue, both as present in the waste package originally and as sourced by the host rock and surrounding geology. Some features of the GDF may help to reduce gas generation rates or the total volume of free gas. For example, in an environment where there is a low water flow rate (such as some lower strength sedimentary rocks) the limited availability of water may reduce the rates of corrosion of some metals and microbial activity, thus reducing the rate at which gas is generated. The conditions imposed on the waste packages by EBS buffer or backfill can limit the rate of microbial action or the rate of corrosion of some metals. The buffer or backfill also allow the passage of gas from the EBS and may also provide some capacity to store gas. Cements and magnesium oxide – possible backfill materials – also absorb carbon dioxide and hence can reduce the total volume of free gas in an EBS containing such materials.

Engineered seals will be installed during closure of disposal areas (for example vaults or tunnels), access ways, shafts and boreholes. These seals, depending on the disposal concept, may need to allow gas to be released from closed disposal areas to prevent excess pressurisation, but restrict the

EURAD (Deliverable n° 6.1) – Initial State of the Art on Gas Transport in Clayey Materials
Dissemination level: PU
Date of issue of this report: 17/11/2021

Page 236

flow of water. Prior to closure of the GDF, low-permeability seals will be placed at suitable locations to limit the flow of water and gas along shafts and boreholes to the biosphere.

The transport of gas is site-specific, as is the persistence of any free gas phase. Gas transport has been compared previously for concepts in higher strength rocks and lower strength sedimentary rocks (Hicks and Baldwin 2007). In a fractured higher strength rock environment, the bulk gases, if formed in sufficient quantity, can migrate from the EBS, not only as dissolved species in the groundwater but also as a free gas phase. Once the gas has left the EBS, its migration to the biosphere will be determined by the physical nature of the geological environment (for example the presence of 'cap rocks'), the amount of contact with deeper groundwater, the degree of dissolution and dilution in near-surface groundwater and the composition of those waters. In some cases, the combination of such site-specific features may remove free gas by dissolution in groundwater and so may prevent the release of free gas to the biosphere. It is also possible that dissolved gas can be released from groundwater during advection towards the surface. This is a consequence of a decrease in gas solubility with the decrease in pressure with decreasing depth.

In lower strength sedimentary rocks (for example clays), the hydraulic conductivity of the host rock will be so low and the pressure for the gas to enter the host rock will be so high that, if all the gas formed cannot be dissolved, it may not be possible for a free gas phase to be transported from the GDF sufficiently quickly by flow through undisturbed clay to relieve a possible build-up of pressure. Clay formations tend to act as cap rocks and trap gas in nature. Depending on the combination of gas generation, water inflow and gas transport in solution, the gas may reach sufficient pressure that it creates micro-fissures in the EBS and / or host rock. These may then close after the gas pressure has fallen, depending on the properties of the material / host rock. Self-sealing is observed in laboratory experiments for some lower strength sedimentary rocks, such as the Boom Clay from Belgium and the Opalinus Clay from Switzerland (Bernier et al. 2007b). Self-sealing is commonly observed over larger scales from tens of metres to the kilometre scale in geological systems. The rate will depend on the type of clay, the amount of hardening (induration) of the clay and the pore water chemistry.

The bulk of the gas is hydrogen, produced by corrosion and radiolysis, which is not radioactive. Its movement also affects the release of radioactive and chemotoxic gases (present at trace volume levels in the bulk gas) from the EBS and their transport to the biosphere. Carbon-14 containing species, such as methane and carbon monoxide, will migrate with bulk gas and may reach the biosphere as gaseous or dissolved species depending on the processes described above for the transport of bulk gas. Carbon dioxide containing carbon-14 ($^{14}CO_2$) is expected to be retained by cementitious grouts within waste packages or cementitious components of an EBS (for example backfill). The formation of insoluble carbonates (for example by carbonation of cements) is one of the processes that minimises the possibility of the conversion of $^{14}CO_2$ to $^{14}CH_4$ by methanogens in the presence of hydrogen (Holtom 1997).

The current RWM understanding of the behaviour of gas after closure of the GDF in different geological environments (Rodwell et al. 1999, 2003b; Norris 2013; Hoch et al. 2008, Hoch and Swift 2010; Baker et al. 1997; UK Nirex 2003) can be summarised as follows:

- Materials in the GDF, including the wastes, will undergo reactions (corrosion, microbial degradation and radiolysis) and thereby generate gas.

- The bulk gas will be comprised largely of hydrogen, and there will be lesser amounts of carbon dioxide and methane. The hydrogen will be generated mainly from the anoxic corrosion of metals in the GDF. Because corrosion is a well-understood process, the rate at which the bulk gas will be generated can be calculated based on experimentally-determined corrosion rates. Uncertainties in such calculations, when applied to materials in the GDF, include those that arise from estimating the total surface area of each metal, the amount of water in contact with the metal surfaces and the effect of the solution chemistry on the corrosion rate. Such

EURAD (Deliverable n° 6.1) – Initial State of the Art on Gas Transport in Clayey Materials
Dissemination level: PU
Date of issue of this report: 17/11/2021

Page 237

uncertainties can be investigated, for example, by calculations for expected bounding conditions.

- A free gas phase may form. If there is sufficient water availability for gas generation from corrosion not to be limited, then it is likely that bulk gas will be generated sufficiently quickly that not all of it will be able to dissolve in the groundwater.

- Although very small volumes of radioactive gases will be produced, these volumes may correspond to significant amounts of radioactivity. The radioactive gases include tritium, molecules containing carbon-14 (including methane and carbon dioxide) and radon-222. There is uncertainty about the rates at which these active gases will be formed, because they depend first on the release of a radionuclide from the waste matrix, and second on the incorporation of the radionuclide into a gas. In developing our understanding of the consequences of gas generated in a GDF, conservative assumptions have been made about the rates at which the active gases will be produced.

- Of the active gases and focusing on the GDF post-closure period, molecules containing carbon-14 other than carbon dioxide (for example methane or carbon monoxide) may be the most important because:

  o Tritium has a short half-life (12.3 years) and so will decay to an insignificant level within a few hundred years of its creation in reactor operations.

  o Assuming a cementitious backfill material is used in constructing a GDF, any carbon dioxide (including ^{14}C-carbon dioxide) that is released from the waste packages will mostly react with the backfill material (carbonation) and will be immobilised in the facility (Harris et al. 2003a, 2003b; Heyes et al. 2015)[28].

  o Although radon-222 will be formed continuously as part of the radioactive decay chain of uranium, it has a very short half-life (3.8 days) and therefore will decay before it can migrate from the GDF to the biosphere. However, radon generated nearer the biosphere from the decay of in-grown radium, resulting from the migration or natural presence of uranium in groundwater, may need to be considered.

- Gas transport from the GDF can occur by successive mechanisms (depending on the geological environment) as the amount of gas increases. Gas dissolution in water, and subsequent transport via advection and diffusion of dissolved species, will be followed by two-phase flow in existing porosity and fractures once the amount of gas generated is greater than the ability of the system to remove it by dissolution and transport of dissolved species.

- Gas transport in bentonite may occur through pressure-induced transient pathways at the nano-to-micro-scale.

- In the case of lower strength sedimentary rocks (for example clay), the rates of gas generation may be limited by the supply of water from the host rock to the GDF. A free gas phase may form, but because clay has very small intergranular pores, the gas will find it difficult to be transport away from a GDF. The pressure will increase, leading to transport through porosity dilation and localised micro-fissuring in un-fractured clays and mudrocks. If the pressure were to continue to increase, and eventually exceed the mechanical stress field, fracturing and gas release would result (Andra 2005; Nagra 2004). Re-sealing of fractures is subsequently likely to occur – such gas migration pathways should be considered as transient. Thus, for concepts in lower strength sedimentary host rocks, one aim is to ensure that the maximum gas

---

[28] Carbonation of cements can lead to a reduction in total alkaline buffering capacity, through the consumption of calcium hydroxide and calcium-silicate-hydrate phases, and the formation of reaction layers that may affect conditioning of pore water.

![eurad logo] European Joint Programme on Radioactive Waste Management

EURAD (Deliverable n° 6.1) – Initial State of the Art on Gas Transport in Clayey Materials
Dissemination level: PU
Date of issue of this report: **17/11/2021**

Page 238

pressurisation of the GDF will not exceed the mechanical stress of the host rock at depth, to prevent fracturing of the host rock. If it is thought possible that gas transport as dissolved species, by two-phase flow and by release through porosity dilation and micro-fissuring, may be insufficient to ensure that the maximum gas pressure is acceptable, then an engineering solution may be considered. For example, the Nagra concept for the disposal of L/ILW in Opalinus Clay includes the option of an 'engineered gas transport system'.

- The geological environment will affect the rate of gas generation through the chemical composition of the groundwater, and through the rate of groundwater supply. The access of water to the wastes may also be influenced by the physical barrier provided by the disposal containers and, where applicable, the waste encapsulation matrix. Therefore, the rate of gas generation (for example from corrosion) may be reduced, although the eventual total amount of gas produced will be unchanged.

- Finally, a possible future human intrusion into the GDF (for example the drilling of a wellbore that penetrates a GDF) may create a pathway by which gas can be transport quickly from the GDF to the biosphere (Hoch and Thorne 2008). An important consequence of a human intrusion into the GDF is the possibility of radon, if it were present, bypassing the geosphere.

4.1.1.3 Consequences of gas generation on water saturation in a lower strength sedimentary rock – UK unshielded intermediate-level waste (UILW) example

Gas generation and multiphase flow processes are complex in very low-permeability rocks (lower strength sedimentary). Higher strength rock with a permeable backfill, or evaporite rock (where there are no significant water sources), could be simpler[29] although e.g. site-specific conditions could significantly affect gas processes. The resaturation behaviour of the EBS in different host rocks can be significantly different. Small-scale features coupled processes and upscaling in lower permeability host rocks are important (Towler and Bond 2011).

A modelling comparison of gas generation[30] and water saturation for UILW vaults in a lower strength sedimentary host rock and a higher strength rock has been made (Towler and Bond 2011). Figure 4-2 shows the calculated water saturation of the waste vaults at closure and 40 years after closure in a higher strength rock (increasing water saturation is shown by the colour changing from blue through green towards red).

The calculated behaviour in a lower strength sedimentary rock is much more complex because resaturation and the generation of gas are strongly coupled.

Figure 4-3a shows the water saturation at three years, when the vaults are backfilled and closed, but the service and transfer tunnels are still open and being dewatered. The closed vaults begin to resaturate, and gas starts to be generated from the wastes. After 30 years the service and transfer tunnels are assumed to be closed. Figure 4-3b shows water saturation at 30 years; the wasteforms 'pull' water in from the backfill and the vault backfill has largely dried out (in reality the containers will remain intact for tens of thousands of years, and will prevent water being drawn into the waste directly since water would have to be drawn in through the container vents).

---

[29] It can be more complex in higher strength rocks, if a low permeability backfill is used, and in halite if water is available (for example, if the wasteform has a significant water content).

[30] Note that the gas generation model used in these post-closure calculations is simpler than SMOGG, for example it does not include radiolysis and assumes methanogenic conditions in the vaults.

EURAD (Deliverable n° 6.1) – Initial State of the Art on Gas Transport in Clayey Materials
Dissemination level: PU
Date of issue of this report: 17/11/2021
Page 239

Once the service and transfer tunnels have been closed, they resaturate more rapidly than the ILW vaults because of their smaller volume (per unit length), and because there is no gas generation in these tunnels. The concrete seals have higher capillary suction than the sand/bentonite tunnel fill, and therefore resaturate more rapidly than the tunnels. After 1 000 years the service and transfer tunnels, concrete plugs, waste packages and some of the vault backfill have largely resaturated. Gas is trapped in the vault 'crown spaces', which are fully desaturated (Figure 4-3c).

Gas generation continues beyond 1 000 years. Gas cannot readily escape from the vault and water saturation starts to decrease. After 10 000 years the backfill is calculated to be fully desaturated (is at its residual saturation); the water saturation in the wastes has decreased and gas is moving into the service and transfer tunnels (Figure 4-3d). The quantity of gas that can be generated is now limited by the amounts of water and gas generating materials remaining in the waste packages.

At 100 000 years the waste packages, vault backfill, service and transfer tunnels are calculated to be fully dry (that is, they are at their residual saturations) (Figure 4-3e). A small amount of water remains in the concrete plugs. Gas generating processes have consumed all the water that remained in the wastes at 10 000 years. However, Figure 4-4 shows that some of the waste is calculated to still be partially saturated.

This arises because in the model the waste is in contact with the rock and is pulling in water by capillary suction (in reality, as mentioned above, the containers may remain intact for tens of thousands of years and would prevent water being drawn into the waste for at least some of the time up to 100 000 years).

EURAD (Deliverable n° 6.1) – Initial State of the Art on Gas Transport in Clayey Materials
Dissemination level: PU
Date of issue of this report: **17/11/2021**

Page 240
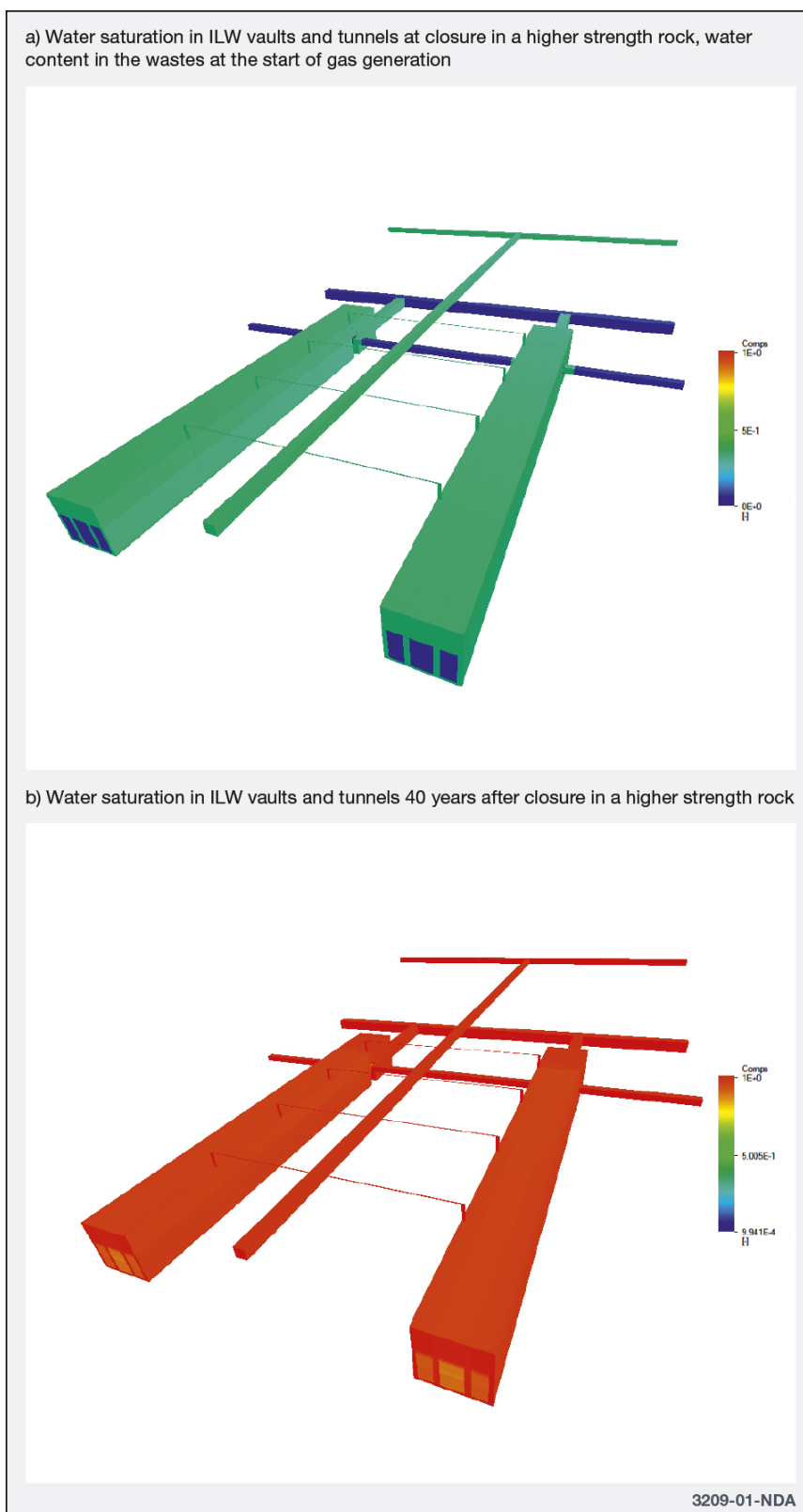
Figure 4-2 – Illustrative calculated results for water saturation in ILW tunnels and vaults at closure and 40 years after closure in a higher strength rock (Towler and Bond 2011).

EURAD (Deliverable n° 6.1) – Initial State of the Art on Gas Transport in Clayey Materials
Dissemination level: PU
Date of issue of this report: **17/11/2021**

Page 241

a) Water saturation in ILW vaults and tunnels at 3 years in a lower strength sedimentary rock. Vaults are closed but transfer and service tunnels remain open.
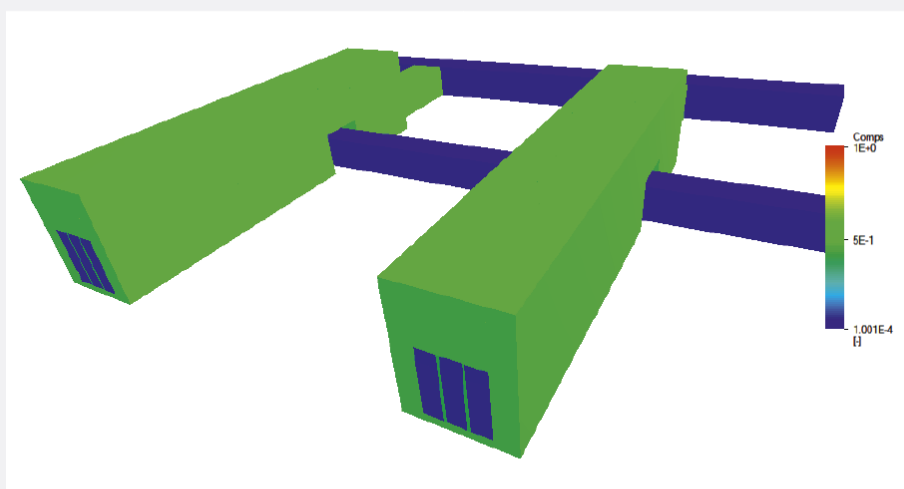
b) Water saturation in ILW vaults and tunnels at 30 years in a lower strength sedimentary rock. Transfer and service tunnels are closed at this time.
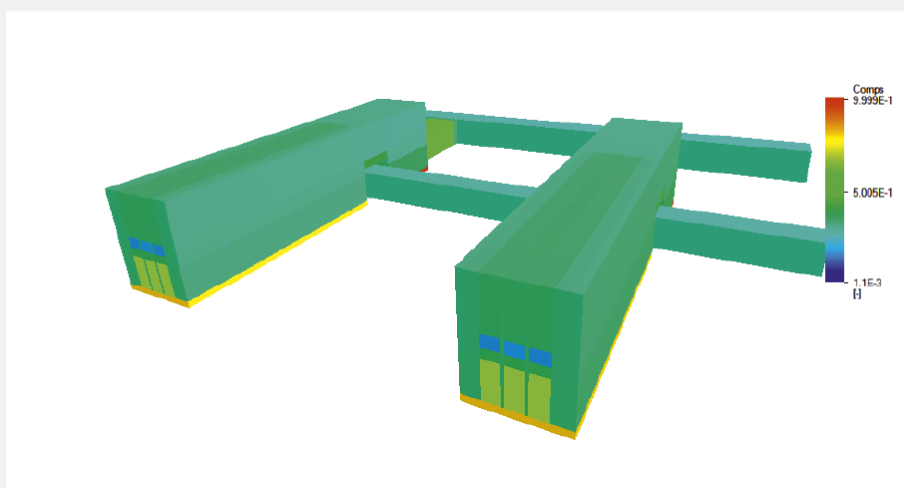
c) Water saturation in ILW vaults and tunnels at 1,000 years in a lower strength sedimentary rock.

3212-01-NDA

EURAD (Deliverable n° 6.1) – Initial State of the Art on Gas Transport in Clayey Materials
Dissemination level: PU
Date of issue of this report: **17/11/2021**

Page 242

d) Water saturation in ILW vaults and tunnels at 10,000 years in a lower strength sedimentary rock.

e) Water saturation in ILW vaults and tunnels at 100,000 years in a lower strength sedimentary rock.
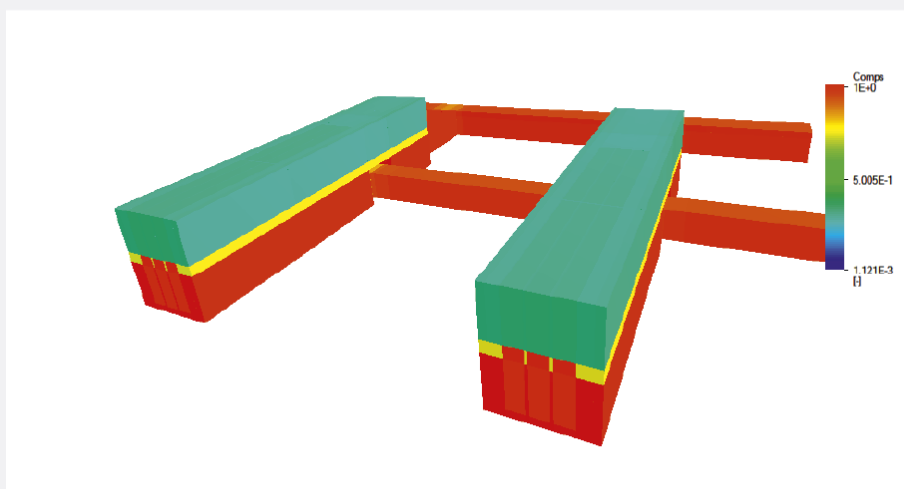
Figure 4-3 – Illustrative calculated results for water saturation in UILW tunnels and vaults in a lower strength sedimentary rock (Towler and Bond 2011).
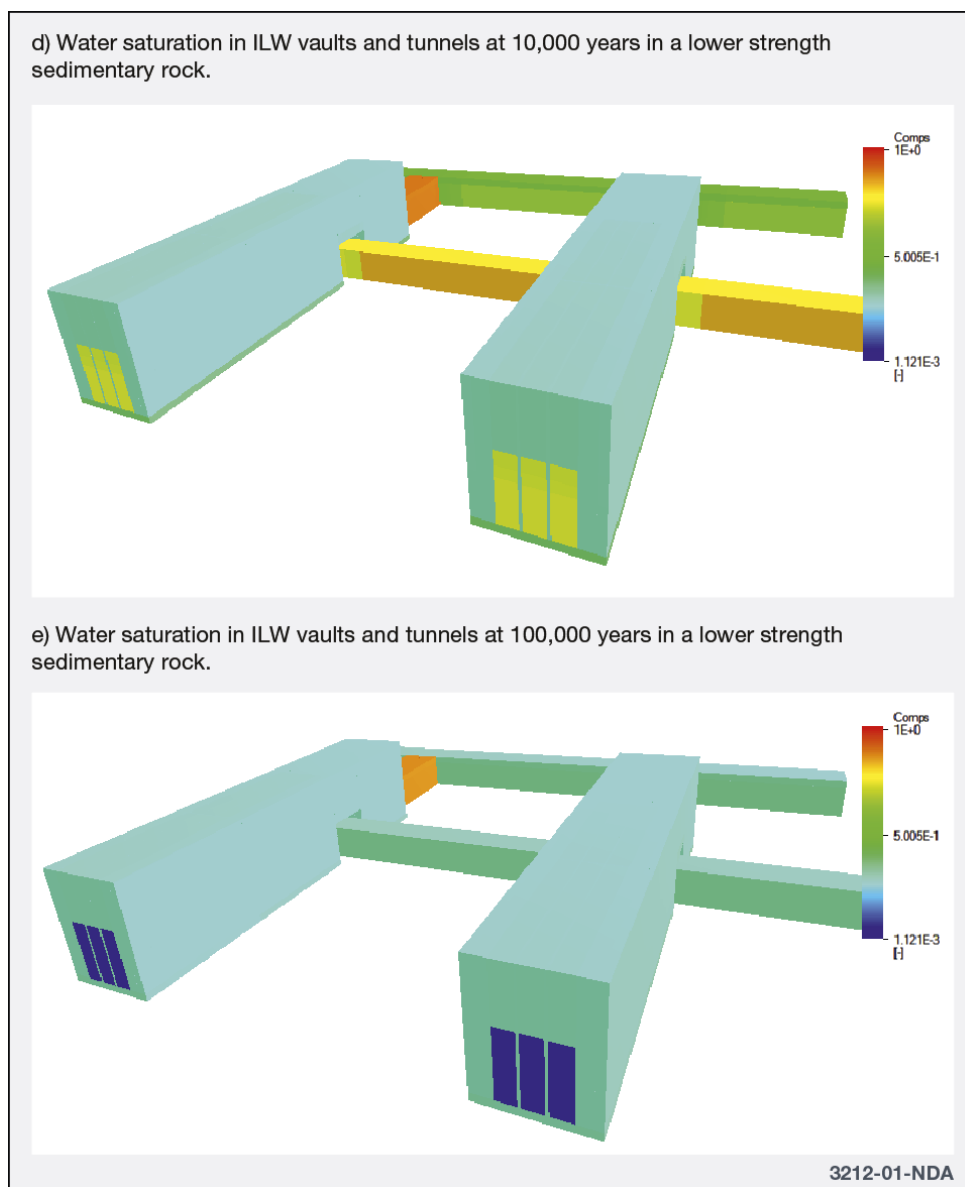
EURAD (Deliverable n° 6.1) – Initial State of the Art on Gas Transport in Clayey Materials
Dissemination level: PU
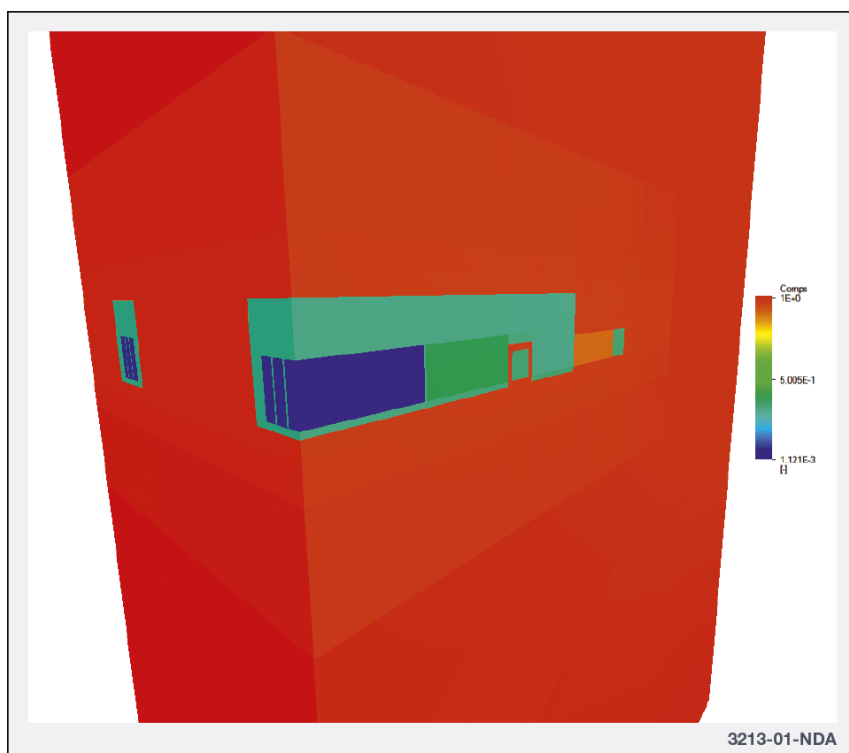Date of issue of this report: 17/11/2021

Page 243

Figure 4-4 – Illustrative calculated water saturation along an ILW vault at 100 000 years in a lower strength sedimentary rock (Towler and Bond 2011).

4.1.1.4 Gas transport in a lower strength sedimentary rock

Clay is being considered as a host rock by a number of waste management organisations. The Swiss concept for Opalinus Clay (Nagra 2004, 2008) is the illustrative disposal concept in the Radioactive Waste Management (RWM) Disposal System Safety Case (DSSC) for both types of waste (L/ILW and HLW/spent fuel in carbon steel containers) in a lower strength sedimentary rock.

RWM's current view, based on references (Nagra 2004, 2008; Andra 2005; Wersin et al. 2003; Hoch and Thorne 2008; Towler and Bond 2011) is that the following processes will be important:

- Because the GDF will be ventilated throughout construction and operation, the host rock in the immediate vicinity of the operational GDF will de-saturate.

- Outside the desaturated zone, there will be a transient pressure build-up around the high heat-generating waste packages, for example HLW and spent fuel (the temperature rise decreases the groundwater density and hence the pressure increases).

- After closure of the GDF, both the desaturated zone and the facility will gradually resaturate.

- The time for saturation of the bentonite surrounding a HLW/SF container will range from about 100 years to many hundreds of years.

- Resaturation will be coupled with hydrogen generation (mainly from corrosion of metal components) and its transport; this will delay the attainment of full saturation in L/ILW emplacement tunnels, which can take tens of thousands of years.

- Any hydrogen generated, as well as air trapped at the time of closure, will dissolve in the water in the engineered barrier system until the solubility limit at the GDF pressure is reached; dissolved gas will then diffuse away from the facility into the host rock.

EURAD (Deliverable n° 6.1) – Initial State of the Art on Gas Transport in Clayey Materials
Dissemination level: PU
Date of issue of this report: **17/11/2021**

Page 244

- If the rate of gas generation is sufficiently high, the gas pressure will rise until a gas phase can be transport away from the GDF.

- A possible pathway will be the excavation disturbed/damaged zone (Ed/DZ)[31], which is likely to contain stress relief fractures that will act as preferential pathways for free gas. However, the host rock around the GDF will creep slowly and the fractures in the Ed/DZ may be sealed as the rock converges under the lithostatic pressure.

- If the gas pressure exceeds the threshold for two-phase flow (the hydraulic pressure plus the gas entry pressure), then a gas phase flow into the host rock.

- A further increase in the gas pressure may create localised porosity dilation and temporary micro-fissuring in the host rock, which closes once the gas pressure drops (depending on the properties of the host rock) and preventing the gas pressure exceeding the strength of the host rock.

- Pore water will be displaced from the L/ILW emplacement tunnels into the host rock once the gas pressure exceeds the hydrostatic pressure. However, pathway dilation will result in little displacement of water when gas is released into the host rock and Nagra have concluded that gas effects on the movement of dissolved contaminants from a L/ILW repository in Opalinus Clay will not compromise safety.

Figure 4-5 shows calculated gas pressures where resaturation is coupled to gas generation for the GDF in a lower strength sedimentary rock. A model that couples together waste evolution and heat / gas production, water inflow, and gas transport away from the facility may be required to simulate this fully.
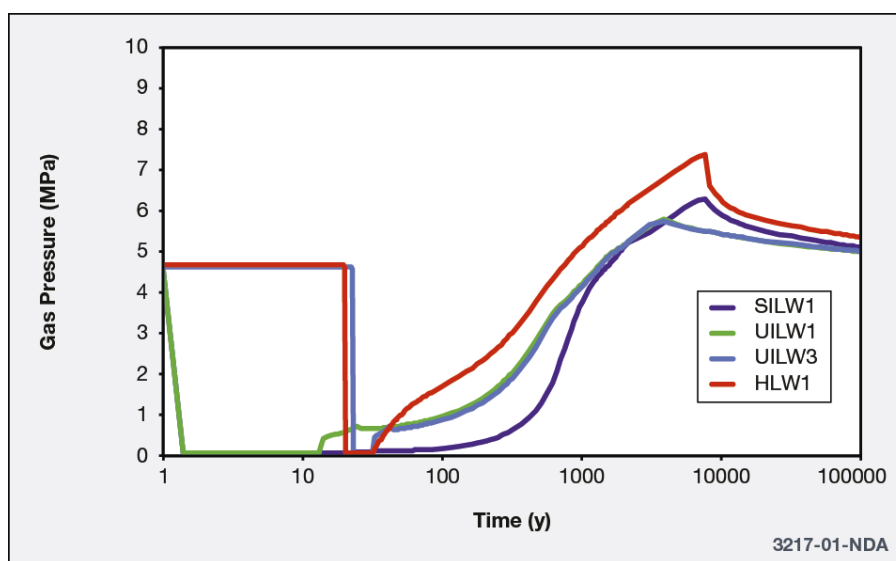
Figure 4-5 – Illustrative gas pressure in different waste modules/areas for the GDF in lower strength sedimentary rock (Towler and Bond 2011).

Clay has very small intergranular pores and the movement of gas through these will be very slow. Figure 4-6 shows the results of an illustrative calculation for a gas phase transported from the GDF

---

[31] The shafts and access tunnels, as well as the EDZ around those features, may provide a preferential pathway for groundwater flow and gas migration; that is because they will be more permeable, and have a lower gas entry pressure, than the undisturbed rock. Sealing of the features will be an important issue for GDF design.

EURAD (Deliverable n° 6.1) – Initial State of the Art on Gas Transport in Clayey Materials
Dissemination level: PU
Date of issue of this report: **17/11/2021**   Page 245

located at 400 metres below ground level in clay. The gas saturation (S_g) (the fraction of the pore space in the rock that is occupied by gas) is colour shaded with colours to the red end of the spectrum corresponding to higher gas saturation. In the model, free gas is released through the top boundary (at z = -280 metres) at approximately 20 000 years after closure. The system then settles down to a pseudo steady-state, in which the gas leaving the model is approximately equal to the gas generated, with the gas crossing the host rock in a relatively short period (of the order of years). Gas dissolves in the groundwater all along the pathway, followed by the transported free gas, as can be seen by comparison of Figure 4-7 with Figure 4-6.

The performance of seals used to close underground spaces and access shafts and tunnels will be important because they represent possible pathways for gas transport. It has been noted that, for lower strength sedimentary host rock, the EDZ may be an important feature for the transport of gas as it can enable gas to bypass low-permeability seals, and may provide a preferential route for the transport of gas (Towler and Bond 2011). The extent of an EDZ around an underground opening in a lower strength sedimentary rock is limited and, although some lower strength rocks respond to stress change in the short term by fracturing, there is much evidence for longer term creep which causes these fractures to self-seal (RWM 2016a) so that the initial properties of intact rock are partially restored[32]. Therefore, the effects are considered to be largely or wholly reversible. In a lower strength sedimentary rock the EDZ should be considered in conjunction with interfaces between seals and rock that may provide a preferential pathway for gas transport.
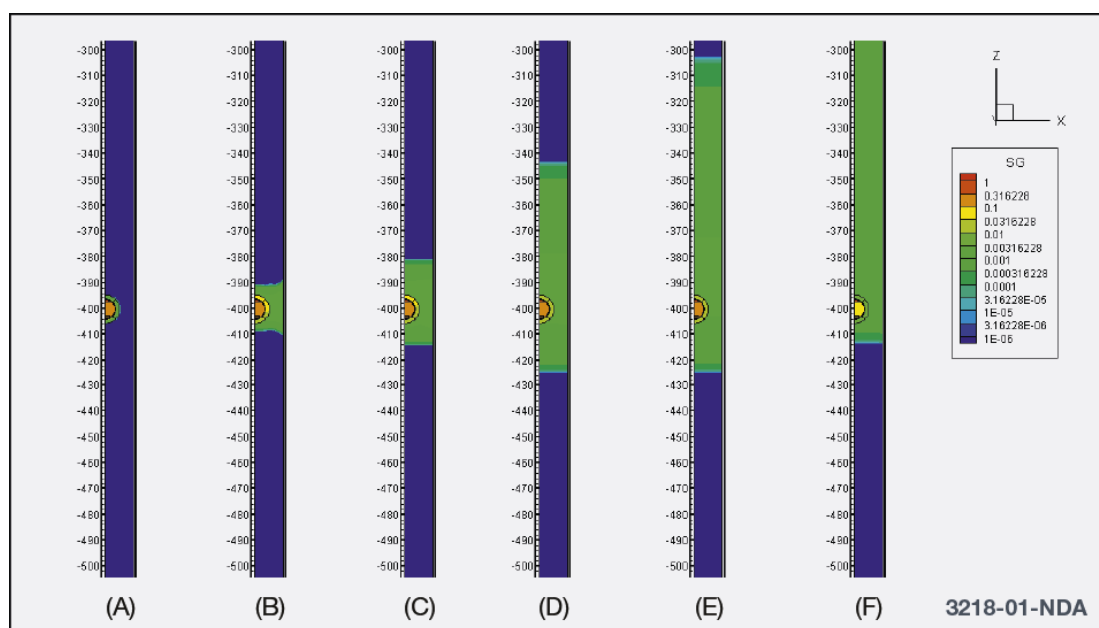
Figure 4-6 – Illustrative calculation of gas saturation post-closure for gas migration from the GDF in clay (Hoch and Swift 2010). The colour corresponds to the degree of gas saturation (denoted by SG in legend) with increasing gas saturation towards the red end of the spectrum, (a) is at closure; (b) is at 100 years post-closure; (c) is at 1 000 years post-closure; (d) is at 10 000 years post-closure; (e) is at 20 000 years post-closure; and (f) is at 100 000 years post-closure.

---

[32] Healing of the fracture zone is generally not demonstrated. There is evidence of weakness of the self-sealed materials with regards to mechanical properties. For gas, many observations indicate that gas entry pressure is lower in previously fractured clay than in the intact one even after self-sealing and recovery of the original water permeability.

EURAD (Deliverable n° 6.1) – Initial State of the Art on Gas Transport in Clayey Materials
Dissemination level: PU
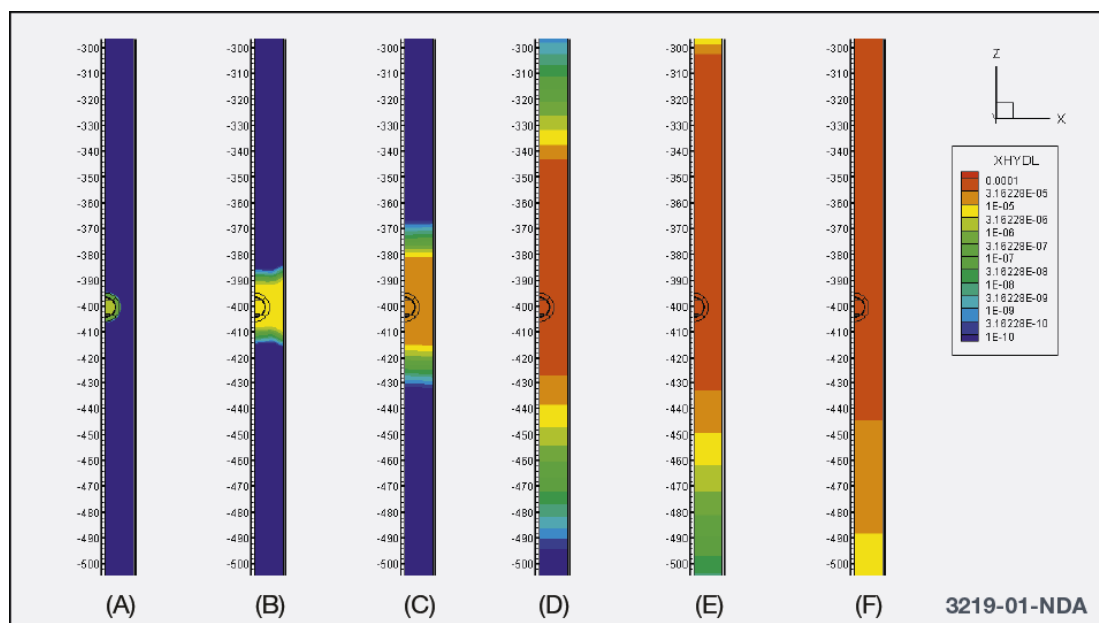Date of issue of this report: 17/11/2021

Page 246

Figure 4-7 – Illustrative calculation of mass fraction of gas dissolved in liquid for gas migration from the GDF in clay (Towler and Bond 2011). The colour corresponds to the mass fraction of gas dissolved in liquid (denoted by XHYDL in legend) with increasing mass fraction towards the red end of the spectrum. (a) is at closure; (b) is at 100 years post-closure; (c) is at 1 000 years post-closure; (d) is at 10 000 years post-closure; (e) is at 20 000 years post-closure; and (f) is at 100 000 years post-closure.

Aside from potential radioactive and chemotoxic consequences that could arise post-closure from waste-derived gas uptake by receptors, were transport from GDF to biosphere to occur, other possible consequences of gas in this geological environment include:

- Pressurisation of the GDF. For the clay host rocks being investigated as potential sites by Nagra and Andra, experimental data suggest that gas will enter the rock at pressures below those required for macroscopic fracturing. However, the option of engineered design features can be considered if excess over-pressurisation were to be a possible issue.

- Gas-induced movement of contaminated water in the vicinity of a GDF.

4.1.1.5 Summary

Processes that contribute to gas generation during the transport of waste packages to the GDF, during the operational phase of the GDF and after closure of the GDF are generally understood (RWM 2016b); there is significant work ongoing nationally and internationally to enhance the associated knowledge base and build confidence in understanding the relevance of waste-derived gas to the safety case for a GDF. Gas transport from the GDF after closure will be site-specific and will need to be addressed in detail after a site has been chosen. Specifically:

- Gases will be generated during transport, operations and after closure of the GDF. The key gas generation processes applicable to a GDF are the corrosion of metals, microbial action and radiolysis. The relative importance of the various generation processes, and hence the rates of gas formation and the gas composition, depend partly on the type of wasteform and also on the disposal concept.

- Most of the volume of gas generated will not be radioactive and will consist of hydrogen, with lesser amounts of methane and carbon dioxide. A small fraction of the gas volume will be radioactive and some non-radiological chemotoxic species may also be formed.

EURAD (Deliverable n° 6.1) – Initial State of the Art on Gas Transport in Clayey Materials
Dissemination level: PU
Date of issue of this report: 17/11/2021

Page 247

- The radioactive / chemotoxic gases of potential importance are: tritium; gaseous molecules containing carbon-14, such as methane, carbon dioxide and carbon monoxide; and radon-222. Of these, carbon-14 is the only one with a sufficiently long half-life to be of post-closure interest with respect to its release as gas from waste packages.

- Carbon-14 may be present in irradiated metals, irradiated graphite, spent ion-exchange resins and organic compounds. Only a small fraction of the carbon-14 in irradiated graphite is released to the gas phase when leached in alkaline solution and there is some evidence for the release of gaseous carbon-14 from the corrosion of irradiated metals.

- Waste packages must satisfy limits on the generation rates of both bulk gas and active gases during transport.

- During the operational phase of the GDF lifecycle, flammable and radioactive / chemotoxic gases, similar to those arising during interim surface storage, will be generated. These can be removed by adequate ventilation, and the subsequent discharge of air containing radioactive gases from the GDF to atmosphere will be controlled to meet regulatory limits on authorised discharges.

- After closure of a GDF, gases will continue to be generated. The bulk gas will be comprised largely of hydrogen, but there will be lesser quantities of carbon dioxide and methane. The generation of bulk gases may impact on the performance of the GDF, through reactions such as carbonation of cements and possible delayed resaturation, or the formation of preferential flow paths due to pressurisation. The formation of radioactive gases depends on the release of a radionuclide from the waste matrix, the incorporation of the radionuclide into a gas and the disposal concept. Of these, molecules that contain carbon-14 may be the most important if free gas migrates from the GDF after closure because of its relatively long half-life. Tritium has a short half-life and will have decayed significantly within a few hundred years of packaging. Although radon will be formed continually as part of the radioactive decay chain of uranium, it has a very short half-life and any originating from the waste packages will decay in the GDF. However, naturally-occurring radon may be released from some rocks.

- In a lower strength sedimentary host rock, the rates of gas generation may be limited by the supply of water from the host rock to the GDF. It will be difficult for any free gas phase formed to be transport from the GDF by flow through undisturbed rock because of high gas entry pressure. Depending on the precise combination of gas generation, water inflow and gas transport in solution, the gas may be released through a combination of dilation and micro-fissuring in the clay. These pathways are then expected to close after the gas pressure has fallen, depending on the properties of the host rock.

- Gas transport from the GDF will be site-specific (that is, geology and disposal concept specific) and will need to be addressed in detail after the site has been selected.

EURAD (Deliverable n° 6.1) – Initial State of the Art on Gas Transport in Clayey Materials
Dissemination level: PU
Date of issue of this report: **17/11/2021**

Page 248

4.1.2 Gas storyboard in Boom Clay by ONDRAF/NIRAS (Belgian context)

4.1.2.1 Belgian generic geological disposal facility concept

In its reference concept for a geological repository in Belgium, ONDRAF/NIRAS plans to dispose of two types of disposal packages: the supercontainers containing the high-level waste and the monoliths, containing the intermediate-level, long-lived waste. Besides facilitating the operational phase, these packages have significantly different functions, tailored to specificities of the waste types.

4.1.2.1.1 Supercontainer

In the supercontainer design, the primary waste packages of high-level waste (i.e. the category C waste in the Belgian concept) are surrounded by a carbon steel overpack, a buffer made of concrete containing Portland cement and a stainless steel envelope (Figure 4-8, Figure 4-9). The length of the supercontainers varies from 4 metres up to 6.5 metres to accommodate the lengths of the different types of waste.

The supercontainer fulfils several functions, contributing to the operational and long-term safety of man and the environment:

- to provide permanent shielding for workers (25 µSV/h at 1 metre from the disposal waste package) (operational safety);

- to provide sufficient mechanical strength (for handling, gallery support, accidental fall, retrievability, etc.) (operational safety);

- to contain the radionuclides and other contaminants through at least the thermal phase. The overpack should show a low sensitivity to localised corrosion and an acceptable uniform passive corrosion rate in its cementitious (high pH) environment. This implies that there would be no premature penetration of the overpack due to localised corrosion but that, over an extended period of time, there may be gradual loss of wall thickness (long-term safety).

The supercontainer is assembled at the surface before being transported underground for disposal. The first stage of supercontainer assembly consists of inserting the waste packages into an overpack. The overpack either contains two vitrified high-level waste packages emplaced end-to-end, four boxes containing UOX irradiated fuel assemblies positioned in parallel, spaced by an 8 centimetres thick cross-shaped cast iron separator or one box with a MOX irradiated fuel assembly, should the direct disposal of the latter fuel type be considered. Carbon steel has been chosen for the overpack because its corrosion behaviour is well known and because, under the high pH conditions expected in the buffer, it will undergo general corrosion, rather than the less predictable localised corrosion. Furthermore, it is easy to weld in reasonable thicknesses. The void space between waste packages and overpack is filled with an inert material before the overpack is sealed by welding (ONDRAF/NIRAS 2019a).

The filled overpack is then inserted in the prefabricated concrete buffer, which is closed and sealed by a (cast) concrete lid. The roles of the buffer are to act as a radiation shield and pH controller in order to create favourable conditions with regards to passivation of carbon steel so that the overpack will fully contains the waste for thousands of years (at least for the duration of the thermal phase). The buffer is made of concrete containing Portland cement because this provides a highly alkaline chemical environment, which lasts thousands of years. In this highly alkaline chemical environment, the external surface of the overpack will be passivated and corrosion will be inhibited (GALSON 2005). The formation of a passive layer on the surface of an embedded carbon steel body under the influence of a high pH environment is a well-known phenomenon and guarantees a low uniform corrosion rate (Chivot 2004; Macdonald 2011).

EURAD (Deliverable n° 6.1) – Initial State of the Art on Gas Transport in Clayey Materials
Dissemination level: PU
Date of issue of this report: 17/11/2021

Page 249
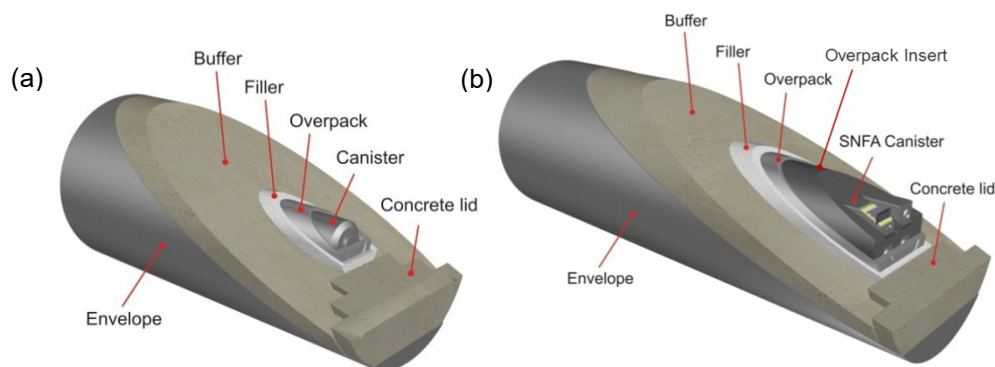
Figure 4-8 – Supercontainer for (a) vitrified high-level waste and (b) UOX spent fuel (ONDRAF/NIRAS 2013a).
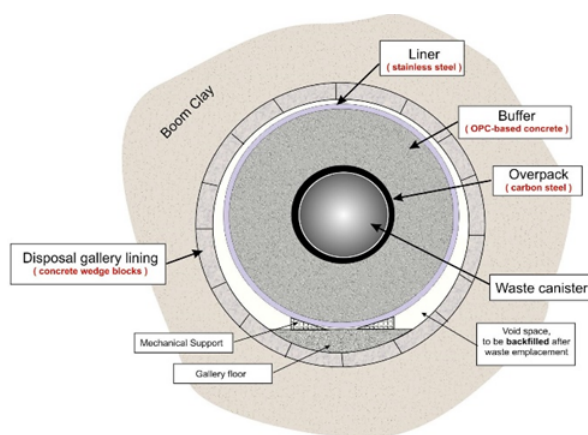
Figure 4-9 – Supercontainer design in a geological repository, disposal waste package, concrete lining and host clay formation (ONDRAF/NIRAS 2013a).

4.1.2.1.2   Monolith B

The disposal packages for intermediate-level and long-lived waste (i.e. the category B waste in the Belgian concept) are called monoliths B. In the reference design, the primary waste packages of this type of waste are immobilised in mortar in concrete caissons made with Portland cement. Several monolith B designs exist to accommodate the large variety of primary waste packages (Figure 4-10). The outside diameter is always 2.8 metres, the length of the different monolith designs ranges from 1.9 to 2.9 metres, and their mass ranges from 32 to 39 tonnes (ONDRAF/NIRAS 2019b).
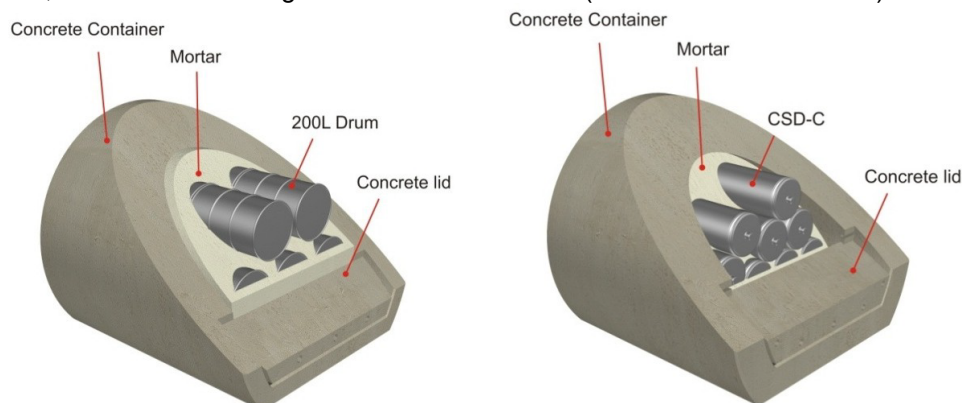
Figure 4-10 – Disposal waste packages for intermediate-level and long-lived waste (monoliths B) (ONDRAF/NIRAS 2013a).

EURAD (Deliverable n° 6.1) – Initial State of the Art on Gas Transport in Clayey Materials
Dissemination level: PU
Date of issue of this report: 17/11/2021

Page 250

The monolith B fulfils several functions, contributing to the operational and long-term safety of the man and the environment:

- to standardise the dimensions and mass of disposal packages and limit the underground works (operational safety);

- to provide permanent shielding for workers (25 µSV/h at 1 metre from the disposal waste package) (operational safety);

- to provide sufficient mechanical strength (for handling, gallery support, accidental fall, retrievability, etc.) (operational safety).

The monolith B is constructed at the surface before being transported underground for disposal. At the post-conditioning facility, primary waste packages are inserted in a pre-cast caisson, then mortar is poured in (eventually through the concrete lid) to fill up and close (i.e. cover) the disposal package (ONDRAF/NIRAS 2019b). This way of post conditioning category B waste allows standardising transportation and handling operations for disposal and disposal gallery backfilling operations. The thicknesses of the lid and the caisson walls are determined by the shielding criterion. In the current reference design, the standardised outside diameter of the monoliths B is maximised to the disposal gallery diameter. It follows that the number of primary waste packages inside a monolith is determined by the dimensions of these packages and by their radiological activity. If the primary packages are relatively short, a second layer of primary packages can be stacked on top of the first one. However, in order to maintain the weight and dimensions of all monoliths within a certain range, to allow standardising transportation and handling operations, no second layer is stacked if it would lead to the total length of the monolith B becoming much larger than its diameter.

4.1.2.1.3   Geological disposal facility layout

The reference solution considered in Belgium for RD&D purposes is a geological disposal in a poorly indurated clay layer at a depth between 200 and 600 metres and being at least 100 metres thick. This reference solution implies either the Boom Clay or the Ypresian clays as reference host rock formation. This reference layout of the GDF is given in Figure 4-11 and described in detail in ONDRAF/NIRAS (2020).

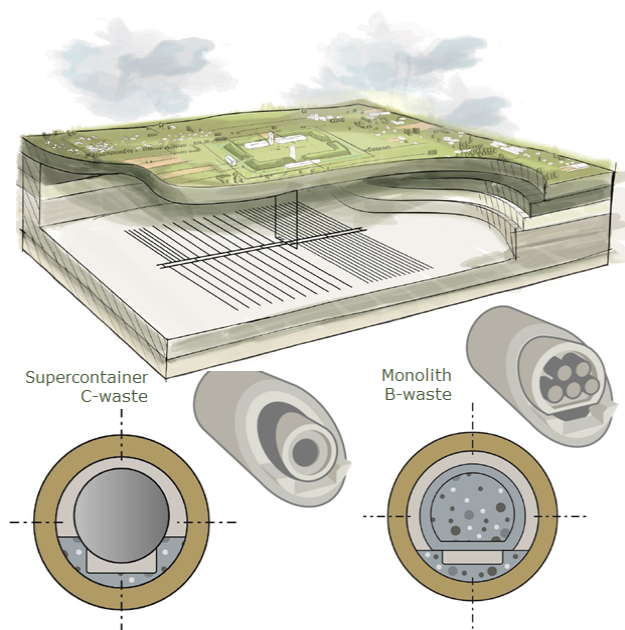*Figure 4-11 – Artistic view of a geological disposal facility (ONDRAF/NIRAS 2020).*

EURAD (Deliverable n° 6.1) – Initial State of the Art on Gas Transport in Clayey Materials
Dissemination level: PU
Date of issue of this report: 17/11/2021
Page 251

The reference layout of the GDF is split in two separated areas, constructed and operated successively: one for the category B waste and another one for the category C waste. It is composed of two access galleries for each area and a network of maximum 1 km long disposal galleries built perpendicularly to the access galleries. The distance between disposal galleries depends on the waste type, it is 50 metres for those containing category B waste and vitrified waste and 120 metres for those containing heat-generating category C waste to limit temperature increase in the clay and the surrounding aquifers. The GDF is operated and ventilated by two shafts.

Considering the outer diameter of the disposal waste packages (DWP, 2 m) and the space required for the ventilation ducts, the internal diameter of the disposal galleries is 3.5 metres. To allow rotation of the longest DWP at the T-crossing, the diameter of the access galleries is 7.0 metres. Galleries are supported by thick, structural concrete lining. A concrete end plug of 20 metres is foreseen at the end of the disposal galleries to avoid direct contact between the disposal waste package and the Boom Clay. Access and disposal galleries will be outfitted with a concrete floor, specifically designed to provide a path for the transportation. Within the disposal gallery, the floor will serve as a mechanical support to dispose the disposal waste packages. A cementitious material with a high water/cement ratio mortar will be used to progressively backfill remaining gaps in each disposal gallery. The backfill will reduce the voids and, consequently, the amount of free water in the repository. Furthermore, the backfill will provide mechanical stability to the gallery lining and limits the risk of human intrusion. Disposal galleries will be sealed after complete backfilling by cementitious plugs of 25 metres long, for reasons of operational safety. Access galleries and shafts will be hydraulically sealed with bentonite-based materials.

4.1.2.1.4   Safety functions

The disposal system has to provide three main safety functions (ONDRAF/NIRAS 2013a, Figure 4-12):

1. Engineered containment (only for category C waste). It consists in preventing the release of contaminants from the waste disposal package during the thermal phase, where the thermal phase is the time frame during which the temperature of the host formation is expected to lie above the range of temperatures within which nominal transport properties can be relied upon, by using one or several engineered barriers. This containment is ensured by the supercontainer components, namely the overpack and its favourable environment provided by the cementitious buffer.

2. Delay and attenuate the releases in order to retain the contaminants for as long as required within the disposal system. The components contributing to this safety function are the waste forms, the engineered barrier system and the host formation. Three subfunctions are defined:

   o Limitation of contaminant releases from the waste forms: This function consists of limiting and spreading in time the releases of contaminants from the waste packages.

   o Limitation of the water flow through the disposal system: This function consists of limiting the flow of water through the disposal system as much as possible, thus preventing or limiting the advective transport to the environment of the contaminants released from the waste packages.

   o Retardation of contaminant migration: This function consists of retarding and spreading in time the migration to the environment of the contaminants released from the waste packages.

3. Isolation of the waste from man and the environment for as long as required, by preventing direct access to the waste and by protecting the repository from the potential detrimental processes occurring in its environment. The host formation and its geological coverage provide this safety function. Two subfunctions are defined:

EURAD (Deliverable n° 6.1) – Initial State of the Art on Gas Transport in Clayey Materials
Dissemination level: PU
Date of issue of this report: **17/11/2021**

Page 252

- o Reduction of the likelihood of inadvertent human intrusion and of its possible consequences: This function consists of limiting the likelihood of inadvertent human intrusion and, in case such intrusion does occur, of limiting its possible consequences in terms of radiological and chemical impact on humans and the environment.

- o Ensuring stable conditions for the disposed waste and the system components: This function consists of protecting the waste and the engineered barrier system (EBS) from changes and perturbations occurring in the environment of the facility, such as climatic variations, erosion, uplifting, seismic events or relatively rapid changes in chemical and physical conditions.
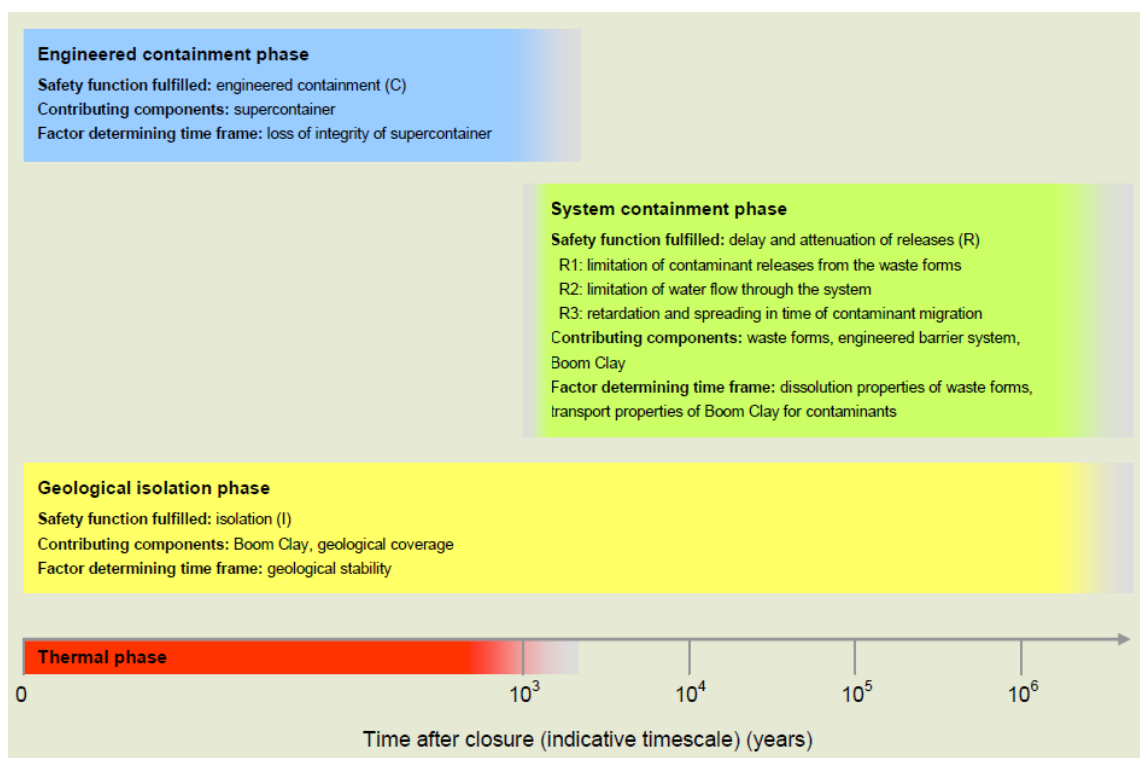
Figure 4-12 – Safety functions provided by the main components of the disposal system in Boom Clay and its geological coverage and the time frames over which they are expected to be fulfilled. The engineered containment phase is specific to heat-generating waste (category C waste, that is, vitrified high-level waste and irradiated fuel) (ONDRAF/NIRAS 2013a).

The dominant component of the disposal system from the point of view of long-term safety if the system evolves as expected is the host formation. The poorly indurated clays studied in Belgium are efficient natural barriers to the migration of radionuclides and chemical contaminants towards the surface environment:

- They have a very low permeability. There is therefore practically no water movement in these clays. As a result, transport is essentially diffusive, which means species migrate under the influence of their concentration gradient, not under the influence of the pore water movement.

- They have a strong retention capacity for many radionuclides and chemical contaminants (e.g. sorption capacity, favourable geochemical properties). Their migration through the clay is thus considerably delayed.

- They have a capacity of self-sealing. Fractures such as those induced by excavation works seal within weeks in Boom Clay and Ypresian clays.

EURAD (Deliverable n° 6.1) – Initial State of the Art on Gas Transport in Clayey Materials
Dissemination level: PU
Date of issue of this report: 17/11/2021

Page 253

The EBS fulfils three main functions:

- Next to operational safety aspects, it limits perturbations of the host formation by repository construction, operation and closure and it contains the category C waste during the thermal phase.

- It contributes to the delay and attenuation of the releases.

- The presence of backfill and seals will ensure that transport within the repository after closure will also be diffusion-dominated.

The current safety concept and repository design have not been optimised with respect to gas. So far, the main focus was to ensure the containment of all contaminants inside the overpack till at least the end of the thermal phase (category C waste). The design was focused on ease of operation (e.g. supercontainer and monolith provide shielding) and feasibility of excavation and construction. In the current Safety and Feasibility Case, gas is not included in reference scenario but only considered as a perturbation that should not affect barrier integrity or performance.

4.1.2.2 Conceptualisation of gas transport at the level of the repository

The generation of gas is inevitable after closure of the disposal gallery, due to (i) the anaerobic corrosion of metals contained in waste, container materials, overpacks …, (ii) the microbial degradation of waste, (iii) the radiolysis of organic components, and, to a lesser degree, (iv) the alpha decay. Gas generated within the GDF are mainly hydrogen, methane, helium and radon. In quantity the major gas generated is the hydrogen as a result of the corrosion of metal components.

Initially, gas generated in the near field of a geological repository in clay will dissolve in the pore water and will be transported away from the repository by diffusion as dissolved species. However, if the gas generation exceeds the capacity for diffusive transport of dissolved gas, a free gas phase will be formed, leading to a gas pressure build-up and eventually to gas breakthrough events. During gas breakthrough, some water could be displaced by the gas phase. Depending on the timing of gas breakthrough, dissolved radionuclides and contaminants could be driven through the disposal system and, ultimately, out of the clay faster than by the normally expected diffusive transport of these radionuclides and contaminants.

The study of possible gas transport modes through Boom Clay is being carried out in the WP GAS of EURAD. In this section, the ONDRAF/NIRAS's conceptualisation of gas transport is presented at repository scale. It is based on the state of knowledge of gas transport processes available at the beginning of the project and described in the previous chapters of this state-of-the-art report of the WP GAS.

4.1.2.2.1   Main controls on gas transport modes

The system characteristics and processes controlling the transport modes of gas in a poorly indurated clay like the Boom Clay are mainly related to:

1. <u>The fast saturation of disposal galleries.</u> As the permeability of the Boom Clay is about 10^{-19} m², the Boom Clay will on the one hand never be unsaturated (even by ventilation of the galleries) and on the other hand water will easily enter in the components of the GDF after gallery closure (as the permeability of these components is higher than the one of Boom Clay).

2. <u>The generation of gases in disposal galleries</u> by corrosion of metallic components. This production of gas starts in presence of water, after the gallery closure, and depends on the chemical conditions (pH and temperature) imposed by DWP. In the Belgian context, both

EURAD (Deliverable n° 6.1) – Initial State of the Art on Gas Transport in Clayey Materials
Dissemination level: PU
Date of issue of this report: 17/11/2021

Page 254

monoliths and supercontainers are in a high pH concrete environment (pH about 12.5–13.5) to allow a passive corrosion from initial stage, and a depassivation by concrete lixiviation at very long term.

3. The evacuation capacity of dissolved gases. With reasonably conservative estimates of the gas source terms of category C waste, gas is expected to be evacuated entirely by dissolution and diffusion. A gas phase is only likely to be formed within the EBS without penetrating into the Boom Clay for the maximum gas production rates (Yu L. and Weetjens 2012). However, current estimates of diffusive evacuation capacity and source terms suggest that a gas phase will develop and pressurise the system for some category B waste (Yu L. and Weetjens 2012). For those, gas pathways could be active and there is a need to evaluate their consequences on repository components.

4. The high gas entry pressure in intact Boom Clay, higher than in situ stresses at HADES URL level, is not favourable to the development of a gas phase through the Boom Clay beyond the EDZ without perturbing it (Yu L. and Weetjens 2009).

4.1.2.2.2 Main features of the transport of gas in Boom Clay at repository scale: storyboards

The state of knowledge on gas transport is detailed in the previous chapters of this state-of-the-art report of the WP GAS of EURAD and partly summarised in Yu L. and Weetjens (2009). Here, only the potential gas transport modes expected in the Boom Clay at repository scale are described.

Before gallery backfilling, no significant quantities of gas are expected to be generated by the DWPs. If any gas is produced, it will dilute into the ventilation air.

After gallery backfilling, water mostly enters the GDF through the joints between lining segments. Backfill porosity being high, it is the first EBS component to be water saturated. Saturation of DWP and lining concrete elements takes more time as their permeability is lower. Once metallic components are in contact with water, corrosion starts and, as a result, so does generation of gas. The processes occurring during the post-closure phase and related to the generation and the transport of gas are illustrated in Figure 4-13.

Because of the thickness of metallic components and the low anaerobic corrosion rate of steel in undisturbed concrete in Boom Clay environment, gas generation is expected to last for several hundred thousands of years. Once gas generation stops, several thousands of years might be likely necessary to dissipate all remaining gas (Yu L. and Weetjens 2012).

First, the gas produced dissolves in water and migrates out of the repository components by diffusion of dissolved gas. The effective diffusion coefficient of gases in the intact saturated Boom Clay is about 10^{-10} m²/s (Jacops et al. 2015).

Once the evacuation capacity by diffusion of dissolved gas is reached, the excess gas forms a free gas phase and its pressure progressively increases. While two-phase flow has been considered in the past as a possible representation of the transport of free gas through Boom Clay, it now seems likely that the creation or activation of gas-specific conductive pathways will be necessary for the free gas to be transport into water-saturated Boom Clay (Yu L. and Weetjens 2009). If so, depending on the in situ conditions at that time, gas might be transported in Boom Clay through (Figure 4-14):

1. The excavation damaged zone (EDZ). If gas pressure is sufficient, gas entry in this zone of potentially lower strength is possible and gas might be transport through the disturbed, near field Boom Clay (Ortiz et al. 2002).

EURAD (Deliverable n° 6.1) – Initial State of the Art on Gas Transport in Clayey Materials
Dissemination level: PU
Date of issue of this report: 17/11/2021

Page 255

2. The interface between the GDF and the host rock. Depending on the contact stress between the clay and the gallery lining and of the properties of this interface, the gas might be transported along it (Ortiz et al. 2002).

3. The bedding planes of the intact Boom Clay. Because of the anisotropic properties of the Boom Clay, if gas pressure is sufficient for gas pathways to develop up to the intact Boom Clay, it may be transported preferentially along the bedding planes (Gonzalez-Blanco 2017).

For all of these possible gas transport modes, the amount of (possibly contaminated) pore water that can be displaced by gas flow is expected to be minimal. This is illustrated in part by Jacops et al. (2011).

(a)

Early post-closure phase
(engineered barriers intact)
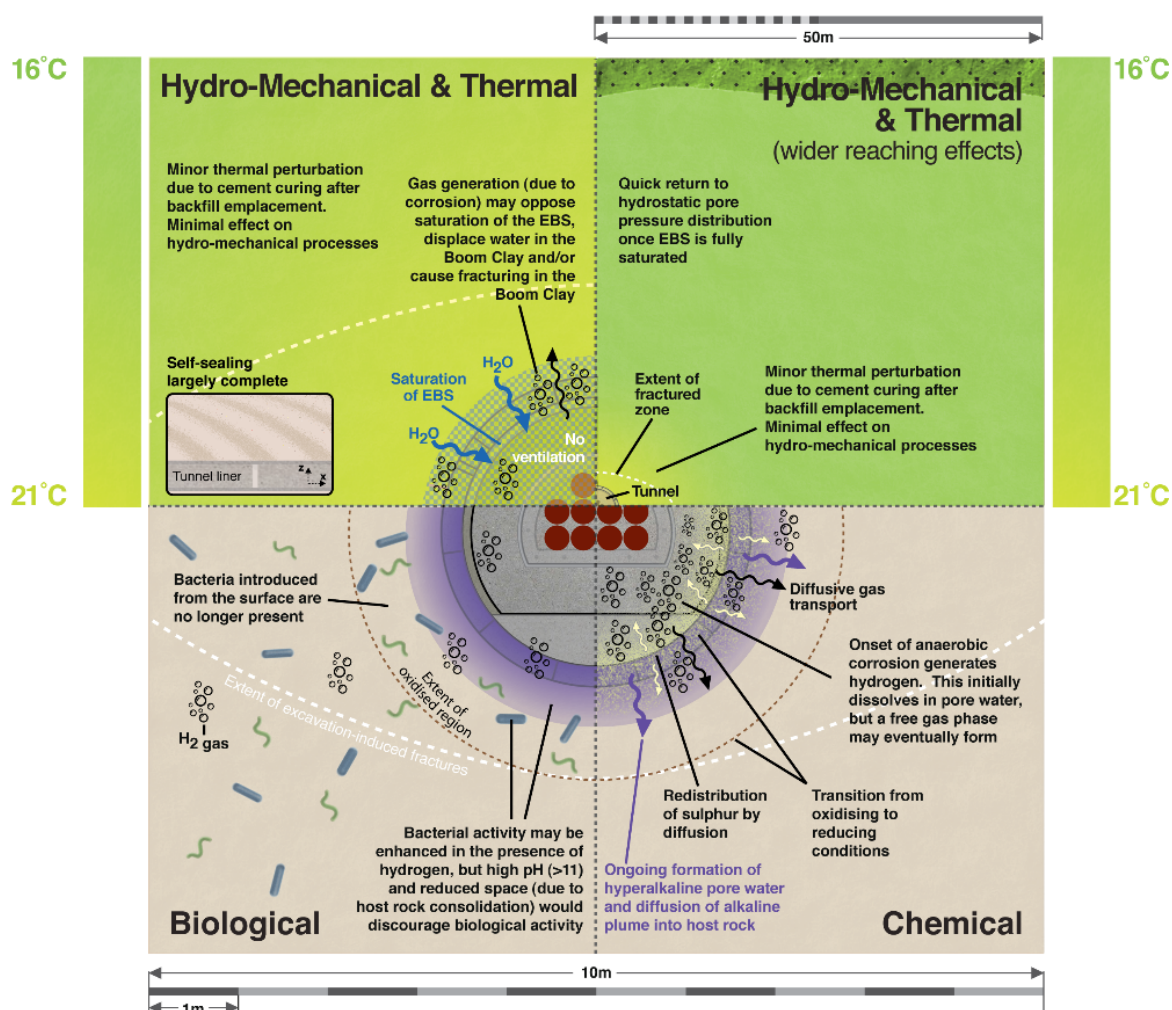
EURAD (Deliverable n° 6.1) – Initial State of the Art on Gas Transport in Clayey Materials
Dissemination level: PU
Date of issue of this report: 17/11/2021

Page 256
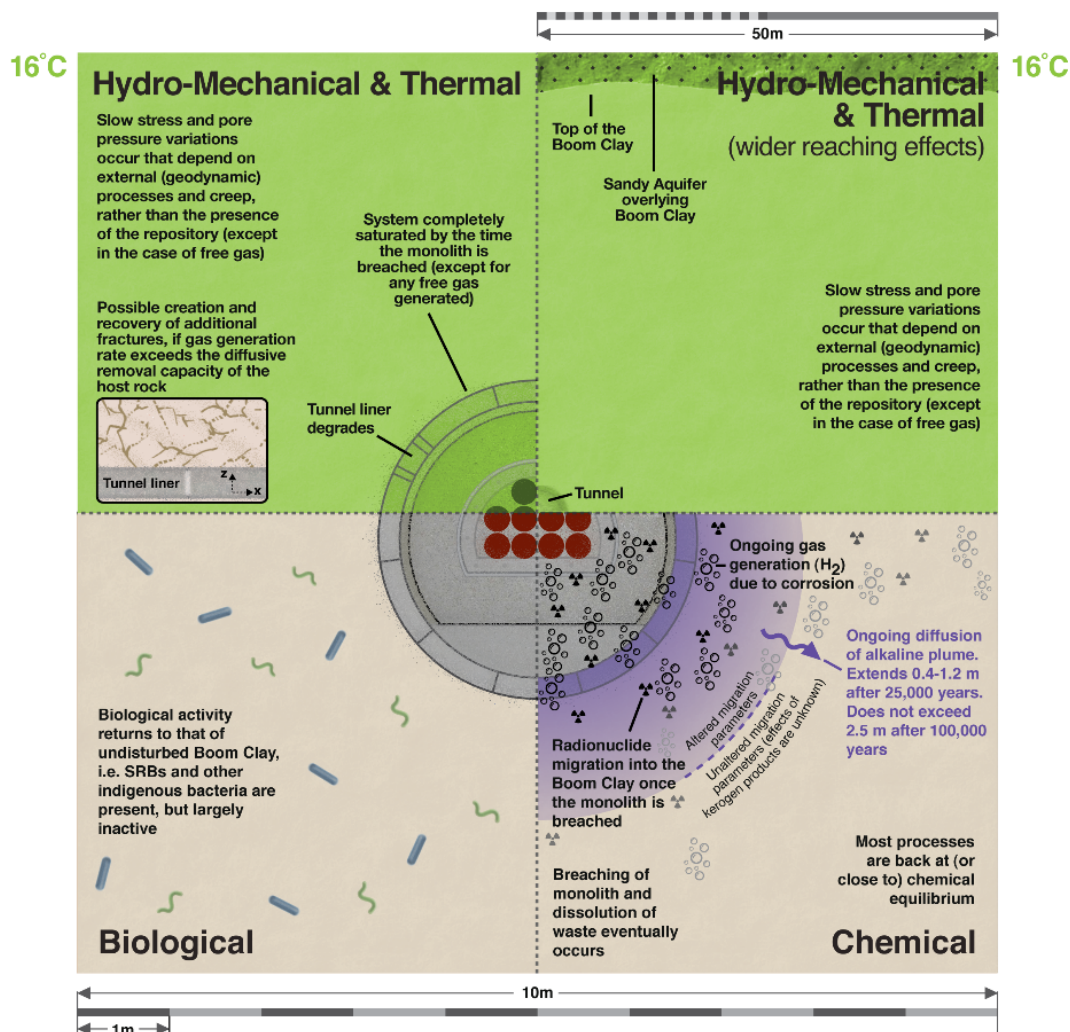
Figure 4-13 – Transverse cross-sections through a disposal gallery filled with category B waste and the surrounding Boom Clay illustrating the processes occurring during (a) early and (b) late post-closure phase (ONDRAF/NIRAS).
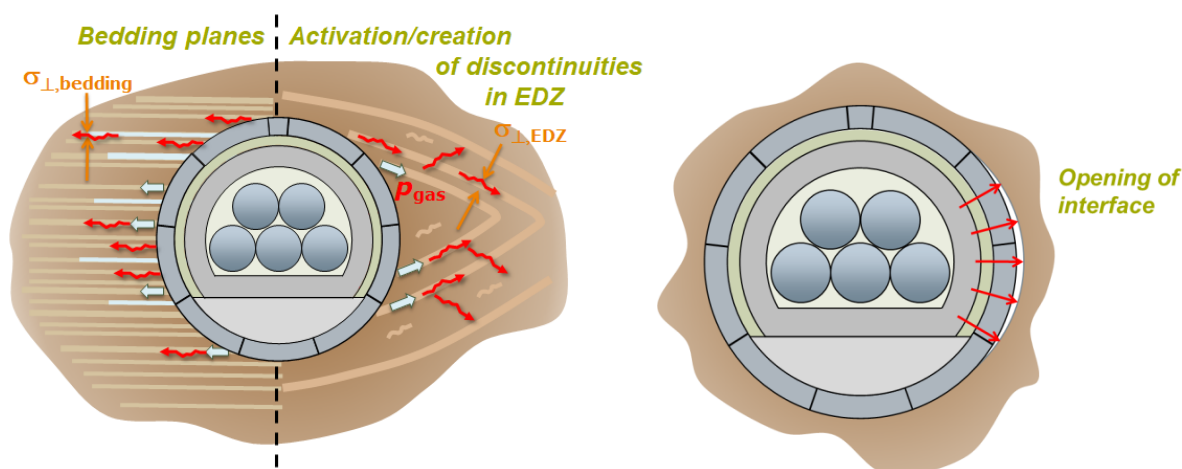
Figure 4-14 – Potential expected gas transport modes in the Boom Clay at repository scale (ONDRAF/NIRAS).

EURAD (Deliverable n° 6.1) – Initial State of the Art on Gas Transport in Clayey Materials
Dissemination level: PU
Date of issue of this report: 17/11/2021

Page 257

4.1.2.2.3   Situations that may affect gas transport in Boom Clay

Gas generation depends on evolving conditions affecting the gas source term as for instance the water availability, the corrosion rates and the microbial activity that in some case might reduce the amount of gas.

Gas transport parameters depend on the properties of the Boom Clay and on the properties of the EBS, e.g.:

1. Transport of gas through the lining blocks is unlikely as diffusion coefficient in structural concrete is very small and breakthrough pressure very high compared to the other components of the GDF. Gas can probably move through the joints between lining segments.

2. The convergence of the Boom Clay around GDF will:

    o   Induce a continuous evolution of the state of stress around galleries modifying the characteristics of the EDZ and of the interfaces GDF/Boom Clay, affecting the gas transport properties in the area surrounding galleries. Estimation of the state of the sealed EDZ and interfaces at the time of gas migration is an open question.

    o   Cause clay to intrude into the lining joints. On the long-term, the properties of the joints might be related to the properties of the clay, limiting water or gas flows through the GDF. Estimation of the actual sealing of these joints by clay is an open question.

3. The diffusion coefficient of dissolved gas through the intact DWP materials (supercontainer or monolith) is one order of magnitude lower than in the Boom Clay (Jacops et al. 2021). This will limit the capacity of the DWP to evacuate gas by dissolution and diffusion. This limited capacity of evacuation by diffusion may be also reinforced by the potential carbonation of cementitious components. The possible pressurisation of the DWP and its consequences on gas release and transport still have to be considered.

4. The backfill of the galleries presents a high porosity that allows to store a large amount of gas. However, because of its weak mechanical strength, the risk of backfill damage and its consequences on gas transport still have to be considered. The impact of carbonation of the cementitious backfill also remains to be taken into account.

5. Galleries of the GDF are closed by seals/plugs. There is not yet a specific design for these and their characteristics are thus currently unknown. As they could affect the capacity of the GDF to manage gas transport, the requirements on the seals and plugs and their impacts on gas transport have to be refined.

Furthermore, the gas production rate due to corrosion rate might modify properties and conditions characterising the initiation of gas transport modes (dilatant gas pathways or gas fracturing). Such situations have to be examined.

4.1.2.2.4   The key properties assumed to control gas transport

Regarding the storyboards of gas transport and the situations that may affect gas transport in Boom Clay described previously, the key properties assumed to control gas transport are:

*   In the Boom Clay, both in intact and perturbed conditions:
    o   the diffusion coefficient dissolved gas in saturated conditions,
    o   the gas entry pressure,
    o   the hydraulic conductivity,
    o   the permeability to gas.

EURAD (Deliverable n° 6.1) – Initial State of the Art on Gas Transport in Clayey Materials
Dissemination level: PU
Date of issue of this report: **17/11/2021**

Page 258

- In the EBS, for each component (lining, backfill, DWP materials):
    - the diffusion coefficient of dissolved gas,
    - the gas entry pressure,
    - the hydraulic conductivity,
    - the permeability to gas as a function of the degree of saturation of the porous media.
- At the interface between the Boom Clay and the GDF:
    - the diffusion coefficient of dissolved gas in saturated conditions,
    - the gas entry pressure,
    - the hydraulic and gas transmissivity.

All known properties for the considered clayey materials are provided in the previous chapters of this state-of-the-art report. These values have to be taken with care as they strongly depend on material microstructure and heterogeneities. Their identifications are scale and stress dependant. In addition to these properties, the possible presence (or creation) of discrete features should be taken into account.

4.1.2.2.5   Expected effects of gas on the Boom Clay and on the barrier integrity

The current knowledge on the transport of gas in Boom Clay does not permit at this stage a robust identification of the gas transport modes and conditions that may be active at repository scale. An experimental and modelling programme is still ongoing to improve current knowledge and specify conditions that will allow to bound gas pressures and determine which gas pathways are the most plausible in in the various components of the EBS and in the Boom Clay.

Providing quantitative estimates of the effects of gas on the Boom Clay and the consequences of gas on the integrity of barriers would currently be premature. Specific investigations are needed to evaluate the consequences of limitations imposed by each component (e.g. the monolith B, the backfill, the lining, the near field and far-field clay) on the functioning of the adjacent components. Once possible mechanisms are well understood at component level, they have to be examined in the light of more advanced storyboards of gas transport. The WP GAS of EURAD investigates process of gas transport in clayey materials and their potential impact on a disposal system. Laboratory experiments and in situ tests will be conducted on Boom Clay in order to investigate in particular the possible free gas transport modes and to confirm that no significant pore water displacement is associated with the transport of free gas (if any). Numerical modelling will be performed to analyse potential effects of increasing gas pressures on clayey materials properties. The results of this project will contribute to the further evaluation of the effects of gas on the behaviour of the Boom Clay.

Furthermore, as the design of the Belgian disposal is not yet fixed, the estimation of gas transport modes can only be indicative and various possibilities have to be considered. Disposal functioning in relation to gas transport will be revised iteratively based on new insights on gas transport and its consequence and possible design modifications.

EURAD (Deliverable n° 6.1) – Initial State of the Art on Gas Transport in Clayey Materials
Dissemination level: PU
Date of issue of this report: **17/11/2021**

Page 259

4.1.3 Gas storyboard in Boom Clay by COVRA (Dutch context)

The Dutch programme for geological disposal is in a preliminary phase as the waste will be stored for an extended period before disposal. Suitable clay and salt formations are present in the Netherlands (I&E 2016). The clay host rocks in COVRA's programme are limited to poorly indurated clay formations at suitable disposal depth. The research efforts are focused on the definition of the disposal concept and characterising its associated costs in order to collect sufficient budget through the waste fees upon acceptance of the waste by COVRA. The generation of gas has not yet been included in the post-closure safety assessment. Some limited performance assessment calculations have been performed and are presented in this contribution. Assumptions in the construction and operational phase have been made for these calculations and are therefore presented first.

4.1.3.1 Disposal facility in clay for Dutch waste

During construction of the disposal galleries and access galleries, emplacement of hardened concrete segments is immediately required due to the fast convergence of poorly indurated clays. The following figure shows an artist's impression of such a concrete-supported disposal facility in which all Dutch waste envisaged in 2130 can be emplaced. The facility has 53 disposal galleries with a length of 45 metres for high-level waste (HLW) and 101 disposal galleries with a length of 200 metres for low- and intermediate-level waste (LILW). The external diameters of HLW disposal galleries and LILW galleries are respectively 3.2 and 4.8 metres.
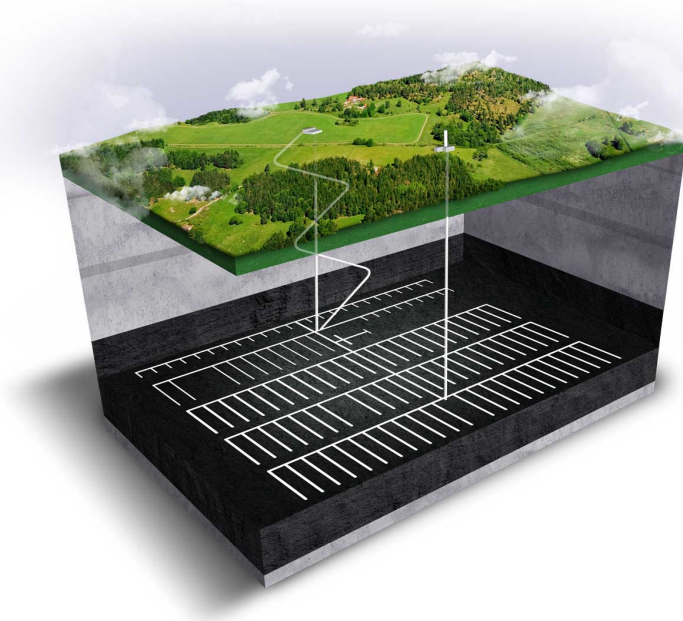
Figure 4-15 – Artist's impression of a geological disposal facility in poorly indurated clay (Boom Clay) in the operational phase (Verhoef et al. 2017).

4.1.3.2 Impact of construction

Fractures are generated in the clay in the vicinity of the tunnel boring machines during the excavation of clay. The characterisation of the Excavated Damaged Zones in clay host rocks has been investigated in the 5th framework programme SELFRAC (Bernier et al. 2007b). The EDZ is characterised as a zone with a larger porosity and permeability than the virgin host rock. The values for hydraulic conductivity or permeability are largest near the interface between concrete and clay (Bock et al. 2010). The driving forces for the closure of the generated fractures during construction are compressive load or confining

EURAD (Deliverable n° 6.1) – Initial State of the Art on Gas Transport in Clayey Materials
Dissemination level: PU
Date of issue of this report: 17/11/2021

Page 260

pressure and access to water. The closure of fractures can be measured as the increase in pore water pressure. The conceptual understanding has been provided in the Swiss programme (Alcolea et al. 2014) in which water suction towards the generated fractures occurs; these fractures have an atmospheric pressure immediately after excavation. The necessary immediate emplacement of the concrete segments prevents further drying and growth of these fractures. Equilibrium has been achieved when the formation pressure is achieved.

Poorly indurated clays have a high self-sealing capacity due to their high content of swelling clay minerals such as smectite of which montmorillonite is the most famous species. The research activities performed in the HADES URL in Mol (Belgium) provide the best available knowledge concerning the speed of the self-sealing process. Table 1-5 in Chapter 1 provides the hydraulic properties of Boom Clay. The extent of the fractures around the galleries depends on the excavation technique and excavated diameter. The connecting gallery was constructed with a larger overcut than the PRACLAY gallery (ONDRAF/NIRAS 2013a). The PRACLAY gallery has an external diameter of 2.5 metres and the connecting gallery 4.6 metres. The measured hydraulic properties near the interface between concrete and clay at the PRACLAY gallery has been measured to be similar to these properties measured further away from this interface (Dizier et al. 2017). It is therefore tentatively assumed that the hydraulic properties in the vicinity of the concrete-clay interface are similar to virgin Boom Clay for the HLW disposal galleries in Figure 4-15. A larger hydraulic conductivity than virgin Boom Clay has been measured for clay near the concrete lining for the larger gallery of 4.6 metres i.e. less than a factor of 3 at less than 1.5 metres from the interface between concrete and clay i.e. outside the interconnected fracture zone after a few months. After 8 years, less than twice as large of a hydraulic conductivity than virgin clay has been measured (Bernier et al. 2007b; ONDRAF/NIRAS 2013a).

The waste packages are emplaced after finishing the construction of the underground facility i.e. construction and emplacement of waste packages will not be envisaged to be parallel activities in the current disposal concept. The necessary time to seal the excavated zone is therefore envisaged to be significantly smaller than the envisaged construction time of 30 years for the Dutch inventory. A twice as large permeability than the virgin host rock for zone of 1.5 metres surrounding the clay-concrete interfaces seems therefore to be a conservative approach for the LILW disposal galleries in Figure 4-15.

4.1.3.3 Negligible impact of operation

In the operational phase, ventilation is expected to be sufficient to keep the underground facility dry. Salts have been deposited at the intrados of the concrete lining especially at joints between concrete segments; these salt deposits can be shown clearly in the HADES URL in Figure 4-16. These deposits are less clearly to be observed in traffic tunnels that are constructed in poorly indurated clay since material as a fire protection measure is usually applied in these tunnels. An indication of the length of the applied concrete segments can however be made by these salt deposits since they appear as white spots on the dark grey fire protection material in which the joints are located at most white parts.

EURAD (Deliverable n° 6.1) – Initial State of the Art on Gas Transport in Clayey Materials
Dissemination level: PU
Date of issue of this report: 17/11/2021

Page 261

Figure 4-16 – (a) salt deposits at joints of concrete segments in HADES URL and (b) traffic tunnel – Westerschelde tunnel – constructed in Boom (Rupel) Clay in the Netherlands.

The salt deposits indicate the preferential path of ingress of clay pore water into the disposal facility. The necessary ventilation in the operational phase may have an impact on the saturation degree of the intrados of the concrete lining at the start of the post-closure phase but is not expected to have an impact on the clay i.e. there is no drying or oxidation of the clay by ventilation. The porosity of the concrete segments is about 12 vol.%, a representative value for well-engineered concrete. This porosity in concrete is smaller than the porosity of poorly indurated clays such as Boom Clay, for example 35–40 vol.% for Boom Clay in Belgium at HADES at 223 metres depth (De Craen et al. 2004), 31–35 vol.% for Boom Clay in the Netherlands at around 500 metres depth (Verweij et al. 2016). The initial saturation of concrete segments is about 90%. The extrados of the concrete lining i.e. concrete interfacing the clay host rock, becomes 100% saturated in the operational phase. The saturation degree of the concrete lining at the intrados i.e. interfacing air, may follow the seasonal variation in relative humidity in the operational phase until the disposal gallery is backfilled. An example of the relative humidity of a research laboratory built in indurated clay i.e. Opalinus Clay is Mont Terri with a seasonal variation in relative humidity between 63% during winter and 94% during summer (Wild et al. 2017).

The porosity of concrete made with blended cements is similar to concrete made with OPC based cement with the same factors such as cement content, water/cement ratio, curing conditions etc but CEM I (i.e. OPC) based concrete has a relative open pore structure compared to blended cements containing slag. Concrete made with these blended cements are called low-permeability concretes due to the refined pore structure (Atkins et al. 1991; Atabek et al. 1991; Jackson et al. 2017). The concrete segments are to be made with blended cement. Aggregates have a negligible porosity for well-engineered concrete. Diffusion values of water in concrete are about 100 times smaller than these diffusion values for virgin Boom Clay.

The disposal galleries will be backfilled with a porous cementitious material e.g. about 28 vol.% porosity, after emplacement of the waste packages. Contact-handled waste is envisaged to be disposed in the Dutch disposal concept. Disposal packages for HLW have been adopted from the Belgian programme: the HLW canisters are to be encapsulated in the carbon steel overpack that is surrounded by a cementitious buffer. Currently, it is investigated whether the gas generated by anaerobic corrosion of a stainless envelope surrounding the cementitious buffer may lead to an acceptable perturbation of the clay host rock in the post-closure phase. Figure 4-17 shows the envisaged disposal cells for Dutch

EURAD (Deliverable n° 6.1) – Initial State of the Art on Gas Transport in Clayey Materials
Dissemination level: PU
Date of issue of this report: 17/11/2021

Page 262

HLW: Spent research reactor fuel (SRRF) and a vitrified waste product that arises from recycling of spent nuclear power fuel.
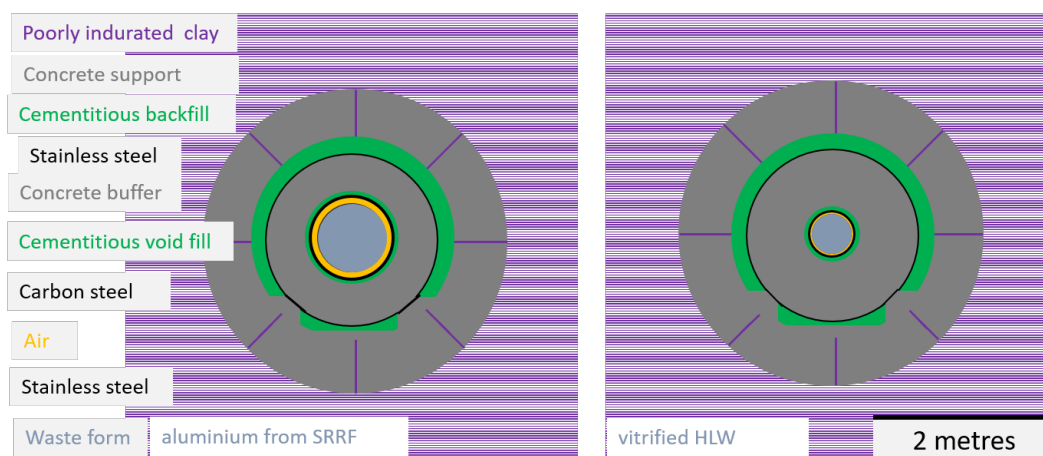

Figure 4-17 – HLW disposal cells envisaged in the Dutch disposal concept, it is uncertain whether an stainless steel envelope will surround the disposal waste packages.

All cementitious materials in the underground facility will be made with sulphate resistant cement since the clay pore water in suitable Dutch poorly indurated clays is expected to be as at least as saline as seawater. COVRA's current experience – it is a certified concrete supplier – is used for the definition of cement recipes. The current choice is to use cement with Blast Furnace Slag (BFS) content of at least 66% blended with Ordinary Portland Cement. Interfaces between carbon steel and cement blended with BFS have been known to form magnetite since the nineties (Naish et al. 1991). Magnetite can only be formed during anaerobic corrosion of carbon steel. These anaerobic conditions are provided by the traces of pyrite that are present in cement blended with BFS. Anaerobic conditions at the interface between the concrete buffer and carbon steel overpack and thereby gas generation is therefore assumed to start in the operational phase.

4.1.3.4 Post-closure phase

Impact of thermal phase

The waste form, overpack, concrete buffer, backfill and clay host rock will be heated by the heat produced by the heat emitting waste, leading to a rise of temperatures followed by a slow cooldown later in the post-closure phase as heat production diminishes due to radioactive decay. The temperatures as a function of time have been calculated as a function of time for the vitrified HLW for a 2D axi-symmetric case. SRRF has a smaller heating power. The following figure shows the calculated results for a cooling period of the waste at the start of the post-closure phase of 130 years.

EURAD (Deliverable n° 6.1) – Initial State of the Art on Gas Transport in Clayey Materials
Dissemination level: PU
Date of issue of this report: **17/11/2021**

Page 263
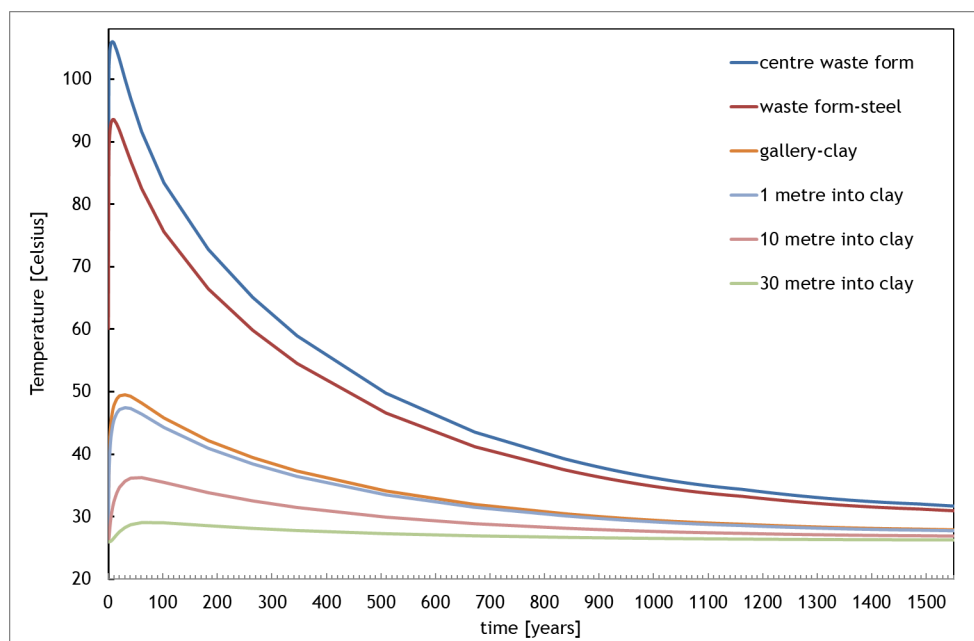
Figure 4-18 – Calculated temperatures at different interfaces after a storage period above ground of 130 years for CSD-V; at midpoints; 2D axi-symmetry with thermal power as supplied by AREVA.

Figure 4-18 shows that the temperature of the clay remains below 50°C in the Dutch case. Minor hydro-mechanical perturbations are therefore expected in the clay host rock in the vicinity of the concrete lining. The heating reduces the saturation degree in the concrete buffer and thereby the availability of water for anaerobic corrosion. This reduction in saturation degree may lower the corrosion rate. The increase in temperature may increase the corrosion rate since the diffusion of water through the passivating layer, magnetite, is larger. So far, there is no evidence that heating increases the corrosion rate in alkaline media if the temperature remains below 80°C. Irradiation has also been found to have no impact if the dose rate remains below 25 Gy per hour (Smart et al. 2017) which is the situation for the Dutch HLW with a cooling period of about 130 years, a dose rate of 5.2 Gy/hr at the surface of the carbon steel overpack containing CSD-V has been calculated.

Considered gas transport mechanisms

The MEGAS EC project has investigated gas transport. Within this project, Volckaert et al. (1995) have identified three zones of gas behaviour in Boom Clay that are visualised in Figure 4-19:

- transport of gas dissolved in the pore water,
- two-phase flow,
- dilatancy-controlled gas flow and tensile failure.

EURAD (Deliverable n° 6.1) – Initial State of the Art on Gas Transport in Clayey Materials
Dissemination level: PU
Date of issue of this report: **17/11/2021**

Page 264

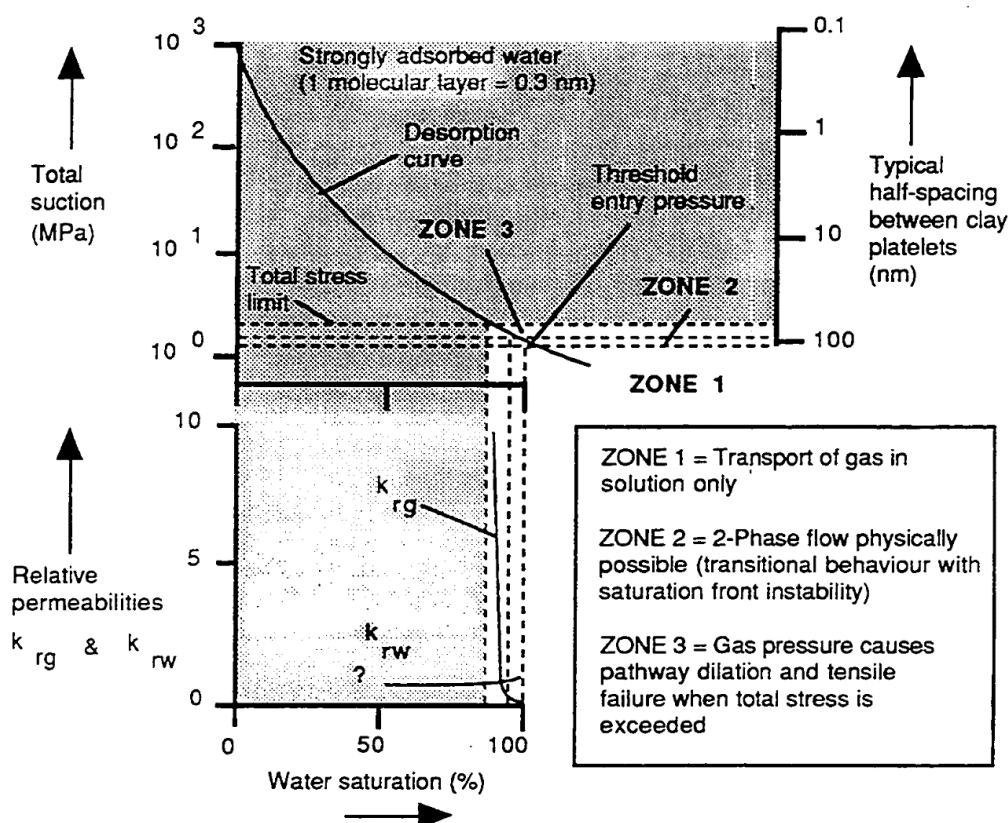*Figure 4-19 – Mechanisms of gas migration in Boom Clay (Volckaert et al. 1995) revised from Volckaert et al. (1994).*

Transport of gas in solution

As long as the gas solubility is not exceeded, gas can be dissipated by advection and diffusion. Advection is considered when a load is applied on the host rock for example during an ice age. For the first 100 000 years, such a climate is not expected in the Netherlands. Initially, only diffusion is considered i.e. pore water is stagnant. The diffusion values along the bedding planes are larger than the diffusion values perpendicular to the bedding planes.

Usually, the gas solubility is determined by the hydrostatic pressure e.g. 5 MPa at 500 metres depth. For the Dutch case, clay pore water can at least be as saline as seawater and the solubility of gas decreases with increasing salinity. The International Union of Pure and Applied Chemistry (IUPAC) evaluate and publish recommended data. The evaluation of available data for the solubility of hydrogen can be found in volume 5/6 in which it was concluded that sufficient data of good quality are available to recommend data for hydrogen pressures below 200 kPa but too limited high quality data were available for above 200 kPa (IUPAC 1981). As a first approximation, the ideal gas law is assumed. The gas solubility depends on the ionic strength of the clay pore water, temperature and the lithostatic pressure i.e. the depth of the clay host rock. The solubility of hydrogen in mol H_2 per m^3 is calculated by:

$$n_{H_2} = x_{H_2}(101.325\ kPa, T)\frac{\alpha_{H_2}(\%, T, P)}{\alpha_{H_2}(0, T, P)}P_{H_2}\frac{1}{V_m(H_2O)}\phi_{clay} \tag{4-1}$$

EURAD (Deliverable n° 6.1) – Initial State of the Art on Gas Transport in Clayey Materials
Dissemination level: PU
Date of issue of this report: **17/11/2021**

Page 265

where x_{H_2} is the recommend hydrogen solubility by IUPAC in mole fractions of the gas in solution at one atmosphere of the gas. The recommended fit for the selected data is:

$$\ln x_{H_2}(101.325 kPa, T) = -48.1611 + 55.2845/(T/100K) + 16.8893 \ln(T/100K) \qquad (4\text{-}2)$$

The gas solubility ratio can be given as the Bunsen coefficient ratio (α) and defined as the volume of gas absorbed by unit volume solvent as a function of salinity (%), temperature (T) and pressure (P). This ratio in measured values for the Bunsen coefficients as measured by Crozier and selected by IUPAC becomes

$$\frac{\alpha_{H_2}(3.9927\%, 297.55K)}{\alpha_{H_2}(0\%, 297.92K)} = \frac{0.0147}{0.017789}.$$

The disposal depth is converted to a potential hydrogen pressure in atmosphere (P_{H_2}), $V_m(H_2O)$ is the molar volume of the solvent H₂O and ϕ_{clay} is the porosity of clay. Figure 4-20 shows the calculated solubility of hydrogen as a function of depth with the same porosity.
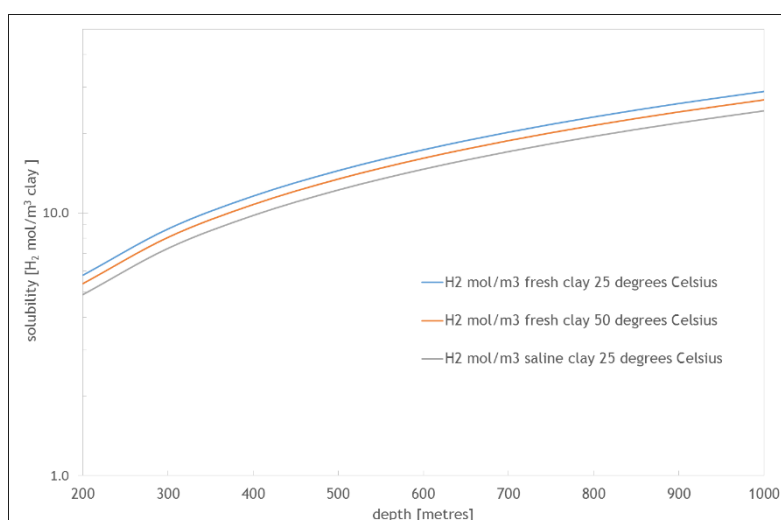
Figure 4-20 – Calculated hydrogen gas solubility in clay; saline as seawater is calculated as clay pore water; porosity 37%.

Please note that the hydrogen concentration on the y-axis is on a log scale. The temperature of 50°C is the calculated maximum in temperature in the thermal phase at the interface between the gallery and clay for Dutch waste. The porosity of about 37% is the measured porosity in Boom Clay in Mol at HADES URL (Jacops et al. 2016) which is at a depth of 223 metres. Salinity is therefore envisaged to have a higher impact on the solubility of gas in the Dutch programme than temperature.

Two-phase flow

The clay host rock in the vicinity from the concrete and beyond is expected to be saturated at the start of the post-closure phase due to:

1) the fast achievement of the pore water pressure after emplacement of the concrete segments in the construction phase
2) the prevention of drying in the operational phase by the concrete liner.

EURAD (Deliverable n° 6.1) – Initial State of the Art on Gas Transport in Clayey Materials
Dissemination level: PU
Date of issue of this report: **17/11/2021**

Page 266

Consequently, the relative gas permeability in the clay host rocks is assumed to be zero at start of the post-closure phase. Visco-capillary two-phase flow is also used when the amount of dissolved gas exceeds the solubility limit. This transport mechanism has however been known to be an impossible mechanism for bentonite (Horseman et al. 1999). Poorly indurated clays may also have a too high smectite content to have a sufficient rigid skeleton of pores. The compressibility of the clay matrix needs to be included in order to calculate permeability values with variable porosity values that gave reasonable steady-state results i.e. a change of the clay pore structure in the first phase of MEGAS (Volckaert et al. 1995). The experimentally observed transient behaviour could not be modelled with solely changing the permeability of gas and liquid. The capillary bundle model was used in the second phase of MEGAS (Ortiz et al. 1997) and the trend in transient behaviour as experimentally observed could be simulated but the model should be extended with variable pore radius with gas pressure.

Dilatant flow and fracture flow

For dilatant gas flow, it may be necessary to include the swelling pressure or another material property that takes the dynamic response of the clay pore fabric into account in order to understand this transport mechanism for poorly indurated clays. The bedding planes are the preferential pathway for this gas transport mechanism since the smallest breakthrough pressures are present there as measured in MEGAS. Steady-state flow rates were possible to be measured experimentally when the preferential gas pathway could be between the bedding planes (Ortiz et al. 1997). There is a variation in the measured breakthrough pressures since the size of the sample cannot accommodate the scale of the heterogeneities within clay but a variation of 1 MPa excess pressure has been measured. Fitting of experimental results led to an understanding of the effective gas permeability by opening of these preferential pathways. On the scale of the disposal system, trapping of gas between the bedding planes of sedimentary formations is envisaged since this trapping is observed in seismic sections as bright spots as shown in Figure 4-21.

EURAD (Deliverable n° 6.1) – Initial State of the Art on Gas Transport in Clayey Materials
Dissemination level: PU
Date of issue of this report: 17/11/2021

Page 267
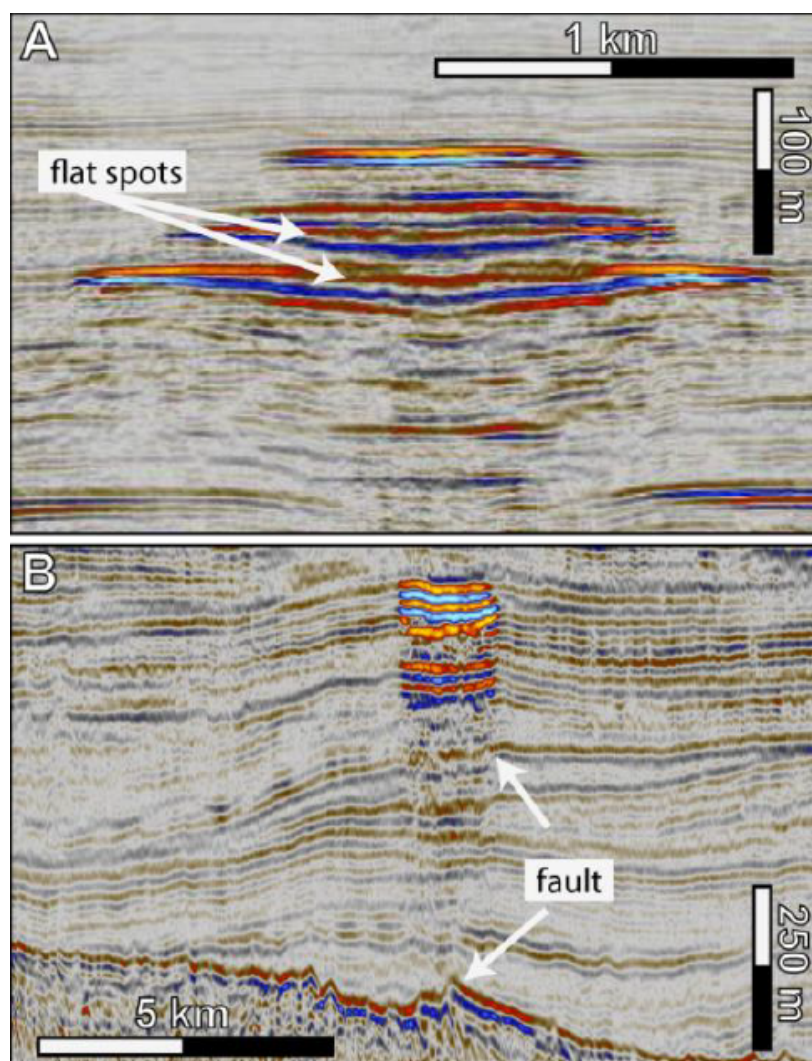
Figure 4-21 – Seismic sections of the northern Dutch offshore with various types of bright spots: (a) stacked bright spots indicative of multi-layered gas fields, each with their own gas-water contact (seen as flat spots); (b) multi-layered bright spots above acoustic turbulence zone that hint at gas expulsion from a faulted zone below (Ten Veen 2015).

Faults perpendicular to the bedding planes results into release of this trapped gas. Gas experiments performed perpendicular to the bedding planes show much higher breakthrough pressures and achieved only very small, perhaps even negligible steady-state gas flow rates. This type of gas breakthrough requires gas pressures till the total or lithostatic pressure (Ortiz et al. 1997; Volckaert and Mallants 2001) e.g. 10 MPa at 500 metres depth.

4.1.3.5 Preliminary performance assessments

In the post-closure phase, the preferential pathway for clay pore water transport is along the joints between concrete segments into the cementitious backfill. The backfill is more porous than the concrete buffer of the supercontainer i.e. shielded container so there will be initially a dissipation of water within the backfill until saturation. The intrados of the concrete lining – that was dried due to ventilation in a relative humidity below 100% – becomes saturated. The relative permeability of gases in concrete becomes zero and the preferential gas pathways out of the disposal facility becomes the joints between concrete segments as indicated in Figure 4-22.

EURAD (Deliverable n° 6.1) – Initial State of the Art on Gas Transport in Clayey Materials
Dissemination level: PU
Date of issue of this report: **17/11/2021**

Page 268

Figure 4-22 – Preferential pathways of clay pore water (purple), hydrogen gas (yellow) and leaching of dissolved species in cementitious pore water (grey) (a) spent fuel from research reactor; (b) vitrified HLW.
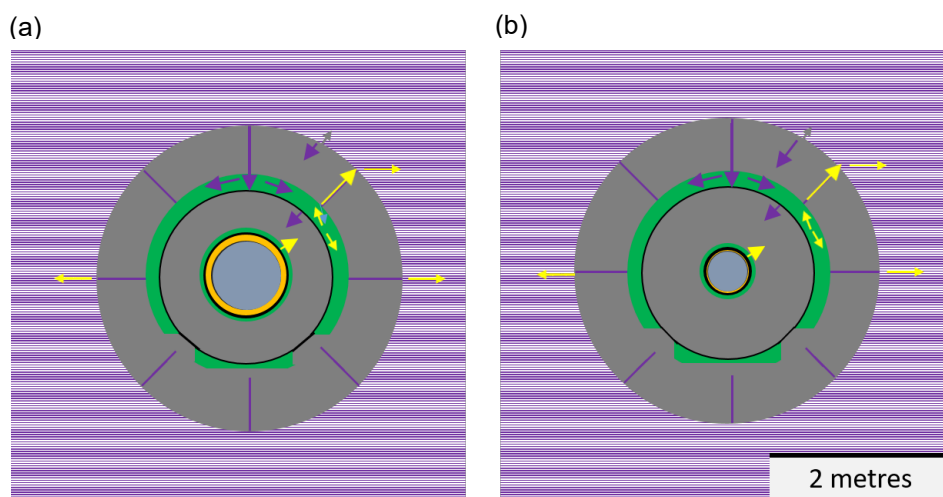
The chemical interaction between clay host rock and concrete causes some cementation of the clay by precipitation of calcite by the reaction between the bicarbonate ions from the clay pore water and leached calcium ions from the concrete segments. The preferential pathways of the generated gas are envisaged to be the bedding planes.

Stationary hydrogen concentrations for a 1D axi-symmetric case containing vitrified HLW in Figure 4-23 have been made for an anaerobic corroding stainless steel envelope and carbon steel overpack. The preferential gas pathway between concrete segments has initially been excluded, these pathways will be included at a later stage. For this simulation, the hydrogen diffusion value in the concrete buffer and concrete segments is assumed to be 100 times larger than in clay. The calculations show that the hydrogen generation by radiolysis has a negligible contribution to the hydrogen flux into the clay host rock if shielding by the concrete is included. Potential cracks in the concrete buffer will increase these diffusion values but these are limited to the diffusion values in clay. The calculated hydrogen concentration in the clay becomes larger due to the envisaged higher corrosion rate but the gas solubility in the clay host rocks may still not be exceeded. Microbial induced corrosion cannot be excluded at the interface between the stainless steel envelop and porous backfill. The gas solubility in the clay host rock is expected to be exceeded by the anaerobic corrosion of this steel as the bottom figure shows.

EURAD (Deliverable n° 6.1) – Initial State of the Art on Gas Transport in Clayey Materials
Dissemination level: PU
Date of issue of this report: **17/11/2021**

Page 269
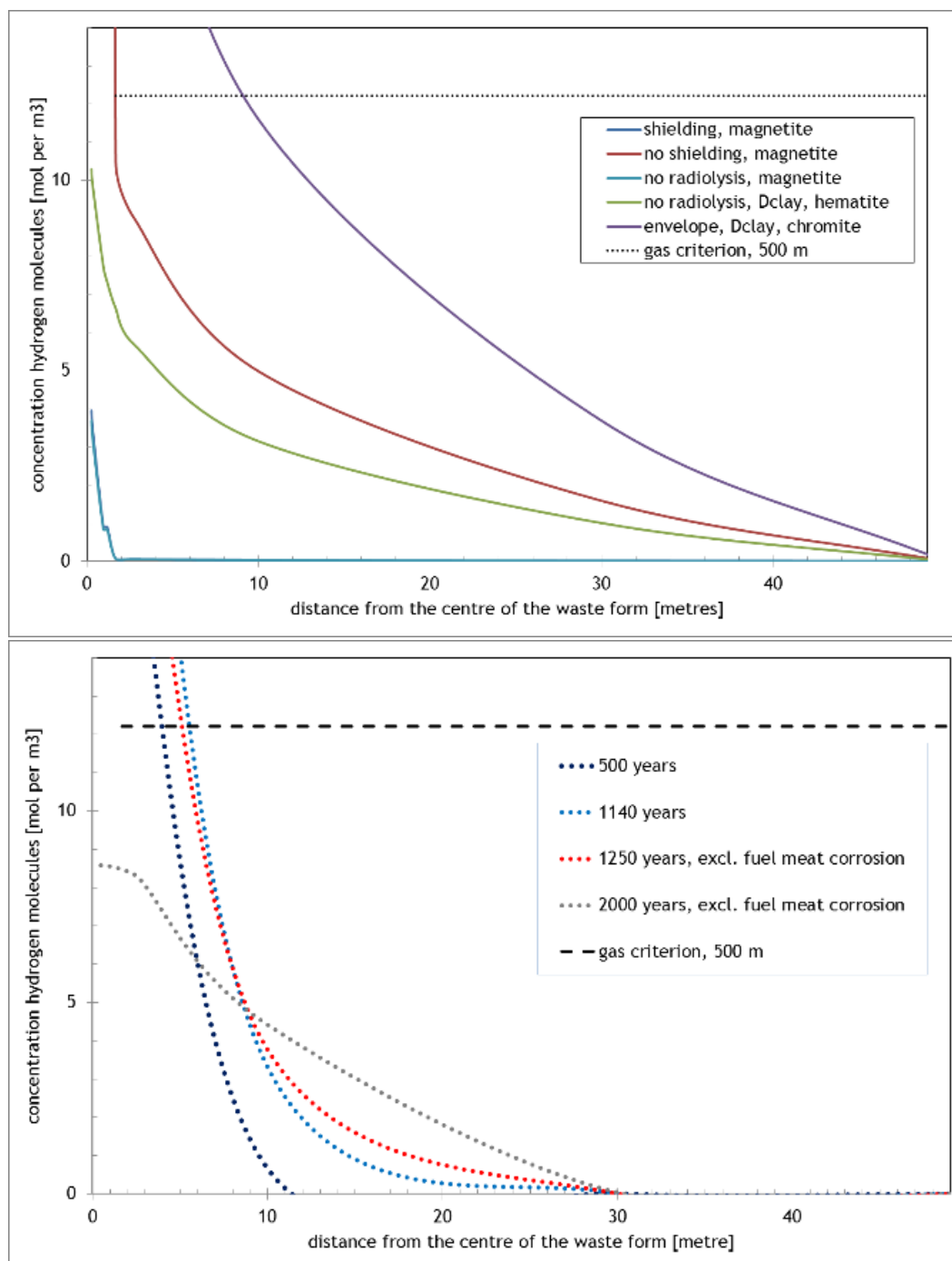
Figure 4-23 – Preliminary stationary calculations for vitrified HLW and transient gas transport calculations for spent fuel from research reactor (SRRF).

The potential transport of radionuclides from the vitrified waste form in the clay host rock is not expected to be enhanced by gas transport since no gas is generated during degradation of glass. Spent fuel from a research reactor (SRRF) contains aluminium claddings and the fuel meat in alloy between uranium and aluminium. The reactive surface area is large as the fuel filaments are small. An additional hydrogen source is the anaerobic corrosion of aluminium after fracture of the carbon steel overpack. Lower image in Figure 4-23 shows that the gas solubility would be exceeded in that case. The potential transport of radionuclides in the clay host rock that are left from this fuel is therefore expected to be enhanced by gas pressure.

EURAD (Deliverable n° 6.1) – Initial State of the Art on Gas Transport in Clayey Materials
Dissemination level: PU
Date of issue of this report: **17/11/2021**

Page 270

4.1.4 Gas storyboard in Opalinus Clay by Nagra (Swiss context)

This section considers conceptualisation of the gas-related evolution of the deep geological repositories for L/ILW and SF/HLW according to the Swiss disposal concept.

4.1.4.1 Background

The overall approach to implementing deep geological disposal in Switzerland is set out in the Waste Management Programme (Nagra 2016b). This programme foresees two deep geological repositories: a high-level waste repository (HLW repository) for spent fuel (SF), vitrified high-level waste (HLW) and long-lived intermediate-level waste (ILW); and a repository for low- and intermediate-level waste (L/ILW repository)[33].

Within a deep geological repository, in the absence of oxygen and in the presence of water, corrosion of various metals and alloys will lead to the formation of hydrogen. If present, organic materials may slowly degrade and generate carbon dioxide, methane, and other gaseous species. Radiolysis of water will produce small additional amounts of gas. Depending on local conditions, gaseous species can be consumed by chemical reactions or by microbial activity. If the resulting gas generation rate exceeds the rate of migration due to processes such as advection and diffusion of dissolved gas molecules in the pores of the engineered barriers or the host rock, the solubility limit of the gas will eventually be exceeded. This will lead to the formation of a discrete gas phase. Gases could continue to accumulate until the pressure becomes sufficient to be released through the engineered barriers and the host rock in gaseous form.

The effects of post-disposal gas generation in, and gas release from, deep geological repositories in Opalinus Clay have been assessed in recent synthesis reports (Nagra 2016a; Papafotiou and Senger 2016a, 2016b). The report describes and evaluates the evolution of safety-relevant processes related to gas that can influence the long-term behaviour and safety of L/ILW and HLW repositories constructed in Opalinus Clay. A state-of-the-art synthesis of processes and phenomena is presented, aimed at assessing the influence of repository-produced gases on repository performance. The report provides an overview of the currently available understanding of gas sources, reactions and interactions, generation, consumption, and transport.

Nagra's Model Inventory for Radioactive Materials (MIRAM) characterises and quantifies all Swiss radioactive materials, accounting for existing waste as well as expected future waste. A new version of MIRAM will be elaborated in year 2021; all information presented in this document is based on the former MIRAM 14 (Nagra 2014b), dated 31st of December 2013, assuming a 60-year operating lifetime for the existing Swiss nuclear power plants and the collection of waste from medicine, industry and research until 2065, which is conservative from the point of view of waste amounts. The masses and volumes of conditioned waste for geological disposal according to the base scenario are given in Table 4-1. The vast majority (96%) of the available waste, either by mass or by volume, will be disposed of in the L/ILW repository. Considerably smaller amounts of SF/HLW (3%) and of ILW (1%) will be disposed of in the HLW repository.

---

[33] There is also the possibility to construct the HLW repository and the L/ILW repository at the same site, i.e. to construct a so-called combined repository. Such a combined repository is, however, not dealt with in the present report.

EURAD (Deliverable n° 6.1) – Initial State of the Art on Gas Transport in Clayey Materials
Dissemination level: PU
Date of issue of this report: 17/11/2021

Page 271

Table 4-1 – Masses and volumes of conditioned radioactive waste according to the MIRAM 14 base scenario.

Category of waste	Mass [kg]	Volume [m³]
SF/HLW	4.87×10^6	1 479
ILW	2.33×10^6	891
L/ILW	1.58×10^8	53 060
Total	$\mathbf{1.66 \times 10^8}$	**55 430**

According to the Swiss radioactive waste management programme, the procedure and the criteria for the selection of sites for deep geological repositories are specified in the concept part of the 'Sectoral Plan for Deep Geological Repositories' (BFE 2008, 2011). The procedure consists of three stages and will ultimately lead to the identification of the sites for repository implementation, the definition of the main features of the repositories and the submission of the general licence. In the context of the current Stage 3 of the Sectoral Plan, site-specific repository layouts will be elaborated by the end of 2021, exhibiting an updated waste allocation concept and minor modifications of the safety concept (e.g. placement and detailed design of repository seals).

This document refers to the former version of the overall approach to implementing deep geological disposal in Switzerland, which has been set out in the Waste Management Programme (Nagra 2016b). It is noteworthy, that several features of the previous safety concept will not be pursued in the upcoming version of the Swiss radioactive waste management programme (e.g. compartmentalisation seals in the SF/HLW tunnels).

4.1.4.2 Low- and intermediate-level waste repository

Description of the repository

Layout and design

A schematic layout of the L/ILW repository in Opalinus Clay according to the current Swiss disposal concept is shown in Figure 4-24, displaying the main elements of the underground structures, namely the access tunnel, the operation and ventilation shafts, the operation and ventilation tunnels, the pilot facility, the test area, branch tunnels and the emplacement caverns. Table 4-2 displays the geometries and derived void space volumes of the repository components.

The disposal containers with L/ILW will be emplaced in caverns with a cross-section of approximately 11 m × 13 m (Figure 4-25), while the length of the caverns is approximately 200 metres. The caverns are supported using rock bolts and sprayed concrete lining, including reinforcement (steel wire mesh). Each cavern is connected to the operation tunnel via a branch tunnel. The disposal containers will be transported to the branch tunnels by rail. At the interface with the emplacement cavern, each branch tunnel is enlarged to provide sufficient space for the transfer of the disposal containers from the railway wagon to the overhead crane used for emplacement. The lower part of the cavern ('cavity') is partitioned into disposal sections of approx. 28 metres length by reinforced concrete walls ('bulkheads'). The void space between the disposal containers, between the crane columns and between the disposal containers in the upper part of the cavern ('top heading') will be filled with mono-grain cementitious mortar.

EURAD (Deliverable n° 6.1) – Initial State of the Art on Gas Transport in Clayey Materials
Dissemination level: PU
Date of issue of this report: 17/11/2021

Page 272
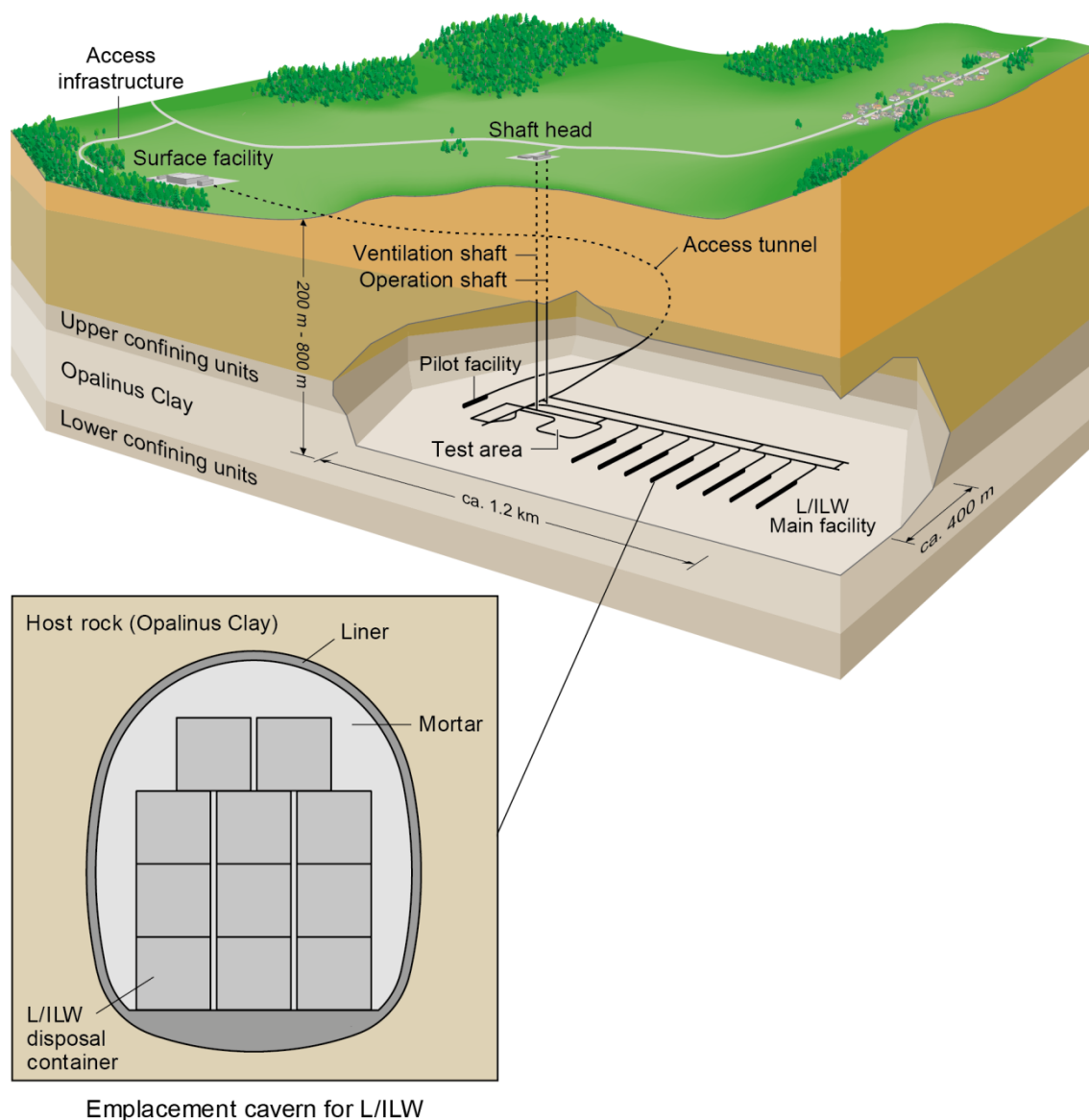
Figure 4-24 – Schematic layout of the L/ILW repository (Nagra 2016a).

Table 4-2 – Repository element geometries and derived void space volumes (L/ILW repository).

	Profile type[2]	Cross-section for storage[2] [m²]	Length [m]	Volume [m³]	Porosity [–]	Void space volume[6] [m³]
L/ILW caverns	K09	102.2	1 800[1] (9*200m)	183 960	0.25[5]	45 990.0
V5 seals	M, I	46.6	180[2] (9*20m)	8 388	0.30[3]	2 516.4
Branch tunnels	L	20.5	960[2]	19 680	0.35[4]	6 888.0
Operation gallery	L	20.5	1 162[2]	23 821	0.35[4]	8 337.4
Ventilation tunnel	D5	19.9	1 060[2]	21 094	0.35[4]	7 382.9
Pilot cavern	K09	102.2	42[2]	4 292	0.25[5]	1 073.1
V5 seal PIL	M, I	46.6	20[2]	932	0.30[3]	279.6

EURAD (Deliverable n° 6.1) – Initial State of the Art on Gas Transport in Clayey Materials
Dissemination level: PU
Date of issue of this report: **17/11/2021**

Page 273

	Profile type[2]	Cross-section for storage[2] [m²]	Length [m]	Volume [m³]	Porosity [–]	Void space volume[6] [m³]
Pilot branch tunnel	L	20.5	100[2]	2 050	0.35[4]	717.5
Test facility	L, D5	20.1	1 584[2]	31 839	0.35[4]	11 143.4
Observation gallery	D5	19.9	372[2]	7 403	0.35[4]	2 591.0
Access tunnels in OPA	A5	31.8	375[2]	11 925	0.35[4]	4 173.8
Pilot operation tunnel	A5	31.8	375[2]	16 970	0.35[4]	4 173.8
Shafts (V3) in OPA	S3	28.3	94[2] (2*47m)	2 660	0.30[3]	798.1
Shafts (UCU)	S3	28.3	100[2] (2*50m)	2 830	0.35[4]	990.5

[1] Nagra 2014c

[2] from reference layout (Nagra 2016b)

[3] Well compacted sand/bentonite mixture, according to the generic repository configuration

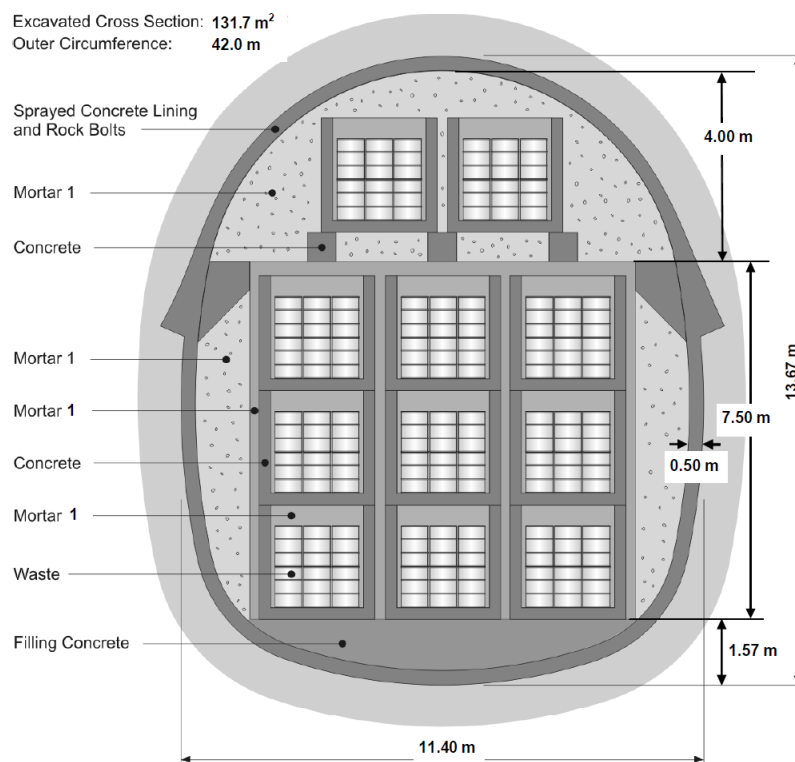[4] Lowly compacted sand/bentonite mixture, according to the generic repository configuration

[5] Effective porosity

[6] Product of porosity and volume

Figure 4-25 – Cross-section of L/ILW emplacement cavern of type K09 after closure.

EURAD (Deliverable n° 6.1) – Initial State of the Art on Gas Transport in Clayey Materials
Dissemination level: PU
Date of issue of this report: **17/11/2021**

Page 274

The M1 mortar used to backfill the emplacement cavern has high hydraulic conductivity and high porosity. The lining consists of shotcrete with a typical porosity of 25%. Disposal containers, reinforced concrete walls, etc. are made of normal building concrete and high performance concrete. Six different container types are currently foreseen. All container types are made of concrete with steel reinforcement and small amounts of organic materials (cement additives). Figure 4-26 illustrates the packing of twelve 200-litre drums into a single disposal container. The remaining space around the drums will be backfilled with cement mortar.

Comprehensive characterisation programmes were conducted for these backfill materials (Nagra, 2008). Back-of-the-envelope estimates of the volume fractions and porosities of the backfill materials in the emplacement caverns and corresponding permeabilities are given in Table 4-3.
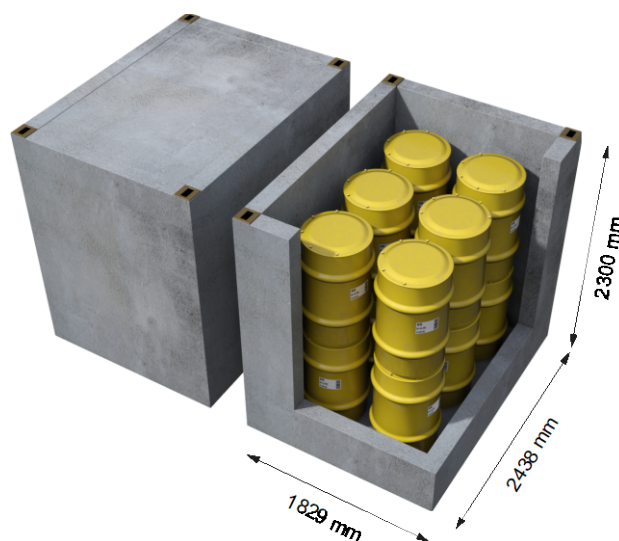

Figure 4-26 – Example of the packing of 200-litre drums into one standard disposal container.

Table 4-3 – Categories of cementitious materials applied for the backfill of the emplacement caverns and typical parameter values for the gas-related properties.

	Material group	Volume fraction [%]	Porosity [–]	Permeability [a] [m²]
Mortar M1		36	~0.30	~1×10^{-10}
Construction concrete	Shotcrete	28	~0.25	~1×10^{-17}
	Normal building concrete		~0.20	~1×10^{-18}
	High performance concrete		0.15	~1×10^{-19}
Waste fixation concrete		36	0.20 [b]	~1×10^{-19}

[a] Permeability tests performed with water.

[b] The effective pore volume of the backfilled waste drums is significantly higher than high performance concrete because the waste drums are not filled up completely.

As soon as the emplacement of disposal containers in one disposal section of a cavern is completed, the voids between the containers and the cavern lining will be backfilled with cementitious mortar. Once all sections of the cavern and the top heading are backfilled, the enlarged section of the branch tunnel at the cavern entrance will also be backfilled with the same cementitious mortar. Each cavern will be

EURAD (Deliverable n° 6.1) – Initial State of the Art on Gas Transport in Clayey Materials
Dissemination level: PU
Date of issue of this report: **17/11/2021**

Page 275

closed with a concrete plug (V5; Figure 4-27). It is foreseen that a dedicated backfill and sealing concept, called the 'engineered gas transport system' (EGTS), will be constructed to enable the controlled release of gases along the access structures (Nagra 2008). The EGTS is the total of all branch and access tunnels that are backfilled with a clay-based material (e.g. processed excavated Opalinus Clay, sand/bentonite mixtures). Also at this stage, a seal (V4) will be placed within the access tunnel at the intersection of Opalinus Clay with the overlying geological formation. The seal is approximately 40 metres long and consists of highly compacted bentonite blocks. Furthermore, a concrete plug (V3) will be placed at repository level at the end of the operation tunnel adjacent to the ventilation shaft. Final closure of the facility involves the emplacement of seals within the shafts, also made of highly compacted bentonite.
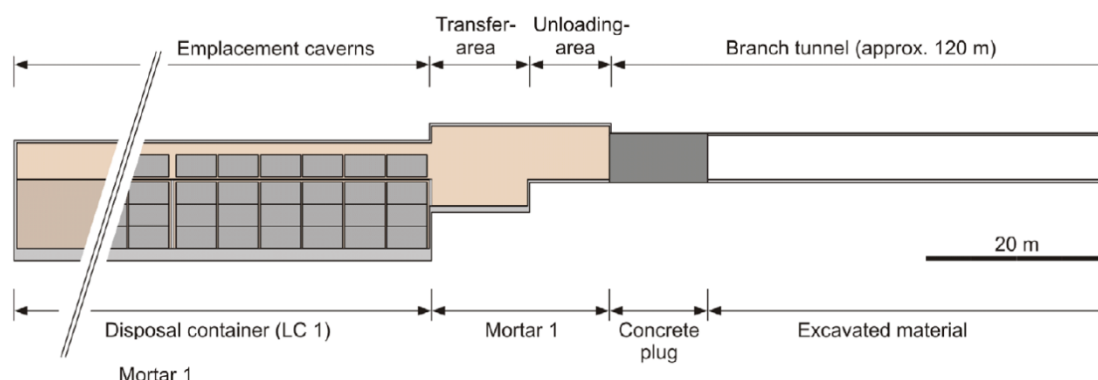

Figure 4-27 – Longitudinal section of L/ILW emplacement cavern after closure (Nagra 2008).

It is assumed that all other underground structures in the host rock formation are backfilled with sand/bentonite mixtures or with crushed Opalinus Clay. A typical porosity of 0.35 can be assumed for a lowly compacted sand/bentonite mixture (80% sand, 20% bentonite). For a well compacted sand/bentonite mixture, i.e. used in the seal sections, the assumed porosity is 0.30 (Nagra 2008). Based on the aforementioned considerations, the void space volumes available for gas storage and transport in individual components as well as for the entire repository are summarised in Table 4-2 (see also Nagra 2008).

Construction, operation and closure of the L/ILW repository

Due to the vertical dimension of the emplacement cavern has to be excavated in segments as shown in Figure 4-28. Subsequent to the branch tunnel, the top heading of the cavern is being excavated and rock support and the sprayed concrete liner with reinforcement is applied in the crown over the total length of 200 metres. Subsequently the core of the bench can be excavated by ripping work before the remaining rock slopes on either side are removed by roadheader and continuously underpinned (Figure 4-28). Preferably the invert is excavated, and the ring of the outer liner is closed shortly after. A typical excavation sequence may achieve advance rate at top heading of 50 to 80 metres per month followed by an enlargement (bench and invert) with similar rates. According to the overall realisation schedule all 10 emplacement tunnels need to be completed within approximately 3 years. In order to perform, 2 to 3 caverns are being excavated concurrently. Prior to the construction of the emplacement tunnels, a construction period of 3 years is anticipated for the rock laboratory.

EURAD (Deliverable n° 6.1) – Initial State of the Art on Gas Transport in Clayey Materials
Dissemination level: PU
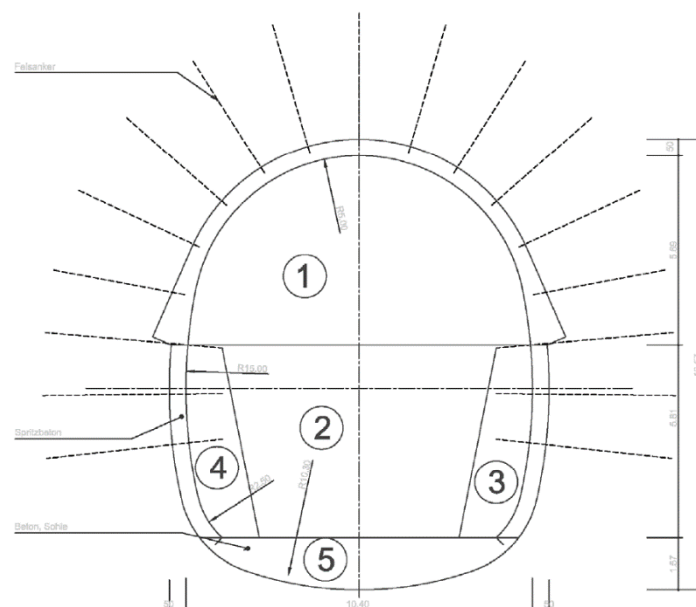Date of issue of this report: **17/11/2021**

Page 276

Figure 4-28 – Excavation sequence of the L/ILW emplacement cavern K09 using top heading (1) with area 55 m², bench core (2) and wall (3, 4) with area 65 m², and invert (5) with area 11 m².

The concept of repository operation envisages emplacing disposal containers in two caverns concurrently whereas the other caverns remain empty. The gaps are filled with cementitious mortar M1 as soon as a single layer of disposal containers within one compartment are emplaced. Once waste packages are emplaced at the upper part (top heading) and backfilled with mortar, the access to the cavern is plugged with concrete (V5) seal or with an EGTS seal that consists of bentonite / sand mixture at the cavern entrance. When all caverns and V5 seals are filled (including the pilot cavern) the branch tunnels are also backfilled, and the monitoring phase of the main repository begins. Consequently, parts of the operations and ventilations tunnels, as well as the access tunnels are backfilled for the repository observation phase. A concrete plug (V2) separates the backfilled underground facilities from the shafts, the observation gallery and the test facility. A long-term seal is placed within the access tunnel (V4) at the transition of Opalinus Clay with the overlying geological formation. At the end of the observation phase, the entire underground facility will be closed; this involves backfilling of the remaining repository elements and placement of the necessary seals. The repository timeline and associated construction, operations, and post-closure phases can be summarised in the following consecutive phases:

- *2029 – 2033*: construction of rock laboratory.
- *2033 – 2042*: operation of rock laboratory.
- *2042 – 2050*: construction of main repository.
- *2050 – 2065*: emplacement of L/ILW.
- *2065 – 2075*: first monitoring phase; the emplacement rooms are backfilled and sealed, the construction / operations tunnels, however, remain open and ventilated.
- *2075 – 2115*: second monitoring phase; the construction / operations tunnels, as well as the main underground access structures are backfilled and sealed. Only the URL and the pilot repository are accessible.
- *2115 –   *: all underground structures are backfilled and sealed.

During operation, all open underground structures are ventilated via ventilation shafts and the access ramp. For simplicity, a constant air temperature of 28°C and a relative humidity of 60% are assumed in

EURAD (Deliverable n° 6.1) – Initial State of the Art on Gas Transport in Clayey Materials
Dissemination level: PU
Date of issue of this report: 17/11/2021

Page 277

all open tunnel sections. After backfilling of the underground structures, humidity is assumed to increase instantly, and the temperature begins to equilibrate towards ambient temperature. Pore pressure in the backfilled structures is assumed to be atmospheric as long as the repository is open. After repository closure (placement of the repository seal), the repository starts to re-pressurise under the action of resaturation and gas generation respectively.

4.1.4.2.1 Waste inventory and source terms

Waste inventory

The following sections summarise the waste amounts and materials in the L/ILW repository. All waste amounts refer to conditioned waste unless it is specifically stated otherwise.

The conditioned masses and volumes of the L/ILW inventory[34] are presented according to MIRAM category and according to origin in Table 4-4. Considering first the waste volumes, the majority (68%) of the L/ILW volume is decommissioning waste. In addition, there is operational waste (31%) and reactor waste (1%). More than half of the waste (60%) is produced by the nuclear power plants and by the centralised interim storage facility. The research facilities CERN (European Organisation for Nuclear Research) and PSI contribute 40% of the total L/ILW volume. Considering next the masses, there is a similar distribution of the waste among the different categories. The majority (73%) of the L/ILW mass is decommissioning waste, with the remaining amount consisting of operational waste (25%) and reactor waste (2%). A little more than half of the waste mass (54%) is produced by the nuclear power plants and the interim repository Zwilag. CERN and PSI contribute 46%.

Table 4-4 – L/ILW conditioned amounts, presented according to MIRAM category.

MIRAM category	Mass [kg]	Volume [m³]
Decommissioning waste	1.17×10^8	36 282
Operational waste	3.94×10^7	16 304
Reactor waste	2.30×10^6	473
Total	$\mathbf{1.58 \times 10^8}$	**53 060**

Table 4-5 shows the masses of L/ILW materials, which are presented according to material group (inorganic, metallic, and organic materials) and also according to their origin within the waste packages. The L/ILW inventory consists of 58% inorganic, 40% metallic, and 2% organic materials. The inorganic materials mainly arise from disposal containers (44%), followed by filler materials (30%) and the waste (26%). The majority of the metals originate from the waste (80%). The organic materials are almost exclusively part of the waste (95%). A more detailed description of the organic and metallic material groups is given in Figure 4-29 and Figure 4-30, respectively.

---

[34] The conditioned masses and volumes refer to the filled waste containers, including raw wastes, additives, containers, filler materials, and fittings. L/ILW disposal containers (described previously) are not included.

EURAD (Deliverable n° 6.1) – Initial State of the Art on Gas Transport in Clayey Materials
Dissemination level: PU
Date of issue of this report: **17/11/2021**
Page 278

Table 4-5 – L/ILW masses [kg] presented according to material group and according to their origin within the waste packages.

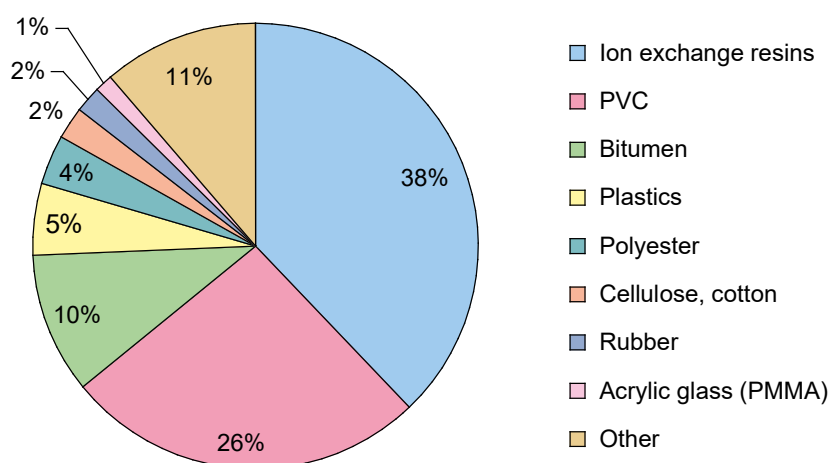| Material group	L/ILW masses [kg]				
	Waste	**Container**	**Filler material**	**Fittings**	**Total mass**
Inorganic	2.37×10^7	4.00×10^7	2.70×10^7	1.31×10^4	9.08×10^7
Metallic	5.07×10^7	1.06×10^7	0	2.43×10^6	6.38×10^7
Organic	2.83×10^6	2.44×10^4	1.16×10^5	8.58×10^2	2.97×10^6
Total	**7.72×10^7**	**5.07×10^7**	**2.72×10^7**	**2.45×10^6**	**1.58×10^8**

Figure 4-29 – L/ILW organics inventory shown as percentage of total conditioned mass.
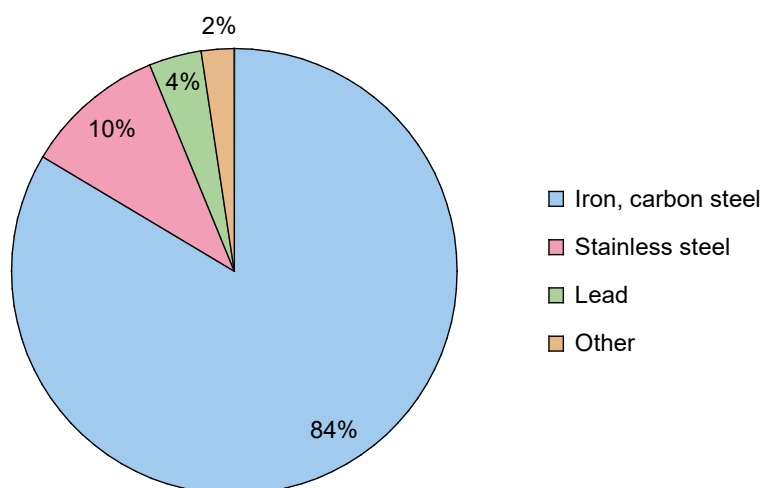
Figure 4-30 – L/ILW metal inventory shown as percentage of total conditioned mass.

EURAD (Deliverable n° 6.1) – Initial State of the Art on Gas Transport in Clayey Materials
Dissemination level: PU
Date of issue of this report: **17/11/2021**

Page 279

Gas generation – source terms

For the simulations of gas release, the following assumptions are made:

- Only H_2 and CH_4 are released from the L/ILW caverns. The cement backfill is carbonated by CO_2.

- The gas sources associated with the support structures (H_2 only) are uniformly distributed along the underground structures outside the emplacement caverns.

The gas production rates from materials emplaced in the underground structures (H_2 only) are shown for the different tunnel types in Figure 4-31. The gas rates from L/ILW (sum of H_2 and CH_4) are compared to the gas rate produced by emplaced materials in the K09 cavern in Figure 4-32. Figure 4-33 shows averaged gas rates from waste assuming 7 caverns emplaced with waste type L/ILW-1 and 2 caverns emplaced with L/ILW-2.

For modelling the gas release, it is assumed that waste-generated gas with the generation rates shown in Figure 4-31 through Figure 4-33 has the properties of H_2 in terms of viscosity, density and solubility. The gas generation rates are prescribed uniformly to the grid cells representing the backfill material of the L/ILW and pilot caverns.
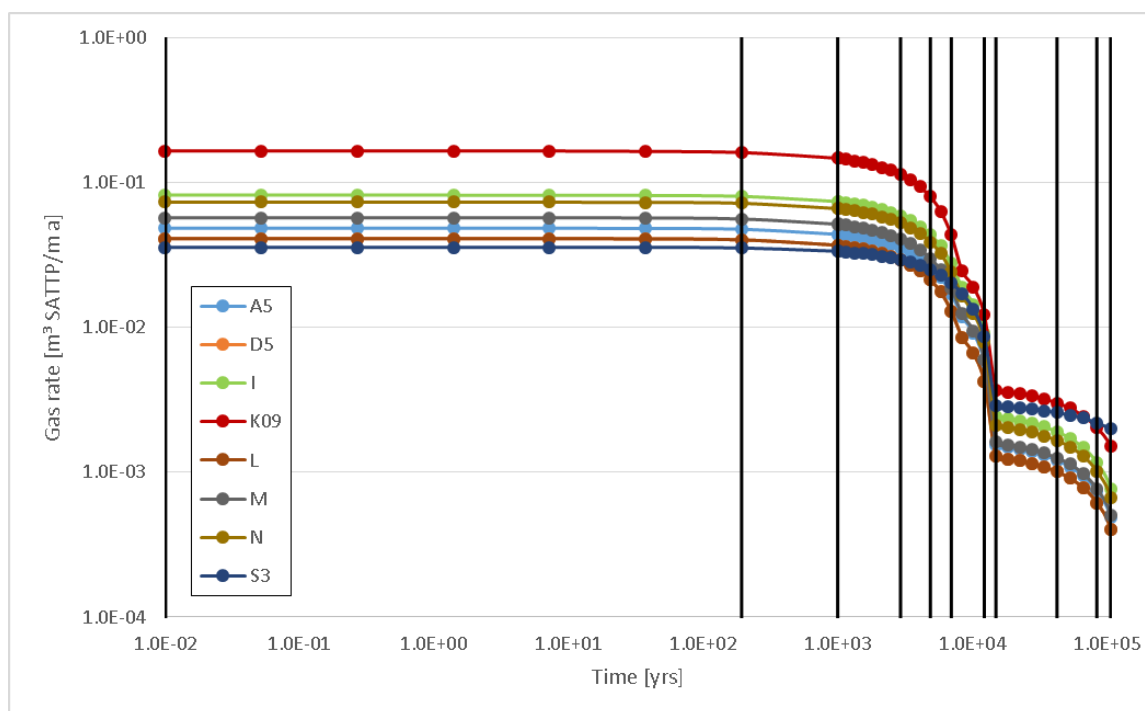
Figure 4-31 – Gas production for different tunnel types as a function of time. (A5: access tunnels in OPA, pilot operation tunnel; D5: ventilation tunnel; I: V5 Seals; K09: L/ILW caverns; L: pilot branch tunnel; M: V5 seals/pilot; S3: Shafts).

EURAD (Deliverable n° 6.1) – Initial State of the Art on Gas Transport in Clayey Materials
Dissemination level: PU
Date of issue of this report: **17/11/2021**

Page 280

Figure 4-32 – Gas production for L/ILW as a function of time.

Figure 4-33 – Averaged gas production for L/ILW as a function of time assuming 7 caverns with L/ILW-1 and 2 caverns with L/ILW-2.

EURAD (Deliverable n° 6.1) – Initial State of the Art on Gas Transport in Clayey Materials
Dissemination level: PU
Date of issue of this report: **17/11/2021**

Page 281

4.1.4.2.2   Gas transport modelling

Two-phase flow simulator

Model-based analysis of gas release in the L/ILW repository requires the modelling of (non-) isothermal two-phase flow through the repository structures and surrounding host rock. For this, a numerical model is used with the equation-of-state module EOS5 for water and hydrogen of TOUGH2 (Pruess et al. 1999). Diffusive transport of dissolved gas is neglected in this study, providing a conservative approach with respect to gas pressure build-up.
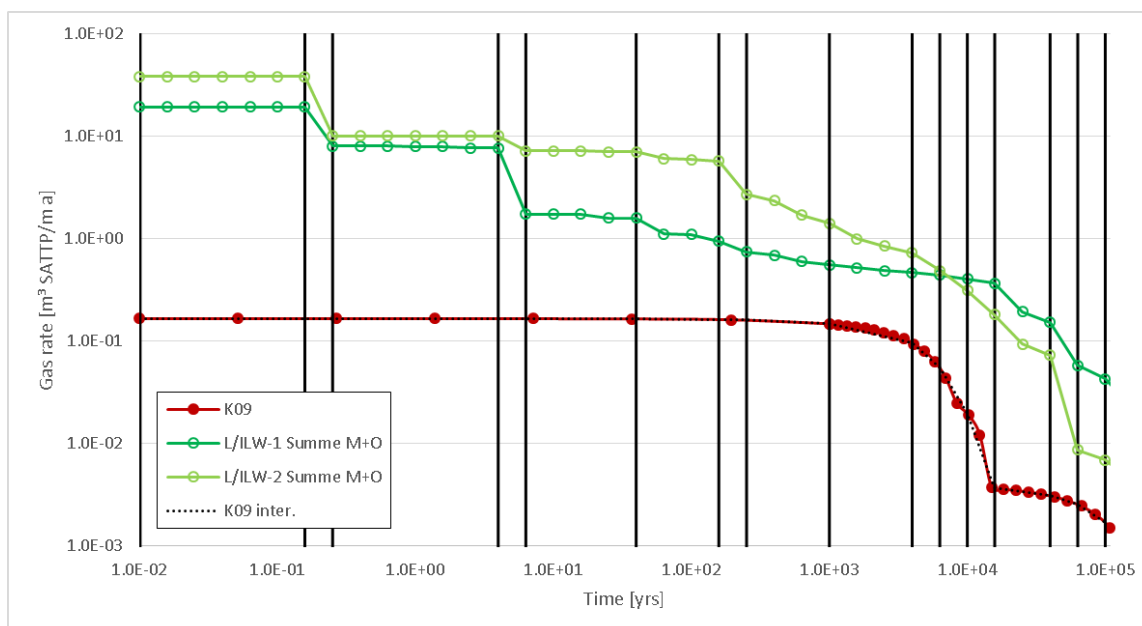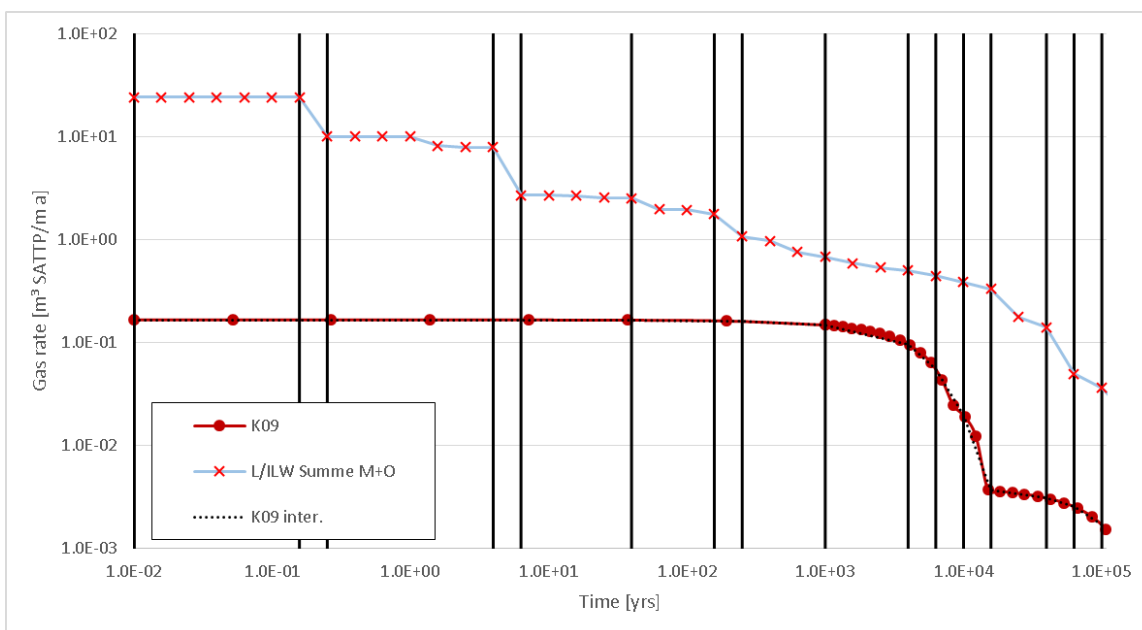
Two-phase flow parameter models

It is assumed that the rock mass always behaves like an elastic medium. The propagation of gas phase through the porous medium is controlled by the gas entry pressure, also known as the capillary threshold pressure, which represents the difference between gas pressure and water pressure needed to displace the pore water from the initially fully saturated medium. Once the gas entry pressure has been exceeded, the gas mobility is controlled mostly by the intrinsic permeability k of the formation, the permeability-saturation relationship (commonly known as relative permeability), and the relationship between the capillary pressure and the water saturation (also known as suction or water retention curve). As detailed in Chapter 2, the functional dependency between the pore space saturation and the relative permeability or the capillary pressure is commonly described with parametric models, such as the one of van Genuchten (1980), given in Equation 2-11.

Relative gas and liquid permeability k_{rg} and k_{rw} can be derived by integration of the capillary pressure curve following the approach of Mualem (1976) (see also Helmig 1997), represented by the van Genuchten model using the same shape parameters obtained from the permeability-saturation relationship given in Equation 2-15.

Enhanced gas mobility is described by the Grant model (Grant 1977), where the relative permeability of the gas phase is given by:

$$k_{rg} = 1 - k_{rw} \tag{4-3}$$

With the Grant model, the gas and liquid phases tend to move independently of each other, which is typical for fracture-porous rocks where liquid tend to migrate primarily through the matrix due to higher capillary pressures, and gas migrates through the higher-permeable fractures characterised by lower capillary pressures. This has been used for upscaling a discrete-fracture network (DFN) model of the fractured EDZ to a homogeneous continuous porous media (CPM) model with effective two-phase flow parameters based on the Grant model for the gas relative permeability (Senger et al. 2008).

The hydraulic and two-phase flow parameters for the intact host rock (Opalinus Clay) are a described in detail in the following paragraph.

Reference values of gas-related properties of the host rock

Hydraulic properties of the host rock formations in the candidate siting regions are a key input for modelling the gas transport through the repository elements and surrounding host rock. In order to derive reference geodata sets comprising hydraulic properties of the host rocks, a comprehensive survey of available hydrogeological and hydro-mechanical laboratory and field data was integrated into a traceable interpretation methodology developed in Senger et al. (2013). The interpretation and synthesis performed for the Opalinus Clay indicated that:

EURAD (Deliverable n° 6.1) – Initial State of the Art on Gas Transport in Clayey Materials
Dissemination level: PU
Date of issue of this report: 17/11/2021

Page 282

- The intact rock matrix of the Opalinus Clay is characterised by very low hydraulic conductivity typically in the range between 1.0×10^{-14} and 1.0×10^{-13} m/s. Variability of rock matrix conductivity is also low. Laboratory experiments carried out with core samples indicate anisotropy related to bedding with matrix permeability parallel to bedding typically a factor 5 greater than permeability normal to bedding.

- Discrete water-conducting features or faults in the Opalinus Clay are not hydraulically active. The inventory of brittle structures recovered from boreholes was integrated into the analyses of packer tests, revealing that discontinuities in the Opalinus Clay do not exhibit hydraulic conductivities higher than those of the intact rock matrix.

A compilation of reference parameters as well as alternative values for the shallow and deep repository configurations is given in Table 4-6.

Table 4-6 – Values for gas-related parameters of the undisturbed Opalinus Clay for a deep L/ILW repository in northern Switzerland (500–900 metres below ground level) (RV: reference value, AV: alternative value) from Senger et al. (2013).

Parameter	RV	AV	Remarks
Intrinsic permeability normal to bedding $k_\perp$ [m²]	2×10^{-21}	1×10^{-21}	RV: corresponds to the reference value for hydraulic conductivity at Benken. AV: corresponds to the lower range for hydraulic conductivity at Benken.
Anisotropy factor $k_\parallel/k_\perp$	5	1	RV: according to Senger et al. (2013). AV: no significant anisotropy
Capillary pressure - saturation relationship			Parametric model according to van Genuchten
Capillary strength P_o [MPa] deep (>500 m)			RV: derived from capillary pressure measurements (drying path)
	34	60	AV: derived from capillary pressure measurements (drying path)
		18	AV: from shallow OPA
Shape parameter n [–], with $n = 1/(1-m)$			RV: derived from capillary pressure measurements (drying path)
	1.6	1.8	AV: derived from capillary pressure measurements (drying path – high P_o)
Relative permeability – saturation relationship			Parametric model according to van Genuchten / Mualem using the shape parameter n from the Pc-S curve
Residual liquid (water) saturation S_{lr} [–]	0.5	0.1	RV: according to the results of adsorption / desorption measurements, suggesting that 50% of the total pore space can be classified as micro- and mesopores. AV: assuming that most of the pore water is mobile
Residual gas saturation S_{gr} [–]	0.00	0.003	RV: effective gas entry pressure of the rock is infinitesimal. AV: the residual gas saturation determines the effective gas entry value. Effective gas entry values were determined by gas permeability testing at Mont Terri and Benken
Total porosity ϕ [%]	12	10	RV: Porosity measurements from Schlattingen core (OPA-20) (avg. value between different core samples) 16%. AV: corresponds to the lower value in OPA-of about 10%
Lower bound of fracture pressure [MPa]	$\sigma_v = \rho_s \cdot g \cdot z$		RV: lithostatic pressure or vertical stress σ_v at repository level (ρ_s = 2.5 Mg/m³, overburden z in metres below ground level) AV: -

EURAD (Deliverable n° 6.1) – Initial State of the Art on Gas Transport in Clayey Materials
Dissemination level: PU
Date of issue of this report: 17/11/2021

Page 283

Parameter	RV	AV	Remarks
Threshold pressure for pathway dilation [% of σ_v]		80%	RV: the onset of pathway dilation is assumed at about 80% of the lithostatic pressure. AV: -

Relationship between intrinsic permeability and hydraulic conductivity:

$$k\,[m^2] = \frac{\mu_w}{\rho_w\,g}\,K \approx 1 \times 10^{-7}\,K\,\left[\frac{m}{s}\right] \qquad for\ T = 20°C$$

μ_w	dynamic viscosity of water [Pa·s]
ρ_s	solid density [Mg/m^3]
ρ_w	density of water [kg/m^3]
g	gravitational acceleration [m/s^2]

Model parameters for the repository components

The hydraulic and two-phase properties for the repository components are based on the compilations in Nagra (2008) and summarised in Table 4-7.

Table 4-7 – Hydraulic and two-phase flow properties assigned to the repository components (Nagra 2008, Papafotiou and Senger 2014).

	Permeability k [m²]	Pore compressibility C_p [1/Pa]	van Genuchten model parameters			
			P_0 [Pa]	n [–]	S_{lr} [–]	S_{gr} [–]
L/ILW caverns	1.0×10^{-15}	1.0×10^{-9}	$4.0\ 10^3$	2.5	0.3	0.001
Pilot cavern	1.0×10^{-15}	1.0×10^{-9}	$4.0\ 10^3$	2.5	0.3	0.001
Shaft (Upper conf. units)	1.0×10^{-18}	1.0×10^{-9}	$4.0\ 10^3$	2.5	0.3	0.001
Shaft (V3)	$5.0 \times 10^{-18\ a}$ $1.0 \cdot 10^{-20} / 2.0 \cdot 10^{-21\ b}$	1.0×10^{-9}	$1.8\ 10^{7\ 1}$ $1.8 \cdot 10^7 / 3.4 \cdot 10^{7\ b}$	1.82	0.01	0.001
V2 seal	$1.0 \times 10^{-16\ a}$ $5.0\ 10^{-18} / 1.0\ 10^{-18\ b}$	1.0×10^{-9}	4.0×10^3	2.5	0.3	0.001
V4 seal	$5.0 \times 10^{-18\ a}$ $1.0 \cdot 10^{-16} / 1.0 \cdot 10^{-18\ b}$	1.0×10^{-9}	4.0×10^3	2.5	0.3	0.001
V5 plug	$1.0 \times 10^{-16\ a}$ $5.0 \cdot 10^{-18} / 1.0 \cdot 10^{-18\ b}$	1.0×10^{-9}	4.0×10^3	2.5	0.3	0.001
All other tunnels	$1.0 \times 10^{-15\ a}$ $1.0 \cdot 10^{-16} / 1.0 \cdot 10^{-17\ b}$	1.0×10^{-9}	4.0×10^3	2.5	0.3	0.001

[a] Base case of EGTS permeabilities

[b] Alternative values of EGTS permeabilities

4.1.4.3 High-level waste repository

4.1.4.3.1   Description of the repository

Layout and design

A schematic layout of the HLW repository in Opalinus Clay according to the current Swiss disposal concept is shown in Figure 4-34 (Nagra 2016a). The repository comprises an array of parallel emplacement drifts containing SF or HLW, while ILW will be emplaced in separate emplacement caverns. Access to the repository will be provided, during construction and operation, by an access tunnel/ramp and/or by shafts. The repository also contains ventilation and construction shafts, ventilation and operation tunnels, a pilot facility and a test area. Table 4-8 displays the geometries and derived void space volumes of the repository components.
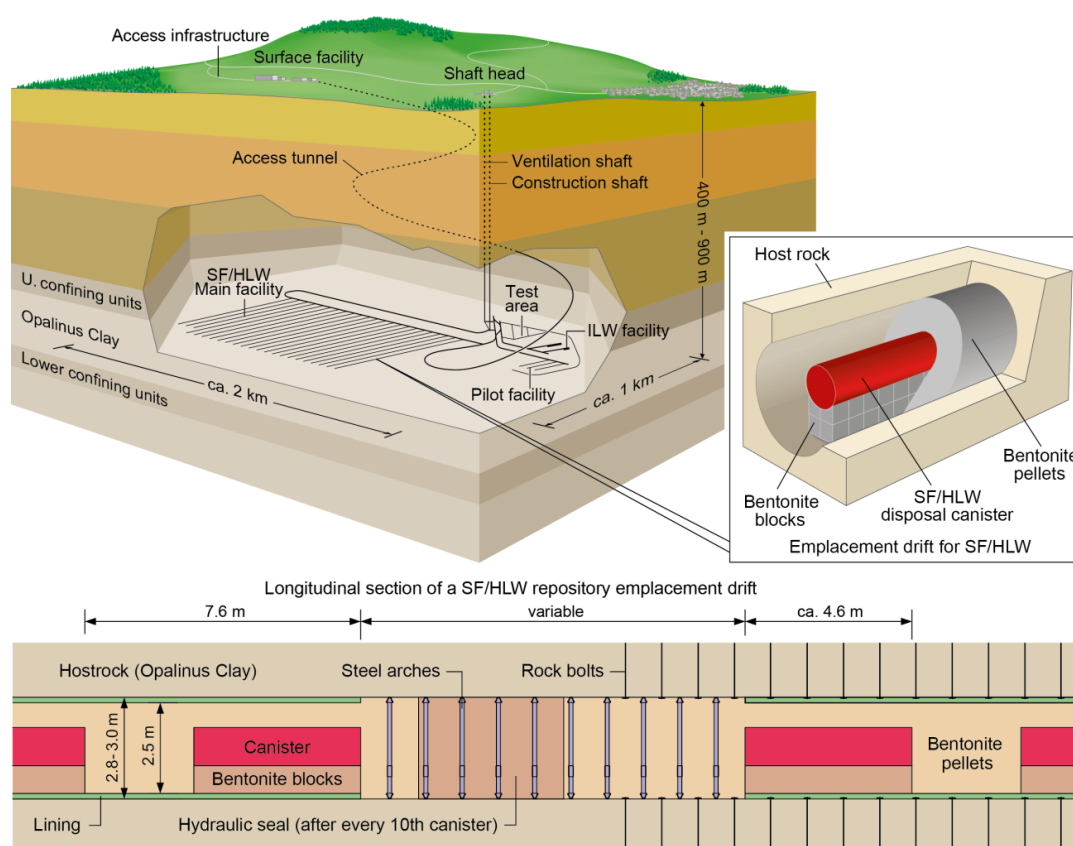
Figure 4-34 – Schematic layout of the HLW repository and of an axial cross-section of the SF/HLW emplacement drifts (note that the compartmentalisation seal with steel arches is part of the previous safety concept and will not be pursued in future safety concepts) (Nagra 2016a).

EURAD (Deliverable n° 6.1) – Initial State of the Art on Gas Transport in Clayey Materials
Dissemination level: PU
Date of issue of this report: 17/11/2021

Page 285

Table 4-8 – Repository element geometries and derived void space volumes (HLW repository).

	Profile type [2]	Cross-section for disposal [2] [m²]	Length [m]	Volume [m³]	Porosity [–]	Specific heat [J/kg °C]	Void space volume [6] [m³]
SF/HLW tunnels	F	4.9	18 900 [1] (27*700m)	92 610	0.40[4]	964	37 044.0
SF/HLW V5 seals	M, N	4.9	1 080 [2] (27*40m)	5 292	0.30[3]	964	1 587.6
Branch tunnels	E	16.2	1 377 [2] (27*51m)	22 307	0.30[3]	920	6 692.2
Operation gallery	L	20.5	1 130 [2]	23 165	0.30[3]	920	6 949.5
Ventilation tunnel	D5	19.9	1 538 [2]	30 606	0.30[3]	920	9 181.9
Pilot tunnels	F	4.9	700 [1] (3*233m)	3 430	0.40[4]	964	1 372.0
Pilot V5 seals	M, N	4.9	120 [2] (3*40m)	588	0.30[3]	964	176.4
Pilot Branch tunnels	E	16.2	154 [2] (3*51m)	2 495	0.30[3]	920	748.4
Pilot operation tunnel	L	20.5	370 [2]	7 585	0.30[3]	920	2 275.5
L/ILW caverns	K04	53.3	171 [2] (154m+17m)	9 114	0.25[5]	920	2 278.6
L/ILW V5 seals	M, I	40.95	40 [2] (2*20m)	1 638	0.30[3]	920	491.4
Test facility	L, A5, D5	20.83	2 148 [2]	44 743	0.30[3]	920	13 422.9
Observation gallery	D5	19.9	930 [2]	18 507	0.30[3]	920	5 552.1
Access tunnels in OPA	A5	31.8	840 [2] (440m CA +400m OPA)	26 712	0.30[3]	920	8 013.6
Pilot access tunnel	A5	31.8	500 [2] (100m CA +400m OPA)	15 900	0.30[3]	920	4 770.0
Shafts (V3) in OPA	S3	28.3	94 [2] (2*47m)	3 736	0.40	964	1 494.2
Shafts (UCU)	S3	28.3	100 [2] (2*50m)	5 037	0.30[3]	920	1 511.2

[1] Nagra 2014c
[2] from reference layout
[3] Well compacted sand/bentonite mixture, according to the reference repository configuration
[4] Effective porosity
[5] Effective porosity of L/ILW
[6] Product of porosity and volume

The disposal canisters containing SF and HLW will be emplaced in 700–800 metres long parallel emplacement drifts with a diameter of about 3 metres, which are supported by rock bolts, steel mesh and low pH shotcrete (Figure 4-35). The disposal canisters will be placed every 3 metres on pedestals

EURAD (Deliverable n° 6.1) – Initial State of the Art on Gas Transport in Clayey Materials
Dissemination level: PU
Date of issue of this report: 17/11/2021

Page 286

made of compacted bentonite blocks with a dry density of about 1.8 Mg/m^3. The region around and between the canisters will be backfilled with granular bentonite with a dry density of about 1.45 Mg/m^3.
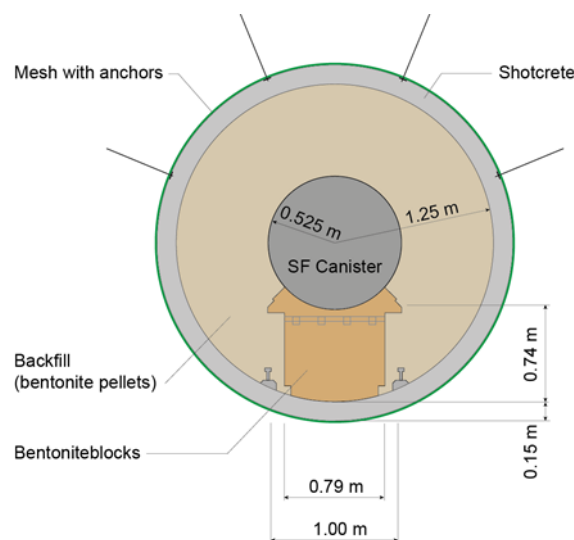

Figure 4-35 – Generic design of the SF/HLW tunnels for a deep repository configuration.

A potential option for the emplacement of the SF/HLW disposal canisters and the backfilling of the respective emplacement drifts is to be carried out using steel rails. However, the corrosion of the steel rails would contribute to the generation of gas, and thus that contribution is evaluated in different assessment cases.

ILW will be emplaced in separate caverns, each about 8 metres in width and up to 200 metres in length. The ILW caverns are supported by concrete liners and backfilled with cementitious mortar. The ILW is embedded within a cementitious matrix or, in some cases, within a matrix of bitumen, polystyrene or borosilicate glass. The waste matrix is usually packed in steel drums, which are then placed in concrete containers. The containers and the emplacement caverns for ILW are essentially the same as those of the L/ILW repository.

The spent fuel assemblies and the flasks containing the vitrified high-level waste will be packed into disposal canisters in the surface facility and then transported to the emplacement drifts of the repository. The present study is based on the current reference SF and HLW disposal canister concept, which foresees the use of thick-walled carbon steel canisters (see Figure 4-36).

It is assumed that each HLW canister contains two HLW flasks, while each SF canister contains either four pressurised water reactor (PWR) or nine boiling water reactor (BWR) spent fuel assemblies[35].

According to the current Nagra reference design, both canister types have a cylindrical shape with flat ends, while the lid of the canister incorporates a handling feature. The disposal canister for HLW contains no internal structure, while the SF disposal canister contains an internal lid and a basket structure, which contains the spent fuel assemblies and which is also made of carbon steel. The basket structure consists of either 4 or 9 boxes with a square cross-section at the required size to hold the fuel

---

[35] Alternative canister concepts containing 3 HLW flasks or 12 BWR fuel assemblies are also under consideration as this could decrease the total number of canisters and the number of handling steps in the surface facility, and also lead to a more efficient use of space in the repository.

EURAD (Deliverable n° 6.1) – Initial State of the Art on Gas Transport in Clayey Materials
Dissemination level: PU
Date of issue of this report: **17/11/2021**
Page 287

assemblies. Design data related to size, weight and reference lifetime for the disposal canisters are given in Table 4-9.
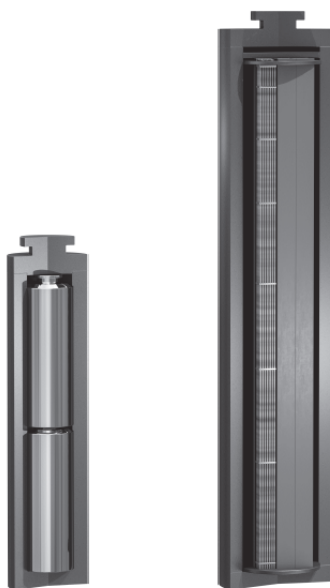

Figure 4-36 – Schematic cross-sections of the current reference design for HLW and SF disposal canisters.

Table 4-9 – Design data related to SF and HLW disposal canisters.

Canister type	HLW	SF
Outer diameter [mm]	720	1 050
Inner diameter [mm]	440	770
Approximate external length [mm]	3 000	5 000
Wall thickness body [mm]	140	
Wall thickness base [mm]	150	180
Wall thickness lid [mm]	170	
Approximate unloaded weight [kg]	6 400	19 500
Number of canisters [–]	317	1 894
Reference lifetime [a]	10 000	

Construction, operation and closure of the L/ILW repository

The concept of repository operation envisages initially the opening of the access and operation tunnels, test facility, and shafts. This is followed by the successive opening of emplacement tunnels, emplacement of the waste, and backfilling. This implies that all emplacement tunnels will remain open for approximately the same time. Once the emplacement tunnel is backfilled, access is plugged with concrete (V5) or with an EGTS seal that consists of bentonite / sand mixture at the tunnel entrance. It is assumed that their emplacement begins in 2065 subsequent to the emplacement of the HLW. According to the current plan, the SF emplacement shall be completed in 2075. That implies that 2.5 SF emplacement tunnels will be filled per year, corresponding to 200 SF emplaced canisters. Based on these considerations, it is estimated that the preceding emplacement of the HLW will last approximately one to two years. It is thus assumed that the starting point for the emplacement of HLW is year 2063. When all tunnels and V5 seals are filled (including the pilot repository) the branch tunnels, operation

EURAD (Deliverable n° 6.1) – Initial State of the Art on Gas Transport in Clayey Materials
Dissemination level: PU
Date of issue of this report: **17/11/2021**

Page 288

tunnels, and ventilation tunnel are also backfilled and the monitoring phase of the main SF/HLW, L/ILW and pilot repositories begins. Consequently, the access tunnels are backfilled for the repository observation phase. A concrete plug (V2) separates the backfilled underground facilities from the shafts, the observation gallery and the test facility. A long-term seal is placed within the access tunnel (V4) at the transition of Opalinus Clay with the overlying geological formation. At the end of the observation phase, the entire underground facility will be closed; this involves backfilling of the remaining repository elements and placement of the necessary seals.

The repository timeline and associated construction, operations, and post-closure phases comprises the following consecutive phases:

- *2029 – 2035*: construction of rock laboratory.

- *2035 – 2050*: operation of rock laboratory.

- *2050 – 2063:* construction of main repository.

- *2063 – 2065*: emplacement of HLW.

- *2065 – 2075*: emplacement of SF (including pilot repository). The average emplacement rate for SF is 2.5 emplacement rooms per year, i.e. 200 SF disposal canisters per year.

- *2075 – 2085:* first monitoring phase; the emplacement rooms are backfilled and sealed, the construction / operations tunnels, however, remain open and ventilated.

- *2085 – 2125:* second monitoring phase; the construction / operations tunnels, as well as the main underground access structures are backfilled and sealed. Only the URL and the pilot repository are accessible.

- *2125 –   :* all underground structures are backfilled and sealed.

During operation, all open underground structures are ventilated via ventilation shafts and the access ramp. For simplicity, a constant air temperature of 28 °C and a relative humidity of 60% are assumed in all open tunnel sections. After backfilling of the underground structures, humidity is assumed to increase instantly and the temperature begins to equilibrate towards ambient temperature. Pore pressure in the backfilled structures is assumed to be atmospheric as long as the repository is open. After repository closure (placement of the repository seal), the repository starts to re-pressurise under the action of resaturation and gas generation respectively.

The evolution of the main processes occurring in the ILW caverns are qualitatively the same as in the L/ILW caverns, as described in Section 4.1.4.2.

Other potentially significant processes include:

- Degradation of the cementitious tunnel liner and migration of high pH pore water a small distance into the host rock and bentonite, where chemical interactions can occur.

- Canister breaching as a result of a combination of wall thickness loss due to corrosion and external stresses, which will lead to the exposure of the internal components of the canister and the SF and HLW to pore water. It is expected that the SF/HLW disposal canisters will breach at different times, with 10 000 years being the expected lower limit of this distribution in time and is also Nagra's design target.

EURAD (Deliverable n° 6.1) – Initial State of the Art on Gas Transport in Clayey Materials
Dissemination level: PU
Date of issue of this report: 17/11/2021

Page 289

4.1.4.3.2   Waste inventory and source terms

Waste inventory

The waste amounts and materials to be disposed of in the HLW repository, consisting of SF, HLW and ILW, are summarised in the following sections. All waste amounts refer to conditioned waste unless specifically mentioned otherwise.

The amounts of waste[36] allocated to the HLW repository are shown in Table 4-10, based on the respective MIRAM categories and origins (Nagra 2014b). The majority (58%) of the waste volume is comprised of fuel elements, followed by operational waste (25%), reprocessing waste (9%), and decommissioning waste (8%).

Table 4-10 – MIRAM categories and respective waste amounts for SF, HLW and ILW (Nagra 2014b).

MIRAM category	Mass [kg]	Volume [m³]
Decommissioning waste	5.03×10^5	200
Operational waste	1.44×10^6	589
Fuel elements	4.56×10^6	1 364
Reprocessing waste	6.95×10^5	217
Total	**7.20×10^6**	**2 370**

In terms of mass, the waste comprises 4.91×10^6 kg (61%) inorganic materials, 3.08×10^6 kg (38%) metals and 3.81×10^4 kg (<1%) organics. The disposal canisters for the packing of SF and HLW increase the abovementioned metal inventory by approximately 3.90×10^7 kg (see Table 4-10).

Figure 4-37 shows the split of the HLW metal inventory (excluding the SF and HLW disposal canisters) into different metals and metal groups. The main contributor is Zircaloy (42%), which derives from the fuel cladding. Iron and carbon steel (28%) mainly derive from the cast iron containers for ILW. Other significant contributors to the HLW metal inventory are stainless steel (18%) and lead (10%). Table 4-11 shows the distribution of inorganic, organic and metallic materials in the waste subcategories.

---

[36] The masses and volumes given here refer to the filled waste containers, including raw wastes, additives, containers, filler materials, and fittings. In the case of spent fuel, masses and volumes refer to unpacked fuel elements. SF/HLW disposal containers are not included.

EURAD (Deliverable n° 6.1) – Initial State of the Art on Gas Transport in Clayey Materials
Dissemination level: PU
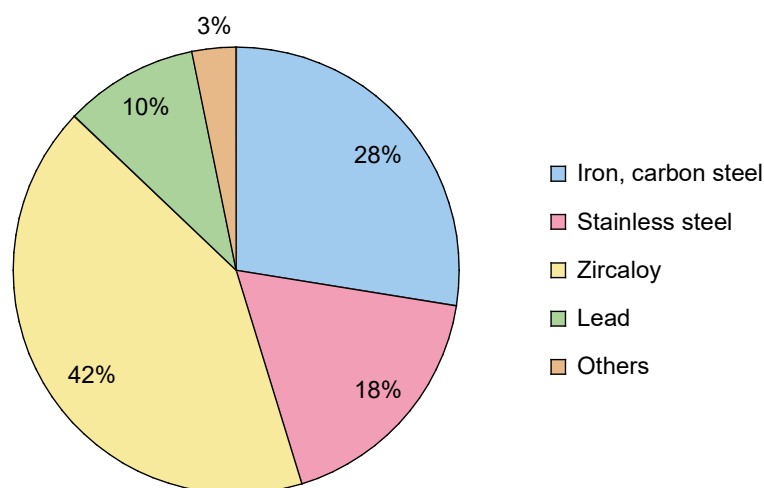Date of issue of this report: **17/11/2021**

Page 290

Figure 4-37 – Metal inventory (wt%) of the waste allocated to the HLW repository, including HLW stainless steel flasks and fuel cladding, but excluding the SF and HLW disposal canisters.

Table 4-11 – Subcategories and material groups of waste allocated to the HLW repository.

Waste subcategory	Material group	Total mass [kg]
Spent fuel	Inorganic	3.32×10^6
	Metallic	1.25×10^6
	Organic	0
HLW	Inorganic	2.47×10^5
	Metallic	5.94×10^4
	Organic	0
ILW	Inorganic	1.35×10^6
	Metallic	1.77×10^6
	Organic	3.81×10^4

Gas generation – source terms

For the simulations of gas release, the following assumptions are made:

- Only H_2 is released from the SF/HLW tunnels.

- Only H_2 and CH_4 are released from the ILW caverns. The cement backfill is carbonised by CO_2.

- The gas sources (H_2 only) associated with the support structures and emplacement materials can be assigned to the entire access / operations tunnel (represented by two element layers) or to the lower element layer of the tunnel. The corresponding source terms are uniformly distributed along the underground structures outside the emplacement caverns.

The gas production rates from materials emplaced in the underground structures are shown for the different tunnel types in Figure 4-38. The gas rates from SF and HLW as well as from ILW are compared to gas rates produced by emplaced materials in corresponding emplacement tunnels in Figure 4-39 and Figure 4-40, respectively. The ILW comprise two waste types, with type ILW-1 emplaced in the 145-m K04 cavern and type ILW-2 emplaced in the 20-m K04 cavern.

EURAD (Deliverable n° 6.1) – Initial State of the Art on Gas Transport in Clayey Materials
Dissemination level: PU
Date of issue of this report: **17/11/2021**

Page 291

For modelling the gas release it assumed that waste-generated gas has the properties of H_2 in terms of viscosity, density and solubility. The gas generation rates are prescribed uniformly to the grid cells representing the backfill material of the SF/HLW tunnels and the ILW and pilot caverns, respectively.
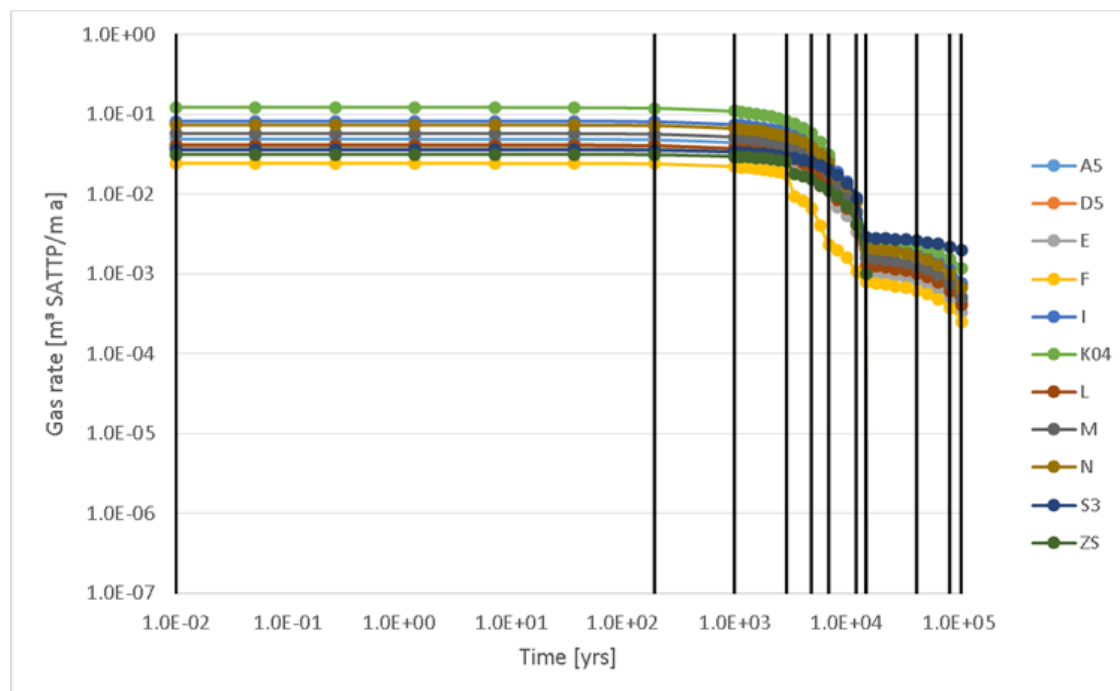

Figure 4-38 – Gas production for different tunnel types as a function of time. (A5: access tunnels in OPA, pilot operation tunnel; D5: ventilation tunnel; I: V5 Seals; K04: SF/HLW tunnels; L: pilot branch tunnel; M: V5 seals/pilot; S3: Shafts).
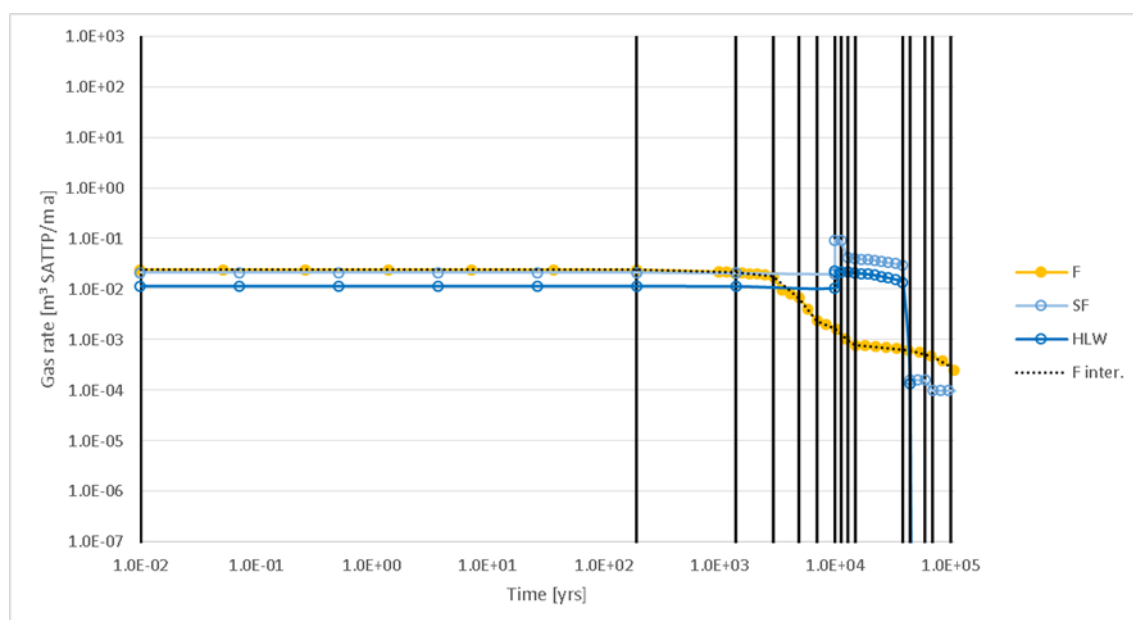

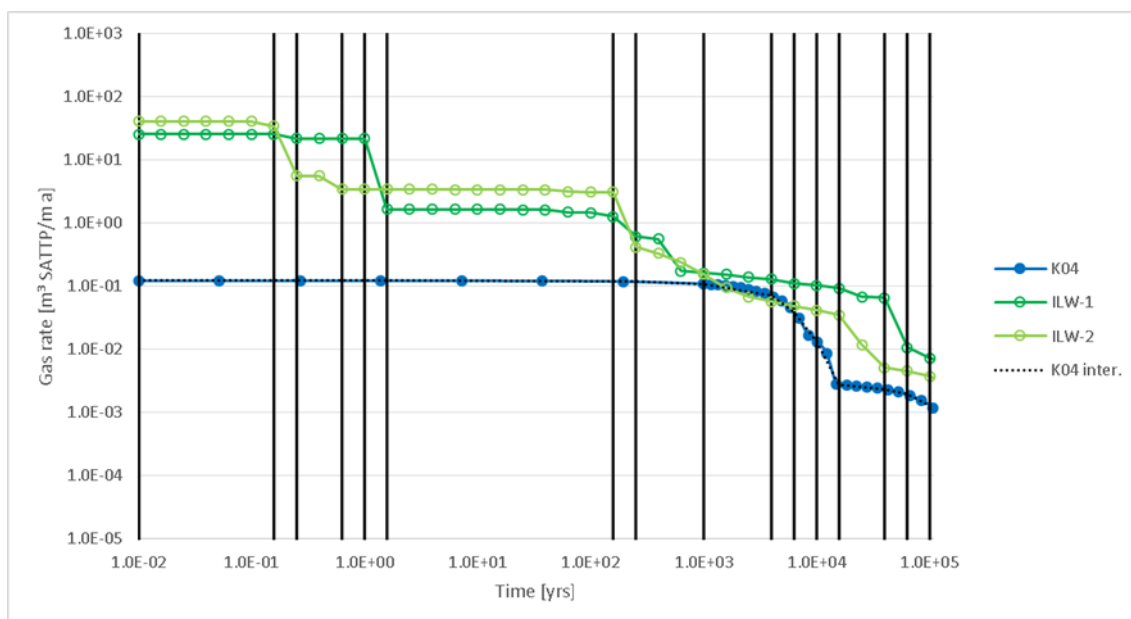*Figure 4-39 – Gas production for SF/HLW as a function of time.*

EURAD (Deliverable n° 6.1) – Initial State of the Art on Gas Transport in Clayey Materials
Dissemination level: PU
Date of issue of this report: 17/11/2021

Page 292

Figure 4-40 – Gas production for ILW as a function of time assuming 1 cavern with waste type ILW-1 and 1 cavern with waste type ILW-2.

4.1.4.3.3   Gas generation modelling

Two-phase flow simulator

A generic 3D model of the HLW repository, similar to that described for the L/ILW repository, was developed using the TOUGH2 code using the equation-of-state module EOS5 for water and hydrogen (Pruess et al. 1999). Diffusive transport of dissolved gas is neglected in this study providing a conservative approach with respect to gas pressure build-up. The thermal evolution of the repository was explicitly considered by introducing heat source terms for the heat emitting waste.

Two-phase flow parameter models

The same two-phase flow parameter models are used as those for the L/ILW repository (see Section 4.1.4.2)

Reference values of gas-related properties of the host rock

The gas-related properties of the host rock are the same as those for the L/ILW repository (see Section 4.1.4.2). The values of the different thermal properties are compiled in Table 4-12.

EURAD (Deliverable n° 6.1) – Initial State of the Art on Gas Transport in Clayey Materials
Dissemination level: PU
Date of issue of this report: **17/11/2021**

Page 293

Table 4-12 – Thermal and mechanical properties for the Opalinus Clay.

	Symbol [unit]	Opalinus Clay	EDZ	Comment
Thermal parameters				
Density - Bulk - grain	ρ [kg/m^3]	2 450 2 700 [a]	2 450 2 700 [a]	[a] Input parameter for TOUGH simulations
Specific heat	C_r [J/(kg.K)]	995.0	995.0	values used in this study
Thermal conduct. - parallel [a/(b)] - perpendicular [a/(b)] - dry [b] - saturated [b]	λ_k [W/m K]	2.15/(2.76) 1.2/(1.32) 1.36 1.8	2.15/(2.76) 1.2/(1.32) 1.36 1.8	[a] Garitte et al. (2014) [b] Wileveau and Rothfuchs (2007)
- Thermal Expansion grain - rock framework - water	Tx [1/ K]	$1.5 \cdot 10^{-6}$ $1.7 \cdot 10^{-5}$ [a] $3.4 \cdot 10^{-4}$	$1.5 \cdot 10^{-6}$ $1.7 \cdot 10^{-5}$ [a] $3.4 \cdot 10^{-4}$	Wileveau and Rothfuchs (2007) [a] Input parameter for TOUGH simulations: rock framework
Rock compressibility				
Young's modulus Poisson ratio Porosity	E [MPa] ν [–] ϕ [–]	6 000 [a] 2 000 [b] 0.27 0.137	6 000 [a] 2 000 [b] 0.27 0.137	[a] Bock (2000, 2002): isotropic linear elastic model (undrained) [b] Giger (2014): drained modulus
Solid compressibility: $\alpha = 3(1-2\ \nu)/E$	α [1/ Pa]	$2.3 \cdot 10^{-10}$ [a] $6.9 \cdot 10^{-10}$ [b]	$2.3 \cdot 10^{-10}$ [a] $6.9 \cdot 10^{-10}$ [b]	Computed from E-modulus
Pore compressibility: $C_p = \alpha/\phi$	C_p [1/ Pa]	$1.7 \cdot 10^{-9}$ [a] $5.0 \cdot 10^{-9}$ [b]	$1.7 \cdot 10^{-9}$ [a] $5.0 \cdot 10^{-9}$ [b]	Input parameter for TOUGH simulations

Model parameters for the repository components

The granular bentonite used to backfill the emplacement tunnels has a high porosity of 45%, whereas the compacted bentonite blocks used for the emplacement of the waste canisters have a lower porosity of 33%. The waste canisters are made of steel and are practically non-permeable, i.e. their volume is typically excluded from estimates of the pore volume available for gas storage in the tunnels. The lining consists of shotcrete with a typical porosity of 25%. Comprehensive characterisation programmes were conducted for the buffer materials (Gaus et al. 2014a, 2014b). In addition, hydraulic and two-phase properties of the buffer materials were characterised as part of the PEBS project, which are summarised in Table 4-13.

It is assumed that all other underground structures in the host rock formation are backfilled with sand/bentonite mixtures or with crushed Opalinus Clay. A typical porosity of 0.35 can be assumed for a lowly compacted sand/bentonite mixture (80% sand, 20% bentonite). For a well compacted sand/bentonite mixture, i.e. used in the seal sections, the assumed porosity is 0.30 (Nagra 2008). The intermediate seal sections in the SF/HLW emplacement tunnels are made of well compacted sand/bentonite. Based on the aforementioned considerations, the void space volumes available for gas storage and transport in individual components as well as for the entire repository are summarised in Table 4-8.

EURAD (Deliverable n° 6.1) – Initial State of the Art on Gas Transport in Clayey Materials
Dissemination level: PU
Date of issue of this report: **17/11/2021**

Page 294

Table 4-13 – Thermal and hydraulic properties for the different bentonite buffer materials from Gaus et al. (2014a, 2014b).

Parameter	Symbol [unit]	Bentonite blocks	Granular bentonite	Canister
Density - dry - bulk - grain	ρ [kg/m^3]	1 806 1 874/1 993 2 699	1492/1 457 1 581/15 431 2 699	 7 850
Thermal parameters				
Specific heat (dry)	C_r [J/(kg K)]	1 058	893	440
at T = 20°C at T = 110°C		800 1 315	856 1 020	775 902
Therm. - dry Cond. - wet	λ_k [W/mK]	0.81 (0.3) 1.3 (1.0)	0.3 1.3 (1.0)	52.5
Thermal expansion	T_x [1/ K]	2.5·10^{-5}	2.5·10^{-5}	1.5·10^{-5}
Hydraulic parameters				
Permeability	k [m^2]	2.5·10^{-21}	3.5·10^{-20}	1.0·10^{-50} [a]
Porosity	ϕ [–]	0.4 0.33	0.45/0.46	0.001
Pore compressibility $C_p = \alpha/\phi$	α [1/Pa] C_p [1/Pa]	1·10^{-9} 3·10^{-9}	1·10^{-9} 3.7·10^{-9}	0
Initial water content	w_r [%]	15.7 10.3	5.95	0
Initial saturation	S_w [–]	0.63	0.20	0
Two-phase flow parameters				
van Genuchten: capillary strength parameter	P_0 [MPa]	21.9	10	10
Temp. effect*	$P = P_0\ \sigma/\sigma_0$	0.072	0.072	
Shape parameters: vG-n (k_r) vG-n (P_c)	vG-n (k_r) vG-n (P_c)	1.42 1.42	1.67 1.67	-
Residual water saturation	S_{lr} (k_r) S_{lr} (P_c)	0.00 0.01	0.00 0.01	-
Residual gas saturation	S_{gr} (k_r)	0	0	0

[a] which is equal to zero numerically.

EURAD (Deliverable n° 6.1) – Initial State of the Art on Gas Transport in Clayey Materials
Dissemination level: PU
Date of issue of this report: 17/11/2021

Page 295

4.1.5   Gas storyboard in Callovo-Oxfordian claystone by Andra (French WMO context)

4.1.5.1   Introduction

Andra founds its assessment of the thermo-hydraulic/gas transient on a deterministic approach based on the related repository architectures and concepts (Figure 4-41), and on the best physical understanding at the moment (in terms of representation model and parameter values). Multiparametric sensitivity analyses are also conducted in relation to the main residual uncertainties, in particular to determine, at the macroscopic component scale (galleries, deposition cells, etc.), operating ranges of characteristic quantities such as maximum gas pressures in the repository.
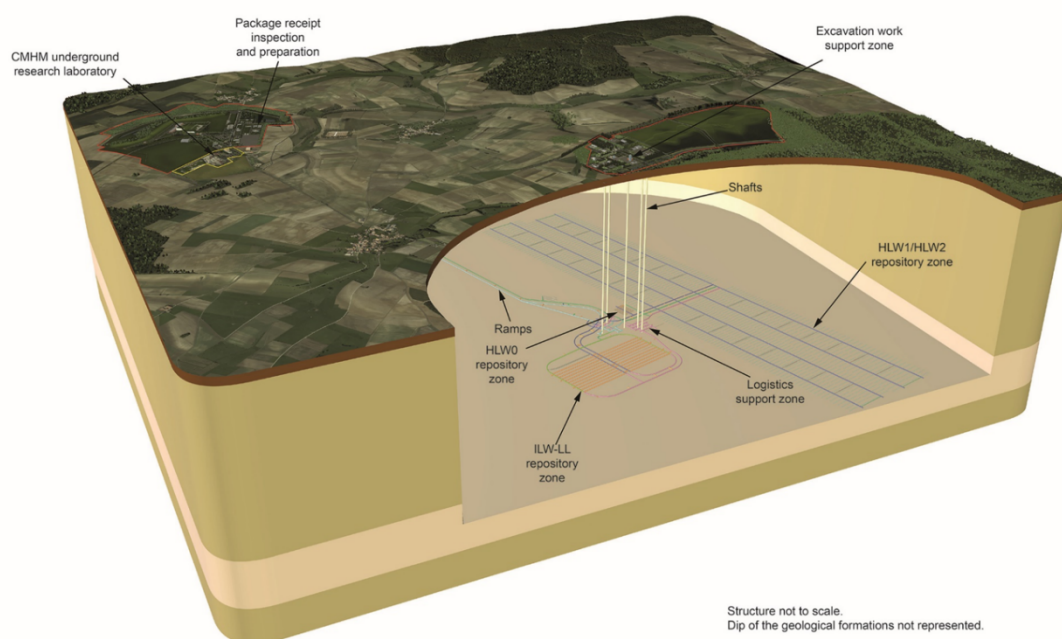
Figure 4-41 – Global architecture of the Cigéo repository.

In order to validate the approach and the numerical tools, Andra has participated and is participating in code intercomparison exercises, has organised and is organising specific exchange meetings with its European counterparts (notably Nagra and ONDRAF/NIRAS whose reference concepts are also developed within clayey sedimentary rocks) and is financing specific developments of calculation code (notably the two-phase TOUGH2-MP code widely used by Andra and its counterparts, in Europe but also in the United States of America and Asia, to conduct quantitative assessments of the hydraulic-gas transient).

EURAD (Deliverable n° 6.1) – Initial State of the Art on Gas Transport in Clayey Materials
Dissemination level: PU
Date of issue of this report: **17/11/2021**

Page 296

4.1.5.2 The main phenomena structuring the hydraulic-gas transient

The characteristics of the hydraulic-gas transient are based on a reduced number of phenomena, represented in blue in Figure 4-42, and detailed in the following paragraphs:
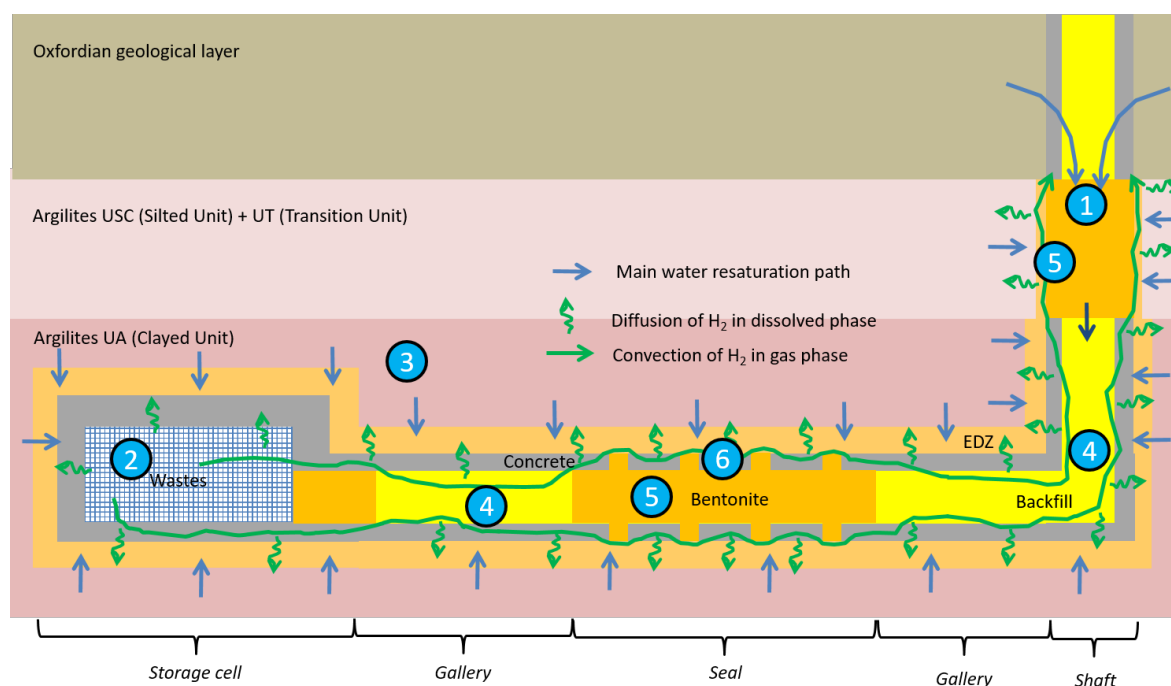

Figure 4-42 – Schematic representation of the repository and of the main phenomena structuring the hydraulic-gas transient (indicated numbers are explained in the text).

1.   A 'rapid' resaturation (within a few decades) of the shafts and ramps seals (Figure 4-43): This resaturation is carried out by the waters of the Oxfordian limestone with which these seals are in contact through their upper section. The calcareous Oxfordian being relatively permeable, the inflow of water is sufficient not to constrain the resaturation which then takes place in a few decades at the most, which leads to an efficiency of these seals that limits the flow of water from the Oxfordian toward the repository. Most galleries and deposition cells are therefore slowly (over several tens of thousands of years at least) radially resaturated by water from the Callovo-Oxfordian claystone.
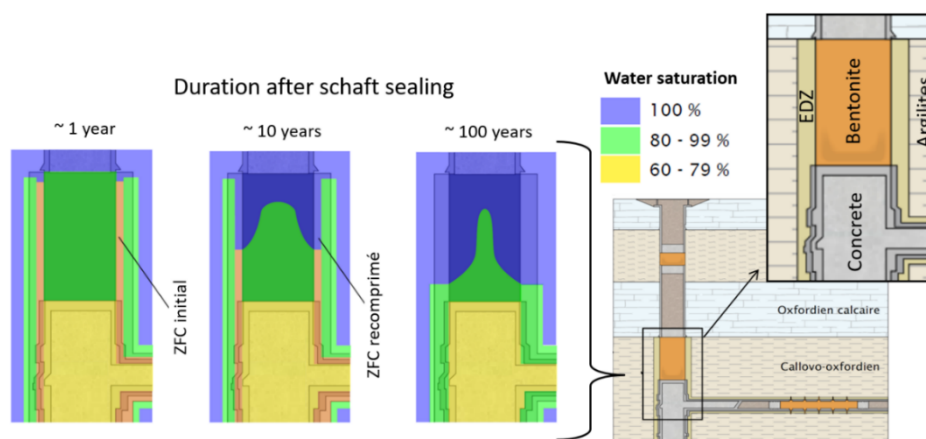

Figure 4-43 – Illustrative representation of the resaturation of a shaft seal.

EURAD (Deliverable n° 6.1) – Initial State of the Art on Gas Transport in Clayey Materials
Dissemination level: PU
Date of issue of this report: **17/11/2021**

Page 297

2.   A significant gas production (mostly hydrogen and mostly in the deposition cells, see Figure 4-44) at the scale of the repository (in the order of tens of billions of moles in total), over periods of up to several hundred thousands of years:

   o   by corrosion: a distinction must be made between reactive metals (aluminium and magnesium alloys), whose corrosion is likely to lead to significant hydrogen flows from the operating phase, and other metal alloys (scrap consisting of steel/nickel alloys/zirconium alloys, steel containers, concrete reinforcement, HLW cell linings, etc.) leading to the production of hydrogen when the repository is closed (under anoxic or very near-anoxic conditions) and with lower corrosion kinetics;

   o   by radiolysis: certain materials in the long-lived intermediate-level waste (ILW) packages (mainly organic materials and the water contained in cement materials) produce hydrogen (but also other gases) under the effect of radiation and therefore influence the hydraulic-gas transient as soon as they are placed in the repository;
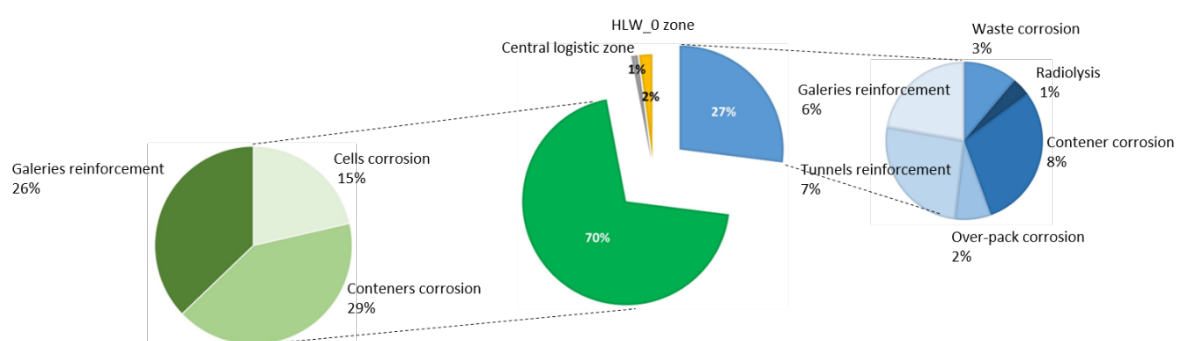

Figure 4-44 – Illustrative representation of the percentage of hydrogen produced in each repository zone (around 10 billion moles at total).

3.   The (very) low diffusion of dissolved hydrogen in the Callovo-Oxfordian claystone, limiting the ability of the Callovo-Oxfordian claystone to evacuate it by diffusion, despite an exchange surface of several million m² between the repository and the Callovo-Oxfordian claystone;

4.   The very high gas entry pressure and very low permeability in the host rock claystone, compared to that of Cigéo's engineered components, thus favouring the transfer of gaseous hydrogen by the components of the repository (mainly backfill and concrete) and not by the Callovo-Oxfordian claystone;

5.   The very low permeability (and the relatively high gas inlet pressure) of the bentonite of the sealing cores;

6.   Favouring at the seals the transfer of gaseous hydrogen by (i) the possible concrete annular rings left in place, (ii) the EDZ and (iii) the interfaces between the different materials.

To a lesser extent than those indicated above, as they only have an influence for a few hundred to thousands of years after closure, the other phenomena involved in the hydraulic-gas transient are as follows:

   •   Desaturation during the operating phase: ventilation by an air that is not saturated with water vapour involves desaturation of the EDZ and the structural concrete. As a result, ventilation influences the hydraulic-gas transient over a period of about a thousand to several thousands of years, corresponding to the time required to balance saturation with the capillary pressures induced by hydrogen production;

EURAD (Deliverable n° 6.1) – Initial State of the Art on Gas Transport in Clayey Materials
Dissemination level: PU
Date of issue of this report: 17/11/2021

Page 298

- The emplacement of the closure materials (backfill, bentonite) at water saturations close to Proctor optimum (in order to obtain a good mechanical coherence) influences the hydraulic-gas transient by a similar process and for a similar duration;

- HLW thermal: the coupling between the hydraulic-gas and the HLW thermal influences the hydraulic-gas transient for several hundred years from the emplacement of the waste packages in the cells, thus including part of the operation phase. This influence is due to the variation in viscosity and density of water as a function of temperature.

4.1.5.3 Storyboard of the hydraulic-gas transient at repository scale

During the operating phase: the hydrogen produced is evacuated by the ventilation system (to protect against the risk of reaching an explosive atmosphere) and therefore does not participate in the hydraulic-gas transient after closure. However, this ventilation contributes to the desaturation of the walls of the ventilated excavations.

Some decades after closure (Figure 4-45): The seals of the shafts and ramps are resaturated in a few decades, mainly by the water from the Oxfordian limestone, thus strongly limiting the flow of water to the disposal excavations. As a result, the latter are mainly radially resaturated by water from the Callovo-Oxfordian claystone. At the same time, the gas produced in the disposal facility dissolves in the Callovo-Oxfordian water and migrates in dissolved form.
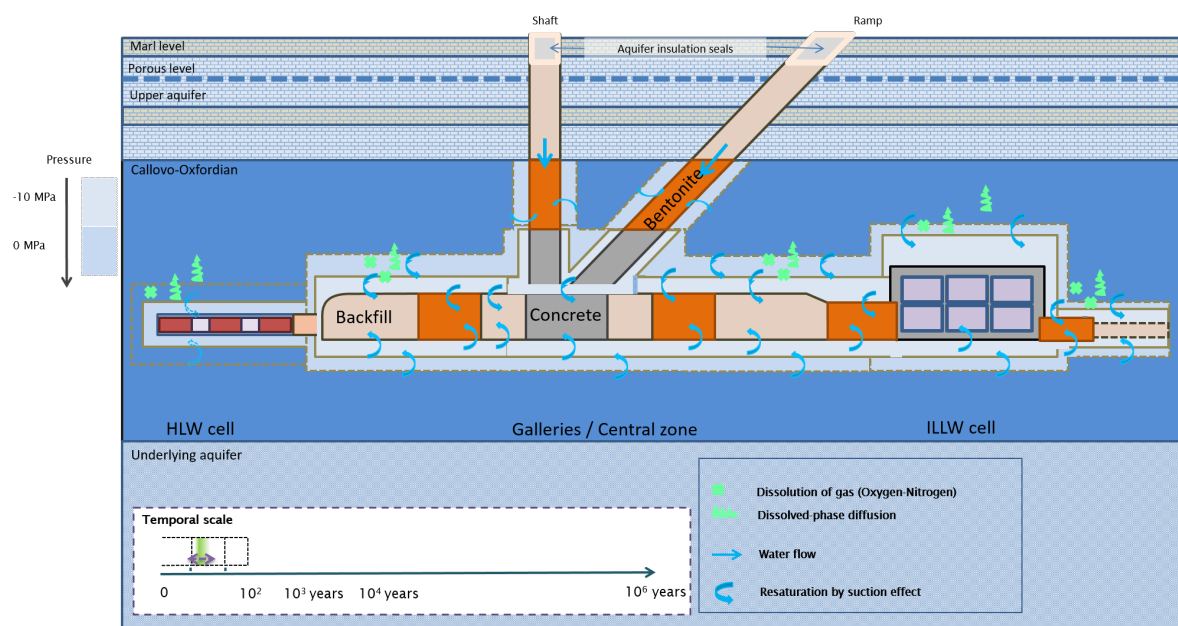

Figure 4-45 – General flow pattern of water and gas in the repository a few decades after closure.

Some hundred years after closure (Figure 4-46): The coupling of hydraulic-gas processes with waste-related thermal (notably due to the decrease in water density with temperature) implies for a few hundred years a peak in water pressure at the half centre distance between cells (with a maximum around 10 MPa) and in gas pressure at the high-activity cells (around several MPa), before the exothermicity of the waste decreases and these overpressures dissipate. This coupling is dominant during this period in the HLW zone because the vitrified high-level waste is highly exothermic, whereas its influence is much less in the ILW areas. In parallel, gas flows from the cells to the galleries at the scale of the disposal zones appear, but the gas pressure is not yet sufficient to allow gas transfers to the central area.
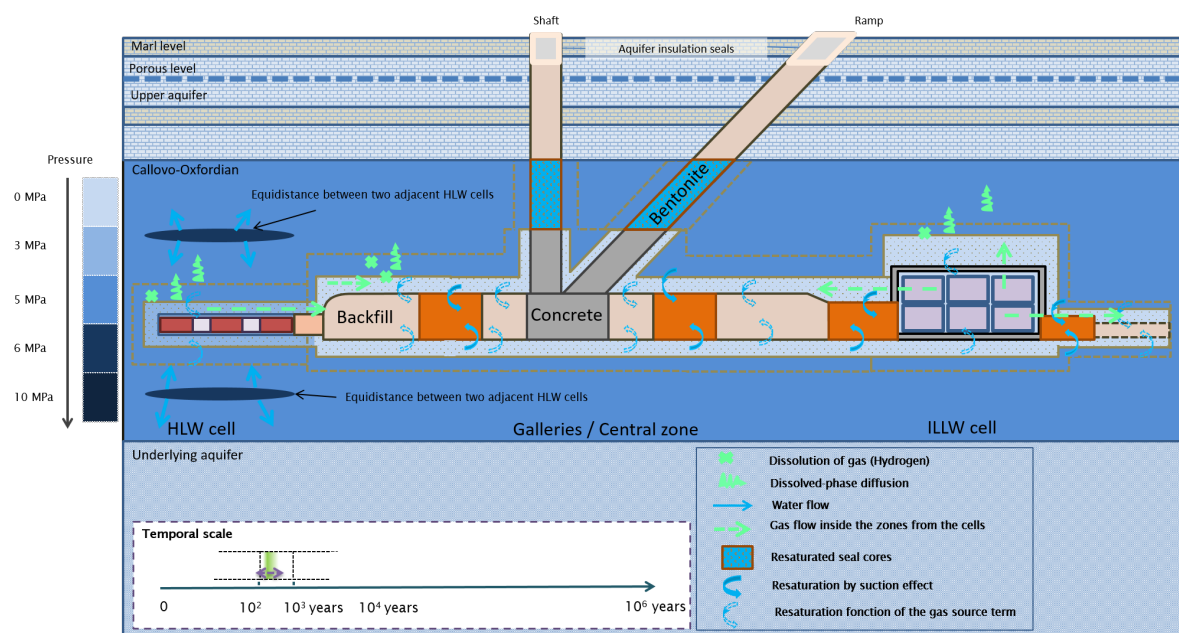
EURAD (Deliverable n° 6.1) – Initial State of the Art on Gas Transport in Clayey Materials
Dissemination level: PU
Date of issue of this report: 17/11/2021

Page 299

Figure 4-46 – General flow pattern of water and gas in the repository a few centuries after closure.

A few thousand of years after closure (Figure 4-47): After closure of the disposal facility, the anoxic corrosion of metals (galleries concrete liner rebars, HLW cell metallic liner, waste packages, …) generates hydrogen which is added to the hydrogen produced by the radiolysis of certain waste types (polymers, bituminous sludge, cementitious matrices, salts, etc.) in the ILW cells. This cumulative production begins to influence the hydraulic transient from a few thousands of years after closure and for several hundred thousands of years. On this time scale, the gas pressures are sufficient for gas transfers from the disposal zone to the central logistics zone but not yet toward the upper aquifer.
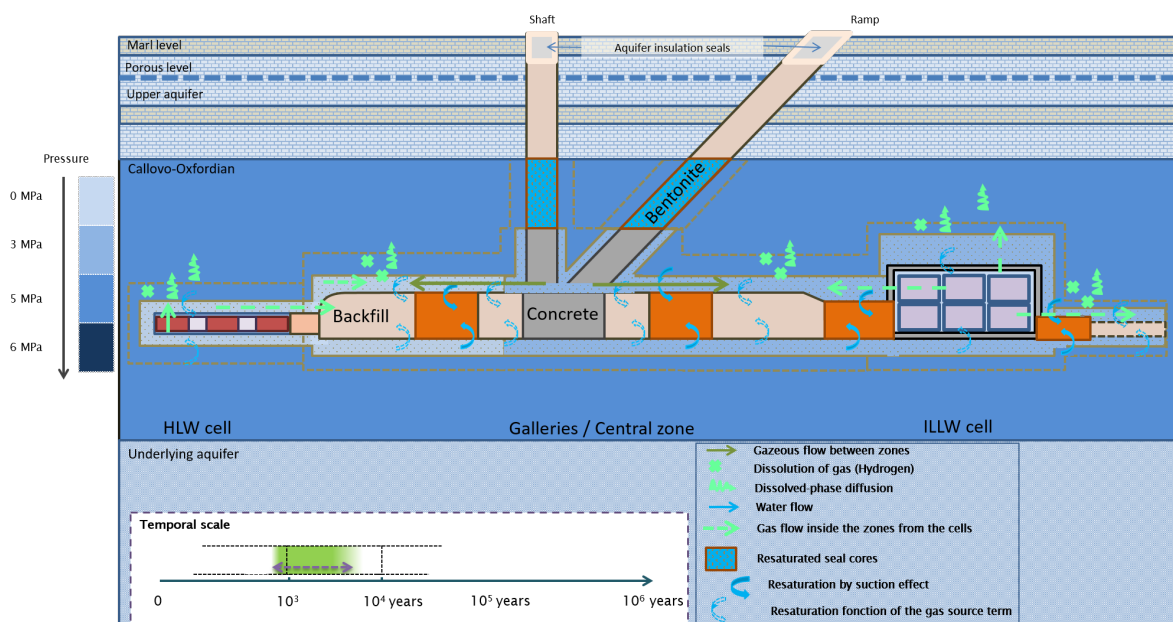

Figure 4-47 – General flow pattern of water and gas in the repository a few thousands of years after closure.

EURAD (Deliverable n° 6.1) – Initial State of the Art on Gas Transport in Clayey Materials
Dissemination level: PU
Date of issue of this report: 17/11/2021
Page 300

The general scheme is then as follows:

- Because of the large amount of hydrogen produced (around 10 billion moles), only part of it dissolves in the waters of the Callovo-Oxfordian claystone and the rest is expressed in gaseous form;

- Due to the very low permeability of the claystone and its high capillarity, the hydrogen expressed in gaseous form does not lead to a desaturation of the Callovo-Oxfordian claystone; it remains confined in the engineered components and migrates towards the shafts and ramps;

- Due to their capillary properties, the sealing cores resaturate before the other materials present in the repository and, by design, they then represent bottlenecks for the passage of the gas, which can only migrate through the EDZ, concrete (retaining annular rings left in place to provide mechanical support for the EDZ) and the interfaces between more permeable materials, thus leading to a rise in pressure upstream;

- Gas flows are set up between the different zones of the repository (HLW zone, ILW zone, central zone) but in the central zone the gas pressure is still too low to allow a flow towards the upper aquifer.

Some tens of thousands of years after closure (Figure 4-48): Gas pressure peaks some tens of thousands of years after closure: During this period, gas flows are organised from the deposition zones toward the central zone and then toward the upper aquifer. The general flow pattern (partial dissolution, two-phase migration towards the accesses, pressure increase upstream of the seals, passage through the seals mainly through the EDZ) continues as long as the hydrogen source terms remain significant, i.e. for at least a hundred thousands of years. Beyond that, the gas pressure decreases and when it reaches that of water, the gas phase disappears. Complete resaturation of the repository is achieved around several hundreds of years after closure.
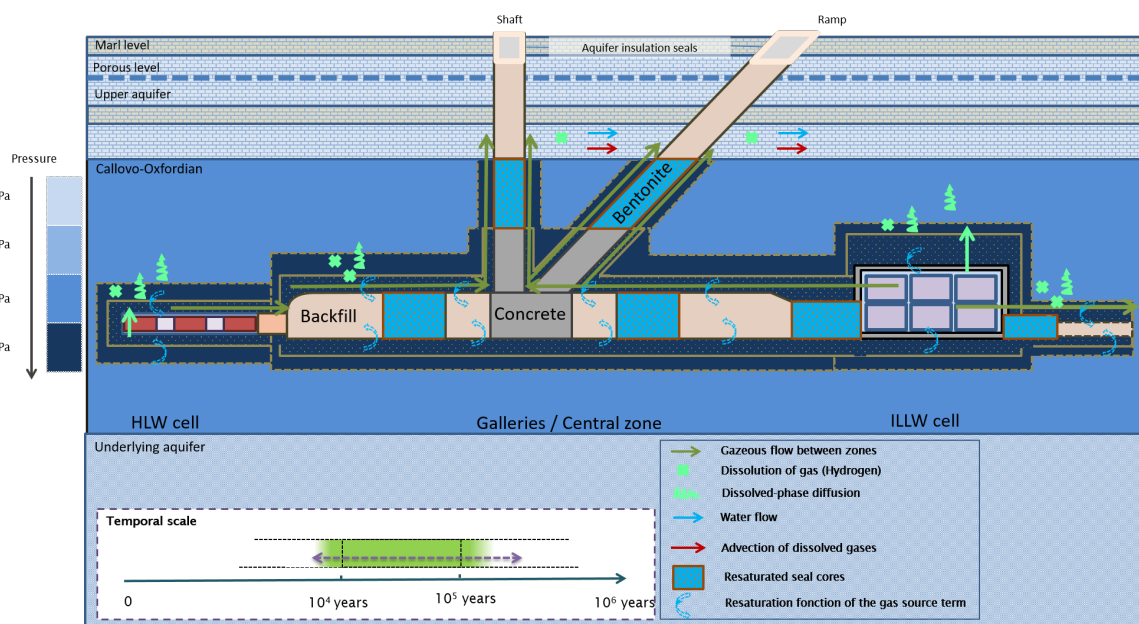

Figure 4-48 – General flow pattern of water and gas in the repository a few tens of thousands of years after closure.

EURAD (Deliverable n° 6.1) – Initial State of the Art on Gas Transport in Clayey Materials
Dissemination level: PU
Date of issue of this report: **17/11/2021**
Page 301

In terms of gas flows:

- The fluxes between zones are relatively low, with peaks of the order of a few tens of thousands of moles per year between the ILW zone and the central logistics zone, then towards the shafts and ramps. The overall flow is mainly distributed among the various wells, which are closer to the central logistics zone than the ramps and are also shorter in length. These maxima are reached a few tens of thousands of years after closure and last for about 100 000 years.

- Of the total hydrogen produced in the repository (around 10 billion moles), about 5% to 10% reaches the upper aquifer in gaseous form via the shafts. The remainder migrating in dissolved form within the Callovo-Oxfordian layer with roughly 40% toward the underlying Dogger aquifer and 55% to 60% toward the upper Oxfordian aquifer (Figure 4-49).
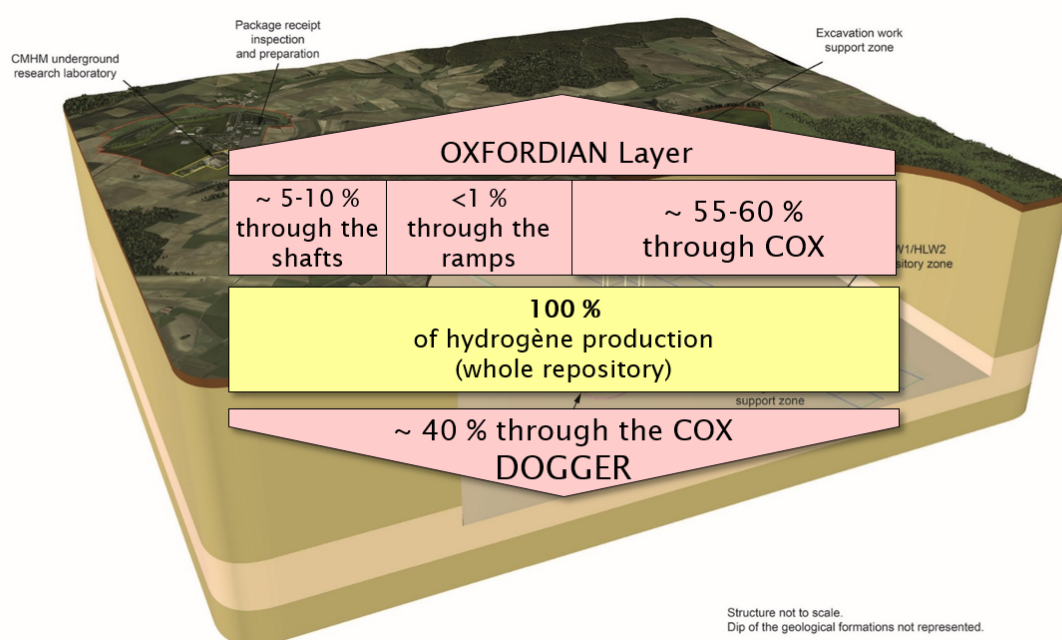

Figure 4-49 – Illustration of the balance of the distribution of hydrogen migration between upper and underlying aquifers via the host rock or the shafts/ramps after one million years.

4.1.6 Gas storyboard in Callovo-Oxfordian claystone by IRSN (French TSO context)

4.1.6.1 Context

The safety assessments conducted by IRSN in the field of geological disposal of HLW and ILW mainly concern the Cigéo project developed in France by Andra in an indurated Callovo-Oxfordian clay host rock (Andra 2015a, 2015b). IRSN is particularly interested, within EURAD, in neglected or unsatisfactorily modelled processes of gas migration that may have an impact on disposal safety. Hence, we will not present here the disposal concept of the Cigéo project nor its overall functioning with regard to gas migration that are already well presented in Andra's chapter. In the following, we focus on the open issues arising in the performance assessment/Safety Assessment of the Cigéo project. For each of them, we also address, at this stage of development of the Cigéo project, their importance regarding the safety of Cigéo. Two general remarks can be made. Firstly, the current understanding of

EURAD (Deliverable n° 6.1) – Initial State of the Art on Gas Transport in Clayey Materials
Dissemination level: PU
Date of issue of this report: 17/11/2021

Page 302

the gas storyboard with respect to major indicators (maximum gas pressures, resaturation times, couplings with other phenomena) shows large uncertainties, and it seems that they cannot be easily reduced with existing approaches. Secondly, the phenomenology to be considered in a quantitative approach depends very much on the disposal concept itself, particularly in terms of the architecture, location and properties of the seals, and the details of the gas source term. These two points justify the pursuit of detailed studies in order to refine the storyboard of gas migration in Cigéo.

4.1.6.2 Performance assessment / safety assessment open issues

It should be remembered that it is difficult to represent experimentally the expected in situ conditions, mainly because of the long characteristic times of the involved phenomena. Thus, the experimental results are extrapolated to conclude on what is expected in a real disposal facility. However, such extrapolation should be based on models taking into account the whole range of parameters, conditions and phenomena. The absence of experimental validation on large time and space scales of such simulations, requires to check carefully the potential impact of all neglected phenomena.

4.1.6.2.1   Mechanical damage associated with the gas flow

According to the conclusions of the FORGE EC project (Norris 2013), for clayey materials with water saturation above 85 to 90%, the gas flow would no longer be governed by the conventional visco-capillary mechanism (Norris 2013) but the gas would flow through localised and unstable pathways. IRSN considers that although international consensus emerged about this phenomenology, the associated models need to be improved. Moreover, the values of their key parameters still have to be specified and it is not yet possible to state about their invariability during the gas migration process. This fundamental difficulty is common to several issues presented in this chapter, but we will discuss it here only once on the basis of the Callovo-Oxfordian (COx) argillite.

The knowledge acquired indicates that COx has a significant total porosity (average porosity 18%). More than 90% of the latter is constituted by pores smaller than 100 nm, the permeability of the claystone is very low (of the order of 10^{-20} m^2). The connectivity, ensured by very small pores (less than 10 nm), and the poral geometry which implies a large exchange surface area, are also particularly favourable to high retention properties. However, the spatial organisation of the porosity remains difficult to characterise experimentally (Song et al. 2015). In this context, the phenomenological modelling of two-phase flows on the macroscopic scale is still a largely open issue (Lefort 2014), on the one hand because of the importance of surface phenomena at the level of submicron pore size, and on the other hand because of the extremely low 'capillary number' that characterises very slow flows ('hyper-slow' flows). The common approach used today to model these flows considers gas migration through a host rock close to complete saturation via localised pathways consisting of temporarily dilated pores. The first models describing this phenomenon are based on the opening of a network of explicitly predefined fractures/cracks (Gerard et al. 2014; Rozhko 2016) with very simplified forms, sizes distributions and connectivity. Due to the quasi absence of small-scale characterisation of the clay particles, some of these parameters are chosen arbitrarily. These choices may have an impact on the transport mechanisms which are active in the micro-scale simulations.

IRSN considers this issue to be of importance as it can influence not only the damage to the clayey materials but also the maximum value of the pressure that will be reached by the gases if they cannot migrate fast enough from the disposal.

EURAD (Deliverable n° 6.1) – Initial State of the Art on Gas Transport in Clayey Materials
Dissemination level: PU
Date of issue of this report: **17/11/2021**

Page 303

4.1.6.2.2   Possibility for gases to lead to a hydraulic overpressure

IRSN questioned the possibility for gases to create a hydraulic gradient in the rock mass that should be taken into account in radioelement transport calculations. The PGZ1 experiment (Harrington et al. 2012b) conducted in the Meuse/Haute-Marne URL showed a very slight hydraulic overpressure (from 5 to 15 kPa at 90 cm from the injection area) for a gas injection pressure of 9.1 MPa. However, it is not certain that this overpressure was due to the percolation of the gas in the sound argillite. This overpressure could be due to the movement of water contained in the damaged zone around the borehole. Besides, during laboratory tests carried out on samples of argillite to measure the breakthrough pressure, only a little of water was displaced. This means that only a very small part of the poral space was desaturated by gas. Thus, at this stage of knowledge, IRSN considers this issue to be less challenging than others regarding Cigéo's safety case. Nevertheless, in both cases (in situ and laboratory tests), the numerical predictions based on a two-phase flow model differed from experimental results. These observations confirm the need for a better model of gas migration in saturated clay rock materials in order to better apprehend the effect of gas migration on water movement in sound argillite (and bentonites).

However, even if the gas phase does not displace much water in the sound claystone of the host rock, the possible effects of gas migration through the more permeable and porous materials of the drifts backfill and EDZ could be more significant. The possibility for the gas to push ahead contaminated water along the drifts has thus been observed by Andra in disposal facility scale simulations. This 'piston effect' is generally considered to be weak (a few tens of metres towards shafts) (IRSN 2014, 2017). Nevertheless, IRSN considers (Saâdi et al. 2020) that this conclusion should be confirmed by assessing the influence of the simplifications that had to be introduced to carry out simulations on the full scale of a disposal facility.

IRSN considers this issue to be relevant for the safety assessment of Cigéo and that simpler simulations from a geometric point of view (compared with a real disposal facility) should be carried out. However, the use of simulation codes, richer in terms of phenomenology, should be encouraged. Some already known macroscopic phenomena, which are usually not accounted for, could already be taken into account: the gas entry pressures (which are now evaluated at several MPa), the hysteresis of the suction curve, the impact of an important suction on gas solubility and a simplified model for intermittent interfaces/voids. By analysing the results of these simulations, it should be possible to better appreciate the importance of all these phenomena and parameters.

4.1.6.2.3   Gas interference with resaturation of bentonite plugs and seals

Plugs and seals made of bentonite are expected to resaturate to some significant saturation levels (95% for plugs) without too much gas disturbances since gas needs some time to accumulate (a few thousands of years) and since the gas percolation pressure increases strongly with the saturation level. However, the gas pressure is expected to eventually exceed this entry pressure value and the gas phase would flow through bentonite in localised pathways, delaying the 100% saturation of the bentonite which can only be reached after the gas production shut down. Thus, despite the presence of gases, the plugs and seals shall be able to reach their nominal swelling pressure, but with a delay in establishing a full saturation. For example, in the PGZ2 experiment (de la Vaissière 2013), a continuous gas pathway persisted in the core of the plug after 600 days of resaturation without being large enough to be explained by some macroscopic initial filling defect. Other experimental evidences indicate that the resaturation process of such a composite material inevitably leads to very heterogeneous resaturation and swelling in space and time, even when saturation becomes almost complete (the Temperature Buffer Test (TBT) in Äspö (Åkesson 2012) and Engineered Barrier (EB) experiment in Mont Terri (Mayor and Velasco 2014). The nominal swelling pressures are generally considered to be asymptotic values that are not necessarily observed in the in situ experiments.

EURAD (Deliverable n° 6.1) – Initial State of the Art on Gas Transport in Clayey Materials
Dissemination level: PU
Date of issue of this report: 17/11/2021

Page 304

The behaviour of pellets and powder mixtures is more complicated and less well understood than that of pre-compacted blocks IRSN considers that understanding the phenomenology associated with the resaturation of pellets-powder mixtures in the presence of gases becomes important for Cigéo insofar as these mixtures are, at this stage, considered for the vertical seals of ramps and shafts, which are the most important seals in the closure system of this project.

4.1.6.2.4   Resaturation of the whole disposal facility

Assessment of the time required to achieve a total resaturation of a disposal facility can only be done by means of large scale simulations. The calculations conducted up to now have been based on pure hydro-gas simulations by neglecting some important two-phase flow phenomena (discussed in Section 4.1.6.2.2). The results obtained present a high degree of uncertainty which makes it almost impossible to identify the expected hydraulic regimes in the different areas of the disposal. It is clear that the results are highly dependent on the detailed disposal design and that the distribution of the results reflects the expected bounds of main parameters. IRSN considers that from a knowledge point of view of the long-term evolution of a disposal, the impact of model simplifications, both in terms of phenomenology and geometry, must be studied. Moreover, the impact of these uncertainties on the safety case needs to be investigated.

4.1.6.2.5   Effect of confinement on pore water properties with dissolved hydrogen

Many analyses of experimental results and many choices of parameters for simulations are based on pure and/or bulk water thermodynamic data, e.g. concerning hydrogen solubility or surface tension in water-hydrogen systems. However, capillary effects can significantly modify the thermodynamic equilibrium of poral water and, in particular, the solubility of gases (hydrogen solubility increases of 10% for a 10 MPa suction) (Dymitrowska et al. 2015). It is also important to continue to refine the knowledge about the effects of desaturation (poral water pressure becomes negative due to high capillarity) and of the massive presence of dissolved hydrogen on the chemical equilibria with clayey materials (Lassin et al. 2011). It would especially of interest to get additional knowledge about the behaviour of radionuclides that could be irreversibly mobilised (speciation change) in the disturbed zone (as a result of a pH change and/or of a high temperature and/or of a negative water pressure).

4.1.6.2.6   Bacteria and hydrogen

IRSN considers that the period during which the hydraulic-gas transient takes place might be of interest in order to evaluate the impact of bacteria on the properties of clays. IRSN notes that the disappearance of hydrogen observed during the HT (Hydrogen Transfer) experiment carried out at Mont Terri (Vinsot et al. 2014) as well as during the diffusion tests carried out at by SCK CEN in the framework of the FORGE EC project, corroborated by the geochemical simulations carried out at IRSN (Devau et al. 2012), show that a chemical disturbance linked to bacterial activity during a prolonged flow of hydrogen cannot be totally excluded and should be investigated further. Some results (Maillet 2012; Chautard 2013; Grousset 2016) suggest that bacterial activity (e.g. sulphate reducing bacteria which use dissolved hydrogen) and the chemical changes they might create locally lead to a higher corrosion rate of metal parts or even, in the long term, to localised corrosion whose location and depth are difficult to assess. Thus, microbial activity may modify the hydrogen production rate (corrosion) and adversely the hydrogen sink term, influencing the overall hydrogen migration pattern in a disposal.

EURAD (Deliverable n° 6.1) – Initial State of the Art on Gas Transport in Clayey Materials
Dissemination level: PU
Date of issue of this report: 17/11/2021

Page 305

4.1.6.2.7   Corrosion under irradiation as a source term for gas

IRSN is also concerned with the effects of irradiation by gamma rays on the anoxic corrosion of steels and on the resulting hydrogen production, a subject that is very little studied elsewhere. The preliminary results obtained by IRSN on experimental tests (Stammose et al. 2013; Giannakandropoulou 2019) raise a number of questions that require further studies in order to identify the processes and mechanisms responsible, for example, of the gradual decline in hydrogen production during the irradiation phase. Such studies should also investigate the coupled impacts of temperature, test solution chemistry and dose rates on the observed phenomena.

4.1.6.3   Conclusion

Assessing the safety of a radioactive waste disposal raises questions, some of which can lead to a great deal of research in case further reducing of uncertainties is at stake. Gas issue is no exception to this point and the impact of these uncertainties on the performance of a disposal concept may also be concept-dependent. In the case of the Cigéo project, IRSN considers that it is necessary to assess the impact of phenomena observed in clayey materials close to a state of total water saturation and usually not taken into account in large scale simulations, such as a non-zero value of the entry pressure of gas (which may influence the maximum value of the calculated gas pressure in the facility), the possibility for gas to push contaminated water along the drifts (piston effect), and the specific behaviour of pellets/powder mixtures envisaged for the construction of the most important seals of the project. The other aspects remain of interest, at this stage of the development of this project, in order to reduce uncertainties related to hydro-chemical conditions prevailing in the disposal facility.

4.1.7   Comparison between end-users approaches

The storyboard elements presented in Sections 4.1.1 to 4.1.6 by RWM (UK), ONDRAF/NIRAS (Belgium), COVRA (The Netherlands), Nagra (Switzerland), Andra and IRSN (France) highlight the following similarities and differences between the repository development approaches in their respective national programmes in relation to gas generation and transport, the phenomenological representations of the hydraulic-gas transient and their consideration in the analysis of the long-term evolution of disposal and finally in the safety assessments.

4.1.7.1   Repository design approaches

Unlike in crystalline and halite host rocks, there is still no geological disposal facility in operation and/or in construction in a clayey host rock. For the moment, only France has selected a site (Bure) in a clayey host rock so it has been possible for Andra to define a complete repository concept for that site. National programmes of other countries considering clay host rocks are at various stages of searching for a site and/or pre-design of a repository concept.

Nevertheless, all those countries are targeting clay layers at a depth of a few hundred metres in their search for a site and all participating WMOs are planning a single level disposal with separate zones for high-level waste disposal and long-lived intermediate-level waste disposal.

For all participating WMOs, the concepts are different for high-level waste and long-lived intermediate-level waste. These differences relate mainly to (i) the geometry of the primary waste packages, (ii) the management of the thermal phase for high-level waste and (iii) the need to delay the migration of radionuclides as long as possible for each type of wastes.

EURAD (Deliverable n° 6.1) – Initial State of the Art on Gas Transport in Clayey Materials
Dissemination level: PU
Date of issue of this report: 17/11/2021

Page 306

All participating WMOs include in their repository concept for high-level waste a disposal overpack made of steel. In order to delay the release and attenuate the migration of radionuclides out of the waste, two main approaches are envisaged:

- Placing the steel overpack in a highly alkaline environment for as long as possible in order to slow down generalised corrosion and to guarantee the longest possible tightness of the overpack. The counterpart being that once the tightness is lost, in case of disposal of vitrified high-level waste, the glass containing the waste may degrade more rapidly if the alkalinity of the water is still elevated and release all the radionuclides over a relatively short period of time.

- Guarantee tightness only during the operating phase (possible safe handling of the waste packages, includes reversibility/retrievability period) and maintain the pH of the water around the packages at values that guarantee, in case of disposal of vitrified high-level waste, slow degradation of the glass once the tightness of the package is lost. The counterpart being that these low-alkaline waters imply a faster corrosion of the steel of the packages and thus an earlier loss of tightness.

As far as gas generation is concerned, the first approach rather implies a lower gas source term (low corrosion rate) but longer in time, whereas the second approach implies a higher gas source term (higher corrosion rate) but of shorter duration.

Regarding long-lived intermediate-level waste, the primary waste packages that have to be dealt with in all national programmes generally have a wider variety of geometries than primary packages of high-level waste, which are generally cylinders of about a few decimetres in diameter and between one and a few metres in length. In contrast, for long-lived intermediate-level waste, the primary packages may be drums of more diverse sizes. More than this, for high-level waste, considerations like criticity and thermal criteria have to be taken into account. As a result:

- High-level waste disposal cells are generally smaller in diameter and the waste disposal packages are disposed horizontally with only one package per cell section;

- Long-lived intermediate-level disposal cells are generally larger in diameter and waste disposal packages are disposed either horizontally or vertically, with several waste packages per cell section, the optimal arrangement being partly driven by cost consideration.

In addition to the above elements that are important for the general architecture of the repository and therefore the expansion volumes available for the gases generated after closure, the following points related to the repository concepts are directly related to the generation of post-closure gases and are common to all programmes:

- High-level waste overpacks are made of steel, which represents an important source of hydrogen generation by anoxic corrosion.

- The lining of the galleries includes metallic elements, mainly reinforcing bolts, and/or concrete reinforcement.

- Some long-lived intermediate-level waste contains (mainly or partially) metallic elements.

- Some long-lived intermediate-level waste (e.g. organic waste) may produce significant quantities of gas by radiolysis and/or (bio-)chemical degradation processes.

The sealing system is also an important component concerning gas migration after repository closure. For most participating WMOs, it is dimensioned (usually by the definition of a water permeability below a certain value) to limit the flow of water containing dissolved radionuclides but with an induced effect on the transport of gases which are also fluids and for which it may represent a bottleneck for gas

EURAD (Deliverable n° 6.1) – Initial State of the Art on Gas Transport in Clayey Materials
Dissemination level: PU
Date of issue of this report: 17/11/2021

Page 307

transport across the system. Therefore some designs take explicitly into account the gas component in the dimensioning and choice of materials of the components of the sealing system.

4.1.7.2 Phenomenological representations of the hydraulic-gas transient

Regarding gas production mechanisms, for all participating WMOs:

- In the repository, other gases than hydrogen are produced but the latter represents by far the main source term and evaluations are conducted assuming that only this gas is produced (except possibly in some sensitivity analyses).

  - The main mechanism producing hydrogen after closure of the repository is corrosion of metals (principally steel) under anoxic conditions.

  - Radiolysis of organic matter and/or water is a secondary but not negligible source term of hydrogen.

- Other production mechanisms (alpha decay which produces helium, bacterial activity which may produce additional gas or convert part of the hydrogen into methane, etc.) are studied but currently neglected in practice (except possibly in some sensitivity analyses).

- Gas consumption processes (bacterial activity, pyrite oxidation, etc.) are generally neglected (except possibly in some sensitivity analyses).

Regarding gas transport mechanisms, for all participating end-users:

- The main mechanisms of transport of hydrogen at repository scale (including the host rock) are advection for the part expressed in gaseous form and diffusion for dissolved gases.

- The main mathematical formulation used for advection is the Darcy formulation generalised to the water-gas two-phase flow. The relative permeability and retention curves are generally represented by van Genuchten / Mualem type relationships, but sensitivity analyses with other relationships are common.

- The main mathematical formulation used for diffusion is that of Fick generalised to water-gas two-phase transport. The impact of porosity and water saturation on diffusion coefficient is generally represented by Millington-Quirk type formulations (Millington and Quirk 1961b) (see Equation 2-47).

- Gas exchanges between the liquid and gas phase are generally represented by a Henry-type formulation (linear relationship between dissolved concentration and gas partial pressure).

- Studies are in progress in order to increase support for the use of these representations and refine these where needed, in particular in connection with phenomena associated with hydro-mechanical couplings (gas capillary thresholds, pathway dilation, degradation of concrete over time due to corrosion of the rebars, etc.) or hydro-chemical coupling (alkaline plume, effect of bacteria, etc.). The WP GAS of EURAD is expected to contribute to these efforts by extending the scientific bases about possible transport modes and couplings in clayey materials and gathering additional data in conditions that are relevant for the repository configurations being considered.

4.1.7.3 Analysis of long-term gas-related repository transient

For countries that already have, if not a site, at least data on the two-phase behaviour of the target geological layer and that have carried out numerical evaluations of the long-term transient evolution of a repository under the action of gases, the overall evolution of the GDF with time includes similar structuring elements:

EURAD (Deliverable n° 6.1) – Initial State of the Art on Gas Transport in Clayey Materials
Dissemination level: PU
Date of issue of this report: 17/11/2021

Page 308

- At the time of closure, the gases are rapidly dissolved in the waters of the host rock and diffusion occurs.

- After a certain period of time, which varies according to the repository concept and the properties of the host rock, dissolution and diffusion may no longer be sufficient to evacuate all the gases produced and a gas phase may appear in part or all of the repository.

- This gas phase generally remains confined to the repository's system of disposal cells and galleries while the host clay layer remains almost saturated with water due to at least one of the following elements: very high gas entry pressure, high capillarity gradient once gas desaturates the media, very low permeability. Desaturation of the host rock, if it is considered to happen, would be restricted to the immediate vicinity of the galleries (metre scale) and saturation would not decrease by more than a few percent in that zone.

- The gas migrates towards the repository access structures (transport galleries, ramps, shafts) mainly by convection but continues to dissolve along the way.

- Along the way, gas flow is slowed down by the repository closure system, mainly by the seals.

- While migrating, the gas is not expected to displace large quantities of water along the galleries mainly (i) because a limited desaturation of the EBS/EDZ is sufficient to obtain high enough transmissivities and (ii) because water is not displaced along the galleries but simply pushed into the surrounding clay (actual analysis, may evolve due to forthcoming WP GAS findings).

- In some evaluations, a significant portion of the gas generated in the repository may reach the geological layer above the host rock under gaseous form through the shafts and/or ramps.

- The duration of transient phenomena linked to gas generation in the repository is of the order of several tens to several hundred thousands of years.

- It cannot generally be excluded that gas pressure may have an impact on the transfer of gases by hydro-mechanical coupling resulting initially in an expansion of the connected pores ('dilatant pathway') and then possibly in fracturing of the host rock (in particular if this pressure exceeds the minor mechanical stress at the site). These effects are investigated in terms of gas transfer, but as the host rock has self-sealing properties due to its high clay content, if a fracture occurs it will close as soon as the gas pressure decreases and the effects on dissolved element transfers are weak. All these effects are generally investigated by sensitivity analyses and are expected to benefit from both the experimental and modelling results of the WP GAS programme.

- The assessments include analyses of the sensitivity to the main parameters recognised as having a strong influence on long-term two-phase flow at repository scale, with respect to gas pressures as the latter determine whether hydro-mechanical couplings, and possibly damage, will play an important role in the functioning of the system. These analyses are ongoing and are expected to benefit from both the experimental and modelling results of the WP GAS programme.

4.1.7.4 Accounting for gases in safety assessments

On the one hand, safety assessments in most national programmes do not currently consider directly the effects of gases on radionuclide transport – at least on soluble radionuclide transport – and thus their potential radiological impact. Indeed, it is assumed that the transport rate of solutes, among which soluble radionuclides, is higher if the 'repository/host rock' system remains saturated with water. It is thus deemed conservative to estimate the transport of radionuclides in water-saturated conditions.

EURAD (Deliverable n° 6.1) – Initial State of the Art on Gas Transport in Clayey Materials
Dissemination level: PU
Date of issue of this report: 17/11/2021

Page 309

Some waste management organisations have put forward numerical evaluations in support of this hypothesis, based on the following hypotheses:

- lower net diffusive fluxes of solutes in partially desaturated media,
- no significant water displacement along the galleries due to gas pressure.

On the other hand, it is recognised that inactive gas produced in large quantities in a repository (essentially H_2) and transported through it could act as a carrier for radionuclides that would also be present in gaseous form. This can be taken into account via a numerical evaluation based on the two-phase phenomenological conceptualisation currently used as a reference (Darcy and Fick generalised for transfers and Henry for phase changes). Alternatively, gaseous radionuclides might be represented as dissolved in the pore water but with specific hypotheses concerning their transport (increased migration parameters values and privileged passage via the interfaces between materials, instantaneous transport from the galleries up to the accesses, etc.).

As far as gas fracturing is concerned, if this mechanism is taken into account, it is generally under the form of an altered evolution scenario or even under the form of a low probability or 'What-If' type scenario. This kind of scenario generally assumes that the system is fully saturated but incorporates the presence of a drain (local or more extensive) connecting the repository galleries to the nearest aquifer above and/or below the host rock.

EURAD (Deliverable n° 6.1) – Initial State of the Art on Gas Transport in Clayey Materials
Dissemination level: PU
Date of issue of this report: **17/11/2021**

Page 310

4.2   Models for total system performance evaluation

This last section is a short overview of the main elements of modelling strategies of gas-related issues as developed for the needs of safety/performance assessments (SA/PA) analyses by ONDRAF/NIRAS, COVRA, Nagra, Andra and IRSN.

4.2.1   ONDRAF/NIRAS's approach to modelling and numerical simulation of gas transport through the repository

ONDRAF/NIRAS has not performed a full modelling of gas transport at the scale of a repository at this stage of the Belgian programme. Instead, the focus has been on a set of scoping calculations to evaluate the capacity of different components of the system to evacuate gas through different possible transport modes. To understand the rationale for the approach chosen by ONDRAF/NIRAS, calculations are briefly presented hereafter. It is important to recall two key features of the Belgian programme, namely the focus on poorly indurated clays (Boom Clay as well as Ypresian clays) as potential host rocks and the choice of a cement-based engineered barrier system (EBS).

Boom Clay and the Ypresian clays share common properties with other clay host rocks considered in Europe, such as very low permeabilities or high sorption capacities for many radionuclides. However, the clays considered in Belgium are also characterised by much higher water content (about 20-30 wt%, close to 40% in volume). While all clay host rocks exhibit some self-sealing capacity, the sealing processes are particularly fast in Boom Clay and probably also in Ypresian clays. From observations and measurements around the HADES URL, it can be seen that closure of open fractures created during gallery excavation occurs in a matter of days or weeks at most and restoration of permeabilities close to those observed in the undisturbed state occurs in a matter of years after gallery construction. Also, as water is available in large quantity, combined with permeability about one order higher than that of, for instance, Callovo-Oxfordian claystone or Opalinus Clay, water saturation of the host rock will be maintained during the construction, operation and closure phases. For the same reasons, the subsequent saturation of the EBS will be relatively quick (a few decades), and will occur before significant quantities of gas can accumulate in the disposal galleries. Hence, the initial gas transport mode will be diffusion of dissolved gas through a (nearly) fully water-saturated system. Also, because the value of the gas entry pressure in the poorly indurated clay is comparable to that of the in situ stress at repository depth, it can be assumed that if dissolution and diffusion are not sufficient to evacuate all produced gas, additional transport would only occur through the creation of discrete or diffuse gas pathways. This would include the re-activation of existing discontinuities (see e.g. Section 4.1.2, Figure 4-14), without significant displacement of pore water from the porous matrix. This is coherent with observations from past in situ gas experiments such as MEGAS (Volckaert et al. 1995). Hence, a Darcian two-phase flow model of gas transport in the near field clay considered as a continuum would not a priori represent the actual gas transport processes. Nevertheless, such a modelling approach based on Darcian two-phase flow models (possibly enhanced with stress- or damage-dependent hydraulic properties) is not entirely dismissed at this stage, but this approach would however require further characterisation of gas transport in a sealed and saturated EDZ.

The EBS design, presented in Section 4.1.2, heavily relies on the use of cementitious materials. It is the result of a multi-criteria analysis of various design options (Bel et al. 2006) in which much emphasis has been given to (1) the containment during the thermal phase, (2) simplicity of underground operations with disposal package that provide adequate shielding and (3) the general feasibility of constructing a repository in poorly indurated clays with relatively weak mechanical characteristics. While gas aspects were not absent from this multi-criteria analysis, these were not seen at the time as key factors for the derivation of functional requirements. In particular, there have been no provisions for actively organising gas transport through the disposal system, even though the material properties of

EURAD (Deliverable n° 6.1) – Initial State of the Art on Gas Transport in Clayey Materials
Dissemination level: PU
Date of issue of this report: 17/11/2021

Page 311

some components such as the backfill and the seal could be later optimised to that effect. Nevertheless, because of the highly alkaline environment provided by the use of cementitious materials, the design ensures that the corrosion rates of the metallic components of the EBS and of the waste will be very low. Therefore, the gas source term is expected to be limited as long as favourable chemical conditions by the cementitious environment (i.e. high pH environment) will prevail.

The maximum gas removal rate that can be obtained from gas dissolution and diffusion as a dissolved species through the host clay layer has been calculated, as a first assessment. This is performed through a straightforward Fickian transport model in a plane perpendicular to a disposal gallery, with simple boundary conditions to account for symmetries and dilution in the geosphere layers above or below the host rock (Figure 4-50a). As an estimate of the maximum removal rate, the solubility of gas (here: hydrogen) in water at repository depth is used as boundary condition, where the host rock contacts the EBS. The concentration of dissolved gas in the host rock at this interface increases with time. Consequently, the concentration gradient between the clay and the EBS and thus also the removal rate decrease in time. The evolution of the removal rate is then compared to the expected gas production rate from different waste families and corresponding EBS configurations (Figure 4-50b). This allows to determine for which of these families a discrete, pressurised gas phase can be expected to develop and, conversely, those families for which dissolution and diffusion would be sufficient to evacuate all the gas produced in the disposal galleries (ONDRAF/NIRAS 2013b).
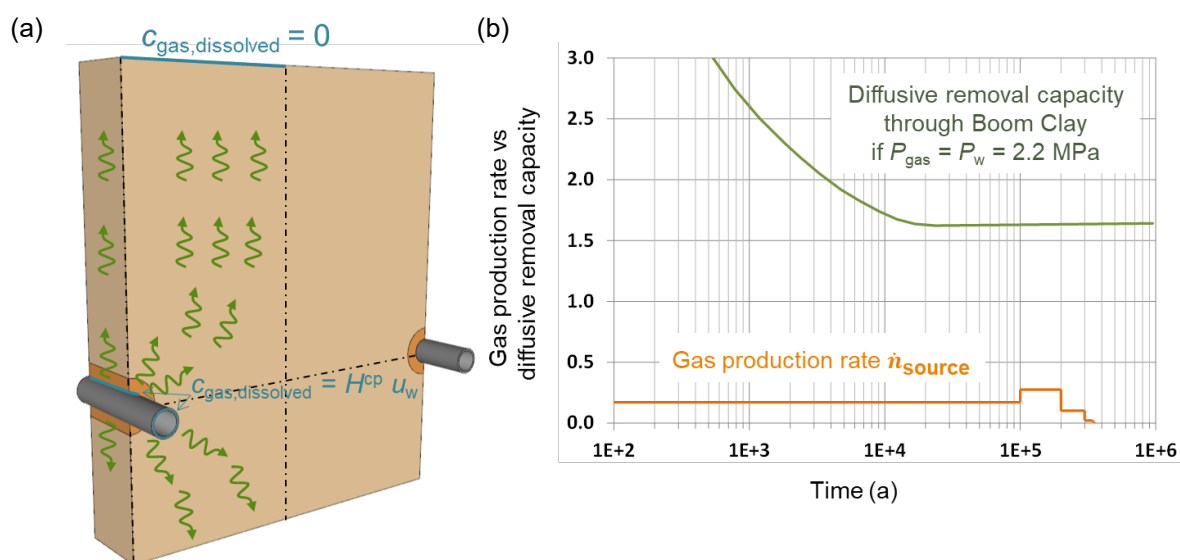

Figure 4-50 – (a) geometry and boundary conditions for a 2D model; (b) maximum possible gas removal rate per metre of disposal gallery by dissolution and diffusion (in green, only diffusion of dissolved gas through the clay domain is calculated and in orange gas source term for a gallery filled with vitrified HLW, over the length of one supercontainer.

To determine gas pressures in the repository, the gas transport capacity of different EBS components and of the clay close to the EBS must be determined. For EBS components such as the seals or the backfill, this can be done through simple steady-state relationships between the gas pressure gradient and flow rate assuming that the discrete gas phase is continuous through the given component (Figure 4-51 and Equation 4-4.

$$\dot{n} = \frac{P_g}{RT} \frac{k_g}{\mu} \frac{\Omega}{\Delta x} \Delta P_g \qquad\qquad (4\text{-}4)$$

EURAD (Deliverable n° 6.1) – Initial State of the Art on Gas Transport in Clayey Materials
Dissemination level: PU
Date of issue of this report: 17/11/2021

Page 312

where $\dot{n}$ is the mass flux [mol/s], P_g is the gas pressure [Pa], ΔP_g is the pressure difference across (the segment of) the component through which gas flows, k_g is the gas permeability [m²], μ is the gas viscosity [Pa·s] and Ω is the cross-section area [m²] and Δx is the length of the component.
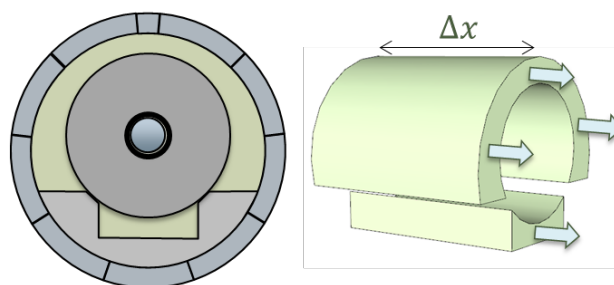

Figure 4-51 – Steady-state Darcian transport model for gas to determine the mass flux through a given repository component (here, a segment of high porosity backfill) as a function of the gas pressure difference across this component, assuming a continuous discrete gas phase.

More detailed component representations can also be evaluated through Darcian multiphase flow calculations (to the extent that these can adequately represent the behaviour of gas through the component) performed, for instance, with computer codes such as TOUGH2 or COMSOL.

Once the relationships between the gas flow rate through each important repository component and its boundary (pressure) conditions have been determined, the global behaviour of the system can be estimated through a network approach in which the links are the components and the pressures are computed at the nodes at which these components connect to each other.

This approach is thought to be sufficient to rapidly evaluate an envelope of maximum pressures that can be reached in different parts of a repository under different assumptions. While it can be used as a basis for a consequence analysis (e.g. can such pressures damage repository components and jeopardise their safety functions?), it is expected that it will need to be upgraded in later safety cases. In particular, knowledge gained through the WP GAS of EURAD on the phenomenology of gas transport through poorly indurated clay will be incorporated, possibly leading to more realistic or at least more defensible representations of the transport through the EDZ in poorly indurated clays, which would in turn require the use of more sophisticated models and tools. As the EBS design will be refined, it is also likely that gas transport aspects will translate into specific functional and material requirements.

4.2.2   COVRA's approach of modelling gas-related issues

The Dutch approach is to investigate first what types of waste and configuration of engineered materials within a specific configuration of the disposal facility would result into a separate gas phase in the clay formation in the post-closure phase. Only poorly indurated clay formations such as Boom and Ypresian clay are considered in the Dutch programme. The characteristic feature of disposal facilities hosted in these clays is that the porosity and hydrogen diffusion values of engineered materials in these facilities are smaller than that of the clay host rock. The generation of a separate gas phase in the clay host rock is an unwanted process in the post-closure phase since the predictability of dilatant gas flow in poorly indurated clays is too uncertain.

The configuration of engineered materials in the disposal facility can be adjusted in order to prevent the formation of a separate gaseous phase in the clay host rock but the associated costs and operational safety for this prevention need to be defined. The best-estimate values for corrosion of metals and associated hydrogen formation as a function of the interfacing environment with these metals with the

EURAD (Deliverable n° 6.1) – Initial State of the Art on Gas Transport in Clayey Materials
Dissemination level: PU
Date of issue of this report: **17/11/2021**

Page 313

current state of knowledge is not yet so well developed in order to define the certainty of a gas problem. The Dutch programme for geological disposal is in a preliminary phase and the certainty whether there is a gas problem is increasing by performing simple stationary and transient gas transport calculations for each type of waste and configuration of engineered materials. These calculations include the porosity and diffusion values of engineered materials and clay host rock and are performed with a software programme COMSOL Multiphysics. Interfaces or other type of features, which can act as fast gas pathways are not yet included but is also possible with this software. Inclusion of these interfaces can draw a different point of view of whether there is a gas problem in the post-closure evolution of Dutch waste in a disposal facility hosted in a poorly indurated clay formation.

Delft University of Technology works as COVRA's Linked Third Party in the WP GAS. They will numerically investigate (using the finite element code Lagamine) the effects of natural heterogeneities and induced discontinuities (including the ability to self-seal) on the gas transport mechanisms. From these detailed numerical investigations, which are aimed to provide understanding of experimental results, an upscaled numerical approach will be defined to model a generic repository configuration with different sets of properties, conditions and scenarios. The intentions of the work are (i) to improve the understanding of the processes that take place after the gas solubility is exceeded in poorly indurated clay host rocks and (ii) to develop sufficiently predictive approaches that can be upscaled and used to assess repository performances.

4.2.3 Nagra's policy to treat the gas issue in the Swiss radioactive waste management framework

Background

The Swiss radioactive waste management programme foresees two deep geological repositories: a high-level waste repository (HLW repository) for spent fuel (SF), vitrified high-level waste (HLW) and long-lived intermediate-level waste (ILW); and a repository for low- and intermediate-level waste (L/ILW repository).

As explained in Section 4.1.4, different gas production and potential removal processes[37] will take place within the repository. If the resulting gas generation rate exceeds the rate of migration due to processes such as advection and diffusion of dissolved gas molecules in the pores of the engineered barriers or the host rock, the solubility limit of the gas will eventually be exceeded. This will lead to the formation of a free gas phase. Gases could continue to accumulate until the pressure becomes sufficient to be released through the engineered barriers and the host rock in gaseous form. Possible detrimental effects are (i) the impact on mechanical integrity of the engineered / geological barriers due to excessive gas overpressures, (ii) the expulsion of contaminated pore water and (iii) the release of volatile radionuclides.

The effects of post-disposal gas generation in, and gas release from, deep geological repositories in Opalinus Clay have been assessed in a recent synthesis report (Diomidis et al. 2016). The report describes and evaluates the evolution of safety-relevant processes related to gas that can influence the long-term behaviour and safety of L/ILW and HLW repositories constructed in Opalinus Clay. It provides a survey of the key elements for mitigating the gas issue in the Swiss repository programme, including

---

[37] e.g. the consumption of gas by chemical reactions or by microbial activities which are studied in MIND EC project (http://www.mind15.eu/)

EURAD (Deliverable n° 6.1) – Initial State of the Art on Gas Transport in Clayey Materials
Dissemination level: PU
Date of issue of this report: 17/11/2021

Page 314

an in-depth evaluation of gas sources and gas generation/consumption mechanisms, gas-related layout optimisation, and gas transport issues.

Gas sources and gas generation

A balanced assessment of long-term repository performance with respect to gas accumulation and gas pressure build-up calls for precise estimation of the gas source terms and the associated uncertainties. For this, comprehensive reviews of the waste inventories of both, the L/ILW and the HLW repository were undertaken. The aims related to the generation of repository gases were (i) to provide precise quantitative estimates of gas generation rates and cumulative gas volume during the post-closure phase, (ii) to review the conservatisms associated with the involved degradation and corrosion mechanisms as well as possible gas consumption processes and (iii) to show the impact of model and parameter uncertainties, and of programme and design options regarding currently available processes that are capable of reducing the amount and rate of generated gas.

Gas-related optimisation of repository structures

A dedicated backfill and sealing concept called the 'engineered gas transport system' (EGTS) is foreseen in the Swiss L/ILW layout to enable the controlled release of gases along the access structures (Nagra 2008). The EGTS consists of the following elements: (i) the L/ILW caverns are backfilled with high porosity mortar, which provides a high gas storage capacity and at the same time sufficient compressive strength to ensure mechanical integrity of the caverns, (ii) gas permeable cavern seals with sand/bentonite mixtures at a mass fraction of 80/20 and (iii) high porosity backfill of clay-based material in all branch and access tunnels of the repository structures in host rock. Only the shaft seals and the main repository seal will be built with highly compacted pure bentonite.

Gas transport modelling

The safety-related assessment of repository performance with respect to gas requires the modelling of (non-) isothermal two-phase flow through the repository structures and surrounding host rock. The numerical code family TOUGH (Pruess et al. 1999; Jung et al. 2018) is Nagra's preferred modelling tool, providing several equation-of-state modules for the simulation of multiphase / multi-component transport.

Performance assessment modelling is conducted on the scale of the individual repository components (seal sections, HLW near field, L/ILW near field, EDZ) but also on the scale of the entire repository. Emphasis of performance assessment on the component level is the detailed understanding of gas transport and transport of volatile radionuclides through the engineered barrier systems. Hydro-mechanical and hydro-chemical couplings are addressed in a simplified manner using functional relationships (e.g. 'pressure dependent permeability') or look-up table approaches. Total system performance assessments on the scale of the entire repository are aimed mainly at evaluating the mechanical integrity of the host rock in response to gas pressure build-up and on the assessment of water fluxes and transport of volatile radionuclides along the backfilled underground structures.

Nagra's expectations regarding Task 4.2

The Task 4.2 definition of the WP GAS involves the simulations of gas transport on the scale of the entire repository and the component scale. Nagra's interest in Task 4.2 concerns benchmarking of the applied codes and models as well as calculation verifications. In this context code verification is seen as the examination of the robustness and reliability of the applied software and to the correctness of the implemented numerical algorithms. Calculation verification aims at the numerical accuracy of the

EURAD (Deliverable n° 6.1) – Initial State of the Art on Gas Transport in Clayey Materials
Dissemination level: PU
Date of issue of this report: 17/11/2021

Page 315

presented results in the light of grid convergence and time convergence. Model validation is dedicated to assessment of the models with regard to the 'intended use', including a 'cost-benefit' evaluation by comparison of CPU-times and the quality of modelling results. A further area of interest is the comparison of the gas-related performance of the different repository concepts.

4.2.4 Andra's approach to modelling of gas transport through the repository

The gas issue has been addressed at Andra since the early 2000s and a first semi-quantitative assessment of the two-phase behaviour of the repository is presented in Cigéo's 2005 Feasibility Report (Andra 2005b). Since then, this issue has become one of Andra's major concerns and is one of the branches of Andra's numerical simulation programme.

As with other important phenomenology, Andra's general policy in terms of numerical simulation is based on an approach that is both phenomenological and deterministic. From a general point of view, for each physical indicator deemed relevant and which cannot be directly estimated by measurements, a numerical simulation programme is set up and the overall approach is based:

- On mathematical models that best represent current knowledge within the possibilities offered by the numerical codes available and the limits of computing platforms. Thus, certain couplings cannot be explicitly taken into account in numerical simulations and certain geometric representations must be simplified in order to keep calculation time within reasonable limits. The impact of these simplifications is systematically evaluated by sensitivity analyses.

- On a deterministic simulation programme including at least a reference simulation and deterministic sensitivities in order to evaluate an operation range of the indicator. In order to estimate this domain, it is necessary to acquire data on the range of variability for each of the parameters taken into account in the mathematical models represented in the calculation codes used. The reference simulation generally corresponds to the simulation in which all the parameters are at their 'best-estimate' value, which is generally close to the mean or median of the available measurements. The boundaries of the domain are generally estimated by assuming that one or more of the parameters are at a limit of the range of variability estimated on the available measurements. In some cases, if Andra considers that the domain of the indicator should be determined more precisely or that the dominant parameters should be prioritised, additional probabilistic type analyses may be carried out.

For the gas issue, several indicators have been defined as relevant:

- For a solute, evaluate the difference, in terms of transfer time and concentration at the shafts/ramps, between a transfer under the hypothesis of a saturated hydraulic field at equilibrium (conceptualisation used up to now in long-term safety evaluations) and a transfer taking explicitly into account the hydraulic-gas transient;

- For a gas produced by the waste, evaluate (in terms of transfer time and concentration) the transfer from the disposal areas to the shafts/ramps taking explicitly into account the hydraulic-gas transient;

- Evaluate the maximum gas pressures that can be reached in the repository during the hydraulic-gas transient.

As solute and gas transfers are carried out on the scale of the repository as a whole as well as on the scale of the host layer, the numerical model used covers the entire repository plain area, i.e. several tens of km^2, and represents all the excavations of the underground facility, i.e. more than one hundred kilometres of galleries and disposal cells (Figure 4-52).
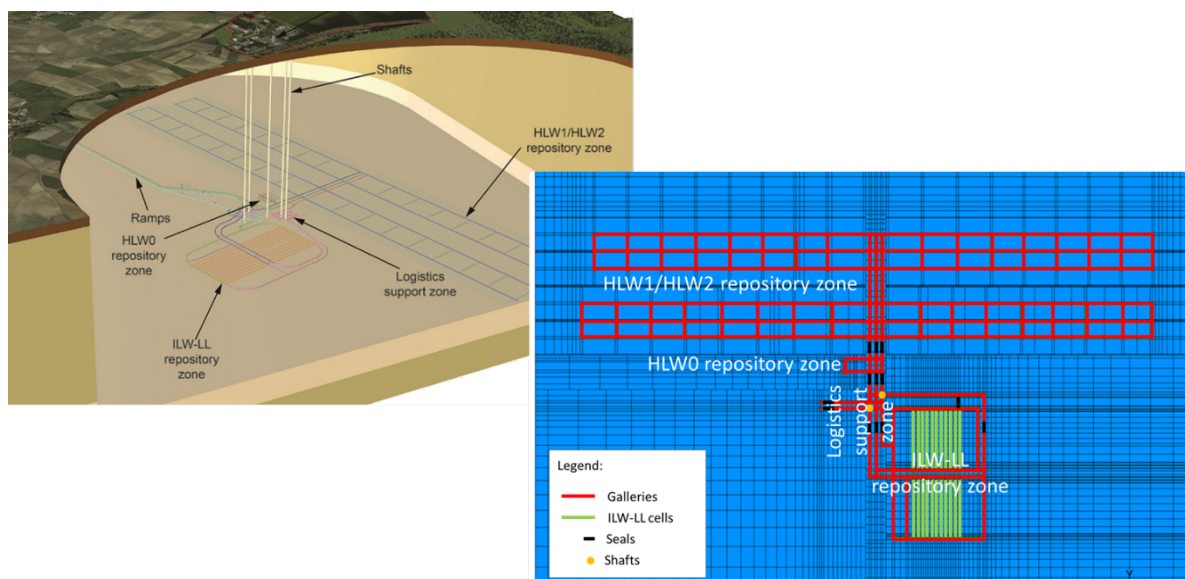
EURAD (Deliverable n° 6.1) – Initial State of the Art on Gas Transport in Clayey Materials
Dissemination level: PU
Date of issue of this report: 17/11/2021

Page 316

Figure 4-52 – Schematic representation of the mesh used to simulate two-phase flow transient at Cigéo scale.

As far as the phenomenology of gas and solute transfers is concerned, the main models used are:

- diffusion according to Fick's Law generalised with a variable diffusion coefficient depending on saturation,

- two-phase flow according to generalised Darcy's Law,

- mass phases exchange according to Henry's law.

Couplings between phenomenologies (Figure 4-53) are managed:

- Directly regarding the couplings between thermal and hydraulic. These couplings are only significant a few hundred years after closure at most.

- Directly concerning the coupling between hydrogen production by anoxic corrosion and the generation of a gaseous phase in the repository. In the current simulations some couplings are not taken into account (in particular water consumption during gas production) because preliminary simulations have shown that they could be neglected (they represent less than 10% of the water flows during the hydraulic-gas transient).

- Indirectly regarding the couplings between hydraulics and mechanics or hydraulics and chemistry through sensitivity analyses of the parameters that may be affected by these couplings.

Studies are under way to assess whether it is necessary to integrate more direct couplings and/or greater representativeness of spatial and temporal discretisation. In this framework, the results of the work carried out within the WP GAS will be closely studied with the aim of optimising the representation of hydro-mechanical-gas couplings.

EURAD (Deliverable n° 6.1) – Initial State of the Art on Gas Transport in Clayey Materials
Dissemination level: PU
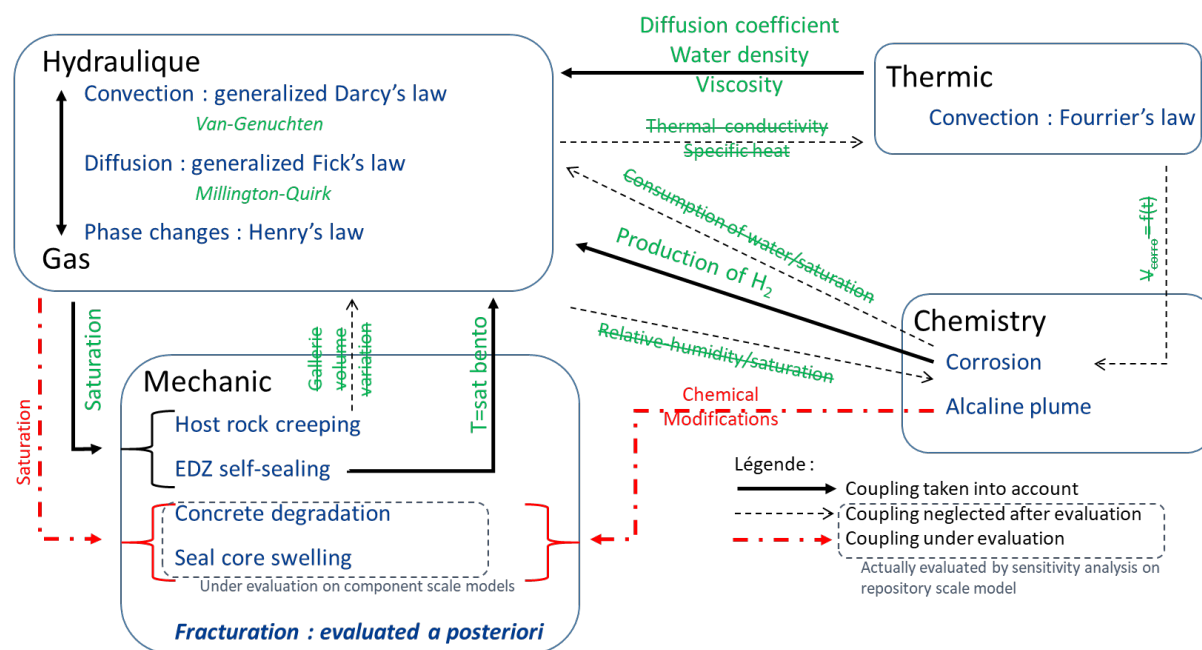Date of issue of this report: 17/11/2021

Page 317

Figure 4-53 – Schematic representation of the type of coupling used in two-phase flow simulations and types of coupling that are still under investigation.

4.2.5 IRSN's modelling strategy on gas-related issues at the scale of repository components

In the past, IRSN participated to several EC projects like PAMINA and FORGE within which was developed a new simulation tool taking into account classical incompressible-compressible two-phase flow with mass exchange in non-deformable porous media. However, in order to avoid problems related to switching models from saturated to unsaturated zones, this code was based on unique primary variables (gas pressure and molar fraction of dissolved gas). It was applied to 2D calculations on a HLW cell scale benchmark proposed within FORGE (Dymitrowska et al. 2015). Using this tool, it was very easy to introduce some sensitivity analysis related to non-zero entry pressure for gas into the host rock (an argillite) and the dissolution equation taking into account the difference of pressure between phases (due to capillarity). Both have shown to be important with respect to the maximal gas pressure and the extent of desaturated zone in the host-hock.

On the major interests of IRSN is related to the so-called piston effect in the transport of radionuclides. In this mechanism, the gas phase displaces the contaminated water, along backfilled but still relatively permeable drifts, towards the main shafts. The precise quantification of such a displacement is still a challenging task because it involves simulations at the scale of a GDF and only few studies were dedicated to this subject. In the IRSN work (Saâdi et al. 2020) an attempt has been made to verify, through a simplified GDF model based on TOUGH2/EOS5 for water and hydrogen if the usual parametrisations could give rise to a substantial and continuous water movement during the first 100 000 years after the closure of a GDF, when a significant H_2-flux reaches its main drift. The assessment of the piston effect importance, related to the H_2 production and release, is evaluated in terms of cumulative liquid phase travel distance (CLTD) within the main drift and its persistence in time. Scenarios simulated by our model show that, in the investigated conditions, piston effect is not negligible (i.e. CLTD-values are greater than 100 m) and that water would be displaced towards the main shafts. However, this work is focused on the mechanisms involved, and the results obtained cannot therefore be generalised to any disposal concept.

EURAD (Deliverable n° 6.1) – Initial State of the Art on Gas Transport in Clayey Materials
Dissemination level: PU
Date of issue of this report: 17/11/2021

Page 318

The purpose of IRSN recently is to develop models of hydrogen transfer at large scale (disposal or module with hundreds of waste cells) based on the code TOUGH2-MP with focus on module EOS5 in particular, which is designed to perform parallel simulation on multi-CPU computational platforms. TOUGH2-MP uses Domain decomposition methods (DDM) as a 'divide and conquer' strategy for solving large or time-consuming problems. Therefore, the METIS software package for the grid domain partitioning with a possible choice between three algorithms (K-way, VK-way, recursive partitioning) is used. TOUGH2-MP uses the finite volume method for space discretisation and a fully implicit scheme for time discretisation. This space-time discretisation results in a set of coupled non-linear algebraic equations that are solved by Newton-Raphson iteration method in each subdomain of the subdivision. Through simultaneous local solutions on subdomains, a global solution is formed. The resulting linearised equations are solved by a parallel linear solver from the AZTEC package. However, the classical version of this code cannot handle the problem of the discontinuity of the derivatives of Van Genuchten model functions near the gas entry pressure value. Therefore, the numerical approach adopted in TOUGH2-MP has been modified by changing the primary variable 'gas saturation' to 'capillary pressure' for solving the compositional two-phase flow problem.

The modified version of TOUGH2-MP will be verified numerically through non-regression tests and exact analytical solutions of Richards' equation (special case of two-phase flow equations). Moreover, the stability of this new numerical solution will be studied for the simulation of water infiltration and drainage, water or gas injection in different porous materials during long time periods. First results (Saâdi et al. 2020) of the simulation of the advance of water front position in a clay soil column showed the importance of the effect of air entry pressure during water infiltration at the surface or capillary rise from the bottom of the column. In fact, uncertainty on the waterfront position in the column reaches 65% when zero gas entry pressure is considered in the case of the infiltration (Figure 4-54). Future work will be dedicated to the validation of this new version of TOUGH2-MP on PGZ-experiment by adding an adequate hysteresis model in the compositional two-phase flow and transport equations.

IRSN is participating in the generic repository exercise in the WP GAS Task 4.2 and the main expectations with respect to its general outcomes are related to the possibility to compare the different approaches with respect to their capability of reproducing the same trends in main indicators of interest for the safety assessment of a deep underground radioactive waste repository.
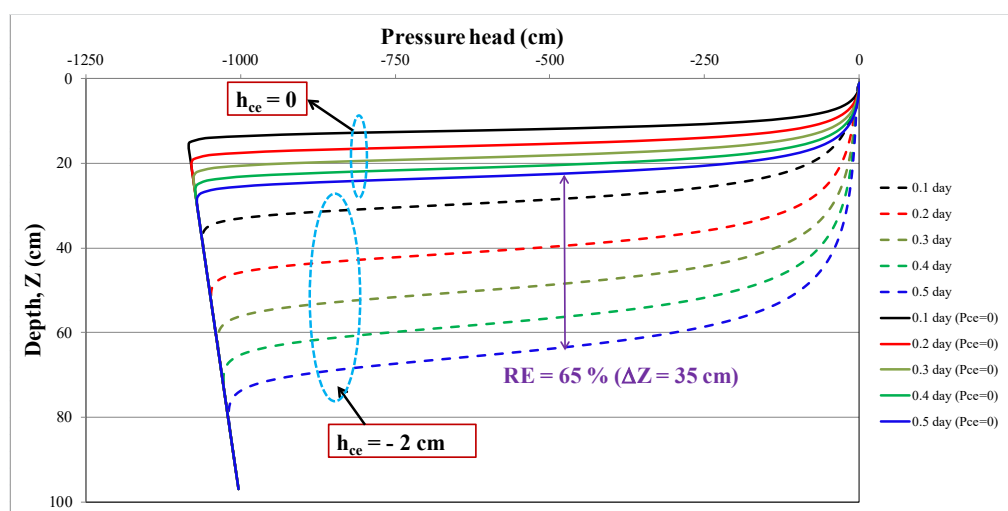

Figure 4-54 – Advance of water front inside a clay column of 1 metre height submitted to zero pressure head at the soil surface (infiltration), simulated with a zero and non-zero gas entry pressure with a modified version of iTOUGH2.

EURAD (Deliverable n° 6.1) – Initial State of the Art on Gas Transport in Clayey Materials
Dissemination level: PU
Date of issue of this report: 17/11/2021

Page 319

5. The way ahead: rationale and programme of the WP GAS of EURAD

This state-of-the-art report summarises the current knowledge on the transport of gas through clayey materials and how this knowledge is currently being used in the context of the development of geological disposal systems in several European countries. Experimental data and insights from modelling are provided for three clayey host formations: the Boom Clay, the Callovo-Oxfordian claystone and the Opalinus Clay, and for three bentonites: the granular Wyoming sodium bentonite (MX-80), the FEBEX bentonite and the Czech bentonite BCV.

Starting from an overview of the main gas transport mechanisms which are expected to take place in a disposal system in the post-closure phase (Chapter 2), the present document dealt with the description of mechanistic understanding of the hydro-mechanical phenomena and processes associated with gas-induced failure of clay barriers, and the effectiveness of self-sealing processes along gas-induced pathways in the clay barriers of a geological repository (Chapter 3). The existing knowledge base was then used for phenomenological evaluation of gas transport and its likely consequences on barrier integrity and radionuclides transport at repository scale (Chapter 4). At each stage of the description of gas transport mechanisms, particular attention was paid to emphasising the interests and needs of the end-users in the context of geological disposal, as well as to highlighting the common understanding of these mechanisms and listing the knowledge gaps as these stood at the beginning of the WP GAS of EURAD. The compilation of all the research on the transport of gas in clayey materials detailed in this SOTA reveals a great diversity of experimental results in terms of observed phenomena and processes. The comparison of results (and experiments) is not trivial and different interpretations are sometimes possible to explain the observations of the same experiment. The lack of reproducibility and/or replication further compounds the experimental uncertainties. Next to their consolidation, the output of laboratory tests need to be transposed to the conditions, in particular the stress fields, prevailing in a deep geological repository. With respect to modelling of gas transfer in saturated clay materials, continuum and discrete approaches exist. For both, the transition from the laboratory to the in situ scale is still a challenging task. It is the ambition of the WP GAS to address these issues. This SOTA is thus a baseline for the research activities carried out within the WP GAS of EURAD and a yardstick to measure its progress.

5.1 What is the WP GAS?

The Work Package 6 of the EURAD European Joint Programme 'Mechanistic understanding of gas transport in clayey materials' (WP GAS) aims to increase the understanding and predictability of gas transport in different host formations and clayey engineered barriers of geological disposal systems. It also aims to support the stepwise integration of the knowledge on gas transport and of its effects in conceptualisations of the functioning of a disposal system, in support to the safety case.

This WP will provide new data and develop new process-level models to improve mechanistic understanding of transport processes in natural and engineered clayey materials, including couplings with mechanical behaviour and impact on the material properties. Experimental work will determine, for each identified gas transport regime, the conditions under which that regime is possible, in clay materials representative of host formation and clayey EBS components. Data will be obtained that are pertinent from low (diffusion) to high (advection) gas transport rates.

EURAD (Deliverable n° 6.1) – Initial State of the Art on Gas Transport in Clayey Materials
Dissemination level: PU
Date of issue of this report: 17/11/2021

Page 321

This WP will also illustrate how knowledge gained from laboratory and in situ experiments can be integrated in the conceptualisation of gas transport through different components of a disposal system and how gas could affect (or not) the performance of the system. This will involve (i) the development of phenomenological descriptions of gas transport and of its likely consequences at the relevant scale and (ii) the testing of different approaches to represent the effects of gas at repository scale and bounding its consequences in terms of repository performance.

At the end of the project, a second state-of-the-art report will be written to present an integrated view of the new insights acquired in the framework of the WP GAS, of the relevant findings from other WPs and of the knowledge on gas transport in clay that could emerge between 2019 and 2024 outside EURAD, but also to clearly identify and formulate, with all participants to this WP (REs, WMOs and TSOs), the uncertainties of all types with sufficient context and full transparency in order to make it as practical as possible for the end-users to later assess which of those uncertainties are the most relevant within their national programme and to devise the best ways to handle these (Deliverable 6.2).

5.2   Why a RD&D WP on gas transport issues within EURAD?

In Theme 4 of the EURAD Roadmap (Geoscience to understand rock properties, radionuclide transport and long-term geological evolution), increasing the understanding of gas migration has been identified by the mandated actors of EURAD (WMOs, REs, TSOs) as a high priority topic. Gas generation and transport is a key issue as it is possible that gas could be generated at a faster rate than it can be removed through clay host formations (and clayey EBS components – Theme 3 of the EURAD Roadmap) without creating discrete, gas-specific pathways through these low-permeability components. Consequently, a raison d'être of this WP is to answer two key end-users' questions:

- How can gas be transported throughout the disposal system and which water soluble and volatile radionuclides could be associated with it?

- How and to what extend could the hydro-mechanical perturbations induced by gas affect barrier integrity and performance?

This WP will build mainly on the outcomes of the FORGE EC project. Experiments in FORGE revealed complex mechanisms and emphasised the importance of the mechanical control exerted by the porous material on gas transport. Another raison d'être of this WP is to provide results that are applicable to a wide range of national programmes. This is possible because the results of previous efforts on the identification and characterisation of the possible gas transport processes suggest that the mechanisms at play in different clays are generally similar, while the conditions (gas pressure, stresses/deformations, saturations, …) for the transition from one transport regime (diffusion, two-phase flow, pathway dilation and fracturing) to another strongly depend on the specific properties of a given clayey material.

It was suggested that the complexity of gas transport and related processes can be addressed as long as one can bound the effects of these processes using simple and robust descriptions for evaluation purposes (e.g. two-phase flow models for gas transient representation at repository scale, identified as a medium priority under Theme 4). A necessary condition for this is that the scientific bases are integrated properly, in a traceable way throughout the system conceptualisation process. Hence, the structure of this WP follows this process, imposing interactions at each step to ensure close cooperation between experimentalists, process modellers and those involved in evaluation of system performance. This should allow the development of robust evaluation approaches that support the expert judgment formulated at the end of FORGE: gas is not an issue challenging the feasibility and long-term performance of geological disposal but more a challenge of managing uncertainties.

EURAD (Deliverable n° 6.1) – Initial State of the Art on Gas Transport in Clayey Materials
Dissemination level: PU
Date of issue of this report: 17/11/2021

Page 322

5.3 WP GAS work programme

To reach the objectives of the WP GAS, the work programme of the WP is defined through three scientific tasks: Task 2 dealing with the 'Transport mechanisms', Task 3 dealing with the 'Barrier integrity' and Task 4 dealing with 'Repository performance aspects'.

5.3.1 Task 2: transport mechanisms

5.3.1.1 Task 2 objectives

Task 2 'Transport mechanisms' focusses on the main gas transport mechanisms which will take place in a disposal system in the post-closure phase. Different mechanisms are generally expected to be of importance in a geological repository:

- Gas produced within the system can dissolve in the pore water and can then be transported by diffusion. The diffusion of dissolved gas may be retarded by physisorption on the solid phase. Improving the mechanistic understanding of diffusive transport of dissolved gas and retention mechanisms will be the general objective of Subtask 2.1 'Gas diffusion and retardation processes at high level of water saturation'.

- If the gas production rate exceeds the rate at which gas can be dissolved and evacuated by diffusion, a free gas phase will develop. Gas pressure gradients will give rise to the flow of the two immiscible fluids, gas and water. Two primary modes for gas transport as a separate phase are proposed: (i) visco-capillary flow and (ii) the formation and propagation of discrete gas-filled pathways. Exploring which transport mechanisms prevail under which range of conditions and understanding how the coupling between pressure in the liquid and gas phase and the stresses in the solid phase control gas transport will be a general objective of Subtask 2.2 'Multiphase flow (displacement vs. dilation)'.

5.3.1.2 Specific objectives of Subtask 2.1 'Gas diffusion and retardation processes at high level of water saturation'

In order to compare the rates of gas generation and gas evacuation by dissolution and diffusion, knowledge of the diffusion parameters of dissolved gas through the used materials is essential. Up to now, diffusion parameters are available essentially in water-saturated systems. As partial desaturation might occur at some point during the repository evolution, this WP will extend the available experimental data for gas diffusion to partially desaturated conditions. In line with the general objective to improve mechanistic understanding, interpretation of the experimental results will be supported by pore network modelling. The experimental and modelling work programme aims in particular to investigate how petrophysical parameters (e.g. mineralogy and density) and the stress state influence the diffusion parameters.

While diffusing through the pore water, dissolved gas might also interact with the barrier materials. Up to now, interactions (mainly gas sorption) have only been studied under dry conditions. In particular, hydrogen uptake due to sorption processes has only been studied under dry condition. One objective of this subtask is to determine if gas sorption could be a relevant retardation mechanism for diffusive transport under repository conditions, in clays that are partially or fully saturated with pore water. Again, the impacts of the pore network morphologies and the nature of the mineral assemblages on the gas sorption mechanisms will be investigated.

EURAD (Deliverable n° 6.1) – Initial State of the Art on Gas Transport in Clayey Materials
Dissemination level: PU
Date of issue of this report: 17/11/2021

Page 323

Key objectives of Subtask 2.1 are thus:

1. to determine gas diffusion parameters on different clayey materials at different degrees of water saturation and support experimental data interpretation by pore network modelling, and
2. to understand gas physisorption mechanisms in microporous systems.

The gas of interest in this task is chiefly H_2, but other apolar gases such as CH_4 (by-product of bacterial activity), He, Ar (naturally occurring noble gases) and Ne (H_2 proxy) will be also investigated in order to i) avoid artefacts related to bacterial activity triggered by H_2, ii) overcome safety problems especially in underground laboratories, and iii) probe the effect of polarisability and kinetic diameter on apolar gases mobility in porous networks.

5.3.1.3 Specific objectives of Subtask 2.2 'Multiphase flow (displacement vs. dilation)'

From previous work (including work done in the FORGE EC project), two primary modes for advective gas transport through natural mudrocks are proposed; (i) visco-capillary flow, where capillary forces must be overridden in order to allow displacement of the wetting phase, by migrating gas and (ii) the formation of discrete gas-filled pathways. The potential for one specific mechanism to prevail is dependent on a range of factors, including the saturation state of the clay and the ratio of the clay to sand fraction. Natural heterogeneity within clay-hosted repositories may also play an important role in the transport of gas and the mitigation of peak gas pressure. For fully saturated pure bentonite materials, such as those used in engineered barriers, experimental evidence indicates that gas flow by pathway dilation is the preferred mode of transport. In such cases, significant hydro-mechanical coupling is observed, which cannot be satisfactorily explained by visco-capillary flow processes. This hydro-mechanical coupling between the immiscible phase, the interstitial fluid, and the total stress, remains unclear. Understanding these relationships, how they vary from one formation to another, and what impact, if any, they have on the integrity of the host formation, is now a priority research issue.

Through new experimental studies, this subtask aims to:

1. Provide reference data for various natural and engineered clayey materials under a sufficiently broad range of conditions, which will make it possible to investigate in a more systematic way how petrophysical parameters, like mineralogy or density, and conditions such as the stress state influence transport of a free gas phase.
2. Improve understanding of the observed gas transport modes and identifying their main controls, through interpretation of the experimental results by models in which the representation of crack propagation and pathway dilatancy is implemented at process level.
3. Conceptualisations of the transport mechanisms limited to the macro-scale (continuum representation + discrete conducting features) such as those developed, for instance, in the FORGE EC project will be compared to conceptualisations in which the micro-scale is also represented to better improve understanding of how micro-level heterogeneities and deformations affect macro properties.

The experimental and modelling programmes of Subtask 2.2 aim at characterising and understanding gas transport in clayey materials close to saturation. For bentonite, it will benefit from the results of the BEACON EC project that characterises the hydro-mechanical coupling of swelling clay materials during resaturation phase. For bentonite barriers, BEACON EC project, this WP GAS and the WP HITEC are complementary as these together support the global description of hydro-mechanical processes from the installation of materials to their evolution over the long term (including the thermal phase in the case of heat emitting waste) and the consequences of gas flow. The integration of knowledge will be facilitated by involvement in this subtask of the WP GAS of some BEACON and WP HITEC partners.

EURAD (Deliverable n° 6.1) – Initial State of the Art on Gas Transport in Clayey Materials
Dissemination level: PU
Date of issue of this report: **17/11/2021**

Page 324

5.3.2   Task 3: barrier integrity

5.3.2.1 Task objectives

Accumulation of gas in the backfilled structures of a deep geological repository associated with the build-up of excessive gas pressures may impair the long-term safety functions of the repository's multi-barrier system, namely the radionuclide retention and attenuation capacity of the engineered barrier system (EBS) and the geological barriers. Clay-rich rocks and clay-based EBS are particularly prone to failure due to their low mechanical strength. On the other hand, it is well known that clays exhibit the favourable feature to self-seal after sustaining mechanical failure. Task 3 is aimed at gaining a mechanistic understanding of the hydro-mechanical phenomena and processes, associated with:

- the gas-induced failure of clay barriers, i.e. within the engineered barrier system (EBS), within the excavation damaged zone (EDZ) and within the host formation (Subtask 3.1);

- the effectiveness of self-sealing processes along gas-induced pathways in the clay barriers of a geological repository (Subtask 3.2).

The evaluation of achievements is accomplished by model-supported data analyses, predictive modelling, and the application of the newly developed modelling tool on in situ experiments (Subtask 3.3).

As mentioned in Task 2, after the FORGE EC project, the hydro-mechanical coupling between the gas phase, the interstitial fluid, and the total stress, are still a priority research issue. For bentonite barriers, the task will benefit from the BEACON EC project that characterises the hydro-mechanical coupling of swelling clay materials during the resaturation phase. This transfer of knowledge will be facilitated by involvement in this task of some BEACON partners.

5.3.2.2 Specific objectives of Subtask 3.1 'Gas-induced impacts on barrier integrity'

Laboratory experiments will be designed and executed, aimed at investigating the evolution of damage in clayey materials when subjected to excessive water / gas pressures. Different test set-ups and different test procedures will be required for the investigation of argillaceous formation and EBS material, respectively.

Clay host formation material (Boom Clay, Callovo-Oxfordian claystone, Opalinus Clay)

Fracture initiation and fracture propagation processes in the intact host formation and fracture re-activation in the excavation damaged zone (EDZ) as well as the re-activation of tectonic features depend on the rock fabric and on the prevailing in situ conditions (pore pressure and stress). Fracture opening and fracture sliding mechanisms will be investigated along typical stress paths, which are representative for real repository conditions:

- Hydro-mechanical laboratory experiments will be performed on clay host formation samples. The test set-ups ensure the precise control of water/gas flow, pore pressure / total suction, stress state and strains during all test stages (isostatic/triaxial cells). The impact of texture and tectonic overprint on gas-induced damage evolution will be addressed by testing the samples parallel, perpendicular and/or at oblique angles to the principal orientations of micro-fabric, respectively.

- Further phenomenological experiments will be conducted by using a direct-shear-rig for water/gas injection experiments. Shear fractures will be created within the apparatus while tensile fractures will be created externally. Quantitative textural information of all fracture

EURAD (Deliverable n° 6.1) – Initial State of the Art on Gas Transport in Clayey Materials
Dissemination level: PU
Date of issue of this report: 17/11/2021

Page 325

surfaces will be determined prior, and after, detailed gas testing. The evolution of damage and self-sealing processes in the sample during gas injection and after shut-in will be followed by using a high-resolution X-ray CT scanner and/or by microstructural analyses.

Clayey buffer materials (including compacted granular bentonite, bentonite blocks, sand/bentonite mixtures)

Long-term water/gas injection tests in oedometric/isostatic cells will be conducted to investigate pathway dilation and particle mobilisation. The laboratory experiments shall reveal the impact of the as-compacted state (e.g. dry density, grain size distribution, initial water content) and the hydration process (e.g. imbibition process, water chemistry) on the gas breakthrough pressure of the hydrated material and on the fraction of mobilised bentonite.

Microstructural analyses of the investigated geomaterials (damaged or intact host formations and EBS materials, respectively) before and after gas injection will be conducted to get insight in the prevailing failure mechanisms. This includes the evaluation of apertures, extensions and surface roughness of the induced fractures and statistical descriptions of the pore networks of the intact and of the damaged material.

5.3.2.3 Specific objectives of Subtask 3.2 'Pathway closure and sealing processes'

From a mechanistic point of view, the self-sealing capacity of clay-bearing materials is associated with various (thermo-)hydro-mechanical and chemical processes and controlled by the prevailing state conditions. Mechanical closure of fractures (e.g. crack closure, fracture sliding), hydro-chemical interactions of the pore water with the clay-bearing solid phase of the geomaterial (e.g. swelling, disaggregation) and colloidal transport processes (e.g. sedimentation, clogging) have been identified as typical self-sealing mechanisms in clay-rich materials. In this context, it is important to consider also phenomena and processes that could prevent fracture closure, such as mineral transformations and hydro-mechanical reorganisations of the fabric caused by gas seepage through the clayey barriers over long time periods of several 10 000 years.

- The self-sealing capacity of the clayey materials will be investigated with the same test configurations as used for the gas injection experiments. After termination of the gas injection experiments, the test specimen will be subjected to different pressure recovery conditions including resaturation with different water compositions and different total stress scenarios. Subsequently, final water permeability testing will be conducted to qualify the loss of hydraulic barrier function of the test specimen. Different host formations and different fracture modes will be addressed. Visualisation techniques such as micro-CT or SEM will allow revealing the microstructural changes of the investigated test samples at the end of the self-sealing stage.

- The phenomenological gas injection experiments will also be extended beyond the shut-in phase to visualise at pore scale the complex HM-C interactions, which are associated with the self-sealing process.

The self-sealing studies of this subtask are closely connected to the ones planned in the Subtask 2.1 of the WP HITEC ('Clay host rock' task – 'Experiment near field with EDZ' subtask). The aim of these tasks in these two WPs will be to characterise (T)HM(-C)(+gas) processes associated to self-sealing mechanisms in clayey materials. Hence, tests will be performed jointly during the duration of the WP under various thermal and chemical conditions to provide a complete characterisation of self-sealing processes in clayey materials. To facilitate a broad information exchange between the two WPs on these aspects, joint workshops will be organised each year with the WP HITEC.

EURAD (Deliverable n° 6.1) – Initial State of the Art on Gas Transport in Clayey Materials
Dissemination level: PU
Date of issue of this report: 17/11/2021

Page 326

5.3.2.4 Specific objectives of Subtask 3.3 'Model-based interpretation and synthesis of results'

Subtask 3.3 is dedicated to the interpretation of the experimental results and the synthesis of the scientific achievements (development of process models for pathway dilation and self-sealing). The modelling teams will contribute to the experimental design of the laboratory experiments and the model-based interpretation of the acquired experimental results. Back-analysis of the experiments will feed in the development of conceptual process models of gas-induced damage evolution and self-sealing processes for damaged or intact host formations and EBS materials, respectively. Validation of these models will take place in a series of prediction-evaluation exercises, covering different loading paths in different geometric configurations (host formations: isostatic / triaxial; EBS material: oedometric / isostatic). Eventually, the validated process models will be applied for the back-analysis of selected in situ experiments in URLs.

5.3.3 Task 4: repository performance aspects

5.3.3.1 Task objectives

This task aims at fulfilling the second high-level objective of the WP, which is to evaluate the gas transport regimes that can be active at the scale of a geological disposal system and their potential impact on repository performance. It is dedicated in particular to end-users' questions concerning:

- the effects of the presence of gas and its transport on the transfer of soluble and volatile radionuclides,

- the consequences of gas-induced hydro-mechanical perturbations on barrier integrity and long-term performance.

From past evaluations, it is known that gas generated by corrosion and/or radiolysis in large quantities may result in the development of a gas phase within the existing porosity of the EBS, within the EDZ and, to some extent, within the host formation. Experimental evidence suggests that discrete, transient, gas-specific pathways may also form through (or between) EBS materials, the EDZ and the host formation in the form of subcritical (pathway dilation) or supercritical (fracturing) cracks. The transient nature of such phenomena is to be emphasised. Desaturation can have a significant effect on soluble radionuclide migration: it may limit the extent of diffusion of soluble radionuclides but may also result in advective transport of radionuclides, if groundwater is displaced one way or another by gas as a consequence of pressurisation or suction. High levels of desaturation may even affect the gas source term by decreasing the availability of water for gas production processes. Continuous gas pathways, possibly evolving and unstable, may form from the deposition zones to the repository access. These would affect the migration of volatile radionuclides. Finally, high gas pressures may possibly result in mechanical damage to the engineered and natural barriers, including the host formation, and could affect the global functioning of the repository. It is important to assess if this could occur in practice and if such damage would be transient only or would have a lasting effect and how this would affect (or not) the outcome of a safety case.

Task 4 will build and improve from the FORGE EC project in several ways, by:

- including in the analysis hydro-mechanical couplings,

- including in the analysis the transfer of soluble and volatile radionuclides,

- promoting the use of multiple assessment approaches, supported by different numerical modelling tools,

- being driven from an end-user perspective of gas-induced effects.

EURAD (Deliverable n° 6.1) – Initial State of the Art on Gas Transport in Clayey Materials
Dissemination level: PU
Date of issue of this report: 17/11/2021

Page 327

This task will also benefit from recent advances in phenomenological understanding from the CAST (CArbon-14 source term and fate) and BEACON (bentonite mechanical evolution) EC projects allowing respectively (i) a better understanding of potential release mechanisms of carbon-14 (in the form of methane for instance) from radioactive waste materials under conditions relevant to geological disposal facilities and (ii) a better characterisation of hydro-mechanical coupling in swelling clayey materials (from the installation of materials to their evolution over the long term).

Task 4 will be mainly end-users oriented. Based on the input from Tasks 2 and 3 of this WP and relevant input from other WPs of EURAD, the objective of Subtask 4.1 will be to assemble phenomenological descriptions of gas transport and its likely consequences on barrier integrity and radionuclide transfer at repository relevant scale, in the form of storyboards. The resulting conceptualisations of gas transport and of its possible consequences for typical repository configurations in clayey host formations will be passed on to Subtask 4.2, which will be dedicated to the assessment of different approaches and tools (e.g. numerical modelling) that can be used for evaluating the effect of gas on repository performance.

5.3.3.2 Specific objectives of Subtask 4.1 'Conceptualisation of gas migration at repository scale'

Subtask 4.1 will be system oriented and will be carried out by end-users (i.e. WMO and TSO). REs will be involved through reviews of this work in Tasks 2 and 3 to ensure that good use is made of available scientific knowledge.

Current conceptualisations of gas migration through clayey host formation geological disposal systems and tools used for describing gas transport and its consequences at repository scale (e.g. numerical modelling) will be compiled and compared by the end-user partners involved to highlight in particular:

- the gas transport processes and related processes considered as relevant at repository scale by each organisation, shedding light on the similarities and differences between national programmes;

- the key properties and conditions assumed to control these processes;

- the expected effects of gas on host formation, groundwater, radionuclide transfer and barrier integrity;

- the different modelling approaches that can be used to evaluate gas transport and related aspects (e.g. fully coupled at repository scale, lumping/homogenisation, compartment modelling, …), how these are related to the storyboards and the rationale for using one or another approach.

The storyboards/conceptualisations describing gas transport through typical repositories and its impact on system components will be phenomenologically-based. Special attention will be given to explain how the conceptualisations have been derived from the available scientific bases (references to experimental data, prioritisation of processes for instance). First conceptualisations will be produced early on in the course of the WP and will be reviewed by the participants to Tasks 2 and 3 to (i) check that repository-scale concepts are consistent with the scientific bases and, (ii) to inform the experimentalists / process-level modellers about the configurations and ranges of conditions that are relevant for repositories. An interaction will be organised at this stage with the WP ACED, which also develops storyboards (of the chemical evolution of a disposal cell) to exchange information and ensure consistency.

This first conceptualisation phase will be completed by the definition of (i) a generic repository configuration and sets of properties and conditions on which Subtask 4.2 will test various evaluation approaches and (ii) a proposal for a set of indicators, covering the range of needs of various end-users

EURAD (Deliverable n° 6.1) – Initial State of the Art on Gas Transport in Clayey Materials
Dissemination level: PU
Date of issue of this report: 17/11/2021

Page 328

in Europe for clay-based host formation repository, representative of the processes to be evaluated (transport of radionuclides, volatile and soluble, barrier integrity for instance). An interaction will also be organised at this stage with WP DONUT to identify possible benchmark studies for the WP DONUT and to exchange on numerical challenges and abstraction methodologies.

In a second phase, the focus will shift to the integration and understanding of the significance of the findings of Task 2 'Transport Mechanisms' and Task 3 'Barrier integrity' during the course of the WP. The phenomenological description improvements will be evaluated for transfer to the repository scale via updates to the storyboards. Uncertainties about which gas transport modes will effectively be active or about other gas-related aspects of the evolution of the system will be identified and evaluated in terms of possible scenarios to be investigated. Additional indicators may be proposed. These conceptualisation updates and alternative scenarios will be passed on to Subtask 4.2 as input for the assessment of gas-induced effects.

This integration task will imply strong interactions between the Task 4 and other tasks of the WP to ease the transfer of concepts from laboratory experiments and process-level models to the relevant configurations and scales. Interactions will also be organised again with other WPs in order to take into account or provide input that can be relevant and/or appropriate (e.g. with the modelling WP DONUT and the chemical evolution assessment WP ACED). Along the course of this subtask, interactions will also be organised with the UMAN Strategic Study on understanding of uncertainty, risk and safety on the basis of the contribution of this subtask to the SOTAs. These interactions will focus on the identification, characterisation, potential significance and treatment of uncertainties in the abstraction process for gas transport (e.g. propagation of parameter uncertainties, scenario uncertainties…) and the evaluation of their consequences.

5.3.3.3 Specific objectives of Subtask 4.2 'Model assisted assessment of gas-induced effects'

Building on the storyboards, the definition of a generic repository and sets of properties and conditions, indicators and scenarios proposed in Subtask 4.1, different approaches will be assessed to numerically describe disposal system behaviour in response to gas accumulation and pressure build-up. This assessment will compare:

- the use of coupled high-resolution models taking into account the full complexity at repository scale of gas-related process understanding towards total system performance;

- the application of traceable, component-based model upscaling techniques, i.e. establishing detailed models of components, accounting for the complexity of the mechanistic understanding embodied in the process-level models, then simplifying the representation of the components in the total system performance models.

To assess the relevancy of these different levels of complexity, several modelling teams will apply various numerical approaches to a generic repository configuration with different sets of properties and conditions and with the scenarios defined in Subtask 4.1.

The main objective of Subtask 4.2 is not to perform a formal performance assessment or a code benchmarking exercise, but to highlight the inherent strengths and limitations of each approach and assessing its suitability in different contexts depending on which system is being evaluated (host formation/concept) or what is the quality of available data/what is the magnitude of uncertainties. The analysis of the results of numerical evaluations will focus on gas-oriented indicators, developed in cooperation with Subtask 4.1, related to volatile and soluble radionuclides transfer and barrier integrity, which are of direct relevance to performance assessment.

EURAD (Deliverable n° 6.1) – Initial State of the Art on Gas Transport in Clayey Materials
Dissemination level: PU
Date of issue of this report: 17/11/2021

Page 329

Interactions will be organised with other WPs and especially with the modelling WP DONUT to address the challenges of building and operating large (or multi-)scale coupled process models of a full disposal system and with the networking Strategic Study UMAN on understanding of uncertainty, risk and safety for aspects related to the treatment of uncertainties (e.g. propagation of parameter uncertainty) in the abstraction process.

5.4 Expected impacts of the WP GAS

5.4.1 Regarding implementation needs for radioactive waste management

This WP GAS is expected to provide input to implementers that may inspire design measures that further reduce the gas impact on the disposal system, or the uncertainties associated with gas flow through geological disposal systems.

5.4.2 Regarding safety

The WP GAS will allow testing various approaches for the treatment of gas in the safety case, identifying the inherent strengths and limitations of each approach and assessing its suitability in different contexts, as this may depend on the disposal system that is being evaluated (host formation/concept) or even the advancement of the (national) programme. Similarities of approaches between national programmes will be identified and the rationale behind possible differences explained.

It will also permit to address the key questions that are common to all end-users, as per the second WP objective and confirm the insight from FORGE that gas is not a showstopper for the safety case but a question of managing uncertainties.

5.4.3 Regarding increasing scientific and technical knowledge (beyond state of the art) in the field of radioactive waste management

Interactions between the participants of the WP GAS will bridge the gap between experimentalists and modellers. Building on the lessons learned from FORGE, no separate (sub)task is assigned to 'modelling' issues. Modellers are embedded with the experimentalists in subtasks of Tasks 2 and 3 to encourage dialogue in the design of experiments and the development of shared conceptualisations of the observed behaviour.

The WP GAS will enhance confidence in and extend the scientific basis on the fundamental principles of gas transport in clayey materials. Previous works suggest that the fundamental gas transport mechanisms that can develop in different clays are similar. Because a wide enough, but realistic, range of conditions will be explored for representative clayey materials, this WP will provide data which will be of relevance for all disposal concepts that include clayey barriers. Testing over a range of conditions spanning low (diffusion) to high (advection) gas generation rates, we will obtain a better understanding of processes, which then has broader end-user appeal.

Through the strong interactions between the three main scientific tasks of this WP, the transfer of knowledge between the scientific community (REs) and the end-users (WMOs and TSOs) will be fostered. Guidance by end-users will ensure that the experimental and model development work programme in Tasks 2 and 3 remains focused on materials and conditions that are relevant. Scientists (REs) will be asked to review the work performed in Task 4 to ensure that the evaluation of gas transport, its consequences and the treatment of residual uncertainties are consistent with the body of scientific knowledge.

EURAD (Deliverable n° 6.1) – Initial State of the Art on Gas Transport in Clayey Materials
Dissemination level: PU
Date of issue of this report: 17/11/2021

Page 330

Appendix – Numerical codes

Code_Aster: is an open source software (www.code_aster.org) developed mainly by the mechanical analysis department (ERMES, ElectRo – MEchanics Studies) of EDF's research and development. Code_Aster is a solver, based on the theory of the mechanics of the continuous media, which uses the method of the finite elements to solve different types of mechanical, thermal, acoustic, seismic, etc. problems. It is general software for simulation in mechanics and calculation of structures. Besides the standard functions of simulation software in thermo-mechanics, Code_Aster has many laws of behaviour, finite elements, and types of loadings. Its modelling, algorithms and solvers are constantly under construction to improve and complete them (1 200 000 lines of code, 200 operators). The Aster quality criteria, which are governing the development and distribution of the code, are based on a regularly audited quality frame of reference meeting the requirements set by the EDF Nuclear Structures Safety Authority. These criteria constitute the Aster Software Quality Plan and are defined in the code Administration Manual. Moreover, the theoretical foundations of Aster models are documented in the Reference Manuals. A porous media modulus dedicated to thermo-hydro-mechanical modelling (https://www.code-aster.org/V2/doc/default/en/man_r/r7/r7.01.11.pdf) has been developed over 25 years including formulation in total/effective stresses, constitutive laws in kit form, etc. Several constitutive laws for concrete, soils and rocks are available. Beyond their diversity, they all share the property of representing the deterioration of materials under shear according to confinement and accompanied by perceptible volume variations. The formulation framework will vary depending on whether it is a case of a concrete, silt, sand, clay or rock. A specific law has been developed for clay rock and is frequently used to model Callovo-Oxfordian rock (Raude et al. 2016; Cuvilliez et al. 2017). Code_Aster meets the variety of hydraulic phenomena in porous media with simple models for drying and hydrating concrete, or more complex ones based on coupled integration of two non-linear flow laws and the integration of the energy conservation law (fully coupled THM model). With Code_Aster, EDF has developed significant experience in geological nuclear waste disposal simulation: in HADES URL, Äspö HRL, Mont Terri URL and MHM URL. Some investigations have recently been made concerning links between two-phase flow transfer terms and mechanical properties (Mahjoub et al. 2018). In recent years, in the framework of two PhD thesis, the formalism of HM couplings in Code_Aster has been integrated in the eXtended finite element method (X-FEM) modules of Code_Aster. So far, the so-called HM_XFEM model is able to consider crack propagation in a fully saturated medium (Faivre et al. 2016). The model can deal with crack propagation on non-predefined pathways, multiple cracks interactions and crack junctions (Paul et al. 2018). Current developments concern the extension of the model to the partially saturated case.

CODE_BRIGHT: The program described here is a tool designed to handle coupled problems in geological media. The computer code, originally, was developed on the basis of a new general theory for saline media. Then the program has been generalised for modelling thermo-hydro-mechanical (THM) processes in a coupled way in geological media. Basically, the code couples mechanical, hydraulic and thermal problems in geological media. The theoretical approach consists in a set of governing equations, a set of constitutive laws and a special computational approach. The code is written in FORTRAN and it is composed by several subroutines. The program does not use external libraries. CODE_BRIGHT uses GiD system for pre-processing and post-processing. GiD is developed by the International Centre for Numerical Methods in Engineering (CIMNE). GiD is an interactive graphical user interface that is used for the definition, preparation and visualisation of all the data related to numerical simulations. This data includes the definition of the geometry, materials, conditions, solution information and other parameters. The program can also generate the finite element mesh and write the information for a numerical simulation program in its adequate format for CODE_BRIGHT. For geometry definition, the

EURAD (Deliverable n° 6.1) – Initial State of the Art on Gas Transport in Clayey Materials
Dissemination level: PU
Date of issue of this report: 17/11/2021

Page 331

program GiD works quite like a Computer Aided Design system. The most important difference is that the geometry is developed in a hierarchical mode. This means that an entity of higher level (e.g. a volume) is constructed over entities of lower level (e.g. a surface); two adjacent entities (e.g. two volumes) will then share the same lower level entity (e.g. a surface). All materials, conditions and solution parameters can also be defined on the geometry without the user having any knowledge of the mesh. The meshing is performed once the problem has been fully defined. The advantages of doing this are that, using associative data structures, modifications can be made on the geometry and all other information will be updated automatically. Full graphic visualisation of the geometry, mesh and conditions is available for comprehensive checking of the model before the analysis run is started. More comprehensive graphic visualisation features are provided to evaluate the solution results after the analysis has been performed. This post-processing user interface is also customisable depending on the analysis type and the results provided.

Lagamine FE: The Lagamine computer code is a non-linear finite element tool initially elaborated at the University of Liège, which has been constantly evolving with time since the 1980s (Charlier 1987; Habraken 1989), supported by successive doctoral research and developments. The code has been primarily developed in two different fields namely the behaviour of metals and geomechanics. The latter more specifically explores multiple facets of the geomechanical environment, which requires Chemo-thermo-hydro-mechanical coupled models. Accordingly, the code compiles both highly coupled constitutive laws based on elasto-plastic, elasto-visco-plastic frameworks, second gradient models (Collin et al. 2006) or on a multi-scale approach on the one hand, and coupled finite elements (Gerard et al. 2008) (monolithic approach) dedicated to the modelling of multiphase or multiphysical problems (Collin et al. 2002b) on the other hand. This way, the Lagamine software constitutes an advanced numerical tool to tackle civil engineering problems involving soil-structure interactions (Gerard et al. 2008) or soils and rocks mechanics problems, with specific applications to the modelling of nuclear waste disposal (Figure 3-55), slope stability, reservoir engineering. The Lagamine solution basically involves two parts: the pre-processor that reads data's from an engineer-type data file, converts them into finite element-type data's and checks their consistency, and the non-linear solution code that performs the non-linear analysis based on some additional data's regarding the solution strategy. The current version of Lagamine runs on any computer running under Windows operating system (from Windows 95 to Windows 10) with a minimum screen resolution of 800 by 600 pixels. Routines in the Lagamine environment are written in FORTRAN. The Lagamine code has recently migrated to the collaborative management platform GitLab, resting on Visual Studio development environment and Intel Parallel Studio compiler. A detailed manual describing the laws and the elements is also available to the community of users through DokuWiki application. Lagamine is currently being used by researchers and engineering students at the University of Liège, along with other universities, and research centres close to the industry. All the past and ongoing enhancement work throughout the world has maintained the code at the cutting edge of technology and research.

OpenGeoSys (OGS) (www.opengeosys.org) is a scientific open source initiative for the numerical simulation of thermo-hydro-mechanical-chemical (THMC) processes in porous and fractured media. The basic concept of OGS consist of providing a flexible numerical framework, using primarily the finite element method (FEM) for solving multi-field coupled processes with application in different scientific and technical disciplines. The development history of OGS with its roots in ROCKFLOW and FEFLOW started in the 1980ties (a more detailed description can be found in Kolditz et al. (2012). Provided years are indicating starting points of related software developments. OGS has been successfully applied in the fields of regional, contaminant and coastal hydrology, technical and geothermal energy systems, geotechnical engineering, energy storage, CO_2 sequestration/storage and nuclear waste management and disposal. The actual version OGS-6 is providing complete workflows starting from data integration, HPC for coupled process simulation and using virtual reality (VR) concepts for data analytics. OGS-6 is developed and maintained platform-independently using professional software engineering tools such as version management (GitHub) and containerisation (e.g. Docker, Singularity). A strict code review is conducted for quality assurance completed by unit testing and comprehensive benchmarking. OGS

EURAD (Deliverable n° 6.1) – Initial State of the Art on Gas Transport in Clayey Materials
Dissemination level: PU
Date of issue of this report: 17/11/2021

Page 332

provides open interfaces for combining with other simulators (e.g. GEMS, iPhreeqc for geochemical processes) including Python bindings. A recent overview of OGS software engineering can be found in Bilke et al. (2019).

After a more general introduction of OGS above, we briefly list some recent work in THM modelling such as: Error-controlled elasto-visco-plastic constitutive models for rock salt (Zhang and Nagel 2020), multi-scale approaches for fluid inclusions in salt rock (Shao et al. 2019), brittle-ductile transitions and related processes in volcanic systems (Parisio et al. 2019a, 2019b), variational phase field methods for fracture mechanics (Yoshioka et al. 2019; Miao et al. 2019), non-local integral plastic-damage constitutive theory (Parisio et al. 2018, 2019c), pressure solution and stress corrosion processes in crystalline rocks (Lu et al. 2018), two-phase flow reactive transport processes (Huang et al. 2018), and introducing novel visualisation concepts for THM analyses (Blecha et al. 2019).

EURAD (Deliverable n° 6.1) – Initial State of the Art on Gas Transport in Clayey Materials
Dissemination level: PU
Date of issue of this report: **17/11/2021**

Page 333

References

Abdullah W. S., Alshibli K. A. and Al-Zou'bi M. S. (1999). Influence of pore water chemistry on the swelling behavior of compacted clays. Applied Clay Science 15 (5), 447–462.

Aertsens M. (2009). Re-evaluation of the experimental data of the MEGAS experiment on gas migration through Boom Clay. ER-106, SCK•CEN, Mol.

Aertsens M., Wemaere I. and Wouters L. (2004). Spatial variability of transport parameters in the Boom Clay. Applied Clay Science 26, 37–45.

Aertsens M., De Cannière P., Moors H. and Van Gompel M. (2009). Effect of ionic strength on the transport parameters of tritiated water, iodide and H14CO3- in Boom Clay. MRS Proceedings 1193, 497–504.

Åkesson M. (2012). Temperature buffer test. SKB. Technical Report TR-12-04.

Alcolea A., Kuhlmann U., Lanyon GW. and Marschall P. (2014). Hydraulic conductance of the EDZ around underground structures of a geological repository for radioactive waste - A sensitivity study for the candidate host rocks in the proposed siting regions Northern Switzerland. Nagra. Arbeitsbericht 13–94.

Alcolea A., Kuhlmann U., Marschall P., Lisjak A., Grasselli G., Mahabadi O., de La Vaissière R., Leung H. and Shao H. (2017). A pragmatic approach to abstract the excavation damaged zone around tunnels of a geological radioactive waste repository: application to the HG-A experiment in Mont Terri. Geological Society, London, Special Publications 443 (1), 127–147.

Alkan H. and Müller W. (2006). GASTON - Evaluation of modelling approaches of gas transport in clay formations (Auswertung von Modellierungsansätzen zum Gastransport in Tonformationen). Institut für Sicherheitstechnologie (ISTec) GmbH.

Alonso E. E., Gens A. and Josa A. (1990). A constitutive model for partially saturated soils. Géotechnique 40, No. 3, 405–430.

Alonso E. E., Vaunat J. and Gens A. (1999). Modelling the mechanical behaviour of expansive clays. Engineering Geology 54, No. 1–2, 173–183.

Alonso E. E., Olivella S., Arnedo D. (2006) Mechanisms of gas transport in clay barriers. Journal of Iberian Geology. 32, n°2, 175-196.

Alonso J., García-Siñeriz J. L., Bárcena I., Alonso M. C., Fernández L., García J. L., Fries T., Pettersson S., Bodén A. and Salo J. P. (2008). ESDRED. Module 4 (Temporary sealing technology). European Commission. Final Technical Report Deliverable 9 of Module 4, WP4.

Andra (2005). Dossier 2005 Argile - Phenomenological evolution of a geological repository.

Andra (2005). Dossier 2005 Argile - Synthesis - Evaluation of the feasibility of a geological repository in an argillaceous formation - Meuse/Haute-Marne site. Andra.

Andra (2009). Rapport mi-parcours pour le Groupement de Laboratoires "Transferts de Gaz." C.RP.ASCM.09.0002.

Andra (2015a). Safety options report - Operating part (DOS-Expl). Andra. Technical Note CG-TE-D-NTE-AMOA-SR1-0000-15-0060.

Andra (2015b). Safety options report - Post-closure part (DOS-AF). Andra. Technical Note CG-TE-D-NTE-AMOA-SR2-0000-15-0062.

Armand G., Conil N., Talandier J. and Seyedi D. M. (2017). Fundamental aspects of the hydromechanical behaviour of Callovo-Oxfordian claystone. From experimental studies to model calibration and validation. Computers and Geotechnics 85, 277–286.

Arnedo D., Alonso E.E., Olivella S. and Romero E. (2008). Gas injection tests on sand/bentonite mixtures in the laboratory. Experimental results and numerical modelling. Physics and Chemistry of the Earth, 33, pp.237–247.

Arnedo D., Alonso E.E. and Olivella S. (2013). Gas flow in anisotropic claystone. Modelling triaxial experiments. International Journal for Numerical and Analytical Methods in Geomechanics, 37, pp.2239–2256.

EURAD (Deliverable n° 6.1) – Initial State of the Art on Gas Transport in Clayey Materials
Dissemination level: PU
Date of issue of this report: 17/11/2021

Page 335

Atabek R., Beziat A., Coulon H., Dardaine M., Debrabant P., Eglem A., Farcy C., Fontan N., Gatabin C., Gegout P., Lajudie A., Landoas O., Lechelle J., Plas F., Proust D., Raynal J. and Revertegat E. (1991). Nearfield behaviour of clay barriers and their interaction with concrete, Task 3. Characterization of radioactive waste forms. A series of final reports. No. 26. EUR. EUR 13877.

Atkins M., Beckley N., Carson S., Cowie J., Glasser J. P., Kindness A., Macphee D., Pointer C., Rahman A, Jappy JG, Evans PA, McHugh G, Natingley NJ and Wilding C (1991). Medium-active waste form characterization: the performance of cement-based systems Task 3 Characterization of radioactive waste forms A series of final reports (1985-89) No. 1. European Commission. EUR 13542.

Auvray C. and Giot R. (2018). Characterization of hydromechanical damage of claystones using X-ray tomography. In Geomechanics and Geodynamics of Rock Masses, Volume 1. Proceedings of the 2018 European Rock Mechanics Symposium, p. 193. CRC Press.

Auvray C., Grgic D., Morlot C., Fourreau E. and Talandier J. (2015). X-ray tomography applied to self-sealing experiments on argillites. In ISRM 2015. The 13th International Congress of ISRM, Innovations in Applied and Theoretical Rock Mechanics.

Bachmat Y. and Bear J. (1986). Macroscopic modelling of transport phenomena in porous media. 1. The continuum approach. Transport in Porous Media 1, No. 3, 213–240.

Bagnoud A., Leupin O., Schwyn B. and Bernier-Latmani R. (2016). Rates of microbial hydrogen oxidation and sulfate reduction in Opalinus Clay rock. Applied Geochemistry 72, 42–50.

Baker A. J., Lever D. A., Rees J. H., Thorne M. C., Tweed C. J. and Wikramaratna R. S. (1997). Nirex 97. An assessment of the post-closure performance of a deep waste repository at Sellafield, Volume 4. The gas pathway. UK Nirex Science report S/97/012.

Baldi G., Hueckel T., Pellegrini R. (1988). Thermal volume changes of the mineral-water system in low-porosity clay soils. Canadian Geotechnical Journal, 25(4), 807-825.

Bandis S. C., Lumsden A. C. and Barton N. R. (1983). Fundamentals of rock joint deformation. International Journal of Rock Mechanics and Mining Sciences & Geomechanics Abstracts 20 (6), 249–268.

Bárcena I., García-Siñeriz J. L. and Huertas F. (2006). FEBEX Project Final Report. Addendum sensors data report. In situ experiment. Publicación Técnica ENRESA 05-5/2006.

Bardelli F., Mondelli C., Didier M., Vitillo J. G., Cavicchia D. R., Robinet J.-C., Leone L. and Charlet L. (2014). Hydrogen uptake and diffusion in Callovo-Oxfordian clay rock for nuclear waste disposal technology. Applied Geochemistry 49, 168–177.

Baryla P., Bernachy-Barbe F., Bosch J. A., Campos G., Carbonell B., Daniels K. A., Ferrari A., Guillot W., Gutiérrez-Álvarez C., Harrington J. F., Iglesias R. J., Kataja M., Mašín D., Najser J., Rinderknecht F., Schäfer T., Sun H., Tanttu J., Villar M. V. and Wieczorek K. (2019). Bentonite mechanical evolution – experimental work for the support of model development and validation. European Commission. Project BEACON Deliverable D4.1/2.

Bastiaens W., Bernier F. and Li X. L. (2007). SELFRAC: Experiments and conclusions on fracturing, self-healing and self-sealing processes in clays. Physics and Chemistry of the Earth 32, 600–615.

Baumgarten N. and Wieners C. (2020). The parallel finite element system M++ with integrated multilevel preconditioning and multilevel Monte Carlo methods. Computers and Mathematics with Applications. https://doi.org/10.1016/j.camwa.2020.03.004.

Bear J. (1972). Dynamics of fluids in porous media. American Elsevier Pub., New York

Been K. and Sills G. C. (1981). Self-weight consolidation of soft soils. an experimental and theoretical study. Geotechnique 31, 519–535.

Bel J. J. P., Wickham S. M. and Gens R. (2006). Development of the Supercontainer Design for Deep Geological Disposal of High-Level Heat Emitting Radioactive Waste in Belgium. MRS Proceedings 932.

Bennethum L.S., Murad M. A. and Cushman J. H. (1997). Modified Darcy's law, Terzaghi's effective stress principle and Fick's law for swelling clay soils. Computers and Geotechnics 20 (3–4), 245–266.

Bensenouci F., Michelot J. L., Matray J. M., Savoye S., Lavielle B., Thomas B. and Dick P. (2011). A profile of helium-4 concentration in pore-water for assessing the transport phenomena through an argillaceous formation (Tournemire, France). Physics and Chemistry of the Earth, Parts A/B/C 36 (17–18), 1521–1530.

Benson C. H., Chiang I., Chalermyanont T. and Sawangsuriya A. (2014). Estimating van Genuchten Parameters α and n for Clean Sands from Particle Size Distribution Data. In From Soil Behavior Fundamentals to Innovations in Geotechnical Engineering. Geo-Congress 2014. American Society of Civil Engineers, Atlanta, Georgia. 410–427.

Bernachy-Barbe F., Conil N., Guillot W. and Talandier J. (2020). Observed heterogeneities after hydration of MX-80 bentonite under pellet/powder form. Applied Clay Science 189, 105542.

EURAD (Deliverable n° 6.1) – Initial State of the Art on Gas Transport in Clayey Materials
Dissemination level: PU
Date of issue of this report: 17/11/2021

Page 336

European Joint Programme on Radioactive Waste Management

Bernier F., Li X. L. and Bastiaens W. (2007). Twenty-five years' geotechnical observation and testing in the Tertiary Boom Clay formation. Géotechnique 57 (2), 229–237.

Bernier F., Li X. L., Bastiaens W., Ortiz L., Van Geet M., Wouters L., Frieg B., Blümling P., Desrues J., Viaggiani G., Coll C., Chanchole S., De Greef V., Hamza R., Malinsky L., Vervoort A., Vanbrabant Y., Debecker B., Verstraelen J., Govaerts A., Wevers M., Labiouse V., Escoffier S., Mathier J.-F., Gastaldo L. and Bühler C. (2007b). Fractures and Self-Healing Within the Excavation Disturbed Zone in Clays. European Commission, Nuclear Science and Technology. Final Report EUR 22585.

Berre I., Doster F. and Keilegavlen E. (2019). Flow in Fractured Porous Media. A Review of Conceptual Models and Discretization Approaches. Transport in Porous Media 130 (1), 215–236.

BFE (2008). Sachplan geologische Tiefenlager. Konzeptteil. Swiss Federal Office of Energy SFOE, Bern, Switzerland.

BFE (2011). Sachplan geologische Tiefenlager. Ergebnisbericht zu Etappe 1. Festlegungen und Objekt¬blätter. 30th November 2011. Swiss Federal Office of Energy SFOE, Bern, Switzer¬land.

Bhatt A., Valentic T., Reimer A., Lamarche L., Reyes P. and Cosgrove R. (2020). Reproducible Software Environment. A tool enabling computational reproducibility in geospace sciences and facilitating collaboration. Journal of Space Weather and Space Climate 10.

Bigler T., Ilhy B., Lehmann B. and Waber H. (2005). Helium Production and Transport in the Low-Permeability Callovo-Oxfordian Shale at the Site Meuse/Haute Marne, France. Nagra. Nagra Arbeitsbericht NAB 05-07

Bilke L., Flemisch B., Kalbacher T., Kolditz O., Helmig R. and Nagel T. (2019). Development of Open-Source Porous Media Simulators. Principles and Experiences. Transport in Porous Media 130 (1), 337–361.

Billiotte J., Yang D. and Su K. (2008). Experimental study on gas permeability of mudstones. Physics and Chemistry of the Earth, Parts A/B/C 33, S231–S236.

Biot M. A. (1941). General theory of three-dimensional consolidation. Journal of Applied Physics 12, No. 2, 155–164.

Biot M. A. (1956). The theory of propagation of elastic waves in a fluid-saturated porous solid. I. Low-frequency range. Journal of the Acoustical Society of America 28, No. 2, 168–178.

Biot M. A. (1962). Mechanics of deformation and acoustic propagation in porous media. Journal of Applied Physics 33, No. 4, 1482–1498.

Biot M. A. and Temple G. (1972). Theory of finite deformations of porous solids. Indiana University Mathematics Journal 21 (7), 597–620.

Birkholzer J. T., Tsang C.-F., Bond A. E., Hudson J. A., Jing L. and Stephansson O. (2019). 25 years of DECOVALEX - Scientific advances and lessons learned from an international research collaboration in coupled subsurface processes. International Journal of Rock Mechanics and Mining Sciences 122.

Bishop A. W. (1959). The principle of effective stress. Tecnisk Ukeblad 39, 859–863.

Bishop A. W. and Blight G. E. (1963). Some aspects of effective stress in saturated and partially saturated soils. Géotechnique 13, No. 3, 177–197.

Bjerrum L. (1967). Progressive failure in slopes of overconsolidated plastic clay and clay shales. Journal of Soil Mechanics and Foundation Divisions, ASCE, vol. 93, No. SM5, 1-49. https://trid.trb.org/view/126870

Blecha C., Raith F., Scheuermann G., Nagel T., Kolditz O. and Maßmann J. (2019). Analysis of coupled thermo-hydro-mechanical simulations of a generic nuclear waste repository in clay rock using fiber surfaces. In IEEE Pacific Visualization Symposium. 189–201.

Bock H. (2000). RA experiment: review of rock mechanical in-situ and laboratory tests. Swiss Nat. Hydrol. Geol. Survey. Mont Terri Project - Technical Note 2000-28: 1-87.

Bock H. (2002). RA experiment – rock mechanics analyses and synthesis: conceptual model of the Opalinus Clay. Mont Terri Technical Report 2001–03.

Bock H., Dehandschutter B., Derek Martin C., Mazurek M., de Haller A., Skoczylas F. and Davy C. (2010). Self-sealing of fractures in argillaceous formations in the context of geological disposal of radioactive waste. Review and synthesis. NEA, Radioactive Waste Management. OECD/NEA Report NEA No. 6184.

Bolzon G., Schrefler B. and Zienkiewicz O. (1996). Elastoplastic soil constitutive laws generalized to partially saturated states. Géotechnique 46 (2), 279–289.

Boudreau B. (1996). The diffusive tortuosity of fine-grained unlithified sediments. Geochimica Et Cosmochimica Acta 60, 3139-3142.

Boudreau B. (1997). Diagenetic models and their implementation. Springer, Berlin.

EURAD (Deliverable n° 6.1) – Initial State of the Art on Gas Transport in Clayey Materials
Dissemination level: PU
Date of issue of this report: 17/11/2021

Page 337

Boulin P. (2008). Expérimentation et modélisation du transfert d'hydrogène à travers des argiles de centre de stockage de déchets radioactifs. PhD thesis, Institut Polytechnique de Grenoble.

Boulin P.F., Angulo-Jaramillo R., Daian J.F., Talandier J. and Berne P. (2008a). Experiments to estimate gas intrusion in Callovo-oxfordian argillites. Physics and Chemistry of the Earth, Parts A/B/C 33, S225–S230.

Boulin P.F., Angulo-Jaramillo R., Daian J.F., Talandier J. and Berne P. (2008b) Pore gas connectivity analysis in Callovo-Oxfordian argillite. Applied Clay Science. 42, 276-283.

Bowen R. M. (1980). Incompressible porous media models by use of the theory of mixtures. International Journal of Engineering Science 18, No. 9, 1129–1148.

Bowen R. M. (1982). Compressible porous media models by use of the theory of mixtures. International Journal of Engineering Science 20, No. 6, 697–735.

Bradbury M. H., Berner U., Curti E., Hummel W., Kosakowski G. and Thoenen T. (2014). The long term geochemical evolution of the nearfield of the HLW repository. Nagra. Technical Report NTB 12-01.

Bucher F. and Müller-Vonmoos M. (1989). Bentonite as a containment barrier for the disposal of highly radioactive wastes. Applied Clay Science 4 (2), 157–177.

Burland J. B. (1990). On the compressibility and shear strength of natural clays. Geotechnique 40, 329–378.

Busch A. and Amann-Hildenbrand A. (2013). Predicting capillarity of mudrocks. Marine and Petroleum Geology 45, 208–223.

Carbonell B., Villar M. V., Martín P. L. and Gutiérrez-Álvarez C. (2019). Gas transport in compacted bentonite after 18 years under barrier conditions. Geomechanics for Energy and the Environment 17, 66–74.

Carey J. W., Lei Z., Rougier E., Mori H. and Viswanathan H. (2015). Fracture-permeability behavior of shale. Journal of Unconventional Oil and Gas Resources 11, 27–43.

Caulk R., Scholtès L., Krzaczek M. and Chareyre B. (2020). A pore-scale thermo–hydro-mechanical model for particulate systems. Computer Methods in Applied Mechanics and Engineering 372, 113292.

Cerfontaine B., Dieudonné, A. C., Radu, J. P., Collin, F. and Charlier, R. (2015). 3D zero-thickness coupled interface element. Formulation and application. Computers and Geotechnics 69, 124–140.

Červinka R., Vašíček R. a kolektiv (2018), Kompletní charakterizace bentonitu BCV 2017, SÚRAO TZ 419/2019

Chan S. and Elsheikh A. H. (2020). Data-driven acceleration of multiscale methods for uncertainty quantification. application in transient multiphase flow in porous media. GEM - International Journal on Geomathematics 11 (1).

Charlier R., Collin F., Pardoen B., Talandier J., Radu J. P. and Gerard P. (2013). An unsaturated hydromechanical modelling of two in-situ experiments in Callovo-Oxfordian argillite. Engineering geology 165, 46–63.

Charlier R. (1987). Approche unifiée de quelques problèmes non linéaires de mécanique des milieux continus par la méthode des éléments finis (grandes déformations des métaux et des sols, contact unilatéral de solides, conduction thermique et écoulements en milieu poreux). PhD thesis, Université de Liège.

Chautard C. (2013). Interactions fer/argile en conditions de stockage géologique profond . Impact d'activités bactériennes et d'hétérogénéités. PhD thesis, Ecole Nationale Supérieure des Mines de Paris.

Chen G. (2018). In-situ hydraulic conductivity measurement for the Boom Clay around CG and PG. EURIDICE Report EUR-18-014

Chen G., Maes T., Vandervoort F., Sillen X., Van Marcke P., Honty M., Dierick M. and Vanderniepen P. (2014). Thermal Impact on Damaged Boom Clay and Opalinus Clay. Permeameter and Isostatic Tests with µCT Scanning. Rock Mechanics and Rock Engineering 47 (1), 87–99.

Chivot J. (2004). Thermodynamique des produits de corrosion - fonctions thermodynamiques, diagrammes de solubilité, diagrammes E-pH des systèmes Fe-H2O, Fe-CO2-H2O, Fe-S-H2O, Cr-H2O et Ni-H2O en fonction de la température. Collection Sciences & Techniques, Andra, Paris, France.

Churakov S. V. (2013). Mobility of Na and Cs on Montmorillonite Surface under Partially Saturated Conditions. Environmental Science and Technology 47, 9816-9823.

Churakov S. V., Gimmi T., Unruh T., Van Loon L. R. and Juranyi F. (2014). Resolving diffusion in clay minerals at different time scales: Combination of experimental and modeling approaches. Applied Clay Science 96, 36–44.

Clayton C.J. and Hay S.L. (1994). Gas migration mechanisms from accumulation to surface. Bull. Geol. Soc. Denmark 41, 12-23

Coleman J. D. (1962). Stress strain relations for partially saturated soil. Géotechnique 12, No. 4, 348–350.

EURAD (Deliverable n° 6.1) – Initial State of the Art on Gas Transport in Clayey Materials
Dissemination level: PU
Date of issue of this report: 17/11/2021

Page 338

Coll C. (2005). Endommagement des roches argileuses et perméabilité induite au voisinage d'ouvrages souterrains. PhD thesis, Université Joseph Fourier - Grenoble I.

Collin F. (2003). Couplages thermo-hydro-mécaniques dans les sols et les roches tendres partiellement saturés. Ph.D. thesis, Université de Liège.

Collin F., Li X.L., Radu J.-P., Charlier R. (2002a) Thermo-hydro-mechanical coupling in clay barriers. Engineering Geology. 64, 179-193.

Collin F., Cui Y. J., Schroeder C. and Charlier R. (2002b). Mechanical behaviour of Lixhe chalk partly saturated by oil and water. experiment and modelling. International Journal for Numerical and Analytical Methods in Geomechanics 26, No. 9, 897–924.

Collin F., Chambon R. and Charlier R. (2006). A finite element method for poro mechanical modelling of geotechnical problems using local second gradient models. International Journal for Numerical Methods in Engineering 65 (11), 1749–1772.

Collins D. J. and Zhou H.-C. (2007). Hydrogen storage in metal–organic frameworks. Journal of Materials Chemistry 17 (30), 3154–3160.

Conil N., Talandier J., Djizanne H., de La Vaissière R., Righini-Waz C., Auvray C., Morlot C. and Armand G. (2018). How rock samples can be representative of in situ condition. A case study of Callovo-Oxfordian claystones. Journal of Rock Mechanics and Geotechnical Engineering 10 (4), 613–623.

Coussy O. (1995). Mechanics of porous continua. Wiley-Blackwell. Dormieux, L., Barboux, P., Coussy, O. and Dangla, P. (1995). A macroscopic model of the swelling phenomenon of a saturated clay. European Journal of Mechanics. A. Solids 14, No. 6, 981–1004.

Croisé J., Mayer G., Marschall P., Matray J.M., Tanaka T. and Vogel, P. (2006). Gas threshold pressure test performed at the Mont Terri Rock Laboratory (Switzerland). Experimental data and data analysis, Oil and Gas Science and Technology 61(5), 631-645.

Cui Y. J. and Delage P. (1996). Yielding and plastic behaviour of an unsaturated compacted silt. Géotechnique 46, No. 2, 291–311.

Cui Y. J., Delage P. and Sultan N. (1995). An elasto-plastic model for compacted soils. In Proceedings of the First International Conference on Unsaturated Soils, UNSAT 1995 (Alonso, E. E. and Delage, P., Eds.), Paris, France, pp. 703–709.

Cuss R. J. and Harrington J. F. (2010). Effect of stress field and mechanical deformation on permeability and fracture self-sealing. Progress Report on the Stress Path Permeameter experiment conducted on Callovo-Oxfordian Claystone. British Geological Survey ID -CR/10/151.

Cuss R. J. and Harrington J. F. (2011). Update on Dilatancy Associated with Onset of Gas Flow in Callovo-Oxfordian Claystone. Progress report on test SPP_COx-2. British Geological Survey. CR/11/110.

Cuss R. J., Harrington J. F. and Noy D. J. (2010). Large Scale Gas Injection Test (Lasgit) Performed at the Aspo Hard Rock Laboratory. Summary Report 2008. SKB. Technical Report TR-10-38.

Cuss R. J., Milodowski A. and Harrington J.F. (2011a). Fracture transmissivity as a function of normal and shear stress. First results in Opalinus Clay. Physics and Chemistry of the Earth, 36(17 – 18), 1960 – 1971. https://doi.org/10.1016/j.pce.2011.07.080

Cuss R. J., Harrington J. F., Noy D. J., Wikman A. and Sellin P. (2011b). Large-scale gas injection test (LASGIT). results from two gas injection tests. Physics and Chemistry of the Earth, Parts A/B/C 36 (17–18), 1729–1742.

Cuss R. J., Harrington J. F. and Noy D. J. (2012). Final report of FORGE WP4. 1.1. The stress-path permeameter experiment conducted on Callovo-Oxfordian Claystone.

Cuss R. J., Harrington J., Giot R. and Auvray C. (2014). Experimental observations of mechanical dilation at the onset of gas flow in Callovo-Oxfordian claystone. Geological Society, London, Special Publications 400 (1), 507–519.

Cuss R. J., Harrington J. F., Sathar S., Norris S. and Talandier J. (2017). The role of the stress-path and importance of stress history on the flow of water along fractures and faults; an experimental study conducted on kaolinite gouge and Callovo-Oxfordian mudstone. Applied Clay Science 150, 282–292.

EURAD (Deliverable n° 6.1) – Initial State of the Art on Gas Transport in Clayey Materials
Dissemination level: PU
Date of issue of this report: 17/11/2021

Page 339

European Joint Programme
on Radioactive Waste Management

Cuvilliez S., Djouadi I. and Raude S. (2017). An elastoviscoplastic constitutive model for geomaterials. Application to hydromechanical modelling of claystone response to drift excavation. Computers and Geotechnics 85, 321–340.

Daïan J.F. (2010). Equilibre et transferts en milieux poreux, première partie. Etats d'équilibre. Archives-ouvertes.fr hal-00452876v1. 188p.

Daneshy A., Blümling P., Marschall P. and Zuidema P. (2004). Interpretation of Field Experiments and Observation of Fracturing Process. In Proceedings of SPE International Symposium and Exhibition on Formation Damage Control. SPE International Symposium and Exhibition on Formation Damage Control. Society of Petroleum Engineers.

Davies P. B. (1991). Evaluation of the role of threshold pressure in controlling flow of waste-generated gas into bedded salt at the Waste Isolation Pilot Plant. Sandia National Laboratories.

Davy C. A., Skoczylas F., Barnichon J. D. and Lebon P. (2007). Permeability of macro-cracked argillite under confinement. gas and water testing. Physics and Chemistry of the Earth, Parts A/B/C 32 (8–14), 667–680.

Davy C. A., Skoczylas F., Lebon P. and Dubois T. (2009). Gas migration properties through a bentonite/argillite interface. Applied Clay Science 42 (3–4), 639–648.

De Craen M., Wang L., Van Geet M. ajd Moors H. (2004). Geochemistry of Boom Clay pore water at the Mol site. Scientific report, SCK•CEN-BLG-990.

de La Vaissière R. (2013). Hydration versus gas percolation in bentonite. In-situ experiment PGZ2. Experimental borehole results. FORGE report Report D3.17 – D3.18, 99p.

de la Vaissière R., Conil N., Morel J., Leveau F., Gatabin C. (2014a). Design and construction of a large-scale sand-bentonite seal in the Meuse/Haute Marne underground research laboratory. NSC experiment. International conference on the performance of engineered barriers, Feb2014, Hanovre, Germany.pp.133-135 .ineris-01862255

de La Vaissière R., Gerard P., Radu J.-P., Charlier R., Collin F., Granet S., Talandier J., Piedevache M. and Helmlinger B. (2014b). Gas injection test in the Callovo-Oxfordian claystone. data analysis and numerical modelling. Geological Society, London, Special Publications 400 (1), 427–441.

de La Vaissière R., Armand G. and Talandier J. (2015). Gas and water flow in an excavation-induced fracture network around an underground drift. A case study for a radioactive waste repository in clay rock. Journal of Hydrology 521. 141-156

de La Vaissière R., Talandier J., Armand G., Vu M.-N. and Cornet F. H. (2019). From Two-Phase Flow to Gas Fracturing into Callovo-Oxfordian Claystone. In ARMA-2019-1723. 53rd U.S. Rock Mechanics/Geomechanics Symposium. American Rock Mechanics Association, ARMA. 9.

de la Vaissière R., Armand G., Vu N.-G., Talandier J. and Cornet F. H. (2020). Effect of gas flow rate on gas fracturing in Callovo-Oxfordian claystone. ISRM, ISBN 978-0-367-42284-4

de Marsily (1986). Quantitative hydrogeology for engineers. New York Academic Press.

de Rango P., Marty P. and Fruchart D. (2016). Hydrogen storage systems based on magnesium hydride: from laboratory tests to fuel cell integration. Applied Physics A 122 (2).

Dehandschutter B., Vandycke S., Sintubin M., Vandenberghe N., Gaviglio P., Sizun J.-P. and Wouters L. (2004). Microfabric of fractured Boom Clay at depth. a case study of brittle-ductile transitional clay behaviour. Applied Clay Science 26. 389-401.

Delahaye C.H. and Alonso E.E. (2002). Soil heterogeneity and preferential paths for gas migration. Engineering Geology. 64, 251-271.

Della Vecchia G., Jommi C. and Romero E. (2013). A fully coupled elastic–plastic hydromechanical model for compacted soils accounting for clay activity. International Journal for Numerical and Analytical Methods in Geomechanics 37, No. 5, 503–535.

Derjaguin B. V., Churaev N. V. and Muller V. M. (1987). Surface Forces (Translated from Russian). 1st ed. ed. J. A. Kitchener, Consultants Bureau.

Desbois G., Urai J. L. and De Craen M. (2010). In-situ and direct characterization of porosity in Boom Clay (Mol site, Belgium) by using novel combination of ion beam cross-sectioning, SEM and cryogenic methods. Motivations, first results and perspectives. SCK•CEN. External Report ER-124.

Descostes M., Blin V., Bazer-Bachi F., Meier P., Grenut B., Radwan J., Schlegel M. L., Buschaert S., Coelho D. and Tevissen E. (2008). Diffusion of anionic species in Callovo-Oxfordian argillites and Oxfordian limestones (Meuse/Haute–Marne, France). Applied Geochemistry 23 (4), 655–677.

EURAD (Deliverable n° 6.1) – Initial State of the Art on Gas Transport in Clayey Materials
Dissemination level: PU
Date of issue of this report: 17/11/2021

Page 340

Devau N., Tremosa J., Pettenati M., Parmentier M., André L., Sbai A. and Lassin A. (2012). Geochemical reactivity of non water-saturated argillites, submitted to conditions of storage of radioactive wastes in presence of high partial hydrogen pressures. Final report of the ZNS-H2 project phase II INIS-FR--20-0923.

Dewhurst D. N., Aplin A. C. and Sarda J. P. (1999). Influence of clay fraction on porescale properties and hydraulic conductivity of experimentally compacted mudstones. Journal of Geophysical Research 104, 29261–29274.

Di Donna A., Charrier P., Salager S. and Bésuelle P. (2019). Self-sealing capacity of argillite samples eds. A. Tarantino and E. Ibraim. E3S Web of Conferences 92, 03005.

Diamond S. (2000). Review - Mercury porosimetry: An inappropriate method for the measurement of pore size distributions in cement-based materials. Cement and Concrete Research 30, 1517–1525.

Didier M. (2012). Etude du transfert réactif de l'hydrogène au sein de l'argilite. PhD, Université de Grenoble 1, Institut des Sciences de la Terre.

Didier M., Leone L., Greneche J.-M., Giffaut E. and Charlet L. (2012). Adsorption of Hydrogen Gas and Redox Processes in Clays. Environmental Science & Technology 46 (6), 3574–3579.

Dieudonné A.-C. (2016). Hydromechanical behaviour of compacted bentonite: from micro-scale analysis to macro-scale modelling. PhD thesis, Université de Liège.

Dieudonné A.-C., Della Vecchia G. and Charlier R. (2017). Water retention model for compacted bentonites. Canadian Geotechnical Journal 54 (7), 915–925.

Dinca M. and Long J. R. (2006). Strong H2 binding and selective gas adsorption within the microporous coordination solid Mg3(O2C-C10H6-CO2)3. Journal of the American Chemical Society 127 (26), 9376–9377.

Ding C., Zhang Y., Teng Q., Hu D., Zhou H., Shao J. and Zhang C. (2020). A method to experimentally investigate injection-induced activation of fractures. Journal of Rock Mechanics and Geotechnical Engineering. https://doi.org/10.1016/j.jrmge.2020.04.002.

Diomidis, N., Cloet, V., Leupin, O.X., Marschall, P., Poller, A., Stein, M. (2016). Production, consumption and transport of gases in deep geological repositories according to the Swiss disposal concept. Nagra Technical Report NTB 16-01.

Dixon D. A., Gray M. N. and Thomas A. W. (1985). A study of the compaction properties of potential clay-sand buffer mixtures for use in nuclear fuel waste disposal. Engineering Geology 21 (3–4), 247–255.

Dizier D., Chen G., Li XL and Rypens J. (2017). The PRACLAY heater test after two years of the stationary phase. EURIDICE report EUR_PH_17_043.

DOE. (2020). Office of Energy Efficiency and Renewable Energy, "Fuel Cell Technologies Office," U.S. Department of Energy, https://energy.gov/eere/fuelcells/fuel-cell-technologies-office. Website accessed on June 2020.

Dolbow J., Moës N. and Belytschko T. (2000). Discontinuous enrichment in finite elements with a partition of unity method. Finite Elements in Analysis and Design 36 (3–4), 235–260.

Dormieux L., Barboux P., Coussy O. and Dangla P. (1995). A macroscopic model of the swelling phenomenon of a saturated clay. European journal of mechanics. A. Solids 14 (6), 981–1004.

Draper D., Pereira A., Prado P., Saltelli A., Cheal R., Eguilior S., Mendes B. and Tarantola S. (1999). Scenario and parametric uncertainty in GESAMAC. A methodological study in nuclear waste disposal risk assessment. Computer Physics Communications 117 (1), 142–155.

Dueck A. (2004) Hydro-mechanical properties of a water unsaturated sodium bentonite. PhD Thesis. University of Lund, Sweden.

Dvorkin E. N., Cuitiño A. M. and Gioia G. (1990). Finite elements with displacement interpolated embedded localization lines insensitive to mesh size and distortions. International Journal for Numerical Methods in Engineering 30 (3), 541–564.

Dymitrowska M., Smaï F. and Bourgeat A. (2015). Thermodynamic Modeling of Hydrogen Migration in Argillite for a Deep Geological Radioactive Waste's Fortune. Irsn Contribution to Forge. Geological Society Special Publication 1, 415.

Dzevanshir R. D., Buryakovskiy L. A. and Chilingarian G. V. (1986). Simple quantitative evaluation of porosity of argillaceous sediments at various depths of burial. Sedimentary Geology 46, 169–175.

Edge J. S., Skipper N. T., Fernandez-Alonso F., Lovell A., Srinivas G., Bennington S. M., Garcia Sakai V. and Youngs T. G. A. (2014). Structure and Dynamics of Molecular Hydrogen in the Interlayer Pores of a Swelling 2:1 Clay by Neutron Scattering. J. Phys. Chem. C 118 (44), 25740–25747.

Eiermann M., Ernst O. G. and Ullmann E. (2007). Computational aspects of the stochastic finite element method. In Computing and Visualization in Science.

EURAD (Deliverable n° 6.1) – Initial State of the Art on Gas Transport in Clayey Materials
Dissemination level: PU
Date of issue of this report: 17/11/2021

Page 341

ENRESA 2006. FEBEX Full-scale Engineered Barriers Experiment. Updated Final Report 1994-2004. Publicación Técnica ENRESA 05-0/2006, Madrid, 590 pp.

Espinosa R. M. and Franke L. (2006). Influence of the age and drying process on pore structure and sorption isotherms of hardened cement paste. Cement and Concrete Research 36, 1969–1984.

EURIDICE. (2020). Experiments - Overview. https://www.euridice.be/en/content/experiments-overview (website accessed 2020-09-23)

Ewen J. and Thomas H. R. (1989). Heating unsaturated medium sand. Géotechnique 3, No. 1, 455–470.

Faivre M., Paul B., Golfier F., Giot R., Massin P. and Colombo D. (2016). 2D coupled HM-XFEM modeling with cohesive zone model and applications to fluid-driven fracture network. Engineering Fracture Mechanics 159, 115–143.

Fall M., Nasir O. and Nguyen T. (2014). A coupled hydro-mechanical model for simulation of gas migration in host sedimentary rocks for nuclear waste repositories. Engineering Geology 176, 24–44.

Fang Y., Elsworth D., Wang C., Ishibashi T. and Fitts J. P. (2017). Frictional stability-permeability relationships for fractures in shales: Friction-Permeability Relationships. Journal of Geophysical Research: Solid Earth 122 (3), 1760–1776.

Fernández A.M. (2004). Caracterización y modelización del agua intersticial en materiales arcillosos:

Estudio de la bentonita de Cortijo de Archidona. PhD thesis. CIEMAT, Madrid, 505 pp.

Ferrari A. and Laloui, L. (2012). Advances in testing the hydro-mechanical behaviour of shales. In L. Laloui and A. Ferrari editors. Multiphysical Testing of Soils and Shales, pages 57-68, Springer, 2012.

Ferrari A., Favero V., Manca D. and Laloui L. (2013). Geotechnical characterization of core samples from the geothermal well Schlattingen SLA-1. Nagra. Arbeitsbericht NAB 12-50.

Ferrari A., Favero, V., Marschall, P. and Laloui, L. (2014). Experimental analysis of the water retention behaviour of shales. Int. J. Rock Mech. Min. Sci. 72, 61–70.

Fourar M., Bories S., Lenormand R. and Persoff P. (1993). Two-phase flow in smooth and rough fractures. Measurement and correlation by porous-medium and pipe flow models. Water Resources Research 29 (11), 3699–3708.

Franče J. (1992). Bentonity ve východní části Doupovských hor, Sborník geologických věd 30, 43-90.

Frederickx L. (2019). An advanced mineralogical study of the clay mineral fraction of the Boom Clay. PhD thesis. KULeuven

Fredlund D. G. and Morgenstern N. R. (1977). Stress state variables for unsaturated soils. Journal of the Geotechnical Engineering Division 103, No. GT5, 447–466.

Fredlund D. G. and Rahardjo H. (1993). Soil mechanics for unsaturated soils. Wiley.

Freni A., Cipiti F. and Cacciola G. (2009). Finite element-based simulation of a metal hydride- based hydrogen storage tank. International Journal of Hydrogen Energy 34, 8574–8582.

Gallé C. (1998). Migration des gaz et pression de rupture dans une argile compactée destinée à la barrière ouvragée d'un stockage profond. Bulletin de la Société Géologique de France 169 (5), 675–680.

Gallé C. and Tanai K. (1998). Evaluation of gas transport properties of backfill materials for waste disposal. H2 migration experiments in compacted Fo-Ca clay. Clays and Clay Minerals 46 (5), 498–508.

Galson (2005). "Belgian Supercontainer Design for HLW and Spent Fuel Disposal. Evaluation of the Reference Design." 0460–5. Galson Sciences.

Garitte B., Gens A., Vaunat J. and Armand G. (2014). Thermal conductivity of argillaceous rocks: determination methodology using in situ heating tests. Rock Mechanics and Rock Engineering 47 (1), 111–129.

Garrels R. M. and Christ C. L. (1965). Solutions, minerals, and equilibra. Harper and Row.

Gaucher E., Robelin C., Matray J. M., Négrel G., Gros Y., Heitz J. F., Vinsot A., Rebours H., Cassagnabère A. and Bouchet A. (2004). ANDRA underground research laboratory: interpretation of the mineralogical and geochemical data acquired in the Callovian–Oxfordian formation by investigative drilling. Physics and Chemistry of the Earth, Parts A/B/C 29 (1), 55–77.

Gaucher E., Blanc P., Bardot F., Braibant G., Buschaert S., Crouzet C., Gautier A., Girard J. P., Jacquot E., Lassin A., Negrel G., Tournassat C., Vinsot A. and Altmann S. (2006). Modelling the porewater chemistry of the Callovian-Oxfordian formation at a regional scale. Comptes Rendus Geoscience 338, 917-930.

EURAD (Deliverable n° 6.1) – Initial State of the Art on Gas Transport in Clayey Materials
Dissemination level: PU
Date of issue of this report: 17/11/2021

Page 342

Gaus I., Garitte B., Senger R., Gens A., Vasconcelos R., Garcia-Sineriz J.-L., Trick T., Wieczorek K., Czaikowski O., Schuster K., Mayor J.C., Velasco M., Kuhlmann U. and Villar M.V. (2014a). The HE-E Experiment. Layout, Interpretation and THM Modelling Combining D2.2-11. Final Report on the HE-E Experiment and D3.2-2. Modelling and Interpretation of the HE-E Experiment of the PEBS Project. Long-term Performance of Engineered Barrier Systems PEBS. European Commission. 180p.

Gaus I., Wieczorek K., Schuster K., Garitte B., Senger R., Vasconcelos R. and Mayor J. C. (2014b). EBS behaviour immediately after repository closure in a clay host rock: HE-E experiment (Mont Terri URL). Geological Society, London, Special Publications 400 (1), 71–91.

Gawin D. and Sanavia L. (2010) Modelling of cavitation in water saturated porous media considering effects of dissolved air. Transport in Porous Media. 81, n°1, 141-160.

Gens A. (1996). Constitutive modelling. application to compacted soils. In Proceedings of the First International Conference on Unsaturated Soils, UNSAT 1996 (Alonso, E. E. and Delage, P., Eds.), Paris, France, pp. 1179–1200.

Gens A. (2013). On the hydromechanical behaviour of argillaceous hard soils-weak rocks. Proceedings of the 15th European Conference on Soil Mechanics and Geotechnical Engineering. Geotechnics of Hard Soils – Weak Rocks (Part 4).

Gens A. (Eds) (2018). Description of the Constitutive Models Available at the Start of the Project. Conceptual Bases, Mathematical Description and Capabilities and Shortcomings. BEACON Project. Technical Report Deliverable D3.1.

Gens A. and Alonso E. E. (1992). A framework for the behaviour of unsaturated expansive clays. Canadian Geotechnical Journal 29 (6), 1013–1032.

Gens A., Sánchez M. and Sheng D. (2006). On constitutive modelling of unsaturated soils. Acta Geotechnica 1, No. 3, 137–147.

Gerard P. (2011). Impact des transferts de gaz sur le comportement poro-mécanique des matériaux argileux. PhD Thesis, Université de Liège.

Gerard P., Charlier R., Chambon R. and Collin F. (2008). Influence of evaporation and seepage on the convergence of a ventilated cavity. Water Resources Research 44 (7).

Gerard P., Harrington J., Charlier R. and Collin F. (2014). Modelling of localised gas preferential pathways in claystone. International Journal of Rock Mechanics and Mining Sciences, 67, pp.104–114.

Ghanem R. G. and Spanos P. D. (1991). Stochastic Finite Elements. A Spectral Approach.

Giannakandropoulou L. (2019). Hydrogen production by steel anoxic corrosion under gamma irradiation. In oral presentation in The Miller Conference on Radiation Chemistry, 9 – 14 Sep 2019, Cumbria, United Kingdom.

Gibson R. E. and Henkel D. (1954). Influence of duration of tests at constant rate of strain on measured 'drained' strength. Geotechnique 4, 6–15.

Giger S. and Marschall P. (2014). Geomechanical properties, rock models and in-situ stress conditions for Opalinus Clay in Northern Switzerland. Nagra. Arbeitsbericht NAB 14-01.

Gimmi T. and Fernández A. M. (2017). Physical characterisation of pores and pore water of samples from the Schlattingen borehole. Nagra. NAB 16-71.

Giot R., Auvray C. and Talandier J. (2019) Self-sealing of claystone under X-ray nanotomography. Geological Society, London, Special Publications, 482, 213-223

Glass R. J., Conrad S. H. and Yarrington L. (2001). Gravity-destabilized non-wetting phase invasion in macro-heterogeneous porous media. Near-pore-scale macro modified percolation simulation of experiments. Water Resources Research 77 (5), 1197–1207.

Glaus M. A., Frick S. and Van Loon L.R. (2017). Diffusion of selected cations and anions in compacted montmorillonite and bentonite. Nagra Technical Report NTB 17-12

Gómez-Hernández J.J. (2000). Technical Note 2000-40. FM-C experiment. Part A) Effective diffusivity and accessible porosity derived from in-situ He-4 tests Part B) Prediction of HE-3 concentration in a cross-hole experiment.

Gonzalez-Blanco L. (2017). Gas migration in deep argillaceous formations: Boom Clay and indurated clays. PhD thesis, Universitat Politècnica de Catalunya

Gonzalez-Blanco L. and Romero E. (2019). Hydro-mechanical processes associated with gas transport in MX-80 Bentonite in the context of Nagra's RD&D programme (results by May 2019). Nagra Arbeitsbericht, NAB 19-16, Nagra, Switzerland

EURAD (Deliverable n° 6.1) – Initial State of the Art on Gas Transport in Clayey Materials
Dissemination level: PU
Date of issue of this report: 17/11/2021

Page 343

Gonzalez-Blanco L., Romero E., Jommi C., Li X. and Sillen X. (2016a), Gas migration in a Cenozoic clay. Experimental results and numerical modelling. Geomechanics for energy and Environment, 6, 81-100.

Gonzalez-Blanco L., Romero E., Li X., Sillen X. and Jommi C. (2016b). Air injection tests in two argillaceous rock formations: Experimental results and modelling. In: Proceedings of the 1st International Conference on Energy Geotechnics, ICEGT 2016, Kiel, Germany, 29–31 August 2016. CRC Press, ISBN 9781138032996, pp. 715–721

Gonzalez-Blanco L., Romero E., Jommi C., Sillen X. and Li X. (2017). Exploring fissure opening and their connectivity in a cenozoic clay during gas injection. In Advances in Laboratory Testing and Modelling of Soils and Shales (ATMSS). (eds. A. Ferrari and L. Laloui). Springer International Publishing. 288–295.

Gonzalez-Blanco L., Romero E. and Marschall P. (2017). Pathway development and connectivity during gas injection/dissipation tests: experimental results and numerical modelling. In Interpore 2017: 9th International Conference on Porous Media and Annual Meeting.

Gonzalez-Blanco L., Romero E. and Marschall P. (2018). Effect of spatial heterogeneity on gas transport in compacted MX-80. In International Symposium on Energy Geotechnics 2018, Lausanne, Switzerland.

Goodman R.E. (1974). The mechanical properties of joints. Proceed. 3rd Congr. Int. Soc. Mech., Denver, Vol. 1, Part A. 127-140, Washington (Nat. Acad. Sciences).

Graham C., Harrington J., Cuss R. and Sellin P. (2012). Gas migration experiments in bentonite. Implications for numerical modelling. Mineralogical Magazine 76, 3279–3292.

Graham C. C., Harrington J. F. and Cuss R. J. (2014). Hydraulic and Gas Transport Testing of Brauner Dogger and Opalinus Clay. In Fourth EAGE Shale Workshop, April 2014.

Graham C. C., Harrington J. F. and Sellin P. (2016). Gas migration in pre-compacted bentonite under elevated pore-water pressure conditions. Applied Clay Science 132, 353–365.

Graham J., Oswell J. M. and Gray M. N. (1992). The effective stress concept in saturated sand–clay buffer. Canadian Geotechnical Journal 29, No. 6, 1033–1043.

Graham J., Halayko K.G., Hume H., Kirkham T., Gray M. and Oscarson D. (2002). A capillarity-advective model for gas break-through in clays. Engineering Geology 64/2, 273-286.

Grant M.A. (1977). Permeability Reduction Factors at Wairakei, paper 77-HT-52, presented at AICHE-ASME Heat Transfer Conference, Salt Lake City, Utah, August 1977.

Grathwohl P. (1998). Diffusion in Natural Porous Media. Contaminant Transport, Sorption/desorption and Dissolution Kinetics. Springer, US.

Grindrod P., Impey M.D., Saddique S.N. and Takase H. (1994) Saturation and gas migration within clay buffers. Proceedings of Conference on High Level Radioactive Waste Management, Las Vegas, United States, April 1994.

Grousset S. (2016). Détermination de la composition isotopique du soufre pour l'étude de l'origine, biotique ou abiotique, des sulfures de fer en corrosion anoxique. PhD thesis, Université Pierre & Marie Curie – Paris 6.

Guiducci C., Pellegrino A., Radu J.-P., Collin F. and Charlier R. (2002a) Numerical modelling of hydro-mechanical fracture behavior. Numerical Models in Geomechanics – Proceedings of NUMOG VIII. Eds. Pande G.N. and Pietruszczak S. Swets and Zeitlinger. Lisse, pp. 293–299.

Guiducci C., Pellegrino A., Radu J.-P., Collin F., Charlier R. (2002b) Hydro-mechanical behavior of fractures. 2D F.E.M. modeling. Poromechanics II – Proceedings of 2nd Biot Conference on Poromechanics. Eds. Auriault J.-L., Geindreau C., Royer P., Bloch G.F. Taylor and Francis. Grenoble, France, pp. 217–224.

Guillon T. (2011). Comportement hydromécanique des argilites du Callovo-Oxfordien lors de cycles de désaturation-resaturation. PhD thesis, Institut National Polytechnique de Lorraine.

Gunzburger Y. and Cornet F. H. (2007). Rheological characterization of a sedimentary formation from a stress profile inversion. Geophysical Journal International, 168, 1, 402–418.

Guo G. and Fall M. (2018). Modelling of dilatancy-controlled gas flow in saturated bentonite with double porosity and double effective stress concepts. Engineering Geology 243, 253–271.

Guo G. and Fall M. (2021). Advances in modelling of hydro-mechanical processes in gas migration within saturated bentonite: A state-of-art review. Engineering Geology 287, 106123.

Gutiérrez M., Øino L. E. and Nygård R. (2000). Stress-dependent permeability of a de-mineralised fracture in shale. Marine and Petroleum Geology 17 (8), 895–907.

Gutiérrez-Rodrigo V. (2018). Transporte de gas en materiales de barrera. PhD thesis. Universidad Complutense de Madrid, p. 303. Colecci´on Documentos CIEMAT. ISBN: 978-84-7834-802-2. Madrid

EURAD (Deliverable n° 6.1) – Initial State of the Art on Gas Transport in Clayey Materials
Dissemination level: PU
Date of issue of this report: 17/11/2021

Page 344

Gutiérrez-Rodrigo V., Villar M. V., Martin P. L. and Romero F. J. (2014). Gas transport properties of compacted bentonite. In Unsaturated soils: research & applications: proceedings of the Sixth International Conference on Unsaturated Soils, UNSAT 2014, Sydney, Australia, 2-4 July 2014. (eds. N. Khalili, A. R. Russell, and A. Khoshghalb). CRC Press, Boca Raton, Fla.

Gutiérrez-Rodrigo V., Villar M. V., Martín P. L., Romero F. J. and Barcala J. M. (2015). Gas-breakthrough pressure of FEBEX bentonite. Geological Society, London, Special Publications 415 (1), 47–57.

Gutiérrez-Rodrigo V., Martín P. L. and Villar M. V. (2021). Effect of interfaces on gas breaktrough pressure in compacted bentonite used as engineered barrier for radioactive waste disposal. Process Safety and Environmental Protection 149, 244–257.

Gygi D., Bloch E. D., Mason J. A., Hudson M. R., Gonzalez M. I., Siegelman R. L., Darwish T. A., Queen W. L., Brown C. M. and Long J. R. (2016). Hydrogen Storage in the Expanded Pore Metal–Organic Frameworks M 2 (dobpdc) (M = Mg, Mn, Fe, Co, Ni, Zn). Chemistry of Materials 28 (4), 1128–1138.

Habraken A. (1989). Contribution à la modélisation du formage des métaux par la méthode des éléments finis. PhD thesis, Université de Liège.

Haijtink B. (1996). Project on Effects of Gas in Underground Storage facilities for radioactive waste (PEGASUS project) - Proceedings of a progress meeting held in Rapolano Terme, Italy on 14 and 15 June 1995. European Commission. Nuclear Science and Technology EUR 16746 EN.

Haijtink B. and McMenamin T. (1993). Project on effects of gas in underground storage facilities for radioactive waste (Pegasus project) - Proceedings of a progress meeting held in Brussels 11-12 June 1992. European Commission. Nuclear Science and Technology EUR 14816 EN.

Haijtink B. and McMenamin T. (1994). Project on effects of gas in underground storage facilities for radioactive waste (Pegasus project) - Proceedings of a progress meeting held in Cologne (D) 3-4 June 1993. European Commission. Nuclear Science and Technology EUR 15734 EN.

Harrington J. F. and Horseman S. T. (1999). Gas transport properties of clays and mud rocks, in A. C. Aplin, A. J. Fleet, and J. H. S. Macquaker, eds., Muds and mudstones. Physical and fluid flow properties. Geological Society (London) Special Publication 158, p. 107 –124

Harrington J. F. and Horseman S. T. (2003). Gas migration in KBS-3 buffer bentonite. Sensitivity of test parameters to experimental boundary conditions. Svensk Kärbränslehantering AB (SKB).

Harrington J., Birchall D., Noy D. and Cuss R. (2008). Large scale gas injection test (Lasgit) performed at the Äspö Hard Rock Laboratory. summary report 2007.

Harrington J. F., Milodowski A. E., Graham C. C., Rushton J. C. and Cuss R. J. (2012a). Evidence for gas-induced pathways in clay using a nanoparticle injection technique. Mineralogical Magazine 76 (8), 465–474.

Harrington J. F., de la Vaissière R., Noy D. J., Cuss R. J. and Talandier J. (2012b). Gas flow in Callovo- Oxfordian clay (COx). results from laboratory and field-scale measurements. Mineralogical Magazine 76, 3303–3318.

Harrington J. F., Volckaert G., Jacobs E., Maes N., Areias L., Charlier R., Collin F., Gerard P., Levasseur S., Radu J.-P., Svoboda J., Granet S., Alcoverro J., Arnedo D., Olivella S., Alonso E., Marschall P., Gaus I., Rüedi J., Cuss R., Sathar S. and Noy D. (2013). Summary report: Experiments and modelling of excavation damage zone (EDZ) behaviour in argillaceous and crystalline rocks (Work Package 4). European Commission. FORGE Milestone D4.24-R.

Harrington J. F., Cuss R. J., Wiseall A. C., Daniels K. A., Graham C. C. and Tamayo-Mas E. (2017a). Scoping study examining the behaviour of Boom Clay at repository depths of interest in OPERA. COVRA Report OPERA-PU-BGS523 and 616.

Harrington J. F., Graham C. C., Cuss R. J. and Norris S. (2017b). Gas network development in a precompacted bentonite experiment. evidence of generation and evolution. Applied Clay Science 147, 80–89.

Harrington J. F., Cuss R. J. and Talandier J. (2017c). Gas transport properties through intact and fractured Callovo-Oxfordian mudstones. Geological Society, London, Special Publications 454 (1), 131–154.

Harrington J. F., Graham C. C., Tamayo-Mas E. and Parkes D. (2018). Stress Controls on Transport Properties of the Mercia Mudstone Group. Importance for Hydrocarbon Depletion and CO2 Injection. Marine and Petroleum Geology 93, 391–408.

Harris A. W., Boult K. A., Manning M. C. and Tearle W. M. (2003a). Experimental study of carbon dioxide uptake by NRVB and 3.1 BFS/OPC. Serco report Serco/ERRA-0453.

Harris A. W., Manning M. C. and Tearle W. M. (2003b). Carbonation of Nirex reference vault backfill. Serco report Serco/ERRA-0454.

Hassanizadeh M. and Gray W. G. (1979a). General conservation equations for multi-phase systems. 1. Averaging procedure. Advances in Water Resources 2, 131–144.

EURAD (Deliverable n° 6.1) – Initial State of the Art on Gas Transport in Clayey Materials
Dissemination level: PU
Date of issue of this report: 17/11/2021

Page 345

Hassanizadeh M. and Gray W. G. (1979b). General conservation equations for multiphase systems. 2. Mass, momenta, energy, and entropy equations. Advances in Water Resources 2, 191–203.

Hassanizadeh M. and Gray W. G. (1980). General conservation equations for multi-phase systems. 3. Constitutive theory for porous media flow. Advances in Water Resources 3, No. 1, 25–40.

Haupt P. (2002). Continuum mechanics and theory of materials., Springer, Heidelberg-Berlin.

Hausmannová L., Hanusová I. and Dohnálková M. (2018). Summary of the research of Czech bentonites for use in the deep geological repository – up to 2018, SÚRAO 309/2018/ENG

Hegde J. and Rokseth B. (2020). Applications of machine learning methods for engineering risk assessment – A review. Safety Science 122.

Helfer T., Bleyer J., Frondelius T., Yashchuk I., Nagel T. and Naumov D. (2020). The \textttMFrontGenericInterfaceSupport project. Journal of Open Source Software 5 (48), 1–8.

Helmig R. (1997). Multiphase flow and transport processes in the subsurface. Springer Ver¬lag, Berlin, Germany.

Helton J. C. (1993). Uncertainty and sensitivity analysis techniques for use in performance assessment for radioactive waste disposal. Reliability Engineering and System Safety 42 (2–3), 327–367.

Henry P., Guglielmi Y., Morereau A., Seguy S., Castilla R., Nussbaum C., Dick P., Durand J., Jaeggi D., Donze F. V. and Tsopela A. (2016). Permeability-fluid pressure-stress relationship in fault zones in shales. In AGU Fall Meeting Abstracts, December 2016.

Henry W. (1803). Experiments on the quantity of gases absorbed by water, at different temperatures, and under different pressures, Phil. Trans. R. Soc. Lond., 93, 29–274.

Heyes D. W., Butcher E. J., Borwick J., Milodowski A. E., Field L. P., Kemp S. J., Mounteney I., Bernal S. A., Corkhill C. L., Hyatt N. C., Provis J. L. and Black L. (2015). Demonstration of Carbonation of the Nirex Reference Vault Backfill. NNL report NNL(14)13296, Issue 4.

Hicks T. W. and Baldwin T. D. (2007). Comparison of gas generation and gas transfer analyses for Nirex, Nagra and Andra ILW, HLW and SF repository concepts. Galson Sciences Report 0573–1 Version 2.

Hildenbrand A., Schlomer S. and Krooss B. M. (2002). Gas breakthrough experiments on fine-grained sedimentary rocks. Geofluids 2 (1), 3–23.

Hildenbrand A., Schlomer S., Krooss B. M. and Littke R. (2004). Gas breakthrough experiments on pelitic rocks. comparative study with N2, CO2 and CH4. Geofluids 4 (1), 61–80.

Hirscher M., Panella B. and Schmitz B. (2010). Metal-organic frameworks for hydrogen storage. Microporous and Mesoporous Materials 129, 335–339.

Hirschfelder J., Curtiss C. and Bird R. (1964). Molecular Theory of Gases and Liquids., Wiley, New York, USA.

Hoch A. R. and Swift B. T. (2010). Post-closure Performance Assessment - Example Approaches for Gas Modelling in Generic Environments. Serco report SERCO/TAS/000472/001, Issue 2.

Hoch A. R. and Thorne M. C. (2008). Gas and the human intrusion pathway. Serco report SA/ENV-0966, issue 2.

Hoch A. R., Cliffe K. A., Swift B. T. and Rodwell W. R. (2004). Modelling gas migration in compacted bentonite: GAMBIT club Phase 3 final report. POSIVA. 2004–02.

Hoch A. R., Thorne M. C., Swift B. T. and Bate F. (2008). Update of the GPA (03) assessment of the consequences of gas. Serco report SA/ENV-0948.

Hokari T., Okihara M., Ishii T. and Ikuse H. (1997). Experimental study on scale effects of bentonite/sand mixtures on gas migration eds. W. J. Gray and I. R. Triay. Materials Research Society Symposia Proceedings, Scientific Basis for Nuclear Waste Management XX Boston, 2-6 Dec., 1996 465, 1019–1026.

Holtom G. J. (1997). The biogenesis of 14C-labelled methane from 14C-labelled barium carbonate in intermediate-level radioactive waste. UK Nirex report NSS/R318.

Homand F., Giraud A., Escoffier S., Koriche A. and Hoxha D. (2004). Permeability determination of a deep argillite in saturated and partially saturated conditions. International Journal of Heat and Mass Transfer 47 (14–16), 3517–3531.

Honty M. and De Craen M. (2012). Boom Clay Mineralogy - qualitative and quantitative aspects. SCK•CEN. External report ER-194.

Horseman S. T. and Harrington J. F. (1994). Migration of repository gases in an overconsolidated clay. British Geological Survey. Technical Report WE/94/7.

Horseman S. T. and Harrington J. F. (2002). Laboratory experiments on gas migration in Opalinus Clay samples from the Benken borehole, Switzerland. NAGRA.

EURAD (Deliverable n° 6.1) – Initial State of the Art on Gas Transport in Clayey Materials
Dissemination level: PU
Date of issue of this report: 17/11/2021

Page 346

Horseman S. T., Winter M. G. and Entwistle D. C. (1987). Geotechnical characterisation of boom clay in relation to the disposal of radioactive waste. European Commission, Nuclear Science and Technology. Final Report EUR 10987 EN.

Horseman S. T., Higgo J. J. W., Alexander J. and Harrington J. F. (1996). Water, gas and solute movement in argillaceous media. Rept. No. CC-96/1 to OECD/NEA Working Group on Measurement and Physical Understanding of Groundwater Flow through Argillaceous Media., Nuclear Energy Agency, OECD.

Horseman S. T., Harrington J. F. and Sellin P. (1997). Gas migration in Mx80 buffer bentonite. Materials Research Society Symposia Proceedings 465, 1003–1010.

Horseman S. T., Harrington J. F. and Sellin P. (1999). Gas migration in clay barriers. Engineering Geology 54, 139–149.

Horseman S. T., Harrington J. F. and Sellin P. (2004). Water and gas flow in MX80 bentonite buffer clay. In Symposium on the Scientific Basis for Nuclear Waste Management XXVII (Kalmar). Materials Research Society. 715–720.

Huang Y., Shao H., Wieland E., Kolditz O. and Kosakowski G. (2018). A new approach to coupled two-phase reactive transport simulation for long-term degradation of concrete. Construction and Building Materials 190, 805–829.

Hueckel T. (1992a). On effective stress concepts and deformation in clays subjected to environmental loads. discussion. Canadian Geotechnical Journal 29, No. 6, 1120–1125.

Hueckel T. (1992b). Water-mineral interaction in hygromechanics of clays exposed to environmental loads. a mixture-theory approach. Canadian Geotechnical Journal 29, No. 6, 1071–1086.

Huertas F., Fuentes-Cantillana J. L., Jullien F., Rivas P., Linares J., Fariña P., Ghoreychi M., Jockwer N., Kickmaier W., Martínez M. A., Samper J., Alonso E. and Elorza F. J. (2000). Full-scale engineered barriers experiment for a deep geological repository for high-level radioactive waste in crystalline host rock (FEBEX project). European Commission. Final Report EUR 19147 EN.

Hume H. B. (1999). Gas breakthrough in compacted avonlea bentonite. MSc Thesis, University of Manitoba.

I&E (2016). The national programme for the management of radioactive waste and spent fuel. Ministry of Infrastructure and Environment (The Netherlands).

IAEA (2012). The safety case and safety assessment for the disposal of radioactive waste. Specific safety guide. IAEA Safety Standards Series No. SSG-23, International Atomic Energy Agency, Vienna, Austria.

IAEA (2014). Characterization of Swelling Clays as Components of the Engineered Barrier System for Geological Repositories. TECDOC Series 1718, International Atomic Energy Agency, Vienna.

Impey M.D., Grindrod P., Takase H. and Worgan K.J. (1997) A capillary network model for gas migration in low-permeability media. Society for Industrial and Applied Mathematics. 57, n°3, 597-608.

IRSN (2014). Projet de stockage Cigéo – Ouvrages de fermeture. IRSN. Rapport IRSN 2014 00006, présenté devant le GPD le 1er juillet 2014.

IRSN (2017). Projet de stockage Cigéo – Examen du Dossier d'Options de Sûreté. IRSN. Rapport IRSN 2017 00013, présenté devant GPD-GPU les 18 19 mai 2017.

Ishida T., Maekawa K. and Kishi T. (2007). Enhanced modeling of moisture equilibrium and transport in cementitious materials under arbitrary temperature and relative humidity history. Cement and Concrete Research 37, 565–578.

IUPAC (1981). Solubility Data Series Hydrogen and Deuterium. Vol. 5/6, International Union of Pure and Applied Chemistry.

IUPAC (1997). Compendium of Chemical Terminology. The Gold Book, Second Edition, McNaught, A. D. and Wilkinson, A., Blackwell Science, London.

Jacinto A., Villar M., Gomezespina R. and Ledesma A. (2009). Adaptation of the van Genuchten expression to the effects of temperature and density for compacted bentonites. Applied Clay Science 42 (3–4), 575–582.

Jackson M., Mulcahy SR, Chen H, Li Y, Li Q, Cappelletti P and Wenk H-R (2017). Philipsite and Al-tobermite mineral cements produced through low-temperature water-rock reactions in Roman marine concrete. American Mineralogist 102, 1435-EP 1450.

Jacops E. (2018). Development and application of an innovative method for studying the diffusion of dissolved gases in porous saturated media. PhD thesis. KU Leuven.

Jacops E. and Maes N. (2015). Measuring the diffusion coefficient for He and Ar in Callovo-Oxfordian Clay. Final Report. SCK-CEN-ER-301, Mol, Belgium.

EURAD (Deliverable n° 6.1) – Initial State of the Art on Gas Transport in Clayey Materials
Dissemination level: PU
Date of issue of this report: 17/11/2021

Page 347

Jacops E., Maes N. and Volckaert G. (2011). Results and interpretation of gas-driven radionuclide transport in undisturbed Boom Clay. SCK•CEN. External Report ER-158.

Jacops E., Volckaert G., Maes N., Weetjens E. and Govaerts J. (2013). Determination of gas diffusion coefficients in saturated porous media. He and CH4 diffusion in Boom Clay. Applied Clay Science 83-84, 217-223.

Jacops E., Volckaert G., Maes N., Charlier R., Collin F., Gerard P., Levasseur S., de La Vaissière R., Talandier J., Granet S., Navarro M., Villar M., Romero F., Martin P., Zandarin M., Olivella S., Alonso E., Marschall P., Harrington J., Cuss R., Noy D. and Woods A. (2014). WP5 Final Report. Experiments and modelling of gas migration processes in undisturbed rocks. European Commission, Euratom 7th Framework Programme. FORGE Report D5.19.

Jacops E., Wouters K., Volckaert G., Moors H., Maes N., Bruggeman C., Swennen R. and Littke R. (2015). Measuring the effective diffusion coefficient of dissolved hydrogen in saturated Boom Clay. Applied Geochemistry 61, 175–184.

Jacops E., Maes N., Bruggeman C. and Grade A. (2016). Measuring diffusion coefficients of dissolved He and Ar in three potential clay host formations: Boom Clay, Callovo-Oxfordian clay and Opalinus Clay. Geological Society, London, Special Publications 443 (1), 349–360.

Jacops E., Aertsens M., Maes N., Bruggeman C., Swennen R., Krooss B., Amann-Hildenbrand A. and Littke R. (2017a). The dependency of diffusion coefficients and geometric factor on the size of the diffusing molecule: observations for different clay-based materials. Geofluids 2017, 1–17.

Jacops E., Aertsens M., Maes N., Bruggeman C., Krooss B. M., Amann-Hildenbrand A., Swennen R. and Littke R. (2017b). Interplay of molecular size and pore network geometry on the diffusion of dissolved gases and HTO in Boom Clay. Applied Geochemistry 76, 182–195.

Jacops E., Rogiers, B., Frederickx, L., Swennen, R., Littke, R., Krooss, B.M., Amann-Hildenbrand, A., Bruggeman, C. (2020a). The relation between petrophysical and transport properties of the Boom Clay and Eigenbilzen Sands. Applied Geochemistry 114, 104527

Jacops E., Swennen R., Janssens N., Seemann T., Amann-Hildenbrand A., Krooss B. M., Littke R., Maes N. and Bruggeman C. (2020b). Linking petrographical and petrophysical properties to transport characteristics: a case from Boom Clay and Eigenbilzen Sands. Applied Clay Science 190, 105568.

Jacops E., Phung Q. T., Frederickx L. and Levasseur S. (2021). Diffusive transport of dissolved gases in potential concretes for nuclear waste disposal. Sustainability 13 (18), 10007.

Jenni A., Wersin P., Thoenen T., Baeyens B., Ferrari A., Gimmi T., Mäder U., Marschall P., Hummel W. and Leupin O. (2019). Bentonite backfill performance in a high-level waste repository. A geochemical perspective. Nagra. Technical Report NTB 19-03.

Jennings J. and Burland J. (1962). Limitations to the use of effective stresses in partly saturated soils. Géotechnique 12 (2), 125–144.

Jirásek M. (2000). Comparative study on finite elements with embedded discontinuities. Computer Methods in Applied Mechanics and Engineering 188 (1–3), 307–330.

Jirásek M. and Zimmermann T. (2001). Embedded crack model. I. Basic formulation. International Journal for Numerical Methods in Engineering 50 (6), 1269–1290.

Johnson D. L., Koplik J. and Schwartz L. M. (1986). New pore-size parameter characterizing transport in porous media. Phys. Rev. Lett. 57 (20), 2564–2567.

Johnson L., Marschall P., Zuidema P. and Gribi P. (2004). Effects of post-disposal gas generation in a repository for spent fuel, high-level waste and long-lived intermediate level waste sited in Opalinus clay. National Cooperative for the Disposal of Radioactive Waste (Nagra).

Jommi C. and di Prisco C. (1994). Un semplice approccio teorico per la modellazione del comportamento meccanico dei terreni granulari parzialmente saturi. In Atto Convegno sul Tema. il ruolo dei fluidi nei problemi di ingegneria geotecnica, Mondovi, Italy, pp. 167–188.

Jung Y., Pau G. S. H., Finsterle S. and Doughty C. (2018). TOUGH3 user's guide. University of California, Berkeley.

Kadono K., Kajiura H. and Shiraishi M. (2003). Dense hydrogen adsorption on carbon subnanopores at 77 K. Applied Physics Letters 83 (16), 3392–3394.

Kamrava S., Tahmasebi P. and Sahimi M. (2020). Linking Morphology of Porous Media to Their Macroscopic Permeability by Deep Learning. Transport in Porous Media 131 (2), 427–448.

Karnland O., Nilsson U., Weber H. and Wersin P. (2008). Sealing ability of Wyoming bentonite pellets foreseen as buffer material – Laboratory results. Physics and Chemistry of the Earth, Parts A/B/C 33, S472–S475.

Katsube T. J. (2000). Shale permeability and pore-structure evolution characteristics.

EURAD (Deliverable n° 6.1) – Initial State of the Art on Gas Transport in Clayey Materials
Dissemination level: PU
Date of issue of this report: 17/11/2021

Page 348

Katsube T. J., Boitnott G. N., Lindsay P. J. and Williamson M. (1996a). Eastern Canada and national and general programs. Current Research. Pore structure evolution of compacting muds from the seafloor, offshore Nova Scotia, Geological Survey of Canada

Katsube T. J., Issler D. R. and Coyner K. (1996b). Petrophysical characteristics of shale from the Beaufort Mackenzie Basin, northern Canada; permeability, formation factor, and porosity versus pressure, interior plains and Arctic Canada. Current Research., Geological Survey of Canada

Keaton R. J., Blacquiere J. M. and Baker R. T. (2007). Base metal catalyzed dehydrogenation of ammonia−borane for chemical hydrogen storage. Journal of the American Chemical Society 129 (7), 1844–1845.

Keller L. M. (2015). On the representative elementary volumes of clay rocks at the mesoscale. Journal of Geology and Mining Research 7 (6), 58–64.

Keller (2019). Microstructural Analysis of MX-80 Bentonite. In. Romero, E., Gonzalez-Blanco, L. (2020). Hydro-mechanical processes associated with gas transport in MX-80 Bentonite in the context of Nagra's RD&D programme. Nagra Arb. Ber. NAB 19-20, Wettingen, Switzerland. (results by May 2019)

Keller L. M., Holzer L., Schuetz P. and Gasser P. (2013a). Pore space relevant for gas permeability in Opalinus clay: Statistical analysis of homogeneity, percolation, and representative volume element. Journal of Geophysical Research: Solid Earth 118 (6), 2799–2812.

Keller L. M., Schuetz P., Erni R., Rossell M. D., Lucas F., Gasser P. and Holzer L. (2013b). Characterization of multi-scale microstructural features in Opalinus Clay. Microporous and Mesoporous Materials 170, 83–94.

Keller L. M., Hilger A. and Manke I. (2015). Impact of sand content on solute diffusion in Opalinus Clay. Applied Clay Science, 112-113, 134-142.

Kenney T., Veen W.V., Swallow M. and Sungaila M. (1992). Hydraulic conductivity of com-pacted bentonite-sand mixtures. Canadian Geotechnical Journal 29/3, 364-374.

Khalili N., Geiser, F. and Blight, G. E. (2004). Effective stress in unsaturated soils. review with new evidence. International Journal of Geomechanics 4, No. 2, 115–126.

Kleppe J., Delaplace P., Lenormand R., Hamon G. and Chaput E. (1997). Representation of capillary pressure hysteresis in reservoir simulation. In. Proceedings - SPE Annual Technical Conference and Exhibition Sigma, pp. 597-604.

Koch T., Gläser D., Weishaupt K., Ackermann S., Beck M., Becker B., Burbulla S., Class H., Coltman E., Emmert S., Fetzer T., Grüninger C., Heck K., Hommel J., Kurz T., Lipp M., Mohammadi F., Scherrer S., Schneider M., Seitz G., Stadler L., Utz M., Weinhardt F. and Flemisch B. (2020). DuMux 3 – an open-source simulator for solving flow and transport problems in porous media with a focus on model coupling. Computers and Mathematics with Applications. https://doi.org/10.1016/j.camwa.2020.02.012.

Kolditz O. and Bauer S. (2004). A process-oriented approach to computing multi-field problems in porous media. Journal of Hydroinformatics 6 (3), 225–244.

Kolditz O., Bauer S., Bilke L., Böttcher N., Delfs J. O., Fischer T., Görke U. J., Kalbacher T., Kosakowski G., McDermott C. I., Park C. H., Radu F., Rink K., Shao H., Shao H. B., Sun F., Sun Y. Y., Singh A. K., Taron J., Walther M., Wang W., Watanabe N., Wu Y., Xie M., Xu W. and Zehner B. (2012). OpenGeoSys. An open-source initiative for numerical simulation of thermo-hydro-mechanical/chemical (THM/C) processes in porous media. Environmental Earth Sciences 67 (2), 589–599.

Kolditz O., Görke U.-J., Shao H., Wang W. and Bauer S. eds. (2016). Thermo-Hydro-Mechanical-Chemical Processes in Fractured Porous Media: Modelling and Benchmarking: Benchmarking Initiatives. Terrestrial Environmental Sciences 1st ed. 2016., Springer International Publishing: Imprint: Springer, Cham.

Kolditz O., Görke U.-J., Shao H., Shao H. and Nagel T. (2019). Workflows in environmental geotechnics: Status-quo and perspectives. In Proceedings of the 8th International Congress on Environmental Geotechnics. ICEG 2018. 119–127. https://doi.org/10.1007/978-981-13-2221-1_6.

Kolditz O., Görke U.-J., Konietzky H., Maßmann J., Nest M., Steeb H., Wuttke F. and Nagel T. eds. (2020). GeomInt - Geomechanical integrity of host and barrier rocks - experiment, modeling and analysis of discontinuities. Terrestrial Environmental Sciences 4, Springer, Heidelberg.

Krooss B.M. and Alles S. (2006). Hydrogeologic analyses and synthesis (HA Experiment): investigation of gas transport processes in the Opalinus Clay. Mont Terri Technical note 2004–73.

EURAD (Deliverable n° 6.1) – Initial State of the Art on Gas Transport in Clayey Materials
Dissemination level: PU
Date of issue of this report: 17/11/2021

Page 349

Krooss B.M. and Alles S. (2008). Experimental studies on caprock sealing efficiency and gas migration in sedimentary rocks. Andra. Internal Report.

Krooss B.M. and Schaefer R.G. (1987). Experimental measurements of the diffusion parameters of light hydrocarbons in water-saturated sedimentary rocks. A new experimental procedure. Organic Geochemistry 11(3). 193-199.

Krooss B.M., Leythaeuser D. and Schäfer R.G. (1992) The quantification of diffusive hydrocarbon losses through cap rocks of natural gas reservoirs – a re-evaluation. The American Association of Petroleum Geologists Bulletin 76, 403–406

Kwon O., Kronenberg A. K., Gangi A. F. and Johnson B. (2001). Permeability of Wilcox Shale and its effective pressure law. Journal of Geophysical Research B, Solid Earth and Planets 106, 19339–19353.

Laloui L. and Nuth M. (2005). An introduction to the constitutive modelling of unsaturated soils. European Journal of Civil Engineering 9, No. 5–6, 651–670.

Laloui L., Ferrari A. and Bosch J. A. (2020). Bentonite clay barriers in nuclear waste repositories eds. J. S. McCartney and I. Tomac. E3S Web of Conferences 205, 01003.

Lambe R. and Whitman V. (1969). Soil mechanics. Wiley.

Langmi H. W., Book D., Walton A., Johnson S. R., Al-Mamouri M. M., Speight J. D., Edwards P. P., Harris I. R. and Anderson P. A. (2005). Hydrogen storage in ion-exchanged zeolites. Journal of Alloys and Compounds vol. 404–406, 637–642.

Langmi H. W., Ren J., North B., Mathe M. and Bessarabov D. (2014). Hydrogen storage in metal-organic frameworks. A review. Electrochimica Acta, 128(2014), 368–392. https://doi.org/10.1016/j.electacta.2013.10.190

Lanyon G. W. (2018). Current understanding of self-sealing of clay-rich rocks for deep geological disposal. Nagra Arbeitsbericht, NAB 18-46, Nagra, Switzerland.

Lanyon G. W., Marschall P., Trick T., de La Vaissière R., Shao H. and Leung H. (2014). Self-sealing experiments and gas injection tests in a backfilled microtunnel of the Mont Terri URL. Geological Society, London, Special Publications 400 (1), 93–106.

Lassin A., Dymitrowska M. and Azaroual M. (2011). Hydrogen solubility in pore water of partially saturated argillites. Application to Callovo-Oxfordian clayrock in the context of a nuclear waste geological disposal. Physics and Chemistry of The Earth - 36 (17–18), 1721–1728.

Le T. T. (2008). Comportement thermo-hydro-mécanique de l'argile de Boom. PhD, Ecole Nationale des Ponts et Chaussées

Le T. T., Delage P., Cui Y.J., Tang a M., Lima A., Romero E.E., Gens A. and Li X.L. (2008). Water retention properties of Boom clay . A comparison between different experimental techniques. In Unsaturated Soils. Advances in Geo-Engineering- Toll et al. (eds). Taylor & Francis Group, London, pp. 229–234.

Leddra M. J., Petley D. N. and Jones M. E. (1992). Fabric changes induced in a cemented shale through consolidation and shear. In The 33rd U.S. symposium on Rock Mechanics. American Rock Mechanics Association.

Lee T.B., Kim D., Jung D.H., Choi S.B., Yoon J.H., Kim J., Choi K. and Choi S.-H. (2007). Understanding the mechanism of hydrogen adsorption into metal organic frameworks. Catalysis Today, v. 120, p. 330-335

Lefort P. (2014). Etude des déplacements eau-gaz dans les argilites du callovo-oxfordien à l'aide de la théorie de la percolation en gradient. PhD thesis, Université de Toulouse.

Lenormand R., Touboul E. and Zarcone C. (1988). Numerical models and experiments on immiscible displacements in porous media. Journal of Fluid Mechanics 189, 165–187.

Leupin O.X., Zeyer J., Cloet V., Smith P. Bernier-Latmani R., Marschall P., Papafotiou A. and Schwyn B. (2016a). An assessment of the fate of L/ILW repository generated gas. Nagra Technical Report NTB 16-05. Nagra, Wettingen, Switzerland.

Leupin O.X., Smith P., Marschall P., Johnson L., Savage D., Cloet V. and Schneider J. (2016b). High-level waste repository-induced effects. Nagra Technical Report NTB 14-13, Nagra, Switzerland.

Levasseur S., Charlier R., Frieg B. and Collin F. (2010) Hydro-mechanical modelling of the excavation damaged zone around an underground excavation at Mont Terri Rock Laboratory. International Journal of Rock Mechanics and Mining Sciences. 47, n°3, 414-425.

Leverett M.C. (1941). Capillary behaviour in porous solids. Trans. AIME 142, 159–172.

EURAD (Deliverable n° 6.1) – Initial State of the Art on Gas Transport in Clayey Materials
Dissemination level: PU
Date of issue of this report: 17/11/2021

Page 350

Lewis R. W. and Schrefler B. A. (1998). The finite element method in the static and dynamic deformation and consolidation of porous media. John Wiley and Sons.

Li Y. and Yang R. T. (2007). Gas Adsorption and Storage in Metal−Organic Framework MOF-177. Langmuir 23 (26), 12937–12944.

Lima A. (2011). Thermo-hydro-mechanical Behaviour of Two Deep Belgian Clay Formations. Boom and Ypresian Clays. PhD, Universitat Politècnica de Catalunya.

Lima A., Romero E. and Piña Y. (2011). Water retention properties of two deep tertiary clay formations within the context of radioactive waste disposal. In VII Brazilian Symposium on Unsaturated Soil, Gitirana, G.F.N. Jr., Mascarenha, M.M.A. & Camapum de Caralho, J. (eds.). Editoria Kelps, Goiania, Prienópolis, Goiania, Brazil. 315–321.

Liu H.H., Rutqvist J. and Berryman J.G. (2009). On the relationship between stress and elastic strain for porous and fractured rock. International Journal of Rock Mechanics and Mining Sciences, 46, pp.289–296.

Liu H.H., Rutqvist J. and Birkholzer J.T. (2011). Constitutive relationships for elastic deformation of clay rock. Data analysis. Rock Mechanics and Rock Engineering, 44, pp.463–468.

Liu J. F. (2013). Etanchéité de l'interface argilite-bentonite re-saturée et soumise à une pression de gaz, dans le contexte du stockage profond de déchets radioactifs. PhD thesis, Ecole Centrale de Lille.

Liu J. F., Davy C. A., Talandier J. and Skoczylas F. (2014a). Effect of gas pressure on the sealing efficiency of compacted bentonite-sand plugs. Journal of Contaminant Hydrology 170, 10–27.

Liu J. F., Skoczylas F. and Liu J. (2014b). Experimental research on water retention and gas permeability of compacted bentonite/sand mixtures. Soils and Foundations 54 (5), 1027–1038.

Lloret A., Villar M. V., Sánchez M., Gens A., Pintado X. and Alonso E. E. (2003). Mechanical behaviour of heavily compacted bentonite under high suction changes. Géotechnique 53 (1), 27–40.

Loret B. and Khalili N. (2000). A three-phase model for unsaturated soils. International Journal for Numerical and Analytical Methods in Geomechanics 24, No. 11, 893–927.

Lu R., Nagel T., Shao H., Kolditz O. and Shao H. (2018). Modeling of Dissolution-Induced Permeability Evolution of a Granite Fracture Under Crustal Conditions. Journal of Geophysical Research. Solid Earth 123 (7), 5609–5627.

Luckner L., van Genuchten M.Th. and Nielsen D. (1989). A consistent set of para-metric models for two-phase flow of immisable fluids in the subsurface. WRR, 25(19).

Luo X.R., Yan J.Z., Zhou B., Hou P., Wang W.and Vasseur G. (2008). Quantitative estimates of oil losses during migration, part II. measurement of the residual oil saturation in migration pathways. J. Pet. Geol. 31, 179-190.

Lux K.-H. and Rutenberg M. (2018). Vorprojekt - Internationales Benchmarking zur Verifizierung und Validierung von TH2M-Simulatoren insbesondere im Hinblick auf fluiddynamische Prozesse in Endlagersystemen (BenVaSim) . Abschlussbericht zum BMWi-Forschungsvorhaben . Zeitraum. 01.07.2016-30.04.2017. Lehrstuhl für Deponietechnik und Geomechanik, Technische Universität Clausthal.

Ma T., Wei C., Yao C. and Yi P. (2020). Microstructural evolution of expansive clay during drying–wetting cycle. Acta Geotechnica 15 (8), 2355–2366.

Macdonald D. D. (2011). The history of the Point Defect Model for the passive state: a brief review of film growth aspects. Eletrochimica Acta 56 (4), 1761–1772.

Madaschi A. and Laloui L. (2018). A stochastic approach to the modelling of gas transport in bentonite. In 7th International Conference on Unsaturated Soils. Hong Kong, China.

Mahjoub M., Rouabhi A., Tijani M., Granet S., M'Jahad S. and Talandier J. (2018). Numerical Study of Callovo-Oxfordian Argillite Expansion due to Gas Injection. . International Journal of Geomechanics 18.

Maillet A. (2012). Interactions argilite de Tournemire / fer métal en contexte in situ . résultats à 10 ans de contact. PhD thesis, Université de Poitiers.

Mainka J., Murad M. A., Moyne C. and Lima S. A. (2014). A modified effective stress principle for unsaturated swelling clays derived from microstructure. Vadose Zone Journal 13, 5.

Makurat A. and Gutiérrez M. (1996). Fracture flow and fracture cross-flow experiments. Proceed. SPE Annual Tech. Conf. and Exhibition, Denver, CO, SPE 36732, pp. 511-519.

Manca D. (2016), Gas Flow Propagation and related Chemo-Hydro-Mechanical Response of Sand Bentonite Mixture. Nagra Technical Report NTB 16-07, Nagra, Switzerland.

Manca D., Ferrari A. and Laloui L. (2016). Fabric evolution and the related swelling behaviour of a sand/bentonite mixture upon hydro-chemo-mechanical loadings. Géotechnique 66 (1), 41–57.

EURAD (Deliverable n° 6.1) – Initial State of the Art on Gas Transport in Clayey Materials
Dissemination level: PU
Date of issue of this report: 17/11/2021

Page 351

Marella M. and Tomaselli M. (2006). Synthesis of carbon nanofibers and measurements of hydrogen storage. Carbon 44 (8), 1404–1413.

Mariani S. and Perego U. (2003). Extended finite element method for quasi-brittle fracture. International Journal for Numerical Methods in Engineering 58 (1), 103–126.

Marinho F. A. M., Take W. A. and Tarantino A. (2009). Measurement of Matric Suction Using Tensiometric and Axis Translation Techniques. In Laboratory and Field Testing of Unsaturated Soils. (eds. Alessandro Tarantino, E. Romero, and Y.-J. Cui). Springer Netherlands, Dordrecht. 3–19. (Originally published in the journal Geotechnical and Geological Engineering, Volume 26, No. 6, 615–631).

Marschall P., Horseman S. and Gimmi T. (2005). Characterisation of gas transport properties of the Opalinus Clay, a potential host rock formation for radioactive waste disposal. Oil and Gas Science and Technology - Revue de l'IFP 60, 121–139.

Marschall P., Lanyon B., Gaus I. and Rüedi J. (2013). Gas transport processes at Mont Terri Test Site (EDZ and host rock) - Field results and conceptual understanding of self-sealing processes. European Commission, Euratom 7th Framework Programme. FORGE Report D4.16 – Final.

Marschall P., Keller L., Giger S.B. and Becker J. (2016). Microstructural insights in petrophysical characteristics of indurated clays. The Clay Minerals Society Workshop Lectures Series, Vol. 21 (2016), Chapter 14, 191–198

Martínez V., Abós H. and García-Siñeriz J. L. (2016). FEBEXe: final sensor data report (FEBEX 'in situ' experiment). Nagra. Arbeitsbericht NAB 16-19.

Masin D. and Khalili N. (2016). Swelling phenomena and effective stress in compacted expansive clays. Canadian Geotechnical Journal 53, 134–147.

Maurer H. and Spillmann T. (2014). HG-D Experiment. Active and passive seismic monitoring and imaging of gas injections. Mont Terri Technical Note 2014-93

Mayor J. C. and Velasco M. (2014). EB dismantling – Synthesis report. European Commission. Long-term Performance of Engineered Barrier Systems PEBS D2.1-8.

Mazurek M., Hurford A.J. and Leu W. (2006). Unravelling the multi-stage burial history of the Swiss Molasse Basin. integration of apatite fission track, vitrinite reflectance and biomarker isomerisation analysis. Basin Research 18(1). 27-50.

Mazurek M., Alt-Epping P., Bath A., Gimmi T., Waber T., Buschaert S., De Cannière P., De Craen M., Gautschi A., Savoye S., Vinsot A., Wemaere I. and Wouters L. (2011). Natural tracer profiles across argillaceous formations. Applied Geochemistry 26, 1035–1064.

Méheust Y., Lovoll G., Maloy K. and Schmittbuhl J. (2002). Interface scaling in a two-dimensional porous medium under combined viscous, gravity, and capillary effects. Phys. Rev. E. 66051603.

Melenk J. M. and Babuška I. (1996). The partition of unity finite element method. Basic theory and applications. Computer Methods in Applied Mechanics and Engineering 139 (1–4), 289–314.

Menaceur H., Delage P., Tang A. M. and Conil N. (2014). Auto-colmatage d'un plan de cisaillement dans l'argilite du Callovo-Oxfordien - Self sealing of shear plane in Callovo-Oxfordian claystone. In Journées Nationales de Géotechnique et de Géologie de l'Ingénieur JNGG2014. Beauvais.

Merrill L. S. (1994). Two-phase flow in fractures, PhD Thesis, University of Denver, Denver, Colorado, U.S.

Mertens J., Vandenberghe N., Wouters L. and Sintubin M. (2003). The Origin and Development of Joints in the Boom Clay Formation (Rupelian) in Belgium. Subsurface Sediment Mobilization 216, 309–321.

Mertens J., Bastiaens W. and Dehandschutter B. (2004). Characterisation of Induced Discontinuities in the Boom Clay Around the Underground Excavations (URF, Mol, Belgium). Applied Clay Science 26 (1–4), 413–428.

Miao X.-Y., Kolditz O. and Nagel T. (2019). Modelling thermal performance degradation of high and low-temperature solid thermal energy storage due to cracking processes using a phase-field approach. Energy Conversion and Management 180, 977–989.

Millington R. J. and Quirk J. P. (1961), Transport in porous media [in soil science], Trans. Int. Congr. Soil Sci., 7(1), 97–106

Minardi A. (2018). Hydro-mechanical characterization of gas shales and Opalinus Clay shale in partially saturated conditions. PhD Thesis No. 8315, École Polytechnique Fédérale de Lausanne, Switzerland

Minardi A., Ferrari A., Ewy R. and Laloui L. (2019). Gas shale water imbibition tests with controlled suction technique. In Energy Geotechnics. (eds. A. Ferrari and L. Laloui). Springer International Publishing, Cham. 250–257.

EURAD (Deliverable n° 6.1) – Initial State of the Art on Gas Transport in Clayey Materials
Dissemination level: PU
Date of issue of this report: 17/11/2021

Page 352

M'Jahad S. (2012). Etude de l'impact de la fissuration sur les propriétés de rétention d'eau et de transport de gaz des bétons, de l'argilite et des interfaces argilite/béton. Application au stockage géologique des déchets radioactifs (PhD thesis (in French)), Ecole Centrale de Lille and Université des Sciences et Technologie de Lille, France.

M'Jahad S., Davy C. Skoczylas F. and Talandier J. (2017) - Characterization of transport and water retention properties of damaged Callovo-Oxfordian claystone, Geological Society, London, Special Publications, 443 (1) 159-177

Moës N. and Belytschko T. (2002). Extended finite element method for cohesive crack growth. Engineering Fracture Mechanics 69 (7), 813–833.

Moës N., Dolbow J. and Belytschko T. (1999). A Finite Element Method for Crack Growth Without Remeshing. International Journal for Numerical Methods in Engineering 46 (1), 131–150.

Molinero Guerra A., Mokni N., Delage P., Cui Y.-J., Tang A. M., Aimedieu P., Bernier F. and Bornert M. (2017). In-depth characterisation of a mixture composed of powder/pellets MX80 bentonite. Applied Clay Science 135, 538–546.

Molinero Guerra A., Aimedieu P., Bornert M., Cui Y.-J., Tang A. M., Sun Z., Mokni N., Delage P. and Bernier F. (2018). Analysis of the structural changes of a pellet/powder bentonite mixture upon wetting by X-ray computed microtomography. Applied Clay Science 165, 164–169.

Mondelli C., Bardelli F., Vitillo J. G., Didier M., Brendle J., Cavicchia D. R., Robinet J.-C. and Charlet L. (2015). Hydrogen adsorption and diffusion in synthetic Na-montmorillonites at high pressures and temperature. International Journal of Hydrogen Energy 40 (6), 2698–2709.

Monfared M. (2011). Couplages température-endommagement-perméabilité dans les sols et les roches argileuses. PhD thesis, Ecole Nationale des Ponts et Chaussées.

Morgenroth J., Khan U. T. and Perras M. A. (2019). An overview of opportunities for machine learning methods in underground rock engineering design. Geosciences (Switzerland) 9 (12).

Mualem Y. (1976). A new model for predicting the hydraulic conductivity of unsaturated porous media. Water Resources Research 12 (3), 513–522.

Muñoz, J.J., Lloret, A., Alonso, E. (2003). "VE Experiment" - Laboratory Report. Characterization of hydraulic properties under saturated and non saturated conditions. VE Experiment Project Deliverable 4, EC contract FIKW-CT2001-00126.

Nagel T., Beckert S., Lehmann C., Gläser R. and Kolditz O. (2016). Multi-physical continuum models of thermochemical heat storage and transformation in porous media and powder beds – A review. Applied Energy 178, 323–345.

Nagra (2002a). Project Opalinus Clay. Safety Report. Demonstration of disposal feasibility (Entsorgungsnachweis) for spent fuel, vitrified high-level waste and long-lived intermediate-level waste. Nagra Tech. Ber. NTB 02-05.

Nagra (2002b). Projekt Opalinuston – Synthese der geowissenschaftlichen Untersuchungs-ergebnisse. Entsorgungsnachweis für abgebrannte Brennelemente, verglaste hochaktive sowie langlebige mittelaktive Abfälle. Nagra Tech. Rep. NTB 02-03. Nagra, Wettingen, Switzerland

Nagra (2004). Effects of post disposal gas generation in a repository for spent fuel, high level waste and long lived intermediate level waste sited in Opalinus Clay. Nagra Technical Report 04–06.

Nagra (2008). Effects of post-disposal gas generation in a repository for low- and intermediate-level waste sited in the Opalinus Clay of Northern Switzerland. Nagra Tech. Rep. NTB 08–07.

Nagra (2014a). SGT Etappe 2. Vorschlag weiter zu untersuchender geologischer Standortgebiete mit zugehörigen Standortarealen für die Oberflächenanlage. Dossier IV /Geomechanische Grundlagen. Nagra Technical Report NTB 14-02

Nagra (2014b). Modellhaftes Inventar für radioaktive Materialien – MIRAM 14. Nagra Technical Report NTB 14-04.

Nagra (2014c). SGT Etappe 2. Vorschlag weiter zu untersuchender geologischer Standortgebiete mit zugehörigen Standortarealen für die Oberflächenanlage. Charakteristische Dosisintervalle und Unterlagen zur Bewertung der Barrierensysteme. Technischer Bericht 14-03

Nagra (2016a). Production, consumption and transport of gases in deep geological repositories according to the Swiss disposal concept. Nagra Technical Report NTB 16-03

Nagra (2016b). Entsorgungsprogramm 2016 der Entsorgungspflichtigen. Nagra Technical Report NTB 16-01.

Nagra (2020). Milestone MS 58. Interim Experimental Design Report comprising a revised detailed work programme of Sub-tasks 3.1, 3.2 and 3.3 Work Package Gas, EURAD (European Joint Programme on Radioactive Waste Management)

EURAD (Deliverable n° 6.1) – Initial State of the Art on Gas Transport in Clayey Materials
Dissemination level: PU
Date of issue of this report: 17/11/2021

Page 353

Naish C.C., Balkwill P. H., O'Brien T. M., Taylor K. J. and Marsh G. P. (1991). The anaerobic corrosion of carbon steel in concrete. European Commission, EUR. Nuclear Science and Technology EUR 13663.

Navarro V., Yustres Á., Asensio L., la Morena G. D., González-Arteaga J., Laurila T. and Pintado X. (2017). Modelling of compacted bentonite swelling accounting for salinity effects. Engineering Geology 223, 48–58.

Neeft E.A.C. (2018). Summary of scientific progress achieved through CAST (D7.24). Carbon-14 Source Term. Work Package 7. Task 7.7. Final report. Cast-2018-D7.24. European Commission.

Nelson P. H. (2009). Pore-throat Sizes in Sandstones, Tight Sandstones, and Shales. AAPG bulletin 93 (3), 329–340.

Neuzil C. E. (1994). How Permeable Are Clays and Shales? Water Resources Research 30 (2), 145–150.

Nicholl M. J., Glass R. J. and Wheatcroft S. W. (1994). Gravity-drive infiltration instability in initially dry nonhorizontal fractures. Water Resources Research 30 (9), 2533–2546.

Noorishad J. and Tsang C.-F. (1996). ROCMAS simulator; A thermohydromechanical computer code. Developments in Geotechnical Engineering 79 (C), 551–558.

Norris S. (Editor) (2013). Synthesis Report. Updated Treatment of Gas Generation and Migration in the Safety Case1 - FORGE Report D1.5R.

Novello E. A. (1988). Geomechanics and the critical state, PhD thesis, Monash University

Nuth M. and Laloui L. (2008). Effective stress concept in unsaturated soils. clarification and validation of a unified framework. International Journal for Numerical and Analytical Methods in Geomechanics 32, No. 7, 771–801.

Olgaard D., Nuesch R. and Ural J. (1995). Consolidation of water saturated shales at great depth under drained conditions, 8th International Symposium on Rock Mechanics. In International Society for Rock Mechanics.

Olivella S. and Alonso E.E. (2008) Gas flow through clay barriers. Géotechnique. 58, n°3, 157-168

Olivella S., Carrera J., Gens A. and Alonso E. E. (1994). Non isothermal multiphase flow of brine and gas through saline media. Transport in Porous Media 15, No. 3, 271–293.

Olivella S., Gens A., Carrera J. and Alonso E.E. (1996). Numerical formulation for a simulator (CODE_BRIGHT) for the coupled analysis of saline media. Engineering Computations, 13(7), pp.87–112.

ONDRAF/NIRAS (2001). Technical Overview of the SAFIR2 report, ONDRAF/NIRAS report NIROND 2001-05E

ONDRAF/NIRAS (2013a). ONDRAF/NIRAS Research, Development and Demonstration Plan for the geological disposal of high-level and/or radioactive waste including irradiated fuel if considered as waste. State-of-the-art report as of December 2012. NIROND-TR 2013–12 E.

ONDRAF/NIRAS (2013b). Verkennende studie van de mogelijke gasproblematiek in geologische berging voor MOSAIK-containers als primaire bergingscolli. NIROND Note 2013–2421.

ONDRAF/NIRAS (2019a). Design and construction of the supercontainer for Category C waste (V3). Category B&C. Technical Report NIROND-TR 2017-11 E V3.

ONDRAF/NIRAS (2019b). Design and Construction of the Monolith B for Category B Waste (V3). Category B&C. Technical Report NIROND-TR 2017-10 E V3.

ONDRAF/NIRAS (2020). Design and Construction of the Geological Disposal Facility for Category B and Category C Wastes (V3). Technical Report NIROND-TR 2017-12 E V3. Category B&C. Brussels, Belgium.

Ortiz L., Volckaert G., De Cannière P., Put M., Horseman S. T., Harrington J. F., Impey M. and Einchcomb S. (1994). MEGAS - Modelling and Experiments on Gas Migration in Repository Host-rocks. EU PEGASUS Meeting Nuclear Science and Technology Series.

Ortiz L., Volckaert G., De Cannière P., Put M, Sen SA, Horseman ST, Harrington JF, Impey M and Einchcomb S (1997). MEGAS Modelling and experiments on gas migration in repository host rocks - Phase II. Nuclear Science and Technology. European Commission, EUR. EUR 17453.

Ortiz L., Impey M. and Einchomb S. (1998) Characterization of Gas Flow in Boom Clay, a Low Permeability Plastic Rock. Proceedings of the Fluid Flow through Faults and Fractures in Argillaceous Formations – Joint NEA/EC Workshop, Berne, Switzerland, 10-12 June 1996.

Ortiz L., Volckaert G. and Mallants D. (2002). Gas Generation and Migration in Boom Clay, a Potential Host Rock Formation for Nuclear Waste Storage. Engineering Geology 64, 287–296.

Palomino G.T., Carayol M.R.L. and Arean C.O. (2006). Hydrogen adsorption on magnesium exchanged zeolites. Journal of Materials Chemistry, v. 16, p. 2884-2885.

Panday S. and Corapcioglu M. Y. (1989). Reservoir transport equations by compositional approach. Transport in Porous Media 4, No. 4, 369–393.

EURAD (Deliverable n° 6.1) – Initial State of the Art on Gas Transport in Clayey Materials
Dissemination level: PU
Date of issue of this report: 17/11/2021

Page 354

Papafotiou A. and Senger R. (2014). Sensitivity analyses of gas release from a L/ILW reposi¬tory in the Opalinus Clay in the candidate siting regions of Northern Switzerland. Nagra Working Report NAB 13-92.

Papafotiou A. and Senger R. (2016a). Sensitivity analyses of gas release from a L/ILW reposi¬tory in the Opalinus Clay including the microbial consumption of hydrogen. Nagra Working Report NAB 16-07.

Papafotiou A. and Senger R. (2016b). Sensitivity analyses of gas release from a SF/HLW reposi¬tory in the Opalinus Clay including the microbial consumption of hydrogen. Nagra Working Report NAB 16-08.

Parisio F., Naumov D., Kolditz O. and Nagel T. (2018). Material forces. An insight into configurational mechanics. Mechanics Research Communications 93, 114–118.

Parisio F., Vilarrasa V., Wang W., Kolditz O. and Nagel T. (2019a). The risks of long-term re-injection in supercritical geothermal systems. Nature Communications 10 (1).

Parisio F., Vinciguerra S., Kolditz O. and Nagel T. (2019b). The brittle-ductile transition in active volcanoes. Scientific Reports 9 (1).

Parisio F., Tarokh A., Makhnenko R., Naumov D., Miao X.-Y., Kolditz O. and Nagel T. (2019c). Experimental characterization and numerical modelling of fracture processes in granite. International Journal of Solids and Structures 163, 102–116.

Parker J.C. (1989). Multiphase flow and transport in porous media. Rev. GeoPhys. 27, 311-328.

Pastusek P., Payette G., Shor R., Cayeux E., Aarsnes U. J., Hedengren J., Menand S., Macpherson J., Gandikota R., Behounek M., Harmer R., Detournay E., Illerhaus R. and Liu Y. (2019). Creating open source models, test cases, and data for oilfield drilling challenges. In SPE/IADC Drilling Conference, Proceedings.

Patchkovskii S., Tse J.S., Yurchenko S.N., Zhechkov L., Heine T. and Seifert G. (2005). Graphene nanostructures as tunable storage media for molecular hydrogen. Proceedings of the National Academy of Sciences of the United States of America, v. 102, p. 10439-10444.

Paul B., Faivre M., Massin P., Giot R., Colombo D., Golfier F. and Martin M. (2018). 3D coupled HM–XFEM modeling with cohesive zone model and applications to non-planar hydraulic fracture propagation and multiple hydraulic fractures interference. Computer Methods in Applied Mechanics and Engineering 342, 321–353.

Pazdniakou A. and Dymitrowska M. (2018). Migration of Gas in Water Saturated Clays by Coupled Hydraulic-Mechanical Model. Geofluids 2018, 1–25.

Pazdniakou A., Tinet A.-J., Golfier F., Kalo K., Gaboreau S. and Gaire P. (2018). Numerical efficiency assessment of the lattice Boltzmann model for digital nano-porous rock applications. Advances in Water Resources 121, 44–56.

Philip J. R. and de Vries D. A. (1957). Moisture movement in porous materials under temperature gradients. Eos, Transactions American Geophysical Union 38, No. 2, 222–232.

Phung Q.T., Maes N. and Jacops E. (2019). Diffusion of dissolved gases in saturated cementitious materials. Does the size matter?, 15th International Congress on the Chemistry of Cement, Prague, Czech Republic.

Pintado X., Ledesma A. and Lloret A. (2002). Backanalysis of thermohydraulic bentonite properties from laboratory tests. Engineering Geology 64 (2–3), 91–115.

Pintado X., Mamunul H. M. and Martikainen J. (2013). Thermo-hydro-mechanical tests of buffer material. POSIVA. 12-49.

Plötze M. and Weber H.P. (2007). ESDRED. Emplacement tests with granular bentonite Wyoming. Laboratory results from ETH Zürich. Nagra Arbeitsber. NAB 07-24. Nagra, Wettingen.

Poller A., Mayer G. and Croisé J. (2007) . Two-phase Flow Analysis of Gas Tests in Opalinus Clay Core Specimen. Complementary Analysis. Mont Terri TN 2007-01.

Poller A., Mayer G. and Croisé J. (2008). Hydrogeologic Analyses and Synthesis (HA) Experiment). Two-phase flow analysis of gas test in Opalinus Clay Core Specimen. Complementary Analysis. Mont Terri Technical report TR 2007-01. St-Ursanne, Switzerland.

Poller A., Mayer G., Darcis M. and Smith P. (2016). Modelling of gas generation in deep geological repositories after closure. Nagra Tech. Rep. NTB 16-04

Popp T., Rölke C. and Salzer K. (2013). Role of interfaces in bentonite-block assemblies as favoured pathways for gas transport. In Gas Generation and Migration International Symposium and Workshop 5th to 7th February 2013 Luxembourg.

Popp T., Rölke C. and Salzer K. (2014). Hydromechanical properties of bentonite-sand block assemblies with interfaces in engineered barrier systems. Geological Society, London, Special Publications 415, 19–33.

EURAD (Deliverable n° 6.1) – Initial State of the Art on Gas Transport in Clayey Materials
Dissemination level: PU
Date of issue of this report: 17/11/2021

Page 355

Prausnitz J., Lichtenthaler R. and de Azevedo E. (1999). Molecular Thermodynamics of Fluid Phase Equilibria, third ed. Prentice Hall, New Jersey.

Pruess K., Oldenburg C. and Moridis G. (1999). TOUGH2 user's guide, version 2. Report LBL-43134. Lawrence Berkeley Laboratories, Berkeley, United States.

Pusch R. and Forsberg T. (1983). Gas Migration through Bentonite Clay. Svensk Karnbranslehantering AB. SKB Technical Report 83-71.

Pusch R. and Hökmark H. (1990). Basic model of water- and gas-flow through smectite clay buffers. Engineering Geology 28 (3–4), 379–389.

Pusch R., Ranhagen L. and Nilsson K. (1985). Gas Migration through Mx-80 Bentonite. Nagra. Technical Report NTB 85-36.

Ramirez-Cuesta A.J. and Mitchell P.C.H. (2007). Hydrogen adsorption in a copper ZSM5 zeolite. An inelastic neutron scattering study. Catalysis Today, v. 120, p. 368-373.

Raude S., Laigle F., Giot R. and Fernandes R. (2016). A unified thermoplastic/viscoplastic constitutive model for geomaterials. Acta Geotechnica 11 (4), 849–869.

Rebour V., Billiotte J., Deveughele M., Jambon A. and le Guen C. (1997). Molecular diffusion in water-saturated rocks. A new experimental method. Journal of Contaminant Hydrology 28, 71-93.

Reitsma S. and Kueper B. H. (1994). Laboratory measurement of capillary pressure-saturation relationships in a rock fracture. Water Resources Research 30 (4), 865–878.

Rieke H. H. and Chilingarian G. V. (1974). Compaction of argillaceous sediments., Elsevier.

Rink K., Bilke L., Raith F., Zänker S., Jaeggi D., Kunz H., Maßmann J., Naumov D., Schefer S., Scheuermann G., Shao H., Wang W. Q., Ziefle G., Bossart P., Nussbaum C., Nagel T. and Kolditz (2020). A Virtual Exploration of the Underground Rock Laboratory Mont Terri. EUROVIS 2020, Eurographics Proceedings, Norrköping, Sweden.

Robinet J.C. (2008). Minéralogie, porosité, et diffusion des solutes dans l'argilite du Callovo-Oxfordien de Bure (Meuse/Haute Marne, France) de l'échelle centimétrique à micrométrique. PhD thesis. Université de Poitiers. France.

Robinet J.C., Yven B., Coelho D. and Talandier J. (2012a). Les distributions de tailles de pores dans les argilites du Callovo-Oxfordien de l'Est de la France. In. Skoczylas, F., Davy, C.A., Agostini, F., Burlion, N. (Eds.) Transfert 2012, Colloque national sur les propriétés de transfert des géomatériaux, Lille, 20-22 Mars 2012. - ISBN. 978-2-915913-28-6, pp. 263-272.

Robinet J.C., Sardini P., Coelho D., Parneix J.-C., Prêt D., Sammartino S., Boller E. and Altmann S. (2012b). Effects of mineral distribution at mesoscopic scale on solute diffusion in a clay-rich rock. Example of the Callovo-Oxfordian mudstone of Bure (France), Water Ressources Research (48), W05554

Rodwell W. R. (2000). Research into gas generation and migration in radioactive waste repository systems (PROGRESS Project). European Commission. Nuclear Science and Technology EUR 19133 EN.

Rodwell W. R. and Nash P.J. (1992) Mechanisms and Modelling of Gas Migration from Deep Radioactive Waste Repositories. Nirex Safety Study Report NSS/R250, June 1992.

Rodwell W. R., Harris A. W., Horseman S. T., Lalieux P., Muller W., Ortiz Amaya L. and Preuss K. (1999). Gas migration and two-phase flow through engineered and geological barriers for a deep repository for radioactive waste. Joint EC/NEA status report. European Commission. EUR 19122EN.

Rodwell W. R., Lineham T. R. and Gardiner M. P. (2000). Gas migration in the geosphere. review of the work undertaken by the Nirex Safety Assessment Research Programme. AEA. AEA Technology Report AEAT/R/ENV/0295.

Rodwell W. R., Hoch A. and Swift B. (2003a). The Modelling of Gas Migration through Compacted Bentonite Buffers in Radioactive Waste Repositories. The Work of the GAMBIT Club. MRS Proceedings 807 (709).

Rodwell W. R., Norris S., Cool W., Cunado M., Johnson L., Mäntynen M., Müller W., Sellin P., Snellam M., Talandier J., Vieno T. and Vines S. (2003). A thematic network on gas issues in safety assessment of deep repositories for radioactive waste (Gasnet). European Commission, Nuclear Science and Technology. Final Report EUR 20620 EN.

Romero E. (1999), Characterisation and thermo-hydro-mechanical behaviour of unsaturated Boom clay. an experimental study, Ph.D. Thesis, Universitat Politècnica de Catalunya, Barcelona, Spain

Romero E. and Gómez R. (2013). Water and air permeability tests on deep core samples from Schlattingen SLA-1 borehole. Nagra Arb. Ber. NAB 13-51. Nagra, Wettingen, Switzerland.

EURAD (Deliverable n° 6.1) – Initial State of the Art on Gas Transport in Clayey Materials
Dissemination level: PU
Date of issue of this report: 17/11/2021

Page 356

Romero E. and Gonzalez-Blanco L. (2015). Complementary water and air permeability tests on core samples from Schlattingen SLA-1 borehole. NAGRA Arbeitsbericht NAB 15-06.

Romero E. and Simms P. H. (2008). Microstructure Investigation in Unsaturated Soils. A Review with Special Attention to Contribution of Mercury Intrusion Porosimetry and Environmental Scanning Electron Microscopy. Geotechnical and Geological Engineering 26 (6), 705–727.

Romero E., Gens A. and Lloret A. (1999). Water permeability, water retention and microstructure of unsaturated compacted Boom clay. Engineering Geology 54 (1–2), 117–127.

Romero E., Alonso E. E. and Knobelsdorf J. (2002). GMT/IR 01-06. laboratory tests on compacted sand- bentonite buffer material for the GMT emplacement project. Nagra.

Romero E., García I. and Alonso E. E. (2003). GMT/IR 02-02. laboratory gas tests on compacted sand- bentonite buffer material used in the GMT in-situ emplacement. Nagra.

Romero E., Della Vecchia G. and Jommi C. (2011). An insight into the water retention properties of compacted clayey soils. Géotechnique 61 (4), 313–328.

Romero E., Senger R. and Marschall P. (2012). Air Injection Laboratory Experiments on Opalinus Clay. Experimental techniques. 3rd EAGE Shale Workshop, Barcelona, Spain, 23-25 January 2012, Results and Analyses.

Romero E., Alvarado C., Lloret A. and Mirsalehi S. (2017). Laboratory tests on the post mortem hydro-mechanical characterisation of FEBEX bentonite. CIMNE-UPC-GEOLAB.

Roscoe K.H. and Burland J. B. (1968). On the generalized stress-strain behaviour of the "wet" clay. In Engineering plasticity (Heyman, J. and Leckic, F., Eds.), Cambridge, UK, pp. 535–609.

Roscoe K.H., Schofield A.N. and Wroth C.P. (1958). On the yielding of soils, Geotechnique, 8, 22–53.

Rousset G. (1988). Comportement mécanique des argiles profondes, application au stockage de déchets radioactifs. PhD thesis, Ecole Nationale des Ponts et Chaussées.

Rozhko A. Y. (2016). Two-phase fluid-flow modeling in a dilatant crack-like pathway. Journal of Petroleum Science and Engineering 146, 1158–1172.

Rubel A., Sonntag C., Lippmann J., Pearson F. and Gautschi A. (2002). Solute transport in formations of very low permeability. Profiles of stable isotope and dissolved noble gas contents of pore water in the Opalinus Clay, Mont Terri, Switzerland. Geochimica Et Cosmochimica Acta 66, 1311-1321.

Rutter E. H. and Mecklenburgh J. (2017). Hydraulic conductivity of bedding-parallel cracks in shale as a function of shear and normal stress. Geological Society, London, Special Publications 454 (1), 67–84.

RWM (2016a). Geological Disposal. Gas Status Report issue 2. Radioactive Waste Management. NDA report DSSC/455/01.

RWM (2016b). Geological Disposal. Geosphere Status Report issue 2. Radioactive Waste Management. DSSC/453/01.

RWM (2016c). Geological Disposal. Generic Environmental Safety Case Main Report. Radioactive Waste Management. RWM Report DSSC/203/01.

Saâdi Z., Dymitrowska M., Deleruyelle F. and Marsal F. (2020). An evaluation model of the impact of hydrogen "piston effect" on water displacement in a deep geological disposal of radioactive waste. Environmental Earth Sciences 79 (18), 434.

Sakintuna B., Lamari-Darkrim F. and Hirscher M. (2007). Metal hydrides for solid hydrogen storage. A review. International Journal of Hydrogen Energy, v. 32, p. 1121-1140

Saltelli A. and Tarantola S. (2002). On the relative importance of input factors in mathematical models. Safety assessment for nuclear waste disposal. Journal of the American Statistical Association 97 (459), 702–709.

Saltelli A., Annoni P., Azzini I., Campolongo F., Ratto M. and Tarantola S. (2010). Variance based sensitivity analysis of model output. Design and estimator for the total sensitivity index. Computer Physics Communications 181 (2), 259–270.

Sammartino S., Bouchet A., Prêt, D., Parneix, J.-C. and Tevissen E. (2003) Spatial distribution of porosity and minerals in clay rocks from the Callovo-Oxfordian formation (Meuse / Haute Marne, Eastern France) implications on ionic species diffusion and rock sorption capability, Applied Clay Science 23, p. 157-166

Sánchez M., Gens A. and Guimarães L. (2005). A double structure generalised plasticity model for expansive materials. International Journal for Numerical and Analytical Methods in Geomechanics 29, No. 8, 751–787.

Sánchez M., Gens A., Villar M. V. and Olivella S. (2016). Fully Coupled Thermo-Hydro-Mechanical Double-Porosity Formulation for Unsaturated Soils. International Journal of Geomechanics 16 (6), D4016015-1-D4016015-17.

EURAD (Deliverable n° 6.1) – Initial State of the Art on Gas Transport in Clayey Materials
Dissemination level: PU
Date of issue of this report: 17/11/2021

Page 357

Sander R. (2015). Compilation of Henry's law constants (version 4.0) for water as solvent. Atmospheric Chemistry and Physics 15 (8), 4399–4981.

Santos J. E., Xu D., Jo H., Landry C. J., Prodanović M. and Pyrcz M. J. (2020). PoreFlow-Net. A 3D convolutional neural network to predict fluid flow through porous media. Advances in Water Resources 138.

Savoye S., Page J., Puente C., Imbert C. and Coelho D. (2010). New experimental approach for studying diffusion through an intact and unsaturated medium: a case study with Callovo-Oxfordian argillite. Environmental Science & Technology 44 (10), 3698–3704.

Savoye S., Beaucaire C., Fayette A., Herbette M. and Coelho D. (2012). Mobility of cesium through the Callovo-Oxfordian claystones under partially saturated conditions. Environmental Science & Technology 46 (5), 2633–2641.

Savoye S., Lefevre S., Fayette A. and Robinet J.-C. (2017). Effect of water saturation on the diffusion/adsorption of 22Na and cesium onto the Callovo-Oxfordian claystones. Geofluids 2017, 17.

Schlömer S. and Krooss B. M. (1997). Experimental characterisation of the hydrocarbon sealing efficiency of cap rocks. Marine and Petroleum Geology 14 (5), 565–580.

Schmertmann J.H. (2012). New concepts for the mobilization of the components of shear resistance in clay. Norwegian Geotechnical Institute, Oslo. Publication 208. 48p.

Schüth F., Bogdanovic B. and Felderhoff M. (2004). Light metal hydrides and complex hydrides for hydrogen storage. Chemical Communications, p. 2249-2258.

Segura J.M. and Carol I. (2008) Coupled HM analysis using zero-thickness interface elements with double nodes. Part I. Theoretical model. International Journal for Numerical and Analytical Methods in Geomechanics. 32, 2083-2101.

Seiphoori A. (2014). Thermo-hydro-mechanical characterisation and modelling of MX-80 granular bentonite. PhD thesis, Ecole Polytechnique Fédérale de Lausanne.

Seiphoori A. (2015). Thermo-hydro-mechanical characterisation and modelling of Wyoming granular bentonite. Nagra Technical Report NTB 15-05, Nagra, Switzerland.

Seiphoori A. (2019). Self-sealing of fractures in Opalinus Clay. experiments and a conceptual framework for quantitative assessments. Nagra Arbeitsbericht NAB 19-07

Seiphoori A., Ferrari A. and Laloui L. (2014). Water retention behaviour and microstructural evolution of MX-80 bentonite during wetting and drying cycles. Géotechnique 64 (9), 721–734.

Sellin P. (editor) (2014). Experiments and modelling on the behaviour of EBS. FORGE Report D3.38. 426pp.

Sellin P. and Leupin O. X. (2013). The use of clay as an engineered barrier in radioactive-waste management – a review. Clays and Clay Minerals 61 (6), 477–498.

Senger R., Enachescu C., Doe T., Distinguin M., Delay J. and Frieg B. (2006) Design and analysis of a gas threshold pressure test in a low permeability clay formation at Andra's underground research laboratory, Bure. PROCEEDINGS, TOUGH Symposium 2006 Lawrence Berkeley National Laboratory, Berkeley, California, May 15–17, 2006

Senger R., Lanyon B., Marschall P., Vomvoris S. and Fujiwara A. (2008). Numerical Modelling of the Gas Migration Test at the Grimsel Test Site (Switzerland). Nuclear Technology Vol. 164, Nov. 2008.

Senger R., Papafotiou A. and Marschall P. (2013). Gas related property distributions in the pro¬posed host rock formations of the candidate siting regions in Northern Switzerland and in the Helvetic Zone. Nagra Working Report NAB 13-83.

Senger R., Romero E., Ferrari A. and Marschall P. (2014). Characterization of gas flow through low-permeability claystone. laboratory experiments and two-phase flow analyses. Geological Society, London, Special Publications (Online), 400, pp.531–543. https://doi.org/10.1144/SP400.15

Senger R., Romero E. and Marschall P. (2015). Modeling of gas migration through low permeability clay using information on pressure and deformation from fast air injection tests. In PROCEEDINGS, TOUGH Symposium 2012 Lawrence Berkeley National Laboratory, Berkeley, California, September 28-30, 2015. pp. 1–5.

Seyedi D. M., Armand G. and Noiret A. (2017). "Transverse Action" – A model benchmark exercise for numerical analysis of the Callovo-Oxfordian claystone hydromechanical response to excavation operations. Computers and Geotechnics 85, 287–305.

Shackelford C. D., Daniel D. E. and Liljestrand H. M. (1989). Diffusion of inorganic chemical species in compacted clay soil. Journal of Contaminant Hydrology 4, No. 3, 441–473.

EURAD (Deliverable n° 6.1) – Initial State of the Art on Gas Transport in Clayey Materials
Dissemination level: PU
Date of issue of this report: 17/11/2021

Page 358

Shao H., Hesser J., Kolditz O. and Wang W. (2019). Hydraulic characterisation of clay rock under consideration of coupled THM properties. Environmental Science and Engineering. https://doi.org/10.1007/978-981-13-2227-3_4.

Shaw R. (ed.) (2013). Gas Generation and Migration, International Symposium and Workshop. In Fault and Top Seals. From Pore to Basin Scale.

Shehata A., Fall M., Detellier C. and Alzamel M. (2020). Effect of groundwater chemistry and temperature on swelling and microstructural properties of sand-bentonite for barriers of radioactive waste repositories. Bulletin of Engineering Geology and the Environment 80, 1857–1873.

Sheng D. (2011). Review of fundamental principles in modelling unsaturated soil behaviour. Computers and Geotechnics 38, No. 6, 757–776.

Sheng D., Sloan S. W. and Gens A. (2004). A constitutive model for unsaturated soils. thermomechanical and computational aspects. Computational Mechanics 33, 453–465.

Sheng D., Gens A., Fredlund D. G. and Sloan S. W. (2008a). Unsaturated soils. From constitutive modelling to numerical algorithms. Computers and Geotechnics 35, No. 6, 810–824.

Sheng D., Fredlund D. G. and Gens A. (2008b). A new modelling approach for unsaturated soils using independent stress variables. Canadian Geotechnical Journal 345, No. 4, 511–534.

Shimura T., Takahashi S., Nishimura M., Koga K. and Owada H. (2017). Study on gas migration behavior through bentonite buffer material, 6th East Asia Forum on Radwaste Management Conference, November 27-29, 2017.

Skempton A. W. (1970). First-time slides in over-consolidated clays. Geotechnique 20, 320–324.

Small J. (ed.) (2019). Final synthesis report for MIND WP1. Deliverable D1.9. Microbiology in Nuclear Waste Disposal. European Commission.

Smart N. R., Rance A. P., Nixon D. J., Fennell P. A. H., Reddy B. and Kursten B. (2017). Summary of studies on the anaerobic corrosion of carbon steel in alkaline media in support of the Belgian supercontainer concept. Corrosion Engineering, Science and Technology 52 (S1), 217–226.

Sobol I. M. (2001). Global sensitivity indices for nonlinear mathematical models and their Monte Carlo estimates. Mathematics and Computers in Simulation 55 (1–3), 271–280.

Song Y., Davy C. A., Troadec D., Blanchenet A.-M., Skoczylas F., Talandier J. and Robinet J. C. (2015). Multi-scale pore structure of COx claystone. Towards the prediction of fluid transport. Marine and Petroleum Geology 65, 63–82.

Song Y., Davy C. A. and Troadec D. (2016). Gas breakthrough pressure (GBP) through claystones: correlation with FIB/SEM imaging of the pore volume. Oil and Gas Science and Technology-Revue d'IFP Energies nouvelles 71 (51).

Sridharan A. and Venkatappa R. G. (1973). Mechanisms controlling volume change of saturated clays and the role of the effective stress concept. Géotechnique 23, No. 3, 359–382.

Srinivasan S., Karra S., Hyman J., Viswanathan H. and Srinivasan G. (2019). Model reduction for fractured porous media. a machine learning approach for identifying main flow pathways. Computational Geosciences 23 (3), 617–629.

Stammose D., Marcillaud B., Berger L. and Raboin M. (2013). Hydrogen production by iron corrosion under gamma-radiation, oral presentation and extended abstract. In Gas Generation and Migration, International Symposium and Workshop. Luxembourg.

Stark T.D. and Eid H.T. (1994). Drained residual strength of cohesive soils. Journal of Geotechnical Engineering 120/5, 856–871.

Steefel C. I., Appelo C. A. J., Arora B., Jacques D., Kalbacher T., Kolditz O., Lagneau V., Lichtner P. C., Mayer K. U., Meeussen J. C. L., Molins S., Moulton D., Shao H., Šimůnek J., Spycher N., Yabusaki S. B. and Yeh G. T. (2015). Reactive transport codes for subsurface environmental simulation. Computational Geosciences 19 (3), 445–478.

Stefanou G. (2009). The stochastic finite element method. Past, present and future. Computer Methods in Applied Mechanics and Engineering 198 (9–12), 1031–1051.

Steurbaut E., Dupuis C. and Jacobs P. (2003). Field Guide to the Ypresian Stratotype. Symposium on the Paleogene – Preparing for Modern Life and Climate, IUGS - ICS, Leuven.

Sultan N. (1997). Etude du comportement thermo-mécanique de l'Argile de Boom . expériences et modélisation. PhD, Ecole Nationale des Ponts et Chaussées.

EURAD (Deliverable n° 6.1) – Initial State of the Art on Gas Transport in Clayey Materials
Dissemination level: PU
Date of issue of this report: 17/11/2021

Page 359

Svensson D., Dueck A., Nilsson U., Olsson S., Sandén T., Lydmark S., Jägerwall S., Pedersen K. and Hansen S. (2011). Alternative buffer material, status of the ongoing laboratory investigation of reference materials and test package 1. SKB. Technical Report TR-11-06.

Tanai K., Kanno T. and Gallé C. (1997). Experimental study of gas permeabilities and breakthrough pressures in clays. In Proceedings of the Fall Meeting of the Material Research Society, Boston, USA. 995–1002.

Taron J., Hickman S., Ingebritsen S. E. and Williams C. (2014). Using a fully coupled, open-source THM simulator to examine the role of thermal stresses in shear stimulation of enhanced geothermal systems. In 48th US Rock Mechanics / Geomechanics Symposium 2014. 525–533.

Ten Veen J. (2015). Future evolution of the geological and geohydrological properties of the geosphere. OPERA-PU-TNO412.

Terzaghi K. (1936). The shearing resistance of saturated soils and the angle between the planes of shear. In Proceedings of the First International Conference on Soil Mechanics and Foundation Engineering, Cambridge, UK, pp. 54–56.

Terzaghi K. (1943). Theoretical soil mechanics. John Wiley and Sons.

Terzaghi K., Peck R. and Mesri G. (1996). Soil Mechanics In Engineering Practice. Third edition., John Wiley and sons, inc.

Thomas K. M. (2007). Hydrogen adsorption and storage on porous materials. Catalysis today, 120(3-4), 389-398

Thomas H.R. and He Y. (1995). Analysis of coupled heat, moisture and air transfer in a deformable unsaturated soil. Géotechnique. 45, n°4, 677-689.

Tindall J. A. and Kunkel J. R. (1999). Unsaturate zone hydrology for scientists and engineers., Prentice Hall, Upper Saddle River, New Jersey.

Tonon F., Bernardini A. and Mammino A. (2000). Reliability analysis of rock mass response by means of Random Set Theory. Reliability Engineering and System Safety 70 (3), 263–282.

Towler G. and Bond A. (2011). Investigation of gas generation and resaturation issues. Input to EC FORGE project. Quintessa report QRS-1378ZC-R2, Version 2.0.

Truche L., Joubert G., Dargent M., Martz P., Cathelineau M., Rigaudier T. and Quirt D. (2018). Clay minerals trap hydrogen in the Earth's crust. Evidence from the Cigar Lake uranium deposit, Athabasca. Earth and Planetary Science Letters 493, 186–197.

Tsang C. and Bernier F. (2005). Definitions of excavation disturbed zone and excavation damaged zone. In Davies C and Bernier F. (eds.). Impact of the excavation disturbed or damaged zone (EDZ) on the performance of radioactive waste geological repositories, EUR 21028 EN. 5-8, Brussels (European Commission)

Tsang C., Bernier F. and Davies C. (2005). Geohydromechanical processes in the Excavation Damaged Zone in crystalline rock, rock salt, and indurated and plastic clays in the context of radioactive waste disposal. International Journal of Rock Mechanics & Mining Sciences 42, 109–125.

UK Nirex (2003). Generic Repository Studies. Generic post-closure performance assessment. UK Nirex report N/080.

Valfouskaya A., Adler P. M., Thovert J.-F. and Fleury M. (2005). Nuclear-magnetic-resonance diffusion simulations in porous media. Journal of Applied Physics 97 (8), 083510.

Valkó P. and Economides M.J. (1995). Hydraulic fracture mechanics. John Wiley, New York.

Van Geet M., Volckaert G., Bastiaens W., Maes N., Weetjens E., Sillen X., Vallejan B. and Gens A. (2007). Efficiency of a borehole seal by means of pre-compacted bentonite blocks. Physics and Chemistry of the Earth 32, 123–134.

Van Geet M., Bastiaens W. and Ortiz L. (2008). Self-sealing capacity of argillaceous rocks: Review of laboratory results obtained from the SELFRAC project. Physics and Chemistry of the Earth 33, S396–S406.

Van Geet M., Bastiaens W., Volckaert G., Weetjens E., Sillen X., Maes N., Imbert C., Billaud P., Touzé G., Filippi M., Plas F., Villar M., Garcia-Gutiérrez M., Mingarro M., Gens A. and Vallejan B. (2009). RESEAL II A large-scale in situ demonstration test for repository sealing in an argillaceous host rock - Phase II. nuclear science and technology EUR 24161 EN, European Commission, Luxembourg.

van Genuchten M.Th. (1980). A Closed-Form Equation for Predicting the Hydraulic Conductivity of Unsaturated Soils, Soil Science Society American Journal 44, 892-898.

Vandenberghe N., De Craen M. and Wouters L. (2014). The Boom Clay geology. From sedimentation to present-day occurrence. A review. Memoirs of the Geological Survey of Belgium 60, 76.

EURAD (Deliverable n° 6.1) – Initial State of the Art on Gas Transport in Clayey Materials
Dissemination level: PU
Date of issue of this report: 17/11/2021

Page 360

Vasilyeva M., Leung W. T., Chung E. T., Efendiev Y. and Wheeler M. (2020). Learning macroscopic parameters in nonlinear multiscale simulations using nonlocal multicontinua upscaling techniques. Journal of Computational Physics 412.

Večerník P., Trpkošová D. and Hofmanová E. (2014). Vývoj aparatur pro charakterizaci materiálů inženýrských bariér hlubinného úložiště radioaktivních odpadů a vyhořelého jaderného paliva - TA04021378. Zpráva ÚJV Řež, a. s. číslo 14422

Verhoef E., Neeft E., Chapman N. and McCombie C. (2017). OPERA safety case. COVRA report.

Verweij H., Nelskamp S. and Valstar J. (2016). Definition of the future boundary conditions for the near-field model_1. OPERA-PU-TNO421_1.

Villar M. V. (2002). Thermo-hydro-mechanical characterisation of a bentonite from Cabo de Grata. A study applied to the use of bentonite as sealing material in high level radioactive waste repositories. PhD thesis, Universidad Complutense de Madrid.

Villar M. V. (2005). MX-80 bentonite. Thermo-hydro-mechanical characterisation performed at CIEMAT in the context of the Prototype Project. Informes Técnicos CIEMAT, 1053.

Villar M. V. (2006). FEBEX project final report. Post-mortem bentonite analysis. Enresa. Publicación Técnica Enresa 05-1/2006.

Villar M. V. (2007). Water retention of two natural compacted bentonites. Clays and Clay Minerals, vol. 55, No. 3, 311-322.

Villar M. V. (2017). FEBEX-DP Postmortem THM/THC Analysis Report. Nagra. Technical Report NAB 16-017.

Villar M. V. and Gómez-Espina R. (2009). Report on thermo-hydro-mechanical laboratory tests performed by CIEMAT on FEBEX bentonite 2004 – 2008. CIEMAT. Informes Técnicos CIEMAT 1178.

Villar M. V. and Lloret A. (2001). Variation of the intrinsic permeability of expansive clays upon saturation. Proceedings of the International Symposium on Suction, Swelling, Permeability and Structure of Clays, Shizuoka. In Clay Science for Engineering. (eds. Adachi and Fukue). Balkema, Rotterdam. 259–266.

Villar M. and Romero F. (2012). Water retention curves of Opalinus Clay. CIEMAT. Technical Report 1262.

Villar M. V., Martín P. L., Romero F. J., Barcala J. M. and Gutiérrez-Rodrigo V. (2012). Gas transport through bentonite: influence of dry density, water content and boundary conditions. In Propriétés de Transfert des Géomatériaux (F. Skoczylas, C.A. Davy, F. Agostini, and N. Burlion, editors). Transfert 2012, Actes du Colloque. 379–389.

Villar M. V., Gutiérrez-Rodrigo V., Martin P. L., Romero F. J. and Barcala J. M. (2013). Gas transport in bentonite. CIEMAT. Technical Report 1301.

Villar M. V., Romero F., Martin P.-L., Gutiérrez-Rodrigo V. and Barcala J. (2015). Gas transport in Opalinus Clay. CIEMAT. Technical Report 1378.

Villar M. V., Iglesias R. J., Abós H., Martínez V., de la Rosa C. and Manchón M. A. (2016). FEBEX-DP onsite analyses report. Nagra. NAB 16-12.

Villar M. V., Carbonell B., Martin P. L., Gutiérrez-Álvarez C. and Barcala J. M. (2018). Gas Permeability of Bentonite Samples of the FEBEX Dismantling Project (FEBEX-DP). CIEMAT. Technical Report 1431.

Villar M. V., Romero F. J., Martín P. L., Gutiérrez-Rodrigo V. and Barcala J. M. (2019). Experimental Investigation of Gas Transport in the Shaly Facies of Opalinus Clay. In Energy Geotechnics. (eds. A. Ferrari and L. Laloui). Springer International Publishing. 434–441.

Villar M. V., Armand G., Conil N., de Lesquen C., Herold P., Simo E., Mayor J. C., Dizier A., Li X., Chen G., Leupin O., Niskanen M., Bailey M., Thompson S., Svensson D., Sellin P. and Hausmannová L. (2020a). D7.1 HITEC. Initial State-of-the-Art on THM behaviour of i) Buffer clay materials and of ii) Host clay materials. EURAD Project HORIZON 2020. Deliverable D7.1 HITEC No 847593.

Villar M. V., Iglesias R. J., García-Siñeriz J. L., Lloret A. and Huertas F. (2020). Physical evolution of a bentonite buffer during 18 years of heating and hydration. Engineering Geology 264, 105408.

Villar M. V., Carbonell B., Martín P. L. and Gutiérrez-Álvarez C. (2021). The role of interfaces in the bentonite barrier of a nuclear waste repository on gas transport. Engineering Geology 286, 106087.

Vinsot A., Appelo C. A. J., Lundy M., Wechner S., Lettry Y., Lerouge C., Fernandez A. M., Labat M., Tournassat C., De Cannière P., Schwyn B., Mckelvie J., Dewonck S., Bossart P. and Delay J. (2014). In situ diffusion test of hydrogen gas in the Opalinus Clay. Geological Society, London, Special Publications 400.

Vinsot A., Appelo C. A. J., Lundy M., Wechner S., Cailteau-Fischbach C., de Donato P., Pironon J., Lettry Y., Lerouge C. and De Cannière P. (2017). Natural gas extraction and artificial gas injection experiments in Opalinus Clay, Mont Terri rock laboratory (Switzerland). Swiss Journal of Geosciences 110 (1), 375–390.

EURAD (Deliverable n° 6.1) – Initial State of the Art on Gas Transport in Clayey Materials
Dissemination level: PU
Date of issue of this report: 17/11/2021

Page 361

Vitillo J. G., Regli L., Chavan S., Ricchiardi G., Spoto G., Dietzel P. D. C., Bordiga S. and Zecchina A. (2008). Role of exposed metal sites in hydrogen storage in MOFs. Journal of the American Chemical Society 130 (26), 8386–8396.

Volckaert G. and Mallants D. (2001). The treatment of gas in the performance assessment for the disposal of HLW and MLW in Boom Clay. In Gas migration and migration in radioactive waste disposal safety-relevant issues, Nuclear Energy Agency Radioactive Waste Management publication. 125–128.

Volckaert G., Put M., Ortiz L., De Cannière P., Horseman S., Harrington J., Fioravante V., Imprey M. and Worgan K. (1994). MEGAS Modelling and experiments on gas migration in repository host rocks. Project on effects of gas in underground storage facilities for radioactive waste (Pegasus project). European Commission, Nuclear Science and Technology. EUR 15734.

Volckaert G., Ortiz L., De Cannière P., Put M., Horseman S. T., Harrington J. F., Fioravante V. and Impey M. (1995). MEGAS - Modelling and Experiments on Gas Migration in Repository Host Rocks. Final Report Phase 1, Contract No. F12-CT91-0076. European Commission. EUR 16235 EN.

Voskuilen T. G., Pourpoint T. L. and Dailly A. M. (2012). Hydrogen adsorption on microporous materials at ambient temperatures and pressures up to 50 MPa. Adsorption 18 (3–4), 239–249.

Wagner G., Birovljev A., Meakin P., Feder J. and Jøssang T. (1997). Fragmentation and migration of invasion percolation clusters: Experiments and simulations. Phys. Rev. E 55 (6), 7015–7029.

Wan M., Delage P., Tang A. M. and Talandier J. (2014). The water retention properties of the Callovo-Oxfordian claystone. In Unsaturated Soils: Research & Applications. (eds. N. Khalili, A. R. Russell, and A. Khoshghalb). CRC Press.

Wang W. and Kolditz O. (2007). Object-oriented finite element analysis of thermo-hydro-mechanical (THM) problems in porous media. International Journal for Numerical Methods in Engineering 69 (1), 162–201.

Wang L., Yao B., Xie H., Winterfeld P. H., Kneafsey T. J., Yin X. and Wu Y. S. (2017). CO2 Injection induced Fracturing in Naturally Fractured Shale Rocks. Energy 139, 1094–1110.

Wareing A., Abrahamsen L., Banford A., Metcalfe M. and von Lensa W. (2008). Final Publishable CARBOWASTE Report. Deliverable D-0.3.12. CARBOWASTE Treatment and Disposal of Irradiated Graphite and Other Carbonaceous Waste. European Commission

Wells G. N. and Sluys L. J. (2001). A new method for modelling cohesive cracks using finite elements. International Journal for Numerical Methods in Engineering 50 (12), 2667–2682.

Wemaere I., Marivoet J. and Labat S. (2008). Hydraulic conductivity variability of the Boom clay in north-east Belgium based on four core drilled boreholes. Physics and Chemistry of the Earth 33, S24–S36.

Wersin P., Johnson L. H., Schwyn B., Berner U. and Curti E. (2003). Redox conditions in the near field of a repository for SF/HLW and ILW in Opalinus Clay. Nagra. NTB 02-13.

Wheeler S. J. and Karube D. (1995). Constitutive modelling. In Proceedings of the First International Conference on Unsaturated Soils, UNSAT 1995 (Alonso, E. E. and Delage, P., Eds.), Paris, France, pp. 1323–1356.

Wheeler S. J. and Sivakumar V. (1995). An elasto-plastic critical state framework for unsaturated soil. Géotechnique 45, No. 1, 35–53.

Wheeler S. J., Sharma R. S. and Buisson M. S. R. (2003). Coupling of hydraulic hysteresis and stress–strain behaviour in unsaturated soils. Géotechnique 53, No. 1, 41–54.

Wild K. M., Walter P. and Amann F. (2017). The response of Opalinus Clay when exposed to cyclic relative humidity variations. Solid Earth 8 (2), 351–360.

Wileveau Y. and Rothfuchs T. (2007). THM behaviour of host rock(HE-D) Experiment. Study of Thermal effects on Opalinus Clay, Mont Terri Technical Report 2006-01

Wileveau Y., Cornet F. H., Desroches J. and Blumling P. (2007). Complete in situ stress determination in an argillite sedimentary formation. Physics and Chemistry of the Earth, 32, 866–878

Wiseall A., Graham C., Zihms S., Harrington J., Cuss R., Gregory S. and Shaw R. (2015). Properties and behaviour of the Boom Clay formation within a Dutch repository concept. COVRA Report OPERA-PU-BGS615.

Wong P.Z. and Pengra D.B. (1995). Pore size, permeability and electrokinetic phenomena. In. Pinnavaia, T.J. and Thorpe, M.F. (eds). Access in Nanoporous Materials, New York Plenum Press, pp 295-317.

Wong-Foy A.G., Matzger A.J. and Yaghi O.M. (2006). Exceptional H2 Saturation Uptake in Microporous Metal−Organic Frameworks. Journal of the American Chemical Society, v. 128, p. 3494-3495.

Xu K., Daian J. and Quenard D. (1997a). Multiscale structures to describe porous media part I: theoretical background and invasion by fluids. Transport in porous media 26 (1), 51–73.

EURAD (Deliverable n° 6.1) – Initial State of the Art on Gas Transport in Clayey Materials
Dissemination level: PU
Date of issue of this report: 17/11/2021

Page 362

Xu K., Daian J.-F. and Quenard D. (1997b). Multiscale structures to describe porous media part II: transport properties and application to test materials. Transport in Porous Media 26 (3), 319–338.

Xu L., Ye W. M., Ye B., Chen B., Chen Y. G. and Cui Y. J. (2015). Investigation on gas migration in saturated materials with low permeability. Engineering Geology 197, 94–102.

Xu L., Ye W. M. and Ye B. (2017). Gas breakthrough in saturated compacted GaoMiaoZi (GMZ) bentonite under rigid boundary conditions. Canadian Geotechnical Journal 54 (8), 1139–1149.

Xu L., Ye W. M., Chen Y. G., Chen B. and Cui Y. J. (2020). Investigation on gas permeability of compacted GMZ bentonite with consideration of variations in liquid saturation, dry density and confining pressure. Journal of Contaminant Hydrology 230, 103622.

Xu W. J., Shao H., Hesser J., Wang W. Q., Kolditz O. and Popp T. (2011). Simulation of dilatancy-controlled gas migration process in saturated argillaceous rock. In Computational Geomechanics, COMGEO II - Proceedings of the 2nd International Symposium on Computational Geomechanics. 693–703.

Xu W. J., Shao H., Hesser J., Wang W., Schuster K. and Kolditz O. (2013). Coupled multiphase flow and elasto-plastic modelling of in-situ gas injection experiments in saturated claystone (Mont Terri Rock Laboratory). Engineering Geology 157, 55–68.

Yamamoto S., Kumagai M., Koga K. and Sato S. (2015). Mechanical Stability of Engineered Barriers in Sub-surface Disposal Facility during Gas Migration Based on Coupled Hydro-Mechanical Modelling. Geological Society, London, Special Publications, 415, pp.213–224.

Yang D. (2008). Caractérisation par la mesure de perméabilité au gaz de l'endommagement mécanique et hydrique dans l'EDZ des argilites du Callovo-Oxfordien. PhD. Thesis Ecole des Mines de Paris, France (208 pp.)

Yang Y. and Aplin A. C. (2010). A permeability–porosity relationship for mudstones. Marine and Petroleum Geology 27 (8), 1692–1697.

Yao X., Liu Y., Cao Q., Li J., Huang R., Woodcock R., Paget M., Wang J. and Li G. (2019). China Data Cube (CDC) for Big Earth Observation Data. Lessons Learned from the Design and Implementation. In BGDDS 2018 - 2018 International Workshop on Big Geospatial Data and Data Science.

Yoshioka K., Parisio F., Naumov D., Lu R., Kolditz O. and Nagel T. (2019). Comparative verification of discrete and smeared numerical approaches for the simulation of hydraulic fracturing. GEM - International Journal on Geomathematics 10 (1).

Yu L. and Weetjens E. (2009). Summary of Gas Generation and Migration. Current State-of-the-Art. External Report ER-106. Mol, Belgium. SCK•CEN.

Yu L. and Weetjens E. (2012). Estimation of the Gas Source Term for Spent Fuel (SF), Vitrified High-Level Waste (VHLW), Compacted Waste and MOSAIK Waste. External Report ER-162. Mol, Belgium. SCK•CEN.

Yu L., Gedeon M., Wemaere I., Marivoet J. and De Craen M. (2011). Boom Clay Hydraulic Conductivity A synthesis of 30 years of research. SCK•CEN. External Report ER-122.

Yu L., Rogiers B., Gedeon M., Marivoet J., De Craen M. and Mallants D. (2013). A critical review of laboratory and in-situ hydraulic conductivity measurements for the Boom Clay in Belgium. Applied Clay Science 75–76, 1–12.

Yu Q.-Y., Bagas L., Yang P.-H. and Zhang D. (2019). GeoPyTool. A cross-platform software solution for common geological calculations and plots. Geoscience Frontiers 10 (4), 1437–1447.

Yven B., Sammartino S., Géraud Y., Homand F. and Villiéras F. (2007). Mineralogy, texture and porosity of Callovo-Oxfordian argilites of Meuse / Haute-Marne (Eastern Paris Bassin). Mémoires de la Société Géologique de France (SGF), 178. 73-90

Zeelmaekers E., Honty M., Derkowski A., Środoń J., De Craen M., Vandenberghe N., Adriaens R., Ufer K. and Wouters L. (2015). Qualitative and quantitative mineralogical composition of the Rupelian Boom Clay in Belgium. Clay Minerals 50 (2), 249–272.

Zhang C.-L. (2013). Sealing of Fractures in Claystone, Journal of Rock Mechanics and Geotechnical Engineering 5, 214-220.

Zhang C.-L. (2015). Investigation of gas migration in damaged and resealed claystone, Proceedings – Gas Generation and Migration in Deep Geological Radioactive Waste Repositories (edited by SHAW, R.P.), The Geological Society of London, 2015.

Zhang C.-L. (2017). Sealing Performance of Fractured Claystone and Clay-Based Materials within the Framework of the German Project THM-TOM and the EC Project DOPAS. Final Report. GRS Report GRS – 451 Gesellschaft für Anlagen- und Reaktorsicherheit (GRS) mbH, Braunschweig

Zhang N. and Nagel T. (2020). Error-controlled implicit time integration of elasto-visco-plastic constitutive models for rock salt. International Journal for Numerical and Analytical Methods in Geomechanics 44 (8), 1109–1127.

EURAD (Deliverable n° 6.1) – Initial State of the Art on Gas Transport in Clayey Materials
Dissemination level: PU
Date of issue of this report: 17/11/2021

Page 363

Zhang C. and Rothfuchs T. (2004). Experimental study of the hydro-mechanical behaviour of the Callovo-Oxfordian argillite. Applied Clay Science 26 (1–4), 325–336.

Zhang C.-L. and Rothfuchs T. (2007). Moisture Effects on Argillaceous Rocks. In. Proceedings 2nd International Conference of Mechanics of Unsaturated Soils (editor T. Schanz), Springer Proceedings in Physics 112, p. 319-326.

Zhang C.-L. and Rothfuchs T. (2008). Damage and sealing of clay rocks detected by measurements of gas permeability. Physics and Chemistry of the Earth, Parts A/B/C 33, Supplement 1, S363–S373.

Zhang C-L., Dittrich J., Muller J. and Rothfuchs T. (2002) – Experimental study of hydromechanical behavior of the Callovo-Oxfordian argillites, GRS-187

Zhang C.-L., Rothfuchs T., Dittrich J., Müller J. (2008) Investigations on self-sealing of indurated clay. GRS Report GRS-230. 1-67, ISBN 978-3-939355-04-5

Zhang C.-L., Czaikowski O., Rothfuchs T. (2010) - Thermo-Hydro-Mechanical Behaviour of the Callovo-Oxfordian Clay Rock, Rapport GRS-266

Zhu C. M., Ye W. M., Chen Y. G., Chen B. and Cui Y. J. (2013). Influence of salt solutions on the swelling pressure and hydraulic conductivity of compacted GMZ01 bentonite. Engineering Geology 166, 74–80.

Zinner M., Rink K., Jäkel R., Feldhoff K., Grunzke R., Fischer T., Song R., Walther M., Jejkal T., Kolditz O. and Nagel W. E. (2018). Revision control and automatic documentation for the development numerical models for scientific applications. International Journal on Advances in Software 11 (3 and 4), 214–226.

Zio E. and Apostolakis G. E. (1996). Two methods for the structured assessment of model uncertainty by experts in performance assessments of radioactive waste repositories. Reliability Engineering and System Safety 54 (2–3), 225–241.

EURAD (Deliverable n° 6.1) – Initial State of the Art on Gas Transport in Clayey Materials
Dissemination level: PU
Date of issue of this report: 17/11/2021

Page 364